frontiers | Research Topics

Ischemic stroke as systemic disorder involving both nervous and immune systems

Edited by
Qingkun Liu, Yan Wang and Jui-Hung Jimmy Yen

Published in
Frontiers in Immunology
Frontiers in Cellular Neuroscience

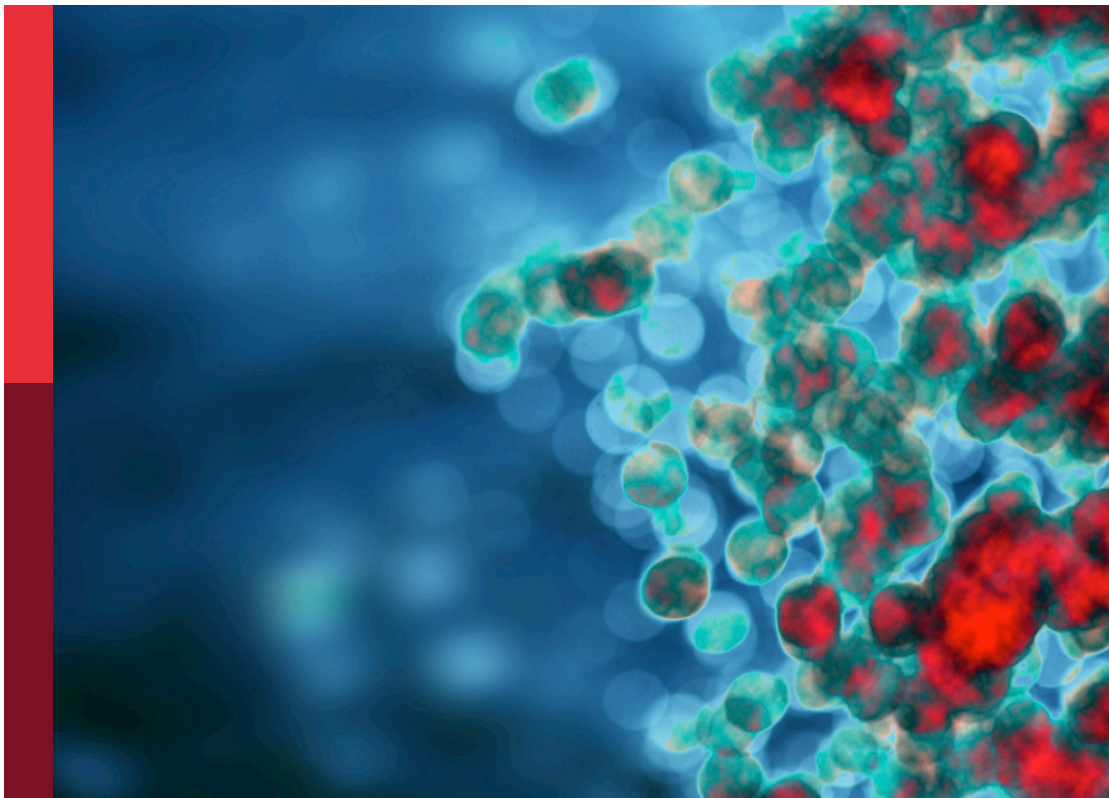

ISSN 1664-8714
ISBN 978-2-8325-2531-9
DOI 10.3389/978-2-8325-2531-9

About Frontiers

Frontiers is more than just an open access publisher of scholarly articles: it is a pioneering approach to the world of academia, radically improving the way scholarly research is managed. The grand vision of Frontiers is a world where all people have an equal opportunity to seek, share and generate knowledge. Frontiers provides immediate and permanent online open access to all its publications, but this alone is not enough to realize our grand goals.

Frontiers journal series

The Frontiers journal series is a multi-tier and interdisciplinary set of open-access, online journals, promising a paradigm shift from the current review, selection and dissemination processes in academic publishing. All Frontiers journals are driven by researchers for researchers; therefore, they constitute a service to the scholarly community. At the same time, the *Frontiers journal series* operates on a revolutionary invention, the tiered publishing system, initially addressing specific communities of scholars, and gradually climbing up to broader public understanding, thus serving the interests of the lay society, too.

Dedication to quality

Each Frontiers article is a landmark of the highest quality, thanks to genuinely collaborative interactions between authors and review editors, who include some of the world's best academicians. Research must be certified by peers before entering a stream of knowledge that may eventually reach the public - and shape society; therefore, Frontiers only applies the most rigorous and unbiased reviews. Frontiers revolutionizes research publishing by freely delivering the most outstanding research, evaluated with no bias from both the academic and social point of view. By applying the most advanced information technologies, Frontiers is catapulting scholarly publishing into a new generation.

What are Frontiers Research Topics?

Frontiers Research Topics are very popular trademarks of the *Frontiers journals series*: they are collections of at least ten articles, all centered on a particular subject. With their unique mix of varied contributions from Original Research to Review Articles, Frontiers Research Topics unify the most influential researchers, the latest key findings and historical advances in a hot research area.

Find out more on how to host your own Frontiers Research Topic or contribute to one as an author by contacting the Frontiers editorial office: frontiersin.org/about/contact

Ischemic stroke as systemic disorder involving both nervous and immune systems

Topic editors

Qingkun Liu — Icahn School of Medicine at Mount Sinai, United States

Yan Wang — Peking University Third Hospital, China

Jui-Hung Jimmy Yen — Indiana University School of Medicine, United States

Citation

Liu, Q., Wang, Y., Yen, J.-H. J., eds. (2023). *Ischemic stroke as systemic disorder involving both nervous and immune systems*. Lausanne: Frontiers Media SA.

doi: 10.3389/978-2-8325-2531-9

Table of contents

frontiers | Frontiers in Cellular Neuroscience

TYPE Editorial
PUBLISHED 10 May 2023
DOI 10.3389/fncel.2023.1208787

OPEN ACCESS

EDITED AND REVIEWED BY
Dirk M. Hermann,
University of Duisburg-Essen, Germany

*CORRESPONDENCE
Qingkun Liu
✉ qkliu.lisa@gmail.com
Yan Wang
✉ yanwang2019@bjmu.edu.cn
Jui-Hung Jimmy Yen
✉ jimyen@iu.edu

RECEIVED 19 April 2023
ACCEPTED 25 April 2023
PUBLISHED 10 May 2023

CITATION
Liu Q, Wang Y and Yen J-HJ (2023) Editorial: Ischemic stroke as systemic disorder involving both nervous and immune systems.
Front. Cell. Neurosci. 17:1208787.
doi: 10.3389/fncel.2023.1208787

Editorial: Ischemic stroke as systemic disorder involving both nervous and immune systems

Qingkun Liu[1]*, Yan Wang[2,3]* and Jui-Hung Jimmy Yen[4]*

[1]Nash Family Department of Neuroscience, Icahn School of Medicine at Mount Sinai, New York, NY, United States, [2]Institute of Medical Innovation and Research, Peking University Third Hospital, Beijing, China, [3]Medical Research Center, Peking University Third Hospital, Beijing, China, [4]Department of Microbiology and Immunology, Indiana University School of Medicine, Fort Wayne, IN, United States

KEYWORDS

ischemic stroke, systemic immune responses, microglia, peripheral immune cells, biomarker for stroke diagnosis

Editorial on the Research Topic
Ischemic stroke as systemic disorder involving both nervous and immune systems

As a systemic disorder, ischemic stroke affects millions of people worldwide with devastating consequences, including disabilities and death. Although extensive effects have been made to investigate potential clinical treatments, the time window for vascular intervention after stroke, using either thrombolytic therapy or endovascular surgery, is limited and neuroprotective approaches have failed in clinical trials. Therefore, it is critical to discover novel treatments with extended time window or to identify novel clinical biomarkers for ischemic stroke diagnosis for prompt treatments. As a multiphasic process, ischemic stroke progression is associated with long-lasting innate and adaptive immune responses, which offer appropriate time frames and targets for therapeutic interventions. To this end, this Research Topic creates a platform for researchers to (1) reveal the mechanisms of systemic immune responses and nervous system damages in ischemic stroke; and (2) discover novel biomarkers for clinical diagnosis of ischemic stroke. By including five original research articles and four comprehensive reviews, this topic covers additional critical topics in ischemic stroke, including systemic immune functions in the central nervous system and periphery, neuronal damage mechanisms, and the discovery of novel diagnostic biomarkers. These findings were categorized and summarized as follows.

The immune functions of microglia in ischemic stroke were discussed intensively in this topic. Microglia have long been taken as a main contributor to the progression of ischemic stroke. However, the dynamic functions of microglia make it challenging to revolve its exact role in different phases of ischemic stroke. In this topic, two studies investigate the mechanisms of microglial polarization in pre-clinical models. The study by Kuo et al. demonstrates a novel mechanism of IFNβ on the modulation of microglial polarization in which they identified IFNβ attenuates inflammatory and augments anti-inflammatory phenotypes of microglia in ischemic stroke mice subjected to delayed tPA treatment. They found that IFNβ-mediated modulation of microglial phenotypes plays an essential role in attenuating tPA-exacerbated ischemic brain injury and alleviating tPA-augmented BBB disruption in ischemic stroke. The study by Kong et al. showed the inhibition of stimulator of interferon genes (STING) diminishes ischemic brain infarction, edema, and neuronal injury after ischemic stroke. Mechanistically, they identified STING promotes microglial

polarization toward inflammatory phenotype. In addition, a specific review of the functions and mechanisms of microglial phagocytosis is included. Jia et al. demonstrated the microglial phagocytosis as a double-sword to stroke recovery by several potential receptors sensing "eat-me" signals. On the one hand, microglia engulf live neurons and endothelial cells, resulting in excessive neuronal death and BBB leakage. On the other hand, microglia restrict inflammatory damage via engulfing cell debris, cleaning infiltrating neutrophils, and creating an optimal microenvironment for neurogenesis.

In addition to microglia, peripheral immune cells have been shown to play a systemic role in ischemic stroke. Unlike microglia, leukocytes could either infiltrate into the brain or maintain in the peripheral organs to exert both detrimental and beneficial effects on the outcomes of ischemic stroke (Benakis et al., 2016; Liu et al., 2019). In this topic, Weber et al. evaluated the transcriptomic gene changes, vascular quantification, and behavior tests among Reg2$^{-/-}$, NSG, and tacrolimus immunosuppressed mouse as well as wild type (WT) C57BL/6J mouse stroke model. Firstly, the study indicated that the immune-deficiency mice had less macrophage infiltration and microglia activation. Secondly, although the genetic immunosuppression model is reliable for graft survival, pharmacological immunosuppression with tacrolimus could provide more accurate results with the least variation in gene expression compared to WT control group. This conclusion provides valuable baseline data for researchers to consider which mouse model would best suit for studies. In addition, a review by Zhang et al. summarized the effects and mechanisms of infiltrating peripheral immune cells, immune cell-released cytokines, and cell-cell interactions in the neurological recovery after ischemic stroke. Specifically, monocytes and macrophages actively participate in neurogenesis and oligodendrogenesis via polarization and phagocytotic function. Neutrophils can impair revascularization by releasing extracellular traps. T regulatory cells facilitate functional recovery, and B cells may regulate neurological function by antibodies. These cells and brain resident cells can also interact and communicate with each other to exert complicated effects on functional recovery.

Another topic that attracts attention is how systemic immunity involving both CNS and periphery affects ischemic stroke outcomes. The study by Weng et al. evaluated the therapeutic potential of 4-ethylguaiacol (4-EG) known as methoxyphenols in ischemic stroke. They found that 4-EG ameliorates ischemic brain injury and lessens BBB disruption in the ischemic brain. They further identified that 4-EG suppresses microglial activation, peripheral inflammatory immune cell infiltration, and brain endothelial cell adhesion molecule upregulation in the ischemic brain. These protective effects are attributed to the induction of anti-oxidant and anti-inflammatory Nrf2/HO-1 pathway. As a group of cytokines, interleukins can be expressed and secreted by both leukocytes and microglia. It plays a significant role in modulating the functions of immune cells systemically. The review by Zhu et al. divided interleukins into two categories: pro-inflammation and anti-inflammation. Another difference between these two categories is the time points they function. Specifically, pro-inflammatory IL-1 functions during the acute phase, whereas anti-inflammatory IL-10 starts to express 4 days after the brain injury. Currently, the therapeutic potential of interleukins has been well-applied in both basic and translational cancer research (Briukhovetska et al., 2021). As it has been shown, interleukins play significant roles in both acute and sub-acute phases after ischemic stroke; interleukin therapy would be an interesting and exciting future clinical research direction. Cell apoptosis, edema, endoplasmic reticulum stress (ERS), and inflammation are the main events occurring after ischemic stroke. In this topic, the review by Wang et al. summarizes many cytokines and compounds targeting ERS that show effects on alleviating ischemic brain injury.

Identifying clinical biomarkers for stroke diagnosis would benefit thousands of patients by providing prompt treatments. In this topic, Maciejczyk et al. demonstrates the potential utility of salivary xanthine oxidase (XO) in the differential diagnosis of stroke with the stress-free and non-invasive collection. In particular, XO catalyzes the generation of reactive oxygen species, which induce oxidative stress and inflammatory mediators, the leading factors for ischemic brain injury. They demonstrated that XO-specific activity in salivary distinguishes ischemic stroke from hemorrhagic stroke and healthy control with high sensitivity and specificity and therefore serves as a potential biomarker for diagnosis.

In summary, this Research Topic includes studies covering the effects of microglial polarization on ischemic brain injury outcome, the role of peripheral immune cells in the acute injury and recovery phase, roles of cytokines in modulating neuroinflammation and novel brain-protective immunomodulatory treatments. With this regard, this Research Topic contributes important findings that advance our understanding in the field of peripheral and CNS immune system interplay.

Author contributions

QL initiated the Research Topic and drafted the editorial manuscript. YW and J-HY contribute to the writing of the editorial. All authors contribute equally to the editing of the papers in this topic. All authors contributed to the article and approved the submitted version.

Conflict of interest

The authors declare that the research was conducted in the absence of any commercial or financial relationships that could be construed as a potential conflict of interest.

Publisher's note

References

Benakis, C., Brea, D., Caballero, S., Faraco, G., Moore, J., Murphy, M., et al. (2016). Commensal microbiota affects ischemic stroke outcome by regulating intestinal γδ T cells. *Nat. Med.* 22, 516–523. doi: 10.1038/nm.4068

Briukhovetska, D., Dörr, J., Endres, S., Libby, P., Dinarello, C. A., and Kobold, S. (2021). Interleukins in cancer: from biology to therapy. *Nat. Rev. Cancer* 21, 481–499. doi: 10.1038/s41568-021-00363-z

Liu, Q., Johnson, E. M., Lam, R. K., Wang, Q., Ye, H. B., Wilson, E. N., et al. (2019). Peripheral TREM1 responses to brain and intestinal immunogens amplify stroke severity. *Nat. Immunol.* 20, 1023–1034. doi: 10.1038/s41590-019-0421-2

frontiers in Immunology

REVIEW
published: 10 January 2022
doi: 10.3389/fimmu.2021.790201

The Role of Microglial Phagocytosis in Ischemic Stroke

Junqiu Jia[1], *Lixuan Yang*[1], *Yan Chen*[1], *Lili Zheng*[1], *Yanting Chen*[1], *Yun Xu*[1,2,3,4*] *and Meijuan Zhang*[1,2,3,4*]

[1] Department of Neurology, Drum Tower Hospital, Medical School and The State Key Laboratory of Pharmaceutical Biotechnology, Institute of Brain Science, Nanjing University, Nanjing, China, [2] Jiangsu Key Laboratory for Molecular Medicine, Medical School of Nanjing University, Nanjing, China, [3] Jiangsu Province Stroke Center for Diagnosis and Therapy, Affiliated Drum Tower Hospital, Medical School of Nanjing University, Nanjing, China, [4] Nanjing Neuropsychiatry Clinic Medical Center, Affiliated Drum Tower Hospital, Medical School of Nanjing University, Nanjing, China

Microglia are the resident immune cells of the central nervous system that exert diverse roles in the pathogenesis of ischemic stroke. During the past decades, microglial polarization and chemotactic properties have been well-studied, whereas less attention has been paid to phagocytic phenotypes of microglia in stroke. Generally, whether phagocytosis mediated by microglia plays a beneficial or detrimental role in stroke remains controversial, which calls for further investigations. Most researchers are in favor of the former proposal currently since efficient clearance of tissue debris promotes tissue reconstruction and neuronal network reorganization in part. Other scholars propose that excessively activated microglia engulf live or stressed neuronal cells, which results in neurological deficits and brain atrophy. Upon ischemia challenge, the microglia infiltrate injured brain tissue and engulf live/dead neurons, myelin debris, apoptotic cell debris, endothelial cells, and leukocytes. Cell phagocytosis is provoked by the exposure of "eat-me" signals or the loss of "don't eat-me" signals. We supposed that microglial phagocytosis could be initiated by the specific "eat-me" signal and its corresponding receptor on the specific cell type under pathological circumstances. In this review, we will summarize phagocytic characterizations of microglia after stroke and the potential receptors responsible for this programmed biological progress. Understanding these questions precisely may help to develop appropriate phagocytic regulatory molecules, which are promoting self-limiting inflammation without damaging functional cells.

Keywords: phagocytosis, microglia, ischemic stroke, signaling receptors, prognosis

OPEN ACCESS

Edited by:
Yan Wang,
Peking University Third Hospital, China

Reviewed by:
Marlene Wiart,
Centre National de la Recherche Scientifique (CNRS), France
Robert Adam Harris,
Karolinska Institutet (KI), Sweden

****Correspondence:***
Yun Xu
xuyun20042001@aliyun.com
Meijuan Zhang
juanzi1986126@163.com

Specialty section:
This article was submitted to Multiple Sclerosis and Neuroimmunology, a section of the journal Frontiers in Immunology

Received: *06 October 2021*
Accepted: *14 December 2021*
Published: *10 January 2022*

Citation:
Jia J, Yang L, Chen Y, Zheng L, Chen Y, Xu Y and Zhang M (2022) The Role of Microglial Phagocytosis in Ischemic Stroke. Front. Immunol. 12:790201. doi: 10.3389/fimmu.2021.790201

Stroke has a great impact on public health and is still the leading cause of death and disability in the world (1). Obstruction of the blood and oxygen supply after ischemic stroke is the initial reason for cell death. The intense changes of circumstances like accumulation of cell debris or infiltration of immune cells in the brain may induce the secondary progression of cell injury (2). Strategies aiming at restoring cerebral perfusion, namely, intravenous rt-PA injection and emergent endovascular intervention have been written in stroke therapeutic guidelines (3, 4). Plenty of stroke patients

cannot receive this treatment for missing the time windows although sizable efforts have been made to shorten the door to needle time (DNT). Hence, it is imperative to develop drugs that extend the time window through alleviating the secondary injury and promoting rehabilitation of ischemic stroke.

Microglia, the professional phagocyte of the brain, are capable of engulfing cell debris and pruning synapses in developing brain and various cerebral diseases (5). Despite being less commonly known, a growing body of literature has linked microglial phagocytosis with stroke recovery. In this review, we will summarize phagocytic characterizations of microglia after stroke and the potential receptors responsible for this programmed biological progress.

BRIEF INTRODUCTION OF MICROGLIA PROPERTIES AFTER ISCHEMIC STROKE

Microglia Accumulate in Large Numbers After Ischemic Stroke

Originating from myeloid precursors, microglial cells born in the yolk sac invade the central nervous system (CNS) during early embryonic development, which continuously supervises the brain parenchyma and protects against damage-associated pathogens (6). Upon ischemic stroke, microglia are rapidly activated and accumulate in large numbers at the site of infarction, which is also defined as microgliosis (7). Whether microglia are replenished *in situ* or derived from circulatory precursors is the subject of great interest. Taking advantage of a mouse photothrombosis stroke model, Li et al. reported that reactive microglia increased within minutes and were recruited to the infarcted area continuously during the first week after stroke induction (7). Additionally, local resident microglia division rather than recruitment of circulating macrophage was the main source of microgliosis (7, 8). Researchers then begin to search whether microglia progenitors exist in the brain, which gives rise to the newborn microglia after cerebral injury. It is considered that microglia progenitor cells in the adult brain may be lacking. The rapidly proliferated microglia after the injury are solely derived from residual microglia rather than microglia progenitors (9).

Functions of Microglia Were Heterogenous After Ischemic Stroke

It is widely accepted that targeting microglia activation could inhibit inflammatory injury and facilitate better stroke recovery (10). However, depletion of microglial cells exacerbates ischemic injury and dysregulates neuronal network activity (11, 12). It is predicted that detrimental outcomes of excessive microglial activation after ischemia could be counterbalanced by beneficial outcomes, namely, phagocytosis and release of trophic factors. It also provides a hint that microglia demonstrate great heterogeneity, which calls for further investigations regarding microglia subtypes or specific functions. Upon the challenge of ischemic stroke, rest microglia can be activated in response to the inflammatory triggers and differentiates into two phenotypes like macrophage: M1 and M2. M1 macrophages (classically activated) are thought to be neurotoxic and are related to the production of pro-inflammatory cytokines, such as interleukin-6 (IL-6) and tumor necrosis factor-α (TNF-α), while M2 macrophages (alternatively activated) are neuroprotective and promote tissue repair and stroke recovery (13). It is worth mentioning that M2 microglia are proven to show the ability of phagocytosis and their capability of cleaning neuronal debris reduces brain damage after stroke (14). *In vitro* assays suggest that IL-10-induced M2 microglia present enhanced phagocytosis abilities (15). However, this classification method could not adequately reflect the complicated microglial characteristics in the activated state. In recent studies, researchers even failed to find pure M1 or M2 state *in vivo* (16). With the development of single cell-sequencing techniques, scientists prefer to designate the microglia profile regarding its unique functions in specific diseases. For instance, one unique microglia population with the potential to restrict neurodegeneration of Alzheimer's disease is named neurodegenerative microglia (DAM) (17, 18). Therefore, we also expect to characterize microglia in ischemic stroke from a functional perspective.

Microglia Invade Infarcted Areas Earlier Than Macrophages

Due to similar histological phenotypes, the contribution of activated resident microglia or infiltrated macrophages to stroke pathology has been difficult to distinguish. On Day 1 after focal cerebral ischemia, the microglia amount remains unchanged (19). However, they switch their morphology into an ameboid and rounded shape with acquiring phagocytic properties and phagocytose neuronal cell debris. Thereafter, the microglia continue to proliferate during the first two weeks and show the most powerful phagocytic capacity within the first 2 days of stroke, which proceeds and predominates over phagocytes of hematogenous origin (19). Similarly, histological studies of green fluorescent protein (GFP) transgenic bone marrow chimeric mice with transient or permanent stroke models pointed that blood-derived macrophages infiltrated infarct area with a delay of at least 24 to 48 h after stroke onset (20, 21).

Taken together, studies suggest that macrophages invade the ischemic site of stroke later than microglia. The microglia are the main phagocytes during the first three days after stroke (19–21). In contrast to the rapid microglial response, the macrophages are rarely detected during the first 48 h and then gradually increase with the peak time in the first week after stroke (22). Transcriptomic studies of macrophages at Day 5 post stroke showed that infiltrated macrophages promote efferocytosis and inflammation resolution after ischemic stroke (23).

ENGULFMENT PROPERTIES OF MICROGLIA AFTER STROKE

Whether the phagocytic property of microglia in stroke is harmful or beneficial remains unclear. For instance, some researchers found that upregulating phagocytic capability of

microglia in transient middle cerebral artery occlusion (tMCAO) mouse model promoted efficient clearance of tissue debris, facilitated tissue reconstruction, and reorganized neuronal network (24, 25). Conversely, other scholars suggested that excessively activated microglia engulfed live or stressed neuronal cells in endothelin-1 induced focal cerebral ischemia model, which resulted in function deficits and brain atrophy after stroke (26, 27). Therefore, microglial phagocytosis after stroke is a very interesting and complicated biological progress that may depend on the severity of initial ischemia, the advent or not of reperfusion, the location within the lesion (core or penumbra as defined afterwards), and the considered time points post-ictus. In addition, different experimental techniques and stroke models could be one reason for result discrepancy. Therefore, we summarized the various techniques used to measure phagocytic capability in **Table 1**. Another critical reason is that the comprehensive phagocytic effect of microglia may depend on their swallowing different cells mediated by specific "eat-me" signaling pathways. Understanding these mechanisms of microglia-mediated engulfment upon ischemic injury may open up exciting new therapeutic avenues for combating acute-stage inflammation and late-stage synaptic refinements.

Stroke triggers a cascade of events leading to rapid neuron and oligodendrocyte injury in the infarcted core (unsalvageable infarcted tissue with rCBF values less than 10 ml/100 g/min), and also in the penumbra area (salvageable infarcted tissue with rCBF values of 10 to 22 ml/100 g/min) (41). Initially, stressed neurons or oligodendrocytes release damage associated molecular patterns (DAMPs), which act as eat-me signals attracting microglial phagocytosis. Subsequently, severe or prolonged ischemic injury produces a large number of cell debris. Efficient clearance of cell debris by microglia could be positive feedback for neurogenesis and initiate stroke recovery. Additionally, microglial phagocytosis may destabilize blood–brain barrier (BBB) integrity by engulfing endothelial cells and regulate the inflammatory response by engulfing polymorphonuclear neutrophil granulocytes (PMNs). We here summarized these biological properties.

The Engulfment of Neurons

It is beneficial in part that microglia are capable of rapidly clearing dead or dying neurons within hours after stroke (39). Therefore, microglia play a fundamental role in facilitating the reorganization of neuronal circuits and resolving inflammation, especially in the ischemic core (42). Nevertheless, in areas of penumbra, stressed but alive neurons expose an eat-me signal called phospholipid phosphatidylserine (PS) in a reversible manner. Phagocytosis of these stressed but viable neurons is harmful to recovery, causing brain atrophy and motor dysfunction, which is also defined as phagoptosis (26, 27). Communication between microglia and stressed neurons is interesting. Upon ischemia, stressed neurons express TMEM16F, which mediates the exposure of PS. TMEM16F knockdown blocked microglial phagocytosis of viable neurons in the penumbra and improved functional recovery in rat MCAO model (43). On the other hand, to resist phagoptosis, neurons

TABLE 1 | Different techniques available to assess microglial phagocytosis.

Techniques	Concrete experiment content	Advantages/Limitations	Literature
	In Vivo		
Immunofluorescence (IF): Co-staining with microglial biomarkers, e.g., Iba1	Phagocytosis function: CD68, Lamp1, Phalloidin, Clathrin	The most common method and is suitable for all kinds of phagocytosis, but difficult to show the general view of brain	(28–30)
	Hemocytes: CFSE		(31)
	Neutrophil: NIMP-R14, Ly6G		(31, 32)
	Neuronal cell debris: NeuN, MAP2		(19, 29)
	Endothelial cells: CD31		(33)
	Myelin debris: MBP		(34)
Confocal microscopy and three-dimensional reconstruction	Multiple-immunostaining of Iba1 and other markers followed by orthogonal optical sectioning	Intuitive to show the microglial phagocytosis although the view is small	(27, 33, 32)
Immunohistochemistry	Oil red O staining for myelin debris phagocytosis	Simple and efficient but indirect and non-specific	(35)
Fluorescence activated cell sorting (FCAS)	CD68 expression	A quantitative and overall analysis while nonintuitive	(33)
	Double-positive cells (CD11b and other markers) expression		(32)
Two-photon microscopy	Use transgenic mice visualizing microglia and other cells	Display dynamic phagocytosis process *in vivo* with high technical requirement	(33, 36)
Morphological phenotype: combined with IF	Ball-and-chain microglial buds in developing brain	Only indicating phagocytic activity without definitive evidence	(37)
	In vitro		
Immunofluorescence (IF)	Use different kinds of fluorescent microbeads to assess phagocytic activity	Might be the "gold standard" but is restricted to *in vitro* study	(27, 32, 38, 39)
Fluorescence activated cell sorting (FCAS)	DiO-labeled myelin debris and microglia coculture	Easy to quantify but the experimental conditions are not unified	(34)
Time-lapse video microscopy	PMN–microglia coculture	Display the phagocytosis procedure in a video but only *in vitro*	(40)
	Neuron–microglia coculture		(39)

CD11b, cluster of differentiation molecule 11b; CD31, Platelet endothelial cell adhesion molecule; CD68, Cluster of Differentiation 68; CFSE, Carboxyfluorescein succinimidyl ester; Iba1, Ionized calcium binding adaptor molecule 1; Lamp1, Lysosomal-associated membrane protein 1; MAP2, Microtubule Associated Protein 2; MBP, Myelin Basic Protein; NeuN, neuronal nuclei; NIMP-R14, a Ly-6G/Ly-6C antibody; Ly6G, Lymphocyte antigen 6 complex locus G6D.

may transfer microRNA-98 to microglia *via* extracellular vesicle secretion to prevent the salvageable neurons from microglial phagocytosis in tMCAO model (44).

The Cleaning of Myelin

In the research on remyelination of multiple sclerosis, it was found that the proliferation of oligodendrocyte progenitor cells (OPCs) and their migration to the lesion are not pivotal players in remyelination, while the differentiation of OPCs is more critical for remyelination. The debris from injured myelin and death cells suppress differentiation of OPCs (35, 45). Moreover, the mononuclear phagocytic system mediates debris phagocytosis, improves the immune microenvironment of OPCs differentiation, and plays a necessary role in the restoration of white matter damage (34). Although white matter injury occupies nearly half of ischemic infarct volume, few studies are concerned about microglia mediated myelin clearance in ischemic stroke. Pseudoginsenoside-F11 (PF11), an ocotillol-type saponin, exerts neuroprotective effects against ischemic stroke in a way that accelerates the phagocytosis of myelin debris by microglia (38). Mechanically, metabolic analysis showed that the clearance of cholesterol-rich myelin debris by microglia could synthesize desmosterol and activate liver X receptor (LXR) signaling, which resolves inflammation and creates a favorable environment for oligodendrocyte differentiation (28). Whether this mechanism is applicable to stroke model remains to be studied.

The Cleaning of Cell Debris

Microglia, especially M2 microglia, have the constant ability to clear cell debris in ischemic stroke and consequently attenuate the detrimental effects of inflammation (14, 42). Debris clearance efficiency by microglia could be affected by the local microenvironment. For example, a positive correlation was found between the TNF expression level and phagocytic activity in stroke-lesioned rodent brain (22, 46). The ability of microglia to phagocytize and clean cell debris can be halted by reactive oxygen species (ROS) including superoxide ($O2^-$) (47).

In addition to controlling detrimental inflammation, microglial phagocytosis does a remarkable job of promoting neurogenesis through clearing debris. Neurogenesis takes place in regions like cerebral neocortex, subventricular zone (SVZ), and sub-granular zone (SGZ), which happens immediately after brain ischemic challenge (48). Microglia isolated from the SVZ supported neurosphere generation *in vitro*, indicating the supporting role of microglia in neurogenesis in SVZ. Studies demonstrated that prefrontal stroke disturbed homeostasis of microglial phagocytosis, presenting with accumulating apoptotic cells in the SGZ (49). In early postnatal rats subjected to hemisphere ischemia, microglia accumulated and displayed engulfment properties in the ipsilateral SVZ region (37), while in adult rat stroke brain, it is reported that activated microglia increased in ipsilateral SVZ region concomitant with neuroblast migration into the ischemic region (30). Even though knowledge about the effects of microglial phagocytotic populations in SVZ region of ischemia is still scarce, the phagocytic nature of SVZ microglia in adult has been reported (29, 30, 50). Enhancement of phagocytosis by sevoflurane treatment might lead to a favorable microenvironment for neuroblast survival (29, 50). Consistently, intraperitoneal injection of minocycline (a microglial inhibitor) hampered the activation of microglia and obstructed neurogenesis at the same time (29).

The Engulfment of Polymorphonuclear Neutrophil Granulocytes (PMNs)

PMNs infiltrate the brain parenchyma 1 day after focal ischemia, which induces inflammation and exacerbates neuronal damage through releasing oxygen radicals, proteases, and pro-inflammatory cytokines (51, 52). Thus, the prevention of infiltration and the reduction of the number of PMNs are putatively protective. Applying invading PMNs into organotypic brain slices enhances ischemic neurotoxicity, which could be counteracted by additional application of microglia (31, 53). Several recent studies have shown that microglia can engulf these infiltrating neutrophils (31, 32, 36, 54). In hippocampal slice cultures exposed to oxygen glucose deprivation, microglia engulf apoptotic PMNs and viable, motile, non-apoptotic PMNs, adopting a "chasing behavior" by time-lapse image (40). In the rat ischemic brain, the number of neutrophils is controlled by microglial phagocytosis (31). Two-photon microscopy intuitively presented neutrophils which infiltrated into the ischemic brain parenchyma cross talked with microglia and were engulfed by them. The engulfment of PMNs may prevent the release of neurotoxic compounds because dying PMNs secrete toxic compounds and also living PMNs (31). As such, scavenging PMNs alleviate neuron injury by converting the microenvironment from pro-inflammatory to anti-inflammatory (53).

The Engulfment of Vascular Endothelial Cells

Using two-photon microscopy and $CX3CR1^{+/GFP}$ mice, microglia were detected to expand toward adjacent blood vessels within 24 h post tMCAO (33). Subsequently, these perivascular microglia started to eat up endothelial cells by phagocytosis, which caused the disintegration of blood vessels with an eventual breakdown of the BBB. Accordingly, loss-of-microglia-function studies displayed a reduction in the extravasation of contrast agent into the brain penumbra and a decreased infarct size as measured by MRI.

Engulfment properties of microglia and their potential pathological outcome after ischemic stroke are depicted in **Figure 1**.

SIGNALING MOLECULES RESPONSIBLE FOR MICROGLIA PHAGOCYTOSIS AFTER STROKE

Professional phagocytes constantly fulfill a monitoring role rely on immune molecules to identify targeted pathogens or debris in need of removal. All phagocytic behaviors start with the exposure of "eat-me" signals from the target cells or debris. By sensing

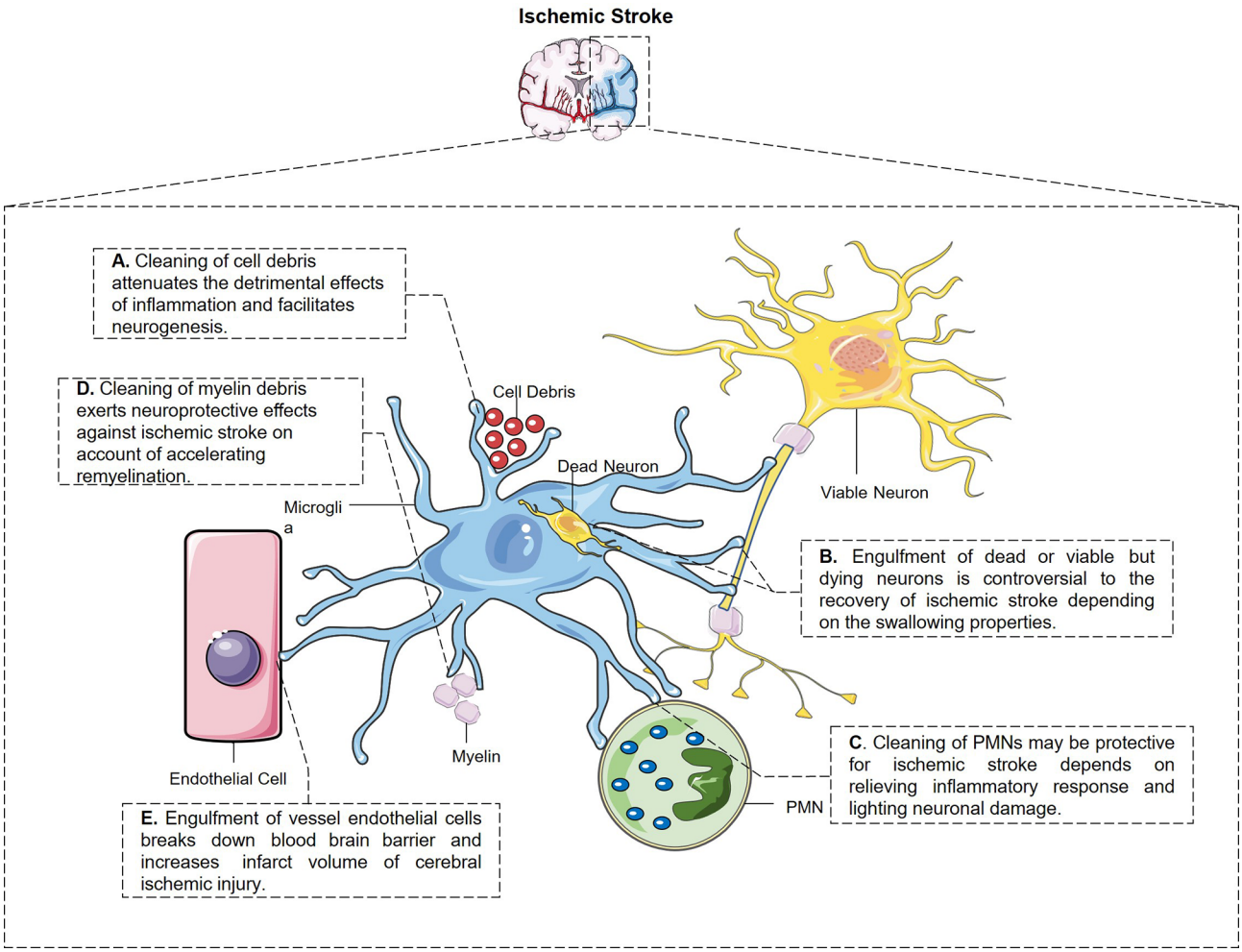

FIGURE 1 | The engulfment properties of microglia and its potential pathological outcome after ischemic stroke. **(A)** Microglia have the constant ability to clear cell debris, which attenuates the detrimental effects of inflammation and facilitates neurogenesis. **(B)** Microglia engulf dead and also stressed but viable neurons after stroke through different signal pathways, which is controversial to the stroke outcome. **(C)** Microglia swallow not only living but also dying PMNs and relieves inflammatory response and neuronal damage from every aspect. **(D)** Microglia swallow myelin debris in MCAO mice which may be protective for ischemic stroke in a way of accelerating remyelination and restoring white matter damage. **(E)** Perivascular microglia eat up endothelial cells after cerebral ischemic injury which breaks down blood–brain barrier and enlarged infarct volume.

exposed "eat-me" signals, microglia begin rapid recognition and engulfment of target cells. PS is the best-known "eat-me" signal. Once exposed on the cell surface, it will modulate a crucial process of phagocytosis. PS appears usually inside of the cellular membrane and translocates to the external side of membrane under various circumstances, such as oxidative stress, inflammation, and growth-factor withdrawal (26). Apart from PS, calreticulin and desialylated cell surface glycoproteins also act as "eat-me" signals. Calreticulin is normally localized in the endoplasmic reticulum and translocates on the cell surface as a result of endoplasmic reticulum stress (55). The chemistry process of desialylation is catalyzed by sialidases (also known as neuraminidases). Sialidases integrate on cytomembrane and remove sialic acid residue after cell stress (56). Opsonins are soluble proteins binding the "eat-me" signal to its corresponding receptor on professional phagocytes, which are engaged subsequent to "eat-me" signal exposure. As an illustration, galectin-3 (Gal-3) is one of the opsonins secreted by macrophages and microglia. Upon LPS stimulation, Gal-3 is rapidly released from activated microglia and binds to Mertk on microglial cells and also desialylated sugar chains of stressed or dying neuronal cells (56). Multiple soluble molecules, namely, growth arrest-specific protein 6 (Gas6) or Protein S, milk fat globule EGF factor 8 (MFG-E8) opsonizes PS-exposing cells or other eat-me signals and is subsequently recognized by unique receptors on professional phagocytes (57). Here, we summarized emergent eat-me/opsonin/phagocytic receptor systems in ischemic stroke in **Figure 2**.

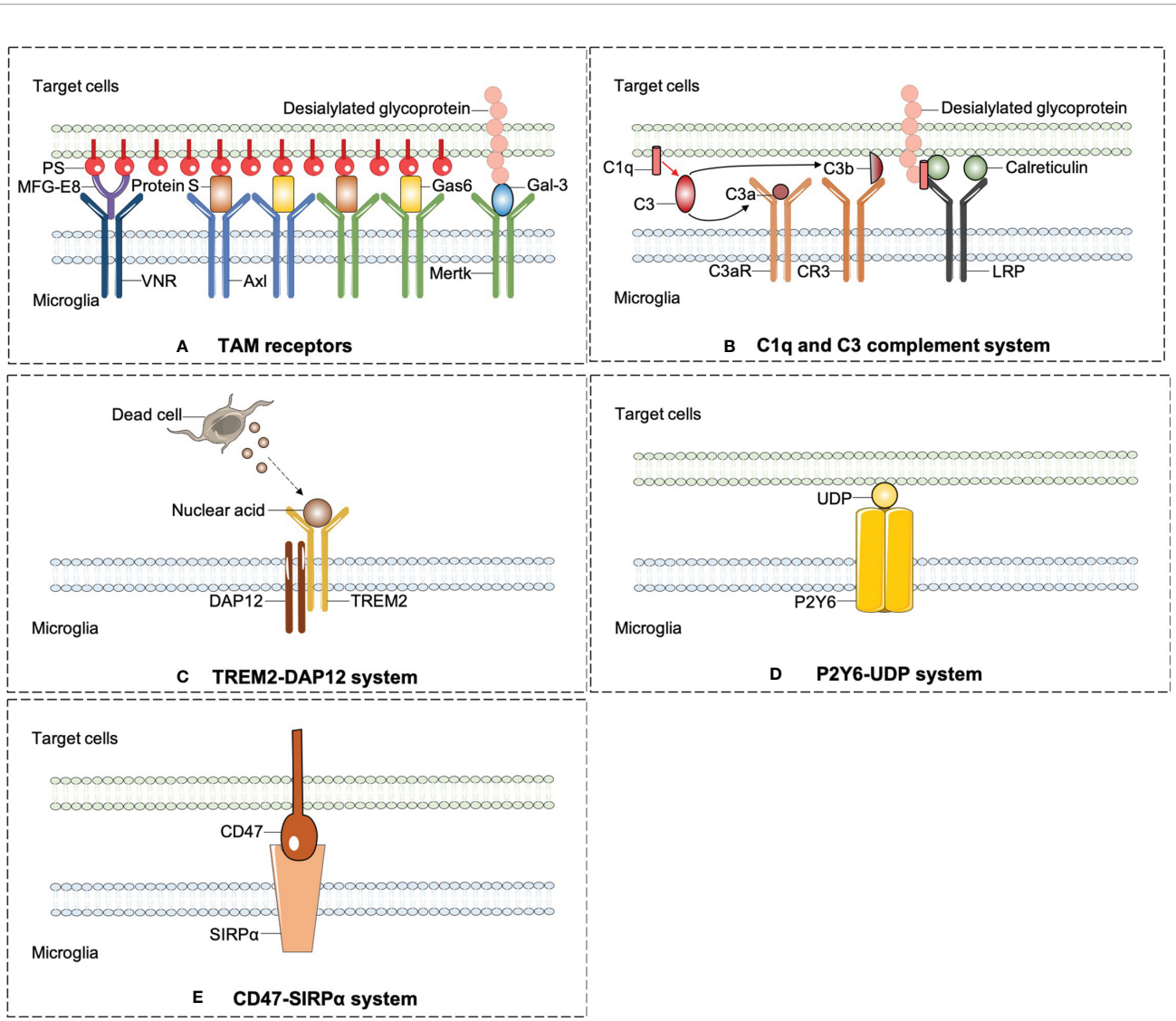

FIGURE 2 | The emergent eat-me/opsonins/phagocytic receptor systems in ischemic stroke. **(A)** Axl and Mertk of TAM receptors were widely expressed on microglia and can identify the best-known "eat-me" signal-PS. PS induces phagocytosis by activating VNR via MFG-E8 or TAM receptors via GAS6 or protein S. In addition to PS, Mertk also binds to desialylated sugar chains of stressed or dying neuronal cells through Gal-3, another opsonin which is rapidly released from activated microglia. **(B)** C1q mediates phagocytic recognition by means of binding to desialylated glycoproteins on targeted cell surface, and cooperatively activates LRP on microglia with the combination of calreticulin. Additionally, C1q triggers a protease cleavage and leads to the deposition of C3b, which directly activates CR3 on microglia. **(C)** TREM2-DAP12 signaling is involved in phagocytosis by microglia and plays a beneficial role in ischemic stroke. **(D)** P2Y6 receptors on microglia is activated by UDP released from damaged neurons and triggers microglial phagocytosis. **(E)** CD47-SIRPαsignaling can inhibit the microglia engulfment property which may aggravate ischemic injury.

TAM Receptors

TAM is an acronym for Tyro3, Axl, and Mer (protein designation Mer, c-Mer, or Mertk), which is widely expressed on the phagocyte surface of central nervous, immune, vascular, mammalian reproductive system, and retina (57). Mice with triple mutations in *Tyro3*, *Axl*, and *Mer* display a severe lymphoproliferative disorder accompanied by broad-spectrum autoimmunity (58). In the human brain, Axl is highest in mature astrocytes, microglia, oligodendrocytes, endothelial cells, and neurons. Mer expression is highest in both microglia and mature astrocytes, still detected in oligodendrocytes (59). Tyro3 is expressed on mature oligodendrocytes and has been implicated in multiple sclerosis susceptibility and myelin production (60).

Protein S is a vitamin K-dependent anticoagulant plasma glycoprotein. Growth arrest-specific protein 6 (Gas6), a structural analog of protein S, acts as a molecular bridge between the TAM receptors and eat-me signals together with protein S. In retinal pigment epithelial cells, either Mer mutation or concerted deletion of Gas6/protein S ligands disrupts

circadian phagocytosis of photoreceptor outer segments (57). As mentioned above, Gal-3 has also been identified as a Mer ligand (61).

The pathological roles of TAM receptors in ischemic stroke have begun to be addressed directly. Protein S blocks endothelial injury and MCAO-induced BBB leakage after ligation of Tyro3 through activating sphingosine 1-phosphate receptor other than Mer or Axl (62). Likewise, protein S obstructs the extrinsic apoptotic cascade through Tyro3-dependent phosphorylation of FKHRL1 which may reduce post-ischemic neuronal toxicity (63). Endogenous expression of Axl and Gas6 increased in microglia/macrophage after stroke, while intranasal injection of recombinant Gas6 (rGas6) reduced the neurological deficits through inhibiting neuroinflammation by inhibiting TLR/TRAF/NF-kappaB pathway (64).

Upon PS exposure, another opsonin molecule MFG-E8 and its microglial receptors vitronectin receptors (VNRs) mediate phagocytosis through activating a CRKII–DOCK180–RAC1 signaling pathway, which results in remodeling of microglial cytoskeleton (26). Previous findings confirmed that microglia express Mer and MFG-E8 in a high-level response to inflammatory stimuli after ischemia stroke. Compared to wild-type mice, mice lacking Mer or MFG-E8 appeared a decreased loss of viable neurons after brain ischemia stroke, which leads to a great improvement of motor function recovery (26, 27). Molecular signaling pathways regarding TAM receptors are summarized in **Figure 2A**.

C1q and C3 Complement System

The complement components C3 and C1q may induce phagocytosis by binding to dying cell surfaces. C3 is activated and cleaved into the small protein C3a and the larger C3b complex by C3 convertase. C3a could attract immune cells and modulate the immune response by interacting with the cellular receptor C3a receptor (C3aR). C3b along with its cellular receptor CR3 mediates the clearance of dying cells and modulates the adaptive immune response (65, 66).

C1q, the biggest protein of the C1 complex, is present in the neutrophils, microglia, and a subset of interneurons (67). Interestingly, C1q can enhance microglial clearance of apoptotic cells independent of C1r and C1s after ischemic stroke (68). On the intact cell surface, sialic acid modification of glycoproteins or glycolipids can act as a "don't-eat-me" signal by preventing complement C3b and C1q binding. On the dying cell surface, glycoproteins or glycolipids could be desialylated. Then, C1q mediates phagocytic recognition by means of binding to desialylated glycoproteins. Apart from desialylated glycoprotein, calreticulin also acts as an opsonin for C1q. When C1q opsonizes dead cells, it could not only mediate engulfment by binding to lipoprotein receptor-related protein (LRP) on microglia, but also promote the conversion of C3 to C3b and trigger C3b-based phagocytosis (26, 69, 70).

In the developing CNS, C1q and C3 have been identified as important factors for controlling synaptic pruning. Microglia engulf presynaptic inputs during peak retinogeniculate pruning is dependent on C3b/CR3 signaling pathway (70, 71). After ischemic stroke, complement activation directs continuous microglia-dependent phagocytosis of hippocampal synapses and penumbral salvageable neurons, leading to cognitive decline. B4Crry is a targeted complement inhibitor inhibiting all complement pathways at the central C3 activation step. B4Crry prevents phagocytosis of penumbral neurons and hippocampal synapses, improving long-term motor and cognitive recovery (72, 73). C3aR antagonist, SB 290157 given intracortically, may limit neuroinflammation and neuronal death after ischemia by restraining microglia transition to the phagocytic type (74). In chronic cerebral hypoperfusion rats, SB290157 decreased the number of microglia adhering to myelin, attenuated white matter injury and cognitive deficits (75). Generally, animal studies suggest that activation of the C1q/C3 system after stroke may be detrimental to recovery.

Molecular signaling pathways regarding complement system are summarized in **Figure 2B**.

Triggering Receptor Expressed on Myeloid Cells-2 (TREM2)-Activating Protein of 12 kDa (DAP12) System

TREM2 was originally described on circulating macrophages, where it is bound to anionic moieties on exogenous pathogens and mediated pathogen clearance (76). DAP12 is an intracellular membrane adaptor of TREM2 (77). Accumulating evidence demonstrated that TREM2-DAP12 signaling is involved in microglial phagocytosis. Human beings with a loss function of either TREM2 or DAP12 develop an inflammatory neurodegenerative disease—Nasu-Hakola disease (NHD), leading to death in the fourth or fifth decade of life (78). TREM2 deficiency in microglia inhibits apoptotic neuronal clearance and increases the production of inflammatory mediators such as TNF-α (79).

TREM2 participates in phagocytic activity following experimental stroke (24, 76). TREM2 deficiency can lead to worsened outcomes after ischemic stroke by decreasing the phagocytosis of injured neurons (24). With the application of bone marrow chimeric mice, this team further addressed that intact microglia TREM2 is more important for beneficial phagocytosis and stroke recovery than that of circulating macrophage (80). Additionally, another research group reported that TREM2 could promote a microglial switch from the detrimental M1 phenotype to the beneficial M2 phenotype, which may affect the short-term outcome in the mouse MCAO model (81). Ligand or opsonin of TREM2 was less reported. It is predicted that the potential endogenous binding partner of TREM2 in ischemic brain is probably high-molecular-weight nucleic acids released by damaged cells (24). In conclusion, the TREM2-DAP12 signaling is mainly considered beneficial in ischemic stroke. Targeting TREM2 signaling especially in microglia has become a therapeutic target as it was shown that the systemic administration of a TREM2 agonist or TREM2 overexpression had a neuroprotective effect in ischemic injury (82).

Molecular signaling pathways regarding TREM2-DAP12 system are summarized in **Figure 2C**.

Nucleotides and P2 Metabolic Purinoceptors

P2 purinoceptors are divided into two families, ionotropic receptors (P2X) and metabotropic receptors (P2Y). P2Y containing eight types (P2Y1, 2, 4, 6, 11, 12, 13, and 14) are activated by nucleotides and couple to intracellular second-messenger systems through heteromeric G-proteins. P2Y6 receptor is actively responsive to UDP and partially responsive to UTP and ADP. It has been demonstrated that microglial purinergic P2Y6 receptor is activated by UDP released from damaged neurons and triggers microglial phagocytosis (83). In other words, UDP, which is released from injured neurons after trauma or ischemia, acts as an "eat-me" signal and meditates the P2Y6-dependent phagocytosis (53). P2Y6 is combined with UDP, and then activates phospholipase C (PLC) which in turn causes the synthesis of inositol 1,4,5-trisphosphate (InsP3) and triggers the booted release of Ca^{2+} from InsP3-receptor-sensitive stores. On top of triggering the intracellular Ca^{2+} over-loading, the P2Y6-receptor-signaling pathway triggers actin cytoskeleton polarization to shape filopodia-like protrusions, thus facilitating the engulfment of cell debris (83).

The research newly reported that the expression of the P2Y6 receptor in microglia increased after tMCAO and P2Y6 receptor antagonist MRS2578 treatment inhibited microglia to swallow apoptosis cell debris, subsequently aggravating neurological function. The possible mechanism of P2Y6 receptor-mediated phagocytosis is related to myosin light chain kinase (84). After all, it indicates that P2Y6/UDP-mediated microglial phagocytosis plays a favorable part in the acute stage of ischemic stroke, which can be a therapeutic target for ischemic stroke.

Apart from P2Y6/UDP signaling pathway, neuronal injury gives rise to the leakage of ATP or ADP that appears to be a "find-me" signal to attract microglia and cause chemotaxis through P2Y12 receptors (85). In the hippocampus regions of young mice, the percentage of apoptotic cell engulfment significantly reduces in P2Y12 deficient mice, which impacts the neurogenesis of hippocampus SGZ (86). Following cerebrovascular damage, P2Y12-mediated chemotaxis of microglia is central to the maintenance of BBB integrity (87).

The P2Y6/UDP and P2Y12/ADP signaling pathways are depicted in **Figure 2D**.

CD47-Signal Regulated Protein Alpha (SIRPα) System

Inhibitory signals can also modulate microglial phagocytosis, so-called "don't-eat-me" signals. In the immune system, SIRPα acts as a "don't-eat-me" signal, which is required for optimal and appropriate microglial engulfment. CD47 is documented to express on synapses, oligodendrocytes, erythrocytes, and microglia. Its receptor SIRPα is an Ig superfamily protein and has been observed on microglia or macrophage in the CNS (88). The expression pattern of CD47-SIRPα is correlated with peak pruning in the developing retinogeniculate system and prevents excess microglial phagocytosis according to literature (89). This inhibitory engulfment property of CD47-SIRPα hindered the maintenance of myelin integrity following mild brain damage (90). In ischemic stroke, a study using CD47 knockout mice suggests that CD47 deletion reduces brain infarct and swelling at an acute stage in MCAO model through decreasing neuroinflammation (91). Notably, it is interpreted that CD47-deficient erythrocytes are more prone to be cleared by microglia/macrophage. Injection of CD47 knockout blood into mouse brain resulted in quicker clot resolution and less brain swelling than WT blood (92). Consistently, CD47 blocking antibody speeded up hematoma clearance (93) and alleviated atherosclerosis through restoring phagocytosis by microglia/macrophage (94). Exempt from cerebral hemorrhage, these findings provide more clues for the treatment of hemorrhagic transformation in stroke patients. The CD47/SIRPα signaling pathway is depicted in **Figure 2E**.

In addition to the molecules described above, several other phagocytic molecules are still being reported and studied, although their functions in ischemic stroke are unknown. For instance, CD22 blocks microglia-mediated engulfment of myelin debris in the aged brain, while CD22 blockade restores microglial homeostasis and cognitive impairment in aged mice (95).

RXR/PPAR-γ is a critical transcription factor in the nuclear receptor superfamily and is responsible for the expression of scavenger receptors. Mice lacking RXR-α in myeloid phagocytes demonstrated worsened late functional recovery and serious brain atrophy in MCAO dependent model (25).

We still have a long way to thoroughly understand the molecular pathways of phagocytosis. We expect to find specific phagocytosis pathways that protect ischemic brain injury without causing excessive alive neuronal clearance in the future.

OTHER IMMUNE CELLS CONTRIBUTING TO PHAGOCYTOSIS IN ISCHEMIC STROKE

The lack of precise discriminating markers between the myeloid populations (macrophage and microglia) has led many studies summarized above to generate conclusions based on the grouping of the two populations. In addition to microglia and macrophage, some other cells, namely, astrocytes, peripheral infiltrated PMNs, monocytes, and pericytes have been reported to present engulfment properties as well (22, 54, 87, 96–107).

It was reported that monocyte infiltration occurs as early as 4 h after stroke. Infiltrating monocytes are primarily involved in early debris clearance and have significantly higher phagocytic capacity at 72 h after stroke compared with microglia (22). An earlier study underscored the importance of monocytes to hemorrhage clearance in a model of intracerebral hemorrhage and highlighted their ability to significantly improve long-term outcomes through phagocytic function early after stroke (96). Cell surface scavenger receptor CD36 on monocyte-derived macrophages mediates phagocytosis during the recovery phase in post-stroke brains and plays a reparative role during the resolution of inflammation in ischemic stroke (97).

PMNs elicit rapid immune responses compared with mononuclear phagocytes. The infiltration of neutrophils can be detected within 3 h after the onset of ischemic stroke (54). One subtype of PMNs named N2 phenotype represents a pro-resolving function by producing anti-inflammatory factors or engulfing cellular debris (98, 99). A further study corroborates that the N2 phenotype facilitates neutrophil clearance by macrophage and does not induce neuronal death after ischemic injury. Meanwhile, skewing neutrophils toward the N2 phenotype before stroke reduced infarct volumes at 1 day after MCAO (100).

As BBB components, pericytes reside in the abluminal side of endothelial cells lining the capillaries in the brain. Pericytes are considered to be multipotent progenitor cells and exhibit microglia-like properties after ischemia insult (101). In response to ischemic insult, pericytes could leave blood vessel wall and migrate into the ischemic brain parenchyma, where they express microglia-specific markers, namely, Iba-1 and gal-3. In human stroke postmortem sections, a portion of gal-3 positive pericytes were found in the peri-infarct area (102). Platelet-derived growth factor receptor-β (PDGFR-β) is a specific marker of pericytes. PDGFR-β^+ pericytes, isolated from ischemic brain tissue, could differentiate into Iba-1^+ ameboid-like microglia and own the capability to phagocytose latex beads (103).

It has been recently observed that astrocytes, acting like non-professional phagocytes, can also contribute to the elimination of apoptotic neurons, synapses, and cell debris after transient focal ischemia in mice (87, 104, 105). Astrocytes become phagocytic during the late stage of ischemia, and ABCA1 along with its downstream molecules plays a pivotal role in this process (106). Phagocytic astrocytes have a distinct role from microglia given that phagocytic astrocytes were observed in the ischemic penumbra region in the late phase of stroke, while phagocytic microglia were located in the infarcted core in the early stage of stroke (105). Judging from the spatiotemporal pattern of astrocytic phagocytosis after stroke, it is predicted that astrocytes would be involved in the elimination of debris and synapses, thereby leading to repairing/remodeling of the ischemic penumbra region (106, 107).

Nevertheless, resident microglia, astrocyte, monocyte/macrophage system, peripheral neutrophils, and pericytes may cooperatively modulate the removal of debris and synapse architecture after stroke.

CONCLUDING REMARKS

Microglial phagocytosis is a double-sword to immunoinflammation and stroke recovery. Microglia engulf live neurons and endothelial cells, which results in excessive neuronal death and BBB leakage respectively. On the other hand, microglia restrict inflammatory damage *via* engulfing cell debris, cleaning infiltrating neutrophils, and creating an optimal microenvironment for neurogenesis. Therefore, understanding the molecular mechanisms and modulating selective microglial phagocytosis represent an attractive target with a long therapeutic window after stroke in the future.

AUTHOR CONTRIBUTIONS

JJ and MZ wrote the first draft and all co-authors revised the manuscript. All authors contributed to the article and approved the submitted version.

FUNDING

This study was supported by the National Natural Science Foundation of China (81971112, 82130036, 81920208017, 81400971, and 81801147), the Natural Science Foundation of Jiangsu Province (BK20191116), the Jiangsu Province Key Medical Discipline (ZDXKA2016020), the Key Research and Development Program of Jiangsu Province of China (BE2020620). The project is sponsored by the "Young Talent Support Program" for the China Stroke Association from the China Association for Science and Technology.

REFERENCES

1. Chen Z, Jiang B, Ru X, Sun H, Sun D, Liu X, et al. Mortality of Stroke and Its Subtypes in China: Results From a Nationwide Population-Based Survey. *Neuroepidemiology* (2017) 48(3-4):95–102. doi: 10.1159/000477494
2. Dirnagl U, Iadecola C, Moskowitz MA. Pathobiology of Ischaemic Stroke: An Integrated View. *Trends Neurosci* (1999) 22(9):391–7. doi: 10.1016/S0166-2236(99)01401-0
3. Jauch EC, Saver JL, Adams HPJr., Bruno A, Connors JJ, Demaerschalk BM, et al. Guidelines for the Early Management of Patients With Acute Ischemic Stroke: A Guideline for Healthcare Professionals From the American Heart Association/American Stroke Association. *Stroke* (2013) 44(3):870–947. doi: 10.1161/STR.0b013e318284056a
4. Powers WJ, Derdeyn CP, Biller J, Coffey CS, Hoh BL, Jauch EC, et al. 2015 American Heart Association/American Stroke Association Focused Update of the 2013 Guidelines for the Early Management of Patients With Acute Ischemic Stroke Regarding Endovascular Treatment: A Guideline for Healthcare Professionals From the American Heart Association/American Stroke Association. *Stroke* (2015) 46(10):3020–35. doi: 10.1161/STR.0000000000000074
5. Wang K, Li J, Zhang Y, Huang Y, Chen D, Shi Z, et al. Central Nervous System Diseases Related to Pathological Microglial Phagocytosis. *CNS Neurosci Ther* (2021) 27(5):528–39. doi: 10.1111/cns.13619
6. Ajami B, Bennett JL, Krieger C, Tetzlaff W, Rossi FM. Local Self-Renewal can Sustain CNS Microglia Maintenance and Function Throughout Adult Life. *Nat Neurosci* (2007) 10(12):1538–43. doi: 10.1038/nn2014
7. Li T, Pang S, Yu Y, Wu X, Guo J, Zhang S. Proliferation of Parenchymal Microglia Is the Main Source of Microgliosis After Ischaemic Stroke. *Brain* (2013) 136(Pt 12):3578–88. doi: 10.1093/brain/awt287
8. Li T, Zhang S. Microgliosis in the Injured Brain: Infiltrating Cells and Reactive Microglia Both Play a Role. *Neuroscientist* (2016) 22(2):165–70. doi: 10.1177/1073858415572079
9. Huang Y, Xu Z, Xiong S, Sun F, Qin G, Hu G, et al. Repopulated Microglia Are Solely Derived From the Proliferation of Residual Microglia After Acute Depletion. *Nat Neurosci* (2018) 21(4):530–40. doi: 10.1038/s41593-018-0090-8

10. Lambertsen KL, Finsen B, Clausen BH. Post-Stroke Inflammation-Target or Tool for Therapy? *Acta Neuropathol* (2019) 137(5):693–714. doi: 10.1007/s00401-018-1930-z
11. Faustino JV, Wang X, Johnson CE, Klibanov A, Derugin N, Wendland MF, et al. Microglial Cells Contribute to Endogenous Brain Defenses After Acute Neonatal Focal Stroke. *J Neurosci* (2011) 31(36):12992–3001. doi: 10.1523/JNEUROSCI.2102-11.2011
12. Szalay G, Martinecz B, Lenart N, Kornyei Z, Orsolits B, Judak L, et al. Microglia Protect Against Brain Injury and Their Selective Elimination Dysregulates Neuronal Network Activity After Stroke. *Nat Commun* (2016) 7:11499. doi: 10.1038/ncomms11499
13. Smolders SM, Kessels S, Vangansewinkel T, Rigo JM, Legendre P, B. Brone. Microglia: Brain Cells on the Move. *Prog Neurobiol* (2019) 178:101612. doi: 10.1016/j.pneurobio.2019.04.001
14. Hu X, Li P, Guo Y, Wang H, Leak RK, Chen S, et al. Microglia/Macrophage Polarization Dynamics Reveal Novel Mechanism of Injury Expansion After Focal Cerebral Ischemia. *Stroke* (2012) 43(11):3063–70. doi: 10.1161/STROKEAHA.112.659656
15. Michelucci A, Heurtaux T, Grandbarbe L, Morga E, Heuschling P. Characterization of the Microglial Phenotype Under Specific Pro-Inflammatory and Anti-Inflammatory Conditions: Effects of Oligomeric and Fibrillar Amyloid-Beta. *J Neuroimmunol* (2009) 210(1-2):3–12. doi: 10.1016/j.jneuroim.2009.02.003
16. Ransohoff RM. A Polarizing Question: Do M1 and M2 Microglia Exist? *Nat Neurosci* (2016) 19(8):987–91. doi: 10.1038/nn.4338
17. Wlodarczyk A, Holtman IR, Krueger M, Yogev N, Bruttger J, Khorooshi R, et al. A Novel Microglial Subset Plays a Key Role in Myelinogenesis in Developing Brain. *EMBO J* (2017) 36(22):3292–308. doi: 10.15252/embj.201696056
18. Keren-Shaul H, Spinrad A, Weiner A, Matcovitch-Natan O, Dvir-Szternfeld R, Ulland TK, et al. A Unique Microglia Type Associated With Restricting Development of Alzheimer's Disease. *Cell* (2017) 169: (7):1276–1290 e17. doi: 10.1016/j.cell.2017.05.018
19. Schilling M, Besselmann M, Muller M, Strecker JK, Ringelstein EB, Kiefer R. Predominant Phagocytic Activity of Resident Microglia Over Hematogenous Macrophages Following Transient Focal Cerebral Ischemia: An Investigation Using Green Fluorescent Protein Transgenic Bone Marrow Chimeric Mice. *Exp Neurol* (2005) 196(2):290–7. doi: 10.1016/j.expneurol.2005.08.004
20. Schilling M, Besselmann M, Leonhard C, Mueller M, Ringelstein EB, Kiefer R. Microglial Activation Precedes and Predominates Over Macrophage Infiltration in Transient Focal Cerebral Ischemia: A Study in Green Fluorescent Protein Transgenic Bone Marrow Chimeric Mice. *Exp Neurol* (2003) 183(1):25–33. doi: 10.1016/S0014-4886(03)00082-7
21. Tanaka R, Komine-Kobayashi M, Mochizuki H, Yamada M, Furuya T, Migita M, et al. Migration of Enhanced Green Fluorescent Protein Expressing Bone Marrow-Derived Microglia/Macrophage Into the Mouse Brain Following Permanent Focal Ischemia. *Neuroscience* (2003) 117 (3):531–9. doi: 10.1016/s0306-4522(02)00954-5
22. Ritzel RM, Patel AR, Grenier JM, Crapser J, Verma R, Jellison ER, et al. Functional Differences Between Microglia and Monocytes After Ischemic Stroke. *J Neuroinflamm* (2015) 12:106. doi: 10.1186/s12974-015-0329-1
23. Zhang W, Zhao J, Wang R, Jiang M, Ye Q, Smith AD, et al. Macrophages Reprogram After Ischemic Stroke and Promote Efferocytosis and Inflammation Resolution in the Mouse Brain. *CNS Neurosci Ther* (2019) 25(12):1329–42. doi: 10.1111/cns.13256
24. Kawabori M, Kacimi R, Kauppinen T, Calosing C, Kim JY, Hsieh CL, et al. Triggering Receptor Expressed on Myeloid Cells 2 (TREM2) Deficiency Attenuates Phagocytic Activities of Microglia and Exacerbates Ischemic Damage in Experimental Stroke. *J Neurosci: Off J Soc Neurosci* (2015) 35 (8):3384–96. doi: 10.1523/JNEUROSCI.2620-14.2015
25. Ting SM, Zhao X, Sun G, Obertas L, Ricote M, Aronowski J. Brain Cleanup as a Potential Target for Poststroke Recovery: The Role of RXR (Retinoic X Receptor) in Phagocytes. *Stroke* (2020) 51(3):958–66. doi: 10.1161/strokeaha.119.027315
26. Brown GC, Neher JJ. Microglial Phagocytosis of Live Neurons. *Nat Rev Neurosci* (2014) 15(4):209–16. doi: 10.1038/nrn3710
27. Neher JJ, Emmrich JV, Fricker M, Mander PK, Thery C, Brown GC. Phagocytosis Executes Delayed Neuronal Death After Focal Brain Ischemia. *Proc Natl Acad Sci USA* (2013) 110(43):E4098–107. doi: 10.1073/pnas.1308679110
28. Berghoff SA, Spieth L, Sun T, Hosang L, Schlaphoff L, Depp C, et al. Microglia Facilitate Repair of Demyelinated Lesions via Post-Squalene Sterol Synthesis. *Nat Neurosci* (2021) 24(1):47–60. doi: 10.1038/s41593-020-00757-6
29. Li L, Saiyin H, Xie J, Ma L, Xue L, Wang W, et al. Sevoflurane Preconditioning Induced Endogenous Neurogenesis Against Ischemic Brain Injury by Promoting Microglial Activation. *Oncotarget* (2017) 8 (17):28544–57. doi: 10.18632/oncotarget.15325
30. Thored P, Heldmann U, Gomes-Leal W, Gisler R, Darsalia V, Taneera J, et al. Long-Term Accumulation of Microglia With Proneurogenic Phenotype Concomitant With Persistent Neurogenesis in Adult Subventricular Zone After Stroke. *Glia* (2009) 57(8):835–49. doi: 10.1002/glia.20810
31. Denes A, Vidyasagar R, Feng J, Narvainen J, McColl BW, Kauppinen RA, et al. Proliferating Resident Microglia After Focal Cerebral Ischaemia in Mice. *J Cereb Blood Flow Metab* (2007) 27(12):1941–53. doi: 10.1038/sj.jcbfm.9600495
32. Otxoa-de-Amezaga A, Miro-Mur F, Pedragosa J, Gallizioli M, Justicia C, Gaja-Capdevila N, et al. Microglial Cell Loss After Ischemic Stroke Favors Brain Neutrophil Accumulation. *Acta Neuropathol* (2019) 137(2):321–41. doi: 10.1007/s00401-018-1954-4
33. Jolivel V, Bicker F, Biname F, Ploen R, Keller S, Gollan R, et al. Perivascular Microglia Promote Blood Vessel Disintegration in the Ischemic Penumbra. *Acta Neuropathol* (2015) 129(2):279–95. doi: 10.1007/s00401-014-1372-1
34. Natrajan MS, de la Fuente AG, Crawford AH, Linehan E, Nunez V, Johnson KR, et al. Retinoid X Receptor Activation Reverses Age-Related Deficiencies in Myelin Debris Phagocytosis and Remyelination. *Brain* (2015) 138(Pt 12):3581–97. doi: 10.1093/brain/awv289
35. Olah M, Amor S, Brouwer N, Vinet J, Eggen B, Biber K, et al. Identification of a Microglia Phenotype Supportive of Remyelination. *Glia* (2012) 60 (2):306–21. doi: 10.1002/glia.21266
36. Neumann J, Henneberg S, von Kenne S, Nolte N, Muller AJ, Schraven B, et al. Beware the Intruder: Real Time Observation of Infiltrated Neutrophils and Neutrophil-Microglia Interaction During Stroke *In Vivo*. *PloS One* (2018) 13(3):e0193970. doi: 10.1371/journal.pone.0193970
37. Fisch U, Bregere C, Geier F, Chicha L, Guzman R. Neonatal Hypoxia-Ischemia in Rat Elicits a Region-Specific Neurotrophic Response in SVZ Microglia. *J Neuroinflamm* (2020) 17(1):26. doi: 10.1186/s12974-020-1706-y
38. Liu Y, Wu C, Hou Z, Fu X, Yuan L, Sun S, et al. Pseudoginsenoside-F11 Accelerates Microglial Phagocytosis of Myelin Debris and Attenuates Cerebral Ischemic Injury Through Complement Receptor 3. *Neuroscience* (2020) 426:33–49. doi: 10.1016/j.neuroscience.2019.11.010
39. Neher JJ, Neniskyte U, Zhao JW, Bal-Price A, Tolkovsky AM, Brown GC. Inhibition of Microglial Phagocytosis Is Sufficient to Prevent Inflammatory Neuronal Death. *J Immunol* (2011) 186(8):4973–83. doi: 10.4049/jimmunol.1003600
40. Neumann J, Sauerzweig S, Ronicke R, Gunzer F, Dinkel K, Ullrich O, et al. Microglia Cells Protect Neurons by Direct Engulfment of Invading Neutrophil Granulocytes: A New Mechanism of CNS Immune Privilege. *J Neurosci* (2008) 28(23):5965–75. doi: 10.1523/JNEUROSCI.0060-08.2008
41. Wu L, Wu W, Tali and W.T. Yuh ET. Oligemia, Penumbra, Infarction: Understanding Hypoperfusion With Neuroimaging. *Neuroimaging Clin N Am* (2018) 28(4):599–609. doi: 10.1016/j.nic.2018.06.013
42. Neumann H, Kotter MR, Franklin RJ. Debris Clearance by Microglia: An Essential Link Between Degeneration and Regeneration. *Brain* (2009) 132(Pt 2):288–95. doi: 10.1093/brain/awn109
43. Zhang Y, Li H, Li X, Wu J, Xue T, Wu J, et al. TMEM16F Aggravates Neuronal Loss by Mediating Microglial Phagocytosis of Neurons in a Rat Experimental Cerebral Ischemia and Reperfusion Model. *Front Immunol* (2020) 11:3389/fimmu.2020.01144. doi: 10.3389/fimmu.2020.01144
44. Yang J, Cao LL, Wang XP, Guo W, Guo RB, Sun YQ, et al. Neuronal Extracellular Vesicle Derived Mir-98 Prevents Salvageable Neurons From Microglial Phagocytosis in Acute Ischemic Stroke. *Cell Death Dis* (2021) 12 (1):23. doi: 10.1038/s41419-020-03310-2
45. Goldman SA, Osorio J. So Many Progenitors, So Little Myelin. *Nat Neurosci* (2014) 17(4):483–5. doi: 10.1038/nn.3685

46. Lambertsen KL, Biber K, Finsen B. Inflammatory Cytokines in Experimental and Human Stroke. *J Cereb Blood Flow Metab* (2012) 32(9):1677–98. doi: 10.1038/jcbfm.2012.88
47. Lauber K, Blumenthal SG, Waibel M, Wesselborg S. Clearance of Apoptotic Cells: Getting Rid of the Corpses. *Mol Cell* (2004) 14(3):277–87. doi: 10.1016/S1097-2765(04)00237-0
48. Bengzon J, Kokaia Z, Elmer E, Nanobashvili A, Kokaia M, Lindvall O. Apoptosis and Proliferation of Dentate Gyrus Neurons After Single and Intermittent Limbic Seizures. *Proc Natl Acad Sci USA* (1997) 94(19):10432–7. doi: 10.1073/pnas.94.19.10432
49. Rudolph M, Schmeer CW, Günther M, Woitke F, Kathner-Schaffert C, Karapetow L, et al. Microglia-Mediated Phagocytosis of Apoptotic Nuclei Is Impaired in the Adult Murine Hippocampus After Stroke. *Glia* (2021) 69 (8):2006–22. doi: 10.1002/glia.24009
50. Dang DD, Saiyin H, Yu Q, Liang WM. Effects of Sevoflurane Preconditioning on Microglia/Macrophage Dynamics and Phagocytosis Profile Against Cerebral Ischemia in Rats. *CNS Neurosci Ther* (2018) 24 (6):564–71. doi: 10.1111/cns.12823
51. Barone FC, Hillegass LM, Price WJ, White RF, Lee EV, Feuerstein GZ, et al. Polymorphonuclear Leukocyte Infiltration Into Cerebral Focal Ischemic Tissue: Myeloperoxidase Activity Assay and Histologic Verification. *J Neurosci Res* (1991) 29(3):336–45. doi: 10.1002/jnr.490290309
52. Hermann DM, Kleinschnitz C, Gunzer M. Implications of Polymorphonuclear Neutrophils for Ischemic Stroke and Intracerebral Hemorrhage: Predictive Value, Pathophysiological Consequences and Utility as Therapeutic Target. *J Neuroimmunol* (2018) 321:138–43. doi: 10.1016/j.jneuroim.2018.04.015
53. Fu R, Shen Q, Xu P, Luo JJ, Tang Y. Phagocytosis of Microglia in the Central Nervous System Diseases. *Mol Neurobiol* (2014) 49(3):1422–34. doi: 10.1007/s12035-013-8620-6
54. Neumann J, Riek-Burchardt M, Herz J, Doeppner TR, Konig R, Hutten H, et al. Very-Late-Antigen-4 (VLA-4)-Mediated Brain Invasion by Neutrophils Leads to Interactions With Microglia, Increased Ischemic Injury and Impaired Behavior in Experimental Stroke. *Acta Neuropathol* (2015) 129(2):259–77. doi: 10.1007/s00401-014-1355-2
55. Fricker M, Oliva-Martin MJ, Brown GC. Primary Phagocytosis of Viable Neurons by Microglia Activated With LPS or Abeta Is Dependent on Calreticulin/LRP Phagocytic Signalling. *J Neuroinflamm* (2012) 9:196. doi: 10.1186/1742-2094-9-196
56. Nomura K, Vilalta A, Allendorf DH, Hornik TC, Brown GC. Activated Microglia Desialylate and Phagocytose Cells *via* Neuraminidase, Galectin-3, and Mer Tyrosine Kinase. *J Immunol* (2017) 198(12):4792–801. doi: 10.4049/jimmunol.1502532
57. Burstyn-Cohen T, Lew ED, Traves PG, Burrola PG, Hash JC, Lemke G. Genetic Dissection of TAM Receptor-Ligand Interaction in Retinal Pigment Epithelial Cell Phagocytosis. *Neuron* (2012) 76(6):1123–32. doi: 10.1016/j.neuron.2012.10.015
58. Lu Q, Lemke G. Homeostatic Regulation of the Immune System by Receptor Tyrosine Kinases of the Tyro 3 Family. *Science* (2001) 293(5528):306–11. doi: 10.1126/science.1061663
59. Shafit-Zagardo B, Gruber RC, DuBois JC. The Role of TAM Family Receptors and Ligands in the Nervous System: From Development to Pathobiology. *Pharmacol Ther* (2018) 188:97–117. doi: 10.1016/j.pharmthera.2018.03.002
60. Blades F, Aprico A, Akkermann R, Ellis S, Binder MD, Kilpatrick TJ. The TAM Receptor TYRO3 Is a Critical Regulator of Myelin Thickness in the Central Nervous System. *Glia* (2018) 66(10):2209–20. doi: 10.1002/glia.23481
61. Caberoy NB, Alvarado G, Bigcas J-L, Li W. Galectin-3 Is a New Mertk-Specific Eat-Me Signal. *J Cell Physiol* (2012) 227(2):401–7. doi: 10.1002/jcp.22955
62. Zhu D, Wang Y, Singh I, Bell RD, Deane R, Zhong Z, et al. Protein s Controls Hypoxic/Ischemic Blood-Brain Barrier Disruption Through the TAM Receptor Tyro3 and Sphingosine 1-Phosphate Receptor. *Blood* (2010) 115 (23):4963–72. doi: 10.1182/blood-2010-01-262386
63. Guo H, Barrett TM, Zhong Z, Fernandez JA, Griffin JH, Freeman RS, et al. Protein s Blocks the Extrinsic Apoptotic Cascade in Tissue Plasminogen Activator/N-Methyl D-Aspartate-Treated Neurons *via* Tyro3-Akt-FKHRL1 Signaling Pathway. *Mol Neurodegener* (2011) 6:13. doi: 10.1186/1750-1326-6-13
64. Wu G, McBride DW, Zhang JH. Axl Activation Attenuates Neuroinflammation by Inhibiting the TLR/TRAF/NF-Kappab Pathway After MCAO in Rats. *Neurobiol Dis* (2018) 110:59–67. doi: 10.1016/j.nbd.2017.11.009
65. van Lookeren Campagne M, Wiesmann C, Brown EJ. Macrophage Complement Receptors and Pathogen Clearance. *Cell Microbiol* (2007) 9 (9):2095–102. doi: 10.1111/j.1462-5822.2007.00981.x
66. Ma Y, Liu Y, Zhang Z, Yang G-Y. Significance of Complement System in Ischemic Stroke: A Comprehensive Review. *Aging Dis* (2019) 10(2):429–62. doi: 10.14336/AD.2019.0119
67. Fonseca MI, Chu S-H, Hernandez MX, Fang MJ, Modarresi L, Selvan P, et al. Cell-Specific Deletion of C1qa Identifies Microglia as the Dominant Source of C1q in Mouse Brain. *J Neuroinflamm* (2017) 14(1):48. doi: 10.1186/s12974-017-0814-9
68. Fraser DA, Pisalyaput K, Tenner AJ. C1q Enhances Microglial Clearance of Apoptotic Neurons and Neuronal Blebs, and Modulates Subsequent Inflammatory Cytokine Production. *J Neurochem* (2010) 112(3):733–43. doi: 10.1111/j.1471-4159.2009.06494.x
69. Linnartz B, Kopatz J, Tenner AJ, Neumann H. Sialic Acid on the Neuronal Glycocalyx Prevents Complement C1 Binding and Complement Receptor-3-Mediated Removal by Microglia. *J Neurosci: Off J Soc Neurosci* (2012) 32 (3):946–52. doi: 10.1523/JNEUROSCI.3830-11.2012
70. Schafer DP, Lehrman EK, Kautzman AG, Koyama R, Mardinly AR, Yamasaki R, et al. Microglia Sculpt Postnatal Neural Circuits in an Activity and Complement-Dependent Manner. *Neuron* (2012) 74(4):691–705. doi: 10.1016/j.neuron.2012.03.026
71. Kettenmann H, Kirchhoff F, Verkhratsky A. Microglia: New Roles for the Synaptic Stripper. *Neuron* (2013) 77(1):10–8. doi: 10.1016/j.neuron.2012.12.023
72. Alawieh A, Langley EF, Tomlinson S. Targeted Complement Inhibition Salvages Stressed Neurons and Inhibits Neuroinflammation After Stroke in Mice. *Sci Transl Med* (2018) 10(441):eaao6459. doi: 10.1126/scitranslmed.aao6459
73. Alawieh AM, Langley EF, Feng W, Spiotta AM, Tomlinson S. Complement-Dependent Synaptic Uptake and Cognitive Decline After Stroke and Reperfusion Therapy. *J Neurosci* (2020) 40(20):4042–58. doi: 10.1523/JNEUROSCI.2462-19.2020
74. Surugiu R, Catalin B, Dumbrava D, Gresita A, Olaru DG, Hermann DM, et al. Intracortical Administration of the Complement C3 Receptor Antagonist Trifluoroacetate Modulates Microglia Reaction After Brain Injury. *Neural Plasticity 2019* (2019) 2019:1071036. doi: 10.1155/2019/1071036
75. Zhang LY, Pan J, Mamtilahun M, Zhu Y, Wang L, Venkatesh A, et al. Microglia Exacerbate White Matter Injury *via* Complement C3/C3ar Pathway After Hypoperfusion. *Theranostics* (2020) 10(1):74–90. doi: 10.7150/thno.35841
76. Daws MR, Lanier LL, Seaman WE, Ryan JC. Cloning and Characterization of a Novel Mouse Myeloid DAP12-Associated Receptor Family. *Eur J Immunol* (2001) 31(3):783–91. doi: 10.1002/1521-4141(200103)31:3<783::AID-IMMU783gt;3.0.CO;2-U
77. Jay TR, von Saucken VE, Landreth GE. TREM2 in Neurodegenerative Diseases. *Mol Neurodegener* (2017) 12(1):56. doi: 10.1186/s13024-017-0197-5
78. Dardiotis E, Siokas V, Pantazi E, Dardioti M, Rikos D, Xiromerisiou G, et al. A Novel Mutation in TREM2 Gene Causing Nasu-Hakola Disease and Review of the Literature. *Neurobiol Aging* (2017) 53:194.e13–194.e22. doi: 10.1016/j.neurobiolaging.2017.01.015
79. Takahashi K, Rochford CD, Neumann H. Clearance of Apoptotic Neurons Without Inflammation by Microglial Triggering Receptor Expressed on Myeloid Cells-2. *J Exp Med* (2005) 201(4):647–57. doi: 10.1084/jem.20041611
80. Kurisu K, Zheng Z, Kim JY, Shi J, Kanoke A, Liu J, et al. Triggering Receptor Expressed on Myeloid Cells-2 Expression in the Brain Is Required for Maximal Phagocytic Activity and Improved Neurological Outcomes Following Experimental Stroke. *J Cereb Blood Flow Metab* (2019) 39 (10):1906–18. doi: 10.1177/0271678X18817282
81. Zhai Q, Li F, Chen X, Jia J, Sun S, Zhou D, et al. Triggering Receptor Expressed on Myeloid Cells 2, a Novel Regulator of

Immunocyte Phenotypes, Confers Neuroprotection by Relieving Neuroinflammation. *Anesthesiology* (2017) 127(1):98–110. doi: 10.1097/ALN.0000000000001628
82. Gervois P, Lambrichts I. The Emerging Role of Triggering Receptor Expressed on Myeloid Cells 2 as a Target for Immunomodulation in Ischemic Stroke. *Front Immunol* (2019) 10:2019.01668. doi: 10.3389/fimmu.2019.01668
83. Koizumi S, Shigemoto-Mogami Y, Nasu-Tada K, Shinozaki Y, Ohsawa K, Tsuda M, et al. UDP Acting at P2Y6 Receptors Is a Mediator of Microglial Phagocytosis. *Nature* (2007) 446(7139):1091–5. doi: 10.1038/nature05704
84. Wen R-X, Shen H, Huang S-X, Wang L-P, Li Z-W, Peng P, et al. P2Y6 Receptor Inhibition Aggravates Ischemic Brain Injury by Reducing Microglial Phagocytosis. *CNS Neurosci Ther* (2020) 26(4):416–29. doi: 10.1111/cns.13296
85. Haynes SE, Hollopeter G, Yang G, Kurpius D, Dailey ME, Gan WB, et al. The P2Y12 Receptor Regulates Microglial Activation by Extracellular Nucleotides. *Nat Neurosci* (2006) 9(12):1512–9. doi: 10.1038/nn1805
86. Diaz-Aparicio I, Paris I, Sierra-Torre V, Plaza-Zabala A, Rodriguez-Iglesias N, Marquez-Ropero M, et al. Microglia Actively Remodel Adult Hippocampal Neurogenesis Through the Phagocytosis Secretome. *J Neurosci* (2020) 40(7):1453–82. doi: 10.1523/JNEUROSCI.0993-19.2019
87. Lou N, Takano T, Pei Y, Xavier AL, Goldman SA, Nedergaard M. Purinergic Receptor P2RY12-Dependent Microglial Closure of the Injured Blood-Brain Barrier. *Proc Natl Acad Sci USA* (2016) 113(4):1074–9. doi: 10.1073/pnas.1520398113
88. Zhang H, Li F, Yang Y, Chen J, Hu X. SIRP/CD47 Signaling in Neurological Disorders. *Brain Res* (2015) 1623:74–80. doi: 10.1016/j.brainres.2015.03.012
89. Lehrman EK, Wilton DK, Litvina EY, Welsh CA, Chang ST. CD47 Protects Synapses From Excess Microglia-Mediated Pruning During Development. *Neuron* (2018) 100(1):120–134 e6. doi: 10.1016/j.neuron.2018.09.017
90. Gitik M, Liraz-Zaltsman S, Oldenborg PA, Reichert F, Rotshenker S. Myelin Down-Regulates Myelin Phagocytosis by Microglia and Macrophages Through Interactions Between CD47 on Myelin and Sirpalpha (Signal Regulatory Protein-Alpha) on Phagocytes. *J Neuroinflamm* (2011) 8:24. doi: 10.1186/1742-2094-8-24
91. Jin G, Tsuji K, Xing C, Yang YG, Wang X, Lo EH. CD47 Gene Knockout Protects Against Transient Focal Cerebral Ischemia in Mice. *Exp Neurol* (2009) 217(1):165–70. doi: 10.1016/j.expneurol.2009.02.004
92. Ni W, Mao S, Xi G, Keep RF, Hua Y. Role of Erythrocyte CD47 in Intracerebral Hematoma Clearance. *Stroke* (2016) 47(2):505–11. doi: 10.1161/STROKEAHA.115.010920
93. Jing C, Bian L, Wang M, Keep RF, Xi and Y. Hua G. Enhancement of Hematoma Clearance With CD47 Blocking Antibody in Experimental Intracerebral Hemorrhage. *Stroke* (2019) 50(6):1539–47. doi: 10.1161/STROKEAHA.118.024578
94. Kojima Y, Volkmer JP, McKenna K, Civelek M, Lusis AJ, Miller CL, et al. CD47-Blocking Antibodies Restore Phagocytosis and Prevent Atherosclerosis. *Nature* (2016) 536(7614):86–90. doi: 10.1038/nature18935
95. Pluvinage JV, Haney MS, Smith BAH, Sun J, Iram T, Bonanno L, et al. CD22 Blockade Restores Homeostatic Microglial Phagocytosis in Ageing Brains. *Nature* (2019) 568(7751):187–92. doi: 10.1038/s41586-019-1088-4
96. Hammond MD, Taylor RA, Mullen MT, Ai Y, Aguila HL, Mack M, et al. CCR2+ Ly6C(Hi) Inflammatory Monocyte Recruitment Exacerbates Acute Disability Following Intracerebral Hemorrhage. *J Neurosci: Off J Soc Neurosci* (2014) 34(11):3901–9. doi: 10.1523/JNEUROSCI.4070-13.2014
97. Woo M-S, Yang J, Beltran C, Cho S. Cell Surface CD36 Protein in Monocyte/Macrophage Contributes to Phagocytosis During the Resolution Phase of Ischemic Stroke in Mice. *J Biol Chem* (2016) 291(45):23654–61. doi: 10.1074/jbc.M116.750018
98. Cuartero MI, Ballesteros I, Moraga A, Nombela F, Vivancos J, Hamilton JA, et al. N2 Neutrophils, Novel Players in Brain Inflammation After Stroke: Modulation by the Pparγ Agonist Rosiglitazone. *Stroke* (2013) 44(12):3498–508. doi: 10.1161/STROKEAHA.113.002470
99. Tsuyama J, Nakamura A, Ooboshi H, Yoshimura A, Shichita T. Pivotal Role of Innate Myeloid Cells in Cerebral Post-Ischemic Sterile Inflammation. *Semin Immunopathol* (2018) 40(6):523–38. doi: 10.1007/s00281-018-0707-8
100. Cai W, Liu S, Hu M, Huang F, Zhu Q, Qiu W, et al. Functional Dynamics of Neutrophils After Ischemic Stroke. *Trans Stroke Res* (2020) 11(1):108–21. doi: 10.1007/s12975-019-00694-y
101. Cheng J, Korte N, Nortley R, Sethi H, Tang Y, Attwell D. Targeting Pericytes for Therapeutic Approaches to Neurological Disorders. *Acta Neuropathol* (2018) 136(4):507–23. doi: 10.1007/s00401-018-1893-0
102. Özen I, Deierborg T, Miharada K, Padel T, Englund E, Genové G, et al. Brain Pericytes Acquire a Microglial Phenotype After Stroke. *Acta Neuropathologica* (2014) 128(3):381–96. doi: 10.1007/s00401-014-1295-x
103. Sakuma R, Kawahara M, Nakano-Doi A, Takahashi A, Tanaka Y, Narita A, et al. Brain Pericytes Serve as Microglia-Generating Multipotent Vascular Stem Cells Following Ischemic Stroke. *J Neuroinflamm* (2016) 13(1):57. doi: 10.1186/s12974-016-0523-9
104. Chung W-S, Clarke LE, Wang GX, Stafford BK, Sher A, Chakraborty C, et al. Astrocytes Mediate Synapse Elimination Through MEGF10 and MERTK Pathways. *Nature* (2013) 504(7480):394–400. doi: 10.1038/nature12776
105. Koizumi S, Hirayama Y, Morizawa YM. New Roles of Reactive Astrocytes in the Brain; an Organizer of Cerebral Ischemia. *Neurochem Int* (2018) 119:107–14. doi: 10.1016/j.neuint.2018.01.007
106. Morizawa YM, Hirayama Y, Ohno N, Shibata S, Shigetomi E, Sui Y, et al. Reactive Astrocytes Function as Phagocytes After Brain Ischemia *via* ABCA1-Mediated Pathway. *Nat Commun* (2017) 8(1):28. doi: 10.1038/s41467-017-00037-1
107. Puig B, Brenna S, Magnus T. Molecular Communication of a Dying Neuron in Stroke. *Int J Mol Sci* (2018) 19(9). doi: 10.3390/ijms19092834

Conflict of Interest: The authors declare that the research was conducted in the absence of any commercial or financial relationships that could be construed as a potential conflict of interest.

frontiers in Immunology

REVIEW
published: 31 January 2022
doi: 10.3389/fimmu.2022.828447

Interleukins and Ischemic Stroke

Hua Zhu[1,2†], Siping Hu[3†], Yuntao Li[1,2], Yao Sun[1], Xiaoxing Xiong[1,2], Xinyao Hu[2], Junjing Chen[4] and Sheng Qiu[1*]*

[1] Department of Neurosurgery, The Affiliated Huzhou Hospital, Zhejiang University School of Medicine (Huzhou Central Hospital), Huzhou, China, [2] Department of Neurosurgery, Renmin Hospital of Wuhan University, Wuhan, China, [3] Department of Anesthesiology, The Affiliated Huzhou Hospital, Zhejiang University School of Medicine (Huzhou Central Hospital), Huzhou, China, [4] Department of General Surgery, The Affiliated Huzhou Hospital, Zhejiang University School of Medicine (Huzhou Central Hospital), Huzhou, China

Ischemic stroke after cerebral artery occlusion is one of the major causes of chronic disability worldwide. Interleukins (ILs) play a bidirectional role in ischemic stroke through information transmission, activation and regulation of immune cells, mediating the activation, multiplication and differentiation of T and B cells and in the inflammatory reaction. Crosstalk between different ILs in different immune cells also impact the outcome of ischemic stroke. This overview is aimed to roughly discuss the multiple roles of ILs after ischemic stroke. The roles of IL-1, IL-2, IL-4, IL-5, IL-6, IL-8, IL-9, IL-10, IL-12, IL-13, IL-15, IL-16, IL-17, IL-18, IL-19, IL-21, IL-22, IL-23, IL-32, IL-33, IL-34, IL-37, and IL-38 in ischemic stroke were discussed in this review.

Keywords: interleukins, ischemic stroke, inflammation, cytokines, neuro-immune

OPEN ACCESS

Edited by:
Yan Wang,
Peking University Third Hospital, China

Reviewed by:
Xinchun Jin,
Capital Medical University, China
Zongjian Liu,
Capital Medical University, China

****Correspondence:***
Junjing Chen
chenjunjing1983@163.com
Sheng Qiu
qius2001@126.com

[†]These authors have contributed equally to this work

Specialty section:
This article was submitted to Multiple Sclerosis and Neuroimmunology, a section of the journal Frontiers in Immunology

Received: *03 December 2021*
Accepted: *12 January 2022*
Published: *31 January 2022*

Citation:
Zhu H, Hu S, Li Y, Sun Y, Xiong X, Hu X, Chen J and Qiu S (2022) Interleukins and Ischemic Stroke. Front. Immunol. 13:828447. doi: 10.3389/fimmu.2022.828447

1 INTRODUCTION

Ischemic stroke after cerebral artery occlusion is one of the major causes of chronic disability worldwide, and there is still a lack of effective methods to improve functional recovery after cerebral stroke (1). After ischemic stroke, a severe shortage of blood supply to the brain leads to the insufficient oxygen supply to the brain, which in turn leads to neuronal death. Inflammatory responses at the blood-endothelial interface of brain capillaries are the basis of ischemic tissue damage. Furthermore, inflammatory interactions at the blood-endothelial interface, including adhesion molecules, cytokines, chemokines and white blood cells, are crucial for the pathogenesis of tissue injury in cerebral infarction (2). Pathophysiological changes after ischemic stroke include ion imbalance, neuroinflammation, and abnormal activation of immune cells, can lead to neuronal death. However, despite extensive research work have been made, the exact mechanisms of stroke damage are not fully understood. It is clear that ILs play a major role in the progression of ischemic stroke disease.

IL, refers to a lymphocyte medium that interacts between white blood cells or immune cells. It is a cytokine in the same category as blood cell growth factor. Both IL and hemocyte growth factor belong to cytokines, and they coordinate and interact with each other to complete hematopoiesis and immune regulation functions together. IL plays a crucial role in information transmission, activation and regulation of immune cells, mediating the activation, multiplication and differentiation of T and B cells and in the inflammatory reaction (3). There is a close relationship between IL and the pathogenesis of ischemic stroke. This review is to discuss the inflammatory effects of IL in the pathogenesis of stroke, the interactions between different IL-mediated pathways,

the cell-type dependent effects of different mediators and how different ILs regulate complex inflammatory cascades. The role of IL-1, IL-4, IL-6, and IL-10 were discussed in more detail.

2 IL-1 FAMILY

IL-1, described earlier as a fever-causing protein called human leukocyte pyrogen, is one of the pro-inflammatory cytokines produced by monocytes, macrophages, and epithelial cells. The IL-1 family consists of IL-1α, IL-1β, and specific receptor antagonist (IL-1RN) (4). The IL-1 gene complex is located on chromosome-14 and consists of three linked genes, namely IL-1α, IL-1β and IL-β (5). IL-1α and IL-1β was regarded as pro-inflammatory cytokines. The sequence homology of IL-1α and IL-1β is not high, but they bind to the same receptor complex and have similar biological activity. IL-1RN is a 16-18 kD protein that binds competitively with IL-1 and its receptor to become an important anti-inflammatory cytokine. There are five alleles for IL-1RN, and IL-1RN*1 is the most common genotype, followed by IL-1RN*2. The incidence of the remaining alleles (IL-1RN*3, IL-1RN*4 and IL-1RN*5) is less than 1% (6). Among them, IL-1RN*2 polymorphism is considered to be a genetic risk factor for coronary artery disease and atherosclerosis, which is closely related to ischemic stroke.

2.1 Mechanism of Pleiotropic Effects of IL-1 on Ischemic Stroke

IL-1 is a multifactorial cytokine with multiple biological effects in many cell types, many of which are associated with stroke risk and outcome. Downstream effects of IL-1 include increased expression of cytokines, chemokines, and growth factors, activation of matrix metalloproteinases, upregulation of adhesion molecules, increased leukocyte infiltration, activation of platelets, alteration of blood flow, increased angiogenesis, decreased neurogenesis, and numerous other effects. We have discussed some of all these effects and related mechanisms in detail, and the rest can be found in the reviews (7, 8).

Stroke-related comorbidities and risk factors are associated with elevated systemic inflammation, mediated in part by IL-1. As shown in **Figure 1**, in acute phase, the increase of IL-1 in the brain after stroke mediates the harmful the inflammatory process, including up-regulation of IL-6, TNF-α, MMP-9 and chemokines in astrocytes; inhibition of neurogenesis (9); increase

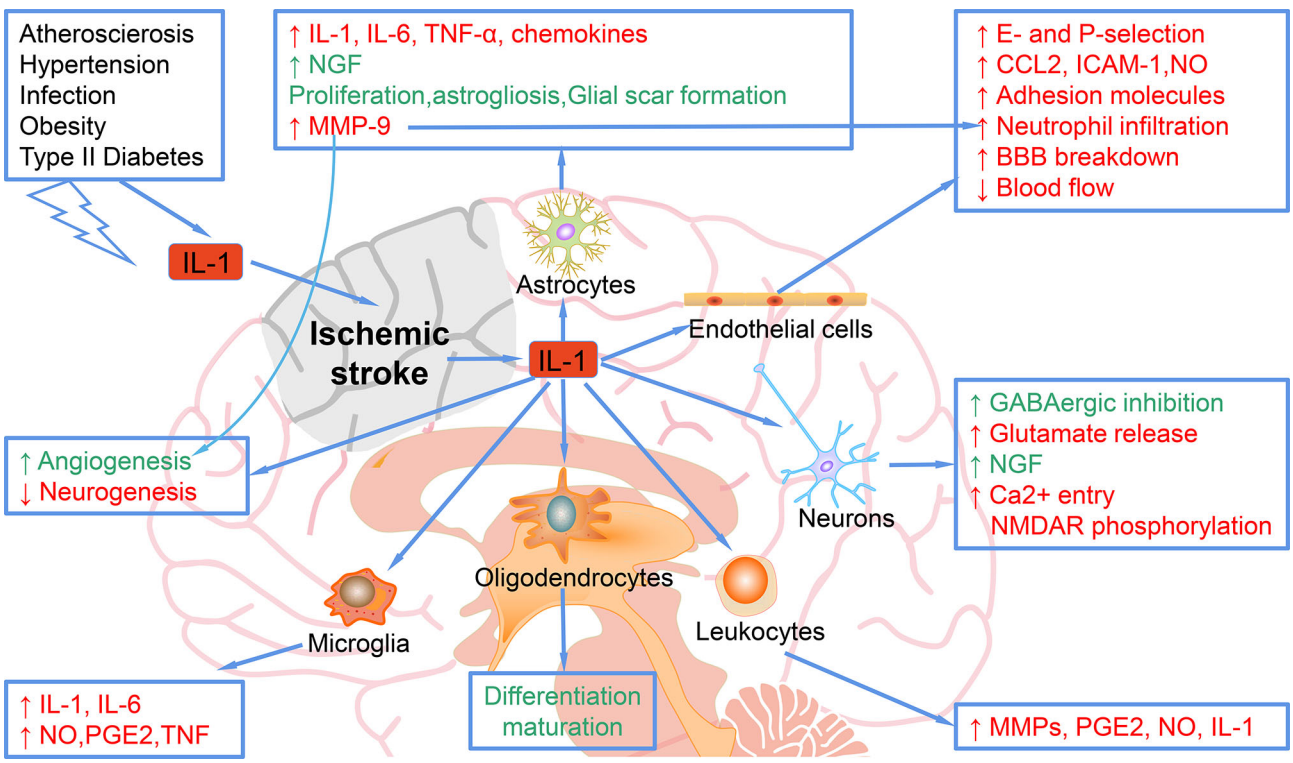

FIGURE 1 | Mechanisms of the role of IL-1 in ischemic stroke. IL-1, elevated after ischemic stroke or other risk factors, can target astrocytes and up-regulate the expression of IL-1, IL-6, TNF-α, MMP-9, and chemokines. IL-1 target astrocytes to promote the NGF, proliferation, astrogliosis, and glial scar formation, which ameliorate ischemic injury. IL-1 targets endothelial cells and increases the E- and P-selection, CCL-2, ICAM-1, NO, adhesion molecules, neutrophil infiltration, blood flow decrease and BBB breakdown, which exacerbate ischemic stroke. When targets neurons, IL-1 increases the GABAergic inhibition and NGF, which rescue ischemic injury, while IL-1 also increases glutamate release and Ca2+ entry NMDAR phosphorylation, which cause more damage in ischemic stroke. Leukocytes can be regulated by IL-1 to secret more MMPs, PGE2, NO, and IL-1. In addition, microglia can be regulated by IL-1 to elevate the expression of IL-1, IL-6, NO, PGE2 and TNF. Oligodendrocytes can also be regulated by IL-1 for differentiation maturation.

of adhesion molecules and neutrophil infiltration, decrease of BBB integrity and blood flow by acting on endothelial cells, leading to worse outcomes. Moreover, IL-1 stimulates the proliferation and activation of astrocytes, leading to astrocyte hyperplasia, which is a typical response to brain injury. Data reported in many studies confirm that IL-1 upregulates a large number of genes in astrocytes, which encode neurotoxic factors including MMPs, chemokines, pro-inflammatory cytokines such as IL-6 and TNFα, but also survival-promoting mediators such as NGF (nerve growth factor) (10). IL-1 also exerts its effects on cerebrovascular endothelial cells to increase the production of chemoattractant and adhesion molecules such as CCL2 (CC chemokine ligand-2), ICAM-1 (intercellular adhesion molecule-1), and E- and P-selectin, and even promotes the breakdown of BBB, events that are associated with recruitment of leukocytes (11). IL-1 can act directly on neurons through an alternative signaling mechanism involving ceramide production and activation of Src kinase that phosphorylates the NMDAR [NMDA (N-methyl-D-aspartate) receptor] subunit 2B, leading to enhanced calcium entry and increased vulnerability to additional injury (12). IL-1 may also induce neurotoxicity indirectly through its action on the vascular endothelium to promote the recruitment of leukocytes, especially neutrophils that damage the neurovascular unit through the release of MMPs and reactive oxygen species (ROS) (11).

However, in the subacute and chronic phases post-stroke, some of the effects of IL-1 may be beneficial. For example, IL-1 promotes the glial scar formation and enhances angiogenesis, thereby promoting ischemic stroke recovery (13). In addition, IL-1 is not toxic to pure neurons in culture and can even promote survival through enhancement of synaptic GABA(γ-aminobutyric acid)ergic inhibition or production of NGF (14, 15).

2.2 The Mechanisms of IL-1β-Induced Brain Damage in Ischemic Stroke

In acute ischemic stroke, blood perfusion to the brain is reduced. In cerebral infarction, when blood flow is 10%-25% lower than normal, nerve cells will suffer irreversible damage or even death, and inflammatory cells in the tissue will release inflammatory factors. As one of the most powerful pro-inflammatory cytokines, IL-1β exerts an essential role in ischemic stroke mainly through the following mechanisms.

2.2.1 IL-1β Aggravates the BBB Dysfunction

After ischemic stroke, increased secretion of IL-1β activates phospholipase A2 to degrade arachidonic acid and destroy the phospholipid bilayer (16). Moreover, the metabolites, prostaglandin and leukotriene, can promote the increase of microvascular permeability, resulting in blood-brain barrier (BBB) dysfunction and the formation of vasogenic brain edema (17). Meanwhile, after ischemic stroke, the reduction of glucose and oxygen supply, insufficient ATP production, and enhanced glycolysis, lead to the occurrence of cytotoxic brain edema. The interaction between the vasogenic brain edema and cytotoxic brain edema causes cranial pressure increase, secondary injury of brain tissue, and the possible occurrence of cerebral hernia in severe cases, endangering the life of the patient. In addition, IL-1β also aggravates ischemic injury by promoting the expression of adhesion molecules between endothelial cells, inducing leukocyte migration to the ischemic area to trigger inflammatory response (18).

2.2.2 IL-1β Mediates the Inflammatory Response in Ischemic Stroke

IL-1β stimulates the activation of microglia, which, as the main effector cells in the neuroinflammatory response, aggravates the inflammatory response and leads to secondary brain damage by secreting and releasing a series of potential neurotoxic substances, such as TNF-α and iNOS. IL-1β activates IκB kinase through the IRAK pathway, resulting in the phosphorylation and ubiquitination of IL-1β-mediated IκB-α, which ultimately upregulates the expression of NF-kB in the cell nucleus and induces the increase of the transcription of target genes such as IL-8 and TNF-α (19). Study has demonstrated that IL-1β regulates the PI3K/AKT pathway to stimulate IL-6 and other cytokines, which synergistically act on ischemic areas and aggravate the damage effect (20). Other studies have shown that up-regulation of IL-6 and other pro-inflammatory cytokines can promote the phosphorylation of JAK2/STAT3 (21, 22). After P-STAT3 enters the nucleus, it will bind to the DNA sequence characteristic of the promoter region of target genes and up-regulate the transcription of IL-1β, IL-6 and TNF-α genes (22). This vicious cycle leads to persistent inflammation, and damaged brain cells fail to recover.

2.2.3 IL-1β Promotes Apoptosis After Ischemic Stroke

After ischemic stroke, a large number of potentially salvageable neurons exist in the ischemic penumbra. However, with the prolongation of ischemia time, IL-1β promotes the apoptosis of the damaged cells by activating the apoptotic molecular mechanism, leading to the original ischemic penumbra gradually becoming the area of cerebral infarction, and finally the aggravated brain damage. Studies have verified that IL-1β plays a crucial role in the process of apoptosis of injured cells. This effect is mainly through the following two aspects: (1) activation of the excitatory toxicity mediated by glutamate (23); (2) activating the apoptotic cascade to activate the JNK/AP-1 pathway (24). Recently, it has been reported that the AIM2 inflammasome-derived IL-1β production activated triggers the expression of FasL in the spleen monocytes which evokes the apoptosis of Fas-dependent extrinsic T cells, causing an increased risk of infection by bacteria after ischemic stroke (25). Therefore, IL-1β may be involved in the signaling cascade activated by AIM2 inflammasome, causing immune suppression and secondary infection after stroke injury.

3 IL-2

Il-2, also known as cell growth factor, is an immunomodulatory lymphocyte secreted by T lymphocytes after being stimulated by antigen. In addition to maintaining the long-term multiplication

and differentiation of T cells *in vitro*, IL also has important biological functions such as enhancing the killing activity of NK cells, promoting the proliferation and differentiation of B cells, and inducing the production of lymphokine-activated killer cells.

3.1 IL-2 Expression Decreased After Ischemic Stroke

Clinical trials showed that the level of serum IL-2 in patients with acute cerebral apoplexy was significantly lower than that in normal control group (26). The mechanism may be related to the following two factors: (1) In acute stroke, the body stress response, the immune stability *in vivo* is destroyed, especially the function of T cell is affected, so that the blood level of IL-2 is significantly decreased; (2) In acute stroke, the brain tissue cells are damaged, and local ischemia and hypoxia reduce the synthesis of IL-2 in the brain.

3.2 The Role of IL-2 in Ischemic Stroke

The IL-2/IL-2 antibody complex (IL-2/IL-2Ab) may improve the prognosis of ischemic stroke by regulating the amount of regulatory T cells (Tregs) in the body (27). Tregs are known to prevent ischemic stroke. However, the small amount of Tregs limits their clinical efficacy.

Previous research has showed that IL-2/IL-2Ab treatment selectively increases the amount of Tregs in the lymph nodes, spleen, and blood, significantly reduces the infarct volume, inhibits neuroinflammation, and improves sensorimotor function compared to stroke mice treated with isotype IgG (27). IL-2mAb has been reported to reduce demyelination after ischemic stroke by suppressing CD8 + T cells (28). The depletion of Tregs by diphtheria toxin eliminated neuroprotective effect provided by IL-2/IL-2Ab. IL-2/IL-2Ab promotes the expression of CD39 and CD73 in expanded Tregs, the deficiency of which may reduce the protective action of Tregs stimulated by IL-2/IL-2Ab in ischemic stroke mice (27). After stroke, increasing Treg cell numbers by delivering IL-2:IL-2 antibody complexes can improve white matter integrity and rescue neurological functions over the long term (29). In addition, Zhao et al. has found that ischemic stroke patients with poor functional outcomes at 3 months have significantly higher levels of IL-2 receptor α (sIL-2Rα) and lower levels of IL-2 than patients with good outcomes. Higher sIL-2Rα and IL-2 levels were associated with an increased and reduced risk of unfavorable outcomes, respectively (30), indicating that increased plasma sIL-2Rα and IL-2 levels manifested opposite correlations with functional outcome, illustrating the importance of IL-2/IL-2R autocrine loops in ischemic stroke.

4 IL-4

IL-4 regulates various immune responses, including the differentiation of T cells and nonspecific transformation of B cells (31). It is also the most characteristic M2 macrophage polarization promoter to date. Numerous evidences suggest that IL-4 plays a critical role in brain function under physiological and pathological conditions. For example, T-cell-derived IL-4 is essential for learning and memory in the normal brain. Levels of IL-4 in the brain tissue decrease with age, which may contribute to cognitive decline in older people and also increase the risk of Alzheimer's disease (32). After ischemic stroke, IL-4 treatment has been shown to enhance white matter integrity (33).

4.1 IL-4 Promotes the M2 Polarization of Microglia/Macrophages

Recent animal and clinical researches have demonstrated the importance of IL-4 in the acute phase of stroke (34, 35). Several hours after the onset of stroke, the level of IL-4 in serum was observably increased (36). In addition, 24 hours after transient middle cerebral artery occlusion (MCAO), IL-4 deficiency resulted in brain injury and neurological dysfunction (37). IL-4 plays an important role in the M2 polarization and long-term recovery of microglia/macrophages after ischemic stroke. Mice lacking IL-4 have more M1-polarized microglia/macrophages, larger infarcts and more severe functional deficits after cerebral ischemia, while recombinant IL-4 can eliminate these effects (38). IL-4-polarized microglia cells may alleviate the ischemic stroke injury by promoting angiogenesis through the secretion of exosomes containing miRNA-26a (39). There is a direct salutary effect of IL-4 on oligodendrocyte differentiation that is mediated by the peroxisome proliferator-activated receptor gamma (PPARγ) axis. Additionally, PPARγ is essential for IL-4-induced oligodendrocyte progenitor cell differentiation and long-term functional improvements after stroke (33).

4.1.1 Inhibition Pro-Inflammatory Cytokines

The neuroprotective effect of IL-4 may be achieved by stimulating IL-4/STAT6 signal transduction and inhibiting pro-inflammatory cytokines. Previous study has showed that IL-4 knockout mice produce more pro-inflammatory cytokines, including IL-1β and TNF-α (40). The loss of IL-4 in mice also increases sensitivity to mechanical pain.

4.1.2 IL-4 Is Essential for Sex Differences in Vulnerability to Stroke

IL-4 protects against cerebral ischemia in male mice. However, female mice generally exhibit less damage in response to the same challenge of cerebral ischemia. Infarct volume in WT female mice in proestrus and estrus phases is markedly smaller than in males. IL-4 is required for female neuroprotection during the estrus phase of the estrus cycle (38). In protected female WT mice, microglia/macrophages were dominated by M2 polarization and inflammatory infiltration was reduced (40). Therefore, increasing macrophage M2 polarization, with or without added inhibition of inflammatory infiltration, may be a novel approach for stroke treatment.

4.1.3 IL-4 Affects Neuronal Excitability

Chen et al. have shown that cortical pyramidal and stellate neurons common for ischemic penumbra after cerebral ischemia-reperfusion injury exhibit intrinsic hyperexcitability and enhanced excitatory synaptic transmissions in IL-4

knockout mice. In addition, upregulation of Nav1.1 channel, and downregulations of KCa3.1 channel and α6 subunit of GABAA receptors are observed in the cortical tissues and primary cortical neurons in IL-4 knockout mice (34), indicating that IL-4 deficiency results in neural hyperexcitability and aggravates cerebral ischemia-reperfusion injury.

5 IL-6

IL-6 is a glycoprotein with a molecular mass of 20 to 30 kDa, depending on the cellular source and preparation, and is a cytokine with pleiotropic, playing a role in central host defense (41). The IL-6 family of cytokines recruits gp130 for signaling. For IL-6 specifically, a hexamer forms (two IL-6, two IL-6R and two gp130) that can activate intracellular tyrosin-kinases such as JAK and, to a lesser extent, TYK, which, in turn, activate a number of proteins including the STAT family of transcription factors, or the RAS-RAF-MAPK pathway, PI3K, or IRS (insulin receptor substrate) (42). IL-6, mainly produced by monocyte macrophages, lymphoid cells, T cells, B cells, granulocytes, mast cells and endothelial cells, is a kind of multi-effector cytokine. IL-6 has critical effect in immune reactions, acute phase response and hematopoiesis regulation, mainly in autocrine or paracrine ways. By activating target genes, IL-6 not only serves as a differentiation and growth factor of hematopoietic cells, B cells, T cells, osteoclasts and endothelial cells, but also plays an important role in the growth, differentiation, regeneration and degradation of peripheral and central nervous system nerve cells. IL-6 activates and recruits neutrophils and monocytes, stimulates vascular endothelial cells to secrete adhesion molecules and other inflammatory transmitters, and enhances local inflammatory response (43). Circulating and local IL-6 production will lead to the state of pre-thrombosis, which can induce the production of platelet derived growth factor, fibroblast growth factor, TNF, macrophage colony stimulating factor, and promote the proliferation of smooth muscle cells (44).

5.1 Dual Role of IL-6 in Ischemic Stroke

The dysregulation of IL-6 is closely related to the occurrence and outcome of many clinical diseases, including coronary heart disease, leukemia, hypertension, ischemic stroke and so on (45). Su et al. demonstrated that elevated IL-6 induced by ischemia and hypoxia, oxidative stress, vascular occlusion and inflammation, partly leads to the production of the acute phase protein in the liver, thereby stimulating leukocyte recruitment and thrombosis, ultimately causing multiple cardio-cerebrovascular diseases including ischemic stroke (46). Elevated serum IL-6 levels are implicated in a higher risk of incident stroke and mediate the racial disparity in stroke *via* inflammatory effects of risk factors (47). Elevated plasma IL-6 has been reported to be a signatures of post-stroke delirium (48). Additionally, high IL-6 levels at 24 hours are associated with futile reperfusion in patients with acute ischemic stroke with large vessel occlusion treated with mechanical thrombectomy (49). Moreover, a lower admission level of IL-6 is positively correlated with the first-pass effect, which is defined as a complete or near-complete reperfusion achieved after a single thrombectomy pass is predictive of favorable outcome in acute ischemic stroke patients (50). These findings indicate that IL-6 may be a predictor of the prognosis of ischemic stroke patients.

IL-6 is a marker of inflammation after stroke, and elevated IL-6 is mainly secreted from neurons, microglia, astrocytes, and endothelia cells in the ischemic hemisphere, traditionally regarding as an adverse prognostic factor (51) (**Figure 2**). In the ischemic brain, IL-6 protein is mainly localized in the neurons of the cerebral cortex. The neuronal expression of IL-6 starts 3.5 h after ischemia, peaks after 24 h of reperfusion, and remains for 7 days. The immunoreactivity of IL-6 was most upregulated in ischemic penumbra. IL-6 released into the cerebrospinal fluid after stroke may lead to impaired cerebrovascular autoregulation and increased histopathology. In addition, IL-6 is related to the inflammation, which contributes to both damage and recovery process after ischemic stroke (52). The high levels of serum IL-6 have been reported to be related to the body temperature, early neurologic deterioration, infarct volume, and a long-term poor outcome. It has been identified that after stroke brain is the main source of IL-6 (53). In addition, inflammatory biomarkers, including C-reactive protein, fibrinogen, IL-1 receptor antagonist, and TNF-α are also elevated in parallel with IL-6 (54).

However, IL-6 is also a neurotrophic cytokines that shares a common receptor subunit, gp130, with other neurotrophic cytokines, such as leukemia inhibitory factor (LIF) and ciliary neurotrophic factor (55). The IL-6 expression is mainly observed in neuronal cells in the ischemic penumbra region, and the expression of LIF shows a similar pattern. The direct injection of these cytokines into the brain tissue after ischemic stroke can reduce cerebral ischemic damage. The main downstream signaling pathway of IL-6 is JAK-STAT, and the activation of STAT3 occurs primarily in neuronal cells after ischemic reperfusion. Since the role of STAT3 in stroke is also diverse and controversial, further studies are needed to explore the accurate action of STAT3 signaling in neuroprotective effect (54). IL-6 secreted from astrocytes promotes Th1 polarize into Th2 to mediate immunosuppressive microenvironment and contribute to the neurogenesis and angiogenesis and neuronal differentiation (51). IL-6 stimulates the phosphorylation of STAT3 and the early transcriptional activation of angiogenesis-related genes, thereby leading to the enhanced angiogenesis and elevated cerebral blood flow in the delayed period after ischemic stroke. IL-6R simultaneously activates the PI3K/AKT and JAK-STAT pathways, which play vital roles in angiogenesis after ischemic stroke (56). Additionally, IL-6 also been reported to facilitate post-traumatic healing in the CNS through repair of endothelial cells, which also demonstrates that IL-6 may enhance revascularization or angiogenesis after ischemic stroke (57). IL-6 increases CNS neuronal survival and decreases excitotoxic neuronal damage against NMDA-mediated injury and protects neurons against apoptosis (54). Continuously injection of recombinant for 7 days IL-6 into the lateral ventricle of gerbils subjected to transient cerebral ischemia, IL-6 injection was found

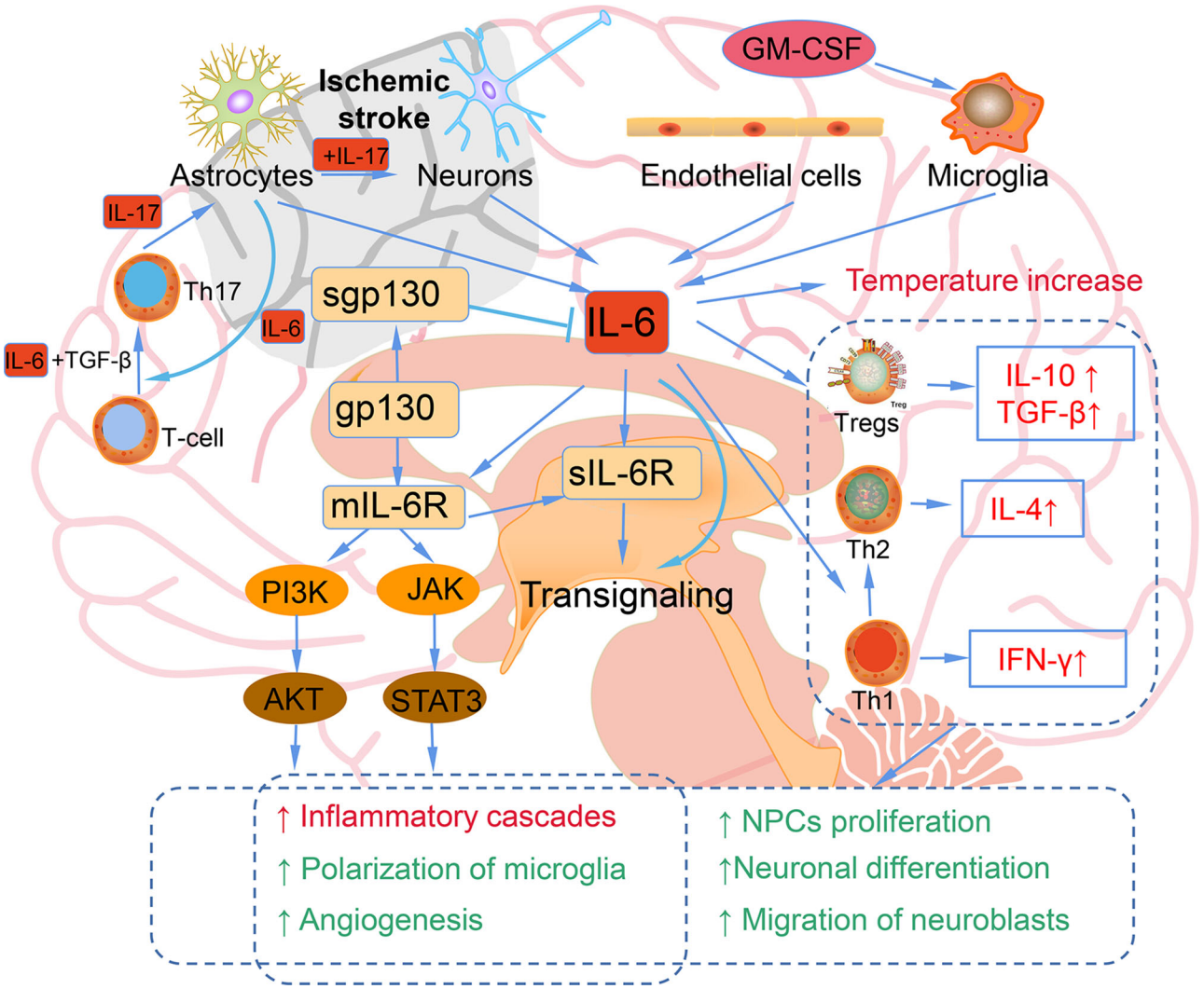

FIGURE 2 | The bidirectional role of IL-6 in ischemic stroke. Astrocytes, neurons, endothelial cells, and microglia can produce IL-6 after ischemic stroke. Elevated IL-6 leads to the temperature increase; inflammatory cascades, microglia polarization, and angiogenesis mediated by JAK/STAT3 and PI3K/AKT pathways; increased IL-10, TGF-β induced by Tregs; Th1 polarizing to Th2; NPCs proliferation; neuronal differentiation; migration of neuroblasts.

to prevent learning disabilities and delayed neuronal loss (58). In conclusion, IL-6 has a dual effect in ischemic stroke, acting as an inflammatory factor in the acute stage and a neurotrophic mediator in the subacute and prolonged phase.

6 IL-8 IN ISCHEMIC STROKE

IL-8 is a chemotactic cytokine that promotes the chemotaxis of inflammatory cells and induces cell proliferation. After ischemic stroke, IL-8 levels are increased (59, 60), mobilizes and activates neutrophils, causing neutrophils to infiltrate into the ischemic area, aggravating the local inflammatory response, leading to the expansion of ischemic lesions, and leading to severe morbidity and disability (2, 61–63). Endothelin-1 may be a stimulator of IL-8 (62). IL-8 may be also involved in recruiting blood polymorphonuclear leukocytes to the sites of cerebral ischemia (59). The expression of pro-inflammatory cytokines (IL-1β, IL-6, IL-8, TNF-α) in the cortex of ischemic stroke mice was detected after the occurrence of cerebral ischemia (64). One study showed that the levels of these pro-inflammatory cytokines in patients with acute cerebral ischemia were observably higher than those in the control normal group, and the degree of disability in early phase of acute stroke was positively correlated with the level of serum IL-8 (65). IL-8 gene knockout has been shown to promote neuroglial cells activation while inhibit neuroinflammation through the PI3K/Akt/NF-κB-signaling pathway in mice with ischemic stroke (66). The high serum IL-8 levels are associated with prognosis. IL-8 exaggerates the ischemic stroke injury through inducing neutrophil-mediated-inflammation (61). The development of new neuroprotective treatments aimed to

prevent neutrophil-mediated-inflammation induced by IL-8 is critical in the treatment of stroke, and prevention of clinical worsening. IL-8 can be used as important indicator to judge the severity of the early condition of acute ischemic stroke patients (67). However, IL-8 stimulates VEGF production in human bone marrow mesenchymal stem cells partially *via* the PI3K/Akt and MAPK/ERK signal transduction pathways and that administration of IL-8-treated human bone marrow mesenchymal stem cells increases angiogenesis after stroke (68).

7 IL-10

IL-10 is a significant anti-inflammatory cytokine that has inhibitory effects on a variety of immune cells. IL-10 was first identified in mouse Th2 cells, and was subsequently found to be secreted in astrocytes, neurons, B cells, monocytes/macrophages, keratinocytes, and human Th1 cells. IL-10 has strong anti-inflammatory and immunosuppressive activity. It can inhibit the production and release of IL-2, IFN-γ and pro-inflammatory factors, reduce the expression of immune receptors, inhibit human Th2 cells, lead to cell proliferation, cytokine production reduction (69). IL-10 binds to IL-10 receptors (IL-10R) to decrease inflammation and limit apoptosis (70). These effects make it a very important role in the protection of cerebral ischemia.

7.1 IL-10 in Ischemic Stroke

The neuroprotection of IL-10 on ischemic stroke has always been a research hotspot. A meta-analysis exploring the relationship between IL-10 gene polymorphism and ischemic stroke risk revealed no overall significant association of IL-10 with ischemic stroke risk, but an association was found with macrovascular disease and microvascular disease (71), demonstrating that certain subtypes of ischemic stroke are correlated to IL-10 gene polymorphisms.

In experimental stroke, the levels of IL-10 mRNA and protein and IL-10R mRNA were elevated, with IL-10 observed in microglia and IL-10R on astrocytes in the ischemic penumbra (72). In transgenic mice that overexpressed IL-10, infarct size was reduced, and apoptosis was limited 4 days post ischemic stroke (73). Additionally, Overexpression of IL-10 enhances the neuroprotective effect of mesenchymal stem cell transplantation through anti-inflammatory regulation, thus supporting the survival of neurons during acute ischemia (74). Both systemic intravenous (IV) and central intracerebroventricular (ICV) exogenous administration of IL-10 reduced infarct size after permanent MCAO (pMCAO) (75). Moreover, low IL-10 levels were related to poor stroke outcomes and a delayed, exacerbated inflammatory response that was alleviated by IL-10 administration after pMCAO (76). Lower levels of IL-10 and IL-33 may also be used to predict post stroke depression (77, 78). The IL-10 expression in the brain tissue increases with pathological changes of the central nervous system, promotes the survival of gliocyte and neurons, and inhibits inflammatory responses through multiple signaling pathways. Previous research showed that the significant decrease of IL-10 was significantly associated with the degree of neurological impairment, and the concentration of IL-10 had a high predictive value on the early neurobehavioral performance post-acute stroke (79). However, stroke patients are susceptible to infection as a result of stroke-induced immunosuppression, and elevated serum IL-10 levels have been identified as an independent predictor of post-stroke infection (80, 81). IL-10 overreaction can lead to immunosuppression and worsening neurological prognosis after stroke, indicating that IL-10 therapy should be used with caution (82). Elevated IL-10 levels may be associated with higher incidence of post-stroke urinary tract infection, leading to poorer recovery after ischemic stroke in women (83, 84). In addition, IL-10 can mediate the function of Th2 cells, exert a protective effect, and lead to the reduction of ischemic infarction lesions (85). Future studies should be aimed at differentiating between central and peripheral IL-10 effects post-stroke.

7.1.1 The Mechanism of IL-10 in Inhibiting Inflammatory Responses After Stroke

Immune cells, including T and B cells, are important in ameliorating neuroinflammation *via* the modulation of varieties of cytokines and chemokines, with IL-10 playing a central immunomodulatory role (86, 87). The protective effect of IL-10 on stroke is mainly achieved by inhibiting inflammatory reactions. Firstly, IL-10 decreased the expression and activity of pro-inflammatory cytokines such as IFN-γ, IL-1β and TNF-α through PI3K and STAT3 activation (**Figure 3**) (88). Secondly, IL-10 inhibits the synthesis and activity of Th1 lymphocytes (89). In addition, IL-10 treatment can effectively down-regulate the up-regulated pro-inflammatory signals in acute ischemic lesions after stroke, and can provide neuroprotection for ischemic stroke (90). IL-10 gene transduction before cerebral artery ischemia can alleviate brain damage induced by ischemia/reperfusion in rats through increasing the expression of heme oxygenase (91). IL-10 also exert its anti-inflammatory effects partially through inhibition of NF-κB (92). Hydrogen sulfide donor administration during reperfusion protects the integrity of BBB after ischemia/reperfusion and is accompanied by increased IL-10 expression, reduced NF-κB nuclear translocation, and MMP-9 and NOX4 activity (93). In MCAO mice, by reducing the release of neuroinflammatory factors (IL-6, IL-1β, TNF-α) and astrocyte activation, IL-32α overexpressing transgenic mice showed reduced cell death of ischemic neurons and enhanced anti-neuroinflammatory factor (IL-10), indicating a crosstalk between IL-32α and IL-6, IL-1β, IL-10 (94). IL-10-secreting $CD4^+$ T cells induced by nasal MOG reduce injury following stroke. IL-10 secreted from $CD4^+$ T cells may be the reason of the neuroprotection of oligodendrocyte glycoprotein administration in MCAO mice (95, 96). Increased IL-10 levels also decreased the number of $CD11b^+$ cells that may contribute to secondary infarct expansion *via* nitric oxide pathways (96). Expansion of the CNS Treg cell population by administration of the CD28 superagonist monoclonal antibody at the start of reperfusion decreased the infarct volume 7 days after MCAO, and its effect was attributed

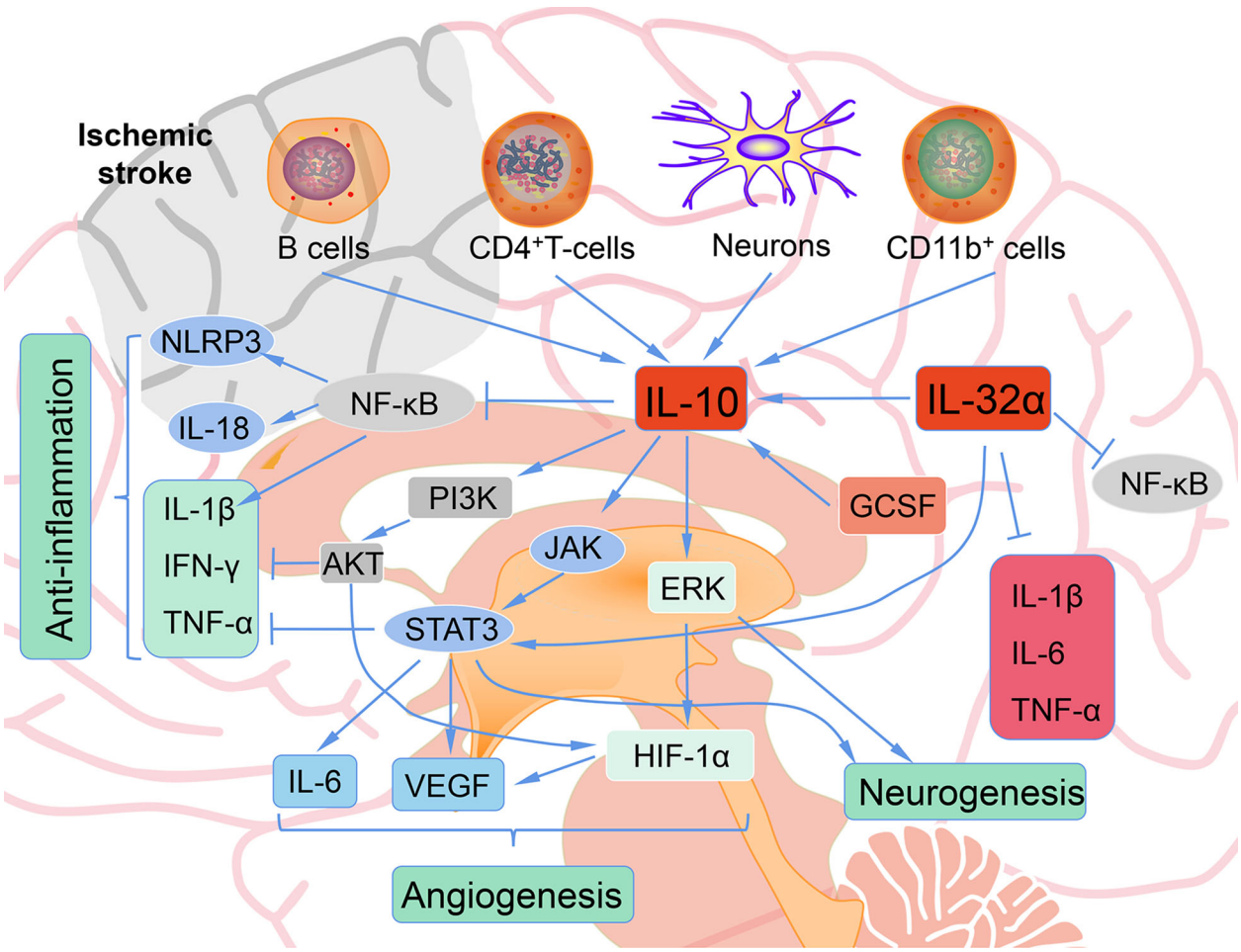

FIGURE 3 | The role of IL-10 after ischemic stroke. B cells, CD4+ T cells, neurons, CD11b+ cells produce IL-10 after ischemic. IL-10 shows anti-inflammatory, angiogenesis, and neurogenesis role after ischemic stroke.

to the increased IL-10 (97). Transfer of IL-10-producing B cells into B cell-deficient mice 24 h after MCAO attenuated cerebral ischemia-reperfusion injury, reduced the amount of T cells and monocytes in cerebral parenchyma, and improved the peripheral proinflammatory homeostasis (87). Interesting, IL-10-producing B cells also upregulated the number of Tregs (87), suggesting that there may be a positive feedback loop between B cells and Tregs, both of which play a neuroprotective role through IL-10 production. These facts indicate a complicated network between IL-10 and immune cells in ischemic stroke. These methods of targeting IL-10 to prevent recurrence of stroke may be realized in the interventional treatment of stroke.

7.1.2 The Role of IL-10 in Neurogenesis After Ischemic Stroke

Injection of activated Tregs into the lateral ventricle of C57BL/6 mice 60 min after of transient ischemia promotes the proliferation of neural stem cell in the subventricular region in ischemic brain tissues. Moreover, this effect was abolished by blocking IL-10 with a neutralizing antibody, suggesting that activated Tregs act through IL-10 to facilitate the proliferation of neural stem cells (98). Hematopoietic cytokines such as GCSF and stem cell factor have been confirmed to promote neurogenesis (99), and also may be required to provide the initial signals for IL-10 production in ischemic stroke (100). Administration of these cytokines early (1–10 days) and later (11–20 days) post MCAO significantly elevated the mRNA expression of IL-10, reduced the activation of microglia/macrophages, and did not change proinflammatory cytokine levels in C57BL/6J mice (100). A study where bone marrow-derived mesenchymal stem cells were transplanted into the lateral ventricle of Sprague-Dawley rats before pMCAO yielded similar results, where IL-10 mRNA and protein levels were elevated 4 days post-stroke, TNFα was reduced, infarct size was smaller, and neurologic function was improved (101). IL-10 targets Nestin$^+$ progenitors and activates neurogenesis by

modulating ERK and STAT3 activity in adult subventricular zone (102). Either administration of stem cells themselves or hematopoietic cytokines may ameliorate ischemic stroke injury partially through the increase of IL-10. Additionally, neuroprotection after dysbiosis depends on IL-10 and IL-17. IL-10 is required for Treg mediated IL-17$^+$ γδ T suppression (103). Recently, it has been reported that IL-10 acts differentially on αβ and γδ T cells. IL-17A producing CD4+ αβ T cells are directly controlled *via* their IL-10-receptor (IL-10R), whereas IL-10 by itself has no direct effect on the IL-17A production in γδ T cells. The control of the IL-17A production in γδ T cells depended on an intact IL-10R signaling in Tregs (104).

8 IL-12 AND ISCHEMIC STROKE

During antigen presentation to naive T cells, IL-12, IL-23, and IL-27 are produced by activated antigen-presenting cells, while IL-35 is a product of B cells and Tregs (105). The primary target cells of IL-12 are NK and T cells, which are stimulated to produce cytokines, proliferative and cytotoxic activities (106). IL-12 is produced early in infection and plays a pro-inflammatory role in the immune response, and serve as a cofactor in the polarization of T cell response to cell-mediated immunity (107).

Previous studies have confirmed that IL-12 plays an essential role in the pathological process of acute ischemic stroke (108). Cytokines are usually released in response to tissue injury, so increase levels of IL-12 in serum in patients with acute cerebral infarction are consistent with a rapid increase IL-12 levels in the serum of patients with acute myocardial infarction and severe brain injury (109). The increase of IL-12 in serum of stroke patients appears to be a local or systemic immune response to ischemic brain injury, and the increase of IL-12 in serum may be caused by the release of cytokines from the infarcted brain region or cerebrospinal fluid to the periphery. On the other hand, stroke-activated cerebral endothelial cells secrete cytokines that may activate peripheral blood monocytes, leading to systemic expression of cytokines (110). An increase in the number of IL-12 secreting monocytes and monocytes isolated from peripheral blood of patients with cerebral ischemia has been demonstrated (111, 112). In this case, the increase in serum IL-12 levels in patients with stroke may be caused by cytokines.

IL-12 may promote the deterioration of ischemic brain injury *via* cytokines by activating the ability of immunoreactive cells and modulating their abilities in response to inflammation. IL-12 increases the production and action of several pro-inflammatory cytokines and chemokines and promotes endothelial cells to release adhesion molecules, which are potent chemical attractors for different subsets of white blood cells, including monocytes and neutrophils (113, 114). Additionally, in a mouse cancer model, IL-12 gene therapy is associated with increased tissue infiltration and apoptosis of NK and T cells, which are important mechanisms of neuronal death induced by aggressive inflammatory cells in the ischemic brain (115). At present, we can know exactly that there is close correlation between increased levels of IL-12 in the ischemic stroke patients and reaction intensity in acute phase, the size of the early brain injury, neurological stroke severity and functional disability, suggesting IL-12 may play a critical role in pathophysiology of cerebral ischemia.

9 IL-13 AND ISCHEMIC STROKE

IL-13 is a protein secreted by activated T cells and is a powerful regulator of human monocyte and B cell function *in vitro* (116). IL-13 shares a common biological activity with IL-4 (117). IL-13 can induce the differentiation of mononuclear cell, inhibit LPS-induced mononuclear factor secretion, control inflammatory response, induce the proliferation of B cell and synthesize IgE antibody, cooperate with IL-2 to stimulate NK cells to produce IFN, thereby promoting mononuclear macrophage activation.

Previous studies have confirmed the indispensable role of IL-13 in ischemic stroke. IL-13 exerts an effect on microglia and infiltrating macrophages in the brain after stroke, and it can regulate the spontaneous polarization transition from anti-inflammatory to pro-inflammatory phenotype of microglia and macrophages (118). As a well-known modulator of immune response *in vitro*, IL-13 has been shown to have neuro-protective abilities in several experimental models of neurodegenerative diseases by significantly reducing the secretion of pro-inflammatory factors, reducing inflammatory cell infiltration, and inhibiting axonal loss as well as inducing anti-inflammatory microglial/macrophage responses (119, 120). Interestingly, interleukin-13 can also improve ischemic liver gluconeogenesis and hyperglycemia in stroke model rats (121), exerting a salutary action. That is, it has been demonstrated that mesenchymal stem cells that continuously secrete IL 13 can differentiate microglia and macrophages into neuroprotective M2 phenotypes in the pro-inflammatory state of ischemic stroke (122).

10 IL-15 AND ISCHEMIC STROKE

IL-15 can be produced by activated mononuclear macrophages, epidermal cells and fibroblasts. Its molecular structure has many similarities with that of IL-2, and it plays a similar biological activity to IL-2 (123). IL-15 also has the ability to chemotaxis and promote survival, and it can be involved in neuroinflammation. IL-15 also acts as an effective chemotactic agent for T cells, promoting the migration of T cells to inflammatory tissues (124). In addition, IL-15 maintains homeostasis and cytotoxic activity in lymphocytes (NK and CD8$^+$ T cells) carrying its receptor (125).

Although recent studies have shown that astrocytes are a major source of IL-15 in the inflammatory central nervous system (126, 127), the potential role of IL-15 in astrocytes in cerebral ischemic injury is not completely clear. However, significant increase in IL-15 expression in astrocytes post ischemia reperfusion has been

observed. Subsequent studies have shown that IL-15 is a key factor for astrocytes to control the degree of central nervous system inflammation and brain injury following ischemic stroke (126). Astrocytes produce inflammatory cytokines such as IL-15, which promote the cell-mediated immune reaction to ischemic stroke, increase the number of $CD8^+$ T cells and NK cells, participating in ischemic nerve injury. In addition, blockage of IL-15 decreased the effector capacity of NK, $CD8^+$ T and $CD4^+$ T cells in WT mice after CIRI, and the elimination of IL-15 response after CIRI improved brain damage in adult mice (127). Moreover, IL-15 as a mediator of the crosstalk between astrocytes and microglia that exacerbates brain injury after intracerebral hemorrhage (128). Recently, IL-15 has been reported to modulates the response of cortical neurons to ischemia through alleviating endoplasmic reticulum stress and increasing cell survival (129). Therefore, therapy targeted IL-15 is a potential strategy for cerebral ischemia.

11 IL-16 IN ISCHEMIC STROKE

IL-16 is a pro-inflammatory cytokine produced by activated $CD8^+$ T cells and activates $CD4^+$ T cells, monocytes, macrophages, and dendritic cells by binding to the CD4 molecule (130). In addition, IL-16 promotes the production of inflammatory cytokines such as TNF-α, IL-1β, and IL-6, which has key effects in immune responses after ischemic stroke (131). Although the mechanism by which IL-16 acts as a mediator of inflammation is not fully understood, previous study has shown that IL-16 is involved in inflammatory disease through the activation of T lymphocytes and the expression of inflammatory cytokines (132). In the early stage of cerebral ischemia, T lymphocytes are activated to release reactive oxygen species, which eventually lead to brain damage. In later stages, T lymphocytes regulate brain recovery and regeneration. The depletion of T cells in the acute phase of ischemia reduces the infarction size and has a sustained protective action against ischemic stroke in the later stages of infarction development (133). IL-16 accumulates during injury-related response areas and perivascular areas through the infiltrated immune cells (e.g., neutrophils, $CD8^+$ lymphocytes, and activated $CD68^+$ microglia/macrophages) (134). The recruitment and activation of immune cells lead to microvascular aggregation and disorder of BBB, leading to secondary injury.

12 IL-18 IN ISCHEMIC STROKE

IL-18 is known as a pro-inflammatory cytokine. IL-18 expression is mainly observed in neuronal cells at early phase and in microglia at a later stage. IL-18 is associated with stroke-induced inflammation and that initial serum IL-18 levels may be predictive of stroke outcome. IL-18 KO mice exhibit the resistance to spatial restraint stress and CIRI (135). Caspase-1 activated by NLRP3 inflammasome, cleavage pro-IL-1β and pro-IL-18 to mature forms (IL-1β and IL-18), and mediate the inflammatory response or initiate the process of inflammatory cell death and pyrolysis. In addition, increased IL-18 in the brain causes depression-like behaviors by promoting the IL-18 receptor/NKCC1 (a sodium-potassium chloride co-transporter) signaling pathway. Hence, agents that inhibits NLRP3 inflammasome exert a neuroprotective effect on ischemic stroke and post-stroke depression *via* suppressing the expression of IL-18.

13 IL-19 AND ISCHEMIC STROKE

IL-19 is a member of the IL-10 family, which includes IL-10, IL-19, IL-20, IL-22, IL-24, and IL-26 (136). IL-19 was first discovered in primary human monocytes stimulated by LPS and GM-CSF (137). Subsequent reports on IL-19 mainly focused on its role as a product of immune cells. In immune cells, IL-19 is mainly secreted by monocytes, and a small part is expressed by B cells. It has been reported that IL-19 treatment can mature human T cell polarize them from pro-inflammatory Th1 phenotype to anti-inflammatory Th2 phenotype (138, 139). In addition, the anti-inflammatory effect of IL-19 on vascular diseases has also been clearly demonstrated (140).

As an anti-inflammatory factor, IL-19 also exerts a critical action in the immune reaction after the onset of ischemic stroke. Studies have shown that IL-19 can reduce infarct size and reduce neurological impairment after ischemic stroke through its anti-inflammatory ability (141). Moreover, IL-19 treatment can significantly reduce the up-regulation of TNF-α and IL-6 mRNA expression after ischemic stroke, inhibit the increase of microglia, macrophages, $CD4^+$ T cells, $CD8^+$ T cells, and B cells, and suppress the activation of macrophages and neutrophils. The administration of IL-19 also contributes to preserve the reduced number of immune cells, including macrophages, $CD4^+$ T cells, $CD8^+$ T cells, and B cells in peripheral blood compared to controls. In conclusion, IL-19 reduces cerebral infarction and neurologic deficits after cerebral ischemia in mice, possibly by inhibiting the infiltration and activation of immune cells and the increased expression of pro-inflammatory cytokine genes. Therefore, IL-19 may be identified as a new therapeutic agent to suppress the development of neuroinflammation after ischemic stroke.

14 IL-20 IN ISCHEMIC STROKE

IL-20 is also a member of the IL-10 family, and is produced by monocytes, epithelial cells, and endothelial cells. IL-20 has been related to a variety of inflammatory diseases, such as psoriasis, rheumatoid arthritis, atherosclerosis, and renal failure (142). IL-20 also induces the production of IL-6 (143), which is also a major pro-inflammatory cytokine. In addition, the levels of IL-6 in serum are correlated with cerebral infarction volume and

stroke severity. IL-20 may be associated with the increased IL-6 levels in serum after ischemic stroke.

14.1 IL-20 Promotes Inflammation After Ischemic Stroke

The pathogenicity of IL-20 in ischemic brain injury has been demonstrated in transient MCAO animal models. After cerebral ischemia reperfusion, the levels of IL-20 in serum and ischemic penumbra were significantly elevated than sham groups, and glial cells were the main source of IL-20. After cerebral ischemia, hypoxia also induces the production of IL-20 in endothelial cells (144). The upregulation of IL-20 on glial pro-inflammatory cytokines and chemokines (may cooperate with IL-1β to promote inflammatory activity) is associated with inflammatory response and brain damage after ischemic stroke (145). Inflammatory cytokines and chemokines such as IL-1β, IL-8 and monocyte chemotactic protein 1 (MCP-1) are involved in the inflammatory response of infarcts (146). In conclusion, IL-20 is a novel hypoxia response factor that is upregulated in gliocyte after experimental ischemic stroke and mediates cell proliferation, signal transduction, and cytokine production. These suggest that IL-20 is related to the pathogenesis of cerebral ischemia, and IL-20 antagonists may have clinical therapeutic effects on ischemic stroke.

15 IL-23/IL-17

The IL-23/IL-17 axis has essential effect on the development of chronic inflammation and host defense against bacterial infection (147). In chronic inflammation, antigen-stimulated dendritic cells and macrophages produce IL-23, promoting the development of Th17 cells (148). Th17 cells produce IL-17, which promotes T cell activation by inducing the expression of various of inflammatory cytokines and triggers a powerful inflammatory response. IL-23 also acts on dendritic cells and macrophages in an autocrine/paracrine manner to promote the production of inflammatory cytokines, such as IL-1, IL-6, and TNF-α (149).

15.1 IL-23/IL-17 in Ischemic Stroke

Studies have shown that routine $CD172a^+/IRF4^+$ 2 type dendritic cells (CDC2s) are the main source of IL-23 in the brain following ischemic stroke, and are essential for IL-17 expression in γδT cells (148). Dendritic cells infiltrate the peri-infarcted area near the blood vessels after stroke. These cells induce γδT cells to produce IL-17, promoting neutrophil recruitment to the ischemic hemisphere (150). However, IL-23R gene knockout has no significant effect on the mortality in mice, suggesting that DC cells exert their adverse effects not only through IL-23, but also through other mechanisms (148). Additionally, IL-23 and IL-17 have been reported to increase after stroke, but there is insufficient clinical discriminatory power to predict the outcome of stroke (151). Vγ4 T cell-derived IL-17A, and IL-1β/IL-23 in infract hemisphere coordinately to exaggerate the inflammatory cascades and exacerbate ischemic tissue injury (152).

16 IL-33 AND ISCHEMIC STROKE

As a member of the IL-1 family, IL-33 can bind to membrane receptors on target cells to mediate downstream signaling pathways, or be transported to the nucleus of target cells to function as a DNA-binding factor. After IL-33 binds to its receptor complex, activated signals transmits into cells, and activates NF-κB and mitogen-activated protein kinase (MAPK) through a series of downstream signaling molecules such as IL-1-associated protein kinase, myeloid differentiation factor 88, and TNF receptor-associated factor 6 (153).

IL-33 has been reported to have neuroprotective effects through inhibiting inflammation *via* ST2 (a member of the IL-1 receptor family)/IL-33 signaling (154, 155). After ischemic brain injury, IL-33 expression in mature oligodendrocytes and astrocytes is increased. Interleukin-33 also protects against ischemic brain injury by regulating microglia and regulatory T cell activity (156). Serum IL-33 has been proved to be a novel predictive biomarker of hemorrhage transformation and outcome in acute ischemic stroke (157). The expression of ST2 on microglia/macrophages increases after MCAO. ST2 deficiency can exacerbate neurobehavioral disorders and brain damage *via* shifting microglial polarization toward M1. Some traditional oriental medicine, such as celastrol, ameliorate ischemic stroke injury through promoting IL-33/ST2 axis-mediated microglia/macrophage M2 polarization (158). IL-33 also protects ischemic stroke injury by regulating specific microglial activities (159). IL-10 is an essential protective factor for the neuroprotection of IL-33/ST2 signaling. In the ischemic brain, intracerebroventricular IL-33 can activate the downstream Foxp3 *via* ST2 receptor to increase Treg proportions, which produce amphiregulin to activate epidermal growth factor receptor located in neurons, leading to better outcomes (160). In addition, systemic administration of Th2 cells to promote cytokines IL-33 and IL-4 can reduce acute brain injury after CIRI (154). Astrocyte lipogenesis increases IL-33 production in the peri-infarct region, which promotes BBB repair in the subacute phase of cerebral ischemic injury and improves long-term functional recovery (161). The long-term protective role of IL-33 in ischemic stroke may be partly associated to its regulation of splenic T-cell immune responses *via* inhibiting Th1 response and promoting Treg response (162). Although IL-17 has these neuroprotective effects, mice treated with IL-33 showed an exacerbation of post-stroke pulmonary bacterial infection associated with greater functional impairment and mortality after 24 hours, suggesting exacerbation of systemic immunosuppression after ischemic stroke (163).

17 OTHER ILS IN ISCHEMIC STROKE

IL-5 and IL-9 are decreased in severe stroke patients acute ischemic stroke patients with poor outcome than mild stroke (164). It had been indicated that IL-5 and IL-7 may be predictors of edema and infarct volume (165). In experimental stroke, expressions of IL-9 and its upstream stimulating factors has

been confirmed to be increased (166). Anti-IL-9-neutralizing antibody can ameliorate ischemic stroke injury partially by alleviating the destruction of the BBB *via* down-regulation of astrocyte-derived VEGF-A (167). In OGD, IL-9 has a destructive effect on the BBB, partly by decreasing eNOS production (168). IL-21 polymorphism is related to the increased susceptibility to ischemic stroke possibly by upregulating gene expression (169). IL-21R-deficient mice have reduced collateral vascular connections and increased brain infarct volume, suggesting that IL-21R regulates collateral vascular anatomy and innate neuroprotection. The neuroprotective effects of IL-21R are mediated through the JAK/STAT signaling pathway and upregulation of caspase 3 (170). IL-22 exerts a protective action through regulating the JAK2-STAT3 pathway to improve oxidative stress, inflammation, and neuronal apoptosis following CIRI (171). IL-32 silence protects PC12 cells against OGD/R-induced injury *via* activation of Nrf2/NF-κB pathway (172). Increased serum IL-34 levels may be a novel diagnostic and prognostic biomarker in patients with acute ischemic stroke (173). Increased serum IL-37 in ischemic stroke patients is correlated with stroke recurrence (174) and 3-month functional prognosis (175). However, another study has illustrated that IL-37 exert protective effects by modulating post-stroke inflammation in the brain and periphery (176). Large randomized controlled trials are needed to further verify the role of IL-37 in ischemic stroke. The lower changes in IL-38 serum level lead to a poorer prognosis, indicating that IL-38 serum changes might be a novel early predictor factor for ischemic stroke prognosis (177) (141).

18 CONCLUSIONS AND PERSPECTIVES

In summary, we have briefly discussed the functional role of interleukins and their relationships with ischemic stroke. Based on the classification of the effect of interleukin on the immune response after stroke, interleukins can be roughly divided into anti-inflammatory and pro-inflammatory categories. IL-1β, IL-6, IL-8, IL-12, IL-15, IL-16, IL-20, IL-18, IL-23/IL-17 and so on play a pro-inflammatory role after ischemic stroke (**Figure 4**). ILs that have anti-inflammatory effects on ischemic stroke include IL-2, IL-4, IL-10, IL-13, IL-19, IL-33 and so on (**Figure 5**). However, the IL family contains so many ILs, the complicated roles of ILs in ischemic stroke cannot be discussed in detail in this brief overview. After ischemic stroke, ischemia leads to vascular endothelial damage and induces immune responses. The action of these ILs on local or systemic immune cells, or the interaction of these ILs, determines the progress of immune response in the ischemic brain. From a macroscopic perspective, it is their interactions that determine the degree of neurological impairment and clinical prognosis of ischemic stroke patients. Therefore, interleukins play an important role in the immune mechanism of ischemic stroke.

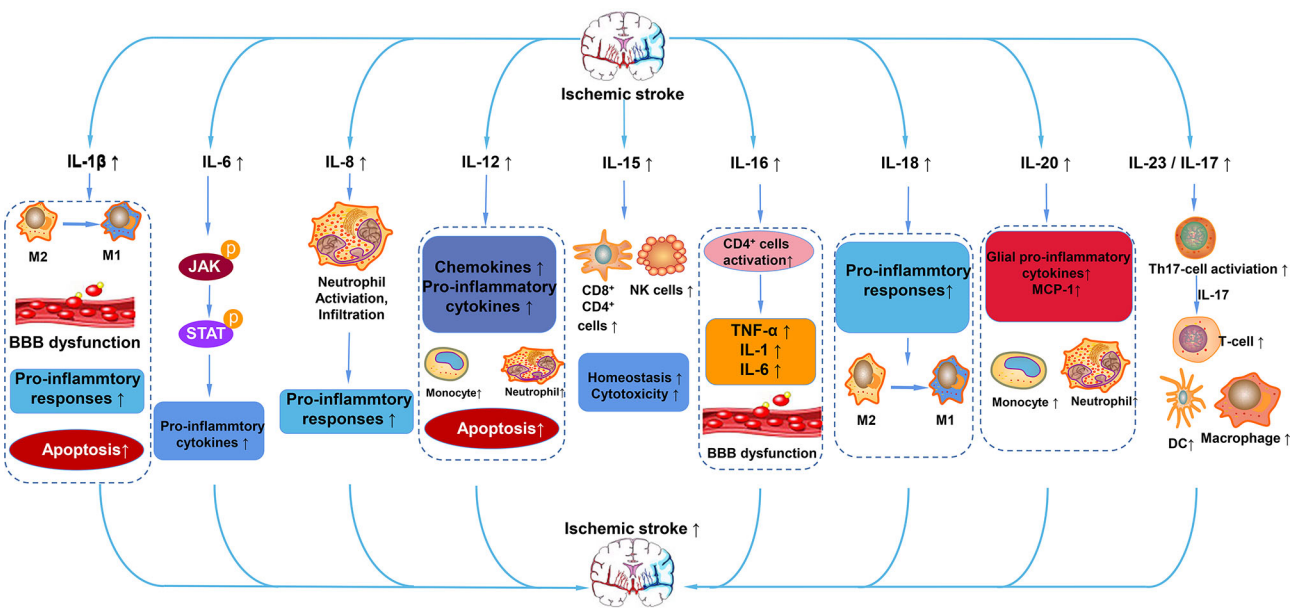

FIGURE 4 | Pro-inflammatory ILs in ischemic stroke. After ischemic stroke, IL-1β aggravates cerebral infarction injury by polarization of microglia/macrophages to M1 phenotype, BBB dysfunction, and apoptosis. IL-6 activates the JAK/STAT pathway to promote the expression of pro-cytokines. IL-8 promotes the activation and infiltration of neutrophils into cerebral infarction. IL-12 promotes the expression of chemokines and pro-inflammatory mediators, promotes apoptosis, exerting a pro-inflammatory effect. IL-15 increases the number of $CD4^+$, $CD8^+$, and NK cells. IL-16 activates $CD4^+$ cells and increases the levels of TNF-α, IL-1, and IL-6. IL-18 promotes the polarization of microglia/macrophages to the M1 phenotype and enhances the pro-inflammatory response. IL-20 promotes the expression of pro-inflammatory cytokines of MCP-1 and glia pro-inflammatory cytokines. IL-23/17 activates Th17 cells, which secrete IL-17 to increase the number of T cells, macrophages, and DC cells.

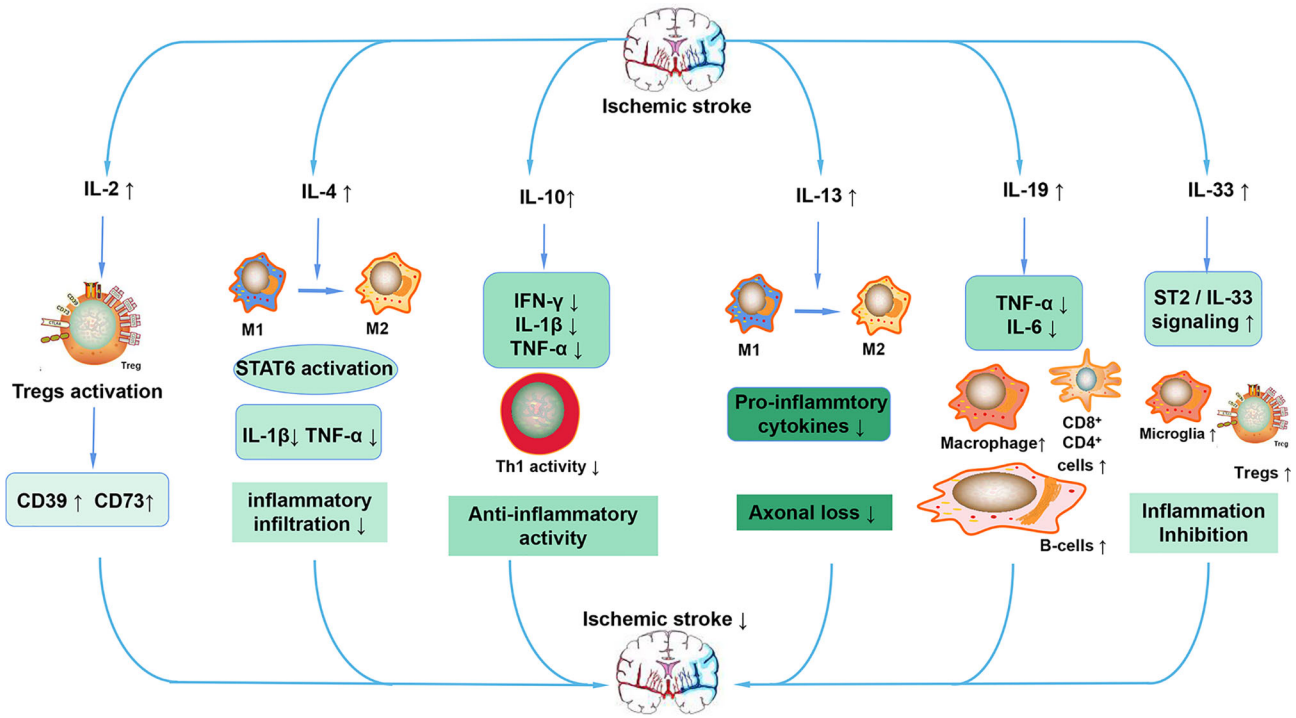

FIGURE 5 | Anti-inflammatory ILs in ischemic stroke. After stroke, increased IL-2 activates Tregs, leading to the increased expression of CD39 and CD73. The increased IL-4 promotes the polarization of macrophages to the M2 phenotype and decreases the expression of pro-inflammatory cytokines such as IL-1β and TNF-α by activating STAT6. IL-10 also reduces the expression of pro-inflammatory cytokines, maintains the activity of Th1, ultimately exerting an anti-inflammatory action. IL-13 also increases the polarization of macrophages to the M2 phenotype, decreases the expression of pro-inflammatory cytokines and decreases the loss of neurons. IL-19 mainly preserves the reduced the number of $CD4^+$, $CD8^+$, and B cells and reduces the expression of pro-inflammatory cytokines. IL-33 inhibits inflammation after stroke mainly through the ST2/IL-33 signaling pathway.

This also urges us to make continuous progress and search in this field, in order to find a breakthrough method for clinical treatment of ischemic stroke, which is a worldwide problem, and bring hope to stroke patients.

AUTHOR CONTRIBUTIONS

HZ wrote the manuscript. JC, SQ, and SH designed this work. The figures were prepared by HZ. YL, YS, XH, and XX revised the manuscript. All authors contributed to the article and approved the submitted version.

FUNDING

This study was supported by the National Natural Science Foundation of China (81870939 to XX).

REFERENCES

1. Campbell BCV, Khatri P. Stroke. *Lancet* (2020) 396:129–42. doi: 10.1016/s0140-6736(20)31179-x
2. Al-Bahrani A, Taha S, Shaath H, Bakhiet M. TNF-Alpha and IL-8 in Acute Stroke and the Modulation of These Cytokines by Antiplatelet Agents. *Curr Neurovasc Res* (2007) 4:31–7. doi: 10.2174/156720207779940716
3. Vignali DA, Kuchroo VK. IL-12 Family Cytokines: Immunological Playmakers. *Nat Immunol* (2012) 13:722–8. doi: 10.1038/ni.2366
4. Smith DE, Renshaw BR, Ketchem RR, Kubin M, Garka KE, Sims JE. Four New Members Expand the Interleukin-1 Superfamily. *J Biol Chem* (2000) 275:1169–75. doi: 10.1074/jbc.275.2.1169
5. Patterson D, Jones C, Hart I, Bleskan J, Berger R, Geyer D, et al. The Human Interleukin-1 Receptor Antagonist (IL1RN) Gene is Located in the Chromosome 2q14 Region. *Genomics* (1993) 15:173–6. doi: 10.1006/geno.1993.1025
6. Tarlow JK, Blakemore AI, Lennard A, Solari R, Hughes HN, Steinkasserer A, et al. Polymorphism in Human IL-1 Receptor Antagonist Gene Intron 2 is Caused by Variable Numbers of an 86-Bp Tandem Repeat. *Hum Genet* (1993) 91:403–4. doi: 10.1007/bf00217368
7. Murray KN, Parry-Jones AR, Allan SM. Interleukin-1 and Acute Brain Injury. *Front Cell Neurosci* (2015) 9:18. doi: 10.3389/fncel.2015.00018
8. Brough D, Tyrrell PJ, Allan SM. Regulation of Interleukin-1 in Acute Brain Injury. *Trends Pharmacol Sci* (2011) 32:617–22. doi: 10.1016/j.tips.2011.06.002
9. Allan SM, Tyrrell PJ, Rothwell NJ. Interleukin-1 and Neuronal Injury. *Nat Rev Immunol* (2005) 5:629–40. doi: 10.1038/nri1664
10. John GR, Lee SC, Song X, Rivieccio M, Brosnan CF. IL-1-Regulated Responses in Astrocytes: Relevance to Injury and Recovery. *Glia* (2005) 49:161–76. doi: 10.1002/glia.20109

11. Konsman JP, Drukarch B, Van Dam AM. (Peri)vascular Production and Action of Pro-Inflammatory Cytokines in Brain Pathology. *Clin Sci (Lond)* (2007) 112:1–25. doi: 10.1042/cs20060043
12. Viviani B, Bartesaghi S, Gardoni F, Vezzani A, Behrens MM, Bartfai T, et al. Interleukin-1beta Enhances NMDA Receptor-Mediated Intracellular Calcium Increase Through Activation of the Src Family of Kinases. *J Neurosci* (2003) 23:8692–700. doi: 10.1523/jneurosci.23-25-08692.2003
13. Sobowale OA, Parry-Jones AR, Smith CJ, Tyrrell PJ, Rothwell NJ, Allan SM. Interleukin-1 in Stroke: From Bench to Bedside. *Stroke* (2016) 47:2160–7. doi: 10.1161/strokeaha.115.010001
14. Simi A, Tsakiri N, Wang P, Rothwell NJ. Interleukin-1 and Inflammatory Neurodegeneration. *Biochem Soc Trans* (2007) 35:1122–6. doi: 10.1042/bst0351122
15. Strijbos PJ, Rothwell NJ. Interleukin-1 Beta Attenuates Excitatory Amino Acid-Induced Neurodegeneration *In Vitro*: Involvement of Nerve Growth Factor. *J Neurosci* (1995) 15:3468–74. doi: 10.1523/jneurosci.15-05-03468.1995
16. Barnes J, Mondelli V, Pariante CM. Genetic Contributions of Inflammation to Depression. *Neuropsychopharmacology* (2017) 42:81–98. doi: 10.1038/npp.2016.169
17. Yang J, Ma K, Zhang C, Liu Y, Liang F, Hu W, et al. Burns Impair Blood-Brain Barrier and Mesenchymal Stem Cells Can Reverse the Process in Mice. *Front Immunol* (2020) 11:578879. doi: 10.3389/fimmu.2020.578879
18. Dinarello CA. Immunological and Inflammatory Functions of the Interleukin-1 Family. *Annu Rev Immunol* (2009) 27:519–50. doi: 10.1146/annurev.immunol.021908.132612
19. Liu G, Tsuruta Y, Gao Z, Park YJ, Abraham E. Variant IL-1 Receptor-Associated Kinase-1 Mediates Increased NF-Kappa B Activity. *J Immunol* (2007) 179:4125–34. doi: 10.4049/jimmunol.179.6.4125
20. Cahill CM, Rogers JT. Interleukin (IL) 1beta Induction of IL-6 is Mediated by a Novel Phosphatidylinositol 3-Kinase-Dependent AKT/IkappaB Kinase Alpha Pathway Targeting Activator Protein-1. *J Biol Chem* (2008) 283:25900–12. doi: 10.1074/jbc.M707692200
21. Kong X, Gong Z, Zhang L, Sun X, Ou Z, Xu B, et al. JAK2/STAT3 Signaling Mediates IL-6-Inhibited Neurogenesis of Neural Stem Cells Through DNA Demethylation/Methylation. *Brain Behav Immun* (2019) 79:159–73. doi: 10.1016/j.bbi.2019.01.027
22. Zhu H, Jian Z, Zhong Y, Ye Y, Zhang Y, Hu X, et al. Janus Kinase Inhibition Ameliorates Ischemic Stroke Injury and Neuroinflammation Through Reducing NLRP3 Inflammasome Activation *via* JAK2/STAT3 Pathway Inhibition. *Front Immunol* (2021) 12:714943. doi: 10.3389/fimmu.2021.714943
23. Chaparro-Huerta V, Rivera-Cervantes MC, Flores-Soto ME, Gómez-Pinedo U, Beas-Zárate C. Proinflammatory Cytokines and Apoptosis Following Glutamate-Induced Excitotoxicity Mediated by P38 MAPK in the Hippocampus of Neonatal Rats. *J Neuroimmunol* (2005) 165:53–62. doi: 10.1016/j.jneuroim.2005.04.025
24. Li W, Zheng S, Tang C, Zhu Y, Wang X. JNK-AP-1 Pathway Involved in Interleukin-1beta-Induced Calcitonin Gene-Related Peptide Secretion in Human Type II Alveolar Epithelial Cells. *Peptides* (2007) 28:1252–9. doi: 10.1016/j.peptides.2007.03.021
25. Roth S, Cao J, Singh V, Tiedt S, Hundeshagen G, Li T, et al. Post-Injury Immunosuppression and Secondary Infections are Caused by an AIM2 Inflammasome-Driven Signaling Cascade. *Immunity* (2021) 54:648–59.e8. doi: 10.1016/j.immuni.2021.02.004
26. Nayak AR, Kashyap RS, Purohit HJ, Kabra D, Taori GM, Daginawala HF. Evaluation of the Inflammatory Response in Sera From Acute Ischemic Stroke Patients by Measurement of IL-2 and IL-10. *Inflammation Res* (2009) 58:687–91. doi: 10.1007/s00011-009-0036-4
27. Zhang H, Xia Y, Ye Q, Yu F, Zhu W, Li P, et al. *In Vivo* Expansion of Regulatory T Cells With IL-2/IL-2 Antibody Complex Protects Against Transient Ischemic Stroke. *J Neurosci* (2018) 38:10168–79. doi: 10.1523/jneurosci.3411-17.2018
28. Zhou YX, Wang X, Tang D, Li Y, Jiao YF, Gan Y, et al. IL-2mab Reduces Demyelination After Focal Cerebral Ischemia by Suppressing CD8(+) T Cells. *CNS Neurosci Ther* (2019) 25:532–43. doi: 10.1111/cns.13084
29. Shi L, Sun Z, Su W, Xu F, Xie D, Zhang Q, et al. Treg Cell-Derived Osteopontin Promotes Microglia-Mediated White Matter Repair After Ischemic Stroke. *Immunity* (2021) 54:1527–42.e8. doi: 10.1016/j.immuni.2021.04.022
30. Zhao H, Li F, Huang Y, Zhang S, Li L, Yang Z, et al. Prognostic Significance of Plasma IL-2 and sIL-2rα in Patients With First-Ever Ischaemic Stroke. *J Neuroinflamm* (2020) 17:237. doi: 10.1186/s12974-020-01920-3
31. Gadani SP, Cronk JC, Norris GT, Kipnis J. IL-4 in the Brain: A Cytokine to Remember. *J Immunol* (2012) 189:4213–9. doi: 10.4049/jimmunol.1202246
32. Derecki NC, Cardani AN, Yang CH, Quinnies KM, Crihfield A, Lynch KR, et al. Regulation of Learning and Memory by Meningeal Immunity: A Key Role for IL-4. *J Exp Med* (2010) 207:1067–80. doi: 10.1084/jem.20091419
33. Zhang Q, Zhu W, Xu F, Dai X, Shi L, Cai W, et al. The Interleukin-4/Pparγ Signaling Axis Promotes Oligodendrocyte Differentiation and Remyelination After Brain Injury. *PloS Biol* (2019) 17:e3000330. doi: 10.1371/journal.pbio.3000330
34. Chen X, Zhang J, Song Y, Yang P, Yang Y, Huang Z, et al. Deficiency of Anti-Inflammatory Cytokine IL-4 Leads to Neural Hyperexcitability and Aggravates Cerebral Ischemia-Reperfusion Injury. *Acta Pharm Sin B* (2020) 10:1634–45. doi: 10.1016/j.apsb.2020.05.002
35. García-Berrocoso T, Giralt D, Bustamante A, Llombart V, Rubiera M, Penalba A, et al. Role of Beta-Defensin 2 and Interleukin-4 Receptor as Stroke Outcome Biomarkers. *J Neurochem* (2014) 129:463–72. doi: 10.1111/jnc.12649
36. Kim HM, Shin HY, Jeong HJ, An HJ, Kim NS, Chae HJ, et al. Reduced IL-2 But Elevated IL-4, IL-6, and IgE Serum Levels in Patients With Cerebral Infarction During the Acute Stage. *J Mol Neurosci* (2000) 14:191–6. doi: 10.1385/jmn:14:3:191
37. Xiong X, Xu L, Wei L, White RE, Ouyang YB, Giffard RG. IL-4 Is Required for Sex Differences in Vulnerability to Focal Ischemia in Mice. *Stroke* (2015) 46:2271–6. doi: 10.1161/strokeaha.115.008897
38. Liu X, Liu J, Zhao S, Zhang H, Cai W, Cai M, et al. Interleukin-4 Is Essential for Microglia/Macrophage M2 Polarization and Long-Term Recovery After Cerebral Ischemia. *Stroke* (2016) 47:498–504. doi: 10.1161/strokeaha.115.012079
39. Tian Y, Zhu P, Liu S, Jin Z, Li D, Zhao H, et al. IL-4-Polarized BV2 Microglia Cells Promote Angiogenesis by Secreting Exosomes. *Adv Clin Exp Med* (2019) 28:421–30. doi: 10.17219/acem/91826
40. Shi Q, Cai X, Shi G, Lv X, Yu J, Wang F. Interleukin-4 Protects From Chemotherapy-Induced Peripheral Neuropathy in Mice Modal *via* the Stimulation of IL-4/STAT6 Signaling. *Acta Cir Bras* (2018) 33:491–8. doi: 10.1590/s0102-865020180060000003
41. Akira S, Taga T, Kishimoto T. Interleukin-6 in Biology and Medicine. *Adv Immunol* (1993) 54:1–78. doi: 10.1016/s0065-2776(08)60532-5
42. Boulanger MJ, Chow DC, Brevnova EE, Garcia KC. Hexameric Structure and Assembly of the Interleukin-6/IL-6 Alpha-Receptor/Gp130 Complex. *Science* (2003) 300:2101–4. doi: 10.1126/science.1083901
43. Uyama N, Tsutsui H, Wu S, Yasuda K, Hatano E, Qin XY, et al. Anti-Interleukin-6 Receptor Antibody Treatment Ameliorates Postoperative Adhesion Formation. *Sci Rep* (2019) 9:17558. doi: 10.1038/s41598-019-54175-1
44. Zimmermann M, Aguilera FB, Castellucci M, Rossato M, Costa S, Lunardi C, et al. Chromatin Remodelling and Autocrine Tnfα are Required for Optimal Interleukin-6 Expression in Activated Human Neutrophils. *Nat Commun* (2015) 6:6061. doi: 10.1038/ncomms7061
45. Erta M, Quintana A, Hidalgo J. Interleukin-6, a Major Cytokine in the Central Nervous System. *Int J Biol Sci* (2012) 8:1254–66. doi: 10.7150/ijbs.4679
46. Su JH, Luo MY, Liang N, Gong SX, Chen W, Huang WQ, et al. Interleukin-6: A Novel Target for Cardio-Cerebrovascular Diseases. *Front Pharmacol* (2021) 12:745061. doi: 10.3389/fphar.2021.745061
47. Jenny NS, Callas PW, Judd SE, McClure LA, Kissela B, Zakai NA, et al. Inflammatory Cytokines and Ischemic Stroke Risk: The REGARDS Cohort. *Neurology* (2019) 92:e2375–84. doi: 10.1212/wnl.0000000000007416
48. Kowalska K, Klimiec E, Weglarczyk K, Pera J, Slowik A, Siedlar M, et al. Reduced Ex Vivo Release of Pro-Inflammatory Cytokines and Elevated Plasma Interleukin-6 are Inflammatory Signatures of Post-Stroke Delirium. *J Neuroinflamm* (2018) 15:111. doi: 10.1186/s12974-018-1156-y
49. Mechtouff L, Bochaton T, Paccalet A, Da Silva CC, Buisson M, Amaz C, et al. Association of Interleukin-6 Levels and Futile Reperfusion After Mechanical

Thrombectomy. *Neurology* (2021) 96:e752–7. doi: 10.1212/wnl.0000000000011268
50. Mechtouff L, Bochaton T, Paccalet A, Crola Da Silva C, Buisson M, Amaz C, et al. A Lower Admission Level of Interleukin-6 Is Associated With First-Pass Effect in Ischemic Stroke Patients. *J Neurointerv Surg* (2021). doi: 10.1136/neurintsurg-2021-017334
51. Yao H, Zhang Y, Shu H, Xie B, Tao Y, Yuan Y, et al. Hyperforin Promotes Post-Stroke Neuroangiogenesis *via* Astrocytic IL-6-Mediated Negative Immune Regulation in the Ischemic Brain. *Front Cell Neurosci* (2019) 13:201. doi: 10.3389/fncel.2019.00201
52. Armstead WM, Hekierski H, Pastor P, Yarovoi S, Higazi AA, Cines DB. Release of IL-6 After Stroke Contributes to Impaired Cerebral Autoregulation and Hippocampal Neuronal Necrosis Through NMDA Receptor Activation and Upregulation of ET-1 and JNK. *Transl Stroke Res* (2019) 10:104–11. doi: 10.1007/s12975-018-0617-z
53. Tarkowski E, Rosengren L, Blomstrand C, Wikkelsö C, Jensen C, Ekholm S, et al. Early Intrathecal Production of Interleukin-6 Predicts the Size of Brain Lesion in Stroke. *Stroke* (1995) 26:1393–8. doi: 10.1161/01.str.26.8.1393
54. Suzuki S, Tanaka K, Suzuki N. Ambivalent Aspects of Interleukin-6 in Cerebral Ischemia: Inflammatory Versus Neurotrophic Aspects. *J Cereb Blood Flow Metab* (2009) 29:464–79. doi: 10.1038/jcbfm.2008.141
55. Rose-John S. Interleukin-6 Family Cytokines. *Cold Spring Harb Perspect Biol* (2018) 10:a028415. doi: 10.1101/cshperspect.a028415
56. Zhu H, Zhang Y, Zhong Y, Ye Y, Hu X, Gu L, et al. Inflammation-Mediated Angiogenesis in Ischemic Stroke. *Front Cell Neurosci* (2021) 15:652647. doi: 10.3389/fncel.2021.652647
57. Swartz KR, Liu F, Sewell D, Schochet T, Campbell I, Sandor M, et al. Interleukin-6 Promotes Post-Traumatic Healing in the Central Nervous System. *Brain Res* (2001) 896:86–95. doi: 10.1016/s0006-8993(01)02013-3
58. Matsuda S, Wen TC, Morita F, Otsuka H, Igase K, Yoshimura H, et al. Interleukin-6 Prevents Ischemia-Induced Learning Disability and Neuronal and Synaptic Loss in Gerbils. *Neurosci Lett* (1996) 204:109–12. doi: 10.1016/0304-3940(96)12340-5
59. Kostulas N, Kivisäkk P, Huang Y, Matusevicius D, Kostulas V, Link H. Ischemic Stroke is Associated With a Systemic Increase of Blood Mononuclear Cells Expressing Interleukin-8 mRNA. *Stroke* (1998) 29:462–6. doi: 10.1161/01.str.29.2.462
60. Kostulas N, Pelidou SH, Kivisäkk P, Kostulas V, Link H. Increased IL-1beta, IL-8, and IL-17 mRNA Expression in Blood Mononuclear Cells Observed in a Prospective Ischemic Stroke Study. *Stroke* (1999) 30:2174–9. doi: 10.1161/01.str.30.10.2174
61. Domac FM, Misirli H. The Role of Neutrophils and Interleukin-8 in Acute Ischemic Stroke. *Neurosci (Riyadh)* (2008) 13:136–41.
62. Zidovetzki R, Chen P, Chen M, Hofman FM. Endothelin-1-Induced Interleukin-8 Production in Human Brain-Derived Endothelial Cells Is Mediated by the Protein Kinase C and Protein Tyrosine Kinase Pathways. *Blood* (1999) 94:1291–9. doi: 10.1182/blood.V94.4.1291
63. Yamasaki Y, Matsuo Y, Matsuura N, Onodera H, Itoyama Y, Kogure K. Transient Increase of Cytokine-Induced Neutrophil Chemoattractant, a Member of the Interleukin-8 Family, in Ischemic Brain Areas After Focal Ischemia in Rats. *Stroke* (1995) 26:318–22; discussion 322-3. doi: 10.1161/01.str.26.2.318
64. Wang HJ, Wei JY, Liu DX, Zhuang SF, Li Y, Liu H, et al. Endothelial Atg7 Deficiency Ameliorates Acute Cerebral Injury Induced by Ischemia/Reperfusion. *Front Neurol* (2018) 9:998. doi: 10.3389/fneur.2018.00998
65. Shaheen HA, Daker LI, Abbass MM, Abd El Fattah AA. The Relationship Between the Severity of Disability and Serum IL-8 in Acute Ischemic Stroke Patients. *Egypt J Neurol Psychiatr Neurosurg* (2018) 54:26. doi: 10.1186/s41983-018-0025-z
66. Lv H, Li J, Che YQ. CXCL8 Gene Silencing Promotes Neuroglial Cells Activation While Inhibiting Neuroinflammation Through the PI3K/Akt/NF-κb-Signaling Pathway in Mice With Ischemic Stroke. *J Cell Physiol* (2019) 234:7341–55. doi: 10.1002/jcp.27493
67. Zhang L, Xu D, Zhang T, Hou W, Yixi L. Correlation Between Interleukin-6, Interleukin-8, and Modified Early Warning Score of Patients With Acute Ischemic Stroke and Their Condition and Prognosis. *Ann Palliat Med* (2021) 10:148–55. doi: 10.21037/apm-20-2200
68. Hou Y, Ryu CH, Jun JA, Kim SM, Jeong CH, Jeun SS. IL-8 Enhances the Angiogenic Potential of Human Bone Marrow Mesenchymal Stem Cells by Increasing Vascular Endothelial Growth Factor. *Cell Biol Int* (2014) 38:1050–9. doi: 10.1002/cbin.10294
69. van Scott MR, Justice JP, Bradfield JF, Enright E, Sigounas A, Sur S. IL-10 Reduces Th2 Cytokine Production and Eosinophilia But Augments Airway Reactivity in Allergic Mice. *Am J Physiol Lung Cell Mol Physiol* (2000) 278:L667–74. doi: 10.1152/ajplung.2000.278.4.L667
70. Sabat R, Grütz G, Warszawska K, Kirsch S, Witte E, Wolk K, et al. Biology of Interleukin-10. *Cytokine Growth Factor Rev* (2010) 21:331–44. doi: 10.1016/j.cytogfr.2010.09.002
71. Kumar P, Yadav AK, Misra S, Kumar A, Chakravarty K, Prasad K. Role of Interleukin-10 (-1082a/G) Gene Polymorphism With the Risk of Ischemic Stroke: A Meta-Analysis. *Neurol Res* (2016) 38:823–30. doi: 10.1080/01616412.2016.1202395
72. Nguyen TV, Frye JB, Zbesko JC, Stepanovic K, Hayes M, Urzua A, et al. Multiplex Immunoassay Characterization and Species Comparison of Inflammation in Acute and Non-Acute Ischemic Infarcts in Human and Mouse Brain Tissue. *Acta Neuropathol Commun* (2016) 4:100. doi: 10.1186/s40478-016-0371-y
73. de Bilbao F, Arsenijevic D, Moll T, Garcia-Gabay I, Vallet P, Langhans W, et al. *In Vivo* Over-Expression of Interleukin-10 Increases Resistance to Focal Brain Ischemia in Mice. *J Neurochem* (2009) 110:12–22. doi: 10.1111/j.1471-4159.2009.06098.x
74. Nakajima M, Nito C, Sowa K, Suda S, Nishiyama Y, Nakamura-Takahashi A, et al. Mesenchymal Stem Cells Overexpressing Interleukin-10 Promote Neuroprotection in Experimental Acute Ischemic Stroke. *Mol Ther Methods Clin Dev* (2017) 6:102–11. doi: 10.1016/j.omtm.2017.06.005
75. Spera PA, Ellison JA, Feuerstein GZ, Barone FC. IL-10 Reduces Rat Brain Injury Following Focal Stroke. *Neurosci Lett* (1998) 251:189–92. doi: 10.1016/s0304-3940(98)00537-0
76. Pérez-de Puig I, Miró F, Salas-Perdomo A, Bonfill-Teixidor E, Ferrer-Ferrer M, Márquez-Kisinousky L, et al. IL-10 Deficiency Exacerbates the Brain Inflammatory Response to Permanent Ischemia Without Preventing Resolution of the Lesion. *J Cereb Blood Flow Metab* (2013) 33:1955–66. doi: 10.1038/jcbfm.2013.155
77. Chi CH, Huang YY, Ye SZ, Shao MM, Jiang MX, Yang MY, et al. Interleukin-10 Level is Associated With Post-Stroke Depression in Acute Ischaemic Stroke Patients. *J Affect Disord* (2021) 293:254–60. doi: 10.1016/j.jad.2021.06.037
78. Chen Z, Zhang R, Wu Y, Fu Q, Qin X. Serum Interleukin-33 is a Predictor of Depression in Patients With Acute Ischemic Stroke. *Curr Neurovasc Res* (2020) 17:719–24. doi: 10.2174/1567202617999210101223635
79. Chang LT, Yuen CM, Liou CW, Lu CH, Chang WN, Youssef AA, et al. Link Between Interleukin-10 Level and Outcome After Ischemic Stroke. *Neuroimmunomodulation* (2010) 17:223–8. doi: 10.1159/000290038
80. Worthmann H, Tryc AB, Dirks M, Schuppner R, Brand K, Klawonn F, et al. Lipopolysaccharide Binding Protein, Interleukin-10, Interleukin-6 and C-Reactive Protein Blood Levels in Acute Ischemic Stroke Patients With Post-Stroke Infection. *J Neuroinflamm* (2015) 12:13. doi: 10.1186/s12974-014-0231-2
81. Chamorro A, Amaro S, Vargas M, Obach V, Cervera A, Torres F, et al. Interleukin 10, Monocytes and Increased Risk of Early Infection in Ischaemic Stroke. *J Neurol Neurosurg Psychiatry* (2006) 77:1279–81. doi: 10.1136/jnnp.2006.100800
82. Conway SE, Roy-O'Reilly M, Friedler B, Staff I, Fortunato G, McCullough LD. Sex Differences and the Role of IL-10 in Ischemic Stroke Recovery. *Biol Sex Differ* (2015) 6:17. doi: 10.1186/s13293-015-0035-9
83. Lambertsen KL, Finsen B, Clausen BH. Post-Stroke Inflammation-Target or Tool for Therapy? *Acta Neuropathol* (2019) 137:693–714. doi: 10.1007/s00401-018-1930-z
84. Bushnell C, McCullough LD, Awad IA, Chireau MV, Fedder WN, Furie KL, et al. Guidelines for the Prevention of Stroke in Women: A Statement for Healthcare Professionals From the American Heart Association/American Stroke Association. *Stroke* (2014) 45:1545–88. doi: 10.1161/01.str.0000442009.06663.48
85. Pelidou SH, Kostulas N, Matusevicius D, Kivisäkk P, Kostulas V, Link H. High Levels of IL-10 Secreting Cells are Present in Blood in Cerebrovascular

Diseases. *Eur J Neurol* (1999) 6:437–42. doi: 10.1046/j.1468-1331.1999.640437.x

86. Liesz A, Zhou W, Na SY, Hämmerling GJ, Garbi N, Karcher S, et al. Boosting Regulatory T Cells Limits Neuroinflammation in Permanent Cortical Stroke. *J Neurosci* (2013) 33:17350–62. doi: 10.1523/jneurosci.4901-12.2013
87. Bodhankar S, Chen Y, Vandenbark AA, Murphy SJ, Offner H. IL-10-Producing B-Cells Limit CNS Inflammation and Infarct Volume in Experimental Stroke. *Metab Brain Dis* (2013) 28:375–86. doi: 10.1007/s11011-013-9413-3
88. Sharma S, Yang B, Xi X, Grotta JC, Aronowski J, Savitz SI. IL-10 Directly Protects Cortical Neurons by Activating PI-3 Kinase and STAT-3 Pathways. *Brain Res* (2011) 1373:189–94. doi: 10.1016/j.brainres.2010.11.096
89. Oleszycka E, McCluskey S, Sharp FA, Muñoz-Wolf N, Hams E, Gorman AL, et al. The Vaccine Adjuvant Alum Promotes IL-10 Production That Suppresses Th1 Responses. *Eur J Immunol* (2018) 48:705–15. doi: 10.1002/eji.201747150
90. Bodhankar S, Chen Y, Vandenbark AA, Murphy SJ, Offner H. Treatment of Experimental Stroke With IL-10-Producing B-Cells Reduces Infarct Size and Peripheral and CNS Inflammation in Wild-Type B-Cell-Sufficient Mice. *Metab Brain Dis* (2014) 29:59–73. doi: 10.1007/s11011-013-9474-3
91. Liang QJ, Jiang M, Wang XH, Le LL, Xiang M, Sun N, et al. Pre-Existing Interleukin 10 in Cerebral Arteries Attenuates Subsequent Brain Injury Caused by Ischemia/Reperfusion. *IUBMB Life* (2015) 67:710–9. doi: 10.1002/iub.1429
92. Driessler F, Venstrom K, Sabat R, Asadullah K, Schottelius AJ. Molecular Mechanisms of Interleukin-10-Mediated Inhibition of NF-kappaB Activity: A Role for P50. *Clin Exp Immunol* (2004) 135:64–73. doi: 10.1111/j.1365-2249.2004.02342.x
93. Wang Y, Jia J, Ao G, Hu L, Liu H, Xiao Y, et al. Hydrogen Sulfide Protects Blood-Brain Barrier Integrity Following Cerebral Ischemia. *J Neurochem* (2014) 129:827–38. doi: 10.1111/jnc.12695
94. Hwang CJ, Yun HM, Jung YY, Lee DH, Yoon NY, Seo HO, et al. Reducing Effect of IL-32α in the Development of Stroke Through Blocking of NF-κb, But Enhancement of STAT3 Pathways. *Mol Neurobiol* (2015) 51:648–60. doi: 10.1007/s12035-014-8739-0
95. Frenkel D, Huang Z, Maron R, Koldzic DN, Moskowitz MA, Weiner HL. Neuroprotection by IL-10-Producing MOG CD4+ T Cells Following Ischemic Stroke. *J Neurol Sci* (2005) 233:125–32. doi: 10.1016/j.jns.2005.03.022
96. Frenkel D, Huang Z, Maron R, Koldzic DN, Hancock WW, Moskowitz MA, et al. Nasal Vaccination With Myelin Oligodendrocyte Glycoprotein Reduces Stroke Size by Inducing IL-10-Producing CD4+ T Cells. *J Immunol* (2003) 171:6549–55. doi: 10.4049/jimmunol.171.12.6549
97. Na SY, Mracsko E, Liesz A, Hünig T, Veltkamp R. Amplification of Regulatory T Cells Using a CD28 Superagonist Reduces Brain Damage After Ischemic Stroke in Mice. *Stroke* (2015) 46:212–20. doi: 10.1161/strokeaha.114.007756
98. Wang J, Xie L, Yang C, Ren C, Zhou K, Wang B, et al. Activated Regulatory T Cell Regulates Neural Stem Cell Proliferation in the Subventricular Zone of Normal and Ischemic Mouse Brain Through Interleukin 10. *Front Cell Neurosci* (2015) 9:361. doi: 10.3389/fncel.2015.00361
99. Kawada H, Takizawa S, Takanashi T, Morita Y, Fujita J, Fukuda K, et al. Administration of Hematopoietic Cytokines in the Subacute Phase After Cerebral Infarction is Effective for Functional Recovery Facilitating Proliferation of Intrinsic Neural Stem/Progenitor Cells and Transition of Bone Marrow-Derived Neuronal Cells. *Circulation* (2006) 113:701–10. doi: 10.1161/circulationaha.105.563668
100. Morita Y, Takizawa S, Kamiguchi H, Uesugi T, Kawada H, Takagi S. Administration of Hematopoietic Cytokines Increases the Expression of Anti-Inflammatory Cytokine (IL-10) mRNA in the Subacute Phase After Stroke. *Neurosci Res* (2007) 58:356–60. doi: 10.1016/j.neures.2007.04.006
101. Liu N, Chen R, Du H, Wang J, Zhang Y, Wen J. Expression of IL-10 and TNF-Alpha in Rats With Cerebral Infarction After Transplantation With Mesenchymal Stem Cells. *Cell Mol Immunol* (2009) 6:207–13. doi: 10.1038/cmi.2009.28
102. Pereira L, Font-Nieves M, Van den Haute C, Baekelandt V, Planas AM, Pozas E. IL-10 Regulates Adult Neurogenesis by Modulating ERK and STAT3 Activity. *Front Cell Neurosci* (2015) 9:57. doi: 10.3389/fncel.2015.00057
103. Benakis C, Brea D, Caballero S, Faraco G, Moore J, Murphy M, et al. Commensal Microbiota Affects Ischemic Stroke Outcome by Regulating Intestinal γδ T Cells. *Nat Med* (2016) 22:516–23. doi: 10.1038/nm.4068
104. Piepke M, Clausen BH, Ludewig P, Vienhues JH, Bedke T, Javidi E, et al. Interleukin-10 Improves Stroke Outcome by Controlling the Detrimental Interleukin-17A Response. *J Neuroinflamm* (2021) 18:265. doi: 10.1186/s12974-021-02316-7
105. Collison LW, Workman CJ, Kuo TT, Boyd K, Wang Y, Vignali KM, et al. The Inhibitory Cytokine IL-35 Contributes to Regulatory T-Cell Function. *Nature* (2007) 450:566–9. doi: 10.1038/nature06306
106. Reading PC, Whitney PG, Barr DP, Wojtasiak M, Mintern JD, Waithman J, et al. IL-18, But Not IL-12, Regulates NK Cell Activity Following Intranasal Herpes Simplex Virus Type 1 Infection. *J Immunol* (2007) 179:3214–21. doi: 10.4049/jimmunol.179.5.3214
107. Noble A, Thomas MJ, Kemeny DM. Early Th1/Th2 Cell Polarization in the Absence of IL-4 and IL-12: T Cell Receptor Signaling Regulates the Response to Cytokines in CD4 and CD8 T Cells. *Eur J Immunol* (2001) 31:2227–35. doi: 10.1002/1521-4141(200107)31:7<2227::aid-immu2227>3.0.co;2-c
108. Zaremba J, Losy J. Interleukin-12 in Acute Ischemic Stroke Patients. *Folia Neuropathol* (2006) 44:59–66.
109. Zykov MV, Barbarash OL, Kashtalap VV, Kutikhin AG, Barbarash LS. Interleukin-12 Serum Level has Prognostic Value in Patients With ST-Segment Elevation Myocardial Infarction. *Heart Lung* (2016) 45:336–40. doi: 10.1016/j.hrtlng.2016.03.007
110. Han D, Liu H, Gao Y. The Role of Peripheral Monocytes and Macrophages in Ischemic Stroke. *Neurol Sci* (2020) 41:3589–607. doi: 10.1007/s10072-020-04777-9
111. Kanazawa M, Ninomiya I, Hatakeyama M, Takahashi T, Shimohata T. Microglia and Monocytes/Macrophages Polarization Reveal Novel Therapeutic Mechanism Against Stroke. *Int J Mol Sci* (2017) 18:2135. doi: 10.3390/ijms18102135
112. Kouwenhoven M, Carlström C, Ozenci V, Link H. Matrix Metalloproteinase and Cytokine Profiles in Monocytes Over the Course of Stroke. *J Clin Immunol* (2001) 21:365–75. doi: 10.1023/a:1012244820709
113. Ogawa H, Nishimura N, Nishioka Y, Azuma M, Yanagawa H, Sone S. Adenoviral Interleukin-12 Gene Transduction Into Human Bronchial Epithelial Cells: Up-Regulation of Pro-Inflammatory Cytokines and its Prevention by Corticosteroids. *Clin Exp Allergy* (2003) 33:921–9. doi: 10.1046/j.1365-2222.2003.01702.x
114. Yago T, Tsukuda M, Fukushima H, Yamaoka H, Kurata-Miura K, Nishi T, et al. IL-12 Promotes the Adhesion of NK Cells to Endothelial Selectins Under Flow Conditions. *J Immunol* (1998) 161:1140–5.
115. Zhu S, Lee DA, Li S. IL-12 and IL-27 Sequential Gene Therapy *via* Intramuscular Electroporation Delivery for Eliminating Distal Aggressive Tumors. *J Immunol* (2010) 184:2348–54. doi: 10.4049/jimmunol.0902371
116. Hart PH, Bonder CS, Balogh J, Dickensheets HL, Vazquez N, Davies KV, et al. Diminished Responses to IL-13 by Human Monocytes Differentiated *In Vitro*: Role of the IL-13Ralpha1 Chain and STAT6. *Eur J Immunol* (1999) 29:2087–97. doi: 10.1002/(sici)1521-4141(199907)29:07<2087::Aid-immu2087>3.0.Co;2-j
117. Zurawski G, de Vries JE. Interleukin 13, an Interleukin 4-Like Cytokine That Acts on Monocytes and B Cells, But Not on T Cells. *Immunol Today* (1994) 15:19–26. doi: 10.1016/0167-5699(94)90021-3
118. Chung HS, Lee BS, Ma JY. Ethanol Extract of Mylabris Phalerata Inhibits M2 Polarization Induced by Recombinant IL-4 and IL-13 in Murine Macrophages. *Evid Based Complement Alternat Med* (2017) 2017:4218468. doi: 10.1155/2017/4218468
119. Hamzei Taj S, Le Blon D, Hoornaert C, Daans J, Quarta A, Praet J, et al. Targeted Intracerebral Delivery of the Anti-Inflammatory Cytokine IL13 Promotes Alternative Activation of Both Microglia and Macrophages After Stroke. *J Neuroinflamm* (2018) 15:174. doi: 10.1186/s12974-018-1212-7
120. Kolosowska N, Keuters MH, Wojciechowski S, Keksa-Goldsteine V, Laine M, Malm T, et al. Peripheral Administration of IL-13 Induces Anti-Inflammatory Microglial/Macrophage Responses and Provides Neuroprotection in Ischemic Stroke. *Neurotherapeutics* (2019) 16:1304–19. doi: 10.1007/s13311-019-00761-0

121. Liao KY, Chen CJ, Hsieh SK, Pan PH, Chen WY. Interleukin-13 Ameliorates Postischemic Hepatic Gluconeogenesis and Hyperglycemia in Rat Model of Stroke. *Metab Brain Dis* (2020) 35:1201–10. doi: 10.1007/s11011-020-00596-1
122. Hawkins KE, Corcelli M, Dowding K, Ranzoni AM, Vlahova F, Hau KL, et al. Embryonic Stem Cell-Derived Mesenchymal Stem Cells (MSCs) Have a Superior Neuroprotective Capacity Over Fetal MSCs in the Hypoxic-Ischemic Mouse Brain. *Stem Cells Transl Med* (2018) 7:439–49. doi: 10.1002/sctm.17-0260
123. Sim GC, Radvanyi L. The IL-2 Cytokine Family in Cancer Immunotherapy. *Cytokine Growth Factor Rev* (2014) 25:377–90. doi: 10.1016/j.cytogfr.2014.07.018
124. Perera LP, Goldman CK, Waldmann TA. IL-15 Induces the Expression of Chemokines and Their Receptors in T Lymphocytes. *J Immunol* (1999) 162:2606–12.
125. Zhou X, Yu J, Cheng X, Zhao B, Manyam GC, Zhang L, et al. The Deubiquitinase Otub1 Controls the Activation of CD8(+) T Cells and NK Cells by Regulating IL-15-Mediated Priming. *Nat Immunol* (2019) 20:879–89. doi: 10.1038/s41590-019-0405-2
126. Li M, Li Z, Yao Y, Jin WN, Wood K, Liu Q, et al. Astrocyte-Derived Interleukin-15 Exacerbates Ischemic Brain Injury *via* Propagation of Cellular Immunity. *Proc Natl Acad Sci USA* (2017) 114:E396–e405. doi: 10.1073/pnas.1612930114
127. Lee GA, Lin TN, Chen CY, Mau SY, Huang WZ, Kao YC, et al. Interleukin 15 Blockade Protects the Brain From Cerebral Ischemia-Reperfusion Injury. *Brain Behav Immun* (2018) 73:562–70. doi: 10.1016/j.bbi.2018.06.021
128. Shi SX, Li YJ, Shi K, Wood K, Ducruet AF, Liu Q. IL (Interleukin)-15 Bridges Astrocyte-Microglia Crosstalk and Exacerbates Brain Injury Following Intracerebral Hemorrhage. *Stroke* (2020) 51:967–74. doi: 10.1161/strokeaha.119.028638
129. Nguyen V, Ameri K, Huynh K, Fredkin M, Grona R, Larpthaveesarp A, et al. Interleukin-15 Modulates the Response of Cortical Neurons to Ischemia. *Mol Cell Neurosci* (2021) 115:103658. doi: 10.1016/j.mcn.2021.103658
130. Liu XL, Du JZ, Zhou YM, Shu QF, Li YG. Interleukin-16 Polymorphism is Associated With an Increased Risk of Ischemic Stroke. *Mediators Inflammation* (2013) 2013:564750. doi: 10.1155/2013/564750
131. Mathy NL, Scheuer W, Lanzendörfer M, Honold K, Ambrosius D, Norley S, et al. Interleukin-16 Stimulates the Expression and Production of Pro-Inflammatory Cytokines by Human Monocytes. *Immunology* (2000) 100:63–9. doi: 10.1046/j.1365-2567.2000.00997.x
132. Skundric DS, Cruikshank WW, Drulovic J. Role of IL-16 in CD4+ T Cell-Mediated Regulation of Relapsing Multiple Sclerosis. *J Neuroinflamm* (2015) 12:78. doi: 10.1186/s12974-015-0292-x
133. Kleinschnitz C, Kraft P, Dreykluft A, Hagedorn I, Göbel K, Schuhmann MK, et al. Regulatory T Cells are Strong Promoters of Acute Ischemic Stroke in Mice by Inducing Dysfunction of the Cerebral Microvasculature. *Blood* (2013) 121:679–91. doi: 10.1182/blood-2012-04-426734
134. Schwab JM, Nguyen TD, Meyermann R, Schluesener HJ. Human Focal Cerebral Infarctions Induce Differential Lesional Interleukin-16 (IL-16) Expression Confined to Infiltrating Granulocytes, CD8+ T-Lymphocytes and Activated Microglia/Macrophages. *J Neuroimmunol* (2001) 114:232–41. doi: 10.1016/s0165-5728(00)00433-1
135. Wu D, Zhang G, Zhao C, Yang Y, Miao Z, Xu X. Interleukin-18 From Neurons and Microglia Mediates Depressive Behaviors in Mice With Post-Stroke Depression. *Brain Behav Immun* (2020) 88:411–20. doi: 10.1016/j.bbi.2020.04.004
136. Wolk K, Kunz S, Asadullah K, Sabat R. Cutting Edge: Immune Cells as Sources and Targets of the IL-10 Family Members? *J Immunol* (2002) 168:5397–402. doi: 10.4049/jimmunol.168.11.5397
137. Gallagher G. Interleukin-19: Multiple Roles in Immune Regulation and Disease. *Cytokine Growth Factor Rev* (2010) 21:345–52. doi: 10.1016/j.cytogfr.2010.08.005
138. Gallagher G, Eskdale J, Jordan W, Peat J, Campbell J, Boniotto M, et al. Human Interleukin-19 and its Receptor: A Potential Role in the Induction of Th2 Responses. *Int Immunopharmacol* (2004) 4:615–26. doi: 10.1016/j.intimp.2004.01.005
139. Oral HB, Kotenko SV, Yilmaz M, Mani O, Zumkehr J, Blaser K, et al. Regulation of T Cells and Cytokines by the Interleukin-10 (IL-10)-Family Cytokines IL-19, IL-20, IL-22, IL-24 and IL-26. *Eur J Immunol* (2006) 36:380–8. doi: 10.1002/eji.200425523
140. England RN, Autieri MV. Anti-Inflammatory Effects of Interleukin-19 in Vascular Disease. *Int J Inflam* (2012) 2012:253583. doi: 10.1155/2012/253583
141. Xie W, Fang L, Gan S, Xuan H. Interleukin-19 Alleviates Brain Injury by Anti-Inflammatory Effects in a Mice Model of Focal Cerebral Ischemia. *Brain Res* (2016) 1650:172–7. doi: 10.1016/j.brainres.2016.09.006
142. Autieri MV. IL-19 and Other IL-20 Family Member Cytokines in Vascular Inflammatory Diseases. *Front Immunol* (2018) 9:700. doi: 10.3389/fimmu.2018.00700
143. Hsu YH, Yang YY, Huwang MH, Weng YH, Jou IM, Wu PT, et al. Anti-IL-20 Monoclonal Antibody Inhibited Inflammation and Protected Against Cartilage Destruction in Murine Models of Osteoarthritis. *PloS One* (2017) 12:e0175802. doi: 10.1371/journal.pone.0175802
144. Chen WY, Chang MS. IL-20 is Regulated by Hypoxia-Inducible Factor and Up-Regulated After Experimental Ischemic Stroke. *J Immunol* (2009) 182:5003–12. doi: 10.4049/jimmunol.0803653
145. Hsu YH, Lin RM, Chiu YS, Liu WL, Huang KY. Effects of IL-1β, IL-20, and BMP-2 on Intervertebral Disc Inflammation Under Hypoxia. *J Clin Med* (2020) 9:140. doi: 10.3390/jcm9010140
146. Lee JS, Hsu YH, Chiu YS, Jou IM, Chang MS. Anti-IL-20 Antibody Improved Motor Function and Reduced Glial Scar Formation After Traumatic Spinal Cord Injury in Rats. *J Neuroinflamm* (2020) 17:156. doi: 10.1186/s12974-020-01814-4
147. Iwakura Y, Ishigame H. The IL-23/IL-17 Axis in Inflammation. *J Clin Invest* (2006) 116:1218–22. doi: 10.1172/jci28508
148. Gelderblom M, Gallizioli M, Ludewig P, Thom V, Arunachalam P, Rissiek B, et al. IL-23 (Interleukin-23)-Producing Conventional Dendritic Cells Control the Detrimental IL-17 (Interleukin-17) Response in Stroke. *Stroke* (2018) 49:155–64. doi: 10.1161/strokeaha.117.019101
149. Gooderham MJ, Papp KA, Lynde CW. Shifting the Focus - the Primary Role of IL-23 in Psoriasis and Other Inflammatory Disorders. *J Eur Acad Dermatol Venereol* (2018) 32:1111–9. doi: 10.1111/jdv.14868
150. Chien YH, Meyer C, Bonneville M. γδ T Cells: First Line of Defense and Beyond. *Annu Rev Immunol* (2014) 32:121–55. doi: 10.1146/annurev-immunol-032713-120216
151. Backes FN, de Souza A, Bianchin MM. IL-23 and IL-17 in Acute Ischemic Stroke: Correlation With Stroke Scales and Prognostic Value. *Clin Biochem* (2021) 98:29–34. doi: 10.1016/j.clinbiochem.2021.09.003
152. Lu L, Wang Y, Zhou L, Li Y, Zhang X, Hu X, et al. Vγ4 T Cell-Derived IL-17A is Essential for Amplification of Inflammatory Cascades in Ischemic Brain Tissue After Stroke. *Int Immunopharmacol* (2021) 96:107678. doi: 10.1016/j.intimp.2021.107678
153. Ali S, Huber M, Kollewe C, Bischoff SC, Falk W, Martin MU. IL-1 Receptor Accessory Protein is Essential for IL-33-Induced Activation of T Lymphocytes and Mast Cells. *Proc Natl Acad Sci USA* (2007) 104:18660–5. doi: 10.1073/pnas.0705939104
154. Drieu A, Martinez de Lizarrondo S, Rubio M. Stopping Inflammation in Stroke: Role of ST2/IL-33 Signaling. *J Neurosci* (2017) 37:9614–6. doi: 10.1523/jneurosci.1863-17.2017
155. Sun Y, Wen Y, Wang L, Wen L, You W, Wei S, et al. Therapeutic Opportunities of Interleukin-33 in the Central Nervous System. *Front Immunol* (2021) 12:654626. doi: 10.3389/fimmu.2021.654626
156. Liu X, Hu R, Pei L, Si P, Wang C, Tian X, et al. Regulatory T Cell is Critical for Interleukin-33-Mediated Neuroprotection Against Stroke. *Exp Neurol* (2020) 328:113233. doi: 10.1016/j.expneurol.2020.113233
157. Chen Z, Hu Q, Huo Y, Zhang R, Fu Q, Qin X. Serum Interleukin-33 is a Novel Predictive Biomarker of Hemorrhage Transformation and Outcome in Acute Ischemic Stroke. *J Stroke Cerebrovasc Dis* (2021) 30:105506. doi: 10.1016/j.jstrokecerebrovasdis.2020.105506
158. Jiang M, Liu X, Zhang D, Wang Y, Hu X, Xu F, et al. Celastrol Treatment Protects Against Acute Ischemic Stroke-Induced Brain Injury by Promoting an IL-33/ST2 Axis-Mediated Microglia/Macrophage M2 Polarization. *J Neuroinflamm* (2018) 15:78. doi: 10.1186/s12974-018-1124-6
159. Luo Q, Fan Y, Lin L, Wei J, Li Z, Li Y, et al. Interleukin-33 Protects Ischemic Brain Injury by Regulating Specific Microglial Activities. *Neuroscience* (2018) 385:75–89. doi: 10.1016/j.neuroscience.2018.05.047

160. Guo S, Luo Y. Brain Foxp3(+) Regulatory T Cells Can Be Expanded by Interleukin-33 in Mouse Ischemic Stroke. *Int Immunopharmacol* (2020) 81:106027. doi: 10.1016/j.intimp.2019.106027
161. Wei H, Zhen L, Wang S, Zhang Y, Wang K, Jia P, et al. *De Novo* Lipogenesis in Astrocytes Promotes the Repair of Blood-Brain Barrier After Transient Cerebral Ischemia Through Interleukin-33. *Neuroscience* (2021) 481:85–98. doi: 10.1016/j.neuroscience.2021.11.026
162. Xiao W, Guo S, Chen L, Luo Y. The Role of Interleukin-33 in the Modulation of Splenic T-Cell Immune Responses After Experimental Ischemic Stroke. *J Neuroimmunol* (2019) 333:576970. doi: 10.1016/j.jneuroim.2019.576970
163. Zhang SR, Piepke M, Chu HX, Broughton BR, Shim R, Wong CH, et al. IL-33 Modulates Inflammatory Brain Injury But Exacerbates Systemic Immunosuppression Following Ischemic Stroke. *JCI Insight* (2018) 3: e121560. doi: 10.1172/jci.insight.121560
164. Li X, Lin S, Chen X, Huang W, Li Q, Zhang H, et al. The Prognostic Value of Serum Cytokines in Patients With Acute Ischemic Stroke. *Aging Dis* (2019) 10:544–56. doi: 10.14336/ad.2018.0820
165. Martha SR, Cheng Q, Fraser JF, Gong L, Collier LA, Davis SM, et al. Expression of Cytokines and Chemokines as Predictors of Stroke Outcomes in Acute Ischemic Stroke. *Front Neurol* (2019) 10:1391:1391. doi: 10.3389/fneur.2019.01391
166. Lin Y, Zhang L, Dai Y, Li H, Wang Y, Zhang B, et al. Expression of Interleukin-9 and its Upstream Stimulating Factors in Rats With Ischemic Stroke. *Neurol Sci* (2015) 36:913–20. doi: 10.1007/s10072-015-2096-2
167. Tan S, Shan Y, Lin Y, Liao S, Zhang B, Zeng Q, et al. Neutralization of Interleukin-9 Ameliorates Experimental Stroke by Repairing the Blood-Brain Barrier *via* Down-Regulation of Astrocyte-Derived Vascular Endothelial Growth Factor-a. *FASEB J* (2019) 33:4376–87. doi: 10.1096/fj.201801595RR
168. Tan S, Shan Y, Wang Y, Lin Y, Liao S, Deng Z, et al. Exacerbation of Oxygen-Glucose Deprivation-Induced Blood-Brain Barrier Disruption: Potential Pathogenic Role of Interleukin-9 in Ischemic Stroke. *Clin Sci (Lond)* (2017) 131:1499–513. doi: 10.1042/cs20170984
169. Li G, Xu R, Cao Y, Xie X, Zheng Z. Interleukin-21 Polymorphism Affects Gene Expression and is Associated With Risk of Ischemic Stroke. *Inflammation* (2014) 37:2030–9. doi: 10.1007/s10753-014-9935-9
170. Lee HK, Keum S, Sheng H, Warner DS, Lo DC, Marchuk DA. Natural Allelic Variation of the IL-21 Receptor Modulates Ischemic Stroke Infarct Volume. *J Clin Invest* (2016) 126:2827–38. doi: 10.1172/jci84491
171. Dong Y, Hu C, Huang C, Gao J, Niu W, Wang D, et al. Interleukin-22 Plays a Protective Role by Regulating the JAK2-STAT3 Pathway to Improve Inflammation, Oxidative Stress, and Neuronal Apoptosis Following Cerebral Ischemia-Reperfusion Injury. *Mediators Inflammation* (2021) 2021:6621296. doi: 10.1155/2021/6621296
172. Yin H, Wu M, Jia Y. Knockdown of IL-32 Protects PC12 Cells Against Oxygen-Glucose Deprivation/Reoxygenation-Induced Injury *via* Activation of Nrf2/NF-κb Pathway. *Metab Brain Dis* (2020) 35:363–71. doi: 10.1007/s11011-019-00530-0
173. Huang X, Li F, Yang T, Li H, Liu T, Wang Y, et al. Increased Serum Interleukin-34 Levels as a Novel Diagnostic and Prognostic Biomarker in Patients With Acute Ischemic Stroke. *J Neuroimmunol* (2021) 358:577652. doi: 10.1016/j.jneuroim.2021.577652
174. Zhang Y, Xu C, Wang H, Nan S. Serum Interleukin-37 Increases in Patients After Ischemic Stroke and Is Associated With Stroke Recurrence. *Oxid Med Cell Longev* (2021) 2021:5546991. doi: 10.1155/2021/5546991
175. Zhang F, Zhu T, Li H, He Y, Zhang Y, Huang N, et al. Plasma Interleukin-37 is Elevated in Acute Ischemic Stroke Patients and Probably Associated With 3-Month Functional Prognosis. *Clin Interv Aging* (2020) 15:1285–94. doi: 10.2147/cia.S230186
176. Zhang SR, Nold MF, Tang SC, Bui CB, Nold CA, Arumugam TV, et al. IL-37 Increases in Patients After Ischemic Stroke and Protects From Inflammatory Brain Injury, Motor Impairment and Lung Infection in Mice. *Sci Rep* (2019) 9:6922. doi: 10.1038/s41598-019-43364-7
177. Zare Rafie M, Esmaeilzadeh A, Ghoreishi A, Tahmasebi S, Faghihzadeh E, Elahi R. IL-38 as an Early Predictor of the Ischemic Stroke Prognosis. *Cytokine* (2021) 146:155626. doi: 10.1016/j.cyto.2021.155626

Conflict of Interest: The authors declare that the research was conducted in the absence of any commercial or financial relationships that could be construed as a potential conflict of interest.

Publisher's Note: All claims expressed in this article are solely those of the authors and do not necessarily represent those of their affiliated organizations, or those of the publisher, the editors and the reviewers. Any product that may be evaluated in this article, or claim that may be made by its manufacturer, is not guaranteed or endorsed by the publisher.

frontiers | Frontiers in Immunology

ORIGINAL RESEARCH
published: 05 April 2022
doi: 10.3389/fimmu.2022.860977

mtDNA-STING Axis Mediates Microglial Polarization *via* IRF3/NF-κB Signaling After Ischemic Stroke

Lingqi Kong[1], Wenyu Li[1], E Chang[2], Wuxuan Wang[1], Nan Shen[1], Xiang Xu[1], Xinyue Wang[1], Yan Zhang[1], Wen Sun[1], Wei Hu[1], Pengfei Xu[1]* and Xinfeng Liu[1]**

[1] Stroke Center and Department of Neurology, The First Affiliated Hospital of USTC, Division of Life Sciences and Medicine, University of Science and Technology of China, Hefei, China, [2] The First Affiliated Hospital of USTC, Division of Life Sciences and Medicine, University of Science and Technology of China, Hefei, China

Neuroinflammation is initiated in response to ischemic stroke, and is usually characterized by microglial activation and polarization. Stimulator of interferon genes (STING) has been shown to play a critical role in anti-tumor immunity and inflammatory diseases. Nevertheless, the effect and underlying mechanisms of STING on microglial polarization after ischemic stroke remain unclarified. In this study, acute ischemic stroke was simulated using a model of middle cerebral artery occlusion (MCAO) at adult male C57BL/6 mice *in vivo* and the BV2 microglia oxygen-glucose deprivation/reperfusion (OGD/R) model *in vitro*. The specific STING inhibitor C-176 was administered intraperitoneally at 30min after MCAO. We found that the expression of microglial STING was increased following MCAO and OGD/R. Pharmacologic inhibition of STING with C-176 reduced the ischemia/reperfusion (I/R)-induced brain infarction, edema and neuronal injury. Moreover, blockade of STING improved neurological performance and cognitive function and attenuated neuronal degeneration in the hippocampus after MCAO. Mechanistically, both *in vivo* and *in vitro*, we delineated that STING could promote the polarization of microglia towards the M1 phenotype and restrain M2 microglia polarization *via* downstream pathways, including interferon regulatory factor 3 (IRF3) and nuclear factor-κB (NF-κB). In addition, mitochondrial DNA (mtDNA), which is released to microglial cytoplasm induced by I/R injury, could facilitate microglia towards M1 modality through STING signaling pathway. Treatment with C-176 abolished the detrimental effects of mtDNA on stroke outcomes. Taken together, these findings suggest that STING, activated by mtDNA, could polarize microglia to the M1 phenotype following MCAO. Inhibition of STING may serve as a potential therapeutic strategy to mitigate neuroinflammation after ischemic stroke.

Keywords: ischemia/reperfusion (I/R) injury, STING, microglia, polarization, neuroinflammation

OPEN ACCESS

Edited by:
Jui-Hung Jimmy Yen, Indiana University School of Medicine, United States

Reviewed by:
Wenhai Chou, National Health Research Institutes, Taiwan
Ping-Chang Kuo, Indiana University Fort Wayne, United States
Gordon Meares, West Virginia University, United States

***Correspondence:**
Xinfeng Liu
xfliu2@ustc.edu.cn
Pengfei Xu
xupengfei1026@126.com
Wei Hu
andinghu@ustc.edu.cn

Specialty section:
This article was submitted to Multiple Sclerosis and Neuroimmunology, a section of the journal Frontiers in Immunology

Received: *24 January 2022*
Accepted: *16 March 2022*
Published: *05 April 2022*

Citation:
Kong L, Li W, Chang E, Wang W, Shen N, Xu X, Wang X, Zhang Y, Sun W, Hu W, Xu P and Liu X (2022) mtDNA-STING Axis Mediates Microglial Polarization via IRF3/NF-κB Signaling After Ischemic Stroke. Front. Immunol. 13:860977. doi: 10.3389/fimmu.2022.860977

INTRODUCTION

Ischemic stroke caused a huge social burden to the world with a high morbidity, disability rate and poor prognosis (1, 2). There is accumulating evidence indicating that post-ischemic inflammation is an essential process in the pathophysiology of ischemic stroke and closely related to the prognosis (3, 4). Therefore, it is important to gain a deeper understanding of neuroinflammation following ischemic stroke.

Microglia, known as the resident immune cell of the central nervous system (CNS), has emerged as a key mediator of neuroinflammation in the setting of ischemic stroke (5, 6). After stimulation, microglia could be polarized into the M1 or M2 form, which plays a dual role in brain injury, repair, and regeneration after ischemic stroke (7). M1 microglia secretes proinflammatory cytokines and chemokines, which can aggravate immune response and brain injury. In contrast, M2 microglia promotes the repair of the damaged tissue by producing anti-inflammatory cytokines (7, 8). Regulating the polarization of microglia and exploring the underlying mechanisms might provide novel insight into a theoretical basis for the study of ischemic stroke.

Stimulator of interferon genes (STING) is an endoplasmic reticulum adaptor protein that facilitates the transcription of numerous host defense genes, including type-I interferons (IFNs) and pro-inflammatory cytokines (9–11). STING can be directly activated by the second messenger cyclic guanosine monophosphate-adenosine monophosphate (cGAMP), which is produced from the cyclic GMP-AMP synthase (cGAS). cGAS, a central cellular cytosolic DNA sensor, can detect and bind to mitochondrial DNA (mtDNA) and nuclear DNA (nDNA) (9–11). STING is also known to bind double-stranded DNA (dsDNA) directly and subsequently instigate primary innate immune genes expression (12). Numerous studies have indicated that STING signaling pathway is involved in innate immune response, anti-tumor immunity and inflammatory diseases (13, 14). Intriguingly, STING has been reported to be expressed in microglia (15, 16). HDAC3-cGAS-STING signaling pathway was activated following ischemic stroke, which promoted the formation of a pro-inflammation microenvironment (17). Damage-associated molecular patterns (DAMPs) activated the microglial cGAS-STING signaling pathway and promoted microglia M1 polarization, while knockdown of cGAS could inhibit these effects (18). Moreover, nuclear dsDNA could drive cGAS signaling and further promote microglial inflammasome activation and pyroptosis to amplify the inflammation during cerebral ischemia (19). Cerebrovascular complications of tPA were aggravated *via* cGAS-STING activation and type I interferon response in ischemic brain (20). However, in these studies, cGAS was more concerned and explored in ischemic stroke, but there is no interfering targeting STING was performed. Whether STING modulates ischemic/reperfusion (I/R)-induced microglia polarization remains to be elucidated.

The mtDNA leakage following tissue injury has been reported to activate STING signaling (9, 21). mtDNA could be released to cytoplasm during the cerebral I/R process and act as a potent DAMPs (22, 23). However, to date, whether mtDNA activates STING after I/R injury has not been clarified. In this study, using the mice middle cerebral artery occlusion (MCAO) model and microglia oxygen-glucose deprivation/reperfusion (OGD/R) model, we examined whether STING could orchestrate neuroinflammation through transforming microglial polarization and explored the underlying mechanisms of STING activation.

METHODS AND MATERIALS

Animals

Adult male C57BL/6 mice weighting 20-25g (6-8 weeks old) were purchased from Beijing Vital River Laboratory Animal Technology. All mice were housed in an environment with controlled light (12 h light/dark), temperature (temperature 23 ± 1°C) and humidity (humidity 55-60%) and provided ad libitum access to food and water. All experimental protocols were approved by the Animal Ethics Review Committee of The First Affiliated Hospital of the University of Science and Technology of China. The study was implemented according to the National Institute of Health Guide for the Care and Use of Laboratory Animals (NIH Publications No. 80-23, revised 1996). All mice were acclimated 1 week to the environment before use and randomized into groups. The experiment scheme is shown in **Supplementary Figure S1**. A total of 466 male mice were used in this study. The animal usage and the excluded reason are shown in **Supplementary Table S1**. At least 4 mice were analyzed for each data point.

Transient Middle Cerebral Artery Occlusion Surgery

The middle cerebral artery occlusion (MCAO) model was induced by occluding the MCA using the intraluminal filament method (24). In brief, mice were anesthetized with 2% isoflurane in O_2 (RWD Life Science, China). The right common carotid artery (CCA), internal carotid artery (ICA), and external carotid artery (ECA) were isolated through a midline cervical incision. The ECA was ligated, and a nylon suture with silicon (Beijing Cinontech Co., Ltd., China) was inserted through the ECA stump and next advanced into the ICA to occlude the origin of the middle cerebral artery (MCA). Mice underwent reperfusion after 90 min of occlusion. The body temperature was maintained at 37 ± 0.5°C by a homoeothermic blanket. To confirm the occlusion of MCA, mice were monitored for cerebral blood flow (CBF) with Laser Speckle Doppler Flowmetry (PeriCam PSI Z; Perimed, Sweden) contrast Imaging before, during, and after surgery (**Supplementary Figure S2**). A decline in regional CBF ≥ 75% of baseline was considered as a successful occlusion. Sham-operated mice were anesthetized and received the same surgical procedures except that the MCA was not occluded.

Cell Culture and OGD/R Model

The mouse BV2 microglial cells and mouse HT22 hippocampal neurons were purchased from the Procell (Wuhan, China). Cells were grown in DMEM (Gibco, USA) medium supplemented

with 10% FBS (Gibco, USA) and 1% penicillin-streptomycin (Gibco, USA) solution in a 37°C, 5% CO_2 incubator. OGD/R was implemented according to our previous methods (24, 25). Briefly, cells were transferred to glucose-free and serum-free DMEM and then incubated in an anaerobic chamber equipped with Anaero Pack-Anaero (MITSUBISHI GAS CHEMICAL CO., INC. Japan). After cells were subjected to OGD for 2 h in the chamber, the medium was replaced by DMEM and returned to normal incubator for reoxygenation. Control microglia cells were cultured with normal oxygen-conditioned incubator for the same periods. For microglia-neuron cocultures, Transwell®plates (0.4-μm pore size, Corning, MA, USA) were used. HT22 cells were seeded in the lower chamber of the Transwell plates and cultured together with microglia, which were pretreated and underwent OGD/R.

Drug Administration

STING inhibitor C-176 (6.1, 12.2, 24.4ug/g, MedChemExpress, USA) or vehicle (1% DMSO+corn oil) were administered intraperitoneally at 30min after MCAO surgery (16, 26). The mtDNA (5mg/kg), extracted from liver tissue by Mitochondrial DNA Isolation Kit (ab65321, Abcam, USA), was intracerebroventricular injected (right lateral ventricle, bregma: 0.23mm posterior, 1mm lateral, and 2.25 mm deep) immediately after MCAO modeling (27). To inhibit STING, BV2 cells were treated with 1 μM C-176 (28). Cells were collected 6 h after mtDNA (100 ng/ml) stimulation and used for subsequent analyses (29). The same volume of PBS was used as the control treatment.

Small Interfering RNA (siRNA) Intracerebroventricular Injection and Cell Transfection

STING small interfering RNA (si-STING, sequence: 5'-CGAA AUAACUGCCGCCUCATT-3') was used in our experiments according to a previous study (17). The 2′OMe+5′Chol+5′Cy5 modified STING siRNA (si-STING) and scrambled siRNA (si-NC) were synthesized by RiboBio (Guangzhou, China) for STING knockdown. After the mice were anesthetized with isoflurane, they were fixed with a stereotaxic apparatus (RWD Life Science, China). A 10μl stainless-steel microsyringe (Shanghai Gaoge Industry & Trade Co., Ltd., China) with siRNAs against STING (si-STING or si-NC, 1.5nmol in 3μl) was inserted into the right lateral ventricle (bregma: 0.23mm posterior, 1mm lateral, and 2.25 mm deep) at a flow rate of 300 nl/min. The injector was administered over 10 min and withdrawn slowly after the infusion, and MCAO surgical procedures were performed 48h after the infusion. After completion of the injection, the burr hole was sealed with bone wax and the incision was closed with sutures. For *in vitro* experiments, 1.25μl siRNA (20μM) and 3μl riboFECT™ CP Reagent (RiboBio, China) were mixed in 30μl riboFECT™ CP Buffer to generate a transfection mixture with a final concentration of 50nM, according to the manufacturer's instruction. Then the 50nM transfection mixture of scrambled siRNA (si-NC) or interfering RNA (si-STING) was added into DMEM and cultured with BV2 microglia for 48 h. Immunofluorescent staining and western blot analysis were performed to examine the transfection efficiency.

Neurobehavioral Test

Modified Neurological Severity Scores (mNSS) and Corner-turning test were performed to assess sensorimotor deficits and motor coordination at day 1, 3, 7, 14, and 21 after cerebral ischemia, as previously described (30). Behavioral function assessments were performed by two researchers who were blinded to the experiments.

Spatial learning and memory was investigated with the Morris Water Maze (MWM) test on days 22-28 after reperfusion (24, 31). Briefly, blind tests were performed on day 22 to exclude blind mice, in which mice were allowed to reach the platform with the flag when the platform was over the water. In the next 5 days, animals were trained to find the platform below the water in four trials. Five days later, the platform was removed and each mouse was explored to search the platform for 90s. The time spent in the target quadrant, the number of platform crossings, the escape latency to find the platform and the swim path length were recorded by the Smart video software (Panlab Harvard Apparatus, USA). The observer and recorder were blinded to animal grouping.

Infarct Volume Evaluation and Brain Water Content

At 24 h after reperfusion, mice were anesthetized, and brains were quickly removed. The brains were frozen rapidly at -80°C with PBS for 6-8min, and coronally sliced in a brain mold and incubated in 2% 2,3,5-triphenyl tetrazolium chloride (TTC, Sigma Aldrich Inc., USA) solution for 10 min at 37°C (25). Then, the brain sections were photographed, and the infarct volume of each slice was determined using Image J software (NIH, USA) by an investigator blinded to the experimental design. To exclude the effects of brain edema, each slice infarct area was calculated as the volume of the contralateral hemisphere minus the non-infarcted volume of the ipsilateral hemisphere and summed to determine the whole infarct volume.

The brain water content was measured with the wet-dry method to evaluate the severity of brain edema at 24 h post-modeling (32). Brains were collected and quickly divided into the left hemisphere and the right hemisphere. Each hemisphere was weighed to get the wet weight and then weighed again at 105°C overnight to get the dry weight. The percentage of water content was calculated according to the following formula: [(wet weight-dry weight)/wet weight] ×100%.

Immunofluorescence

The mice were deeply anesthetized and intracardially perfused with cold PBS and 4% paraformaldehyde (PFA). The brains were removed and fixed in 4% PFA at 4°C for 24 h, and then transferred into 30% sucrose solution until dehydration. Brains were embedded and frozen in the Tissue-Tek O.C.T. compound (Sakura Finetek, USA). The brains were cut into 15 μm or 20 μm frozen coronal sections with a Leica CM1950 cryostat for immunofluorescence staining. Sections were fixed with 4% PFA for 10 min, and then incubated with 10% donkey serum, 1%

bovine serum albumin (BSA) and 0.1% Triton X-100 at room temperature for 1 h. Then the slices were incubated overnight at 4° C with indicated primary antibodies (**Supplementary Table S2**). After three washes with PBS, the slices were incubated for 2 h at room temperature with secondary antibodies (**Supplementary Table S2**). Coverslips were immunostained as brain slices did. Immunofluorescence images were acquired with an Olympus FV3000 fluorescence microscope (Japan). Quantification analysis of positive signals was performed with Image J software (NIH, USA) by an investigator blinded to the experimental design.

TUNEL and Cells Live/Dead Staining

For NeuN and TUNEL co-staining, the frozen sections were first stained with NeuN antibody overnight at 4°C, followed by terminal deoxynucleotidyl transferase-mediated dUTP nick end-labeling (TUNEL) staining with One Step TUNEL Assay Kit (Beyotime, China), according to the manufacturer's protocol. Three brain sections were examined per mouse, with each section containing three microscopic fields from the ischemic boundary zone. The means numbers of target cells were measured in sections per brain, by observers blinded to the experiments. Data were presented with the number of double-positive for TUNEL and NeuN neurons in the fields as cells/mm^2. Meanwhile, HT22 cells death was determined with LIVE/DEAD^{TM} Viability/Cytotoxicity Kit (Thermo Fisher Scientific, USA) after microglia-neuron co-cultures. The percentage of live cells (green) compared with the dead cells (red) was used to assess cell death. Images were captured using a confocal laser scanning microscope (Olympus FV3000, Japan).

Fluoro-Jade C (FJC) Staining

Fluoro-Jade C (FJC, Millipore, USA) was performed at day 1 and day 28 after MCAO induction for identifying degenerated neurons (32, 33). Briefly, brain frozen sections were sequentially immersed in 1% NaOH/80% ethanol solution, 70% ethanol, and 0.06% potassium permanganate solution. Then, the sections were incubated with 0.0001% solution of FJC. Three brain slices were examined per mouse, and the number of FJC-positive neurons was quantified in three different fields of view for each section. Data were presented as TUNEL staining did.

Quantitative Real-Time PCR

Total RNA from cells or tissue was extracted with TRIzol reagent (Invitrogen, USA) according to the manufacturer's instruction and was reverse-transcribed into cDNA using HiScript III RT SuperMix for qPCR Kit (Vazyme, China). Then quantitative real-time PCR was performed using quantitative PCR (Light Cycler 96 System, Roche, China) with corresponding primers (**Supplementary Table S3**) in the presence of a fluorescent dye (AceQ qPCR SYBR Green Master Mix). The levels of mRNA were normalized in relevance to GAPDH.

Western Blot Analysis

Total lysates of peri-infarct tissue or BV2 microglia were prepared using RIPA lysis buffer (Beyotime, China). Protein concentration was quantified by NanoPhotometer-N50 (IMPLEN GMBH, Germany). Equal amounts of protein were loaded and separated by 8-12% SDS-PAGE gel, then electrophoresed and transferred onto PVDF membranes (Millipore, USA). PVDF membranes were blocked with 5% BSA and incubated with primary antibodies overnight at 4°C and then incubated with appropriate HRP-conjugated secondary antibodies at room temperature for 1 h. The used antibodies were listed in **Supplementary Table S2**. Membranes were then incubated with ECL reagents (Willget biotech, China) before visualization using Azure 500 (Azure Biosystems, USA). β-Tubulin was served as the internal control. The immunoblots were analyzed by Image J software (NIH, USA).

Statistical Analysis

All statistical tests were performed using SPSS 22.0 software (IBM, Armonk, NY, USA). Differences between groups were evaluated by the one-way ANOVA followed by Tukey's *post hoc* test. The escape latency and swimming path length in MWM tests were analyzed using two-way ANOVA followed by Tukey's *post hoc* test. All data were presented as mean ± SD. All tests were considered statistically significant at $P < 0.05$.

RESULTS

STING in Microglia Was Upregulated With Stroke

We first investigated the expression change of STING in MCAO mice. Western blot results showed that the protein levels of cGAS, p-STING, and STING were significantly increased with time following MCAO (**Figure 1A**). BV2 microglia OGD/R model was used to mimic the *in vitro* conditions of I/R injury. Immunoblots showed that the expression levels of cGAS, p-STING, and STING in BV2 cells were significantly increased after OGD/R, and continuously increased as the reperfusion time prolongs (**Figure 1B**). Double immunostaining of STING with cell markers (Iba1, GFAP, or NeuN) demonstrated that STING was mainly expressed in microglia cells, rather than neurons or astrocytes and was increased at 1d after MCAO (**Figure 1C** and **Supplementary Figure S3**). Furthermore, STING was co-stained with Iba1 in BV2 cells. STING immunofluorescence signal was enhanced at 24h after reoxygenation (**Figure 1D**). Thus, our data indicated that STING was activated after I/R injury.

Inhibition of STING Attenuated Brain Infarction and Neurological Deficits Following Ischemic Stroke

To investigate the function of STING in the pathophysiological process of ischemic stroke, we intraperitoneally injected mice with C-176 to block STING. TTC staining showed that C-176 administration notably decreased brain infarction and brain edema in a dose-dependent manner 1d post-MCAO (**Figures 2A–C**, for brain infarction: $P = 0.0344$, $P < 0.001$ and $P < 0.001$, for brain edema: $P = 0.0044$, $P < 0.001$ and $P < 0.001$). The dosage of 12.2 and 24.4 ug/g were more effective than the dosage of 6.1 ug/g on brain infarction and cerebral edema 1d

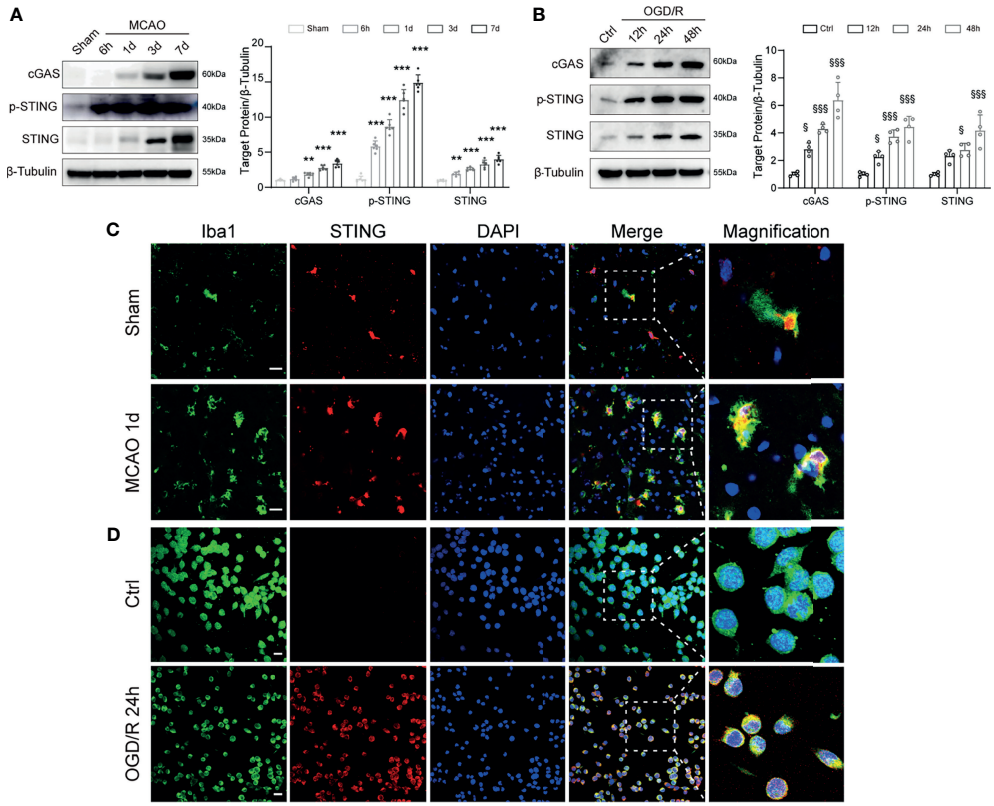

FIGURE 1 | Temporal expression and cellular localization of STING following ischemic stroke. **(A)** Western blot and quantitative analysis of cGAS, p-STING and STING at 6 h, 1d, 3d, and 7d after MCAO. n = 6. **(B)** Western blotting showing cGAS, p-STING and STING expression at 12 h, 24 h, 48h after reoxygenation. n = 4. **(C, D)** STING/Iba1 double immunostaining in Sham and MCAO mice 1d after reperfusion and in Control and OGD/R BV2 microglia 24h after reoxygenation. STING signal was increased after I/R injury both *in vivo* and *in vitro*. n = 4. Data are expressed as mean ± SD. $^{**}P < 0.01$, $^{***}P < 0.001$ vs Sham group. $^{§}P < 0.05$, $^{§§§}P < 0.001$ vs Ctrl group. Scale bar = 20 μm.

post-MCAO (**Figures 2A–C**). However, there were no significant differences between 12.2 ug/g and 24.4 ug/g dose on stroke outcomes (**Figures 2A–C**). Therefore, 12.2 ug/g dose was chosen for subsequent experiments.

We next investigated whether blockade of STING could rescue I/R-induced neuronal injury. TUNEL/NeuN staining was performed to assess neuronal apoptosis at 1d after reperfusion and found a significant decrease (~25%) in the number of apoptotic neurons in the MCAO+C-176 mice compared to the MCAO+vehicle mice (**Figures 2D, E**, $P = 0.0023$). We evaluated neuronal degeneration by FJC staining and found a decrease of ~49% in the number of neuronal degeneration in MCAO+C-176 mice at 1d post-modeling compared with that in MCAO mice (**Figures 2F, G**, $P < 0.001$).

Blockade of STING Improved Long-Term Neurobehavioral Function

The mNSS score was prominently improved in C-176-administered MCAO mice compared to the vehicle-treated MCAO mice on day 7, 14, and 21 post-stroke (**Figure 3A**, $P = 0.0035$, $P < 0.001$ and $P = 0.0047$). Similarly, the C-176-treated group exhibited a significant improvement in sensorimotor function with Corner test compared to the vehicle-treated group at 7 and 14 days after MCAO (**Figure 3B**, $P = 0.0412$, $P = 0.0156$). Cognitive function was assessed by the MWM test on days 22-28 after reperfusion. As shown in **Figures 3C, D**, the escape latency and the path length for the mice to find the hidden platform in the MCAO group were inferior to that of Sham-operated mice, suggesting that I/R injury induced severe learning and memory impairments. C-176-treated MCAO mice displayed a better performance with decreased escape latency and shorter path length on days 3 to 5 (for escape latency: $P = 0.008$, $P < 0.001$ and $P = 0.0012$, for path length: $P = 0.0138$, $P < 0.001$ and $P < 0.001$). Moreover, in the probe phase, treatment with C-176 conspicuously increased the crossovers of the platform and the time spent in the target quadrant compared to the MCAO+vehicle group (**Figures 3E–G**, $P = 0.0096$ and $P = 0.0073$).

We then used FJC staining to test whether STING could affect neuronal degeneration for a long time after ischemic stroke. Robust FJC staining in CA1, CA2, and CA3 regions of the hippocampus were found at 28 d after MCAO. The density of FJC-positive cells was increased after MCAO, while C-176 treatment significantly decreased the number of FJC-positive neurons in CA1, CA2 and CA3 regions of the hippocampus

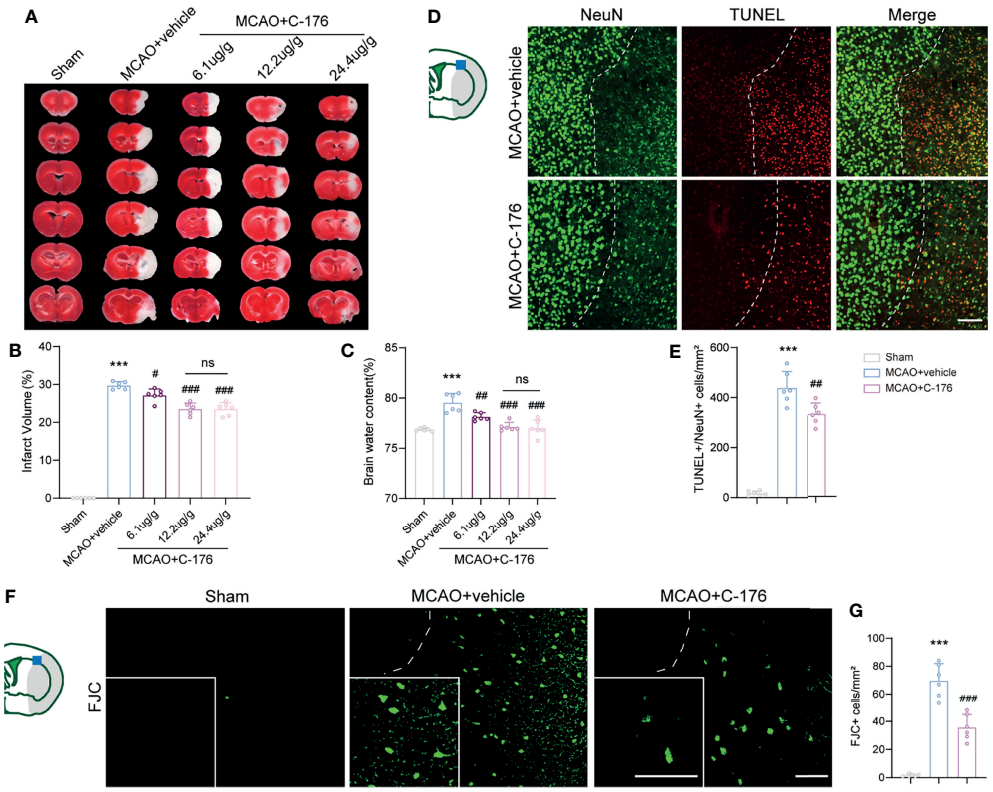

FIGURE 2 | C-176 treatment rescued infarct volume, brain edema, and neuronal injury. **(A)** Representative images for TTC staining in the indicated groups. **(B, C)** Quantitative analysis of infarct volume and brain edema in treated mice 1d post-modeling. **(D, E)** Representative microphotographs and quantitative analysis of NeuN/TUNEL co-staining. The dotted lines designate infarct borderlines. **(F, G)** FJC staining showed that the density of FJC-positive cells was increased in the peri-infarct area, while C-176 treatment reversed this trend. Insets show a higher magnification view. n = 6. Data are expressed as mean ± SD. $^{***}P < 0.001$ vs Sham group; $^{\#}P < 0.05$, $^{\#\#}P < 0.01$, $^{\#\#\#}P < 0.001$ vs MCAO+vehicle group. n. s., no significant difference. Scale bar = 50 μm.

(**Figures 3H, I**, $P = 0.0018$, $P < 0.001$ and $P = 0.0468$). Taken together, blockade of STING may have substantially advantageous effects on long-term behavioral outcomes following ischemic stroke.

Suppression of STING Inhibited Microglial M1 Polarization

Having demonstrated that STING modulates functional outcomes after stroke, we sought to explore whether STING could affect post-ischemic inflammation through microglial polarization. We found that the protein levels of cGAS, p-STING, STING, p-p65, and p-IRF3 were increased substantially in MCAO mice and OGD/R microglia; whilst the STING-related proteins expression levels were remarkably decreased with C-176 administration (**Figures 4A, B**). Moreover, immunoblots showed that the levels of the M1-related marker iNOS decreased and the M2-related marker Arginase-1 increased with C-176 treatment 3d after MCAO and 24h after OGD/R (**Figure 4C**, both $P < 0.001$, **Figure 4D**, $P = 0.0133$ and $P = 0.0018$). Real-time PCR analysis indicated that the levels of M1 phenotype factors (TNF-α, iNOS, IL-1β, IL-6) and the M2 phenotype factors (IL-10 and Arg-1) increased at 3d after reperfusion (**Figure 4E**, $P < 0.001$, $P < 0.001$, $P < 0.001$, $P < 0.001$, $P < 0.001$ and $P = 0.006$). However, C-176 treatment notably mitigated the expression of M1 phenotype related genes and markedly enhanced the expression of M2 phenotype related genes (**Figure 4E**, all $P < 0.001$). Consistent with observation *in vivo*, C-176 incubation markedly upregulated the expression level of M2 phenotype factors and notably suppressed the levels of M1 phenotype factors in BV2 microglia after 24h reoxygenation (**Figure 4F**, all $P < 0.001$).

We then investigated the effects of STING on microglial phenotype transition. CD16/32 and CD206 staining were used to examine the polarization of microglia in the peri-infarct cortex. As depicted in **Figures 4G, H**, the number of CD16/32 and Iba1 double-positive M1-like cells was significantly increased on day 3 after MCAO when compared with the Sham group, which was markedly decreased in the MCAO+C-176 group ($P = 0.0019$). On the other hand, the number of CD206 and Iba1 double-positive M2-like cells was further increased by C-176 administration at 3 days after MCAO (**Figures 4G, H**, $P < 0.001$). Coincident with the observation on day 3 after MCAO, C-176 treatment also notably decreased the CD16/32-positive microglia and increased the CD206-positive

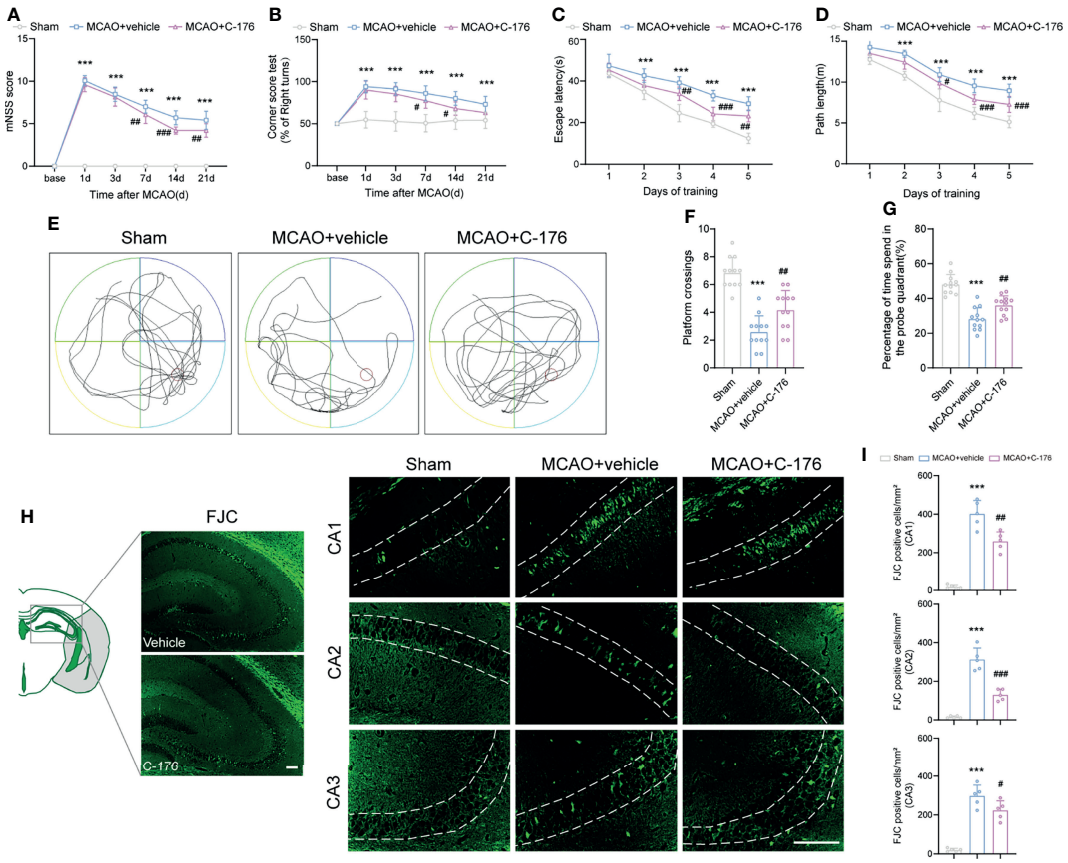

FIGURE 3 | Inhibition of STING improved neurological performance and cognitive function after MCAO. **(A, B)** The mNSS and Corner test were assessed at day 1, 3, 7, 14, and 21 after MCAO. Mice were tested before MCAO surgery. MCAO 1-7 d: n = 15; MCAO 14-21 d: n = 10. Long-term cognitive functions were assessed by the Morris water maze. **(C, D)** The escape latency and swim path length were recorded at days 22-28 after MCAO. n = 12. **(E)** Representative swimming trajectories of the three groups in probe trials. **(F, G)** The crossovers of the platform location and the percentage of time spent in the probe quadrant. n = 12. **(H, I)** FJC staining was performed to assess the neuronal degeneration in hippocampus at day 28 after MCAO. n = 5. Data are expressed as mean ± SD. $^{***}P < 0.001$ vs Sham group; $^{\#}P < 0.05$, $^{\#\#}P < 0.01$, $^{\#\#\#}P < 0.001$ vs MCAO+vehicle group. Scale bar = 100 μm.

microglia on day 7 after MCAO (**Supplementary Figure S4**, $P = 0.0210$ and $P = 0.0007$). We further performed immunostaining for the BV2 cells to evaluate the effects of C-176 on the M1/M2 polarization state at 24h after OGD/R. Blockade of STING reduced the number of $CD16/32^{+}$ microglia cells, and increased the number of $CD206^{+}$ microglia cells (**Figures 4I, J**, $P = 0.0074$ and $P < 0.001$). OGD/R induced a substantial increment of neuronal death as determined by quantification of live/dead staining, while incubation with C-176 maximally preserved neuronal viability (**Supplementary Figure S5**, $P = 0.0026$). These results demonstrated that C-176 alleviated cerebral I/R injury by promoting the microglial polarization to M2 state.

Knockdown of STING in Microglia Attenuated I/R-Induced Neuroinflammation and Brain Injury

To further verify the role of STING post-MCAO, siRNA was administrated i.c.v to silence STING. Double immunostaining images at the siRNA injection site and the surrounding area showed that Cy5-conjugated si-STING was co-stained with microglia (**Figure 5A**). And we found that the levels of p-STING and STING were suppressed by si-STING (**Figures 5B, C**, both $P < 0.001$). Similarly, si-STING transfection could effectively knockdown p-STING and STING expression in BV2 microglia 24h after OGD/R (**Supplementary Figure S6**, $P = 0.0099$ and $P = 0.0087$). These results suggested that si-STING could transfect into microglia and knockdown of STING expression.

Genetic knockdown of STING decreased the infarct volume and brain edema, and alleviated neurological deficits post-MCAO (**Figures 5D–G**, $P < 0.001$, $P = 0.0011$ and $P = 0.0207$). Moreover, administration with si-STING significantly suppressed the mRNA level of M1 phenotype markers (TNF-α, iNOS, IL-1β, and IL-6) 1d post-MCAO when compared to the MCAO+si-NC group (**Figure 5H**, $P < 0.001$, $P = 0.0291$, $P < 0.001$ and $P < 0.001$). We also found that silence STING upregulated the expression of M2 phenotype mRNA markers (IL-10 and Arg-1), while injection si-NC had no such effects (**Figure 5I**, both $P < 0.001$).

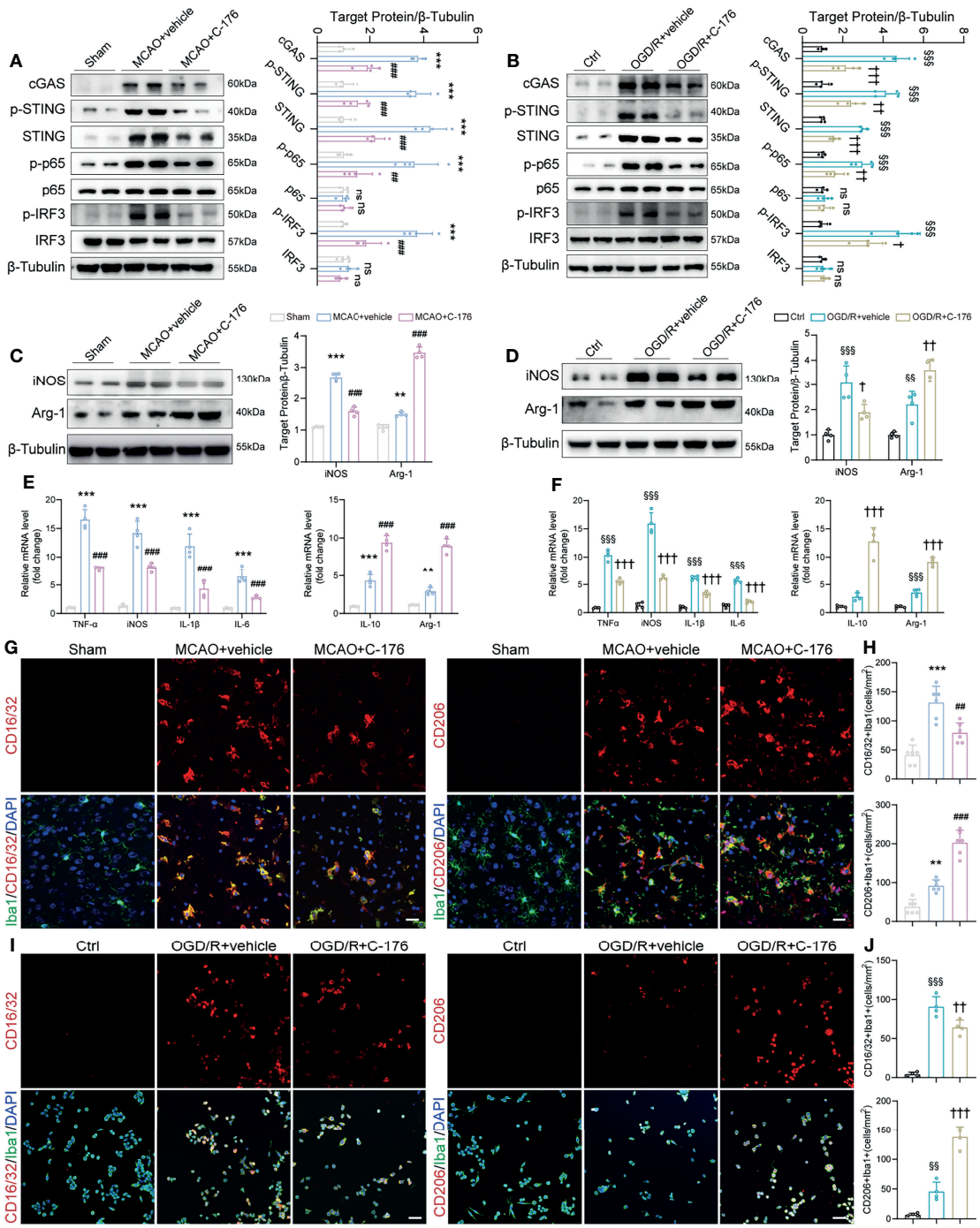

FIGURE 4 | The STING inhibitor C-176 promoted M2 polarization after MCAO. **(A)** Immunoblotting analysis of cGAS, p-STING, STING, p-p65, p65, p-IRF3 and IRF3 in the peri-infract tissue of Sham, MCAO+vehicle and MCAO+C-176 mice 1d post-MCAO. n = 4. **(B)** Immunoblotting images and quantitative analysis of cGAS, p-STING, STING, p-p65, p65, p-IRF3 and IRF3 in BV2 microglia of Ctrl, OGD/R+vehicle and OGD/R+C-176 group 24h after reoxygenation. n = 4. **(C, D)** Western blot and quantification analysis for iNOS and Arginase-1 in treated mice 3d post-MCAO and BV2 microglia 24h post-reoxygenation. n = 4. **(E, F)** mRNA expression of pro-inflammatory genes (TNF-α, iNOS, IL-1β and IL-6) and anti-inflammatory genes (IL-10 and Arg-1) were measured by real-time PCR 3d after MCAO and 24h after OGD/R. n = 4. **(G)** Representative confocal images of two microglia phenotypes were obtained from the peri-infarct cortex. **(H)** Quantification of CD16/32 positive M1 microglia and CD206 positive M2 microglia in the treated mice. n = 6. **(I, J)** Representative immunostained images and statistical analysis of M1 state ($CD16/32^+/Iba1^+$) and M2 state ($CD206^+/Iba1^+$) BV2 microglia. n = 4. Data are expressed as mean ± SD. $^{**}P < 0.01$, $^{***}P < 0.001$ vs Sham group; $^{\#\#}P < 0.01$, $^{\#\#\#}P < 0.001$ vs MCAO+vehicle group. $^{\S\S}P < 0.01$, $^{\S\S\S}P < 0.001$ vs Ctrl group; $^{\dagger}P < 0.05$, $^{\dagger\dagger}P < 0.01$, $^{\dagger\dagger\dagger}P < 0.001$ vs OGD/R+vehicle group. n. s., no significant difference. Scale bar = 20 μm.

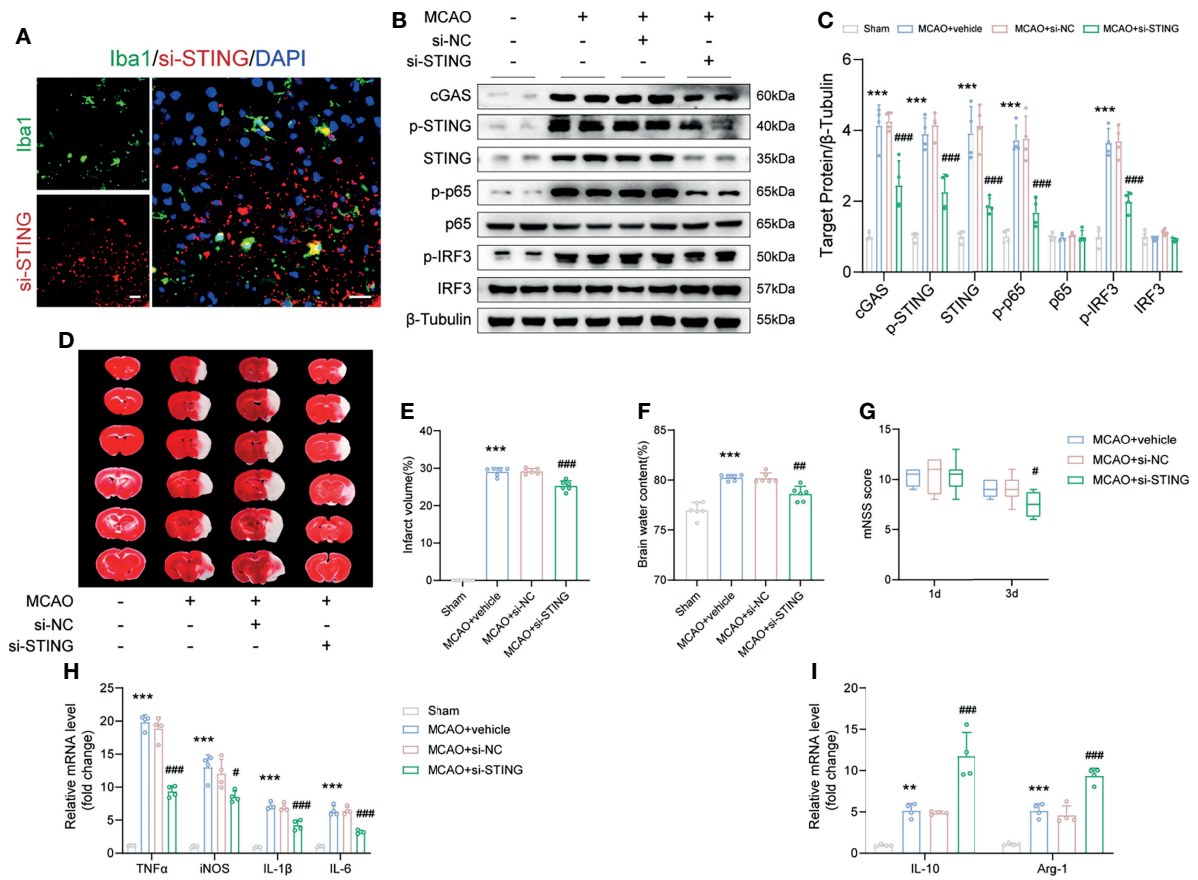

FIGURE 5 | STING knockdown ameliorated brain infarction and edema, promoted neurological recovery and rescued the expression of anti-inflammatory genes. **(A)** si-STING (red) co-stained with Iba1 (green) 1d post-MCAO in mice receiving Cy5-conjugated si-STING. **(B, C)** Immunoblots and quantitative analysis of STING-related proteins, including cGAS, p-STING, STING, p-p65, p65, p-IRF3 and IRF3 of Sham, MCAO+vehicle, MCAO+si-NC and MCAO+si-STING mice 1d after MCAO. n = 4. **(D-F)** Representative images of TTC staining and quantitative analysis of infarct volume and brain edema 1d post-MCAO. n = 6. **(G)** mNSS score of the indicated groups at day 1 and day 3 after MCAO. n = 8. **(H, I)** Relative mRNA expression of M1 microglia-specific transcripts (TNFα, iNOS, IL-1β and IL-6) and M2 microglia-specific transcripts (IL-10 and Arg-1). n = 4. Data are expressed as mean ± SD. $^{**}P < 0.01$, $^{***}P < 0.001$ vs Sham group; $^{\#}P < 0.05$, $^{\#\#}P < 0.01$, $^{\#\#\#}P < 0.001$ vs MCAO+si-NC group. Scale bar = 20 μm.

Inhibition of STING Retarded the Expression of mtDNA After MCAO

Recently, it has been reported that mtDNA could release into the neuronal cytoplasm and participate in the pathogenesis of amyotrophic lateral sclerosis (ALS) (34). As a potent DAMPs, mtDNA is closely involved in the immune process after stroke (35). To this end, we triple-labeled stained against dsDNA, HSP60 (a mitochondrial marker), and Iba1 to assess whether mtDNA could leak into the microglial cytoplasm after I/R injury. Immunofluorescence and 3D-reconstructed images revealed that quantities of mtDNA were released into microglial cytoplasm following MCAO, which were alleviated by treatment with C-176 (**Figures 6A, B**, $P = 0.0016$). A similar trend was found in the cell experiments. Incubation with C-176 remarkably reduced the level of mtDNA, which was released into microglial cytoplasm induced by OGD/R ictus (**Figures 6D, E**, $P < 0.001$). I/R injury also induced the levels of mtDNA mRNA markers (UUR, COXI, ND1, and COX3) to noticeably increase, and these increments were all reversed by C-176 injection (**Figure 6C**, $P = 0.0030$, $P < 0.001$, $P < 0.001$ and $P < 0.001$).

MCAO-Induced mtDNA Was Responsible for Microglial Polarization Through the STING Pathway

mtDNA has been found to be capable of triggering STING signaling (21). We next sought to explore the role of microglial mtDNA in the STING-mediated I/R injury. Mice were received an intracerebroventricular injection of 5 mg/kg mtDNA. Compared with the vehicle-treated MCAO mice, mtDNA injection could markedly enhance the protein levels of cGAS, p-STING, STING, p-p65 and p-IRF3 1d after MCAO, which were alleviated by C-176 administration (**Figures 7A, B**). A similar tendency was observed in BV2 cells that C-176 incubation notably reversed the increments of STING-related proteins induced by mtDNA treatment (**Supplement Figure S7**). In addition, aggravated brain infarction and brain edema were observed as a result of mtDNA

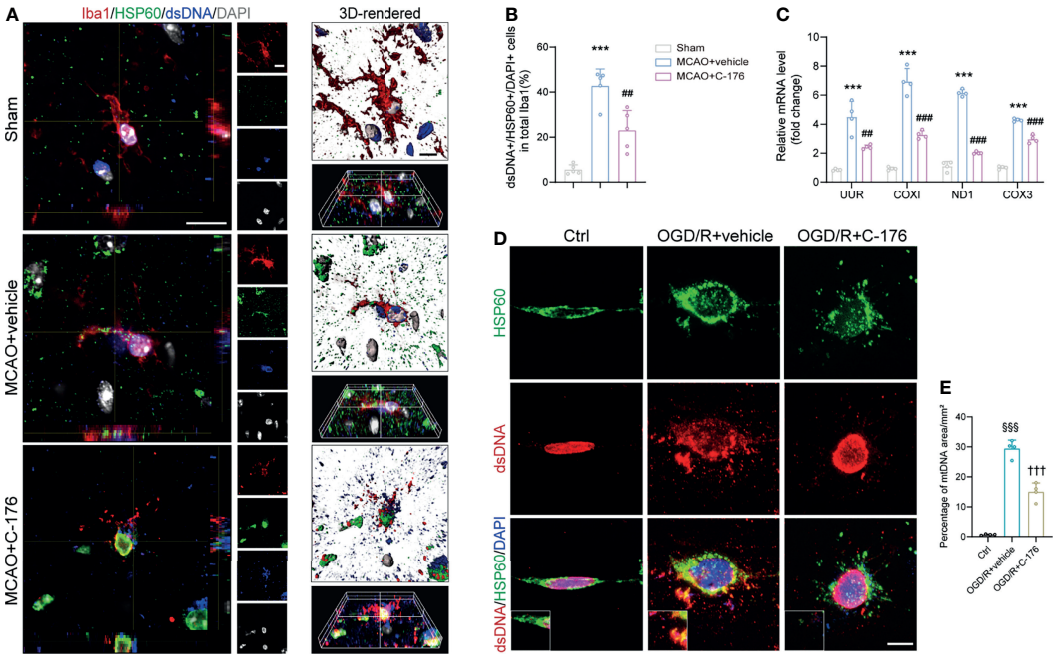

FIGURE 6 | Blockade of STING suppressed microglial mtDNA leakage after MCAO. **(A, B)** Representative confocal, 3D-reconstructed images of dsDNA$^+$/HSP60$^+$/Iba1$^+$ microglia and quantification of microglial mtDNA 1d post-MCAO. Images were reconstructed from confocal images using Imaris software. n = 5. **(C)** Relative mRNA expression of mtDNA-specific genes (UUR, COXI, ND1 and COX3) 1d after MCAO. n = 4. **(D, E)** BV2 microglia cells were stained with anti-dsDNA and anti-HSP60 to detect mtDNA at 24h after reoxygenation. Representative dsDNA/HSP60 double immunostaining images and quantification of mtDNA. n = 4. Data are expressed as means ± SD. $^{***}P < 0.001$ vs Sham group; $^{\#\#}P < 0.01$, $^{\#\#\#}P < 0.001$ vs MCAO+vehicle. $^{\S\S\S}P < 0.001$ vs Ctrl group; $^{\dagger\dagger\dagger}P < 0.001$ vs OGD/R+vehicle group. Scale bar = 10 μm.

administration in MCAO mice, which was reversed by C-176 administration (**Figures 7C–E**, both $P < 0.001$). mtDNA injection remarkably worsened neurobehavioral performance in MCAO mice compared to the MCAO+vehicle group throughout the testing periods (**Figure 7F**, $P = 0.0301$, $P = 0.0317$ and $P = 0.0067$). The mtDNA+C-176 mice displayed significantly better neurological performance than the mice in the mtDNA group on days 7 to 21 post-MCAO (**Figure 7F**, $P < 0.001$, $P < 0.001$ and $P = 0.0036$). As illustrated in **Figures 7G, H**, MCAO mice injected with mtDNA induced the increment of TUNEL-positive cells at 1d after reperfusion, which was alleviated by treatment of C-176 ($P < 0.001$).

We further evaluated the effects of STING activation, which is induced by mtDNA injection, on microglial polarization in ischemic stroke. Immunofluorescent staining results showed that mtDNA treatment increased the numbers of Iba1$^+$CD16/32$^+$ pro-inflammatory microglia and reduced Iba1$^+$CD206$^+$ anti-inflammatory microglia at 3d after MCAO compared with vehicle-treated mice (**Figures 7I–L**, $P < 0.001$ and $P = 0.0040$). However, co-administration of mtDNA and C-176 could suppress the number of the M1-specific marker CD16/32 and increase the number of the M2-specific marker CD206 in microglia after MCAO attack (**Figures 7I–L**, $P < 0.001$ and $P = 0.0040$). These results suggested that mtDNA could trigger microglial phenotype shift towards the M1 modality through activation of STING, resulting in neurological function deterioration following ischemic stroke.

DISCUSSION

In the current study, we found that STING was triggered and mainly located in microglia after ischemic stroke. Pharmacological blockade of STING with C-176 remarkably alleviated brain infarct volume, brain edema, neuronal apoptosis and degeneration, and thus recovered short-term and long-term neurological function. Moreover, inhibition of STING remarkably decreased the number of M1 phenotype microglia and facilitated microglial phenotype towards the M2 phenotype following cerebral I/R injury. In addition, we demonstrated that the microglial mtDNA, which escaped into the cytoplasm under I/R stimulation, could promote microglial polarization switch to M1 phenotype *via* STING signaling pathway. Blockade of STING remarkably shifted microglial polarization towards the M2 phenotype and alleviated neuroinflammation (**Figure 8**).

STING is a dimeric transmembrane protein at the endoplasmic reticulum (ER) with 42-kDa (14). Research on the immune role of the STING pathway in CNS disorders has grown in recent years (34, 36, 37). However, little is known about the role of STING in the pathological process of ischemic stroke. Here we showed that STING expression gradually increased at least 7 days following ischemic stroke. In agreement with our study, in the hypoxic-ischemic encephalopathy (HIE) model, M. Gamdzyk and colleagues demonstrated that the expression of

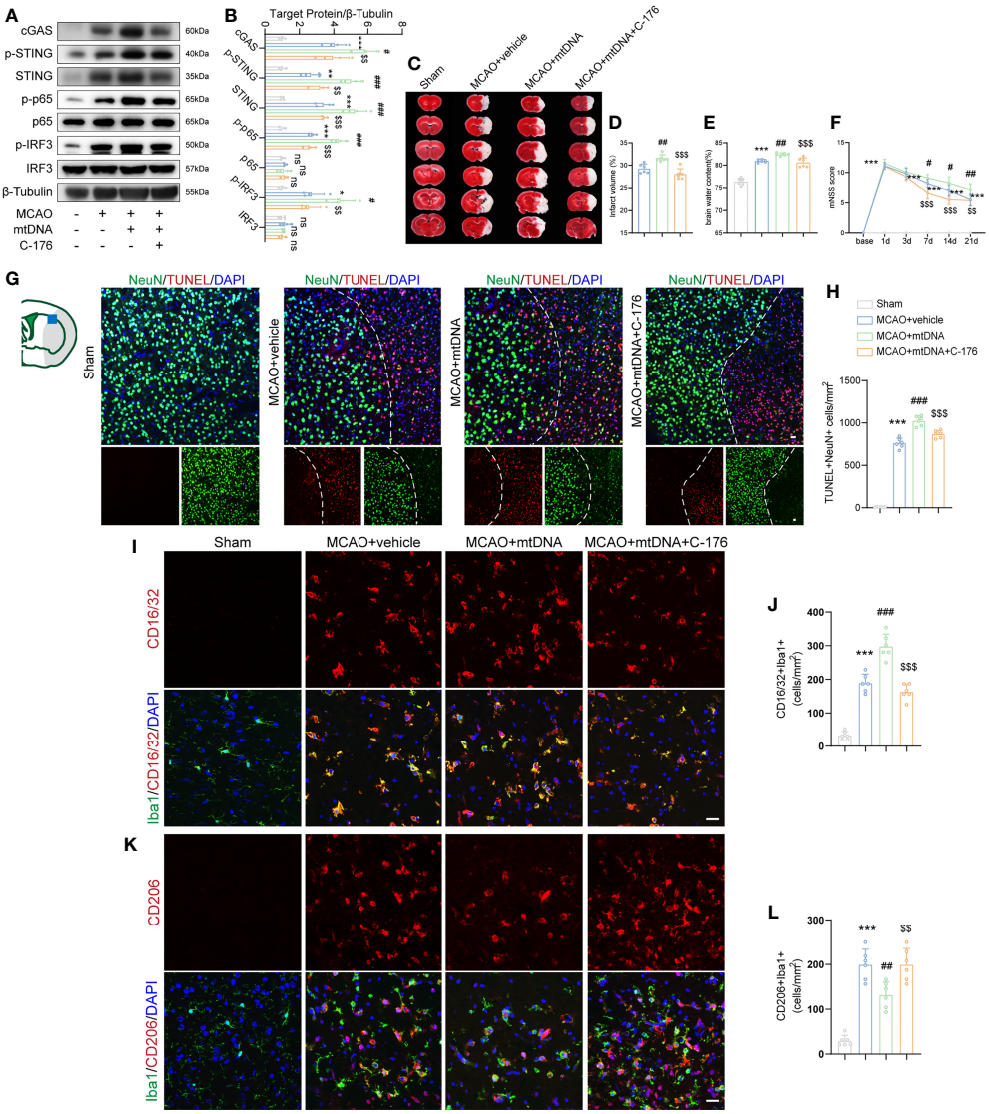

FIGURE 7 | mtDNA induced microglial M1 polarization by activating STING signaling pathway. **(A, B)** Western blot and quantification analysis of cGAS, p-STING, STING, p-p65, p65, p-IRF3 and IRF3 in Sham-, MCAO+vehicle-, MCAO+mtDNA-, and MCAO+mtDNA+C-176-treated mice 1d after reperfusion. n = 4. **(C-E)** Representative TTC staining images and quantification of infarction volume and brain edema 1d post-MCAO. n = 6. **(F)** mNSS score was assessed at day 1, 3, 7, 14 and 21 after MCAO. MCAO 1-7 d: n = 10; MCAO 14-21 d: n = 8. **(G, H)** TUNEL (red) and NeuN (green) double immunostaining with quantitative analysis. Dotted line designates the infarct borderline. n = 6. **(I–L)** Representative confocal images and quantification of M1 modality microglia (CD16/32$^+$/Iba1$^+$) and M2 modality microglia (CD206$^+$/Iba1$^+$) in the indicated groups. n = 6. Scale bar = 20 μm. Data are expressed as mean ± SD. $^*P < 0.05$, $^{**}P < 0.01$, $^{***}P < 0.001$ vs Sham group; $^{\#}P < 0.05$, $^{\#\#}P < 0.01$, $^{\#\#\#}P < 0.001$ vs MCAO+vehicle group; $^{\$\$}P < 0.01$, $^{\$\$\$}P < 0.001$ vs MCAO+mtDNA group. n. s., no significant difference.

STING was significantly increased from 6 h to 7d after HIE (38). Yet, a study examining the function of STING in subarachnoid hemorrhage (SAH) mice showed that the level of STING was increased post-SAH, peaked at 24h and gradually declined (16). Simultaneously, our immunofluorescence staining results confirmed that STING was mainly distributed in microglia after MCAO, which was similarly evaluated by the work of Peng and colleagues under the SAH condition (16). However, there was research showing that STING was located in neurons and astrocytes in HIE and traumatic brain injury (TBI) models (38, 39). The different models and complex microenvironments in the brain may be responsible for the different expression and location patterns of STING.

C-176, a highly potent and selective small molecule antagonist of STING, is widely used to block STING. C-176 could covalently target transmembrane cysteine residue 91 and thereby block the activation-induced palmitoylation of STING (26). It is reported that C-176 could effectively attenuate STING-associated autoinflammatory disease and early brain injury *via* intraperitoneally injection (16). So, intraperitoneally

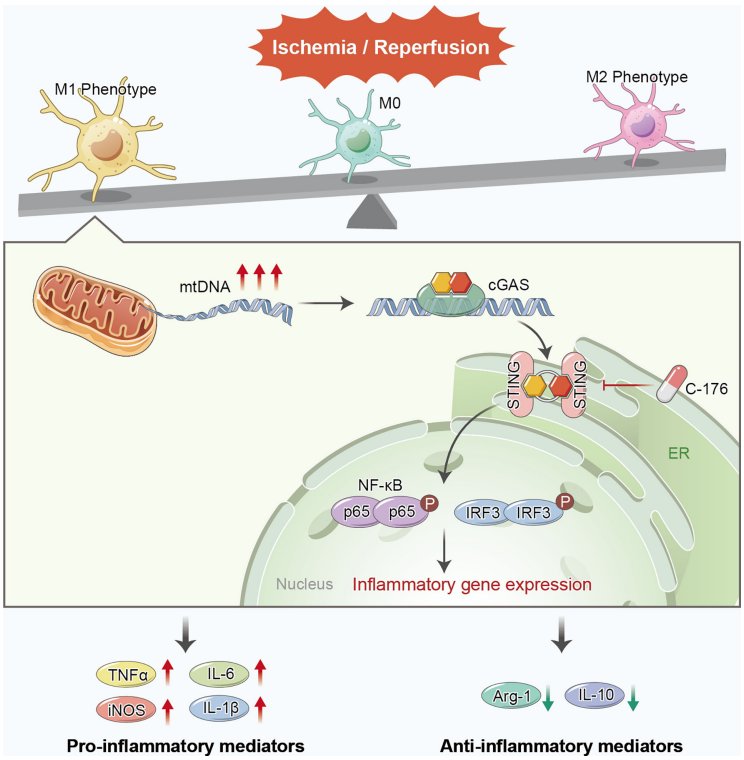

FIGURE 8 | Proposed mechanism of STING-mediated microglial polarization following ischemic stroke. I/R injury induces the leakage of mtDNA to cytoplasm and the activation of STING in microglia. Blockade of STING shifts the microglia toward M2 modality through IFR3 and NF-κB, thereby rescuing neuroinflammation and stroke outcomes. mtDNA can promote microglial polarization to the M1 phenotype *via* activating STING signaling pathway.

delivery of C-176 was applied to inhibit STING in our study. Pharmacological inhibition of STING with C-176 significantly alleviated neuroinflammation, thereby reducing brain water content and neurological deficits in SAH mice (16). Inhibition of STING with C-176 abrogated the increased level of proinflammatory cytokines/chemokines secretion in BMDMs in both young and aged mice (29). In this study, we found that pharmacological inhibition of STING with C-176 could suppress neuroinflammation and improve stroke outcomes. Li et al. showed that activation of cGAS-STING signaling could drive microglial inflammasome production and microglia pyroptosis to amplify the inflammation during cerebral I/R injury (19). However, the exact mechanisms of STING on neuroinflammation in ischemic stroke are not completely understood.

Neuroinflammatory, which responses to post-ischemia, is characterized by rapid activation of resident microglia cells (40). Microglia is the chief innate immune cell within the CNS and the most potent modulator of CNS repair and regeneration (5, 7, 41). But microglia cells play an apparent double-edged sword role in the CNS. Recent studies have reported that regulation of the balance between M1 and M2 phenotypes is a promising therapeutic strategy for brain ischemia (42–44). Considering that STING contributes to microglia/macrophages polariztion in SAH and colitis (16, 45), we speculated that STING might mediate microglial polarization in ischemic stroke. Indeed, our results showed that the gene and protein expressions of M1 phenotype in microglia was increased at 3 days post-MCAO, while the genes and proteins expression of M2 phenotype was suppressed. Additionally, inhibition of STING with C-176 notably promoted the M2 phenotype but reduced the M1 phenotype to exert an anti-inflammatory function. In this study, we chose the third-day time point to analyze microglial polarization states. The reasons are as follows: i) M1 microglia gradually increased over time from day 3 onward and remained elevated for at least 14 days after ischemia; ii) M2 microglia gradually increased beginning 1 to 3 days, peaked by 3 to 5 days and then decreased at 7 days after MCAO (7, 46).

Another major observation in this study was that STING could mediate microglial polarization through activating IRF3 and NF-κB pathways. The phosphorylated STING recruits and activates IRF3, ultimately, IRF3 enters the nucleus and exerts its function in the type-I interferon responses (10, 47). Meanwhile, STING could mediate the production of NF-κB-driven inflammatory genes and subsequently immune responses (48). It is reported that IRF3 and NF-κB could regulate microglial polarization after ischemic stroke (49).We speculated that STING might influence microglial polarization through activating IRF3 and NF-κB pathways following MCAO. Indeed, as depicted in western blot results, the protein expression of p-p65 and p-IRF3 was increased

post-MCAO, and C-176 administration suppressed this increment. Furthermore, we noted that the downregulation of p-p65 and p-IRF3 was accompanied with decreasing microglial M1 phenotype polarization and growing M2 phenotype polarization. Intriguingly, it is reported that STING could recruit and improve NLRP3 localization in the endoplasmic reticulum, and remove NLRP3 polyubiquitination, thereby promoting the inflammasome activation (50). NLRP3 inflammasome has been proposed as a critical mediator of microglial M1/M2 polarization post-ischemic stroke (51). Therefore, NLRP3 inflammasome may be involved in STING-medicated microglial polarization. Accumulating evidences demonstrated that metabolic reprogramming and autophagy could orchestrate microglia activation and polarization (52). A recent investigation has declared that STING could orchestrate metabolic reprogramming of macrophages *via* HIF-1α during bacterial infection (53). Moreover, STING activation induces autophagy dysfunction in TBI and sepsis-related acute lung injury mice (39, 54). In view of these, STING might affect the polarization states of microglial cells through regulating other pathways, such as metabolic reprogramming and autophagy. Further researches are needed to elucidate the specific way of STING mediated microglial polarization.

Mitochondria dysfunction, including mtDNA damage, depletion and release, plays a critical role in ischemic cascades (55). mtDNA could activate the cGAS-STING immune pathway, subsequently regulate innate immune response and sterile inflammation (17, 21, 56). Here, we verified that the mtDNA could be released into the microglial cytoplasm and activated the STING signaling pathway during the cerebral I/R process. Previous studies have shown that STING was able to complex with self or pathogen-related signal-stranded DNA (ssDNA) and dsDNA, possibly by interacting with DNA through its cytoplasmic tail (12).However, as a dsDNA, whether mtDNA can directly bind to STING under ischemia conditions needs further study. Mitochondria are present in varieties of cells in CNS and comprise the intracellular cores for energetics and viability (57). Neurons and astrocytes can exchange damaged mitochondria with each other for disposal and recycling after stroke (58, 59). Furthermore, fragmented mitochondria released from microglia can trigger A1 astrocytic phenotype and propagate neuronal death (60). Thus, the elevated mtDNA in microglial cytoplasm of ishchemic brain may be partly from astrocytes and neurons through cell to cell conmmunication. Follow-up studies to elucidate the source of mtDNA in microglia cytoplasm may be envisioned.

CONCLUSIONS

In summary, the present study demonstrated that STING could orchestrate neuroinflammation after ischemic stroke *via* mediating microglial polarization to M1 phenotype. Blockade of STING could inhibit inflammatory responses and provide a neuroprotective effect following ischemic stroke.These findings indicated that STING might be a therapeutic target for ischemic stroke.

DATA AVAILABILITY STATEMENT

The original contributions presented in the study are included in the article/**Supplementary Material**. Further inquiries can be directed to the corresponding authors.

ETHICS STATEMENT

The animal study was reviewed and approved by The First Affiliated Hospital of the University of Science and Technology of China.

AUTHOR CONTRIBUTIONS

XL and PX designed the research. LK and PX drafted the original manuscript. LK and WL performed the animal experiments. EC and WW performed the cellular experiments. NS, XX, and XW contributed to western blots and immunostaining. WL and LK analyzed the data. WS and YZ gave critical comments for the research. WH, PX, and XL conceptualized and supervised the study. All authors read and approved the final manuscript.

FUNDING

This work was supported by the National Natural Science Foundation of China (Nos. U20A20357 and 82101368), the Anhui Provincial Natural Science Foundation (Nos. 2008085QH368, 2108085MH271 and 2108085MH272), the Fundamental Research Fund for the Central Universities (No. WK9110000056), and the Program for Innovative Research Team of The First Affiliated Hospital of USTC.

SUPPLEMENTARY MATERIAL

The Supplementary Material for this article can be found online at: https://www.frontiersin.org/articles/10.3389/fimmu.2022.860977/full#supplementary-material

Supplementary Figure 1 | Experimental design and animal groups. i.p., intraperitoneal injection; i.c.v, intracerebroventricular injection; MCAO, middle cerebral artery occlusion; RT-PCR, real-time polymerase chain reaction; siRNA, short interfering RNA; STING, Stimulator of IFN genes; TTC, 2,3,5-triphenyl tetrazolium chloride solution; mtDNA, Mitochondrial DNA.

Supplementary Figure 2 | Occlusion of MCA decreased cerebral blood flow (CBF). Representative images and quantitative analyses showed the CBF before ischemia, during ischemia, and 24 hours after reperfusion. Data are expressed as mean ± SD, n = 6. $^{***}P < 0.001$ vs Baseline group. $^{\#\#\#}P < 0.001$ vs Ischemia group.

Supplementary Figure 3 | Colocalization of STING with GFAP or NeuN in the peri-infarct cortex of mice. STING was undetectable in astrocytes and neurons. Scale bar = 20 μm.

Supplementary Figure 4 | Effect of inhibit STING on microglia polarization at 7 days post-MCAO. Representative images of double immunostaining and

quantitative analyses of microglia polarization. M1-phenotype: CD16/32$^+$ (red) and Iba1$^+$ (green); M2-phenotype: CD206$^+$ (red) and Iba1$^+$ (green). Data are expressed as mean ± SD, n = 6. $^{**}P < 0.01$, $^{***}P < 0.001$ vs Sham group; $^{\#}P < 0.05$, $^{\#\#\#}P < 0.001$ vs MCAO+vehicle group. Scale bar = 20 μm.

Supplementary Figure 5 | Pharmacological inhibition of STING suppressed neuronal death *in vitro*. Neurons were co-cultured with Control microglia, OGD/R microglia, or OGD/R microglia treated with C-176 (1 μM) for 24 h. Neuronal viability of the three groups was measured by Live/Dead staining. Data are expressed as mean ± SD, n = 4. $^{\S\S\S}P < 0.001$ vs Ctrl group; $^{\dagger\dagger}P < 0.01$vs OGD/R+vehicle group. Scale bar = 200 μm.

Supplementary Figure 6 | Transfection of siRNA restrained STING expression *in vitro*. **(A)** Colocalization of Cy5-conjugated si-STING with Iba1 24h after OGD. **(B)** Western blotting and quantitative analysis for cGAS, p-STING and STING. Data are expressed as mean ± SD, n = 4. $^{\S\S\S}P < 0.001$ vs Control group; $^{\dagger}P < 0.05$, $^{\dagger\dagger}P < 0.001$ vs OGD/R+si-NC group. Scale bar = 50 μm.

Supplementary Figure 7 | mtDNA pre-treatment promoted STING expression *in vitro*. BV2 cells were pre-treated with mtDNA (100 ng/ml) for 6h before C-176 incubation. Immunoblots and densitometry analysis of cGAS, p-STING, STING, p-p65, p65, p-IRF3 and IRF3 in Ctrl, OGD/R+vehicle, OGD/R+mtDNA, OGD/R+mtDNA+C-176 groups. Data are expressed as mean ± SD, n = 4. $^{\S\S\S}P < 0.001$ vs Ctrl group; $^{\dagger}P < 0.05$, $^{\dagger\dagger}P < 0.01$, $^{\dagger\dagger\dagger}P < 0.001$ vs OGD/R+vehicle group; $^{\$\$}P < 0.01$, $^{\$\$\$}P < 0.001$ vs OGD/R+mtDNA group.

Supplementary Table 1 | Animal usage and mortality of all the experimental groups.

Supplementary Table 2 | Antibodies used in this study.

Supplementary Table 3 | Sequences of the PCR primers used in the study.

REFERENCES

1. Feigin VL, Nichols E, Alam T, Bannick MS, Beghi E, Blake N, et al. Global, Regional, and National Burden of Neurological Disorders, 1990-2016: A Systematic Analysis for the Global Burden of Disease Study 2016. *Lancet Neurol* (2019) 18(5):459–80. doi: 10.1016/s1474-4422(18)30499-x
2. Hankey GJ. Stroke. *Lancet* (2017) 389(10069):641–54. doi: 10.1016/s0140-6736(16)30962-x
3. Moskowitz MA, Lo EH, Iadecola C. The Science of Stroke: Mechanisms in Search of Treatments. *Neuron* (2010) 67(2):181–98. doi: 10.1016/j.neuron.2010.07.002
4. Iadecola C, Anrather J. The Immunology of Stroke: From Mechanisms to Translation. *Nat Med* (2011) 17(7):796–808. doi: 10.1038/nm.2399
5. Xiong XY, Liu L, Yang QW. Functions and Mechanisms of Microglia/Macrophages in Neuroinflammation and Neurogenesis After Stroke. *Prog Neurobiol* (2016) 142:23–44. doi: 10.1016/j.pneurobio.2016.05.001
6. Benarroch EE. Microglia: Multiple Roles in Surveillance, Circuit Shaping, and Response to Injury. *Neurology* (2013) 81(12):1079–88. doi: 10.1212/WNL.0b013e3182a4a577
7. Hu X, Li P, Guo Y, Wang H, Leak RK, Chen S, et al. Microglia/Macrophage Polarization Dynamics Reveal Novel Mechanism of Injury Expansion After Focal Cerebral Ischemia. *Stroke* (2012) 43(11):3063–70. doi: 10.1161/strokeaha.112.659656
8. Hu X, Leak RK, Shi Y, Suenaga J, Gao Y, Zheng P, et al. Microglial and Macrophage Polarization—New Prospects for Brain Repair. *Nat Rev Neurol* (2015) 11(1):56–64. doi: 10.1038/nrneurol.2014.207
9. Hopfner KP, Hornung V. Molecular Mechanisms and Cellular Functions of Cgas-Sting Signalling. *Nat Rev Mol Cell Biol* (2020) 21(9):501–21. doi: 10.1038/s41580-020-0244-x
10. Ishikawa H, Ma Z, Barber GN. Sting Regulates Intracellular DNA-Mediated, Type I Interferon-Dependent Innate Immunity. *Nature* (2009) 461(7265):788–92. doi: 10.1038/nature08476
11. Barber GN. Sting: Infection, Inflammation and Cancer. *Nat Rev Immunol* (2015) 15(12):760–70. doi: 10.1038/nri3921
12. Abe T, Harashima A, Xia T, Konno H, Konno K, Morales A, et al. Sting Recognition of Cytoplasmic DNA Instigates Cellular Defense. *Mol Cell* (2013) 50(1):5–15. doi: 10.1016/j.molcel.2013.01.039
13. Decout A, Katz JD, Venkatraman S, Ablasser A. The Cgas-Sting Pathway as a Therapeutic Target in Inflammatory Diseases. *Nat Rev Immunol* (2021) 21(9):548–69. doi: 10.1038/s41577-021-00524-z
14. Jiang M, Chen P, Wang L, Li W, Chen B, Liu Y, et al. Cgas-Sting, an Important Pathway in Cancer Immunotherapy. *J Hematol Oncol* (2020) 13(1):81. doi: 10.1186/s13045-020-00916-z
15. Reinert LS, Lopušná K, Winther H, Sun C, Thomsen MK, Nandakumar R, et al. Sensing of Hsv-1 by the Cgas-Sting Pathway in Microglia Orchestrates Antiviral Defence in the Cns. *Nat Commun* (2016) 7:13348. doi: 10.1038/ncomms13348
16. Peng Y, Zhuang J, Ying G, Zeng H, Zhou H, Cao Y, et al. Stimulator of Ifn Genes Mediates Neuroinflammatory Injury by Suppressing Ampk Signal in Experimental Subarachnoid Hemorrhage. *J Neuroinflamm* (2020) 17(1):165. doi: 10.1186/s12974-020-01830-4
17. Liao Y, Cheng J, Kong X, Li S, Li X, Zhang M, et al. Hdac3 Inhibition Ameliorates Ischemia/Reperfusion-Induced Brain Injury by Regulating the Microglial Cgas-Sting Pathway. *Theranostics* (2020) 10(21):9644–62. doi: 10.7150/thno.47651
18. Jiang GL, Yang XL, Zhou HJ, Long J, Liu B, Zhang LM, et al. Cgas Knockdown Promotes Microglial M2 Polarization to Alleviate Neuroinflammation by Inhibiting Cgas-Sting Signaling Pathway in Cerebral Ischemic Stroke. *Brain Res Bull* (2021) 171:183–95. doi: 10.1016/j.brainresbull.2021.03.010
19. Li Q, Cao Y, Dang C, Han B, Han R, Ma H, et al. Inhibition of Double-Strand DNA-Sensing Cgas Ameliorates Brain Injury After Ischemic Stroke. *EMBO Mol Med* (2020) 12(4):e11002. doi: 10.15252/emmm.201911002
20. Wang R, Zhu Y, Liu Z, Chang L, Bai X, Kang L, et al. Neutrophil Extracellular Traps Promote Tpa-Induced Brain Hemorrhage *Via* Cgas in Mice With Stroke. *Blood* (2021) 138(1):91–103. doi: 10.1182/blood.2020008913
21. West AP, Khoury-Hanold W, Staron M, Tal MC, Pineda CM, Lang SM, et al. Mitochondrial DNA Stress Primes the Antiviral Innate Immune Response. *Nature* (2015) 520(7548):553–7. doi: 10.1038/nature14156
22. Nakahira K, Hisata S, Choi AM. The Roles of Mitochondrial Damage-Associated Molecular Patterns in Diseases. *Antioxid Redox Signal* (2015) 23(17):1329–50. doi: 10.1089/ars.2015.6407
23. Krysko DV, Agostinis P, Krysko O, Garg AD, Bachert C, Lambrecht BN, et al. Emerging Role of Damage-Associated Molecular Patterns Derived From Mitochondria in Inflammation. *Trends Immunol* (2011) 32(4):157–64. doi: 10.1016/j.it.2011.01.005
24. Xu P, Zhang X, Liu Q, Xie Y, Shi X, Chen J, et al. Microglial Trem-1 Receptor Mediates Neuroinflammatory Injury *Via* Interaction With Syk in Experimental Ischemic Stroke. *Cell Death Dis* (2019) 10(8):555. doi: 10.1038/s41419-019-1777-9
25. Xu P, Liu Q, Xie Y, Shi X, Li Y, Peng M, et al. Breast Cancer Susceptibility Protein 1 (Brca1) Rescues Neurons From Cerebral Ischemia/Reperfusion Injury Through Nrf2-Mediated Antioxidant Pathway. *Redox Biol* (2018) 18:158–72. doi: 10.1016/j.redox.2018.06.012
26. Haag SM, Gulen MF, Reymond L, Gibelin A, Abrami L, Decout A, et al. Targeting Sting With Covalent Small-Molecule Inhibitors. *Nature* (2018) 559(7713):269–73. doi: 10.1038/s41586-018-0287-8
27. Zhang X, Wu J, Liu Q, Li X, Li S, Chen J, et al. Mtdna-Sting Pathway Promotes Necroptosis-Dependent Enterocyte Injury in Intestinal Ischemia Reperfusion. *Cell Death Dis* (2020) 11(12):1050. doi: 10.1038/s41419-020-03239-6
28. Bi X, Du C, Wang X, Wang XY, Han W, Wang Y, et al. Mitochondrial Damage-Induced Innate Immune Activation in Vascular Smooth Muscle Cells Promotes Chronic Kidney Disease-Associated Plaque Vulnerability. *Adv Sci (Weinh)* (2021) 8(5):2002738. doi: 10.1002/advs.202002738
29. Zhong W, Rao Z, Rao J, Han G, Wang P, Jiang T, et al. Aging Aggravated Liver Ischemia and Reperfusion Injury by Promoting Sting-Mediated Nlrp3 Activation in Macrophages. *Aging Cell* (2020) 19(8):e13186. doi: 10.1111/acel.13186

30. Chen J, Li Y, Wang L, Zhang Z, Lu D, Lu M, et al. Therapeutic Benefit of Intravenous Administration of Bone Marrow Stromal Cells After Cerebral Ischemia in Rats. *Stroke* (2001) 32(4):1005–11. doi: 10.1161/01.str.32.4.1005
31. D'Hooge R, De Deyn PP. Applications of the Morris Water Maze in the Study of Learning and Memory. *Brain Res Brain Res Rev* (2001) 36(1):60–90. doi: 10.1016/s0165-0173(01)00067-4
32. Xie Y, Guo H, Wang L, Xu L, Zhang X, Yu L, et al. Human Albumin Attenuates Excessive Innate Immunity *Via* Inhibition of Microglial Mincle/Syk Signaling in Subarachnoid Hemorrhage. *Brain Behav Immun* (2017) 60:346–60. doi: 10.1016/j.bbi.2016.11.004
33. Xu P, Tao C, Zhu Y, Wang G, Kong L, Li W, et al. Tak1 Mediates Neuronal Pyroptosis in Early Brain Injury After Subarachnoid Hemorrhage. *J Neuroinflamm* (2021) 18(1):188. doi: 10.1186/s12974-021-02226-8
34. Yu CH, Davidson S, Harapas CR, Hilton JB, Mlodzianoski MJ, Laohamonthonkul P, et al. Tdp-43 Triggers Mitochondrial DNA Release *Via* Mptp to Activate Cgas/Sting in Als. *Cell* (2020) 183(3):636–649.e618. doi: 10.1016/j.cell.2020.09.020
35. He Z, Ning N, Zhou Q, Khoshnam SE, Farzaneh M. Mitochondria as a Therapeutic Target for Ischemic Stroke. *Free Radic Biol Med* (2020) 146:45–58. doi: 10.1016/j.freeradbiomed.2019.11.005
36. Li F, Wang N, Zheng Y, Luo Y, Zhang Y. Cgas- Stimulator of Interferon Genes Signaling in Central Nervous System Disorders. *Aging Dis* (2021) 12(7):1658–74. doi: 10.14336/ad.2021.0304
37. Sliter DA, Martinez J, Hao L, Chen X, Sun N, Fischer TD, et al. Parkin and Pink1 Mitigate Sting-Induced Inflammation. *Nature* (2018) 561(7722):258–62. doi: 10.1038/s41586-018-0448-9
38. Gamdzyk M, Doycheva DM, Araujo C, Ocak U, Luo Y, Tang J, et al. Cgas/Sting Pathway Activation Contributes to Delayed Neurodegeneration in Neonatal Hypoxia-Ischemia Rat Model: Possible Involvement of Line-1. *Mol Neurobiol* (2020) 57(6):2600–19. doi: 10.1007/s12035-020-01904-7
39. Abdullah A, Zhang M, Frugier T, Bedoui S, Taylor JM, Crack PJ. Sting-Mediated Type-I Interferons Contribute to the Neuroinflammatory Process and Detrimental Effects Following Traumatic Brain Injury. *J Neuroinflamm* (2018) 15(1):323. doi: 10.1186/s12974-018-1354-7
40. Jin R, Yang G, Li G. Inflammatory Mechanisms in Ischemic Stroke: Role of Inflammatory Cells. *J Leukoc Biol* (2010) 87(5):779–89. doi: 10.1189/jlb.1109766
41. Hanisch UK, Kettenmann H. Microglia: Active Sensor and Versatile Effector Cells in the Normal and Pathologic Brain. *Nat Neurosci* (2007) 10(11):1387–94. doi: 10.1038/nn1997
42. He T, Li W, Song Y, Li Z, Tang Y, Zhang Z, et al. Sestrin2 Regulates Microglia Polarization Through Mtor-Mediated Autophagic Flux to Attenuate Inflammation During Experimental Brain Ischemia. *J Neuroinflamm* (2020) 17(1):329. doi: 10.1186/s12974-020-01987-y
43. Wang D, Liu F, Zhu L, Lin P, Han F, Wang X, et al. Fgf21 Alleviates Neuroinflammation Following Ischemic Stroke by Modulating the Temporal and Spatial Dynamics of Microglia/Macrophages. *J Neuroinflamm* (2020) 17(1):257. doi: 10.1186/s12974-020-01921-2
44. Li QQ, Ding DH, Wang XY, Sun YY, Wu J. Lipoxin A4 Regulates Microglial M1/M2 Polarization After Cerebral Ischemia-Reperfusion Injury *Via* the Notch Signaling Pathway. *Exp Neurol* (2021) 339:113645. doi: 10.1016/j.expneurol.2021.113645
45. Martin GR, Blomquist CM, Henare KL, Jirik FR. Stimulator of Interferon Genes (Sting) Activation Exacerbates Experimental Colitis in Mice. *Sci Rep* (2019) 9(1):14281. doi: 10.1038/s41598-019-50656-5
46. Gelderblom M, Leypoldt F, Steinbach K, Behrens D, Choe CU, Siler DA, et al. Temporal and Spatial Dynamics of Cerebral Immune Cell Accumulation in Stroke. *Stroke* (2009) 40(5):1849–57. doi: 10.1161/strokeaha.108.534503
47. Cai X, Chiu YH, Chen ZJ. The Cgas-Cgamp-Sting Pathway of Cytosolic DNA Sensing and Signaling. *Mol Cell* (2014) 54(2):289–96. doi: 10.1016/j.molcel.2014.03.040
48. Abe T, Barber GN. Cytosolic-DNA-Mediated, Sting-Dependent Proinflammatory Gene Induction Necessitates Canonical Nf-κb Activation Through Tbk1. *J Virol* (2014) 88(10):5328–41. doi: 10.1128/jvi.00037-14
49. Zhao SC, Ma LS, Chu ZH, Xu H, Wu WQ, Liu F. Regulation of Microglial Activation in Stroke. *Acta Pharmacol Sin* (2017) 38(4):445–58. doi: 10.1038/aps.2016.162
50. Wang W, Hu D, Wu C, Feng Y, Li A, Liu W, et al. Sting Promotes Nlrp3 Localization in Er and Facilitates Nlrp3 Deubiquitination to Activate the Inflammasome Upon Hsv-1 Infection. *PloS Pathog* (2020) 16(3):e1008335. doi: 10.1371/journal.ppat.1008335
51. Xiao L, Zheng H, Li J, Wang Q, Sun H. Neuroinflammation Mediated by Nlrp3 Inflammasome After Intracerebral Hemorrhage and Potential Therapeutic Targets. *Mol Neurobiol* (2020) 57(12):5130–49. doi: 10.1007/s12035-020-02082-2
52. Jin MM, Wang F, Qi D, Liu WW, Gu C, Mao CJ, et al. A Critical Role of Autophagy in Regulating Microglia Polarization in Neurodegeneration. *Front Aging Neurosci* (2018) 10:378. doi: 10.3389/fnagi.2018.00378
53. Gomes MTR, Guimarães ES, Marinho FV, Macedo I, Aguiar E, Barber GN, et al. Sting Regulates Metabolic Reprogramming in Macrophages *Via* Hif-1α During Brucella Infection. *PloS Pathog* (2021) 17(5):e1009597. doi: 10.1371/journal.ppat.1009597
54. Liu Q, Wu J, Zhang X, Li X, Wu X, Zhao Y, et al. Circulating Mitochondrial DNA-Triggered Autophagy Dysfunction *Via* Sting Underlies Sepsis-Related Acute Lung Injury. *Cell Death Dis* (2021) 12(7):673. doi: 10.1038/s41419-021-03961-9
55. Yang JL, Mukda S, Chen SD. Diverse Roles of Mitochondria in Ischemic Stroke. *Redox Biol* (2018) 16:263–75. doi: 10.1016/j.redox.2018.03.002
56. Zhang X, Wu X, Hu Q, Wu J, Wang G, Hong Z, et al. Mitochondrial DNA in Liver Inflammation and Oxidative Stress. *Life Sci* (2019) 236:116464. doi: 10.1016/j.lfs.2019.05.020
57. Riley JS, Tait SW. Mitochondrial DNA in Inflammation and Immunity. *EMBO Rep* (2020) 21(4):e49799. doi: 10.15252/embr.201949799
58. Hayakawa K, Esposito E, Wang X, Terasaki Y, Liu Y, Xing C, et al. Transfer of Mitochondria From Astrocytes to Neurons After Stroke. *Nature* (2016) 535(7613):551–5. doi: 10.1038/nature18928
59. Davis CH, Kim KY, Bushong EA, Mills EA, Boassa D, Shih T, et al. Transcellular Degradation of Axonal Mitochondria. *Proc Natl Acad Sci USA* (2014) 111(26):9633–8. doi: 10.1073/pnas.1404651111
60. Joshi AU, Minhas PS, Liddelow SA, Haileselassie B, Andreasson KI, Dorn GW2nd, et al. Fragmented Mitochondria Released From Microglia Trigger A1 Astrocytic Response and Propagate Inflammatory Neurodegeneration. *Nat Neurosci* (2019) 22(10):1635–48. doi: 10.1038/s41593-019-0486-0

Conflict of Interest: The authors declare that the research was conducted in the absence of any commercial or financial relationships that could be construed as a potential conflict of interest.

GLOSSARY

ALS	Amyotrophic lateral sclerosis
ANOVA	One-way analysis of variance
Arg-1	Arginase-1
CBF	Cerebral blood flow
CCA	Common carotid artery
cGAMP	Cyclic guanosine monophosphate-adenosine monophosphate
cGAS	Cyclic GMP-AMP synthase
CNS	Central nervous system
DAPI	4',6-Diamidino-2-phenyl-indole
DMEM	Dulbecco's modified Eagle's medium
dsDNA	Double-stranded DNA
ECA	External carotid artery
FJC	Fluoro-Jade C
GAPDH	Glyceraldehyde-3-phosphate dehydrogenase
GFAP	Glial fibrillary acidic protein
HIE	Hypoxic-ischemic encephalopathy
I/R	Ischemia–reperfusion
Iba1	Ionized calcium-binding adaptor molecule 1
ICA	Internal carotid artery
i.c.v	Intracerebroventricular injection
iNOS	Inducible nitric oxide synthase
i.p.	Intraperitoneal injection
IRF3	Transcription factor 3
MCAO	Middle cerebral artery occlusion
mNSS	Modified neurological severity score
mtDNA	Mitochondrial DNA
NeuN	Neuronal nuclei
NF-κB	Nuclear factor-κB
NIH	National Institute of Health
NLRP3	Nucleotide-binding oligomerization domain (Nod)-like receptor pyrin domain containing 3
OGD/R	Microglia oxygen-glucose deprivation/reperfusion
PBS	Phosphate-buffered saline
PFA	Paraformaldehyde
qPCR	Quantitative polymerase chain reaction
SAH	Subarachnoid hemorrhage
SD	Standard deviation
si-NC	Scrambled siRNA
siRNA	Short interfering RNA
ssDNA	Signal-stranded DNA
STING	Stimulator of IFN genes
TBI	Traumatic brain injury
TBST	Tris-buffered saline containing Tween-20
TTC	2,3,5-Triphenyltetrazolium chloride
TUNEL	Terminal deoxynucleotidyl transferase-mediated dUTP nick end-labeling

frontiers | Frontiers in Cellular Neuroscience

REVIEW
published: 04 May 2022
doi: 10.3389/fncel.2022.864426

Endoplasmic Reticulum Stress and the Unfolded Protein Response in Cerebral Ischemia/Reperfusion Injury

Lei Wang[1†], Yan Liu[2†], Xu Zhang[1], Yingze Ye[1], Xiaoxing Xiong[1], Shudi Zhang[1], Lijuan Gu[3], Zhihong Jian[1] and Hongfa Wang[4*]*

[1] Department of Neurosurgery, Renmin Hospital of Wuhan University, Wuhan, China, [2] Department of Anesthesiology, Renmin Hospital of Wuhan University, Wuhan, China, [3] Central Laboratory, Renmin Hospital of Wuhan University, Wuhan, China, [4] Rehabilitation Medicine Center, Department of Anesthesiology, Zhejiang Provincial People's Hospital, Affiliated People's Hospital, Hangzhou Medical College, Hangzhou, China

OPEN ACCESS

Edited by:
Yan Wang,
Peking University Third Hospital, China

Reviewed by:
Xiaoyu Wang,
Zhejiang University, China
Xingchun Gao,
Yale University, United States
Rongjing Ge,
Bengbu Medical College, China

***Correspondence:**
Hongfa Wang
whf033@163.com
Zhihong Jian
zhihong@whu.edu.cn

[†] These authors have contributed equally to this work

Specialty section:
This article was submitted to Cellular Neuropathology, a section of the journal Frontiers in Cellular Neuroscience

Received: 28 January 2022
Accepted: 07 March 2022
Published: 04 May 2022

Citation:
Wang L, Liu Y, Zhang X, Ye Y, Xiong X, Zhang S, Gu L, Jian Z and Wang H (2022) Endoplasmic Reticulum Stress and the Unfolded Protein Response in Cerebral Ischemia/Reperfusion Injury. Front. Cell. Neurosci. 16:864426. doi: 10.3389/fncel.2022.864426

Ischemic stroke is an acute cerebrovascular disease characterized by sudden interruption of blood flow in a certain part of the brain, leading to serious disability and death. At present, treatment methods for ischemic stroke are limited to thrombolysis or thrombus removal, but the treatment window is very narrow. However, recovery of cerebral blood circulation further causes cerebral ischemia/reperfusion injury (CIRI). The endoplasmic reticulum (ER) plays an important role in protein secretion, membrane protein folding, transportation, and maintenance of intracellular calcium homeostasis. Endoplasmic reticulum stress (ERS) plays a crucial role in cerebral ischemia pathophysiology. Mild ERS helps improve cell tolerance and restore cell homeostasis; however, excessive or long-term ERS causes apoptotic pathway activation. Specifically, the protein kinase R-like endoplasmic reticulum kinase (PERK), activating transcription factor 6 (ATF6), and inositol-requiring enzyme 1 (IRE1) pathways are significantly activated following initiation of the unfolded protein response (UPR). CIRI-induced apoptosis leads to nerve cell death, which ultimately aggravates neurological deficits in patients. Therefore, it is necessary and important to comprehensively explore the mechanism of ERS in CIRI to identify methods for preserving brain cells and neuronal function after ischemia.

Keywords: ER stress, unfolded protein response (UPR), cerebral ischemia-reperfusion injury (CIRI), inflammation, apoptosis

INTRODUCTION

Ischemic stroke, which accounts for approximately 87% of all stroke cases (Kuriakose and Xiao, 2020), results in severe symptoms and is responsible for the majority of stroke-related deaths and disabilities. The main cause of ischemic stroke is cerebrovascular blockade, which leads to brain dysfunction in the corresponding region. As the disability rate and mortality rate of ischemic stroke are very high, this disease seriously affects the health of individuals and imposes a large burden on society and the economy (Poustchi et al., 2021). The amount of glucose and glycogen stored in brain tissue is very low, making the brain very sensitive to reduced blood flow, which can lead to

irreversible damage after 20 min (Kristian, 2004). Compared with other organs, the brain is rich in polyunsaturated fatty acids (FAs) but contains very low levels of protective antioxidants such as superoxide dismutase and catalase. Thus, it is very sensitive to oxidative stress injury (Adibhatla and Hatcher, 2010). During ischemic stroke, cerebral blood flow is interrupted or reduced, resulting in hypoxic and ischemic damage to brain cells, cell necrosis, or cell apoptosis. During ischemia, anaerobic metabolism dominates in tissues, and adenosine triphosphate (ATP) levels decrease rapidly. Lactate accumulates, leading to a decrease in the intracellular pH value, leading to an imbalance in ATP-dependent ion transport, overload of intracellular calcium ions, and swelling and rupture of cells, ultimately mediating cell death through necrosis, apoptosis, and autophagy (Kalogeris et al., 2012).

At present, the methods for achieving vascular recanalization in patients with ischemic stroke mainly include the use of recombinant tissue plasminogen activator (rtPA) and vascular interventional thrombectomy. Basic and clinical research has led to improvements in the treatment of ischemic stroke. Intravenous rtPA is the recommended treatment for acute cerebral infarction within 4.5 h of onset (Man et al., 2020; Powers, 2020). However, due to time constraints, the existing treatment methods are limited. Importantly, ischemic stroke may lead to intracranial hemorrhage (ICH), cause additional brain injury, and even endanger the patient's life. When blood flow is restored to the brain after a certain period of time, brain injury and brain dysfunction are often aggravated. This phenomenon, called cerebral ischemia/reperfusion injury (CIRI) (Sun et al., 2018), occurs because although oxygen levels are restored to normal after reperfusion, reactive oxygen species (ROS) are produced during this process, and infiltration of proinflammatory neutrophils into ischemic tissues aggravates ischemic injury, eventually leading to mitochondrial permeability transition (MPT) pore opening and further irreversible damage (Kalogeris et al., 2012). The pathophysiological process of CIRI is complex and involves a variety of different mechanisms, including oxidative stress, inflammation, intracellular Ca^{2+} overload, mitochondrial dysfunction, apoptotic cell death, and excitatory amino acid toxicity (Kalogeris et al., 2016; Campbell et al., 2019; Datta et al., 2020). These factors are interrelated and interact with each other to eventually cause nerve cell death and neurological dysfunction. Recent studies have shown that CIRI can also cause endoplasmic reticulum (ER) damage and dysfunction, activate downstream signaling pathways, contribute to ischemia/reperfusion injury, and have an important impact on nerve cell apoptosis and survival (Hetz and Saxena, 2017).

The ER is an organelle that is found in all eukaryotic cells except mature red blood cells and is mainly responsible for the secretion and folding of proteins, the storage and release of calcium, the synthesis and distribution of lipids, and other functions (Stefan et al., 2011; Oakes and Papa, 2015; Addinsall et al., 2018). However, the ER is also sensitive to the environment. In the presence of abnormal energy metabolism, changes of glycosylation, disorder of calcium balance, drugs, toxins, and other influencing factors, the function of the ER will be impaired, leading to the aggregation of misfolded proteins and endoplasmic reticulum stress (ERS) (Guan et al., 2014). Moreover, the ER is one of the earliest organelles in cells to respond to external stress. There are three responses associated with ERS, namely, the unfolded protein response (UPR), the endoplasmic reticulum overload response (EOR), and the sterol regulatory element-binding protein (SREBP) pathway regulation response (Pahl, 1999). ERS most commonly involves the UPR, which helps cells adapt to changes in the intracellular microenvironment by altering the functional state of the ER (Markouli et al., 2020). When ERS is caused by changes in the internal and external environment, the UPR is initiated to alleviate the harmful effects caused by ERS and maintain intracellular homeostasis. The UPR involves a reduction in translational activity, an increase in protein folding ability, and activation of the protein degradation pathway. Particularly, the ER-associated degradation (ERAD) or the ubiquitin–proteasome system (UPS) (Sanderson et al., 2015; Sprenkle et al., 2017). The function of the UPR depends on the stress level. When the degree of ERS is low or the duration is short, the purpose of the UPR is to restore ER homeostasis, but when the degree of ERS is high or the duration is long, the main purpose of the terminal stage of the UPR is promotion of apoptosis (Walter and Ron, 2011; Hetz and Papa, 2018). The UPR regulates the transcription and translation of proteins in cells to alleviate harm and reduce the probability of protein misfolding. If this mechanism cannot achieve its purpose, inflammatory and apoptotic pathways may be activated, leading to the exacerbation of the inflammatory response in the nervous system, affecting cell survival (Bellezza et al., 2014; Logsdon et al., 2016).

Endoplasmic reticulum stress plays a key role in the progression of CIRI (Xin et al., 2014; Yang and Paschen, 2016). Severe CIRI disrupts ER homeostasis and leads to cell death (Luchetti et al., 2017). The function of early ERS is to restore the stability of the internal environment of the ER and protect cells. Transient and mild ERS helps cells reestablish homeostasis. However, long-term severe ERS disrupts cell homeostasis, leading to apoptosis and aggravating brain injury (Szegezdi et al., 2006; Chi et al., 2019). ERS signals are transmitted through three UPR receptors, i.e., inositol-requiring enzyme 1 (IRE1), protein kinase R-like endoplasmic reticulum kinase (PERK), and activating transcription factor 6 (ATF6), to enter the ER. These receptors bind glucose-regulated protein 78 (GRP78)/Bip (also known as HSP5A) on the ER membrane, which maintains them in an inactive state. Under unstressed conditions, GRP78/Bip binds ATF6, IRE1, and PERK to prevent them from activating downstream signaling events. When the amount of unfolded or misfolded proteins increases, Bip dissociates from these receptors and helps fold unfolded or misfolded proteins, resulting in activation of these receptors and downstream signaling events (Zhang and Kaufman, 2006). Cerebral ischemia causes a series of pathophysiological processes in which ERS-mediated apoptosis eventually leads to brain cell death (Zhao et al., 2018). Therefore, strategies that can effectively regulate ERS may be useful for the treatment of cerebral ischemia. Elucidating the interaction between the ER, cerebral ischemia, and the underlying mechanism is important for the development of effective treatments for cerebral ischemia.

FACTORS RELATED TO CEREBRAL ISCHEMIA/REPERFUSION INJURY-INDUCED ENDOPLASMIC RETICULUM STRESS

Ca^{2+} Overload

Ca^{2+} plays an important role in a variety of pathophysiological processes in cells, such as gene expression, protein synthesis and transport, and cell proliferation and differentiation (Clapham, 2007). The ER and mitochondria interact and influence each other and can form physical contact points called mitochondria-associated endoplasmic reticulum membranes (MAMs) (Hayashi et al., 2009). The ER also contacts the plasma membrane (PM), and the interaction between the ER and PM is controlled by Ca^{2+} levels (Toulmay and Prinz, 2011). In the ER, calcium is needed to activate calcium-dependent molecular chaperones that can stabilize protein folding intermediates (Kim et al., 2008). Thus, it can affect ERS.

Ca^{2+} homeostasis disruption in the ER plays a decisive role in many neurological diseases, including stroke (Paschen and Mengesdorf, 2005). During cerebral ischemia, many mechanisms can cause an increase in the intracellular Ca^{2+} content. During cerebral ischemia occurs, the brain mainly relies on glucose-independent degradation to generate ATP due to the lack of oxygen and energy in nerve cells, leading to the aggregation of lactate, hydrogen ions, and nicotinamide adenine dinucleotide and a decrease in the intracellular pH. To restore a normal pH, H^+ is excreted via Na^+/H^+ exchange, which in turn leads to Na^+ inflow. However, the increase in Na^+ content is prevented by the Na^+/Ca^{2+} exchanger, which increases intracellular Ca^{2+} levels. During hypoxia, the sarco/endoplasmic reticulum Ca^{2+}-ATPase (SERCA) is impaired, reducing the uptake of calcium by the ER and increasing the release of calcium. This further aggravates intracellular calcium overload and seriously affects the calcium storage function of the ER, leading to disruption of ER homeostasis (Sanada et al., 2011). Furthermore, due to the large increase in ROS levels, intracellular Ca^{2+} content is markedly increased during reperfusion (Baines, 2009). In addition, nitric oxide (NO), which promotes the release of calcium ions from the ER into the cytoplasm that eventually leads to calcium overload, is produced during ischemia and hypoxia (Rajakumar et al., 2016).

When the concentration of Ca^{2+} reaches a lethal level in cells, a series of changes are triggered, and damage is aggravated (Kalogeris et al., 2012). First, some Ca^{2+} is transported into the mitochondria through unidirectional transport, but once the concentration of Ca^{2+} in mitochondria exceeds the tolerated level, MPT pore opening occurs. Second, a pathologically high concentration of Ca^{2+} in the cytoplasm leads to activation of Ca^{2+}/calmodulin-dependent protein kinases (CaMKs), which aggravates cell death and organelle dysfunction. Third, a high concentration of Ca^{2+} can increase the activity of calpain, promote protein translation, and lead to cell death. Fourth, a high concentration of calcium in cells can lead to the production of calcium pyrophosphate complexes and uric acid, which can combine with protein complexes in cells to form inflammasomes to promote the production of inflammatory factors and ultimately alter the inflammatory response. A high calcium concentration in the cytoplasm and a low calcium concentration in the ER and extracellular environment causes inactivation of a variety of calcium-dependent proteases, resulting in ERS.

Free Radicals

Free radicals include ROS and reactive nitrogen species (RNS). Normally, ROS and RNS play regulatory roles in ERS. The sources of ROS in different human tissues are different. The main sources of ROS in the brain are NADPH oxidase (NOX), mitochondria, xanthine oxidase (XO), and monoamine oxidase (MAO) (Granger and Kvietys, 2015). In the reperfusion phase of cerebral ischemia, the enzyme NOX uses oxygen as the final electron receptor through NADPH, leading to immediate production of O^{2-} which is involved in the degradation of NO and protein tyrosine nitration (Wu M. Y. et al., 2018). Mitochondria are also a main source of ROS in addition to generating energy and regulating cell signals and apoptosis (Murphy, 2009). MAO is located in the outer mitochondrial membrane and helps increase H2O2 production (Granger and Kvietys, 2015).

During ischemia/reperfusion injury, excessive ROS may lead to cell death through autophagy, necrosis, and apoptosis (Cursio et al., 2015). ROS can effectively trigger ERS, and severe ERS can lead to apoptosis during CIRI (Shi et al., 2019; Wei et al., 2019). Excessive ROS act on the ER, leading to depletion of calcium ions in the ER and entry of calcium ions into cells, which eventually causes calcium overload in cells, thereby aggravating ERS and inducing apoptosis. Some studies have shown that the ER and ROS interact through some factors and signaling pathways, including glutathione (GSH)/glutathione disulfide, NOX4, and Ca^{2+} (Cao and Kaufman, 2014).

After cerebral ischemia/reperfusion, oxygenated blood reenters the ischemic tissue and cause the production of a large amount of ROS. ROS can modify almost all biomolecules in cells, which leads to cell dysfunction (Raedschelders et al., 2012). At present, ROS mainly cause damage in the following three ways. First, they oxidize or nitrify key proteins involved in regulating cell signaling through the formation of covalent bonds (Lima et al., 2010). Second, reactive nitrogen/oxide species (RNOS) directly cause cell damage. Third, oxidants, such as hydrogen peroxide, cause indirect damage via regulation of signals in dysfunctional cells and regulation of the sulfhydryl redox cycle (Go et al., 2010). During ischemia, NO is produced via oxidation of arginine to citrulline, nitrite, nitrite reduction, and mitochondrial cytochrome c (Cyt c) oxidase under hypoxic conditions (Golwala et al., 2009). During the reperfusion stage, the amount of NO produced by ischemic tissue increases, and nitrite peroxide is produced in the ER. Nitrite peroxide is highly toxic and may affect the function of some proteins.

Inflammation

Endoplasmic reticulum stress and non-infectious inflammatory reactions are involved in many diseases. The inflammatory response participates in the pathophysiological process of CIRI, leading to cell death (Su et al., 2017). In contrast, some researchers have found that inhibiting the inflammatory response

can reduce the infarct volume, improve neurological function scores, and protect brain function in rats with middle cerebral artery occlusion (MCAO) (Liu et al., 2018c). Furthermore, a recent study on CIRI showed that local inflammation is one of the main causes of ERS. After cerebral ischemia/reperfusion, microglia release interleukin (IL)-1β, IL-6, and tumor necrosis factor-α (TNF-α). These proinflammatory cytokines promote the aggregation of inflammatory cells and the production of more inflammatory cytokines, which further aggravate brain function impairment (Mo et al., 2020).

Changes in cell permeability, cell edema, inflammation, and ERS are the main processes in early cerebral ischemia. After reperfusion, blood circulation is restored, and oxygen and neutrophils reach the ischemic tissue. However, some tissues are necrotic, leading to aggravation of neutral cell aggregation and the production of ROS-dependent mediators. These mediators can promote leukocyte adhesion to the posterior vein of the capillary wall and enter the tissue to aggravate injury (Kvietys and Granger, 2012). Activation of TNF, IL-6, and IL-8 further induces ERS (Lee et al., 2019). Nuclear factor κB (NF-κB) plays a key role in the immune response and can promote the expression of inflammatory factors. In addition, ERS can promote the activation of the NF-κB signaling pathway and promote inflammation (Adolph et al., 2013). In response to ERS, eukaryotic initiation factor 2α (eIF2α) phosphorylation reduces global mRNA translation and stimulates NF-κB transcription. Inhibition of mRNA translation can reduce the protein levels of inhibitor of nuclear factor κB (IκB) and NF-κB (Deng et al., 2004). Studies have shown that eIF2α phosphorylation can inhibit the expression of IκB and activate the NF-κB pathway. Some scholars speculate that this may be because the half-life ratio of IκB to NF-κB is short, causing an increase in the proportion of NF-κB relative to IκB, leading to NF-κB nuclear translocation (Sprenkle et al., 2017). NF-κB is an inflammation-related cytokine that promotes the inflammatory response, leading to the overexpression of iNOS, IL-1β, and IL-6, aggravating CIRI (Sun et al., 2014). In turn, ERS can also be regulated by the NF-κB signaling pathway. Sphingosine kinase 1 (SPHK1) is a novel regulator of ERS. One study showed that SPHK1 can activate the NF-κB pathway, causing ERS (Zhang et al., 2020).

Endoplasmic reticulum stress can also affect inflammation. Recent studies have reported that ERS can regulate TNF-α, IL-12, and matrix metalloproteinase-12 expression. In addition, a study showed that the inositol-requiring enzyme 1α (IRE1α)-X box-binding protein 1 (XBP1) pathway can activate NLRP3 inflammasome-mediated inflammation. Particularly, XBP1 can activate the NLRP3 inflammasome, convert inactive caspase-1 into active caspase-1, and promote the conversion of IL-1β precursor into the active form of IL-1β, causing its secretion into the extracellular space (Yue et al., 2016). ROS produced by mitochondria can consistently activate the NLRP3 inflammasome and affect the function of mitochondria. Inhibition of NLRP3 activation can reduce neuronal injury and exert a neuroprotective effect after CIRI (Guo et al., 2018), while ERS and autophagy promote the death of neurons after cerebral ischemia through the NLRP3 inflammasome (Xu et al., 2021).

Therefore, ERS and the inflammatory response have a causal relationship. However, the mechanism underlying the interaction between ERS and inflammation in specific environments is still unclear. In addition, the crosstalk between ERS and inflammation in neurons, astrocytes, and microglia continues to be elucidated (Sprenkle et al., 2017). It is worth noting that the role of inflammation in CIRI has received increasing attention.

SIGNAL TRANSDUCTION PATHWAYS INVOLVED IN ENDOPLASMIC RETICULUM STRESS

Blockage of cerebral blood flow causes the initiation of the UPR followed by impairment of ER or cell function. The UPR involves many enzymes and transcription factors. To date, three ER transmembrane receptors, i.e., PERK, IRE1, and ATF6, which mediate three different signaling pathways that affect transcription and translation, have been identified (Schonthal, 2012; Gupta et al., 2016; Almanza et al., 2019). Under physiological conditions, these three proteins bind to the ER chaperone GRP78. The physical binding of GRP78 to these ER transmembrane proteins maintains the proteins in an inactive state. Under physiological conditions, these three transmembrane receptors bind to the ER molecular chaperone GRP78/Bip, inhibiting their functions (Bertolotti et al., 2000). During ERS, GRP78 dissociates from these transmembrane receptors and binds aggregated unfolded proteins. Then, PERK, IRE1, and ATF6 are autophosphorylated, and their signaling pathways are activated, leading to initiation of the UPR and maintenance of ER function (**Figure 1**; Volmer et al., 2013; Ibrahim et al., 2019). The activation of the three branches of the UPR leads to the formation of a complex signaling network that contributes to cellular processes such as protein folding, protein degradation, and cellular redox reactions. Misfolded proteins are degraded in the cellular matrix through a process called ERAD (Lopata et al., 2020). Ubiquitination of a substrate can promote its rapid hydrolysis. This helps to maintain the dynamic balance of the ER. In general, activated IRE1 and cleaved ATF6 are involved in XBP1-induced ERAD (Waldherr et al., 2019). The PERK, IRE1, and ATF6 signaling pathways are protective pathways as they relieve early ERS. When harmful stimuli or long-term stimulation impairs ER function, the ERS-mediated cell death pathway, autophagy, apoptosis, and related inflammatory reactions can be induced.

The PERK Pathway

Protein kinase R-like endoplasmic reticulum kinase is a type I transmembrane protein kinase located on the ER membrane (Harding et al., 1999). Its C-terminus contains a serine/threonine protein kinase domain found in upstream members of the eIF2α kinase family. During ERS, because unfolded or misfolded proteins in the ER competitively bind GRP78, GRP78 dissociates from PERK, resulting in disinhibition of PERK and activation of PERK through dimerization and autophosphorylation (McQuiston and Diehl, 2017). Activated

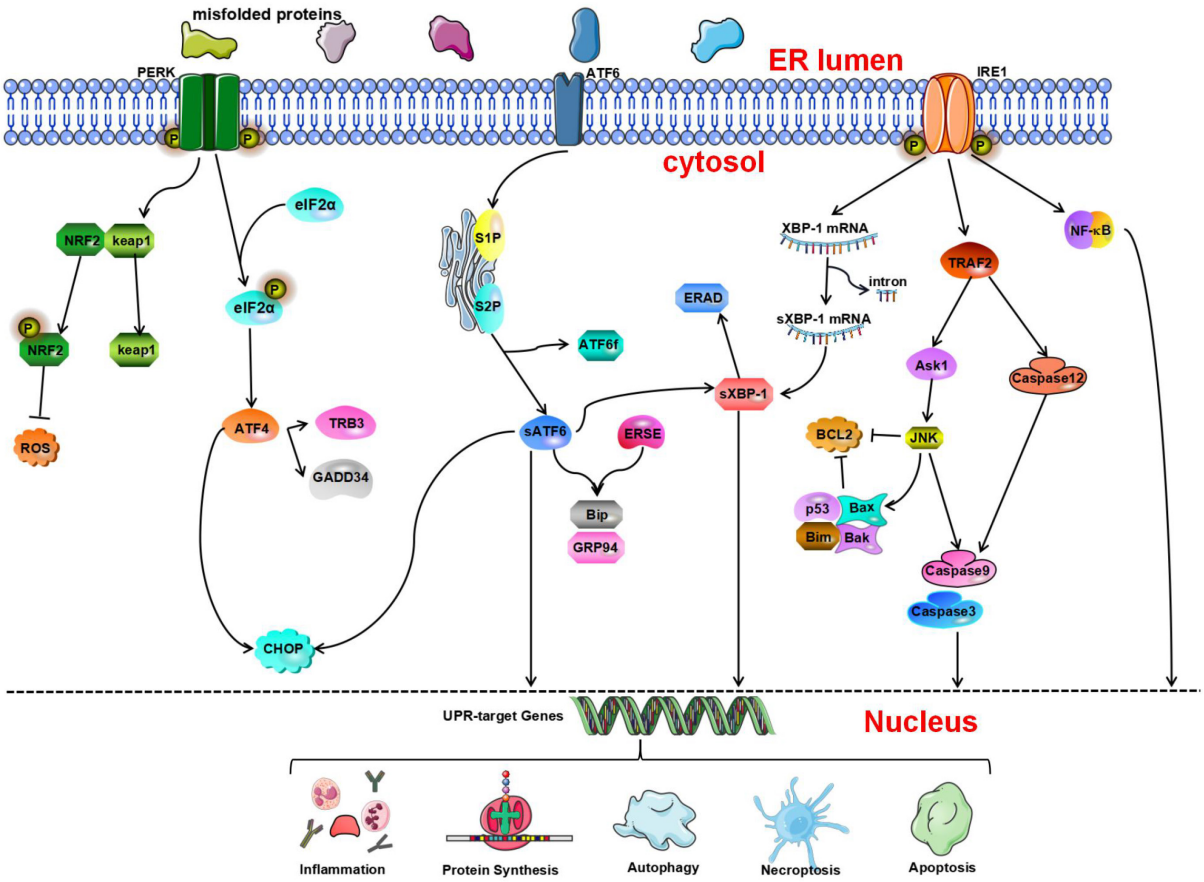

FIGURE 1 | The unfolded protein response (UPR) determines cell fate through the protein kinase R-like endoplasmic reticulum kinase (PERK), inositol-requiring enzyme 1 (IRE1), and activating transcription factor 6 (ATF 6) pathways. Nuclear factor erythroid 2-related factor 2 (NRF2) is phosphorylated by PERK and dissociates from Kelch-like ECH-associated protein 1 (Keap1) under oxidative stress conditions and then activates the expression of NRF2-dependent antioxidant genes. p-eIF2a can inhibit protein synthesis. Activated ATF4 induces the expression of growth arrest and DNA damage-inducible gene 34 (GADD34) and tribbles-related protein 3 (TRB3). ATF6 is cleaved by serene protease site 1 protease and site 2 protease (S1P and S2P, respectively) to generate ATF6f and activated sATF6. Then, it combines with endoplasmic reticulum stress response elements (ERSEs) to regulate and activate the expression of BiP and glucose regulating protein 94 (GRP94). In addition, IRE1 contributes to ERS-mediated apoptosis through the tumor necrosis factor receptor-associated factor 2- activate apoptosis signal-regulating kinase-1-c-Jun N-terminal kinase (TRAF2-ASK1-JNK) and caspase-12 pathways. In addition, inositol-requiring enzyme 1α (IRE1α) can activate the nuclear factor κB (NF-κB) signaling pathway to initiate inflammatory reactions.

PERK phosphorylates eIF2α, inhibits protein translation, and reduces the aggregation of unfolded proteins in the lumen of the ER (Harding et al., 2000). Phosphorylation of eIF2α can prevent the translation of mRNA (Starck et al., 2016). In the ER-related apoptotic pathway, phosphorylated PERK and eIF2α are significantly activated. It has been confirmed that during early ischemia/reperfusion, phosphorylation of eIF2α by PERK, which is the main mechanism through which the translation of proteins is inhibited during stresses, increases markedly (Owen et al., 2005; Gu et al., 2020). In addition to inhibiting protein translation, phosphorylated eIF2α can also activate the expression of activating transcription factor 4 (ATF4) (Harding et al., 2000). ATF4 is a member of the leucine zipper family and activates the basic region of transcription factors. It is a stress response gene and participates in the UPR. Under normal conditions, the content of ATF4 is very low, and ATF4 mRNA is rarely translated. In addition, some studies have shown that the transcription of ATF4 is dependent on phosphorylated eIF2α (Blais et al., 2004). ATF4 can activate two survival and apoptosis pathways during the UPR. ATF4 binds its activator to form a complex, which combines with the promoter of the survival-promoting gene GRP78 (Mamady and Storey, 2008). In addition, activated ATF4 induces the expression of CAAT/enhancer-binding protein (C/EBP) homologous protein (CHOP) (Palam et al., 2011; Han et al., 2013), growth arrest, DNA damage-inducible gene 34 (GADD34) (Ma and Hendershot, 2003), and tribbles-related protein 3 (TRB3) (Ohoka et al., 2005), which promote the initiation of apoptosis. The p-eIF2α-induced decrease in translation reduces the protein load in the lumen of the ER, while adaptive gene expression induced by ATF4 involves amino acid metabolism and protein homeostasis. These two signal regulation mechanisms help cells cope with ERS (Quiros et al., 2017). The PERK-ATF4-CHOP signaling pathway is

involved in neuronal apoptosis (Gu et al., 2020). ATF4 can promote the expression of some genes that are conducive to cell survival, and this coordinated prosurvival response is called the integrated stress response (Young and Wek, 2016; Hetz and Saxena, 2017).

Studies have also shown that phosphorylated PERK/eIF2α is important for activation of ERS-related autophagy. Once eIF2α is phosphorylated, it can promote the conversion of microtubule-associated protein 1A light chain 3 (LC3)-I to LC3-II (Hoyer-Hansen and Jaattela, 2007). During autophagy, LC3-I is transformed into LC3-II by cleavage of amino acids at the hydroxyl end, which activates the autophagy system (Gao et al., 2013). In addition, a recent study showed that PERK signaling participates in oxygen-glucose deprivation/reoxygenation (OGD/R)-induced microglial activation and neuroinflammatory responses following PTP1B inhibitor treatment. After CIRI, the PERK pathway is activated, the expression of ERS marker proteins is increased, and autophagy is activated. In microglia, a PTP1B inhibitor alleviates the deleterious effects of CIRI and plays a neuroprotective role by inhibiting autophagy in rats (Zhu et al., 2021).

Protein kinase R-like endoplasmic reticulum kinase can not only regulate eIF2α but also phosphorylate nuclear factor erythroid 2-related factor 2 (NRF2). NRF2 is involved in the regulation of the cellular stress response and can induce the expression of antioxidant enzymes (Oh and Jun, 2017). Under physiological conditions, NRF2 binds to its negative regulator Kelch-like ECH-associated protein 1 (Keap1) (Hu L. et al., 2018). It is phosphorylated by PERK and dissociates from Keap1 under oxidative stress conditions before translocating into the nucleus where it activates the expression of NRF2-dependent antioxidant genes (Cullinan et al., 2003; Waza et al., 2018). Ultimately, it can reduce apoptosis during ERS and maintain the redox balance in cells (Cullinan and Diehl, 2004). Oxidative stress leads to NRF2 activation, which in turn inhibits the increase in ROS levels and ameliorates cellular damage caused by oxidative stress (Ramezani et al., 2018). Some studies have shown that the levels of NRF2 and HO-1 decrease significantly, indicating that NRF2/HO-1 signaling is involved in CIRI (Tian et al., 2020). Therefore, NRF2 is an important signaling factor related to the PERK signaling pathway, and its downstream signaling pathway should be further studied.

The ATF6 Pathway

In mammals, ATF6 is an n-type membrane protein located in the ER (Haze et al., 1999). Its C-terminal end, which is inserted in the ER lumen, contains a GRP78-binding site and Golgi localization signal. The cytoplasmic N-terminal region contains basic leucine zipper (bZIP) and DNA transcriptional activity domains. ATF-6 has two configurations: ATF-6α and ATF-6β (Zhu et al., 1997). The former plays a leading role in ERS. When ERS occurs in cells, ATF6 is transported into the Golgi apparatus via the Golgi localization signal. Within the Golgi, ATF6 is cleaved by the serine proteases site 1 protease (S1P) and site 2 protease (S2P) to release the cytoplasmic fragment ATF6f, resulting in the activation of the protein (Ye et al., 2000). Activated sATF6 is a transcription factor containing a bZIP domain. After sATF6 leaves the Golgi apparatus and enters the nucleus, it combines with *cis*-acting endoplasmic reticulum stress response elements (ERSEs) in the nucleus to regulate and activate the expression of BiP, GRP94, and calnexin (Yoshida et al., 2001b; Wu et al., 2007; Yamamoto et al., 2007). In addition, ATF6 can stimulate the expression of CHOP and promote initiation of the UPR (Patwardhan et al., 2016).

Many studies have shown that an increase in ATF6 expression can regulate ERS and reduce cellular damage. A recent study showed that ischemic preconditioning can induce ATF6 expression, reduce ERS, and ultimately exert a neuroprotective effect (Lehotsky et al., 2009). Some studies have shown that the neurological function score of sATF6 knock-in mice is significantly increased, suggesting that activation of the ATF6 pathway can improve the outcome of CIRI (Yu et al., 2017). In addition, because the active form of ATF6 is rapidly degraded, the precursor of ATF6 can be used as a marker of early ERS (Thuerauf et al., 2002). Research has shown that ATF6α knockout mice exhibit more severe functional damage and a worse prognosis after myocardial ischemia or cerebral ischemia, indicating that ATF6 deficiency increases organ damage upon exposure to ischemia (Yoshikawa et al., 2015). Recent studies have shown that activation of the ATF6 signaling pathway in the brain after cardiac arrest is conducive to alleviating brain function impairment (Shen et al., 2021). Furthermore, a study showed that decreasing the cleavage of ATF6 in the Golgi apparatus can result in neuroprotection (Gharibani et al., 2013). It was also found that in a cerebral ischemia animal and reoxygenation cell models, taurine can inhibit the activation of ATF6, inhibit ERS, reduce cell apoptosis, and exert a neuroprotective effect after cerebral ischemia/reperfusion (Gharibani et al., 2013). Further molecular biology experiments are needed to validate the regulatory mechanism of ATF6 and its potential for CIRI treatment.

The IRE1 Pathway

Inositol-requiring enzyme 1α is a type 1 transmembrane protein that contains an N-terminal domain, cytoplasmic C-terminal (RNase) domain, and serine/threonine kinase domain (Liu et al., 2003; Lee et al., 2008). There are two IRE1 isoforms in mammals: IRE1α, which is ubiquitously expressed, and IRE1β, which is mainly expressed in the gastrointestinal tract and pulmonary mucosal epithelium (Martino et al., 2013). Both of these isoforms are involved in signal transduction in ERS.

During ERS, unfolded proteins that accumulate in the ER bind GRP78. GRP78 then dissociates from IRE1, causing homodimerization and autophosphorylation of IRE1, which subsequently causes the activation of its RNase domain (Korennykh et al., 2009). Activated IRE1 can cleave XBP1 precursor mRNA, resulting in the generation of active spliced XBP1 (sXBP1) (Yoshida et al., 2001a), which is a bZIP transcription factor (Liou et al., 1990). After entering the nucleus, sXBP1 mRNA is translated to generate a mature protein which can promote the expression of protein folding-related genes and ultimately alleviate ERS (Travers et al., 2000; Chen and Brandizzi, 2013; Hetz and Saxena, 2017). Studies have shown that XBP1 is related to ER-mediated degradation of many components, and that its degradation ability is dependent on

IRE1 (Yoshida et al., 2003). However, it should be noted that sXBP1 mRNA is quickly cleared from cells and is replaced by the uncleaved form (Marciniak et al., 2004). Studies have shown that under pathological conditions *in vitro*, ERS can cause complete cleavage of XBP1 mRNA. However, there have only been a few studies on this phenomenon. Therefore, care should be taken when performing quantitative analysis (Hosoi et al., 2010). sXBP1 is a key transcription factor in the regulation of cell survival (Hetz and Saxena, 2017). Persistent ERS results in sXBP1-mediated initiation of apoptosis via induction of CHOP expression (Dai et al., 2014).

Regarding UPR activation, celecoxib reduces ERS by promoting the IRE1-UPR pathway and ultimately exerts a neuroprotective effect (Santos-Galdiano et al., 2021). In addition, IRE1 contributes to ERS-mediated apoptosis through the c-Jun N-terminal kinase (JNK) and caspase-12 pathways. IRE1 can combine with TRAF2 to activate apoptosis signal-regulating kinase-1 (ASK1) and ultimately activate the JNK pathway and caspase-12, causing apoptosis (Nishitoh et al., 2002; Schonthal, 2013). It has been reported that taurine can significantly inhibit the IRE1 pathway and reduce apoptosis in animals and cell models (Gharibani et al., 2013). In addition, IRE1α can activate the NF-κB signaling pathway to initiate inflammatory reactions. In particular, the RNase domain of IRE1α mediates the degradation of a variety of mRNAs and microRNAs through a process called regulated IRE1-dependent decay (RIDD) and regulates pathological processes such as inflammation and apoptosis (Ghosh et al., 2014; Feldman et al., 2016; Wong et al., 2018).

ENDOPLASMIC RETICULUM STRESS AND CELL APOPTOSIS

Apoptosis is an important cell death pathway. Apoptosis is involved in the pathophysiological process of CIRI (Uzdensky, 2019). However, the process of neuronal apoptosis is complex. Recent studies have shown that three signal transduction pathways are involved in the regulation of apoptosis: the ERS pathway, the mitochondrial pathway, and the death receptor pathway (Ten and Galkin, 2019; Datta et al., 2020). ERS plays a vital role in stroke-induced neuronal apoptosis (Rao et al., 2004; Rozpedek et al., 2017; Mohammed et al., 2020). When cells cannot overcome external stress conditions, the UPR disrupts intracellular homeostasis and promotes apoptosis through CHOP/growth arrest, DNA damage-inducible gene 153 (GADD153), caspase-12, and JNK (**Figure 2**; Xin et al., 2014; Hetz et al., 2015; Hetz and Papa, 2018).

CHOP Signaling

CAAT/enhancer-binding protein (C/EBP) homologous protein, also known as GADD153, is a member of the C/EBP transcription factor family, which some studies have proven to be an important executor of ERS-induced apoptosis (Huang et al., 2017; Hu H. et al., 2018).

Studies have shown that CHOP is involved in apoptosis in the nervous system (Wang et al., 2013; Xin et al., 2014). The process through which CHOP causes apoptosis is described as follows. After GRP78 dissociates from PERK, ATF6, and IRE1, it activates CHOP and the proapoptotic signaling pathway. All three pathways of the UPR can induce CHOP activation. After ERS, ATF4, cleaved ATF6α, and XBP1 undergo nuclear translocation, resulting in the rapid and significant upregulation of CHOP expression (Yang et al., 2017), phosphorylated eIF2α can promote the expression of the transcription factor ATF4. Under stress conditions, the ATF4 signaling pathway can regulate redox reactions, amino acid metabolism, autophagy, and apoptosis. During irreversible cell stress, ATF4 can also activate the expression of the downstream protein CHOP and initiate cell apoptosis. Studies have shown that canopy FGF signaling regulator 2 (CNPY2) is involved in the regulation of ERS (Hong et al., 2017). During ERS, the binding partner of CNPY2 changes from GRP78 to PERK, resulting in activation of the PERK-CHOP pathway and promotion of apoptosis (Urra and Hetz, 2017). Inhibition of the CNPY2 signaling pathway can block neuronal apoptosis induced by CIRI, leading to neuroprotection (Zhao et al., 2021). In addition, a study showed that the transcription of CHOP is regulated by ATF6 (Yoshida et al., 2000). Although moderate ERS helps promote the proper folding and modification of problem proteins, excessive or prolonged ERS may lead to activation of CHOP and caspase-3 signaling and promote apoptosis (Addinsall et al., 2018). Studies have shown that CHOP can increase the expression of the proapoptotic protein Bim and inhibit the expression of the antiapoptotic protein Bcl-2 to play a proapoptotic role (McCullough et al., 2001; Puthalakath et al., 2007; Logue et al., 2013). In a study on CIRI, Tajiri et al. (2004) found that the number of apoptotic neurons is significantly reduced in CHOP knockout mice and that CHOP is involved in the regulation of apoptosis and the expression of antiapoptotic Bcl-2 protein family members. Furthermore, CHOP can induce the expression of death receptor 5 (DR5), which makes cells more sensitive to ER-induced apoptosis, ultimately promoting apoptosis (Yamaguchi and Wang, 2004). Furthermore, after cerebral ischemia, Bax, BAD, and Bak can translocate from the cytoplasm to the outer mitochondrial membrane, resulting in the release of Cyt-c and activation of Caspase-3, resulting in apoptosis (Broughton et al., 2009). Another target gene of CHOP is GADD34. Induction of GADD34 expression can inhibit the downstream PERK signaling pathway. In addition, GADD34 is essential for regulation of protein synthesis during ERS (Walter and Ron, 2011) and can regulate the phosphorylation of eIF2α (Marciniak et al., 2004).

The expression of CHOP during CIRI may depend on the state of the cell and the intensity of ischemia (Osada et al., 2010). CHOP mainly promotes apoptosis during the early stage of reperfusion (Tajiri et al., 2004). A study showed that CHOP protein expression is increased 3 h after cerebral ischemia/reperfusion, peaks at 24 h, and begins to decrease at 48 h, which is consistent with the timeline of neuronal apoptosis. Furthermore, α-difluoromethylornithine (DFMO) treatment can inhibit ERS by inhibiting the expression of CHOP and exert a neuroprotective effect after ischemia/reperfusion (Ding and Ba, 2015). These results prove that drugs that regulate the expression

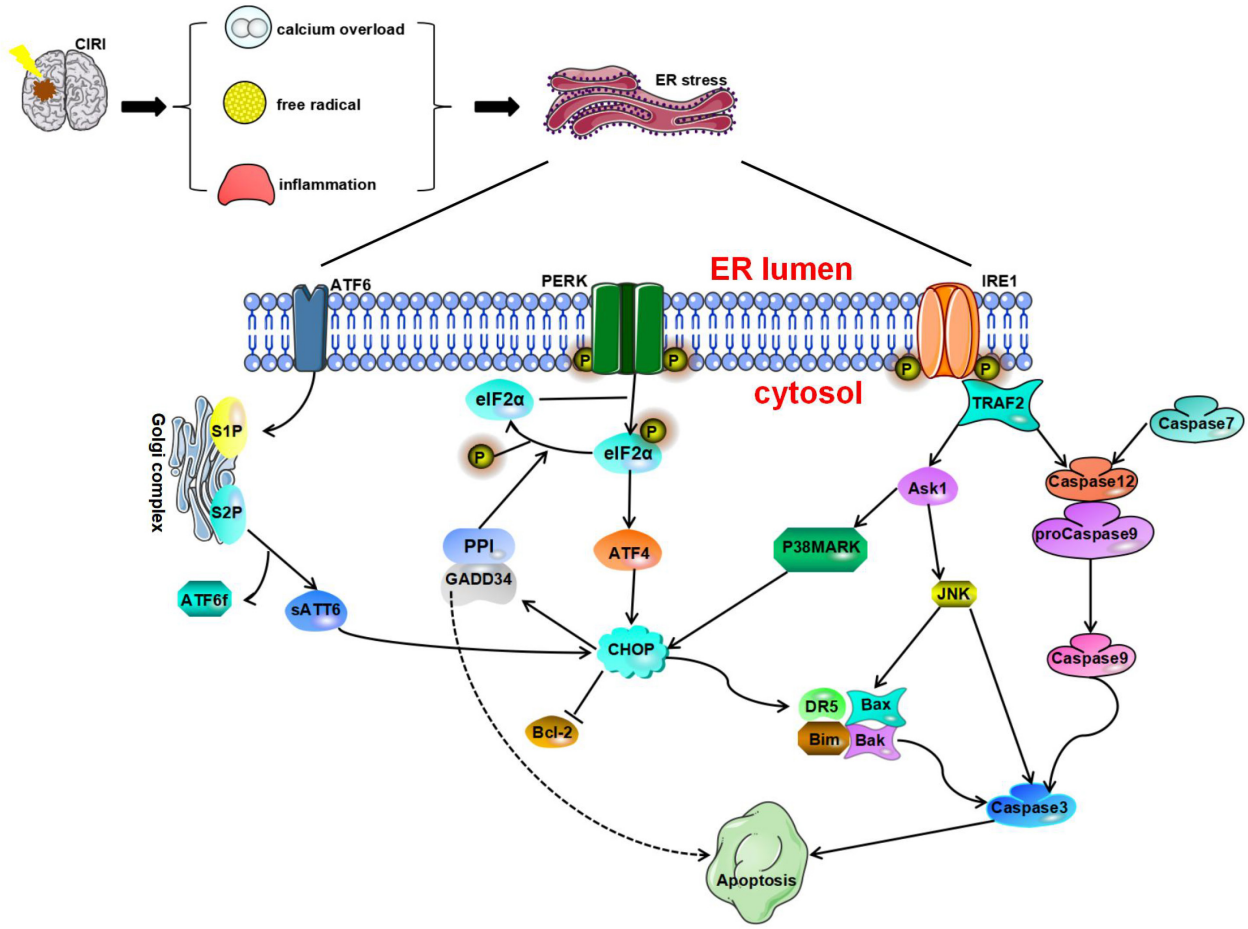

FIGURE 2 | Endoplasmic reticulum stress is a harmful process that induces apoptosis mediated by CAAT/enhancer-binding protein (C/EBP) homologous protein (CHOP), caspase-12, and JNK. Glucose-regulated protein 78 (GRP78) dissociates from protein kinase R-like endoplasmic reticulum kinase (PERK), ATF6, and IRE1 and ultimately initiates proapoptotic signaling pathways by activating CHOP. All three pathways of the UPR can induce CHOP activation. Phosphorylated eukaryotic initiation factor 2α (IF2α) can promote ATF4 expression and then activate the expression of the downstream protein CHOP and induce cell apoptosis. Furthermore, the translation of CHOP is regulated by ATF6. CHOP can increase the expression of Bim, death receptor 5 (DR5), Bax, and Bak and inhibit the expression of Bcl-2 to play a proapoptotic role. The IRE1 pathway and caspase-7 pathway can cause activation of caspase-12. Activated caspase-12 promotes the activation of caspase-3/9 and eventually leads to apoptosis. TRAF2 recruits and activates ASK1, which subsequently phosphorylates and activates JNK.

of CHOP can affect the prognosis of CIRI and that CHOP is a potential target for the treatment of CIRI.

Caspase-12 Signaling

Caspase-12 is a member of the IL-1β-converting enzyme (ICE) caspase subfamily. It is an important regulator of apoptosis and inflammation (García de la Cadena and Massieu, 2016). Caspase-12 usually negatively regulates the inflammatory response. It can inhibit the activation of caspase-1 in the inflammasome and regulate the expression of IL-1β and IL-18. Caspase-12 mRNA can be found in almost all tissues in mice. Under normal physiological conditions, TRAF2 forms a stable complex with procaspase-12. However, under stresses conditions, caspase-12 dissociates from TRAF2 (Yoneda et al., 2001).

It has been found that after alleviation of ischemia in tissues or cells, the levels of CHOP, Bax, activated caspase-12, and caspase-3 increase significantly, while the expression of Bcl-2 decreases (Guo et al., 2021). To date, three main pathways that can activate caspase-12 have been identified: the IRE1 pathway, the m-calpain pathway, and the caspase-7 pathway. IRE1α can trigger caspase-12 activation, while inactive pro-caspase-12 dissociates from the ER membrane and is then cleaved to trigger apoptosis (Sano and Reed, 2013; Yao et al., 2018). On the other hand, caspase-12 can be cleaved by other proteases, such as calpain and caspase-7 (Martinez et al., 2010; de la Cadena et al., 2014). In addition, in human neuroblastoma SK-N-SH cells incubated with thapsigargin (Tg) or Aβ, calpain inhibitors block the cleavage of caspase-12, indicating that calpain can reduce the expression level of caspase-12 (Matsuzaki et al., 2010). After ERS, caspase-7 translocates to the surface of the ER, forms a complex with caspase-12 and GRP78 on the surface of the ER, and mediates the cleavage of caspase-12 (Rao et al., 2001). Further studies have shown that activated caspase-12 is released into the cytoplasm and induces the activation of caspase-3/9 (Morishima et al., 2002;

Datta et al., 2018; Rong et al., 2020). Studies have also shown that cells lacking caspase-12 are resistant to apoptosis elicited by ERS inducers such as tunicamycin (Tm), Tg, and brefeldin A (BFA) (Nakagawa et al., 2000). Shibata et al. reported that caspase-12 is cleaved from 5 to 23 h after reperfusion following 1 h of ischemia in transient middle cerebral artery occlusion (tMCAO) model mice (Shibata et al., 2003). It has also been shown that the expression of PERK and caspase-12 in hippocampal neurons increases rapidly under glucose deprivation. This suggests that glucose deprivation alone can lead to caspase-12-dependent neuronal apoptosis (de la Cadena et al., 2014). Some researchers have suggested that caspase-12 can promote the apoptosis of neuronal cells, mainly during continuous aggravation of reperfusion (Zhu et al., 2012). Selenoprotein K (SELENOK) gene knockout can significantly induce ERS and lead to neuronal apoptosis (Jia S. Z. et al., 2021). However, due to the low proteolytic activity of SELENOK and the lack of related studies, the role of SELENOK in ischemia-induced apoptosis is still controversial (García de la Cadena and Massieu, 2016).

c-Jun N-Terminal Kinase Signaling

c-Jun N-terminal kinase plays an important role in the stress response, is involved in neuronal oxidative stress injury, and can mediate neuronal apoptosis (Ji et al., 2017). Like the CHOP and caspase-12 pathways, the JNK signaling pathway, which is activated during ERS, is considered an apoptosis-promoting pathway.

Phosphorylation of IRE1 in the cytoplasm stimulates the activation of TRAF2, which in turn phosphorylates and activates ASK1 and ultimately activates JNK (Cao and Kaufman, 2012). In addition, nervous system inflammation, ischemia, oxidative stress, and other stimuli can activate the expression of JNK. JNK regulates apoptosis by phosphorylating Stat3, p53, and Bcl-2 (Chen et al., 2003). JNK promotes Cyt c release and regulates caspase activation. Activation of the JNK signaling pathway during CIRI can lead to apoptosis of neuronal cells. It has been found that signals generated by the cytoplasmic kinase domain of IRE1 can regulate the JNK signaling pathway and may affect the regulation of apoptosis (Chakrabarti et al., 2011). Activated JNK can promote the expression of caspase-3 and other apoptosis-related genes and further initiate death receptor or mitochondrial pathways to induce apoptosis (Zhao et al., 2015). One study found that overexpression of aldehyde dehydrogenase 2 (ALDH2) can regulate JNK and caspase-3 activation and transcription in a model of cerebral ischemia, resulting in a significant reduction in mitochondrial-related apoptosis. These results suggest that ALDH2 may affect JNK-mediated mitochondrial apoptosis in ischemic stroke (Xia et al., 2020). It has been found that ischemic brain injury is often accompanied by increased apoptosis of nerve cells and that this cell apoptosis is obviously related to continuous activation of the IRE1α/TRAF2, JNK1/2, and p38 MAPK signaling pathways (Chen et al., 2015).

Drugs and compounds that regulate the JNK pathway, which reduce apoptosis and exerts neuroprotective effects, have been explored in several studies. In the early stage of CIRI, JNK inhibitors can reduce ERS and apoptosis and alleviate CIRI (Zhu et al., 2012). SP600125 is an effective JNK inhibitor that can ameliorate brain injury after CIRI (Khan et al., 2020). Traditional Chinese medicine plays a unique role in the treatment of cerebral ischemia injury, but the components of traditional Chinese medicine compounds are complex. Thus, some studies have focused on the effects of traditional Chinese medicine extracts. A recent study showed that senkyunolide I (SEI), an active constituent of the traditional Chinese medicine Ligusticum chuanxiong Hort. exerts a neuroprotective effect against glutamate-induced cell death. In addition, SEI can significantly inhibit the JNK/caspase-3 signaling pathway (Wang et al., 2021). JLX001 is a novel compound with a structure similar to that of cyclovirobuxine D (CVB-D). Some studies have proven that JLX001 exerts a neuroprotective effect against focal cerebral ischemic injury. Some researchers have studied the protective effects of JLX001 against CIRI and its antiapoptotic effects. The results showed that JLX001 can reduce neuronal apoptosis by inhibiting the JNK signaling pathway, thus exerting a protective effect against ischemia/reperfusion injury (Zhou et al., 2019). Another study showed that butylphthalide exerts an antiapoptotic effect after cerebral ischemic injury and that its effect is related to the regulation of the JNK/p38 MAPK signaling pathway (Bu et al., 2021).

OXIDATIVE STRESS AND CEREBRAL ISCHEMIA/REPERFUSION INJURY

Oxidative stress is characterized by an imbalance between oxidation and antioxidation. Under physiological conditions, ROS and RNS are involved in regulating various redox processes in cells and maintaining homeostasis of the intracellular environment. An increase in free radical levels is the main cause of oxidative stress (Valko et al., 2007). Some exogenous agents can stimulate the production of intracellular free radicals, such as ROS. When the level of ROS exceeds the antioxidant capacity of the cell, oxidative stress impairs intracellular protein synthesis and ER homeostasis and affects the survival of cells (Zeeshan et al., 2016). Excess Ca^{2+} is a source of free radicals in cells. An increase in the Ca^{2+} concentration in neuronal cells leads to activation of neuronal nitric oxide synthase (nNOS), which causes an oxidative stress response, cell homeostasis disruption, or cell injury. Another source of oxygen free radicals is mitochondria (Kalogeris et al., 2014). After cerebral ischemia/reperfusion, activated microglia can promote the production of ROS (Zrzavy et al., 2018). Neurons have high metabolic activity, consume a large amount of oxygen, express relatively low levels of endogenous antioxidant enzymes (such as catalase), and are particularly sensitive to oxidative stress. Thus, oxidative stress can easily cause neuronal cell damage.

Although the pathophysiological mechanism of ischemic stroke is complex, oxidative stress may play a key role in injury caused by ischemic stroke (Manzanero et al., 2013). Moreover, an increasing number of researchers are paying attention to the mechanism by which oxidative stress leads to brain damage after CIRI (Lorenzano et al., 2018). As described earlier, when the levels of ROS and RNS exceed the capacity of

the intracellular antioxidant system, oxidative stress and even cell damage occur. At low levels, ROS can act as signaling molecules in a variety of cellular processes (Scherz-Shouval and Elazar, 2007; Weidinger and Kozlov, 2015). ROS play a key role in the physiological regulation of metabolism and cell survival (Vicente-Gutierrez et al., 2019). However, when the level of ROS exceeds the capacity of the antioxidant and repair systems, ROS can oxidize various intracellular molecules or components, including lipids, DNA, proteins, and mitochondria, causing cell damage. Excessive production of ROS is considered an important mechanism underlying neuronal injury in the brain and impairment of nervous system function during CIRI (Ding et al., 2014). Excessive production of ROS affects the homeostasis of the intracellular environment, damages the normal structure of cells, and affects cell function, ultimately leading to cell necrosis and apoptosis (Cobley et al., 2018). These findings provide a direction for the development of treatments for ischemic stroke. Particularly, some researchers consider redox homeostasis maintenance a method for ischemic stroke treatment.

During reperfusion, the recovery of cerebral blood flow increases the amount of oxygen and nutrients supplied to brain tissue, which is very important for improving cell survival. However, this oxygen may also be used by pro-oxidant enzymes and mitochondria to produce excessive ROS in neuronal tissue, thus contributing to new and exacerbated tissue damage (Chen et al., 2011). This further proves that oxidative stress plays an important role in cerebral ischemic injury. Other studies have shown that oxidative stress can induce the release of Cyt c, leading to mitochondrial dysfunction, alterations in cell energy sources, and, ultimately, apoptosis (Chen et al., 2011). Regarding the specific mechanism, it has been found that cerebral ischemia leads to depolarization of the mitochondrial membrane potential ($\Delta\Psi m$), a reduction in ATP production, extracellular calcium overload, and the release of Cyt c, eventually leading to neuronal death (Liu et al., 2018b; Salehpour et al., 2019). During cerebral ischemia/reperfusion, a large amount of ROS is produced in mitochondria, and these ROS are transported to the outer mitochondrial membrane by Bcl-2 and the proapoptotic protein Bax. These then polymerize to form a membrane channel, which promotes the release of Cyt c from mitochondria into the cytoplasm. Cyt c released into the cytoplasm binds Apaf-1, combines with caspase-9 to form a complex, and finally activates caspase-3. Activated caspase-3 can cleave many nuclear DNA repair enzymes, preventing the repair of nuclear DNA damage during cerebral ischemia and causing apoptosis. CIRI causes mitochondrial edema and fragmentation, further inhibits the synthesis of ATP, and increases the production of ROS, directly leading to necrotic cell death. It has been found that at physiological concentrations, ROS coordinate with the antioxidant system *in vivo* and maintain cell function and the redox state. However, at high concentrations, ROS can inhibit the body's antioxidant defense system (Dasuri et al., 2013). Therefore, after a large amount of ROS passes through the ER membrane, which contains a large amount of lipids, ER function may be further impaired. In addition, oxidative stress can promote the formation of abnormal sulfur bonds, cause the production of a large number of abnormal intermediates, and inhibit the degradation of misfolded proteins.

Oxidative stress and inflammation interact during cerebral ischemia. Adaptive protection of the body during cerebral ischemia stimulates aseptic inflammation in the ischemic area. However, during reperfusion, ROS and blood-derived anti-inflammatory factors enter the ischemic tissue and the surrounding area, aggravating the inflammatory reaction. Furthermore, studies have shown that the UPR can trigger inflammation through its interaction with NF-κB. In turn, inflammation aggravates dysfunction of the internal environment, which can further aggravate ERS (Chaudhari et al., 2014). If this inflammatory response is not alleviated, various factors can trigger the apoptosis pathway mediated by the ER and mitochondria; that is, they can activate caspase-1 and caspase-9, further activate caspase-3 and deoxyribonucleases, induce DNA breaks, activate caspase-12 on the ER, and ultimately mediate apoptosis (Raturi and Simmen, 2013; Ye et al., 2013). Excess ROS may also damage endothelial cells (ECs) and degrade tight junction (TJ) proteins, greatly increasing the permeability of the blood–brain barrier (BBB). As a result, exogenous macromolecules can easily cross the BBB and enter brain tissue, further aggravating brain tissue injury and affecting neuronal function (Zhang et al., 2017). Ischemia/reperfusion facilitates the inflammatory response mediated by oxidative stress in ECs and promotes the recruitment and infiltration of peripheral immune cells into the ischemic area. The accumulation of immune cells and proinflammatory cytokines further promotes BBB disruption and aggravates brain injury (Jin et al., 2019).

Increasing evidence indicates that strategies that eliminate excess free radicals are beneficial in some diseases. Because oxidative stress is the key factor in BBB disruption and neuroinflammation, reducing the production of ROS in cells is a potential strategy for treating cerebral ischemia. Studies have found that some drugs, such as hesperidin, apigenin, and diosmin, can reduce the production of ROS, alleviate brain edema, decrease leukocyte aggregation in the ischemic area, and exert a protective effect against reperfusion injury (Mastantuono et al., 2015). Peroxiredoxin 4 (Prx4), a member of the antioxidant enzyme family (Prx1–6), is an efficient H_2O_2 scavenger. Within the ER, Prx4 can effectively eliminate peroxides (Zhu et al., 2014). Antioxidants can inhibit the production of intracellular ROS, attenuate damage to the BBB, and ameliorate brain injury (Zhang et al., 2017). Therefore, Prx4 may protect neuron function and alleviate CIRI by protecting EC function, reducing BBB damage, and regulating the inflammatory response (Yang et al., 2021). Mitochondria are the main organelles involved in regulation of cellular ROS production (Kausar et al., 2018). In line with this, studies have shown that natural and synthetic polyphenols increase the expression of antioxidant enzymes and cell protective proteins, reduce oxidative stress, inhibit the cellular inflammatory response, and protect cell function (Duong et al., 2014). In addition, these compounds can enhance mitochondrial function and biogenesis (Chen et al., 2019).

Endoplasmic reticulum stress and oxidative stress interact closely. An increase in the amount of unfolded proteins in the lumen of the ER can lead to the release of a large amount of calcium from the ER, and entry of calcium into mitochondria can impair the function of mitochondria, lead to the production of excessive ROS, and promote oxidative stress (Zhang et al., 2016). Furthermore, oxidative stress is an important cause of ERS (Nakka et al., 2016). When cells undergo oxidative stress, the redox balance of the ER is disruption, leading to impairment of ER function and ERS. Therefore, ERS and oxidative stress are closely related and should not be studied in isolation. We look forward to new research on their interaction.

CROSS-TALK BETWEEN ENDOPLASMIC RETICULUM STRESS AND MITOCHONDRIA

The mitochondria generates ATP, contributes to Ca^{2+} homeostasis, and regulation of ROS production. Mitochondrial dysfunction can impair cell energy production and cause oxidative stress, cellular injury, or apoptosis. Furthermore, mitochondrial dysfunction is an important factor in CIRI. In ischemic stroke, local cerebral blood flow is blocked, the supply of nutrients and oxygen is reduced, and the production of ATP is impaired, resulting in cell death. Mitochondrial dysfunction impairs energy generation, increases ROS production, and stimulates Cyt c release into the cytosol (Giorgi et al., 2018). Cells respond to environmental changes through autophagy. As a defense mechanism, autophagy can remove damaged organelles and metabolites in cells. Mitophagy is a selective form of macroautophagy. Its main function is to eliminate superfluous or damaged mitochondria and maintain normal cell function. In recent years, studies have shown that mitophagy can alleviate CIRI and play a neuroprotective role through a variety of mechanisms. However, the role of mitophagy in CIRI remains controversial. Some experts believe that excessive mitophagy can lead to cell death.

The ER is structurally and functionally coupled to mitochondria. In the axons of rodents, approximately 5% of the mitochondrial surface contacts the ER, forming an interconnected network which is conducive to the direct transport of $Ca2^{+}$ from the ER to mitochondria (Wu et al., 2017b). The endoplasmic reticulum-mitochondria encounter structure (ERMES) forms a junction between the mitochondria and the ER, which is involved in maintaining the morphological structure and function of the ER and mitochondria. Four ERMS proteins have been found in yeast, including the ER-anchored protein Mmm1 and three mitochondrial-related proteins, i.e., Mdm10, Mdm12, and Mdm34. Their functions are related to mitochondrial morphology and protein production (Stroud et al., 2011). In addition, the ER and mitochondria are both tubular organelles with dynamic characteristics. Thus, there are many contact points between them, and they interact to form regional membranes, namely, MAMs (Giacomello et al., 2020). MAMs are rich in glycosphingolipid-enriched microdomains (GEMs), which are structures that control $Ca2^{+}$ flow between the ER and mitochondria. In addition, MAMs can regulate lipid metabolism and the inflammatory response (Raturi and Simmen, 2013; Marchi et al., 2014). Inositol 1,4,5-trisphosphate receptors (IP3Rs) are the principal Ca^{2+} channels that regulate Ca^{2+} flux in these regions (Ahumada-Castro et al., 2021). Regarding the transfer of Ca^{2+}, it has been found that the voltage-dependent anion channels (VDACs) help Ca^{2+} released from the ER enter mitochondria (Csordas et al., 2018). IP3R is involved in mediating the release of Ca^{2+} into mitochondria, where Ca^{2+} regulates the activity of several enzymes and transporters.

There is also functional coupling between the ER and mitochondria, and they interact and depend on each other (Giorgi et al., 2009). ATP produced by mitochondrial oxidative phosphorylation is the energy source for correct folding of ER proteins. In addition, lipids produced during the folding of ER proteins are the material basis for the stability of the mitochondrial membrane. As the storage site for neutral lipids, lipid droplets (LDs) play a central role in FA homeostasis. LDs mainly contact the ER, but also contact mitochondria, peroxisomes, and lysosomes (Valm et al., 2017; Shai et al., 2018). Contacts between LDs and these organelles contribute to the maintenance of energy balance and cell survival. In addition, LD and organelles interact to form a metabolic center and regulate the biogenesis, growth, and distribution of LDs (Hariri et al., 2018; Ugrankar et al., 2019; Henne et al., 2020). Therefore, abnormal protein translation at LD contacts leads to various metabolic disorders (Herker et al., 2021).

Moreover, studies have shown that Ca^{2+} underlies the functional coupling between the ER and mitochondria and that Ca^{2+} transport from the ER to mitochondria plays an important role in regulating cell bioenergy, ROS production, autophagy, and apoptosis (Kaufman and Malhotra, 2014). In fact, the regulation of mitochondrial function is closely related to Ca^{2+} (Glancy and Balaban, 2012), and mitochondrial energy balance is regulated by Ca^{2+}(Bustos et al., 2017). Studies have shown that Ca^{2+} levels fluctuate during the cell cycle (Humeau et al., 2018); however, recently, Koval et al. (2019) found that uptake of Ca^{2+} in mitochondria through the mitochondrial Ca^{2+} uniporter (MCU) is necessary for to the production of energy by mitochondria and the maintenance of cell function. After cerebral ischemia, intracellular H^{+} levels increase, and the pH decreases due to anaerobic metabolism. To improve the intracellular environment, the intracellular ion exchange system is activated, resulting in intracellular calcium ion overload. Due to a rapid decrease in ATP content, the function of calcium ion pumps on the ER membrane, such as SERCA pumps, is impaired, and calcium cannot be absorbed. However, calcium ions stored in the ER are released into the cytoplasm, further aggravating intracellular calcium overload, disrupting calcium homeostasis in the ER and triggering or aggravating ERS.

We believe that ERS and mitophagy regulate each other, and that they are involved in the regulation of intracellular homeostasis. At present, the specific mechanisms underlying the interaction between ERS and mitochondria in ischemic stroke are not completely clear. Therefore, further detailed studies are

TABLE 1 | Several cytokines/compounds exacerbate or mitigate cerebral ischemia/reperfusion injury (CIRI) by regulating endoplasmic reticulum stress (ERS).

Cytokine/compound	Animal/cell model(s)	Model(s)	Intervention	Related protein changes	ERS pathway(s)	Effect	References
Taurine	Adult male Sprague–Dawley rats and primary cortical neurons	tMCAO and OGD/R	Taurine	Reduction in ERS (cleaved ATF6 and p-IRE1 levels) and decrease in apoptosis (caspase-3, CHOP, caspase-12, and BCL-2/Bax levels)	The ATF6 and IRE1 pathways	Protective	Gharibani et al., 2013
DETC-MeSO	Adult male Sprague–Dawley rats and primary neurons	tMCAO and OGD/R	DETC-MeSO	Reduction in ERS (p-PERK, p-eIF2α, ATF4, JNK, XBP-1, GADD34, and CHOP levels) and decrease in apoptosis (Bak, Bax, Bad, caspase-3, and BCL-2 levels)	The PERK pathway	Protective	Mohammad-Gharibani et al., 2014
Apelin-13	Adult male Wistar rats and primary cortical neurons	tMCAO and OGD/R	Apelin-13	Reduction in ERS (p-eIF2α, ATF4, CHOP and GRP78 levels) decrease in neuronal apoptosis	The PERK pathway	Protective	Wu F. et al., 2018
Aniline-derived compound (Comp-AD)	Male C57BL/6J mice	tMCAO	Comp-AD	Reduction in ERS (p-PERK and p-IRE1α levels)	The PERK and IRE1 pathways	Protective	Morihara et al., 2018
Dexmedetomidine	Male Sprague–Dawley rats and primary cortical neurons	tMCAO and OGD/R	Dexmedetomidine	Reduction in ERS (GRP78 and p-PERK levels) and decrease in apoptosis (CHOP, Caspase-11 and cleaved Caspase-3 levels)	The PERK pathway	Protective	Liu et al., 2018a
Homer1a	Primary cortical neurons	OGD/R	Homer1a overexpression	Reduction in ERS (p-PERK/PERK and p-IRE1/IRE1 levels) and alleviation of mitochondria dysfunction	The PERK pathway	Protective	Wei et al., 2019
Vascular endothelial growth factor (VEGF) inhibitor	Adult male BALB/C mice and BEND3 microvascular ECs	tMCAO and OGD/R	Intraperitoneal injection of anti-VEGF 30 min before MCAO and transfection with siRNA-VEGF	Reduction in ERS (XBP-1 and GRP78 levels), decrease in apoptosis (cleaved Caspase-3, CHOP and IRE1α levels), and decrease in ROS levels	The IRE1 pathway	Harmful	Feng et al., 2019
RTN1-C	N2a cells and primary neurons	OGD/R	RTN1-C knockdown	Reduction in ERS (GRP78, cleaved caspase-12, CHOP and cleaved caspase-3 levels) and decreases in cell viability and apoptosis	The PERK and IRE1 pathways	Harmful	Lin et al., 2019
Urolithin A	Male C57BL/6 mice, N2a cells and primary neurons	tMCAO and OGD/R	Intraperitoneal injection of Uro-A 24 h and 1 h before surgery	Alleviation of ERS (decreases in ATF6 and CHOP levels) and increase in cell viability	The PERK and ATF6 pathways	Protective	Ahsan et al., 2019

(Continued)

TABLE 1 | (Continued)

Cytokine/compound	Animal/cell model(s)	Model(s)	Intervention	Related protein changes	ERS pathway(s)	Effect	References
Icariin (ICA)	Primary microglia and primary cortical neurons	OGD/R	ICA	Alleviation of ERS (decreases in p-IRE1α, IRE1α, XBP1u, XBP1 s and Cleaved caspase-3 levels), enhancement of cell viability, and reduction in apoptosis	The IRE1 pathway	Protective	Mo et al., 2020
(–)-Clausenamide	Rat primary cortical neurons	OGD/R	(–)-Clausenamide	Inhibition of ERS (decreases in GRP78, eIF2α, ATF4 and CHOP levels) and attenuation of apoptosis (decrease in cleaved caspase-3 levels)	The PERK pathway	Protective	Wu et al., 2020
Ginsenoside Rg1	Sprague–Dawley rats and primary cortical neurons	tMCAO and OGD/R	Intraperitoneal injection of Rg1	Alleviation of ERS (decreases in PERK, eIF2α, ATF4, CHOP and TRB3 levels), inhibition of neuronal apoptosis (decreases in Bax, caspase-3, and BCL-2 levels), and improvement in neuronal viability	The PERK pathway	Protective	Gu et al., 2020
sc-222227	Male Wistar rats	tMCAO	Intracerebroventricular injection of sc-222227	Attenuation of ERS (decreases in p-PERK/total PERK, p-IRE1/total IRE1, and cleaved AFT6/full-length ATF6 levels)	The PERK, IRE1 and ATF6 pathways	Protective	Zhu et al., 2021
Berberine	PC12 cells	OGD/R	Berberine	Decrease in ERS (GRP78, CHOP, Bax and cleaved caspase-3 levels)	The PERK and IRE1 pathways	Protective	Xie et al., 2020
Cilostazol	Male Sprague–Dawley rats and brain microvascular endothelial cells (BMVECs)	tMCAO and OGD/R	Cilostazol	Attenuation of ERS (decreases in p-PERK, PERK, p-IRE1-α, IRE1-α, ATF-6, Bip levels)	The PERK, IRE1 and ATF6 pathways	Protective	Nan et al., 2019
CASP8 and FADD-like apoptosis regulator (CFLAR)	Male C57BL6 mice and primary human brain microvascular endothelial cells (HBMVECs)	tMCAO and OGD/R	CFLAR transfection and knockdown	Alleviation of ERS (decreases in GRP78, PERK, ATF6 and cleaved Caspase-12 levels) and increase in cell viability by CFLAR overexpression and reduction in cell viability by CFLAR silencing	The PERK and ATF6 pathways	Protective	Wang et al., 2019

needed to reveal the complex interaction network between them to provide a theoretical basis for improving CIRI treatments.

ENDOPLASMIC RETICULUM STRESS PLAYS AN IMPORTANT ROLE IN CEREBRAL ISCHEMIA/REPERFUSION INJURY

Endoplasmic reticulum stress is one of the mechanisms involved in CIRI. It may also play different roles in different stages of CIRI. The initial purpose of ERS is to maintain ER homeostasis, but prolonged or severe ERS may be harmful (Martin-Jimenez et al., 2017). Studies have shown that the UPR can promote the degradation of unfolded or incorrectly folded proteins and protect cells in the early stage of ischemia (Xin et al., 2014). However, upon prolongation of ischemia, the UPR can promote apoptosis. ERS and ERS-related apoptosis have been reported to contribute to ischemia/reperfusion injury (Wu et al., 2017a). The ER is sensitive to ischemia. Particularly, ER homeostasis is disrupted by hypoxia-hypoglycemia beginning in the early ischemic period, and ERS and ERS-related apoptosis are triggered and exacerbated in the reperfusion period (Wu F. et al., 2018). Hence, the mitochondrial pathway, the death receptor pathway, and ERS are generally considered the three primary apoptotic pathways (Gillies and Kuwana, 2014).

It has been demonstrated that regulation of the ERS-related signaling pathway is protective during ischemic stroke. Likewise, the PERK pathway may play a protective role in the early stage of ischemic stroke. Yoshikawa et al. (2015) showed that the ATF6 pathway participates in the early stage of ischemia, promotes the survival of neurons and glial cells, and plays a protective role in ischemic stroke. Gharibani et al. (2013) also proved that XBP1 might play a protective role by increasing the Bcl-2/Bax ratio and downregulating Caspase-3 expression *in vitro* during ischemia/reperfusion injury. These findings provide a theoretical basis for the development of related drugs for the treatment of CIRI via regulation of ERS.

Many studies have shown that the UPR can promote apoptosis in the late stage of ischemic stroke and that CHOP, Caspase-12, and JNK are involved in this process, with CHOP playing a leading role (Lopez-Hernandez et al., 2015; Poone et al., 2015). There is further evidence that the PERK pathway plays a major role in the expression of CHOP (Mei et al., 2013; Xin et al., 2014). A study showed that ERS promotes apoptosis through the PERK/eIF2α/caspase-3 pathway and that atorvastatin can reduce the protein expression of PERK, the dephosphorylation of eIF2α, and the activity of caspase-3, thus alleviating CIRI (Yang and Hu, 2015). In particular, excessive ERS can alter the permeability of the BBB (Kwak et al., 2015; Qie et al., 2017; Xu et al., 2019), making it easy for harmful substances to enter brain tissue. A recent study showed that salvinorin A can inhibit the ERS response, inhibit the production of ROS, reduce human brain microvascular endothelial cell (HBMEC) apoptosis, and increase the permeability of the BBB, ultimately alleviating brain injury and protecting neuronal function by activating the AMPK signaling pathway (Xin et al., 2021). Another study showed that adenosine acts as an endogenous neuroprotector by regulating Ca^{2+} homeostasis and glutamate release, reducing excitotoxic cellular damage after cerebral ischemia/reperfusion (Martire et al., 2019).

It has been found that inhibiting ERS can ameliorate CIRI and protect neuronal function (Nakka et al., 2010). Furthermore, studies have shown that hypoxia/reoxygenation (H/R) can induce ERS, increase the expression of ATF6 and GRP78, and ultimately lead to apoptosis. Liquiritin (LQ) treatment can reduce the expression of ATF6 and GRP78, inhibit the ERS pathway, and reduce apoptosis (Li et al., 2021). A study showed that the combination of *S*-methyl-*N,N*-diethyldithiocarbamate sulfoxide (DETC-MeSO) and taurine can reduce ERS in the ipsilateral ischemic penumbra; inhibit the ATF6, PERK, and IRE1 pathways; and reduce apoptosis (Gharibani et al., 2015). It has been found that lncRNAs are closely related to human diseases. Furthermore, some studies have shown that lncRNAs are involved in CIRI. It was found that the expression of MALAT1 is significantly increased during reperfusion in an OGD/R cell model. MALAT1 silencing can inhibit ERS and neuronal apoptosis and reduce neuronal damage (Jia Y. et al., 2021). Nucleotide-binding oligomerization domain 1 (NOD1) activates autophagy and ERS, decreasing cell survival. This suggests that NOD1 ultimately leads to CIRI via activation of ERS-mediated autophagy. Conversely, downregulating the expression of NOD1 can inhibit ERS and increase the viability of cortical neurons (Ma et al., 2020). Hyperhomocysteinemia (HHcy) is a well-known risk factor for stroke. The UPR is activated in a diet-induced HHcy model, and vitamin B supplementation alleviates ERS. HHcy exacerbated cellular injury during OGD/R. These effects can be prevented by vitamin B cotreatment (Tripathi et al., 2016).

In recent years, there have been many studies on CIRI, and it has been found that CIRI can be alleviated via regulation of ERS. Some of these studies are listed (**Table 1**) below. In some studies, cell survival was improved by targeting the apoptosis pathway related to ERS. Therefore, it is necessary to study the role and mechanism of ERS.

CONCLUDING REMARKS

After stroke, the degree of functional damage to nerve cells depends on the degree of tissue hypoperfusion. In the ischemic core, necrotic cells die within a few minutes. However, around the core necrotic area, there is often an ischemic marginal area, namely, the ischemic penumbra. Delayed cell death occurs through apoptosis. The goal of CIRI treatment is to preserve neurons in the ischemic penumbra and restore neuronal function as much as possible. The pathophysiological process of CIRI can trigger ERS, and ERS contributes to the occurrence and development of CIRI. In the present article, we describe various causes of ERS induced by CIRI, including calcium overload, ROS accumulation, and the inflammatory response. These factors not only lead to secondary brain injury but also hinder the recovery of neurological function after treatment. The degree of ERS determines the fate of cells. In the early stage of cerebral

ischemia/reperfusion, ERS can relieve damage to the ER and promote cell survival by initiating the UPR. In this paper, we also discussed the three signal transduction pathways related to ERS in detail. Excessive ERS leads to apoptosis, aggravates CIRI, and promotes apoptosis through the CHOP, caspase-12, and JNK signaling pathways. We also discussed the regulatory mechanism of these three signaling pathways in detail.

In the future, more in-depth research is needed to elucidate the specific mechanism underlying these phenomena. For example, when does ERS protect against and exacerbate ischemic stroke? Is the role of ERS different in different kinds of cells? In addition to considering the mechanisms and treatment effects in neurons, we should also pay attention to other cell populations, such as microglia. Animal studies have proven that inhibiting ERS can reduce the volume of the cerebral infarct, but how far are ERS inhibitors from clinical application? It is important to further determine the interaction between ERS and apoptosis and between ERS and inflammation to identify effective biological strategies for alleviating ERS and preventing brain injury after stroke. A large number of studies on the potential of alleviating CIRI using strategies targeting the apoptosis and inflammation pathways have been carried out, but more research, drug development, and clinical trials are needed. In addition, there are many studies on the molecular mechanism of ERS, but there have been few studies on the interaction between ERS, oxidative stress, and mitochondrial dysfunction. We believe that the interaction between these processes is worthy of in-depth study. At present, it is believed that interventions targeting ERS, including those that alter the expression of ligands in the ERS pathway and their receptors, can ameliorate CIRI and protect neuronal function. In addition, preventing the occurrence and development of brain cell apoptosis induced by ERS, which can protect neuronal function, may alleviate CIRI. We believe that solving these problems will open a new chapter in the treatment of ischemic stroke. Targeting ERS to treat CIRI is an important research direction. There are many mechanisms and answers that are not clear. Future research should focus on solving these problems and translating potential treatments from the laboratory to the clinic as soon as possible. ERS-targeted therapeutic strategies for cerebral ischemia are exciting areas of research as there are many unanswered questions. More careful research is needed in the future to translate such therapies from the laboratory to the clinic. In addition, previous studies focused on individual mechanisms underlying cerebral ischemic injury. We believe that these mechanisms occur simultaneously and synergize after cerebral ischemia. Therefore, we should study them as a whole and pay attention to their interaction.

AUTHOR CONTRIBUTIONS

LW wrote the initial draft. YL contributed to reviewing the literature. XZ and YY prepared the figures and submitted the manuscript. XX and SZ collected the literature and made the tables. ZJ, LG, and HW designed the manuscript and prepared the final version. All authors read and approved the final manuscript.

FUNDING

This work was supported by the Fundamental Research Funds for the Central Universities (No. 2042020kf0079), the Health Commission of Hubei Province Scientific Research Project (No. WJ2021M148), the National Natural Science Foundation of China (Nos. 82171336 and 81870939 to XX and Nos. 82071339 and 81771283 to LG), and the Hubei Province Key Laboratory Open Project (No. 2021KFY044).

REFERENCES

Addinsall, A. B., Wright, C. R., Andrikopoulos, S., Poel, C. V., and Stupka, N. (2018). Emerging roles of endoplasmic reticulum-resident selenoproteins in the regulation of cellular stress responses and the implications for metabolic disease. *Biochem. J.* 475, 1037–1057. doi: 10.1042/bcj20170920

Adibhatla, R. M., and Hatcher, J. F. (2010). Lipid oxidation and peroxidation in CNS health and disease: from molecular mechanisms to therapeutic opportunities. *Antioxid. Redox Signal.* 12, 125–169. doi: 10.1089/ars.2009.2668

Adolph, T. E., Tomczak, M. F., Niederreiter, L., Ko, H. J., Bock, J., Martinez-Naves, E., et al. (2013). Paneth cells as a site of origin for intestinal inflammation. *Nature* 503, 272–276. doi: 10.1038/nature12599

Ahsan, A., Zheng, Y. R., Wu, X. L., Tang, W. D., Liu, M. R., Ma, S. J., et al. (2019). Urolithin A-activated autophagy but not mitophagy protects against ischemic neuronal injury by inhibiting ER stress in vitro and in vivo. *CNS Neurosci. Ther.* 25, 976–986. doi: 10.1111/cns.13136

Ahumada-Castro, U., Bustos, G., Silva-Pavez, E., Puebla-Huerta, A., Lovy, A., and Cárdenas, C. (2021). In the right place at the right time: regulation of cell metabolism by IP3R-mediated inter-organelle Ca^{2+} fluxes. *Front. Cell Dev. Biol.* 9:629522. doi: 10.3389/fcell.2021.629522

Almanza, A., Carlesso, A., Chintha, C., Creedican, S., Doultsinos, D., Leuzzi, B., et al. (2019). Endoplasmic reticulum stress signalling – from basic mechanisms to clinical applications. *FEBS J.* 286, 241–278. doi: 10.1111/febs.14608

Baines, C. P. (2009). The mitochondrial permeability transition pore and ischemia-reperfusion injury. *Basic Res. Cardiol.* 104, 181–188. doi: 10.1007/s00395-009-0004-8

Bellezza, I., Grottelli, S., Mierla, A. L., Cacciatore, I., Fornasari, E., Roscini, L., et al. (2014). Neuroinflammation and endoplasmic reticulum stress are coregulated by cyclo(His-Pro) to prevent LPS neurotoxicity. *Int. J. Biochem. Cell Biol.* 51, 159–169. doi: 10.1016/j.biocel.2014.03.023

Bertolotti, A., Zhang, Y., Hendershot, L. M., Harding, H. P., and Ron, D. (2000). Dynamic interaction of BiP and ER stress transducers in the unfolded-protein response. *Nat. Cell Biol.* 2, 326–332. doi: 10.1038/35014014

Blais, J. D., Filipenko, V., Bi, M. X., Harding, H. P., Ron, D., Koumenis, C., et al. (2004). Activating transcription factor 4 is translationally regulated by hypoxic stress. *Mol. Cell Biol.* 24, 7469–7482. doi: 10.1128/mcb.24.17.7469-7482.2004

Broughton, B. R., Reutens, D. C., and Sobey, C. G. (2009). Apoptotic mechanisms after cerebral ischemia. *Stroke* 40, e331–e339. doi: 10.1161/strokeaha.108.531632

Bu, X. Y., Xia, W. Q., Wang, X. N., Lu, S., and Gao, Y. (2021). Butylphthalide inhibits nerve cell apoptosis in cerebral infarction rats via the JNK/p38 MAPK signaling pathway. *Exp. Ther. Med.* 21:565. doi: 10.3892/etm.2021.9997

Bustos, G., Cruz, P., Lovy, A., and Cárdenas, C. (2017). Endoplasmic reticulum-mitochondria calcium communication and the regulation of mitochondrial metabolism in cancer: a novel potential target. *Front. Oncol.* 7:199. doi: 10.3389/fonc.2017.00199

Campbell, B. C. V., de Silva, D. A., Macleod, M. R., Coutts, S. B., Schwamm, L. H., Davis, S. M., et al. (2019). Ischaemic stroke. *Nat. Rev. Dis. Primers* 5:70. doi: 10.1038/s41572-019-0118-8

Cao, S., and Kaufman, R. (2012). Unfolded protein response. *Curr. Biol.* 22, R622–R626. doi: 10.1016/j.cub.2012.07.004

Cao, S. S., and Kaufman, R. J. (2014). Endoplasmic reticulum stress and oxidative stress in cell fate decision and human disease. *Antioxid. Redox Signal.* 21, 396–413. doi: 10.1089/ars.2014.5851

Chakrabarti, A., Chen, A. W., and Varner, J. D. (2011). A review of the mammalian unfolded protein response. *Biotechnol. Bioeng.* 108, 2777–2793. doi: 10.1002/bit.23282

Chaudhari, N., Talwar, P., Parimisetty, A., Lefebvre d'Hellencourt, C., and Ravanan, P. (2014). A molecular web: endoplasmic reticulum stress, inflammation, and oxidative stress. *Front. Cell. Neurosci.* 8:213. doi: 10.3389/fncel.2014.00213

Chen, H., Yoshioka, H., Kim, G. S., Jung, J. E., Okami, N., Sakata, H., et al. (2011). Oxidative stress in ischemic brain damage: mechanisms of cell death and potential molecular targets for neuroprotection. *Antioxid. Redox Signal.* 14, 1505–1517. doi: 10.1089/ars.2010.3576

Chen, J. H., Kuo, H. C., Lee, K. F., and Tsai, T. H. (2015). Global proteomic analysis of brain tissues in transient ischemia brain damage in rats. *Int. J. Mol. Sci.* 16, 11873–11891. doi: 10.3390/ijms160611873

Chen, R. W., Qin, Z. H., Ren, M., Kanai, H., Chalecka-Franaszek, E., Leeds, P., et al. (2003). Regulation of c-Jun N-terminal kinase, p38 kinase and AP-1 DNA binding in cultured brain neurons: roles in glutamate excitotoxicity and lithium neuroprotection. *J. Neurochem.* 84, 566–575. doi: 10.1046/j.1471-4159.2003.01548.x

Chen, S. N., Sun, M., Zhao, X. H., Yang, Z. F., Liu, W. X., Cao, J. Y., et al. (2019). Neuroprotection of hydroxysafflor yellow A in experimental cerebral ischemia/reperfusion injury via metabolic inhibition of phenylalanine and mitochondrial biogenesis. *Mol. Med. Rep.* 19, 3009–3020. doi: 10.3892/mmr.2019.9959

Chen, Y., and Brandizzi, F. (2013). IRE1: ER stress sensor and cell fate executor. *Trends Cell Biol.* 23, 547–555. doi: 10.1016/j.tcb.2013.06.005

Chi, L., Jiao, D., Nan, G., Yuan, H., Shen, J., and Gao, Y. (2019). miR-9-5p attenuates ischemic stroke through targeting ERMP1-mediated endoplasmic reticulum stress. *Acta Histochem.* 121:151438. doi: 10.1016/j.acthis.2019.08.005

Clapham, D. E. (2007). Calcium signaling. *Cell* 131, 1047–1058. doi: 10.1016/j.cell.2007.11.028

Cobley, J. N., Fiorello, M. L., and Bailey, D. M. (2018). 13 reasons why the brain is susceptible to oxidative stress. *Redox Biol.* 15, 490–503. doi: 10.1016/j.redox.2018.01.008

Csordas, G., Weaver, D., and Hajnoczky, G. (2018). Endoplasmic reticulum-mitochondrial contactology: structure and signaling functions. *Trends Cell Biol.* 28, 523–540. doi: 10.1016/j.tcb.2018.02.009

Cullinan, S., and Diehl, J. (2004). PERK-dependent activation of Nrf2 contributes to redox homeostasis and cell survival following endoplasmic reticulum stress. *J. Biol. Chem.* 279, 20108–20117. doi: 10.1074/jbc.m314219200

Cullinan, S. B., Zhang, D., Hannink, M., Arvisais, E., Kaufman, R. J., and Diehl, J. A. (2003). Nrf2 is a direct PERK substrate and effector of PERK-dependent cell survival. *Mol. Cell. Biol.* 23, 7198–7209. doi: 10.1128/mcb.23.20.7198-7209.2003

Cursio, R., Colosetti, P., and Gugenheim, J. (2015). Autophagy and liver ischemia-reperfusion injury. *Biomed Res. Int.* 2015:417590. doi: 10.1155/2015/417590

Dai, M. X., Zheng, X. H., Yu, J., Yin, T., Ma, M. J., Zhang, L., et al. (2014). The impact of intermittent and repetitive cold stress exposure on endoplasmic reticulum stress and instability of atherosclerotic plaques. *Cell. Physiol. Biochem.* 34, 393–404. doi: 10.1159/000363008

Dasuri, K., Zhang, L., and Keller, J. N. (2013). Oxidative stress, neurodegeneration, and the balance of protein degradation and protein synthesis. *Free Radic. Biol. Med.* 62, 170–185. doi: 10.1016/j.freeradbiomed.2012.09.016

Datta, A., Sarmah, D., Mounica, L., Kaur, H., Kesharwani, R., Verma, G., et al. (2020). Cell death pathways in ischemic stroke and targeted pharmacotherapy. *Transl. Stroke Res.* 11, 1185–1202. doi: 10.1007/s12975-020-00806-z

Datta, D., Khatri, P., Singh, A., Saha, D. R., Verma, G., Raman, R., et al. (2018). *Mycobacterium fortuitum*-induced ER-MItochondrial calcium dynamics promotes calpain/caspase-12/caspase-9 mediated apoptosis in fish macrophages. *Cell Death Discov.* 4:30. doi: 10.1038/s41420-018-0034-9

de la Cadena, S. G., Hernandez-Fonseca, K., Camacho-Arroyo, I., and Massieu, L. (2014). Glucose deprivation induces reticulum stress by the PERK pathway and caspase-7- and calpain-mediated caspase-12 activation. *Apoptosis* 19, 414–427. doi: 10.1007/s10495-013-0930-7

Deng, J., Lu, P. D., Zhang, Y., Scheuner, D., Kaufman, R. J., Sonenberg, N., et al. (2004). Translational repression mediates activation of nuclear factor kappa B by phosphorylated translation initiation factor 2. *Mol. Cell. Biol.* 24, 10161–10168. doi: 10.1128/mcb.24.23.10161-10168.2004

Ding, L., and Ba, X. H. (2015). Role of ornithine decarboxylase/polyamine pathway in focal cerebral ischemia-reperfusion injury and its mechanism in rats. *Int. J. Clin. Exp. Med.* 8, 20624–20630.

Ding, Y., Chen, M. C., Wang, M., Wang, M. M., Zhang, T. J., Park, J. S., et al. (2014). Neuroprotection by acetyl-11-keto-beta-Boswellic acid, in ischemic brain injury involves the Nrf2/HO-1 defense pathway. *Sci. Rep.* 4:7002. doi: 10.1038/srep07002

Duong, T. T., Chami, B., McMahon, A. C., Fong, G. M., Dennis, J. M., Freedman, S. B., et al. (2014). Pre-treatment with the synthetic antioxidant T-butyl bisphenol protects cerebral tissues from experimental ischemia reperfusion injury. *J. Neurochem.* 130, 733–747. doi: 10.1111/jnc.12747

Feldman, H. C., Tong, M., Wang, L. K., Meza-Acevedo, R., Gobillot, T. A., Lebedev, I., et al. (2016). Structural and functional analysis of the allosteric inhibition of IRE1alpha with ATP-competitive ligands. *ACS Chem. Biol.* 11, 2195–2205. doi: 10.1021/acschembio.5b00940

Feng, S. Q., Zong, S. Y., Liu, J. X., Chen, Y., Xu, R., Yin, X., et al. (2019). VEGF antagonism attenuates cerebral ischemia/reperfusion-induced injury via inhibiting endoplasmic reticulum stress-mediated apoptosis. *Biol. Pharm. Bull.* 42, 692–702. doi: 10.1248/bpb.b18-00628

Gao, B., Zhang, X. Y., Han, R., Zhang, T. T., Chen, C., Qin, Z. H., et al. (2013). The endoplasmic reticulum stress inhibitor salubrinal inhibits the activation of autophagy and neuroprotection induced by brain ischemic preconditioning. *Acta Pharmacol. Sin.* 34, 657–666. doi: 10.1038/aps.2013.34

García de la Cadena, S., and Massieu, L. (2016). Caspases and their role in inflammation and ischemic neuronal death. Focus on caspase-12. *Apoptosis* 21, 763–777. doi: 10.1007/s10495-016-1247-0

Gharibani, P., Modi, J., Menzie, J., Alexandrescu, A., Ma, Z., Tao, R., et al. (2015). Comparison between single and combined post-treatment with S-Methyl-N,N-diethylthiolcarbamate sulfoxide and taurine following transient focal cerebral ischemia in rat brain. *Neuroscience* 300, 460–473. doi: 10.1016/j.neuroscience.2015.05.042

Gharibani, P. M., Modi, J., Pan, C. L., Menzie, J., Ma, Z. Y., Chen, P. C., et al. (2013). The mechanism of taurine protection against endoplasmic reticulum stress in an animal stroke model of cerebral artery occlusion and stroke-related conditions in primary neuronal cell culture. *Adv. Exp. Med. Biol.* 776, 241–258. doi: 10.1007/978-1-4614-6093-0_23

Ghosh, R., Wang, L. K., Wang, E. S., Perera, B. G., Igbaria, A., Morita, S. H., et al. (2014). Allosteric inhibition of the IRE1alpha RNase preserves cell viability and function during endoplasmic reticulum stress. *Cell* 158, 534–548. doi: 10.1016/j.cell.2014.07.002

Giacomello, M., Pyakurel, A., Glytsou, C., and Scorrano, L. (2020). The cell biology of mitochondrial membrane dynamics. *Nat. Rev. Mol. Cell Biol.* 21, 204–224. doi: 10.1038/s41580-020-0210-7

Gillies, L. A., and Kuwana, T. (2014). Apoptosis regulation at the mitochondrial outer membrane. *J. Cell. Biochem.* 115, 632–640. doi: 10.1002/jcb.24709

Giorgi, C., De Stefani, S. D., Bononi, A., Rizzuto, R., and Pinton, P. (2009). Structural and functional link between the mitochondrial network and the endoplasmic reticulum. *Int. J. Biochem. Cell Biol.* 41, 1817–1827. doi: 10.1016/j.biocel.2009.04.010

Giorgi, C., Marchi, S., Simoes, I. C. M., Ren, Z., Morciano, G., Perrone, M., et al. (2018). Mitochondria and reactive oxygen species in aging and age-related diseases. *Int. Rev. Cell Mol. Biol.* 340, 209–344. doi: 10.1016/bs.ircmb.2018.05.006

Glancy, B., and Balaban, R. S. (2012). Role of mitochondrial Ca^{2+} in the regulation of cellular energetics. *Biochemistry* 51, 2959–2973. doi: 10.1021/bi2018909

Go, Y. M., Park, H., Koval, M., Orr, M., Reed, M., Liang, Y., et al. (2010). A key role for mitochondria in endothelial signaling by plasma cysteine/cystine redox potential. *Free Radic. Biol. Med.* 48, 275–283. doi: 10.1016/j.freeradbiomed.2009.10.050

Golwala, N. H., Hodenette, C., Murthy, S. N., Nossaman, B. D., and Kadowitz, P. J. (2009). Vascular responses to nitrite are mediated by xanthine oxidoreductase and mitochondrial aldehyde dehydrogenase in the rat. *Can. J. Physiol. Pharmacol.* 87, 1095–1101. doi: 10.1139/y09-101

Granger, D. N., and Kvietys, P. R. (2015). Reperfusion injury and reactive oxygen species: the evolution of a concept. *Redox Biol.* 6, 524–551. doi: 10.1016/j.redox.2015.08.020

Gu, Y., Ren, K. W., Wang, L. M., Jiang, C. Z., and Yao, Q. Q. (2020). Rg1 in combination with mannitol protects neurons against glutamate-induced ER stress via the PERK-eIF2 alpha-ATF4 signaling pathway. *Life Sci.* 263:118559. doi: 10.1016/j.lfs.2020.118559

Guan, B. J., Krokowski, D., Majumder, M., Schmotzer, C. L., Kimball, S. R., Merrick, W. C., et al. (2014). Translational control during endoplasmic reticulum stress beyond phosphorylation of the translation initiation factor eIF2alpha. *J. Biol. Chem.* 289, 12593–12611. doi: 10.1074/jbc.m113.543215

Guo, M., Wang, X., Zhao, Y. X., Yang, Q., Ding, H. Y., Dong, Q., et al. (2018). Ketogenic diet improves brain ischemic tolerance and inhibits NLRP3 inflammasome activation by preventing Drp1-mediated mitochondrial fission and endoplasmic reticulum stress. *Front. Mol. Neurosci.* 11:86. doi: 10.3389/fnmol.2018.00086

Guo, M. M., Qu, S. B., Lu, H. L., Wang, W. B., He, M. L., Su, J. L., et al. (2021). Biochanin A alleviates cerebral ischemia/reperfusion injury by suppressing endoplasmic reticulum stress-induced apoptosis and p38MAPK signaling pathway in vivo and in vitro. *Front. Endocrinol.* 12:646720. doi: 10.3389/fendo.2021.646720

Gupta, M. K., Tahrir, F. G., Knezevic, T., White, M. K., Gordon, J., Cheung, J. Y., et al. (2016). GRP78 interacting partner Bag5 responds to ER stress and protects cardiomyocytes from ER stress-induced apoptosis. *J. Cell. Biochem.* 117, 1813–1821. doi: 10.1002/jcb.25481

Han, J., Back, S. H., Hur, J., Lin, Y. H., Gildersleeve, R., Shan, J. X., et al. (2013). ER-stress-induced transcriptional regulation increases protein synthesis leading to cell death. *Nat. Cell Biol.* 15, 481–490. doi: 10.1038/ncb2738

Harding, H. P., Zhang, Y., and Ron, D. (1999). Protein translation and folding are coupled by an endoplasmic-reticulum-resident kinase. *Nature* 397, 271–274. doi: 10.1038/16729

Harding, H. P., Zhang, Y., Bertolotti, A., Zeng, H., and Ron, D. (2000). Perk is essential for translational regulation and cell survival during the unfolded protein response. *Mol. Cell* 5, 897–904. doi: 10.1016/s1097-2765(00)80330-5

Hariri, H., Rogers, S., Ugrankar, R., Liu, Y. L., Feathers, J. R., and Henne, W. M. (2018). Lipid droplet biogenesis is spatially coordinated at ER-vacuole contacts under nutritional stress. *EMBO Rep.* 19, 57–72. doi: 10.15252/embr.201744815

Hayashi, T., Rizzuto, R., Hajnoczky, G., and Su, T. P. (2009). MAM: more than just a housekeeper. *Trends Cell Biol.* 19, 81–88. doi: 10.1016/j.tcb.2008.12.002

Haze, K., Yoshida, H., Yanagi, H., Yura, T., and Mori, K. (1999). Mammalian transcription factor ATF6 is synthesized as a transmembrane protein and activated by proteolysis in response to endoplasmic reticulum stress. *Mol. Biol. Cell* 10, 3787–3799. doi: 10.1091/mbc.10.11.3787

Henne, M., Goodman, J. M., and Hariri, H. (2020). Spatial compartmentalization of lipid droplet biogenesis. *Biochim. Biophys. Acta Mol. Cell Biol. Lipids* 1865:158499. doi: 10.1016/j.bbalip.2019.07.008

Herker, E., Vieyres, G., Beller, M., Krahmer, N., and Bohnert, M. (2021). Lipid droplet contact sites in health and disease. *Trends Cell Biol.* 31, 345–358. doi: 10.1016/j.tcb.2021.01.004

Hetz, C., Chevet, E., and Oakes, S. A. (2015). Proteostasis control by the unfolded protein response. *Nat. Cell Biol.* 17, 829–838. doi: 10.1038/ncb3184

Hetz, C., and Papa, F. R. (2018). The unfolded protein response and cell fate control. *Mol. Cell* 69, 169–181. doi: 10.1016/j.molcel.2017.06.017

Hetz, C., and Saxena, S. (2017). ER stress and the unfolded protein response in neurodegeneration. *Nat. Rev. Neurol.* 13, 477–491. doi: 10.1038/nrneurol.2017.99

Hong, F., Liu, B., Wu, B. X., Morreall, J., Roth, B., Davieset, C., et al. (2017). CNPY2 is a key initiator of the PERK-CHOP pathway of the unfolded protein response. *Nat. Struct. Mol. Biol.* 24, 834–839. doi: 10.1038/nsmb.3458

Hosoi, T., Ogawa, K., and Ozawa, K. (2010). Homocysteine induces X-box-binding protein 1 splicing in the mice brain. *Neurochem. Int.* 56, 216–220. doi: 10.1016/j.neuint.2009.12.005

Hoyer-Hansen, M., and Jaattela, M. (2007). Connecting endoplasmic reticulum stress to autophagy by unfolded protein response and calcium. *Cell Death Differ.* 14, 1576–1582. doi: 10.1038/sj.cdd.4402200

Hu, H., Tian, M. X., Ding, C., and Yu, S. Q. (2018). The C/EBP homologous protein (CHOP) transcription factor functions in endoplasmic reticulum stress-induced apoptosis and microbial infection. *Front. Immunol.* 9:3083. doi: 10.3389/fimmu.2018.03083

Hu, L., Chen, W., Tian, F., Yuan, C., Wang, H., and Yueet, H. (2018). Neuroprotective role of fucoxanthin against cerebral ischemic/reperfusion injury through activation of Nrf2/HO-1 signaling. *Biomed. Pharmacother.* 106, 1484–1489. doi: 10.1016/j.biopha.2018.07.088

Huang, R. R., Zhang, Y., Han, B., Bai, Y., Zhou, R. B., Gan, G. M., et al. (2017). Circular RNA HIPK2 regulates astrocyte activation via cooperation of autophagy and ER stress by targeting MIR124-2HG. *Autophagy* 13, 1722–1741. doi: 10.1080/15548627.2017.1356975

Humeau, J., Bravo-San Pedro, J. M., Vitale, I., Nuñez, L., Villalobos, C., Kroemer, G., et al. (2018). Calcium signaling and cell cycle: progression or death. *Cell Calcium* 70, 3–15. doi: 10.1016/j.ceca.2017.07.006

Ibrahim, I. M., Abdelmalek, D. H., and Elfiky, A. A. (2019). GRP78: a cell's response to stress. *Life Sci.* 226, 156–163. doi: 10.1016/j.lfs.2019.04.022

Jia, S. Z., Xu, X. W., Zhang, Z. H., Chen, C., Chen, Y. B., Huanget, S. L., et al. (2021). Selenoprotein K deficiency-induced apoptosis: a role for calpain and the ERS pathway. *Redox Biol.* 47:102154. doi: 10.1016/j.redox.2021.102154

Jia, Y., Yi, L., Li, Q. Q., Liu, T. J., and Yang, S. S. (2021). LncRNA MALAT1 aggravates oxygen-glucose deprivation/reoxygenation-induced neuronal endoplasmic reticulum stress and apoptosis via the miR-195a-5p/HMGA1 axis. *Biol. Res.* 54:8. doi: 10.1186/s40659-021-00331-9

Ji, Y. Q., Teng, L., Zhang, R., Sun, J. P., and Guo, Y. L. (2017). NRG-1beta exerts neuroprotective effects against ischemia reperfusion-induced injury in rats through the JNK signaling pathway. *Neuroscience* 362, 13–24. doi: 10.1016/j.neuroscience.2017.08.032

Jin, Z. Q., Liang, J., Li, J. Q., and Kolattukudy, P. E. (2019). Absence of MCP-induced protein 1 enhances blood-brain barrier breakdown after experimental stroke in mice. *Int. J. Mol. Sci.* 20:3214. doi: 10.3390/ijms20133214

Kalogeris, T., Baines, C., Krenz, M., and Korthuis, R. J. (2016). Ischemia/reperfusion. *Compr. Physiol.* 7, 113–170. doi: 10.1002/cphy.c160006

Kalogeris, T., Baines, C. P., Krenz, M., and Korthuis, R. J. (2012). Cell biology of ischemia/reperfusion injury. *Int. Rev. Cell Mol. Biol.* 298, 229–317. doi: 10.1016/b978-0-12-394309-5.00006-7

Kalogeris, T., Bao, Y. M., and Korthuis, R. J. (2014). Mitochondrial reactive oxygen species: a double edged sword in ischemia/reperfusion vs preconditioning. *Redox Biol.* 2, 702–714. doi: 10.1016/j.redox.2014.05.006

Kaufman, R. J., and Malhotra, J. D. (2014). Calcium trafficking integrates endoplasmic reticulum function with mitochondrial bioenergetics. *Biochim. Biophys. Acta* 1843, 2233–2239. doi: 10.1016/j.bbamcr.2014.03.022

Kausar, S., Wang, F., and Cui, H. J. (2018). The role of mitochondria in reactive oxygen species generation and its implications for neurodegenerative diseases. *Cells* 7:274. doi: 10.3390/cells7120274

Khan, M. S., Khan, A., Ahmad, S., Ahmad, R., Rehman, I. U., Ikram, M., et al. (2020). Inhibition of JNK alleviates chronic hypoperfusion-related ischemia induces oxidative stress and brain degeneration via Nrf2/HO-1 and NF-kappaB signaling. *Oxid. Med. Cell. Longev.* 2020:5291852. doi: 10.1155/2020/5291852

Kim, I., Xu, W., and Reed, J. C. (2008). Cell death and endoplasmic reticulum stress: disease relevance and therapeutic opportunities. *Nat. Rev. Drug. Discov.* 7, 1013–1030. doi: 10.1038/nrd2755

Korennykh, A. V., Egea, P. F., Korostelev, A. A., Finer-Moore, J., Zhang, C., Shokat, K. M., et al. (2009). The unfolded protein response signals through high-order assembly of Ire1. *Nature* 457, 687–693. doi: 10.1038/nature07661

Koval, O. M., Nguyen, E. K., Santhana, V., Fidler, T. P., Sebag, S. C., Rasmussen, T. P., et al. (2019). Loss of MCU prevents mitochondrial fusion in G_1-S phase and blocks cell cycle progression and proliferation. *Sci. Signal.* 12:eaav1439. doi: 10.1126/scisignal.aav1439

Kristian, T. (2004). Metabolic stages, mitochondria and calcium in hypoxic/ischemic brain damage. *Cell. Calcium* 36, 221–233. doi: 10.1016/j.ceca.2004.02.016

Kuriakose, D., and Xiao, Z. (2020). Pathophysiology and treatment of stroke: present status and future perspectives. *Int. J. Mol. Sci.* 21:7609. doi: 10.3390/ijms21207609

Kvietys, P. R., and Granger, D. N. (2012). Role of reactive oxygen and nitrogen species in the vascular responses to inflammation. *Free. Radic. Biol. Med.* 52, 556–592. doi: 10.1016/j.freeradbiomed.2011.11.002

Kwak, J. H., Yang, Z. G., Yoon, B., He, Y. X., Uhm, S., Shin, H. C., et al. (2015). Blood-brain barrier-permeable fluorone-labeled dieckols acting as neuronal ER stress signaling inhibitors. *Biomaterials* 61, 52–60. doi: 10.1016/j.biomaterials.2015.04.045

Lee, C. L., Veerbeek, J. H. W., Rana, T. K., van Rijn, B. B., Burton, G. J., and Yung, H. W. (2019). Role of endoplasmic reticulum stress in proinflammatory cytokine-mediated inhibition of trophoblast invasion in placenta-related complications of pregnancy. *Am. J. Pathol.* 189, 467–478. doi: 10.1016/j.ajpath.2018.10.015

Lee, K. P., Dey, M., Neculai, D., Cao, C., Dever, T. E., and Sicheri, F. (2008). Structure of the dual enzyme Ire1 reveals the basis for catalysis and regulation in nonconventional RNA splicing. *Cell* 132, 89–100. doi: 10.1016/j.cell.2007.10.057

Lehotsky, J., Urban, P., Pavlikova, M., Tatarková, Z., Kaminska, B., and Kaplánet, P. (2009). Molecular mechanisms leading to neuroprotection/ischemic tolerance: effect of preconditioning on the stress reaction of endoplasmic reticulum. *Cell. Mol. Neurobiol.* 29, 917–925. doi: 10.1007/s10571-009-9376-4

Li, M. T., Ke, J., Deng, Y. Q., Chen, C. X., Huang, Y. C., Bian, Y. F., et al. (2021). The protective effect of liquiritin in hypoxia/reoxygenation-induced disruption on blood brain barrier. *Front. Pharmacol.* 12:671783. doi: 10.3389/fphar.2021.671783

Lima, B., Forrester, M. T., Hess, D. T., and Stamler, J. S. (2010). S-nitrosylation in cardiovascular signaling. *Circ. Res.* 106, 633–646. doi: 10.1161/circresaha.109.207381

Lin, M. Y., Ling, J., Geng, X. Q., Zhang, J. Q., Du, J., and Chen, L. J. (2019). RTN1-C is involved in high glucose-aggravated neuronal cell subjected to oxygen-glucose deprivation and reoxygenation injury via endoplasmic reticulum stress. *Brain Res. Bull.* 149, 129–136. doi: 10.1016/j.brainresbull.2019.04.010

Liou, H. C., Boothby, M. R., Finn, P. W., Davidon, R., Nabavi, N., Zeleznik-Le, N. J., et al. (1990). A new member of the leucine zipper class of proteins that binds to the HLA DR alpha promoter. *Science* 247, 1581–1584. doi: 10.1126/science.2321018

Liu, C. Y., Xu, Z. H., and Kaufman, R. J. (2003). Structure and intermolecular interactions of the luminal dimerization domain of human IRE1alpha. *J. Biol. Chem.* 278, 17680–17687. doi: 10.1074/jbc.m300418200

Liu, T. L., Liu, M. N., Zhang, T. J., Liu, W. X., Xu, H., Mu, F., et al. (2018c). Z-Guggulsterone attenuates astrocytes-mediated neuroinflammation after ischemia by inhibiting toll-like receptor 4 pathway. *J. Neurochem.* 147, 803–815. doi: 10.1111/jnc.14583

Liu, F., Lu, J., Manaenko, A., Tang, J., and Hu, Q. (2018b). Mitochondria in ischemic stroke: new insight and implications. *Aging Dis.* 9, 924–937. doi: 10.14336/ad.2017.1126

Liu, C., Fu, Q., Mu, R., Wang, F., Zhou, C. J., Zhang, L., et al. (2018a). Dexmedetomidine alleviates cerebral ischemia-reperfusion injury by inhibiting endoplasmic reticulum stress dependent apoptosis through the PERK-CHOP-Caspase-11 pathway. *Brain Res.* 1701, 246–254. doi: 10.1016/j.brainres.2018.09.007

Logsdon, A. F., Lucke-Wold, B. P., Nguyen, L., Matsumoto, R. R., Turner, R. C., Rosen, C. L., et al. (2016). Salubrinal reduces oxidative stress, neuroinflammation and impulsive-like behavior in a rodent model of traumatic brain injury. *Brain Res.* 1643, 140–151. doi: 10.1016/j.brainres.2016.04.063

Logue, S., Cleary, P., Saveljeva, S., and Samali, A. (2013). New directions in ER stress-induced cell death. *Apoptosis* 18, 537–546. doi: 10.1007/s10495-013-0818-6

Lopata, A., Kniss, A., Lohr, F., Rogov, V. V., and Dotsch, V. (2020). Ubiquitination in the ERAD process. *Int. J. Mol. Sci.* 21:5369. doi: 10.3390/ijms21155369

Lopez-Hernandez, B., Cena, V., and Posadas, I. (2015). The endoplasmic reticulum stress and the HIF-1 signalling pathways are involved in the neuronal damage caused by chemical hypoxia. *Br. J. Pharmacol.* 172, 2838–2851. doi: 10.1111/bph.13095

Lorenzano, S., Rost, N. S., Khan, M., Li, H., Lima, F. O., Maas, M. B., et al. (2018). Oxidative stress biomarkers of brain damage: hyperacute plasma F2-isoprostane predicts infarct growth in stroke. *Stroke* 49, 630–637. doi: 10.1161/strokeaha.117.018440

Luchetti, F., Crinelli, R., Cesarini, E., Canonico, B., Guidi, L., Zerbinati, C., et al. (2017). Endothelial cells, endoplasmic reticulum stress and oxysterols. *Redox Biol.* 13, 581–587. doi: 10.1016/j.redox.2017.07.014

Ma, X. D., Zhang, W., Xu, C., Zhang, S. S., Zhao, J. X., Pan, Q., et al. (2020). Nucleotide-binding oligomerization domain protein 1 enhances oxygen-glucose deprivation and reperfusion injury in cortical neurons via activation of endoplasmic reticulum stress-mediated autophagy. *Exp. Mol. Pathol.* 117:104525. doi: 10.1016/j.yexmp.2020.104525

Ma, Y. J., and Hendershot, L. M. (2003). Delineation of a negative feedback regulatory loop that controls protein translation during endoplasmic reticulum stress. *J. Biol. Chem.* 278, 34864–34873. doi: 10.1074/jbc.m301107200

Mamady, H., and Storey, K. B. (2008). Coping with the stress: expression of ATF4, ATF6, and downstream targets in organs of hibernating ground squirrels. *Arch. Biochem. Biophys.* 477, 77–85. doi: 10.1016/j.abb.2008.05.006

Man, S., Xian, Y., Holmes, D., Matsouaka, R. A., Saver, J., Smith, E. E., et al. (2020). Association between thrombolytic door-to-needle time and 1-year mortality and readmission in patients with acute ischemic stroke. *JAMA* 323, 2170–2184. doi: 10.1001/jama.2020.5697

Manzanero, S., Santro, T., and Arumugam, T. V. (2013). Neuronal oxidative stress in acute ischemic stroke: sources and contribution to cell injury. *Neurochem. Int.* 62, 712–718. doi: 10.1016/j.neuint.2012.11.009

Marchi, S., Patergnani, S., and Pinton, P. (2014). The endoplasmic reticulum-mitochondria connection: one touch, multiple functions. *Biochim. Biophys. Acta* 1837, 461–469. doi: 10.1016/j.bbabio.2013.10.015

Marciniak, S. J., Yun, C. Y., Oyadomari, S., Novoa, I., Zhang, Y. H., Jungreis, R., et al. (2004). CHOP induces death by promoting protein synthesis and oxidation in the stressed endoplasmic reticulum. *Genes Dev.* 18, 3066–3077. doi: 10.1101/gad.1250704

Markouli, M., Strepkos, D., Papavassiliou, A. G., and Piperi, C. (2020). Targeting of endoplasmic reticulum (ER) stress in gliomas. *Pharmacol. Res.* 157:104823. doi: 10.1016/j.phrs.2020.104823

Martinez, J. A., Zhang, Z. Q., Svetlov, S. I., Hayes, R. L., Wang, K. K., and Larner, S. F. (2010). Calpain and caspase processing of caspase-12 contribute to the ER stress-induced cell death pathway in differentiated PC12 cells. *Apoptosis* 15, 1480–1493. doi: 10.1007/s10495-010-0526-4

Martin-Jimenez, C. A., Garcia-Vega, A., Cabezas, R., Aliev, G., Echeverria, V., González, J., et al. (2017). Astrocytes and endoplasmic reticulum stress: a bridge between obesity and neurodegenerative diseases. *Prog. Neurobiol.* 158, 45–68. doi: 10.1016/j.pneurobio.2017.08.001

Martino, M. B., Jones, L., Brighton, B., Ehre, C., Abdulah, L., Davis, C. W., et al. (2013). The ER stress transducer IRE1beta is required for airway epithelial mucin production. *Mucosal Immunol.* 6, 639–654. doi: 10.1038/mi.2012.105

Martire, A., Lambertucci, C., Pepponi, R., Ferrante, A., Benati, N., Buccioni, M., et al. (2019). Neuroprotective potential of adenosine A1 receptor partial agonists in experimental models of cerebral ischemia. *J. Neurochem.* 149, 211–230. doi: 10.1111/jnc.14660

Mastantuono, T., Battiloro, L., Sabatino, L., Chiurazzi, M., Maro, M. D., Muscariello, E., et al. (2015). Effects of citrus flavonoids against microvascular damage induced by hypoperfusion and reperfusion in rat pial circulation. *Microcirculation* 22, 378–390. doi: 10.1111/micc.12207

Matsuzaki, S., Hiratsuka, T., Kuwahara, R., Katayama, T., and Tohyama, M. (2010). Caspase-4 is partially cleaved by calpain via the impairment of Ca^{2+} homeostasis under the ER stress. *Neurochem. Int.* 56, 352–356. doi: 10.1016/j.neuint.2009.11.007

McCullough, K. D., Martindale, J. L., Klotz, L. O., Aw, T. Y., and Holbrook, N. J. (2001). Gadd153 sensitizes cells to endoplasmic reticulum stress by down-regulating Bcl2 and perturbing the cellular redox state. *Mol. Cell. Biol.* 21, 1249–1259. doi: 10.1128/mcb.21.4.1249-1259.2001

McQuiston, A., and Diehl, J. A. (2017). Recent insights into PERK-dependent signaling from the stressed endoplasmic reticulum. *F1000Research* 6:1897. doi: 10.12688/f1000research.12138.1

Mei, Y., Thompson, M. D., Cohen, R. A., and Tong, X. Y. (2013). Endoplasmic reticulum stress and related pathological processes. *J. Pharmacol. Biomed. Anal.* 1:1000107.

Mo, Z. T., Liao, Y. L., Zheng, J., and Li, W. N. (2020). Icariin protects neurons from endoplasmic reticulum stress-induced apoptosis after OGD/R injury via suppressing IRE1alpha-XBP1 signaling pathway. *Life Sci.* 255:117847. doi: 10.1016/j.lfs.2020.117847

Mohammad-Gharibani, P., Modi, J., Menzie, J., Genova, R., Ma, Z. Y., Tao, R., et al. (2014). Mode of action of S-methyl-N, N-diethylthiocarbamate sulfoxide

(DETC-MeSO) as a novel therapy for stroke in a rat model. *Mol. Neurobiol.* 50, 655–672. doi: 10.1007/s12035-014-8658-0

Mohammed, T. S., Tsai, S. T., Hung, H. Y., Hu, W. F., Pang, C. Y., Chen, S. Y., et al. (2020). A role for endoplasmic reticulum stress in intracerebral hemorrhage. *Cells* 9:750. doi: 10.3390/cells9030750

Morihara, R., Yamashita, T., Liu, X., Nakano, Y., Fukui, Y., Sato, K., et al. (2018). Protective effect of a novel sigma-1 receptor agonist is associated with reduced endoplasmic reticulum stress in stroke male mice. *J. Neurosci. Res.* 96, 1707–1716. doi: 10.1002/jnr.24270

Morishima, N., Nakanishi, K., Takenouchi, H., Shibata, T., and Yasuhiko, Y. (2002). An endoplasmic reticulum stress-specific caspase cascade in apoptosis. Cytochrome c-independent activation of caspase-9 by caspase-12. *J. Biol. Chem.* 277, 34287–34294. doi: 10.1074/jbc.m204973200

Murphy, M. P. (2009). How mitochondria produce reactive oxygen species. *Biochem. J.* 417, 1–13. doi: 10.1042/bj20081386

Nakagawa, T., Zhu, H., Morishima, N., Li, E., Xu, J., Yankner, B. A., et al. (2000). Caspase-12 mediates endoplasmic-reticulum-specific apoptosis and cytotoxicity by amyloid-beta. *Nature* 403, 98–103. doi: 10.1038/47513

Nakka, V. P., Gusain, A., and Raghubir, R. (2010). Endoplasmic reticulum stress plays critical role in brain damage after cerebral ischemia/reperfusion in rats. *Neurotox. Res.* 17, 189–202. doi: 10.1007/s12640-009-9110-5

Nakka, V. P., Prakash-Babu, P., and Vemuganti, R. (2016). Crosstalk between endoplasmic reticulum stress, oxidative stress, and autophagy: potential therapeutic targets for acute CNS injuries. *Mol. Neurobiol.* 53, 532–544. doi: 10.1007/s12035-014-9029-6

Nan, D., Jin, H. Q., Deng, J. W., Yu, W. W., Liu, R., Sun, W. P., et al. (2019). Cilostazol ameliorates ischemia/reperfusion-induced tight junction disruption in brain endothelial cells by inhibiting endoplasmic reticulum stress. *FASEB. J.* 33, 10152–10164. doi: 10.1096/fj.201900326r

Nishitoh, H., Matsuzawa, A., Tobiume, K., Saegusa, K., Takeda, K., Inoue, K., et al. (2002). ASK1 is essential for endoplasmic reticulum stress-induced neuronal cell death triggered by expanded polyglutamine repeats. *Genes Dev.* 16, 1345–1355. doi: 10.1101/gad.992302

Oakes, S. A., and Papa, F. R. (2015). The role of endoplasmic reticulum stress in human pathology. *Annu. Rev. Pathol.* 10, 173–194. doi: 10.1146/annurev-pathol-012513-104649

Oh, Y. S., and Jun, H. S. (2017). Effects of glucagon-like peptide-1 on oxidative stress and Nrf2 signaling. *Int. J. Mol. Sci.* 19:26. doi: 10.3390/ijms19010026

Ohoka, N., Yoshii, S., Hattori, T., Onozaki, K., and Hayashiet, H. (2005). TRB3, a novel ER stress-inducible gene, is induced via ATF4-CHOP pathway and is involved in cell death. *EMBO J.* 24, 1243–1255. doi: 10.1038/sj.emboj.7600596

Osada, N., Kosuge, Y., Ishige, K., and Ito, Y. (2010). Characterization of neuronal and astroglial responses to ER stress in the hippocampal CA1 area in mice following transient forebrain ischemia. *Neurochem. Int.* 57, 1–7. doi: 10.1016/j.neuint.2010.03.017

Owen, C. R., Kumar, R., Zhang, P. C., McGrath, B. C., Cavener, D. R., and Krauseet, G. S. (2005). PERK is responsible for the increased phosphorylation of eIF2alpha and the severe inhibition of protein synthesis after transient global brain ischemia. *J. Neurochem.* 94, 1235–1242. doi: 10.1111/j.1471-4159.2005.03276.x

Pahl, H. L. (1999). Signal transduction from the endoplasmic reticulum to the cell nucleus. *Physiol. Rev.* 79, 683–701. doi: 10.1152/physrev.1999.79.3.683

Palam, L. R., Baird, T. D., and Wek, R. C. (2011). Phosphorylation of eIF2 facilitates ribosomal bypass of an inhibitory upstream ORF to enhance CHOP translation. *J. Biol. Chem.* 286, 10939–10949. doi: 10.1074/jbc.m110.216093

Paschen, W., and Mengesdorf, T. (2005). Endoplasmic reticulum stress response and neurodegeneration. *Cell Calcium* 38, 409–415. doi: 10.1016/j.ceca.2005.06.019

Patwardhan, G., Beverly, L., and Siskind, L. (2016). Sphingolipids and mitochondrial apoptosis. *J. Bioenerg. Biomembr.* 48, 153–168. doi: 10.1007/s10863-015-9602-3

Poone, G. K., Hasseldam, H., Munkholm, N., Rasmussen, R. S., Grønberg, N. V., and Johansen, F. F. (2015). The hypothermic influence on CHOP and Ero1-alpha in an endoplasmic reticulum stress model of cerebral ischemia. *Brain Sci.* 5, 178–187. doi: 10.3390/brainsci5020178

Poustchi, F., Amani, H., Ahmadian, Z., Niknezhad, S. V., Mehrabi, S., Santos, H. A., et al. (2021). Combination therapy of killing diseases by injectable hydrogels: from concept to medical applications. *Adv. Healthc. Mater.* 10:e2001571. doi: 10.1002/adhm.202001571

Powers, W. J. (2020). Acute ischemic stroke. *N. Engl. J. Med.* 383, 252–260. doi: 10.1056/nejmcp1917030

Puthalakath, H., O'Reilly, L. A., Gunn, P., Lee, L., Kelly, P. N., Huntington, N. D., et al. (2007). ER stress triggers apoptosis by activating BH3-only protein Bim. *Cell* 129, 1337–1349. doi: 10.1016/j.cell.2007.04.027

Qie, X. J., Wen, D., Guo, H. Y., Xu, G. J., Liu, S., Shen, Q. C., et al. (2017). Endoplasmic reticulum stress mediates methamphetamine-induced blood-brain barrier damage. *Front. Pharmacol.* 8:639. doi: 10.3389/fphar.2017.00639

Quiros, P. M., Prado, M. A., Zamboni, N., D'Amico, D., Williams, R. W., Finleyet, D., et al. (2017). Multi-omics analysis identifies ATF4 as a key regulator of the mitochondrial stress response in mammals. *J. Cell Biol.* 216, 2027–2045. doi: 10.1083/jcb.201702058

Raedschelders, K., Ansley, D. M., and Chen, D. D. (2012). The cellular and molecular origin of reactive oxygen species generation during myocardial ischemia and reperfusion. *Pharmacol. Ther.* 133, 230–255. doi: 10.1016/j.pharmthera.2011.11.004

Rajakumar, S., Bhanupriya, N., Ravi, C., and Nachiappan, V. (2016). Endoplasmic reticulum stress and calcium imbalance are involved in cadmium-induced lipid aberrancy in *Saccharomyces cerevisiae*. *Cell Stress Chaperones* 21, 895–906. doi: 10.1007/s12192-016-0714-4

Ramezani, A., Nahad, M. P., and Faghihloo, E. (2018). The role of Nrf2 transcription factor in viral infection. *J. Cell. Biochem.* 119, 6366–6382. doi: 10.1002/jcb.26897

Rao, R. V., Ellerby, H. M., and Bredesen, D. E. (2004). Coupling endoplasmic reticulum stress to the cell death program. *Cell Death Differ.* 11, 372–380. doi: 10.1038/sj.cdd.4401378

Rao, R. V., Hermel, E., Castro-Obregon, S., del Rio, G., Ellerby, L. M., Ellerby, H. M., et al. (2001). Coupling endoplasmic reticulum stress to the cell death program. Mechanism of caspase activation. *J. Biol. Chem.* 276, 33869–33874. doi: 10.1074/jbc.m102225200

Raturi, A., and Simmen, T. (2013). Where the endoplasmic reticulum and the mitochondrion tie the knot: the mitochondria-associated membrane (MAM). *Biochim. Biophys. Acta* 1833, 213–224. doi: 10.1016/j.bbamcr.2012.04.013

Rong, C., Wei, W., and Yu-Hong, T. (2020). Asperuloside exhibits a novel anti-leukemic activity by triggering ER stress-regulated apoptosis via targeting GRP78. *Biomed. Pharmacother.* 125:109819. doi: 10.1016/j.biopha.2020.109819

Rozpedek, W., Nowak, A., Pytel, D., Diehl, J. A., and Majsterek, I. (2017). Molecular basis of human diseases and targeted therapy based on small-molecule inhibitors of ER stress-induced signaling pathways. *Curr. Mol. Med.* 17, 118–132. doi: 10.2174/1566524017666170306122643

Salehpour, F., Farajdokht, F., Mahmoudi, J., Erfani, M., Farhoudi, M., Karimi, P., et al. (2019). Photobiomodulation and coenzyme Q10 treatments attenuate cognitive impairment associated with model of transient global brain ischemia in artificially aged mice. *Front. Cell. Neurosci.* 13:74. doi: 10.3389/fncel.2019.00074

Sanada, S., Komuro, I., and Kitakaze, M. (2011). Pathophysiology of myocardial reperfusion injury: preconditioning, postconditioning, and translational aspects of protective measures. *Am. J. Physiol. Heart. Circ. Physiol.* 301, H1723–H1741. doi: 10.1152/ajpheart.00553.2011

Sanderson, T. H., Gallaway, M., and Kumar, R. (2015). Unfolding the unfolded protein response: unique insights into brain ischemia. *Int. J. Mol. Sci.* 16, 7133–7142. doi: 10.3390/ijms16047133

Sano, R., and Reed, J. C. (2013). ER stress-induced cell death mechanisms. *Biochim. Biophys. Acta* 1833, 3460–3470. doi: 10.1016/j.bbamcr.2013.06.028

Santos-Galdiano, M., Gonzalez-Rodriguez, P., Font-Belmonte, E., Ugidos, I. F., Anuncibay-Soto, B., Pérez-Rodríguez, D., et al. (2021). Celecoxib-dependent neuroprotection in a rat model of transient middle cerebral artery occlusion (tMCAO) involves modifications in unfolded protein response (UPR) and proteasome. *Mol. Neurobiol.* 58, 1404–1417. doi: 10.1007/s12035-020-02202-y

Scherz-Shouval, R., and Elazar, Z. (2007). ROS, mitochondria and the regulation of autophagy. *Trends Cell Biol.* 17, 422–427. doi: 10.1016/j.tcb.2007.07.009

Schonthal, A. (2013). Pharmacological targeting of endoplasmic reticulum stress signaling in cancer. *Biochem. Pharmacol.* 85, 653–666. doi: 10.1016/j.bcp.2012.09.012

Schonthal, A. H. (2012). Endoplasmic reticulum stress: its role in disease and novel prospects for therapy. *Scientifica* 2012:857516. doi: 10.6064/2012/857516

Shai, N., Yifrach, E., van, R. C., Cohen, N., Bibi, C., IJlst, L., et al. (2018). Systematic mapping of contact sites reveals tethers and a function for the peroxisome-mitochondria contact. *Nat. Commun.* 9:1761.

Shen, Y. T., Li, R., Yu, S., Zhao, Q., Wang, Z. R., Sheng, H. X., et al. (2021). Activation of the ATF6 (Activating Transcription Factor 6) signaling pathway in neurons improves outcome after cardiac arrest in mice. *J. Am. Heart Assoc.* 10:e020216. doi: 10.1161/jaha.120.020216

Shi, W. Z., Tian, Y., and Li, J. (2019). GCN2 suppression attenuates cerebral ischemia in mice by reducing apoptosis and endoplasmic reticulum (ER) stress through the blockage of FoxO3a-regulated ROS production. *Biochem. Biophys. Res. Commun.* 516, 285–292. doi: 10.1016/j.bbrc.2019.05.181

Shibata, M., Hattori, H., Sasaki, T., Gotoh, J., Hamada, J., and Fukuuchi, Y. (2003). Activation of caspase-12 by endoplasmic reticulum stress induced by transient middle cerebral artery occlusion in mice. *Neuroscience* 118, 491–499. doi: 10.1016/s0306-4522(02)00910-7

Sprenkle, N. T., Sims, S. G., Sanchez, C. L., and Meares, G. P. (2017). Endoplasmic reticulum stress and inflammation in the central nervous system. *Mol. Neurodegener.* 12:42. doi: 10.1186/s13024-017-0183-y

Starck, S. R., Tsai, J. C., Chen, K., Shodiya, M., Wang, L., Yahiro, K., et al. (2016). Translation from the 5' untranslated region shapes the integrated stress response. *Science* 351:aad3867. doi: 10.1126/science.aad3867

Stefan, C. J., Manford, A. G., Baird, D., Yamada-Hanff, J., Mao, Y., and Emr, S. D. (2011). Osh proteins regulate phosphoinositide metabolism at ER-plasma membrane contact sites. *Cell* 144, 389–401. doi: 10.1016/j.cell.2010.12.034

Stroud, D. A., Oeljeklaus, S., Wiese, S., Bohnert, M., Lewandrowski, U., Sickmann, A., et al. (2011). Composition and topology of the endoplasmic reticulum-mitochondria encounter structure. *J. Mol. Biol.* 413, 743–750. doi: 10.1016/j.jmb.2011.09.012

Su, L., Zhang, R., Chen, Y., Zhu, Z., and Ma, C. (2017). Raf kinase inhibitor protein attenuates ischemic-induced microglia cell apoptosis and activation through NF-kappaB pathway. *Cell. Physiol. Biochem.* 41, 1125–1134. doi: 10.1159/000464119

Sun, B. Z., Chen, L., Wu, Q., Wang, H. L., Wei, X. B., Xiang, Y. X., et al. (2014). Suppression of inflammatory response by flurbiprofen following focal cerebral ischemia involves the NF-kappaB signaling pathway. *Int. J. Clin. Exp. Med.* 7, 3087–3095.

Sun, M. S., Jin, H., Sun, X., Huang, S., Zhang, F. L., Guo, Z. N., et al. (2018). Free radical damage in ischemia-reperfusion injury: an obstacle in acute ischemic stroke after revascularization therapy. *Oxid. Med. Cell. Longev.* 2018:3804979. doi: 10.1155/2018/3804979

Szegezdi, E., Logue, S. E., Gorman, A. M., and Samali, A. (2006). Mediators of endoplasmic reticulum stress-induced apoptosis. *EMBO Rep.* 7, 880–885. doi: 10.1038/sj.embor.7400779

Tajiri, S., Oyadomari, S., Yano, S., Morioka, M., Gotoh, T., Hamada, J. I., et al. (2004). Ischemia-induced neuronal cell death is mediated by the endoplasmic reticulum stress pathway involving CHOP. *Cell Death Differ.* 11, 403–415. doi: 10.1038/sj.cdd.4401365

Ten, V., and Galkin, A. (2019). Mechanism of mitochondrial complex I damage in brain ischemia/reperfusion injury. A hypothesis. *Mol. Cell. Neurosci.* 100:103408. doi: 10.1016/j.mcn.2019.103408

Thuerauf, D. J., Morrison, L. E., Hoover, H., and Glembotski, C. C. (2002). Coordination of ATF6-mediated transcription and ATF6 degradation by a domain that is shared with the viral transcription factor, VP16. *J. Biol. Chem.* 277, 20734–20739. doi: 10.1074/jbc.m201749200

Tian, Y., Su, Y., Ye, Q., Chen, L., Yuan, F., and Wang, Z. Y. (2020). Silencing of TXNIP alleviated oxidative stress injury by regulating MAPK-Nrf2 axis in ischemic stroke. *Neurochem. Res.* 45, 428–436. doi: 10.1007/s11064-019-02933-y

Toulmay, A., and Prinz, W. A. (2011). Lipid transfer and signaling at organelle contact sites: the tip of the iceberg. *Curr. Opin. Cell Biol.* 23, 458–463. doi: 10.1016/j.ceb.2011.04.006

Travers, K. J., Patil, C. K., Wodicka, L., Lockhart, D. J., Weissman, J. S., and Walter, P. (2000). Functional and genomic analyses reveal an essential coordination between the unfolded protein response and ER-associated degradation. *Cell* 101, 249–258. doi: 10.1016/s0092-8674(00)80835-1

Tripathi, M., Zhang, C. W., Singh, B. K., Sinha, R. A., Moe, K. T., Desilva, D. A., et al. (2016). Hyperhomocysteinemia causes ER stress and impaired autophagy that is reversed by vitamin B supplementation. *Cell Death Dis.* 7:e2513. doi: 10.1038/cddis.2016.374

Ugrankar, R., Bowerman, J., Hariri, H., Chandra, M., Chen, K., Bossanyi, M. F., et al. (2019). *Drosophila* Snazarus regulates a lipid droplet population at plasma membrane-droplet contacts in adipocytes. *Dev. Cell* 50, 557–572.e5. doi: 10.1016/j.devcel.2019.07.021

Urra, H., and Hetz, C. (2017). Fine-tuning PERK signaling to control cell fate under stress. *Nat. Struct. Mol. Biol.* 24, 789–790. doi: 10.1038/nsmb.3478

Uzdensky, A. B. (2019). Apoptosis regulation in the penumbra after ischemic stroke: expression of pro- and antiapoptotic proteins. *Apoptosis* 24, 687–702. doi: 10.1007/s10495-019-01556-6

Valko, M., Leibfritz, D., Moncol, J., Cronin, M. T., Mazur, M., and Telser, J. (2007). Free radicals and antioxidants in normal physiological functions and human disease. *Int. J. Biochem. Cell Biol.* 39, 44–84. doi: 10.1016/j.biocel.2006.07.001

Valm, A. M., Cohen, S., Legant, W. R., Melunis, J., Hershberg, U., Wait, E., et al. (2017). Applying systems-level spectral imaging and analysis to reveal the organelle interactome. *Nature* 546, 162–167. doi: 10.1038/nature22369

Vicente-Gutierrez, C., Bonora, N., Bobo-Jimenez, V., Jimenez-Blasco, D., Lopez-Fabuel, I., Fernandez, E., et al. (2019). Astrocytic mitochondrial ROS modulate brain metabolism and mouse behaviour. *Nat. Metab.* 1, 201–211. doi: 10.1038/s42255-018-0031-6

Volmer, R., van der Ploeg, K., and Ron, D. (2013). Membrane lipid saturation activates endoplasmic reticulum unfolded protein response transducers through their transmembrane domains. *Proc. Natl. Acad. Sci. U.S.A.* 110, 4628–4633. doi: 10.1073/pnas.1217611110

Waldherr, S. M., Strovas, T. J., Vadset, T. A., Liachko, N. F., and Kraemer, B. C. (2019). Constitutive XBP-1s-mediated activation of the endoplasmic reticulum unfolded protein response protects against pathological tau. *Nat. Commun.* 10:4443. doi: 10.1038/s41467-019-12070-3

Walter, P., and Ron, D. (2011). The unfolded protein response: from stress pathway to homeostatic regulation. *Science* 334, 1081–1086. doi: 10.1126/science.1209038

Wang, M., Hayashi, H., Horinokita, I., Asada, M., Iwatani, Y., Liu, J. X., et al. (2021). Neuroprotective effects of senkyunolide I against glutamate-induced cells death by attenuating JNK/caspase-3 activation and apoptosis. *Biomed. Pharmacother.* 140:111696. doi: 10.1016/j.biopha.2021.111696

Wang, X. H., Zhao, J., Guo, H. M., and Fan, Q. Q. (2019). CFLAR is a critical regulator of cerebral ischaemia-reperfusion injury through regulating inflammation and endoplasmic reticulum (ER) stress. *Biomed. Pharmacother.* 117:109155. doi: 10.1016/j.biopha.2019.109155

Wang, Z. F., Zhang, C. Y., Hong, Z. H., Chen, H. X., Chen, W. F., and Chen, G. F. (2013). C/EBP homologous protein (CHOP) mediates neuronal apoptosis in rats with spinal cord injury. *Exp. Ther. Med.* 5, 107–111. doi: 10.3892/etm.2012.745

Waza, A. A., Hamid, Z., Bhat, S. A., Naseer, U. D., Bhat, M., and Ganai, B. (2018). Relaxin protects cardiomyocytes against hypoxia-induced damage in in-vitro conditions: involvement of Nrf2/HO-1 signaling pathway. *Life Sci.* 213, 25–31. doi: 10.1016/j.lfs.2018.08.059

Wei, J. L., Wu, X. Q., Luo, P., Yue, K. Y., Yu, Y., Pu, J. N., et al. (2019). Homer1a attenuates endoplasmic reticulum stress-induced mitochondrial stress after ischemic reperfusion injury by inhibiting the PERK pathway. *Front. Cell. Neurosci.* 13:101. doi: 10.3389/fncel.2019.00101

Weidinger, A., and Kozlov, A. V. (2015). Biological activities of reactive oxygen and nitrogen species: oxidative stress versus signal transduction. *Biomolecules* 5, 472–484. doi: 10.3390/biom5020472

Wong, M. Y., DiChiara, A. S., Suen, P. H., Chen, K., Doan, N. D., and Shoulders, M. D. (2018). Adapting secretory proteostasis and function through the unfolded protein response. *Curr. Top. Microbiol. Immunol.* 414, 1–25. doi: 10.1007/82_2017_56

Wu, F., Qiu, J., Fan, Y., Zhang, Q. L., Cheng, B. H., Wu, Y. L., et al. (2018). Apelin-13 attenuates ER stress-mediated neuronal apoptosis by activating Galphai/Galphaq-CK2 signaling in ischemic stroke. *Exp. Neurol.* 302, 136–144. doi: 10.1016/j.expneurol.2018.01.006

Wu, F., Zhang, R. M., Feng, Q. Z., Cheng, H. J., Xue, J. J., and Chen, J. (2020). (−)-Clausenamide alleviated ER stress and apoptosis induced by OGD/R in

primary neuron cultures. *Neurol. Res.* 42, 730–738. doi: 10.1080/01616412.2020.1771040

Wu, J., Rutkowski, D. T., Dubois, M., Swathirajan, J., Saunders, T., Wang, J. Y., et al. (2007). ATF6alpha optimizes long-term endoplasmic reticulum function to protect cells from chronic stress. *Dev. Cell* 13, 351–364. doi: 10.1016/j.devcel.2007.07.005

Wu, M. Y., Yiang, G. T., Liao, W. T., Tsai, A. P., Cheng, Y. L., Cheng, P. W., et al. (2018). Current mechanistic concepts in ischemia and reperfusion injury. *Cell. Physiol. Biochem.* 46, 1650–1667. doi: 10.1159/000489241

Wu, Y., Whiteus, C., Xu, C. S., Hayworth, K. J., Weinberg, R. J., Hess, H. F., et al. (2017b). Contacts between the endoplasmic reticulum and other membranes in neurons. *Proc. Natl. Acad. Sci. U.S.A.* 114, E4859–E4867. doi: 10.1073/pnas.1701078114

Wu, Y., Wang, X., Zhou, X., Cheng, B., Li, G., and Bai, B. (2017a). Temporal expression of Apelin/Apelin receptor in ischemic stroke and its therapeutic potential. *Front. Mol. Neurosci.* 10:1. doi: 10.3389/fnmol.2017.00001

Xia, P. P., Zhang, F., Yuan, Y. J., Chen, C., Huang, Y., Li, L. Y., et al. (2020). ALDH 2 conferred neuroprotection on cerebral ischemic injury by alleviating mitochondria-related apoptosis through JNK/caspase-3 signing pathway. *Int. J. Biol. Sci.* 16, 1303–1323. doi: 10.7150/ijbs.38962

Xie, P., Ren, Z. K., Lv, J., Hu, Y. M., Guan, Z. Z., and Yu, W. F. (2020). Berberine ameliorates oxygen-glucose deprivation/reperfusion-induced apoptosis by inhibiting endoplasmic reticulum stress and autophagy in PC12 cells. *Curr. Med. Sci.* 40, 1047–1056. doi: 10.1007/s11596-020-2286-x

Xin, J. H., Ma, X. X., Chen, W. Y., Zhou, W., Dong, H. P., Wang, Z., et al. (2021). Regulation of blood-brain barrier permeability by Salvinorin A via alleviating endoplasmic reticulum stress in brain endothelial cell after ischemia stroke. *Neurochem. Int.* 149:105093. doi: 10.1016/j.neuint.2021.105093

Xin, Q., Ji, B., Cheng, B., Wang, C., Liu, H., Chen, X., et al. (2014). Endoplasmic reticulum stress in cerebral ischemia. *Neurochem. Int.* 68, 18–27. doi: 10.1016/j.neuint.2014.02.001

Xu, Q. X., Zhao, B., Ye, Y. Z., Li, Y. N., Zhang, Y. G., Xiong, X. X., et al. (2021). Relevant mediators involved in and therapies targeting the inflammatory response induced by activation of the NLRP3 inflammasome in ischemic stroke. *J. Neuroinflammation* 18:123. doi: 10.1186/s12974-021-02137-8

Xu, W. L., Li, T., Gao, L. S., Zheng, J. W., Yan, J., Zhang, J. M., et al. (2019). Apelin-13/APJ system attenuates early brain injury via suppression of endoplasmic reticulum stress-associated TXNIP/NLRP3 inflammasome activation and oxidative stress in a AMPK-dependent manner after subarachnoid hemorrhage in rats. *J. Neuroinflammation* 16:247. doi: 10.1186/s12974-019-1620-3

Yamaguchi, H., and Wang, H. G. (2004). CHOP is involved in endoplasmic reticulum stress-induced apoptosis by enhancing DR5 expression in human carcinoma cells. *J. Biol. Chem.* 279, 45495–45502. doi: 10.1074/jbc.m406933200

Yamamoto, K., Sato, T., Matsui, T., Sato, M., Okada, T., Yoshida, H., et al. (2007). Transcriptional induction of mammalian ER quality control proteins is mediated by single or combined action of ATF6alpha and XBP1. *Dev. Cell* 13, 365–376. doi: 10.1016/j.devcel.2007.07.018

Yang, J. P., Wang, Z. R., Liu, X. Y., and Lu, P. C. (2021). Modulation of vascular integrity and neuroinflammation by peroxiredoxin 4 following cerebral ischemia-reperfusion injury. *Microvasc. Res.* 135:104144. doi: 10.1016/j.mvr.2021.104144

Yang, J. W., and Hu, Z. P. (2015). Neuroprotective effects of atorvastatin against cerebral ischemia/reperfusion injury through the inhibition of endoplasmic reticulum stress. *Neural. Regen. Res.* 10, 1239–1244. doi: 10.4103/1673-5374.162755

Yang, W., and Paschen, W. (2016). Unfolded protein response in brain ischemia: a timely update. *J. Cereb. Blood Flow Metab.* 36, 2044–2050. doi: 10.1177/0271678x16674488

Yang, Y., Liu, L., Naik, I., Braunstein, Z., Zhong, J. X., and Ren, B. X. (2017). Transcription factor C/EBP homologous protein in health and diseases. *Front. Immunol.* 8:1612. doi: 10.3389/fimmu.2017.01612

Yao, W. J., Yang, X. W., Zhu, J. Y., Gao, B., Shi, H. T., and Xu, L. P. (2018). IRE1alpha siRNA relieves endoplasmic reticulum stress-induced apoptosis and alleviates diabetic peripheral neuropathy in vivo and in vitro. *Sci. Rep.* 8:2579. doi: 10.1038/s41598-018-20950-9

Ye, J., Rawson, R. B., Komuro, R., Chen, X., Davé, U. P., Prywes, R., et al. (2000). ER stress induces cleavage of membrane-bound ATF6 by the same proteases that process SREBPs. *Mol. Cell* 6, 1355–1364. doi: 10.1016/s1097-2765(00)00133-7

Ye, Z., Wang, N., Xia, P. P., Wang, E., Liao, J., and Guo, Q. L. (2013). Parecoxib suppresses CHOP and Foxo1 nuclear translocation, but increases GRP78 levels in a rat model of focal ischemia. *Neurochem. Res.* 38, 686–693. doi: 10.1007/s11064-012-0953-4

Yoneda, T., Imaizumi, K., Oono, K., Yui, D., Gomi, F., Katayama, T., et al. (2001). Activation of caspase-12, an endoplastic reticulum (ER) resident caspase, through tumor necrosis factor receptor-associated factor 2-dependent mechanism in response to the ER stress. *J. Biol. Chem.* 276, 13935–13940. doi: 10.1074/jbc.m010677200

Yoshida, H., Matsui, T., Hosokawa, N., Kaufman, R. J., Nagata, K., and Mori, K. (2003). A time-dependent phase shift in the mammalian unfolded protein response. *Dev. Cell* 4, 265–271. doi: 10.1016/s1534-5807(03)00022-4

Yoshida, H., Okada, T., Haze, K., Yanagi, H., Yura, T., Negishi, M., et al. (2001b). Endoplasmic reticulum stress-induced formation of transcription factor complex ERSF including NF-Y (CBF) and activating transcription factors 6alpha and 6beta that activates the mammalian unfolded protein response. *Mol. Cell. Biol.* 21, 1239–1248. doi: 10.1128/mcb.21.4.1239-1248.2001

Yoshida, H., Matsui, T., Yamamoto, A., Okada, T., and Mori, K. (2001a). XBP1 mRNA is induced by ATF6 and spliced by IRE1 in response to ER stress to produce a highly active transcription factor. *Cell* 107, 881–891. doi: 10.1016/s0092-8674(01)00611-0

Yoshida, H., Okada, T., Haze, K., Yanagi, H., Yura, T., Negishi, M., et al. (2000). ATF6 activated by proteolysis binds in the presence of NF-Y (CBF) directly to the cis-acting element responsible for the mammalian unfolded protein response. *Mol. Cell. Biol.* 20, 6755–6767. doi: 10.1128/mcb.20.18.6755-6767.2000

Yoshikawa, A., Kamide, T., Hashida, K., Ta, H. M., Inahata, Y., Takarada-Iemata, M., et al. (2015). Deletion of Atf6alpha impairs astroglial activation and enhances neuronal death following brain ischemia in mice. *J. Neurochem.* 132, 342–353. doi: 10.1111/jnc.12981

Young, S. K., and Wek, R. C. (2016). Upstream open reading frames differentially regulate gene-specific translation in the integrated stress response. *J. Biol. Chem.* 291, 16927–16935. doi: 10.1074/jbc.r116.733899

Yu, Z., Sheng, H. X., Liu, S., Zhao, S. L., Glembotski, C. C., Warneret, D. S., et al. (2017). Activation of the ATF6 branch of the unfolded protein response in neurons improves stroke outcome. *J. Cereb. Blood Flow Metab.* 37, 1069–1079. doi: 10.1177/0271678x16650218

Yue, S., Zhu, J. J., Zhang, M., Li, C. Y., Zhou, X. L., Zhou, M., et al. (2016). The myeloid heat shock transcription factor 1/beta-catenin axis regulates NLR family, pyrin domain-containing 3 inflammasome activation in mouse liver ischemia/reperfusion injury. *Hepatology* 64, 1683–1698. doi: 10.1002/hep.28739

Zeeshan, H., Lee, G. H., Kim, H. R., and Chae, H. J. (2016). Endoplasmic reticulum stress and associated ROS. *Int. J. Mol. Sci.* 17:327. doi: 10.3390/ijms17030327

Zhang, K., and Kaufman, R. J. (2006). The unfolded protein response: a stress signaling pathway critical for health and disease. *Neurology* 66, S102–S109. doi: 10.1212/01.wnl.0000192306.98198.ec

Zhang, M. M., Zhou, D. Z., Ouyang, Z., Yu, M. Q., and Jiang, Y. G. (2020). Sphingosine kinase 1 promotes cerebral ischemia-reperfusion injury through inducing ER stress and activating the NF-kappaB signaling pathway. *J. Cell. Physiol.* 235, 6605–6614. doi: 10.1002/jcp.29546

Zhang, Q. Y., Wang, Z. J., Sun, D. M., Wang, Y., Xu, P., Wu, W. J., et al. (2017). Novel therapeutic effects of leonurine on ischemic stroke: new mechanisms of BBB integrity. *Oxid. Med. Cell. Longev.* 2017:7150376. doi: 10.1155/2017/7150376

Zhang, Y., Zhou, H., Wu, W. B., Shi, C., Hu, S. Y., Yin, T., et al. (2016). Liraglutide protects cardiac microvascular endothelial cells against hypoxia/reoxygenation injury through the suppression of the SR-Ca^{2+}-XO-ROS axis via activation of the GLP-1R/PI3K/Akt/survivin pathways. *Free Radic. Biol. Med.* 95, 278–292. doi: 10.1016/j.freeradbiomed.2016.03.035

Zhao, L., Li, H. M., Gao, Q., Xu, J., Zhu, Y. J., Zhai, M. L., et al. (2021). Berberine attenuates cerebral ischemia-reperfusion injury induced neuronal apoptosis by

down-regulating the CNPY2 signaling pathway. *Front. Pharmacol.* 12:609693. doi: 10.3389/fphar.2021.609693

Zhao, Q., Wang, X., Chen, A., Cheng, X., Zhang, G., Sun, J., et al. (2018). Rhein protects against cerebral ischemic/reperfusioninduced oxidative stress and apoptosis in rats. *Int. J. Mol. Med.* 41, 2802–2812. doi: 10.3892/ijmm.2018.3488

Zhao, Y. N., Li, J. M., Chen, C. X., Zhang, P., and Li, S. X. (2015). Hypertension-mediated enhancement of JNK activation in association with endoplasmic reticulum stress in rat model hippocampus with cerebral ischemia-reperfusion. *Genet. Mol. Res.* 14, 10980–10990. doi: 10.4238/2015.september.21.10

Zhou, L., Ao, L. Y., Yan, Y. Y., Li, W. T., Ye, A. Q., Li, C. Y., et al. (2019). JLX001 ameliorates ischemia/reperfusion injury by reducing neuronal apoptosis via down-regulating JNK signaling pathway. *Neuroscience* 418, 189–204. doi: 10.1016/j.neuroscience.2019.08.053

Zhu, C., Johansen, F. E., and Prywes, R. (1997). Interaction of ATF6 and serum response factor. *Mol. Cell. Biol.* 17, 4957–4966. doi: 10.1128/mcb.17.9.4957

Zhu, H. Y., Zhu, H. Y., Xiao, S. P., Su, H. Y., Xie, C. L., and Ma, Y. W. (2012). Activation and crosstalk between the endoplasmic reticulum road and JNK pathway in ischemia-reperfusion brain injury. *Acta. Neurochir.* 154, 1197–1203.

Zhu, L., Yang, K., Wang, X. E., Wang, X., and Wang, C. C. (2014). A novel reaction of peroxiredoxin 4 towards substrates in oxidative protein folding. *PLoS One* 9:e105529. doi: 10.1371/journal.pone.0105529

Zhu, Y., Yu, J. B., Gong, J. B., Shen, J., Ye, D., Chenget, D. X., et al. (2021). PTP1B inhibitor alleviates deleterious microglial activation and neuronal injury after ischemic stroke by modulating the ER stress-autophagy axis via PERK signaling in microglia. *Aging* 13, 3405–3427. doi: 10.18632/aging.202272

Zrzavy, T., Machado-Santos, J., Christine, S., Baumgartner, C., Weiner, H. L., and Butovskyet, O. (2018). Dominant role of microglial and macrophage innate immune responses in human ischemic infarcts. *Brain Pathol.* 28, 791–805. doi: 10.1111/bpa.12583

Conflict of Interest: The authors declare that the research was conducted in the absence of any commercial or financial relationships that could be construed as a potential conflict of interest.

Publisher's Note: All claims expressed in this article are solely those of the authors and do not necessarily represent those of their affiliated organizations, or those of the publisher, the editors and the reviewers. Any product that may be evaluated in this article, or claim that may be made by its manufacturer, is not guaranteed or endorsed by the publisher.

GLOSSARY

ER, endoplasmic reticulum; ER stress, endoplasmic reticulum stress; CIRI, cerebral ischemia-reperfusion injury; rtPA, recombinant tissue plasminogen activator; ICH, intracranial hemorrhage; ROS, reactive oxygen species; RNS, reactive nitrogen species; RNOS, reactive/nitrogen oxide species; UPR, unfolded protein response; EOR, ER over-load response; SREBP, sterol regulatory element binding protein; GRP78, glucose-related protein 78; ERAD, ER-associated degradation; UPS, ubiquitin proteasome system; MAMs, mitochondria-associated endoplasmic reticulum membranes; PM, plasma membrane; GRPs, glucose-regulated proteins; SERCA, sarco/endoplasmic reticulum Ca^{2+}-ATPase; MPT, mitochondrial permeability transition; NOX, NADPH oxidase; XO, xanthine oxidase; MAO, monoamine oxidase; Cyt *c*, cytochrome *c*; MCAO, middle cerebral artery occlusion; IL-1 β, interleukin-1 β; IL-6, interleukin-6; TNF-α, tumor necrosis factor-α; NF-κB, nuclear factor κB; eIF2α, eukaryotic initiation factor 2α; IκB, inhibitors of nuclear factor κB; PGRN, progranulin; NLRP3, NLR family, pyrin domain-containing 3; PERK, protein kinase RNA-like endoplasmic reticulum kinase; IRE-1, inositol-requiring protein 1; ATF6, activating transcription factor 6; GRP78, glucose regulated protein 78; XBP1, X-box binding protein 1; NRF2, nuclear factor erythroid 2-related factor 2; GADD34, growth arrest and DNA damage 34; CHOP, CAAT/enhancer-binding protein (C/EBP) homologous protein; ATF4, activating transcription factor 4; TRB3, tribbles-related protein 3; OGD/R, oxygen-glucose deprivation/reoxygenation; PTP1B, protein tyrosine phosphatase 1B; Keap1, Kelch-like ECH associating protein 1; S1P, site 1 protease; S2P, site 2 protease; b ZIP, basic leucine zipper; JNK, c-Jun N-terminal kinase; ASK1, apoptosis signal-regulating kinase-1; TRAF2, tumor necrosis factor receptor-associated factor 2; RIDD, Regulated IRE1-Dependent Decay; DR5, death receptor 5; MPTP, mitochondrial permeability transition pore; OMM, outer mitochondrial membrane; LDs, lipid Droplets; DETC-MeSO, S-Methyl-*N*, *N*-diethyldithiocarbamate sulfoxide; NOD1, nucleotide-binding oligomerization domain 1.

frontiers | Frontiers in Immunology

ORIGINAL RESEARCH
published: 06 May 2022
doi: 10.3389/fimmu.2022.897413

Salivary Xanthine Oxidase as a Potential Biomarker in Stroke Diagnostics

Mateusz Maciejczyk[1], Miłosz Nesterowicz[2], Anna Zalewska[3], Grzegorz Biedrzycki[4], Piotr Gerreth[5,6], Katarzyna Hojan[7,8] and Karolina Gerreth[9]*

[1] Department of Hygiene, Epidemiology and Ergonomics, Medical University of Bialystok, Bialystok, Poland, [2] Students Scientific Club "Biochemistry of Civilization Diseases" at the Department of Hygiene, Epidemiology and Ergonomics, Medical University of Bialystok, Bialystok, Poland, [3] Experimental Dentistry Laboratory, Medical University of Bialystok, Bialystok, Poland, [4] Hospital Pharmacy, Provincial Hospital in Olsztyn, Olsztyn, Poland, [5] Private Dental Practice, Poznan, Poland, [6] Postgraduate Studies in Scientific Research Methodology, Poznan University of Medical Sciences, Poznan, Poland, [7] Department of Occupational Therapy, Poznan University of Medical Sciences, Poznan, Poland, [8] Department of Rehabilitation, Greater Poland Cancer Centre, Poznan, Poland, [9] Department of Risk Group Dentistry, Chair of Pediatric Dentistry, Poznan University of Medical Sciences, Poznan, Poland

OPEN ACCESS

Edited by:
Qingkun Liu,
Mount Sinai Hospital, United States

Reviewed by:
Qiang Liu,
Tianjin Medical University General Hospital, China
Adina Bianca Bosca,
Iuliu Haţieganu University of Medicine and Pharmacy, Romania
Xingping Qin,
Harvard University, United States

***Correspondence:**
Mateusz Maciejczyk
mat.maciejczyk@gmail.com

Specialty section:
This article was submitted to Multiple Sclerosis and Neuroimmunology, a section of the journal Frontiers in Immunology

Received: *16 March 2022*
Accepted: *11 April 2022*
Published: *06 May 2022*

Citation:
Maciejczyk M, Nesterowicz M, Zalewska A, Biedrzycki G, Gerreth P, Hojan K and Gerreth K (2022) Salivary Xanthine Oxidase as a Potential Biomarker in Stroke Diagnostics. Front. Immunol. 13:897413. doi: 10.3389/fimmu.2022.897413

Stroke is one of the most common cerebrovascular diseases. Despite significant progress in understanding stroke pathogenesis, cases are still increasing. Thus, laboratory biomarkers of stroke are sought to allow rapid and non-invasive diagnostics. Ischemia-reperfusion injury is an inflammatory process with characteristic cellular changes leading to microvascular disruption. Several studies have shown that hyperactivation of xanthine oxidase (XO) is a major pathogenic factor contributing to brain dysfunction. Given the critical role of XO in stroke complications, this study aimed to evaluate the activity of the enzyme and its metabolic products in the saliva of stroke subjects. Thirty patients in the subacute phase of stroke were included in the study: 15 with hemorrhagic stroke and 15 with ischemic stroke. The control group consisted of 30 healthy subjects similar to the cerebral stroke patients regarding age, gender, and status of the periodontium, dentition, and oral hygiene. The number of individuals was determined *a priori* based on our previous experiment (power of the test = 0.8; α = 0.05). The study material was mixed non-stimulated whole saliva (NWS) and stimulated saliva (SWS). We showed that activity, specific activity, and XO output were significantly higher in NWS of ischemic stroke patients than in hemorrhagic stroke and healthy controls. Hydrogen peroxide and uric acid levels were also considerably higher in NWS of ischemic stroke patients. Using receiver operating curve (ROC) analysis, we demonstrated that XO-specific activity in NWS distinguishes ischemic stroke from hemorrhagic stroke (AUC: 0.764) and controls (AUC: 0.973) with very high sensitivity and specificity. Saliva collection is stress-free, requires no specialized medical personnel, and allows continuous monitoring of the patient's condition through non-invasive sampling multiple times per day. Salivary XO also differentiates with high accuracy (100%) and specificity (93.75%) between stroke patients with mild to moderate cognitive decline (AUC = 0.988). Thus, salivary XO assessment may be a potential screening tool for a

comprehensive neuropsychological evaluation. To summarize, our study demonstrates the potential utility of salivary XO in the differential diagnosis of stroke.

Keywords: stroke, saliva, xanthine oxidase, diagnostics, biomarkers

INTRODUCTION

Stroke is one of the most common cerebrovascular diseases. It is a sudden onset of focal or generalized brain dysfunction that lasts more than 24 hours and is caused by vascular disorders related to cerebral blood flow. Oxygen and glucose deprivation in the brain leads to decreased ATP synthesis and impaired synaptic conduction, causing neuronal malfunction and subsequent apoptosis or necrosis (1). The most common stroke causes include atherosclerotic lesions in extracranial and intracranial vessels, cardioembolism, carotid and vertebral artery dissections, hypercoagulable syndromes, and multiple systemic diseases. There are two types of strokes: ischemic (80%) and hemorrhagic (20%). Ischemic stroke is caused by closure/constriction of intracerebral vessels and hemodynamic abnormalities resulting in slowed cerebral flow, whereas hemorrhagic stroke occurs due to blood extravasation within the brain tissue (2). It is estimated that one person dies every 6 seconds due to stroke, which annually accounts for more than 5-6 million people worldwide. Thus, stroke is the third cause of death after heart disease and cancer (3). It is also the most common reason for permanent disability in people over 40 years old, with severe clinical, social, and economic consequences (4).

Many studies have shown that early revascularization treatment significantly improves patient prognosis (5–10). Although imaging studies such as CT, MRI, ultrasonography, arteriography, and echocardiography are the mainstay of the diagnosis, they may not be sufficient in some groups of stroke patients. Indeed, many other diseases have similar symptoms, making the differential diagnosis of stroke include brain tumors, migraine, epileptic seizure, hypoglycemia, hyperglycemia, hyponatremia, hypertensive encephalopathy, and hepatic encephalopathy (11–14). Not all patients are also treated at specialized stroke/neurology centers. Therefore, it is not surprising that rapid and non-invasive biomarkers of the disease are still being sought (15). Their source may be saliva containing numerous substances that pass from the brain into the blood (16–20). It is well known that the blood-brain barrier (BBB) is disrupted in stroke pathophysiology. The main factors damaging the BBB are mechanical failures or hypoxia damaging the cerebrovascular endothelium. These also include increased activity of matrix metalloproteinases (MMPs), enhanced secretion of cytokines, chemokines, and growth factors, and overproduction of reactive oxygen (ROS)/nitrogen (RNS) species by neuronal, glial, and immune cells. The damaged BBB becomes permeable to leukocytes inducing inflammatory processes and promoting the release of brain biomolecules into the blood (2, 21–29). Subsequently, circulating biomarkers can pass into saliva by passive, facilitated, or active diffusion, making saliva highly attractive in laboratory diagnostics. Saliva's advantages are also evidenced by its easy availability, non-invasive and painless collection, and relatively high durability compared to blood and cerebrospinal fluid (16–18, 20, 30–35).

Recent studies suggest the potential use of saliva in ischemic stroke diagnosing or assessing the stress severity in stroke patients (36–38). However, there is a lack of non-invasive biomarkers to differentiate between different types of strokes. Given the critical role of xanthine oxidase (XO) in ischemic stroke pathomechanism (22, 24, 29, 39–41), we decided to compare the XO activity in saliva of patients with ischemic and hemorrhagic stroke. Ischemia-reperfusion injury is an inflammatory process with characteristic cellular changes leading to microvascular disruption. In ischemic stroke, ROS overproduction by XO hyperactivation is a major pathogenic factor contributing to brain dysfunction. XO catalyzes the conversion of hypoxanthine to xanthine and xanthine to uric acid (UA), generating high amounts of superoxide radicals, hydrogen peroxide (H_2O_2), and peroxynitrite (**Figure 1**). Higher formation of ROS/RNS in stroke brain results in neuronal oxidative stress responsible for altering the fluidity of biological membranes, modifying enzyme activity, uncoupling membrane transport, or deregulating membrane potential (24, 26, 29, 42–44). Although previous studies have not confirmed the clinical usefulness of serum/plasma XO in stroke diagnostics (45), evaluation of enzyme activity in saliva may bring new light to this issue. The results of many studies showed that saliva has the highest correlation with the brain, not the blood (46–48). When the BBB is breached, several glial, neuronal, and pericyte biomarkers appear in the blood, which then passes into saliva (22, 49–51). This is caused by the robust vascularization of the salivary glands allowing the efficient exchange of blood-derived components (52, 53). Since saliva can be collected non-invasively multiple times a day, it is a particularly attractive material for diagnosing cerebrovascular diseases (18, 32). Therefore, the present study aimed to compare XO activity and the enzyme products (e.g., hydrogen peroxide and UA) in non-stimulated and stimulated saliva of patients with hemorrhagic and ischemic stroke.

MATERIAL AND METHODS

Study Subjects

From June to September 2019, the research was carried out in the health center (Bonifraterskie Centrum Zdrowia) in Piaski–Marysin (Piaski, Poland). At this center, patients with numerous disorders, e.g., brain injury, spinal cord injury, vascular brain damage, polyneuropathy, myelopathy, sclerosis multiplex, surgically treated patients with a brain tumor, and

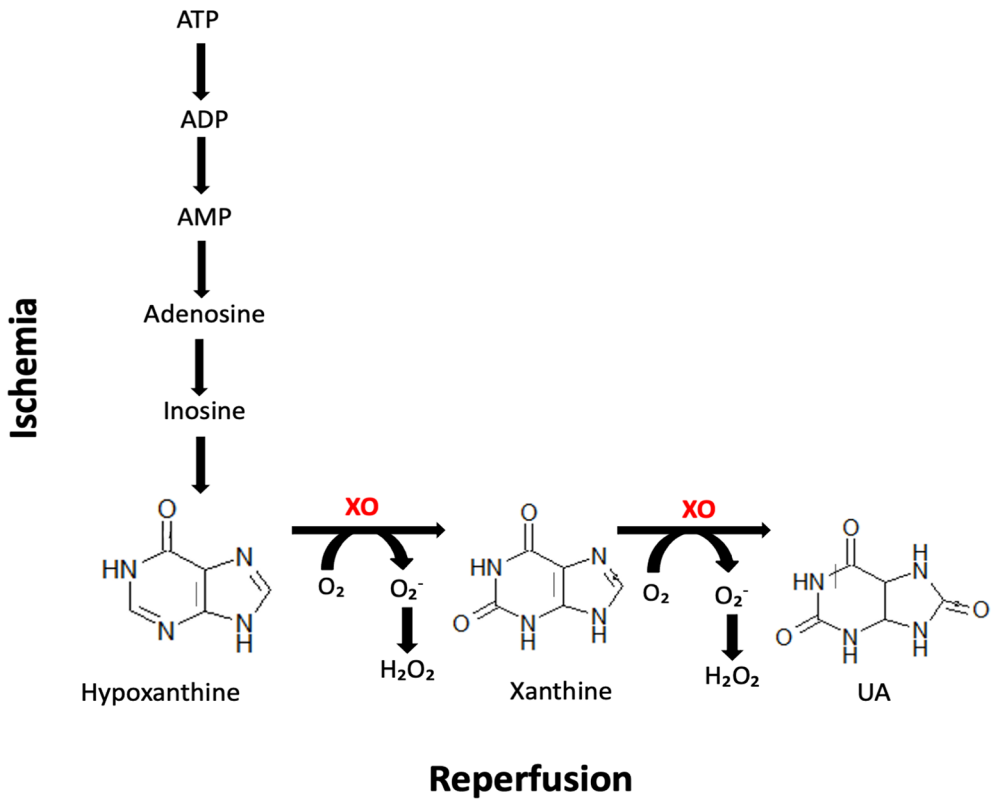

FIGURE 1 | Biochemical reactions occurring in the stroke brain during ischemia and reperfusion. Xanthine oxidase (XO) catalyzes the conversion of hypoxanthine to xanthine and xanthine to uric acid (UA), generating high amounts of superoxide radicals and hydrogen peroxide (H_2O_2).

those after cerebral stroke are hospitalized. Those individuals come from different provinces of the country.

The participation of each patient in the research was voluntary. According to its criteria, one experienced doctor, a specialist in neurorehabilitation, qualified all the subjects for the research.

Stroke patients in the subacute phase of the disease were included in the study group. All of the individuals were admitted to the neurorehabilitation unit immediately after the acute phase cessation and directly from the hospital. Each patient after the medical assessment was subjected to comprehensive individual and similar rehabilitation. It was established that during the time of the research, 385 patients were hospitalized in the neurorehabilitation ward due to different incidents, with 253 (65.71%) individuals who were stroke survivors. Most cerebral stroke individuals were able to cooperate, communicate, and understand instructions.

Data on the patients' general health status and condition were obtained from their files and referred to gender, age, medications used, medical history, and time since diagnosis of cerebral stroke.

The functional status of the subjects was measured using the following scales:

1. Addenbrooke's Cognitive Examination III (ACE III) for differentiation of patients with and without cognitive impairment (54).
2. The Barthel Index (BI) for measurement of individual's everyday function, particularly performance in activities of daily living (ADL) (55).
3. The Berg Balance Scale (BBS) for determining a patient's ability or inability to safely balance during a series of predetermined tasks (56).
4. The functional independence measure (FIM) explores the person's social, psychological, and physical functioning (57).

Numerous patients (117 individuals - 30.39%) declined to participate in the study, including 34 (8.83%) subjects who did not come for saliva and examination sampling, even though they previously gave informed consent and were reminded from three to four times. Moreover, 48 patients (12.47%) were excluded from the analysis because they were uncooperative, i.e., they could not communicate and give conscious written informed consent for participation in the study. In addition, 3 (0.78%) patients were taken from the center to the other hospital because of deterioration of general health, 7 (1.82%) patients were not able for a sampling of the saliva because of general difficulties in understanding the procedure due to language and/or cognitive deficits, and 14 (3.64%) individuals abandoned the study after non-stimulated saliva sampling due to psychological and/or physiological tiredness.

Therefore, ultimately, 30 (11.86% of cerebral stroke patients, i.e., 7.79% of all hospitalized individuals at the rehabilitation

health center) completed the dental examination and saliva sampling and were considered in the analysis.

Most patients received the same meals at the center divided into a baseline diet for most individuals or a diet for diabetes mellitus patients. All the meals were prepared in the center and distributed to the patients every day at the same time.

Study Criteria

The inclusion and exclusion criteria of cerebral stroke subjects to the study are presented in **Table 1**.

Control Group

The control group consisted of 30 generally healthy subjects similar to the cerebral stroke patients (study group) regarding age, gender, and status of the periodontium, dentition, and oral hygiene. This group included individuals reporting for dental examination to the Department of Restorative Dentistry of the Medical University of Bialystok (Bialystok, Poland) from March to September 2020. All individuals were provided with information concerning the research and gave their informed and written consent. Subjects used a regular and balanced diet (not restricted). They were also recommended to have routine physical activity.

Sampling of Saliva

The study material was mixed non-stimulated whole saliva (NWS) and stimulated saliva (SWS). The secretion of saliva was stimulated by utilizing 10 μL of 2% citric acid applied on the central part of the tongue every 30 seconds. Both types of saliva samples were gathered *via* spitting between 7:30 a.m. and 9:00 a.m. Before the dental examination, saliva sampling was performed in the health center in Piaski, from June to September 2019, i.e., during summertime, to keep similar weather conditions outside.

Before saliva gathering, patients were informed not to intake any solid and/or liquid food other than clean water at least two hours before saliva sampling. The individuals were also instructed not to have intensive physical activity for the preceding 12 hours and restrain to carry out any oral hygienic procedures (i.e., mouth rinsing, teeth brushing, gum chewing, etc.) (19, 58). All patients were in the subacute phase of stroke. Therefore, they had to take medicines regularly. However, the time from the last dose of any medication was minimally 2 hours before saliva sampling. In contrast, the subjects from the control group were not allowed to take any medication 8 hours before gathering saliva. Before sampling, the oral cavity was rinsed two times with distilled water at room temperature to avoid possible contamination from other sources. The saliva was collected in a separate, private room after a 5-minute adaptation to the environment. The patients were situated in an adjustable chair that was individually adapted to the height of each individual. The subject's head was slightly bent downwards and resting in a convenient position. Patients were asked to limit face and lips movements during the procedure (19, 58). The saliva samples were gathered into a sterile Falcon tube, and the amounts collected during the first minute were ejected. The NWS was accumulated for 10 minutes to avoid the individuals' physiological and/or psychological tiredness, while SWS was gathered in the same manner for 5 minutes.

Afterward, the saliva volume was measured with a calibrated pipette (accuracy of 0.1 mL) (59). The salivary flow rate (SFR) of

TABLE 1 | Inclusion and exclusion criteria for the subjects in the study group.

Inclusion criteria	Exclusion criteria
confirmed cerebral hemorrhage or cerebral infarction based on magnetic resonance imaging (MRI) and computed tomography (CT)	unconfirmed cerebral infarction or cerebral hemorrhage based on magnetic resonance imaging (MRI) and computed tomography (CT)
good general condition	poor general condition
age of consent, i.e., over the age of 18 years	patients under the age of 18 years
no legal guardianship	legal guardianship
recovery from the acute phase of hemorrhagic or ischemic stroke in all brain areas	no recovery from the acute phase of hemorrhagic or ischemic stroke in all brain areas
the first admission to cure stroke unit was more than 5–6 (to 10) hours from the onset of the early neurological symptoms	the first admission to cure stroke unit was less than 5–6 hours from the onset of the early neurological symptoms and treated with thrombolysis
consciousness and giving of informed and written consent for a sampling of saliva and oral examination	unconsciousness and inability to give informed consent for saliva sampling and oral examination
adequate capacity to follow instructions, i.e., being able to answer questions during the study and understanding how to perform the procedures	inadequate capacity to follow instructions (insufficient cooperation due to cognitive and/or language deficits)
ability to gather a saliva sample	inability to gather a saliva sample
no stroke recurrence during the subacute phase	stroke recurrence during the subacute phase
ischemic stroke treated without thrombolysis or thrombectomy	ischemic stroke treated with thrombolysis or thrombectomy
patients without malnutrition (no weight loss over 10% during the previous three months or having body mass index higher than 18 kg/m^2)	patients suffering from malnutrition (with weight loss over 10% during the previous three months or having body mass index lower than 18 kg/m^2)
no heart failure (NYHA > II)	heart failure (NYHA < II)
no autoimmune disease (e.g., rheumatoid arthritis, systemic lupus erythematosus)	autoimmune disease (e.g., rheumatoid arthritis, systemic lupus erythematosus)
no psychiatric or cognitive disorders	psychiatric or cognitive disorders
no lung disease (chronic obstructive pulmonary disease) or cardiovascular disease (angina or uncontrolled hypertension)	lung disease (chronic obstructive pulmonary disease) or cardiovascular disease (angina or uncontrolled hypertension)
no XO inhibitors such as Allopurinol, Febuxostat, and Topiroxostat	XO inhibitors for the last three months
no vitamins and dietary supplements for the last three months	vitamins and dietary supplements for the last three months
non-smokers	smokers

NWS and SWS was estimated by dividing their volume by the time necessary for the secretion, and finally, it was expressed in mL/min.

After sampling, the saliva was centrifuged (+4°C, 20 min, 3000 × g; MPW 351, MPW Med. Instruments, Warsaw, Poland), and butylated hydroxytoluene (BHT, Sigma-Aldrich, Saint Louis, MO, USA) was added to the acquired supernatants, in the amount of 10 μL 0.5 M BHT in acetonitrile (ACN)/1 mL of saliva, to protect the samples from oxidation processes (60). Subsequently, saliva samples were situated in a container with dry ice, with a temperature of approximately –80°C, and stored for no more than three months for analysis.

Examination of Oral Cavity

The oral examination was performed in a separate room, subsequently after sampling of saliva. The dentition was assessed in artificial light, using a plain mouth mirror and a dental probe, following the World Health Organization (WHO) criteria (61, 62). All accessible tooth surfaces were evaluated, and finally, they were scored as healthy, decayed (DT), extracted due to caries (MT), or filled because of caries (FT). The data collected were used in the calculation of the DMFT index (dental caries experience). It is the sum of DT, MT, and FT. The prevalence of dental caries was also determined. This index is calculated as a percentage of patients with DMFT > 0. Status of gingiva and oral hygiene was evaluated with the use of Gingival Index (GI) and Plaque Index (PlI), respectively, on the teeth, 16 (right permanent maxillary first molar), 12 (right permanent maxillary lateral incisor), 24 (left permanent maxillary first premolar), 36 (left permanent mandibular first molar), 32 (left permanent mandibular lateral incisor), and 44 (right permanent mandibular first premolar), using 4-degree scales (with scores from 0 to 3) (63). Before examining subjects' oral cavity, calibration and training of two researchers who are dentists (P.G. and K.G.) was done by another experienced dental specialist (A.Z.). The intra-examiner and inter-examiner agreement for PlI and GI was assessed by another dental examination in ten subjects (κ >0.9). The dental evaluation was carried out subsequently after NWS and SWS whole saliva collection.

Consent of the Bioethics Committee and Patients

All subjects, i.e., stroke patients (study group) and healthy individuals (control group), received written information on the study's purpose, benefits, risks, and procedures. Full written and informed consent was obtained from all subjects following the Declaration of Helsinki for saliva sampling and dental examination.

The research was also approved by the Bioethics Committee of the Poznan University of Medical Sciences (resolutions 59/19 and 890/19).

XO Assays

The activity of salivary XO (EC 1.17.3.2) was estimated using two biochemical methods. Firstly, the enzyme activity was measured colorimetrically based on the XO-catalyzed conversion of xanthine into UA. XO activity was calculated by the rise in absorbance at 293 nm. The activity of the enzyme was measured in pmol of UA/h/mL (64, 65). Secondly, XO activity was assessed fluorometrically using a commercial Amplex® Red Xanthine/Xanthine Oxidase Assay Kit (Invitrogen, Waltham, MA, USA). In this method, XO catalyzes the oxidation of xanthine/hypoxanthine to superoxide radical and UA. Superoxide anion is then reduced to H_2O_2, which reacts 1:1 with Amplex Red reagent. The reaction occurs with horseradish peroxidase (HRP) and produces red-fluorescent compound resorufin. The absorbance of resorufin was measured at 540/590 nm wavelength. One unit of XO activity was assumed as 1 μmol of UA formed from hypoxanthine at 25°C.

The 96-well microplate reader BioTek Synergy H1 (Winooski, VT, USA) was used to measure the sample's absorbance and fluorescence. All determinations were performed in triplicate samples. The results were presented as enzyme activity (μU/mL), specific activity (nU/mg protein), and salivary output (μU/min). Total protein content (TPC) was assayed colorimetrically using bicinchoninic acid (BCA) assay with bovine serum albumin (BSA) as a standard (Thermo Scientific PIERCE BCA Protein Assay Kit, Rockford, IL, USA).

XO Products

To assess hydrogen peroxide (H_2O_2) concentration, Amplex® Red Hydrogen Peroxide/Peroxidase Assay Kit (Invitrogen, Waltham, MA, USA) was used. The Amplex® Red reagent reacts stoichiometrically with H_2O_2. The product of H_2O_2 oxidation is the fluorescent resorufin, which was measured at 540/590 nm.

UA concentration was estimated by the colorimetric method. Commercial QuantiChrom™ Uric Acid Assay Kit (BioAssay Systems, Hayward, CA, USA) was used. In this assay, iron reacts with UA and 2,4,6-tripyridyl-s-triazine generating a blue-colored complex. UA level is directly proportional to the intensiveness of the samples' color estimated at 590 nm.

All determinations were performed in triplicate samples. The results were presented as nmol/L (H_2O_2) or μmol/L (UA).

Statistical Analysis

Sample size calculation was assumed *a priori* based on our anterior clinical study. For this purpose, the online sample size calculator *ClinCalc* was utilized. The level of statistical significance was determined on 0.05, and the power of the study was 0.8. XO specific activity and UA level in NWS were used for analysis. Patients' minimal number amounted to 12 (per one group).

In order to assess the inter-and intracorporeal agreement of dental examinators, the online *Cohen Kappa* calculator was used.

Statistical analysis was conducted using GraphPad Prism 8 for macOS (Graph- Pad Software, La Jolla, CA, USA). The examined variable distribution was assessed by the Kolmogorov–Smirnov test, while the homogeneity of variance was by Levene's test. The student's t-test was used to compare two groups, while analysis of variance (ANOVA) with Tukey's *post hoc* test was performed to compare three groups. The defined statistical significance was $p < 0.05$. p-Values were computed with correction for multiple

comparisons. The results were expressed as mean ± standard deviation (SD) and 95% confidence intervals (95% CI). Correlations between clinical data and salivary biomarkers were carried out with the Pearson correlation coefficient. Multivariate analysis of the simultaneous impacts of many independent variables on one quantitative dependent variable was made using linear regression. Stroke type, ACE III, BI, FIM, BBS, and SFR were included as independent variables, and 95% CI were reported along with regression parameters. The diagnostic utility of salivary biomarkers was evaluated using receiver operating curve (ROC) analysis. The area under the curve (AUC) and the cut-off point, characterized by the highest sensitivity and specificity, were calculated.

RESULTS

Clinical Characteristics

Clinical characteristics of the groups are shown in **Table 2**. Thirty patients with stroke in the subacute phase were divided into two groups according to the stroke type: hemorrhagic and ischemic. There are no significant differences between both studies and control groups. Only functional and cognitive performance measured by the BI, FIM, BBS, and ACE III scores were significantly lower in stroke patients than controls. Oral examination and saliva collection were carried through between 30 and 35 days since the occurrence of stroke.

Salivary Gland Function

The hemorrhagic stroke group showed significantly lower SFR in SWS (-31%), and significantly lower TPC both in NWS (-19%) and SWS (-29%) regarding the control group. Patients after ischemic stroke incidents also presented significantly lower SFR in SWS (-24%), and TPC both in NWS (-27%) and SWS (-23%) relative to the control group (**Table 3**).

Stomatological Examination

The dental characteristics of the study group in comparison to the control group were shown in **Table 3**. Oral hygiene and periodontal status did not differ between groups.

Salivary Ischemia Biomarkers

The standard colorimetric method failed to assess XO activity in saliva samples. Therefore, XO activity was measured fluorometrically using a commercial Amplex® Red Xanthine/ Xanthine Oxidase Assay Kit.

The group of patients suffering hemorrhagic stroke demonstrated significantly higher XO activity in NWS (+14%), XO specific activity in NWS (+45%) and SWS (+62%), H_2O_2 concentration in SWS (+20%), and UA concentration in NWS (+31%) concerning control group. The patients who suffered from hemorrhagic stroke shown significantly higher XO activity in NWS (+36%), XO specific activity in NWS (+89%) and SWS (+52%), XO output in NWS (+87%), H_2O_2 concentration in NWS (+109%) and SWS (+30%), and UA concentration in NWS (+73%) in comparison to the control group. Significantly differences between the ischemic and hemorrhagic stroke groups were observed in the case of the following parameters: XO activity (+20%), XO specific activity (+31%), XO output (+49%), H_2O_2 concentration (+65%), and UA concentration, all only in NWS (+32%) (**Table 4**).

Correlations

XO specific activity with UA concentration (r = -0.57, p = 0.001) and XO output with H_2O_2 level (r = -0.5, p = 0.005) were negatively correlated, and also H_2O_2 level was positively correlated with the BBS scale (r = 0.57, p = 0.001) in control group in NWS.

SWS in the control group showed a positive relationship only between H_2O_2 level and dynamic balance abilities in BBS (r = 0.57, p = 0.001).

Curiously enough, XO activity was positively correlated with UA ($r = 0.49, p = 0.006$) and H_2O_2 ($r = 0.61, p < 0.001$) concentrations in stroke group in NWS. XO specific activity presented positive interconnections with UA (r = 0.43, p = 0.017) and H_2O_2 (r = 0.49, $p = 0.006$) levels, and negative interconnections with ACE III (r = -0.71, $p < 0.001$), BI (r = -0.58, $p = 0.001$) and BBS (r = -0.61, $p < 0.001$) scores. Moreover, a positive relation between XO output and UA level (r = 0.46, p = 0.011) was shown. UA concentration corresponded positively with H_2O_2 concentration (r = 0.4, p = 0.027).

Interestingly, the study group showed negative correlations between UA concentration and dynamic balance abilities in BI (r = -0.42, p = 0.02), and BBS scales (r = -0.46, p = 0.011) in SWS.

The above correlations were encapsulated in **Figure 2**.

Regression Analysis

XO activity in NWS depends on stroke type, XO specific activity – stroke type and cognitive functions in ACE III, and XO output – stroke type and SFR. Furthermore, H_2O_2 and UA concentrations in NWS are affected by stroke type. In SWS, the variable influencing XO output is SFR, while UA level is affected by the FIM scale (**Table 5**).

ROC Analysis

Results of ROC analysis were shown in **Table 6**. Only XO specific activity was significantly different between hemorrhagic stroke and control groups, both in NWS and SWS. Statistically significant differences between patients with ischemic stroke and healthy controls were presented by XO activity in NWS, XO specific activity in NWS and SWS, H_2O_2 concentration in NWS and SWS, and UA level in NWS. Patients with ischemic stroke were significantly differentiated from those with hemorrhagic by XO activity, XO specific activity, and H_2O_2 level, all of them only in NWS.

Summarizing, the specific activity of XO in NWS is of particular diagnostic utility. This biomarker differentiated with high sensitivity and specificity hemorrhagic and ischemic strokes from control subjects. Moreover, it differentiates between both stroke types (**Table 6** and **Figure 3**).

Clinical Utility of Salivary XO

XO specific activity in NWS correlates negatively with ACE III total score (r = -0.71, p < 0.001) and its several cognitive abilities: attention and orientation (r = -0.57. p = 0.001), memory (r = -0.63, p < 0.001), visual perception (r = -0.54, p = 0.002),

TABLE 2 | Clinical characteristics of the studies and control groups.

		Group			p-Value			
		C ***n*** **= 30**	**HS** ***n*** **= 15**	**IS** ***n*** **= 15**	**ANOVA**	**HS vs. C**	**IS vs. C**	**IS vs. HS**
Sex	Male *n* (%)	15 (50)	7 (46.66)	7 (46.66)		ND		
	Female *n* (%)	15 (50)	8 (53.33)	8 (53.33)				
Age *		63.07 ± 10.74 [59.06 - 67.08]	64.53 ± 8.123 [60.04 - 69.03]	61.6 ± 12.97 [54.42 - 68.78]	0.7586	0.9032	0.9032	0.7377
Education	Primary *n* (%)	2 (6.66)	1 (6.66)	1 (6.66)		> 0.9999		
	Vocational *n* (%)	15 (50)	7 (46.66)	6 (40)				
	Secondary *n* (%)	9 (30)	6 (40)	6 (40)				
	University *n* (%)	4 (13.33)	1 (6.66)	2 (13.33)				
Place of residence	Urban center *n* (%) *	10 (33.33)	6 (40)	7 (46.66)		> 0.9999		
	Small town *n* (%) *	8 (26.66)	4 (26.66)	3 (20)				
	Rural area or small village *n* (%) *	12 (40)	6 (40)	6 (40)				
		Cognitive and physical functional status						
ACE III *		97.47 ± 1.48 [96.91 - 98.02]	69.47 ± 25.04 [55.6 - 83.33]	61.47 ± 22.33 [49.1 - 73.84]	< 0.0001	< 0.0001	< 0.0001	0.3929
BI*		20 ± 0 [20 - 20]	10.73 ± 4.166 [8.426 - 13.04]	10.47 ± 3.62 [8.46 - 12.47]	< 0.0001	< 0.0001	< 0.0001	0.9615
FIM*		125.2 ± 0.68 [125 - 125.5]	81.8 ± 34.16 [62.88 - 100.7]	83.47 ± 33.48 [64.93 - 102]	< 0.0001	< 0.0001	< 0.0001	0.9798
BBS*		55.53 ± 0.51 [55.34 - 55.72]	31.53 ± 18.91 [21.06 - 42.01]	28.47 ± 17.6 [18.72 - 38.21]	< 0.0001	< 0.0001	< 0.0001	0.7899
Comorbidities								
Diabetes *n* (%)		13 (43.33)	7 (46.66)	6 (40)		> 0.9999		
Hypertension *n* (%)		16 (53.33)	8 (53.33)	8 (53.33)		> 0.9999		
Arteriosclerosis *n* (%)		13 (43.33)	7 (46.66)	7 (46.66)		> 0.9999		
Limb thrombosis *n* (%)		4 (13.33)	2 (13.33)	2 (13.33)		> 0.9999		
Atrial fibrillation *n* (%)		5 (16.66)	2 (13.33)	3 (20)		> 0.9999		
Drugs								
< 5 drugs/day *n* (%)		16 (53.33)	7 (46.66)	6 (40)		> 0.9999		
≥ 5 drugs/day *n* (%)		14 (46.66)	8 (53.33)	9 (60)				

*Results were analyzed using ANOVA analysis of variance followed by Tukey's post hoc test; ACE III, Addenbrooke's Cognitive Examination III; BBS, the Berg Balance Scale; BI, Barthel Index; C, Control group (n = 30); FIM, functional independence measure; HS, hemorrhagic stroke group (n = 15); IS, ischemic stroke group (n = 15); n, number of patients; ND, no data. *Expressed as mean ± standard deviation (SD) [95% confidence interval (95% CI)].*

language (r = -0.56, p = 0.001) and visuospatial skills (r = -0.53, p = 0.003) (**Figures 4A, B**).

XO specific activity was significantly higher in stroke patients with moderate cognitive impairment compared with mild cognitive decline and subjects with normal cognitive function (**Figure 4C**). ROC analysis also confirms the clinical relevance of this biomarker. XO specific activity in NWS differentiates with high accuracy and specificity between moderate and mild cognitive impairment and healthy subjects (**Table 7** and **Figures 4C–F**).

DISCUSSION

Vascular brain diseases are one of the most common causes of death and disability worldwide. Despite significant progress in understanding stroke pathogenesis, the number of cases is still increasing (1, 66, 67). Therefore, laboratory biomarkers of stroke are sought to allow rapid and non-invasive diagnostics (15). Although diagnosis is based primarily on clinical examination and CT scans, it is not always possible to rule out conditions mimicking strokes, such as subdural or epidural hematoma, brain tumors, craniocerebral or cervical spine injury, infections (meningitis, encephalitis, brain abscess), seizures, migraine complications, and metabolic disturbances. Moreover, the sensitivity of CT in newly diagnosed ischemic stroke is less than 30-35%, which, in the absence of widespread availability of MRI and CT perfusion, indicates the need to search for new diagnostic strategies (12, 14). The ideal stroke biomarker should differentiate between ischemic and hemorrhagic stroke, have high sensitivity and specificity (at least 75-85%), capture disease dynamics/treatment effectiveness, and be easily

TABLE 3 | Salivary gland function and stomatological characteristics of the studies and control groups.

		Group			p-Value			
		C	HS	IS	ANOVA	HS vs. C	IS vs. C	IS vs. HS
		n = 30	*n* = 15	*n* = 15				
SFR (mL/min)	NWS*	0.34 ± 0.09 [0.31 - 0.37]	0.39 ± 0.26 [0.24 - 0.52]	0.47 ± 0.25 [0.34 - 0.61]	0.1028	0.7393	0.084	0.4339
	SWS*	0.91 ± 0.26 [0.82 - 1.01]	0.63 ± 0.25 [0.5 - 0.77]	0.69 ± 0.29 [0.54 - 0.87]	0.0022	0.0039	0.0335	0.7732
TPC (μg/mL)	NWS*	1121 ± 188.4 [1050 - 1191]	904.5 ± 246.6 [768 - 1041]	817 ± 1 68.7 [723.5 - 910.4]	< 0.0001	0.0033	< 0.0001	0.4587
	SWS*	1240 ± 166.4 [1178 - 1303]	883.6 ± 250 [745.1 - 1022]	952.4 ± 225.4 [827.6 - 1077]	< 0.0001	< 0.0001	0.0001	0.6295
DMFT*		24.63 ± 7.25 [21.92 - 27.34]	22 ± 9.67 [16.64 - 27.36]	24.27 ± 3.84 [22.14 - 26.4]	0.5123	0.494	0.9862	0.674
GI*		0.74 ± 0.79 [0.44 - 1.04]	0.91 ± 0.77 [0.49 - 1.33]	0.6 ± 0.61 [0.26 - 0.94]	0.522	0.7598	0.8128	0.4906
PII*		1.28 ± 1 [0.89 - 1.67]	1.45 ± 0.94 [0.93 - 1.96]	1.01 ± 0.9 [0.51 - 1.51]	0.464	0.8551	0.6607	0.4402

Results were analyzed using ANOVA analysis of variance followed by Tukey's post hoc test; C, Control group (n = 30); DMFT, dental caries experience; GI, Gingival Index; HS, hemorrhagic stroke group (n = 15); IS, ischemic stroke group (n = 15); n, number of patients; NWS, non-stimulated whole saliva; PII, Plaque Index; SFR, salivary flow rate; SWS, stimulated whole saliva; TPC, total protein content.

**Expressed as mean ± standard deviation (SD) [95% confidence interval (95% CI)].*

quantifiable (68). In addition, the collection of biological material should be non-invasive, uncomplicated, and inexpensive. Therefore, saliva has become of increasing interest in the diagnosis of neurovascular diseases (69). Saliva collection is stress-free, requires no specialized medical personnel, and allows continuous monitoring of the patient's condition through non-invasive sampling multiple times per day (18, 32).

The main factors leading to ischemic brain injury are inhibition of ATP production, excitotoxicity, inflammation, and cerebral oxidative/nitrosative stress. Indeed, lack of energy substrates disrupts depolarization of the neuronal membrane and increases intracellular levels of Na^+, Cl^- and Ca^{2+} ions. This leads to activation of Ca^{2+}-dependent enzymes such as protein kinase C (PKC), phospholipase A2, and other cellular proteases

TABLE 4 | Salivary ischemia biomarkers of the studies and control groups.

		Group			p-Value			
		C	HS	IS	ANOVA	HS vs. C	IS vs. C	IS vs. HS
		n = 30	*n* = 15	*n* = 15				
XO activity (μU/mL)	NWS*	41.24 ± 6.61 [38.77 - 43.71]	46.99 ± 7.12 [43.05 - 50.93]	56.17 ± 7.75 [51.88 - 60.46]	< 0.0001	0.0325	< 0.0001	0.0021
	SWS*	38.37 ± 8.23 [35.29 - 41.44]	40.67 ± 8.74 [35.83 - 45.52]	42.99 ± 7.57 [38.79 - 47.18]	0.2039	0.6488	0.1851	0.7218
XO specific activity (nU/mg protein)	NWS*	37.99 ± 9.6 [34.4 - 41.57]	55.06 ± 14.56 [47 - 63.13]	71.94 ± 20.24 [60.73 - 83.15]	< 0.0001	0.0009	< 0.0001	0.0051
	SWS*	31.25 ± 6.8 [28.71 - 33.79]	50.59 ± 20.73 [39.11 - 62.07]	47.35 ± 12.89 [40.21 - 54.48]	< 0.0001	< 0.0001	0.0007	0.7751
XO output (μU/min)	NWS*	14 ± 3.96 [12.52 - 15.48]	17.62 ± 11.67 [11.15 - 24.08]	26.22 ± 14.65 [18.11 - 34.33]	0.0009	0.4701	0.0006	0.0474
	SWS*	34.93 ± 11.63 [30.59 - 39.28]	25.82 ± 12.12 [19.11 - 32.54]	29.75 ± 12.86 [22.63 - 36.88]	0.0562	0.0522	0.3697	0.6473
H_2O_2 concentration (nmol/L)	NWS*	239.7 ± 82.36 [208.9 - 270.5]	302.7 ± 72.37 [262.6 - 342.8]	500.9 ± 85.86 [453.3 - 548.4]	< 0.0001	0.7467	< 0.0001	< 0.0001
	SWS*	291.8 ± 77.43 [262.9 - 320.7]	351.1 ± 56.04 [320.1 - 382.1]	377.9 ± 89.92 [328.1 - 427.7]	0.0015	0.0438	0.0021	0.6024
UA concentration (μmol/L)	NWS*	58.83 ± 13.3 [53.86 - 63.8]	77.15 ± 23.25 [64.27 - 90.02]	102 ± 35.51 [82.37 - 121.7]	< 0.0001	0.0391	< 0.0001	0.0125
	SWS*	63.4 ± 18.34 [56.55 - 70.24]	57.87 ± 27.49 [42.65 - 73.1]	65.38 ± 31.49 [47.95 - 82.82]	0.6781	0.7571	0.9644	0.6804

ANOVA, analysis of variance; C, Control group (n = 30); H_2O_2, hydrogen peroxide; HS, hemorrhagic stroke group (n = 15); IS, ischemic stroke group (n = 15); n, number of patients; NWS, non-stimulated whole saliva; SWS, stimulated whole saliva; UA, uric acid; XO, xanthine oxidase.

**Expressed as mean ± standard deviation (SD) [95% confidence interval (95% CI)].*

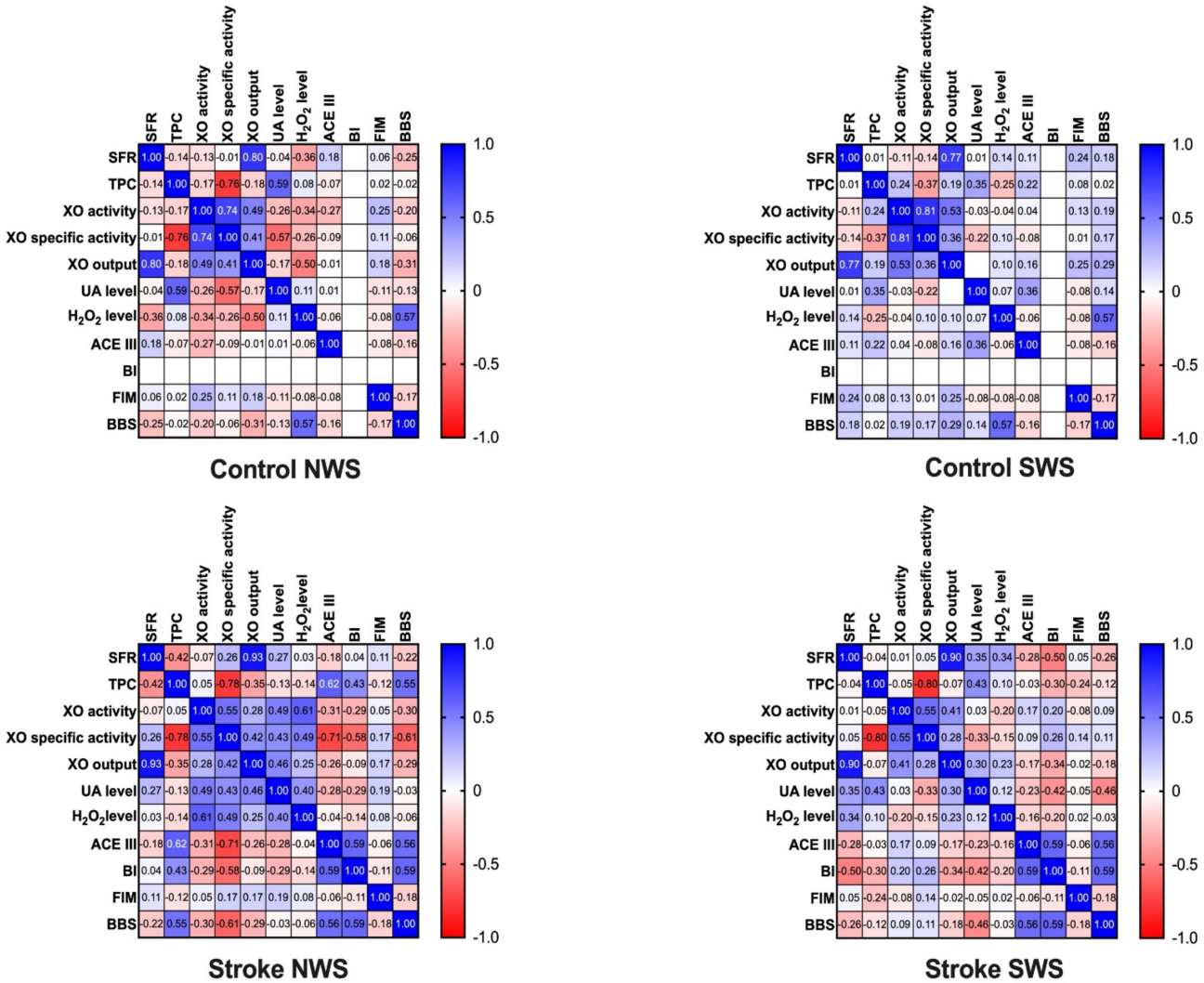

FIGURE 2 | Correlations between salivary gland function, salivary ischemia biomarkers, and clinical parameters. ACE III, Addenbrooke's Cognitive Examination III; BBS, the Berg Balance Scale; BI, Barthel Index; FIM, functional independence measure; H_2O_2, hydrogen peroxide; NWS, non-stimulated whole saliva; SFR, salivary flow rate; SWS, stimulated whole saliva; TPC, total protein content; UA, uric acid; XO, xanthine oxidase.

initiating neuronal apoptosis and necrosis. Simultaneously, there is a conversion of xanthine dehydrogenase to XO, which is crucial in post-stroke complications. The substrate for the enzyme is hypoxanthine (a breakdown product of ATP), which accumulates in the ischemic brain. When O_2 is delivered under reperfusion, XO causes the conversion of hypoxanthine to xanthine accompanied by the release of superoxide radicals (O_2-•) *via* reduction of molecular oxygen. Subsequently O_2-• induces the formation of more toxic ROS (e.g., H_2O_2) and stimulates the production of inflammatory mediators (24, 70, 71). However, XO also catalyzes the conversion of xanthine to UA (**Figure 1**). In ischemic stroke animal models, cerebral XO activity correlates with infarct volume and severity of neurological complications, thus postulating the use of XO in the identification/differentiation of the disease. Because assessment of XO activity in the blood is not diagnostically relevant (72), we were the first to investigate the usefulness of salivary XO in stroke patients.

We demonstrated that XO activity is significantly higher in NWS of ischemic stroke patients compared to hemorrhagic stroke and healthy subjects. However, statistically important differences were not observed in SWS. Indeed, the composition of stimulated saliva depends not only on the salivary gland but also on the environmental stimuli. Under resting conditions, 2/3 of the saliva is produced by the submandibular glands, whose filtrate generally reflects the composition of blood plasma. However, this ratio shifts during food/smell stimulation in favor of the parotid glands (52, 53, 73). These glands are also the primary source of antioxidants in the oral cavity, making SWS more protective against salivary oxidative stress (17, 74).

TABLE 5 | Multiple regression analysis of salivary ischemia biomarkers in all involved objects.

		NWS					SWS				
		XO activity	XO specific activity	XO output	H_2O_2 concentration	UA concentration	XO activity	XO specific activity	XO output	H_2O_2 concentration	UA concentration
β1: stroke type	Estimate	8.42	16.45	4.21	202.1	21.66	-0.008267	2.015	1.044	20.13	-13.56
	95% CI	2.49 - 14.35	8.67 - 24.23	0.47 - 7.95	137.2 - 267.1	0.09 - 43.23	-6.706 - 6.689	-11.4 - 15.43	-3.38 - 5.47	-55.59 - 95.85	-31.62 - 4.5
	p-Value	0.0074	0.0002	0.0291	< 0.0001	0.0491	0.998	0.7589	0.6302	0.5877	0.1341
β2: ACE III	Estimate	-0.02829	-0.2998	0.003936	1.435	-0.1792	-0.019	-0.03557	0.009605	-0.54	-0.4134
	95% CI	-0.19 - 0.14	-0.52 - -0.07	-0.1 - 0.11	-0.41 - 3.28	-0.79 - 0.43	-0.24 - 0.21	-0.48 - 0.41	-0.13 - 0.15	-3.07 - 1.99	-1.01 - 0.19
	p-Value	0.7317	0.0101	0.9397	0.122	0.5517	0.8623	0.8712	0.8944	0.6634	0.1706
β3: BI	Estimate	-0.3106	-1.223	-0.4194	-10.09	-3.855	-0.4503	0.4518	-0.2671	3.151	-2.186
	95% CI	-1.38 - 0.76	-2.63 - 0.18	-1.09 - 0.25	-21.83 - 1.64	-7.75 - 0.04	-1.67 - 0.76	-1.99 - 2.89	-1.07 - 0.54	-10.63 - 16.93	-5.48 - 1.1
	p-Value	0.5542	0.0848	0.212	0.0884	0.0522	0.4526	0.7055	0.4994	0.6407	0.1823
β4: FIM	Estimate	0.0008364	0.03768	0.01982	0.1577	0.1575	-0.009847	0.08176	-0.009425	-0.3358	-0.3762
	95% CI	-0.09 - 0.09	-0.08 - 0.16	-0.03- 0.07	-0.84 - 1.15	-0.18 - 0.49	-0.11 - 0.09	-0.12 - 0.29	-0.07 - 0.05	-1.5 - 0.83	-0.65 - -0.09
	p-Value	0.985	0.5199	0.4821	0.7463	0.3347	0.845	0.4209	0.777	0.5567	0.0101
β5: BBS	Estimate	-0.07378	-0.1856	-0.001744	0.4655	0.7937	0.1786	0.361	0.103	-0.7422	0.3472
	95% CI	-0.29 - 0.14	-0.48 - 0.1	-0.14 - 0.13	-1.97 - 2.9	-0.01 - 1.6	-0.06 - 0.42	-0.13 - 0.85	-0.05 - 0.27	-3.52 - 2.03	-0.31 - 1
	p-Value	0.5	0.2018	0.9797	0.6969	0.0545	0.146	0.1425	0.2017	0.5855	0.2893
β6: SFR	Estimate	-3.899	12.23	50.6	54.62	43.15	0.2419	5.205	41.9	119.2	17.25
	95% CI	-16.44 - 8.64	-4.22 - 28.69	42.69 - 58.52	-82.83 - 192.1	-2.47 - 88.77	-14.65 - 15.14	-24.63 - 35.04	32.06 - 51.74	-49.16 - 287.6	-22.92 - 57.43
	p-Value	0.5264	0.1377	< 0.0001	0.4195	0.0626	0.9735	0.7215	< 0.0001	0.1565	0.3836

ACE III, Addenbrooke's Cognitive Examination III; BBS, the Berg Balance Scale; BI, Barthel Index; CI, confidence interval; FIM, functional independence measure; H_2O_2, hydrogen peroxide; NWS, non-stimulated whole saliva; SFR, salivary flow rate; SWS, stimulated whole saliva; UA, uric acid; XO, xanthine oxidase.

The results of our previous studies support this. In SWS of stroke patients, we have shown higher activity/concentration of enzymatic and non-enzymatic antioxidants, which is an adaptive response to ROS overproduction in the parotid glands. These facts may explain the lack of differences in XO activity in SWS, especially if the concentration of enzyme substrates (xanthine and hypoxanthine) is very low in saliva samples. SWS is also much more dilute than NWS, making it less useful in laboratory medicine (33). Indeed, the main limitation of diagnostic applicability of saliva is the low biomarker concentration/activity compared to other bioliquids and tissues (75). Also in our study, salivary XO activity assessed by a standard enzyme assay was below the detection level in both NWS and SWS. However, using the Amplex Red xanthine/XO fluorometric method, XO can be detected at levels as low as 0.1 mU/mL. The use of a commercial kit has particular advantages in diagnostics, as it allows the comparison of results obtained in different laboratories.

The biomarkers found in saliva can be divided into compounds produced in the salivary glands and those outside of them (33, 74, 76). The ability to pass into saliva depends on the mechanism of transport and occurs *via* intracellular (diffusion, filtration, facilitated transport, active transport) or extracellular routes. Since most salivary proteins have a molecular weight between 20 and 60 kDa (low molecular weight proteins) (77), XO can migrate into saliva through ultrafiltration or damaged cellular membranes (78). XO is a homodimer composed of two subunits with an approximate molecular weight of 150-155 kDa (79). During BBB injury, XO can penetrate the brain into the circulation and then into the oral cavity. The salivary glands are very well vascularized resulted in a very efficient secretion of many substances into saliva (52). This may explain the higher correlation of many biomarkers between brain and NWS compared to blood (33). It may also result from a common developmental origin, or it may simply reflect the more significant variability of XO in the saliva (46). It should not be forgotten that XO can also be produced in the salivary glands (79). However, in some stroke patients, salivary gland dysfunction manifests as decreased salivary secretion (hyposalivation) or subjective dryness of the oral mucosa (xerostomia) (62, 80). Since the activity/concentration of salivary biomarkers is highly dependent on salivary gland function, we standardized XO measurement on total protein content and salivary flow rate. Our study indicates that XO activity should be standardized to total protein concentration, as with other salivary enzymes. Specific XO activity (nU/mg protein) better differentiates ischemic from hemorrhagic stroke and from healthy subjects.

The brain is particularly vulnerable to oxidation because it uses more than 20% of O_2 supplied to the body (81). Neurons also show a very unfavorable surface-to-volume ratio, a high content of unsaturated fatty acids, and low efficiency of enzymatic antioxidant systems (82). Therefore, the main cause of brain damage during ischemia and reperfusion is the increased

TABLE 6 | ROC analysis of salivary ischemia biomarkers.

		Cut off	AUC	95% CI	Sensitivity %	95% CI	Specificity %	95% CI
					HS vs. C			
XO activity	NWS	> 44.78	0.747	0.59 - 0.91	80	54.81% - 92.95%	66.67	48.78% - 80.77%
	SWS	> 40.56	0.593	0.41 - 0.78	60	35.75% - 80.18%	66.67	48.78% - 80.77%
XO specific activity	NWS	> 45.94	0.858	0.74 - 0.97	73.33	48.05% - 89.1%	83.33	66.44% - 92.66%
	SWS	> 37.54	0.824	0.67 - 0.99	80	54.81% - 92.95%	86.67	70.32% - 94.69%
XO output	NWS	< 14.18	0.502	0.28 - 0.73	53.33	30.12% - 75.19%	50	33.15% - 66.85%
	SWS	< 30.95	0.693	0.53 - 0.86	66.67	41.71% - 84.82%	63.33	45.51% - 78.13%
H_2O_2 concentration	NWS	> 251.6	0.704	0.56 - 0.86	66.67	41.71% - 84.82%	56.67	39.2% - 72.62%
	SWS	> 325.4	0.733	0.59 - 0.88	73.33	48.05% - 89.1%	70	52.12% - 83.34%
UA concentration	NWS	> 65.44	0.735	0.59 - 0.89	66.67	41.71% - 84.82%	66.67	48.78% - 80.77%
	SWS	< 57.01	0.609	0.42 - 0.8	66.67	41.71% - 84.82%	73.33	55.55% - 85.82%
					IS vs. C			
XO activity	NWS	> 49.61	0.92	0.82 - 1	86.67	62.12% - 97.63%	93.33	78.68% - 98.82%
	SWS	> 38.78	0.649	0.47 - 0.82	66.67	41.71% - 84.82%	56.67	39.2% - 72.62%
XO specific activity	NWS	> 50.3	0.973	0.94 - 1	93.33	70.18% - 99.66%	90	74.38% - 96.54%
	SWS	> 36.77	0.871	0.74 - 1	86.67	62.12% - 97.63%	83.33	66.44% - 92.66%
XO output	NWS	> 17.46	0.747	0.55 - 0.94	73.33	48.05% - 89.1%	83.33	66.44% - 92.66%
	SWS	< 32.65	0.607	0.43 - 0.79	53.33	30.12% - 75.19%	56.67	39.2% - 72.62%
H_2O_2 concentration	NWS	> 357.6	0.998	0.99 - 1	100	79.61% - 100%	96.67	83.33% - 99.83%
	SWS	> 328.5	0.762	0.61 - 0.92	66.67	41.71% - 84.82%	73.33	55.55% - 85.82%
UA concentration	NWS	> 68.82	0.873	0.74 - 1	86.67	62.12% - 97.63%	80	62.69% - 90.49%
	SWS	< 58.37	0.538	0.34 - 0.73	60	35.75% - 80.18%	66.67	48.78% - 80.77%
					IS vs. HS			
XO activity	NWS	> 49.08	0.836	0.68 - 0.99	86.67	62.12% - 97.63%	73.33	48.05% - 89.1%
	SWS	> 40.87	0.551	0.34 - 0.77	53.33	30.12% - 75.19%	46.67	24.81% - 69.88%
XO specific activity	NWS	> 59.75	0.764	0.6 - 0.93	66.67	41.71% - 84.82%	66.67	41.71% - 84.82%
	SWS	< 46.92	0.516	0.3 - 0.73	53.33	30.12% - 75.19%	53.33	30.12% - 75.19%
XO output	NWS	> 20.09	0.684	0.5 - 0.9	66.67	41.71% - 84.82%	66.67	41.71% - 84.82%
	SWS	> 26.62	0.591	0.38 - 0.8	66.67	41.71% - 84.82%	53.33	30.12% - 75.19%
H_2O_2 concentration	NWS	> 392.6	0.96	0.9 - 1	93.33	70.18% - 99.66%	86.67	62.12% - 97.63%
	SWS	> 368.5	0.6	0.39 - 0.82	60	35.75% - 80.18%	66.67	41.71% - 84.82%
UA concentration	NWS	> 76.44	0.724	0.54 - 0.91	73.33	48.05% - 89.1%	66.67	41.71% - 84.82%
	SWS	> 53.19	0.587	0.38 - 0.8	66.67	41.71% - 84.82%	53.33	30.12% - 75.19%

AUC, the area under the curve; C, Control group (n = 30); CI, confidence interval; H_2O_2, hydrogen peroxide; HS, hemorrhagic stroke group (n = 15); IS, ischemic stroke group (n = 15); NWS, non-stimulated whole saliva; SWS: stimulated whole saliva; UA, uric acid; XO, xanthine oxidase.

formation of ROS by XO (42). The superoxide radical generated by XO is enzymatically reduced to H_2O_2, with the simultaneous conversion of xanthine to uric acid. Although UA has strong antioxidant properties, in high concentrations, it also has a robust pro-oxidant effect. UA can generate free radicals by reaction with peroxynitrite or alkylate cellular biomolecules disrupting their structure and function (40). Thus, increased synthesis/release of proinflammatory cytokines, chemokines, and growth factors promotes neuronal apoptosis and necrosis under XO overexpression (83). In the acute phase of stroke, the BBB is disrupted, causing many biomarkers to infiltrate the blood and saliva (50). In our study, UA and H_2O_2 levels were significantly higher in stroke patients' saliva than controls, whereas they did not differentiate between stroke types. Although XO activity correlated strongly with uric acid and hydrogen peroxide levels in stroke cases, their source in saliva may also be diffusion from blood plasma (UA) or exposure to environmental factors (84). Indeed, the oral cavity is the only place in the body exposed to many pro-oxidant agents such as diet, xenobiotics, oral microbiota, dental procedures, and materials (85–87).

An essential part of our study was also to evaluate the saliva's usefulness for assessing XO activity in stroke patients. For this purpose, we used ROC curves, which are a graphical relationship between a test's sensitivity and specificity. Of all the parameters evaluated, the specific activity of XO has the best clinical utility. We have shown that this biomarker differentiates ischemic stroke from hemorrhagic stroke (AUC: 0.764) and controls (AUC: 0.973) with very high sensitivity (IS vs. HS: 66.67%; IS vs. C: 93.33%) and specificity (IS vs. HS: 66.67%; IS vs. C: 90%). It is also noteworthy that XO specific activity correlates negatively with cognitive impairment according to ACE III scale, postural balance in BBS scale and performance in living activities using BI scale. Importantly, these relationships were observed only in the NWS of stroke patients. Unfortunately, we do not have clinical data on stroke location, brain infarct volume, and severity of neurological symptoms, making further clinical studies necessary. Although this undoubtedly represents limitations of the study, we are the first to demonstrate the utility of salivary XO in the differential diagnosis of stroke and for assessing patients' functional status.

Stroke is the most common cause of cognitive impairment in people over 65 years old. Cognitive deficits include all areas of daily functioning affecting treatment and rehabilitation outcomes and quality of patient's life (88). In our study, XO specific activity correlated highly negatively with cognitive abilities in the ACE III score. In detail, this biomarker

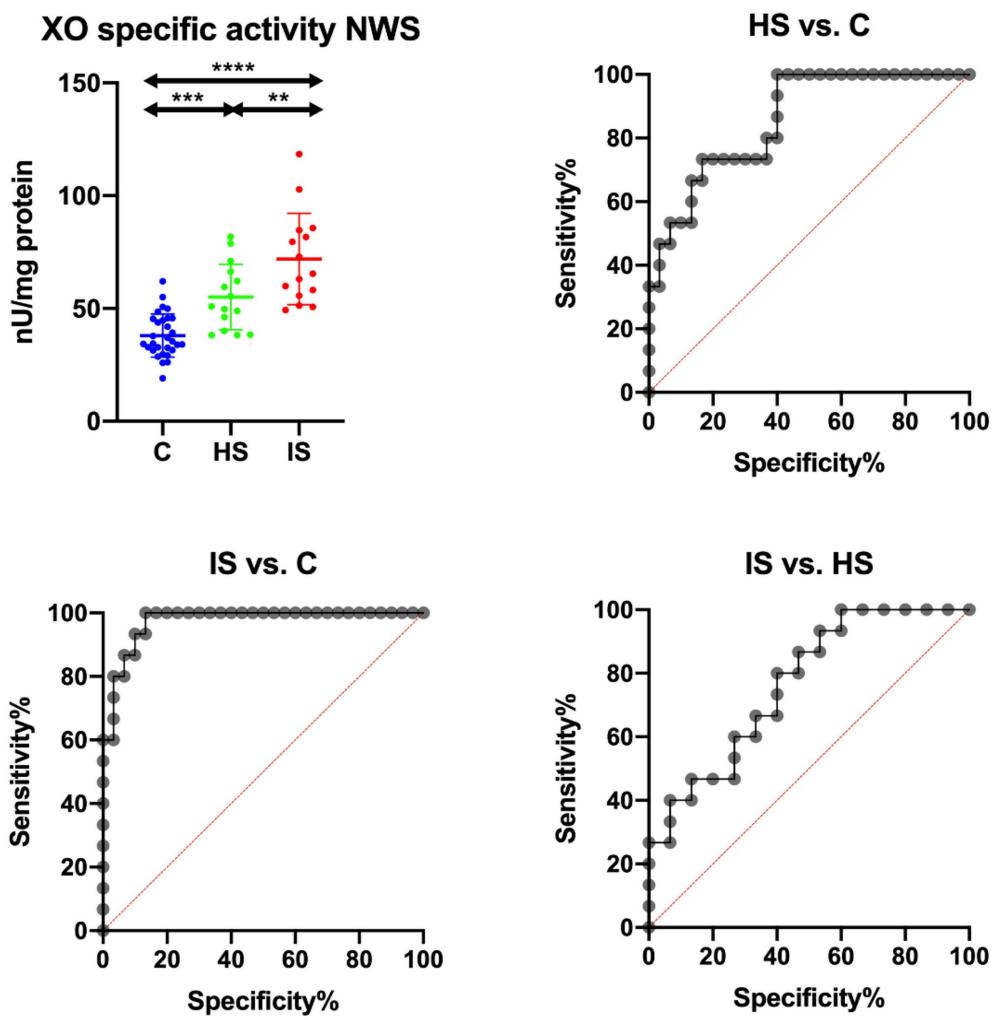

FIGURE 3 | Results of ROC analysis for salivary XO specific activity in NWS. C, Control group (*n* = 30); HS, hemorrhagic stroke group (*n* = 15); IS, ischemic stroke group (*n* = 15); NWS, non-stimulated whole saliva; XO, xanthine oxidase. Differences statistically significant at: **p < 0.005; ***p < 0.0005; ****p < 0.0001.

wasadversely associated with attention and orientation (r = -0.57, p = 0.001), memory (r = -0.63, p = 0.0002), visual perception (r = -0.54, p = 0.002), language (r = -0.56, p = 0.001) and visuospatial functions (r = -0.53, p = 0.003). ACE III is a comprehensive screening tool for cognitive function assessment, useful for early detection of cognitive impairment, differential diagnosis of dementia, and monitoring of the disease progression (54). Therefore, in the next step, we divided stroke patients into three subgroups based on the severity of cognitive decline: normal cognition (100-89 in the ACE III), mild cognitive impairment (88-61 in the ACE III), and moderate cognitive dysfunction (< 61 in the ACE III) (89, 90). We have demonstrated that XO specific activity differentiates with high accuracy (100%) and specificity (93.75%) between stroke patients with mild to moderate cognitive decline (AUC = 0.988). Thus, salivary XO assessment may be a potential screening tool for a comprehensive neuropsychological evaluation. Unfortunately, this parameter did not distinguish cognitively mild patients from those without cognitive impairment, which may be due to the small number of patients.

The ideal diagnostic biomarker should be detectable at an early stage of the disease. Our study involves patients in the acute phase of stroke (30-35 days after the incident), and therefore, it is essential to evaluate salivary XO activity in newly diagnosed cases. Since ischemia-reperfusion is most severe at this time, assessment of XO activity may have even greater diagnostic value (91).

In conclusion, our study demonstrates the utility of salivary xanthine oxidase in the differential diagnosis of stroke. The biological material for assessing XO activity should be non-stimulated saliva, and the results must be standardized to total protein content. We have shown that XO specific activity distinguishes, with very high sensitivity and specificity, between ischemic and hemorrhagic strokes and controls, as

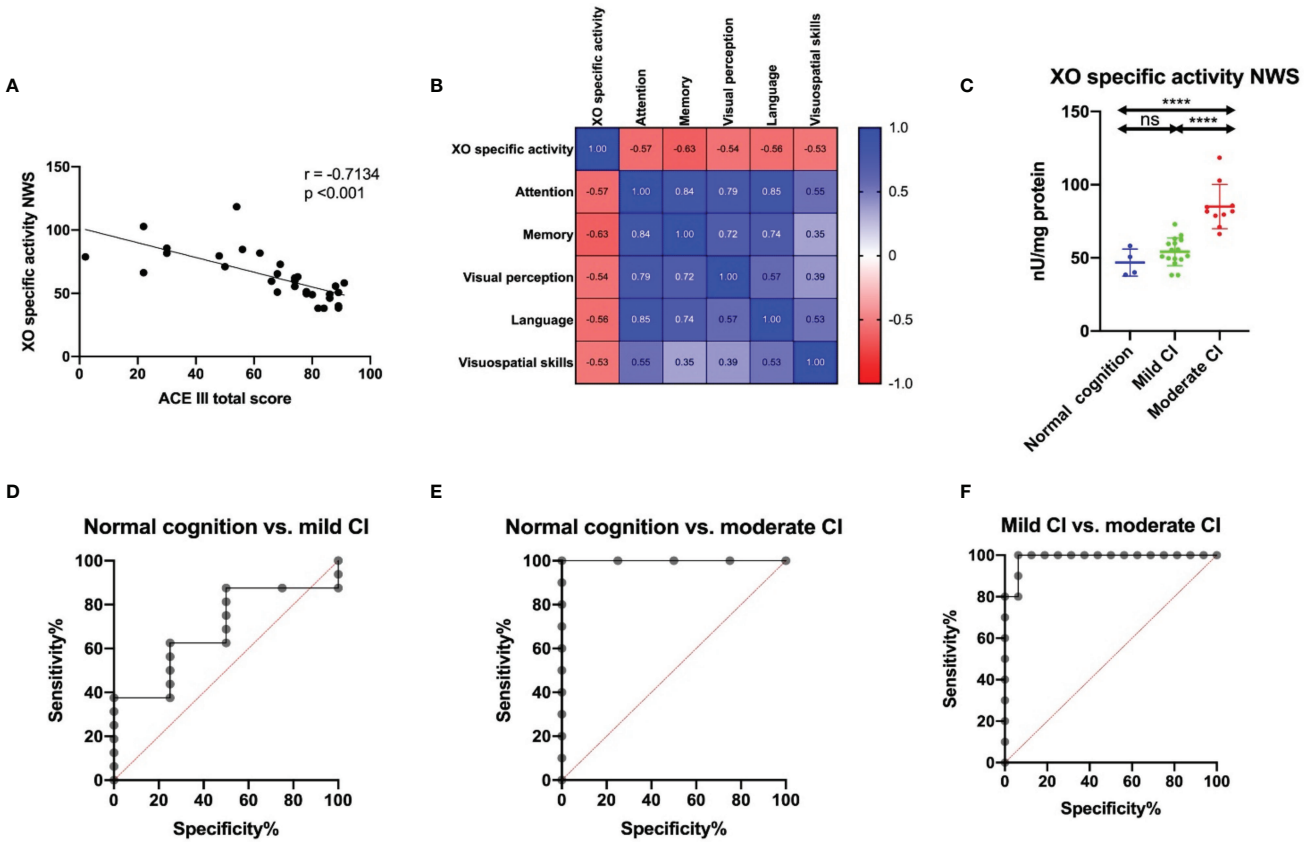

FIGURE 4 | Correlation between salivary XO specific activity and cognitive function in ACE III scale **(A)**, correlations between XO specific activity and several parameters of ACE III score **(B)**; results of ROC analysis for salivary XO specific activity in relation to cognitive function status in ACE III scale in NWS **(C–F)**. ACE III, Addenbrooke's Cognitive Examination III; mild CI, mild cognitive impairment; moderate CI, moderate cognitive impairment; NWS, non-stimulated whole saliva; XO, xanthine oxidase. Differences statistically significant at ****p < 0.0001. ns, non significance.

TABLE 7 | Results of ROC analysis for salivary XO specific activity in relation to cognitive function status in ACE III scale in NWS.

	Cut off	AUC	95% CI	Sensitivity %	95% CI	Specificity %	95% CI
Normal cognition vs. mild CI	> 50.79	0.688	0.42 - 0.95	62.5	38.64% - 81.52%	75	30.06% - 98.72%
Normal cognition vs. moderate CI	> 62.22	1	1 - 1	100	72.25% - 100%	100	51.01% - 100%
Mild CI vs. moderate CI	> 65.86	0.988	0.95 - 1	100	72.25% - 100%	93.75	71.67% - 99.68%

AUC, the area under the curve; CI, confidence interval; mild CI, mild cognitive impairment; moderate CI, moderate cognitive impairment.

well as patients with mild and moderate cognitive impairment. Currently, there is no generally available and sensitive diagnostic test for stroke, which is a major limitation in its early diagnosis as well as its treatment. Salivary XO may be the first potential biomarker used in the differential diagnosis of stroke and to assess the functional status of patients.

Our study also has some limitations. Although appropriate statistical tests determined the sample size calculation, further studies on a larger patient population are needed. It is also necessary to evaluate XO activity in cases with periodontal and other oral and systemic diseases, which may affect the parameters assessed in saliva. It would also be interesting to perform a more extended follow-up of the patients, to investigate the possible correlation between evolution of XO salivary levels and the improvement of cognitive and physical functions, during the recovery after the acute phase of the stroke. To assess biomarker specificity, evaluation of salivary XO activity in patients with other neurological diseases [e.g., small vessel disease and transient ischemic attack (TIA)] is also essential.

DATA AVAILABILITY STATEMENT

The original contributions presented in the study are included in the article/supplementary material. Further inquiries can be directed to the corresponding author.

ETHICS STATEMENT

The studies involving human participants were reviewed and approved by Local Ethics Committee at the Poznan University of Medical Sciences. The patients/participants provided their written informed consent to participate in this study.

AUTHOR CONTRIBUTIONS

MM: conceptualized, did laboratory determinations, performed statistical analysis, interpreted data, did performance of the graphic part of the manuscript, wrote the manuscript, reviewed the article, final approval of the version to be published, coordination of the project. MN: did laboratory determinations, interpreted data. AZ: conceptualized, did laboratory determinations, reviewed the article, final approval of the version to be published. GB: did laboratory determinations. PG: performed clinical examination, qualified patients to the study, collected material. KH: performed clinical examination, qualified patients to the study, collected material. KG: conceptualized, did laboratory determinations, reviewed the article, final approval of the version to be published. All authors contributed to the article and approved the submitted version.

FUNDING

This work was supported by the Medical University of Bialystok, Poland (Grant No. SUB/1/DN/22/002/3330).

REFERENCES

1. Guzik A, Bushnell C. Stroke Epidemiology and Risk Factor Management. *Contin (Minneap Minn)* (2017) 23:15–39. doi: 10.1212/CON.0000000000000416
2. Kuriakose D, Xiao Z. Pathophysiology and Treatment of Stroke: Present Status and Future Perspectives. *Int J Mol Sci* (2020) 21:7609. doi: 10.3390/ijms21207609
3. Feigin VL, Norrving B, Mensah GA. Global Burden of Stroke. *Circ Res* (2017) 120:439–48. doi: 10.1161/CIRCRESAHA.116.308413
4. Johnson W, Onuma O, Owolabi M, Sachdev S. Stroke: A Global Response Is Needed. *Bull World Health Organ* (2016) 94:634–634A. doi: 10.2471/BLT.16.181636
5. Herpich F, Rincon F. Management of Acute Ischemic Stroke. *Crit Care Med* (2020) 48:1654–63. doi: 10.1097/CCM.0000000000004597
6. Zaidat OO, Yoo AJ, Khatri P, Tomsick TA, von Kummer R, Saver JL, et al. Recommendations on Angiographic Revascularization Grading Standards for Acute Ischemic Stroke. *Stroke* (2013) 44:2650–63. doi: 10.1161/STROKEAHA.113.001972
7. Wu S, Yuan R, Wang Y, Wei C, Zhang S, Yang X, et al. Early Prediction of Malignant Brain Edema After Ischemic Stroke. *Stroke* (2018) 49:2918–27. doi: 10.1161/STROKEAHA.118.022001
8. Peisker T, Koznar B, Stetkarova I, Widimsky P. Acute Stroke Therapy: A Review. *Trends Cardiovasc Med* (2017) 27:59–66. doi: 10.1016/j.tcm.2016.06.009
9. Lew JH, Naruishi K, Kaijura Y, Nishikiwa Y, Ikuta T, Kido JI, et al. High Glucose-Mediated Cytokine Regulation in Gingival Fibroblasts and THP-1 Macrophage: A Possible Mechanism of Severe Periodontitis With Diabetes. *Cell Physiol Biochem* (2018) 50:987–1004. doi: 10.1159/000494481
10. Jung S, Stapf C, Arnold M. Stroke Unit Management and Revascularisation in Acute Ischemic Stroke. *Eur Neurol* (2015) 73:98–105. doi: 10.1159/000365210
11. Musuka TD, Wilton SB, Traboulsi M, Hill MD. Diagnosis and Management of Acute Ischemic Stroke: Speed Is Critical. *Can Med Assoc J* (2015) 187:887–93. doi: 10.1503/cmaj.140355
12. Rowley H, Vagal A. "Stroke and Stroke Mimics: Diagnosis and Treatment.," In: Hodler J., Kubik-Huch R., von Schulthess G. (eds) *Diseases of the Brain, Head and Neck, Spine 2020–2023* IDKD Springer Series. Cham:Springer (2020). 25–36. doi: 10.1007/978-3-030-38490-6_3
13. Lin MP, Liebeskind DS. Imaging of Ischemic Stroke. *Contin Lifelong Learn Neurol* (2016) 22:1399–423. doi: 10.1212/CON.0000000000000376
14. Kamalian S, Lev MH. Stroke Imaging. *Radiol Clin North Am* (2019) 57:717–32. doi: 10.1016/j.rcl.2019.02.001
15. Yang C, Fan F, Sawmiller D, Tan J, Wang Q, Xiang Y. C1q/TNF-Related Protein 9: A Novel Therapeutic Target in Ischemic Stroke? *J Neurosci Res* (2019) 97:128–36. doi: 10.1002/jnr.24353
16. Choromańska M, Klimiuk A, Kostecka-Sochoń P, Wilczyńska K, Kwiatkowski M, Okuniewska N, et al. Antioxidant Defence, Oxidative Stress and Oxidative Damage in Saliva, Plasma and Erythrocytes of Dementia Patients. *AGE Be a Marker of Dementia. Int J Mol Sci* (2017) 18:2205. doi: 10.3390/ijms18102205
17. Sawczuk B, Maciejczyk M, Sawczuk-Siemieniuk M, Posmyk R, Zalewska A, Car H. Salivary Gland Function, Antioxidant Defence and Oxidative Damage in the Saliva of Patients With Breast Cancer: Does the BRCA1 Mutation Disturb the Salivary Redox Profile? *Cancers (Basel)* (2019) 11:1–22. doi: 10.3390/cancers11101501
18. Kułak-Bejda A, Waszkiewicz N, Bejda G, Zalewska A, Maciejczyk M. Diagnostic Value of Salivary Markers in Neuropsychiatric Disorders. *Dis Markers* (2019) 2019:1–6. doi: 10.1155/2019/4360612
19. Klimiuk A, Maciejczyk M, Choromańska M, Fejfer K, Waszkiewicz N, Zalewska A. Salivary Redox Biomarkers in Different Stages of Dementia Severity. *J Clin Med* (2019) 8:840. doi: 10.3390/jcm8060840
20. Maciejczyk M, Szulimowska J, Taranta-Janusz K, Werbel K, Wasilewska A, Zalewska A. Salivary FRAP as a Marker of Chronic Kidney Disease Progression in Children. *Antioxidants* (2019) 8:1–18. doi: 10.3390/antiox8090409
21. Pawluk H, Woźniak A, Grześk G, Kołodziejska R, Kozakiewicz M, Kopkowska E, et al. The Role of Selected Pro-Inflammatory Cytokines in Pathogenesis of Ischemic Stroke. *Clin Interv Aging* (2020) 15:469–84. doi: 10.2147/CIA.S233909
22. Yang C, Hawkins KE, Doré S, Candelario-Jalil E. Neuroinflammatory Mechanisms of Blood-Brain Barrier Damage in Ischemic Stroke. *Am J Physiol Physiol* (2019) 316:C135–53. doi: 10.1152/ajpcell.00136.2018
23. Jayaraj RL, Azimullah S, Beiram R, Jalal FY, Rosenberg GA. Neuroinflammation: Friend and Foe for Ischemic Stroke. *J Neuroinflamm* (2019) 16:142. doi: 10.1186/s12974-019-1516-2
24. Doyle KP, Simon RP, Stenzel-Poore MP. Mechanisms of Ischemic Brain Damage. *Neuropharmacology* (2008) 55:310–8. doi: 10.1016/j.neuropharm.2008.01.005
25. Shi K, Tian D-C, Li Z-G, Ducruet AF, Lawton MT, Shi F-D. Global Brain Inflammation in Stroke. *Lancet Neurol* (2019) 18:1058–66. doi: 10.1016/S1474-4422(19)30078-X
26. Sinha N, Dabla P. Oxidative Stress and Antioxidants in Hypertension–A Current Review. *Curr Hypertens Rev* (2015) 11:132–42. doi: 10.2174/1573402111666150529130922
27. Kumar P, Yadav AK, Misra S, Kumar A, Chakravarty K, Prasad K. Role of Interleukin-10 (-1082a/G) Gene Polymorphism With the Risk of Ischemic Stroke: A Meta-Analysis. *Neurol Res* (2016) 38:823–30. doi: 10.1080/01616412.2016.1202395
28. Huda S, Akhter N. Modulation of Oxidative Stress by Enalapril and Valsartan in Adrenaline Treated Rats: A Comparative Study. *Bangladesh Med Res Counc Bull* (2014) 40:25–30. doi: 10.3329/bmrcb.v40i1.20333
29. Durukan A, Tatlisumak T. Acute Ischemic Stroke: Overview of Major Experimental Rodent Models, Pathophysiology, and Therapy of Focal Cerebral Ischemia. *Pharmacol Biochem Behav* (2007) 87:179–97. doi: 10.1016/j.pbb.2007.04.015

30. Choromańska B, Myśliwiec P, Łuba M, Wojskowicz P, Dadan J, Myśliwiec H, et al. A Longitudinal Study of the Antioxidant Barrier and Oxidative Stress in Morbidly Obese Patients After Bariatric Surgery. Does the Metabolic Syndrome Affect the Redox Homeostasis of Obese People? *J Clin Med* (2020) 9:976. doi: 10.3390/jcm9040976
31. Maciejczyk M, Zalewska A, Gerreth K. Salivary Redox Biomarkers in Selected Neurodegenerative Diseases. *J Clin Med* (2020) 9:497. doi: 10.3390/jcm9020497
32. Yoshizawa JM, Schafer CA, Schafer JJ, Farrell JJ, Paster BJ, Wong DTW. Salivary Biomarkers: Toward Future Clinical and Diagnostic Utilities. *Clin Microbiol Rev* (2013) 26:781–91. doi: 10.1128/CMR.00021-13
33. Malathi N, Mythili S, Vasanthi HR. Salivary Diagnostics: A Brief Review. *ISRN Dent* (2014) 2014:1–8. doi: 10.1155/2014/158786
34. Pfaffe T, Cooper-White J, Beyerlein P, Kostner K, Punyadeera C. Diagnostic Potential of Saliva: Current State and Future Applications. *Clin Chem* (2011) 57:675–87. doi: 10.1373/clinchem.2010.153767
35. Matczuk J, Żendzian-Piotrowska M, Maciejczyk M, Kurek K. Salivary Lipids: A Review. *Adv Clin Exp Med* (2017) 26:1023–31. doi: 10.17219/acem/63030
36. Yang NY, Shi L, Zhang Y, Ding C, Cong X, Fu FY, et al. Ischemic Preconditioning Reduces Transplanted Submandibular Gland Injury. *J Surg Res* (2013) 179:265–73. doi: 10.1016/j.jss.2012.02.066
37. Gerreth P, Maciejczyk M, Zalewska A, Gerreth K, Hojan K. Comprehensive Evaluation of the Oral Health Status, Salivary Gland Function, and Oxidative Stress in the Saliva of Patients With Subacute Phase of Stroke: A Case-Control Study. *J Clin Med* (2020) 9:2252. doi: 10.3390/jcm9072252
38. Maciejczyk M, Mil KM, Gerreth P, Hojan K, Zalewska A, Gerreth K. Salivary Cytokine Profile in Patients With Ischemic Stroke. *Sci Rep* (2021) 11:17185. doi: 10.1038/s41598-021-96739-0
39. Dawson J, Broomfield N, Dani K, Dickie DA, Doney A, Forbes K, et al. Xanthine Oxidase Inhibition for the Improvement of Long-Term Outcomes Following Ischaemic Stroke and Transient Ischaemic Attack (XILO-FIST) – Protocol for a Randomised Double Blind Placebo-Controlled Clinical Trial. *Eur Stroke J* (2018) 3:281–90. doi: 10.1177/2396987318771426
40. Britnell SR, Chillari KA, Brown JN. The Role of Xanthine Oxidase Inhibitors in Patients With History of Stroke: A Systematic Review. *Curr Vasc Pharmacol* (2018) 16:583–8. doi: 10.2174/1570161115666170919183657
41. Ngarashi D, Fujikawa K, Ferdaus MZ, Zahid HM, Ohara H, Nabika T. Dual Inhibition of NADPH Oxidases and Xanthine Oxidase Potently Prevents Salt-Induced Stroke in Stroke-Prone Spontaneously Hypertensive Rats. *Hypertens Res* (2019) 42:981–9. doi: 10.1038/s41440-019-0246-2
42. Sun M-S, Jin H, Sun X, Huang S, Zhang F-L, Guo Z-N, et al. Free Radical Damage in Ischemia-Reperfusion Injury: An Obstacle in Acute Ischemic Stroke After Revascularization Therapy. *Oxid Med Cell Longev* (2018) 2018:1–17. doi: 10.1155/2018/3804979
43. Orellana-Urzúa S, Rojas I, Líbano L, Rodrigo R. Pathophysiology of Ischemic Stroke: Role of Oxidative Stress. *Curr Pharm Des* (2020) 26:4246–60. doi: 10.2174/1381612826666200708133912
44. Gauberti M, Lapergue B, Martinez de Lizarrondo S, Vivien D, Richard S, Bracard S, et al. Ischemia-Reperfusion Injury After Endovascular Thrombectomy for Ischemic Stroke. *Stroke* (2018) 49:3071–4. doi: 10.1161/STROKEAHA.118.022015
45. Aygul R, Kotan D, Demirbas F, Ulvi H, Deniz O. Plasma Oxidants and Antioxidants in Acute Ischaemic Stroke. *J Int Med Res* (2006) 34:413–8. doi: 10.1177/147323000603400411
46. Smith AK, Kilaru V, Klengel T, Mercer KB, Bradley B, Conneely KN, et al. DNA Extracted From Saliva for Methylation Studies of Psychiatric Traits: Evidence Tissue Specificity and Relatedness to Brain. *Am J Med Genet B Neuropsychiatr Genet* (2015) 168B:36–44. doi: 10.1002/ajmg.b.32278
47. Thomas M, Knoblich N, Wallisch A, Glowacz K, Becker-Sadzio J, Gundel F, et al. Increased BDNF Methylation in Saliva, But Not Blood, of Patients With Borderline Personality Disorder. *Clin Epigenet* (2018) 10:109. doi: 10.1186/s13148-018-0544-6
48. Martin J, Kagerbauer SM, Gempt J, Podtschaske A, Hapfelmeier A, Schneider G. Oxytocin Levels in Saliva Correlate Better Than Plasma Levels With Concentrations in the Cerebrospinal Fluid of Patients in Neurocritical Care. *J Neuroendoc* (2018) 30:e12596. doi: 10.1111/jne.12596
49. Sifat AE, Vaidya B, Abbruscato TJ. Blood-Brain Barrier Protection as a Therapeutic Strategy for Acute Ischemic Stroke. *AAPS J* (2017) 19:957–72. doi: 10.1208/s12248-017-0091-7
50. Abdullahi W, Tripathi D, Ronaldson PT. Blood-Brain Barrier Dysfunction in Ischemic Stroke: Targeting Tight Junctions and Transporters for Vascular Protection. *Am J Physiol Physiol* (2018) 315:C343–56. doi: 10.1152/ajpcell.00095.2018
51. Chen A-Q, Fang Z, Chen X-L, Yang S, Zhou Y-F, Mao L, et al. Microglia-Derived TNF-α Mediates Endothelial Necroptosis Aggravating Blood Brain–Barrier Disruption After Ischemic Stroke. *Cell Death Dis* (2019) 10:487. doi: 10.1038/s41419-019-1716-9
52. Porcheri C, Mitsiadis T. Physiology, Pathology and Regeneration of Salivary Glands. *Cells* (2019) 8:976. doi: 10.3390/cells8090976
53. Proctor GB. The Physiology of Salivary Secretion. *Periodontol 2000* (2016) 70:11–25. doi: 10.1111/prd.12116
54. Matias-Guiu JA, Cortés-Martínez A, Valles-Salgado M, Rognoni T, Fernández-Matarrubia M, Moreno-Ramos T, et al. Addenbrooke's Cognitive Examination III: Diagnostic Utility for Mild Cognitive Impairment and Dementia and Correlation With Standardized Neuropsychological Tests. *Int Psychoger* (2017) 29:105–13. doi: 10.1017/S1041610216001496
55. Liu W, Unick J, Galik E, Resnick B. Barthel Index of Activities of Daily Living. *Nurs Res* (2015) 64:88–99. doi: 10.1097/NNR.0000000000000072
56. Louie D, Eng J. Berg Balance Scale Score at Admission can Predict Walking Suitable for Community Ambulation at Discharge From Inpatient Stroke Rehabilitation. *J Rehabil Med* (2018) 50:37–44. doi: 10.2340/16501977-2280
57. Chumney D, Nollinger K, Shesko K, Skop K, Spencer M, Newton RA. Ability of Functional Independence Measure to Accurately Predict Functional Outcome of Stroke-Specific Population: Systematic Review. *J Rehabil Res Dev* (2010) 47:17. doi: 10.1682/JRRD.2009.08.0140
58. Maciejczyk M, Taranta-Janusz K, Wasilewska A, Kossakowska A, Zalewska A. A Case-Control Study of Salivary Redox Homeostasis in Hypertensive Children. Can Salivary Uric Acid Be a Marker of Hypertension? *J Clin Med* (2020) 9:837. doi: 10.3390/jcm9030837
59. Skutnik-Radziszewska A, Maciejczyk M, Fejfer K, Krahel J, Flisiak I, Kołodziej U, et al. Salivary Antioxidants and Oxidative Stress in Psoriatic Patients: Can Salivary Total Oxidant Status and Oxidative Status Index Be a Plaque Psoriasis Biomarker? *Oxid Med Cell Longev* (2020) 2020:1–12. doi: 10.1155/2020/9086024
60. Toczewska J, Maciejczyk M, Konopka T, Zalewska A. Total Oxidant and Antioxidant Capacity of Gingival Crevicular Fluid and Saliva in Patients With Periodontitis: Review and Clinical Study. *Antioxidants* (2020) 9:450. doi: 10.3390/antiox9050450
61. WHO. Oral Health Surveys: Basic Methods, in: *World Health Organization* (2013). World Heal Organ. Available at: https://books.google.pl/books?hl=pl&lr=&id=8rEXDAAAQBAJ&oi=fnd&pg=PP1&dq=World+Health+Organization.+Oral+Health+Surveys:+Basic+Methods+(World+Health+Organization,+2013).&ots=fDGES4xy1s&sig=bzmQkFp3oyaZZBgHNFQ3lakNrN8&rediresc=y#v=onepage&q=World HealthO (Accessed September 9, 2021).
62. Gerreth P, Gerreth K, Maciejczyk M, Zalewska A, Hojan K. Is an Oral Health Status a Predictor of Functional Improvement in Ischemic Stroke Patients Undergoing Comprehensive Rehabilitation Treatment? *Brain Sci* (2021) 11:338. doi: 10.3390/brainsci11030338
63. Silness J, Löe H. Periodontal Disease in Pregnancy II. Correlation Between Oral Hygiene and Periodontal Condition. *Acta Odontol Scand* (1964) 22:121–35. doi: 10.3109/00016356408993968
64. Prajda N, Weber G. Malignant Transformation-Linked Imbalance: Decreased Xanthine Oxidase Activity in Hepatomas. *FEBS Lett* (1975) 59:245–9. doi: 10.1016/0014-5793(75)80385-1
65. Zalewska A, Szarmach I, Żendzian-Piotrowska M, Maciejczyk M. The Effect of N-Acetylcysteine on Respiratory Enzymes, ADP/ATP Ratio, Glutathione Metabolism, and Nitrosative Stress in the Salivary Gland Mitochondria of Insulin Resistant Rats. *Nutrients* (2020) 12:458. doi: 10.3390/nu12020458
66. Ferrer I, Vidal N. *"Neuropathology of Cerebrovascular Diseases,"*. (2018). Elsevier B.V. pp. 79–114. doi: 10.1016/B978-0-12-802395-2.00007-9
67. Graff-Radford J. Vascular Cognitive Impairment. *Contin Lifelong Learn Neurol* (2019) 25:147–64. doi: 10.1212/CON.0000000000000684
68. Kamtchum-Tatuene J, Jickling GC. Blood Biomarkers for Stroke Diagnosis and Management. *NeuroMol Med* (2019) 21:344–68. doi: 10.1007/s12017-019-08530-0
69. Maciejczyk M, Bielas M, Zalewska A, Gerreth K. Salivary Biomarkers of Oxidative Stress and Inflammation in Stroke Patients: From Basic Research to

Clinical Practice. *Oxid Med Cell Longev* (2021) 2021:5545330. doi: 10.1155/2021/5545330
70. Crack PJ , Taylor JM. Reactive Oxygen Species and the Modulation of Stroke☆. *Free Radic Biol Med* (2005) 38:1433–44. doi: 10.1016/j.freeradbiomed.2005.01.019
71. Shirley R, Ord E, Work L. Oxidative Stress and the Use of Antioxidants in Stroke. *Antioxidants* (2014) 3:472–501. doi: 10.3390/antiox3030472
72. Lewis SE, Rosencrance CB, De Vallance E, Giromini A, Williams XM, Oh J-Y, et al. Human and Rodent Red Blood Cells Do Not Demonstrate Xanthine Oxidase Activity or XO-Catalyzed Nitrite Reduction to NO. *Free Radic Biol Med* (2021) 174:84–8. doi: 10.1016/j.freeradbiomed.2021.07.012
73. Pedersen AML, Sørensen CE, Proctor GB, Carpenter GH, Ekström J. Salivary Secretion in Health and Disease. *J Oral Rehabil* (2018) 45:730–46. doi: 10.1111/joor.12664
74. Battino M, Ferreiro MS, Gallardo I, Newman HN, Bullon P. The Antioxidant Capacity of Saliva. *J Clin Periodontol* (2002) 29:189–94. doi: 10.1034/j.1600-051X.2002.290301x.x
75. Pernot E, Cardis E, Badie C. Usefulness of Saliva Samples for Biomarker Studies in Radiation Research. *Cancer Epidemiol Biomarkers Prev* (2014) 23:2673–80. doi: 10.1158/1055-9965.EPI-14-0588
76. Dąbrowska Z, Bijowski K, Dąbrowska E, Pietruska M. Effect of Oxidants and Antioxidants on Oral Health. *Med Ogólna i Nauk o Zdrowiu* (2020) 26:87–93. doi: 10.26444/monz/122255
77. Zalewska A, Klimiuk A, Zięba S, Wnorowska O, Rusak M, Waszkiewicz N, et al. Salivary Gland Dysfunction and Salivary Redox Imbalance in Patients With Alzheimer's Disease. *Sci Rep* (2021) 11:23904. doi: 10.1038/s41598-021-03456-9
78. Benn AML, Thomson WM. Saliva: An Overview. *N Z Dent J* (2014) 110:92–6.
79. Tai LA, Hwang KC. Cooperative Catalysis in the Homodimer Subunits of Xanthine Oxidase †. *Biochemistry* (2004) 43:4869–76. doi: 10.1021/bi035467b
80. Maciejczyk M, Gerreth P, Zalewska A, Hojan K, Gerreth K. Salivary Gland Dysfunction in Stroke Patients Is Associated With Increased Protein Glycoxidation and Nitrosative Stress. *Oxid Med Cell Longev* (2020) 2020:6619439. doi: 10.1155/2020/6619439
81. Fan AP, An H, Moradi F, Rosenberg J, Ishii Y, Nariai T, et al. Quantification of Brain Oxygen Extraction and Metabolism With [15O]-Gas PET: A Technical Review in the Era of PET/MRI. *Neuroimage* (2020) 220:117136. doi: 10.1016/j.neuroimage.2020.117136
82. Falkowska A, Gutowska I, Goschorska M, Nowacki P, Chlubek D, Baranowska-Bosiacka I. Energy Metabolism of the Brain, Including the Cooperation Between Astrocytes and Neurons, Especially in the Context of Glycogen Metabolism. *Int J Mol Sci* (2015) 16:25959–81. doi: 10.3390/ijms161125939
83. Boehme AK, Esenwa C, Elkind MSV. Stroke Risk Factors, Genetics, and Prevention. *Circ Res* (2017) 120:472–95. doi: 10.1161/CIRCRESAHA.116.308398
84. Nam Y, Kim Y-Y, Chang J-Y, Kho H-S. Salivary Biomarkers of Inflammation and Oxidative Stress in Healthy Adults. *Arch Oral Biol* (2019) 97:215–22. doi: 10.1016/j.archoralbio.2018.10.026
85. Żukowski P, Maciejczyk M, Waszkiel D. Sources of Free Radicals and Oxidative Stress in the Oral Cavity. *Arch Oral Biol* (2018) 92:8–17. doi: 10.1016/j.archoralbio.2018.04.018
86. Zieniewska I, Maciejczyk M, Zalewska A. The Effect of Selected Dental Materials Used in Conservative Dentistry, Endodontics, Surgery, and Orthodontics as Well as During the Periodontal Treatment on the Redox Balance in the Oral Cavity. *Int J Mol Sci* (2020) 214:1–27. doi: 10.3390/ijms21249684
87. Zięba S, Maciejczyk M, Zalewska A. Ethanol- and Cigarette Smoke-Related Alternations in Oral Redox Homeostasis. *Front Physiol* (2022) 12:793028. doi: 10.3389/fphys.2021.793028
88. Kalaria RN, Akinyemi R, Ihara M. Stroke Injury, Cognitive Impairment and Vascular Dementia. *Biochim Biophys Acta - Mol Bas Dis* (2016) 1862:915–25. doi: 10.1016/j.bbadis.2016.01.015
89. Takenoshita S, Terada S, Yoshida H, Yamaguchi M, Yabe M, Imai N, et al. Validation of Addenbrooke's Cognitive Examination III for Detecting Mild Cognitive Impairment and Dementia in Japan. *BMC Geriatr* (2019) 19:123. doi: 10.1186/s12877-019-1120-4
90. Bruno D, Schurmann Vignaga S. Addenbrooke's Cognitive Examination III in the Diagnosis of Dementia: A Critical Review. *Neuropsychiatr Dis Treat* (2019) 15:441–7. doi: 10.2147/NDT.S151253
91. Morotti A, Poli L, Costa P. Acute Stroke. *Semin Neurol* (2019) 39:061–72. doi: 10.1055/s-0038-1676992

Conflict of Interest: The authors declare that the research was conducted in the absence of any commercial or financial relationships that could be construed as a potential conflict of interest.

Publisher's Note: All claims expressed in this article are solely those of the authors and do not necessarily represent those of their affiliated organizations, or those of the publisher, the editors and the reviewers. Any product that may be evaluated in this article, or claim that may be made by its manufacturer, is not guaranteed or endorsed by the publisher.

frontiers | Frontiers in Immunology

ORIGINAL RESEARCH
published: 01 July 2022
doi: 10.3389/fimmu.2022.887000

4-Ethylguaiacol Modulates Neuroinflammation and Promotes Heme Oxygenase-1 Expression to Ameliorate Brain Injury in Ischemic Stroke

*Wen-Tsan Weng[1], Ping-Chang Kuo[1], Barbara A. Scofield[1], Hallel C. Paraiso[2], Dennis A. Brown[3], I-Chen Yu[2] and Jui-Hung Yen[1]**

[1] Department of Microbiology and Immunology, Indiana University School of Medicine, Fort Wayne, IN, United States, [2] Department of Anatomy, Cell Biology and Physiology, Indiana University School of Medicine, Fort Wayne, IN, United States, [3] Department of Pharmaceutical Sciences, Manchester University College of Pharmacy, Natural and Health Sciences, Fort Wayne, IN, United States

OPEN ACCESS

Edited by:
Xiaofeng Jia,
University of Maryland, United States

Reviewed by:
Shupeng Li,
Peking University, China
Kaibin Huang,
Southern Medical University, China

***Correspondence:**
Jui-Hung Yen
jimyen@iu.edu

Specialty section:
This article was submitted to Multiple Sclerosis and Neuroimmunology, a section of the journal Frontiers in Immunology

Received: *01 March 2022*
Accepted: *12 May 2022*
Published: *01 July 2022*

Citation:
Weng W-T, Kuo P-C, Scofield BA, Paraiso HC, Brown DA, Yu I-C and Yen J-H (2022) 4-Ethylguaiacol Modulates Neuroinflammation and Promotes Heme Oxygenase-1 Expression to Ameliorate Brain Injury in Ischemic Stroke. Front. Immunol. 13:887000. doi: 10.3389/fimmu.2022.887000

Ischemic stroke is caused by a sudden reduction in cerebral blood flow that subsequently induces a complex cascade of pathophysiological responses, leading to brain inflammation and irreversible infarction. 4-ethylguaiacol (4-EG) is reported to suppress inflammatory immune responses. However, whether 4-EG exerts anti-inflammatory effects in ischemic stroke remains unexplored. We evaluated the therapeutic potential of 4-EG and examined the cellular and molecular mechanisms underlying the protective effects of 4-EG in ischemic stroke. The effect of 4-EG in ischemic stroke was determined by using a transient middle cerebral artery occlusion (MCAO) animal model followed by exploring the infarct size, neurological deficits, microglia activation, inflammatory cytokine production, blood–brain barrier (BBB) disruption, brain endothelial cell adhesion molecule expression, and microglial heme oxygenase-1 (HO-1) expression. *Nrf2*$^{-/-}$ and HO-1 inhibitor ZnPP-treated mice were also subjected to MCAO to evaluate the role of the Nrf2/HO-1 pathway in 4-EG-mediated protection in ischemic stroke. We found that 4-EG attenuated infarct size and neurological deficits, and lessened BBB disruption in ischemic stroke. Further investigation revealed that 4-EG suppressed microglial activation, peripheral inflammatory immune cell infiltration, and brain endothelial cell adhesion molecule upregulation in the ischemic brain. Finally, we identified that the protective effect of 4-EG in ischemic stroke was abolished in *Nrf2*$^{-/-}$ and ZnPP-treated MCAO mice. Our results identified that 4-EG confers protection against ischemic stroke and reveal that the protective effect of 4-EG in ischemic stroke is mediated through the induction of the Nrf2/HO1 pathway. Thus, our findings suggest that 4-EG could be developed as a novel therapeutic agent for the treatment of ischemic stroke.

Keywords: 4-EG, HO-1, microglia, blood–brain barrier, ischemic stroke

1 INTRODUCTION

Stroke is ranked as the second leading cause of death worldwide with annual mortality more than 5 million. The burden of stroke not only lies on the high mortality but also high morbidity, resulting in up to 50% of survivors being chronically disabled (1). More than 80% of stroke cases belong to ischemic stroke, in which the occlusion of cerebral blood vessels initiates the acute phase of cerebral injury followed by neuronal excitotoxicity and oxidative damage. Following cerebral ischemia, the central nervous system (CNS) resident immune cells, microglia (MG), are rapidly activated in the injured brain. In addition, peripheral immune cells are recruited into the injured brain, leading to the secondary brain injury (2). In the CNS, MG maintain homeostasis; however, they can quickly respond to ischemic stress (3–5). Ischemic stress triggers MG activation and phagocytosis of damaged neurons in and around the infarct. Following reperfusion, macrophages play an important role in post-stroke inflammation in the ischemic brain (2). Infiltrating macrophages are activated and produce various inflammatory cytokines, including tumor necrosis factor alpha (TNFα) and Interleukin-1β (IL-1β) that promote neuronal cell death in the ischemic brain (5). In addition, there is a growing body of evidence demonstrating that blood–brain barrier (BBB) dysfunction is one of the major pathological causes following ischemic stroke (6). The function of BBB is known to protect the CNS and regulate peripheral leukocyte infiltration into the brain parenchyma through several molecules associated with brain endothelium (7). Among those regulatory molecules, tight junction proteins (TJPs), such as zonula occludens-1 (ZO-1) and occludin, and adhesion molecules, including intercellular adhesion molecule 1 (ICAM-1), vascular cell adhesion molecule 1 (VCAM-1), and E-selection, play important roles in regulating peripheral leukocyte recruitment and modulating the permeability of BBB following ischemic stroke (8).

4-ethylguaiacol (4-EG), a phenolic compound with the molecular formula $C_9H_{12}O_2$, belongs to the class of organic compounds known as methoxyphenols (9, 10). 4-EG is produced along with 4-ethylphenol in wine and beer by the spoilage yeast Brettanomyces. In addition, 4-EG has been found in several different foods, such as green, yellow and orange bell peppers, corns, sesames, and coffee (10). Studies have demonstrated that phenolic compounds possess anti-inflammatory effects through inhibiting the expression of IL-1β, TNFα, IL-6, and cyclooxygenase-2 (9, 11). 4-EG has also been shown to exert anti-inflammatory effects through inhibiting nuclear factor kappa B (NFκB) and inflammasome activation as well as suppressing inflammatory cytokine production in THP-1 human monocytic cells (9, 11). Moreover, we have recently shown that 4-EG modulated neuroinflammation and inhibited Th1/Th17 differentiation to ameliorate disease severity in experimental autoimmune encephalomyelitis (EAE), the animal model of multiple sclerosis (12), further demonstrating the anti-inflammatory effect of 4-EG in the CNS diseases.

Currently, whether 4-EG possesses an anti-inflammatory effect on modulating acute neuroinflammation, such as ischemic stroke, remains unknown. Thus, we explored the potential protective effect of 4-EG in ischemic stroke and investigated the cellular and molecular mechanisms underlying the protective effect of 4-EG in ischemic stroke. We found that 4-EG attenuated brain injury, mitigated neurological deficits, and decreased mortality in mice subjected to ischemic stroke. Further investigations revealed that 4-EG inhibited MG activation and suppressed neuroinflammation in the ischemic brain. Moreover, 4-EG lessened BBB disruption, repressed the cell infiltration of the CNS, and suppressed brain endothelial adhesion molecule upregulation in ischemic stroke animals. Finally, mechanistic studies revealed that 4-EG induced HO-1 expression in MG, and the inhibition of the Nrf2/HO-1 pathway abolished the protective effect of 4-EG in ischemic stroke. Thus, our findings provide the first evidence that 4-EG could be developed as a novel therapeutic agent for the treatment of ischemic stroke.

Abbreviations: CNS, central nervous system; MG, microglia; 4-EG, 4-ethylguaiacol; BBB, blood–brain barrier; PBS, phosphate-buffered saline; 7-AAD, 7-aminoactinomycin D; HO-1, heme oxygenase-1; CBF, cerebral blood flow; CCA, common carotid artery; ECA, external carotid artery; IHC, immunohistochemistry; MCAO, middle cerebral artery occlusion; RT, room temperature; TJP, tight junction proteins; ZO-1, zonula occludens-1; TTC, triphenyltetrazolium chloride; ZnPP, zinc protoporphyrin.

2 MATERIALS AND METHODS

2.1 Mice

All animal procedures were approved by the Purdue Animal Care and Use Committee and conducted in accordance with the National Institutes of Health Guidelines for the Care and Use of Laboratory Animals. C57BL/6 and *Nrf2*$^{-/-}$ mice were purchased from the Jackson Laboratory (Bar Harbor, ME, USA) and bred in the animal facility with controlled humidity, temperature, and 12 h:12 h light–dark cycle with free access to food and water. The genotyping was performed routinely to ensure the phenotypes of Nrf2 deficiency (**Supplementary Figure 1**).

2.2 Reagents

4-EG, triphenyltetrazolium chloride (TTC), Alexa Fluor 594 goat-anti rabbit IgG secondary antibody, Evans blue, Ficoll PM 400, and LPS (*Escherichia coli* O55:B5) were purchased from MilliporeSigma (St. Louis, MO, USA). Zinc protoporphyrin (ZnPP) was purchased from Alfa Aesar (Haverhill, MA, USA). 7-aminoactinomycin D (7-AAD), Alexa Fluor 488-conjugated anti-mouse CD45 (clone: 30-F11), APC-conjugated anti-mouse CD45 (clone: 30-F11), PE/Cy7-conjugated anti-mouse CD11b (clone: M1/70), PE-conjugated anti-mouse CD11b (clone: M1/70), PE/Cy7-conjugated anti-mouse CD86 (clone: GL-1), PE/Cy7-conjugated anti-mouse CD68 (clone: FA-11), Alexa Fluor 647-conjugated anti-mouse CD31 (clone: MEC13.3), PE/Cy7-conjugated anti-mouse ICAM-1 (clone: HA58), and PE/Cy7-conjugated anti-mouse VCAM-1 (clone: 429, MVCAM.A) antibodies for flow cytometer analysis were purchased from BioLegend (San Diego, CA, USA). PE-conjugated anti-mouse E-selectin (clone: 10E9.6) antibody for flow cytometry analysis was purchased from BD Biosciences (San Diego, CA, USA). Alexa Fluor 488 anti-mouse Iba1 (EPR16588) antibody for immunohistochemistry (IHC) was purchased from Abcam

(Cambridge, MA, USA). Anti-mouse HO-1 (10701-1-AP) antibody for flow cytometer and IHC was purchased from Proteintech (Chicago, IL, USA).

2.3 Middle Cerebral Artery Occlusion Model

Male and female C57BL/6 and *Nrf2*$^{-/-}$ mice (8–12 weeks old) were used for cerebral ischemia experiments as previously described (13). The intraluminal suture occlusion model was carried out to induce transient ischemic stroke. Briefly, mice were anesthetized by isoflurane, and the body temperature was controlled at ~37 ± 0.5° C during the surgical procedure. Cerebral blood flow (CBF) was measured before, during, and after ischemia by laser Doppler flowmetry (Moor Instrument VMS-LDF2) at the parietal bone (2 mm posterior and 3 mm lateral from Bregma). The right common carotid artery (CCA) was clamped by a microvascular clamp, and the right external carotid artery (ECA) was exposed. A minimal incision was made in the ECA stump followed by the insertion of a silicon-coated 6.0 nylon monofilament (Doccol Corp, Sharon, MA, USA) through ECA to MCA. After 40 min (male) or 1 h (female) of occlusion, the intraluminal suture was removed to reestablish CBF. Mouse was then placed in the recovery cage with the temperature maintaining at 37°C for 1 h. Mice with a total reduction of CBF more than 75% were included and randomly assigned to different treatment groups. The sham surgery was conducted with the same procedures without the insertion of a suture. At 2 h post-reperfusion, 4-EG 100 mg/kg suspended in 100 µl phosphate-buffered saline (PBS) was i.v. administered to MCAO mice, and the same amount of PBS was i.v. administered to MCAO mice as vehicle controls. For the ZnPP treatment experiments, mice were i.p. administered vehicle (10% solutol) or ZnPP (30 mg/kg, dissolved in 10% solutol) overnight and 1 h prior to MCAO. At 2 h post-reperfusion, vehicle-treated MCAO mice were then subjected to vehicle or 4-EG 100 mg/kg treatment, and ZnPP-treated MCAO mice were subjected to 4-EG 100 mg/kg treatment. The investigators who conducted experiments were blinded to the animal groups.

2.4 Infarct Volume Measurement and Neurological Assessment

The cerebral infarct volume was measured to assess the severity of ischemic brain injury. Briefly, MCAO mice were anesthetized and transcardially perfused with PBS. The ischemic brain was then harvested and subjected to 2 mm coronal slicing with a rodent brain matrix followed by 1% TTC staining. After staining, the brain sections were scanned and the infarct volume was calculated by ImageJ as previously described (13). The neurological score was assessed at 48 h after injury using a six-point scale (0–5): score 0: normal; score 1: mild circling behavior with or without inconsistent rotation when picked up by the tail, <50% attempts to rotate to the contralateral side; score 2: mild consistent circling, >50% attempts to rotate to contralateral side; score 3: consistent strong and immediate circling, the mouse holds a rotation position for more than 1–2 sec with its nose almost reaching its tail; score 4: severe rotation progressing into barreling, the loss of walking, or righting reflex; and score 5: comatose or moribund.

2.5 Isolation of Mononuclear Cells From the Mouse Brain

Mononuclear cells were isolated from the mouse brain after ischemic stroke as previously described (14). MCAO mice were anesthetized and transcardially perfused with PBS. The brain was harvested and homogenized with 1X Hanks' balanced salt solution (HBSS) buffer followed by filtration through a 70-µm nylon cell strainer. After centrifugation, cells were resuspended in 30% Percoll underlayering with 70% Percoll. Following centrifugation, the mononuclear cells were then isolated from the interface between 30% and 70% Percoll. The isolated mononuclear cells were subjected to the surface staining of CD45 and CD11b to detect peripheral immune cell infiltrates or to the surface staining of CD45, CD11b, and CD86 in the presence of 7-AAD to assess MG activation. To detect CD68 expression, the mononuclear cells subjected to the surface staining of CD45 and CD11b in the presence of 7-AAD were fixed and permeabilized followed by CD68 staining. To measure HO-1 expression, the mononuclear cells subjected to the surface staining of CD45 and CD11b in the presence of 7-AAD were fixed and permeabilized and then incubated with the primary HO-1 antibody followed by the Alexa Fluor 546 secondary antibody. The stained cells were then analyzed by flow cytometer (BD FACSVerse).

2.6 Immunohistochemistry

Brain samples were sectioned and fixed with 4% paraformaldehyde in PBS at 4°C overnight. After 6% and 30% sucrose dehydration, brain sections were embedded in optimal cutting temperature compound and cut into 16 µm cryosections. Sections were then permeabilized in PBS containing 0.5% Triton X-100 for 30 min. Following blocking with goat serum (5% goat serum and 0.25% Triton X-100 in PBS) at room temperature (RT) for 1 h, sections were incubated with the primary HO-1 antibody at 4°C overnight. After washing, sections were then stained with the secondary antibody for 2 h followed by the Alexa Fluor 488 anti-mouse Iba1 antibody staining for 2 h at RT. After washing, samples were coverslipped with ProLong Gold antifade mountant containing DAPI. Immunofluorescence images were captured with a fluorescence microscope (×20x BX53, Olympus). The slides stained with only secondary antibodies served as negative controls. The number of Iba1^{+} cells per square millimeter was counted, and Iba1^{+} cells were determined based on the cells with the morphology of large cell body and short dendrites, representing the stage 3–5 of MG activation (15). To determine HO-1 fluorescence intensity, negative controls were used to set up the color threshold of HO-1 fluorescence signals, and the mean of HO-1 fluorescence signals (fluorescence intensity) detected on the brain slides prepared from vehicle- and 4-EG-treated MCAO mice was calculated by ImageJ.

2.7 Evans Blue Extravasation Assay

The BBB permeability was assessed based on the leakage of Evans blue as previously described (14). Briefly, mice were i.v. injected with 2% Evans blue solution (4 ml/kg) at 2.5 h after reperfusion. After 1 h of Evans blue circulation, animals were anesthetized and transcardially perfused with PBS to remove intravascular

Evans blue. The brains were then harvested, sliced, and scanned. The hemispheres were then separated and homogenized in 50% trichloroacetic acid solution. After centrifugation, supernatants were harvested and diluted with 95% ethanol in a ratio of 1:3. The amount of extravascular Evans blue in the supernatant was then determined by measuring the fluorescence with excitation at 540/25 nm and emission at 645/40 nm (BioTek Synergy™ HT microplate reader).

2.8 Isolation of Microvasculature From the Mouse Brain

The microvasculature harvested from the ischemic brains was subjected to the analysis of adhesion molecule expression on brain endothelial cells as previously described (16). The brains harvested from MCAO mice were subjected to the removal of olfactory bulbs and cerebellum followed by homogenization by using an electrical drill (Milwaukee drill connected to the Staco Energy Products Autotransformer, 3PN1010B). The homogenized tissues were then mixed with an equal volume of 40% Ficoll solution to a final concentration of 20% Ficoll. Following centrifugation at 5,800x g, 4°C for 20 min, the pellet containing enriched microvessels was harvested and resuspended with 1X HBSS containing 0.5 mg/ml collagenase at 4°C for 20 min. After adding 10% fetal bovine serum medium to stop the reaction, the mixtures were subjected to filtration through a 70 μm nylon cell strainer followed by centrifugation. Cells were then collected and stained with anti-CD31 in the presence of anti-ICAM-1, anti-E-selectin, or anti-VCAM-1 antibodies followed by flow cytometry analysis.

2.9 Cell Culture

Primary MG were generated from P1–P2 neonatal mice as previously described (14). Briefly, cerebral cortical cells were harvested from P1–P2 neonatal mice and then plated in 75 cm^2 culture flasks with a complete Dulbecco's modified eagle medium: nutrient mixture F-12 (DMEM/F12) medium. At day 4 and 8 after cell plating, the medium was removed and replenished with complete media containing 10 ng/ml of granulocyte-macrophage colony-stimulating factor (GM-CSF). At day 12, MG were harvested from supernatants after the flasks were shaken at 37°C for 30 min. The mouse microglial cell line BV2 cells were grown in 25 cm^2 flasks. After the cells were grown to confluence, they were trypsinized and seeded on tissue culture plates for experiments. Primary macrophages were generated from bone marrow cells as previously described (17). Briefly, the bone marrow cells were cultured in a complete roswell park memorial institute (RPMI) 1640 medium containing 10 ng/ml of macrophage colony-stimulating factor (M-CSF). The cells were replenished with fresh media containing 10 ng/ml of M-CSF at day 3 and harvested at day 7 for experiments. The mouse brain endothelial cell line bEnd.3 cells were grown in 25 cm^2 flasks. After the cells were grown to confluence, they were trypsinized and seeded onto tissue culture plates for experiments.

2.10 Statistical Analysis

All results are given as mean ± SEM. The sample size was determined to be adequate based on our previous studies and also prior literature using similar experimental paradigms. The normal distribution of the data in each group was confirmed by the Shapiro–Wilk normality test. Comparisons between two groups were done by an unpaired *t*-test, whereas comparisons among multiple groups were done by one-way ANOVA (one variable) or two-way ANOVA (two variables) followed by the Tukey *post-hoc* test. For samples that did not pass the normality test, comparisons among multiple groups were done by the Kruskal–Wallis test followed by Dunn's multiple comparison test. The statistical significance was determined as $p<0.05$.

3 RESULTS

3.1 4-EG Ameliorates Brain Injury and Increases Survival in Ischemic Stroke

To determine whether 4-EG offered protection against ischemic stroke, C57BL/6 mice were subjected to MCAO and then administered vehicle or different doses of 4-EG (50, 100, or 150 mg/kg). At 48 h post-injury, mice were sacrificed and the ischemic brains were harvested and subjected to TTC staining to determine the infarct volume. We observed that the dose of 4-EG 50 mg/kg did not confer protection against ischemic stroke (**Supplementary Figures 2A, B**). In contrast, the doses of 4-EG 100 and 150 mg/kg conferred comparable protection against ischemic stroke, as MCAO mice treated with 4-EG 100 and 150 mg/kg displayed a similar level of cerebral infarct (**Supplementary Figures 2A, B**). However, 4-EG 150 mg/kg exerted a toxic effect, resulting in increased mortality in MCAO mice (**Supplementary Figure 2C**). Thus, the dose of 4-EG 100 mg/kg was selected to carry out the rest of studies.

Upon the administration of MCAO mice with 4-EG 100 mg/kg, we observed that 4-EG not only attenuated cerebral infarct volumes (4-EG 45.7 ± 9.5 mm^3 vs. vehicle 95.4 ± 8.1 mm^3, **Figures 1A, B**) but also lowered neurological scores compared to vehicle-treated MCAO controls (**Figure 1C**). We further evaluated the long-term therapeutic effect of 4-EG on the survival of MCAO mice. Our results showed that 4-EG treatment increased long-term survival in MCAO mice in which vehicle-treated MCAO mice had a survival rate of 66.6%, whereas 4-EG-treated MCAO mice had a survival rate of 100% at day 7 post-injury (**Figure 1D**). We also compared the body weight changes between vehicle- and 4-EG-treated MCAO mice and observed that 4-EG-treated MCAO mice started to gain weight at day 3 post-injury, indicating that animals started to recover from ischemic brain injury. In contrast, vehicle-treated MCAO mice did not gain weight until day 5 post-injury and that could potentially contribute to decreased survival at day 7 post-injury (**Figure 1E**).

Finally, the effect of 4-EG in ischemic stroke was also evaluated in female C57BL/6 mice. Our results showed that 4-EG also conferred protection against ischemic brain injury in female MCAO mice, as 4-EG-treated female MCAO mice displayed a smaller infarct size compared to vehicle-treated female MCAO mice (4-EG 74.13 ± 8.6 mm^3 vs. vehicle 99.9 ± 7.6 mm^3, **Figures 1F, G**). Taken together, our results demonstrate that 4-EG attenuates ischemic brain injury, lessens neurological deficits, and increases

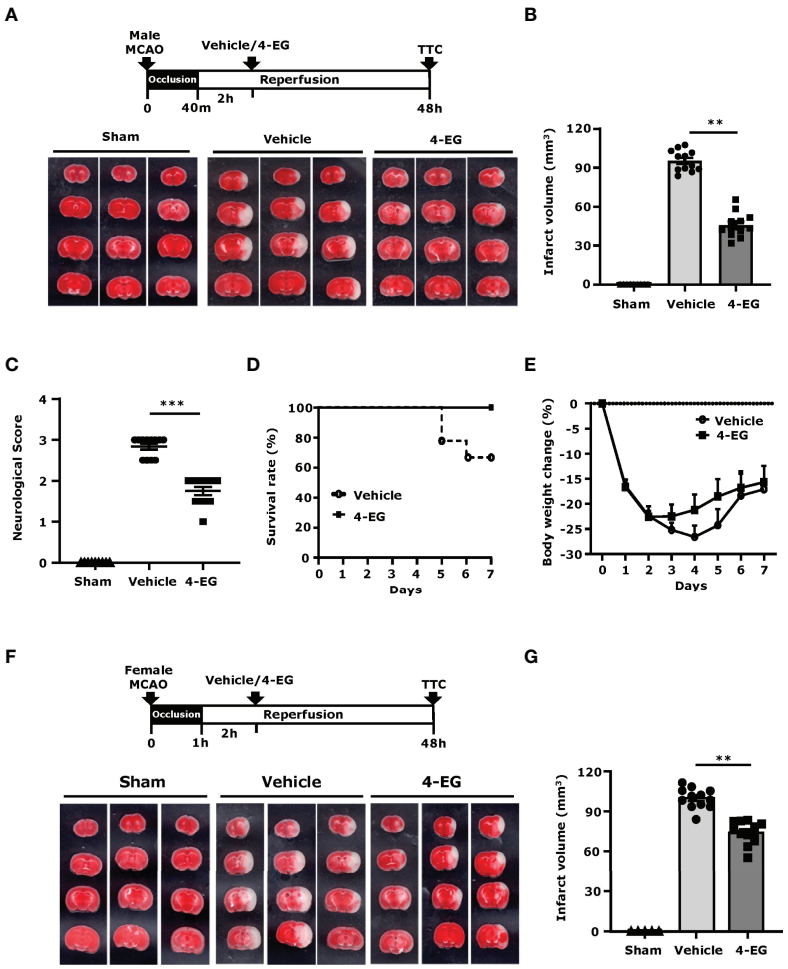

FIGURE 1 | 4-EG ameliorates brain injury and increases survival in ischemic stroke. **(A–E)** C57BL/6 male mice were subjected to sham or 40 min MCAO followed by vehicle or 4-EG (100 mg/kg) i.v. administration at 2 h post-reperfusion. **(A)** At 48 h post-injury, mice were sacrificed, and the ischemic brains were harvested and sliced (2 mm) followed by TTC staining. Three representative TTC-stained brain samples of sham, and vehicle- and 4-EG-treated MCAO mice are shown. **(B)** The infarct volumes and **(C)** neurological scores of sham (n=10), and vehicle- and 4-EG-treated MCAO mice (n=12/group) were evaluated. ***p<0.01*, ****p<0.001* by the Kruskal–Wallis test. **(D)** The survival rate and **(E)** body weight change of vehicle- and 4-EG-treated MCAO mice were evaluated up to day 7 post-injury (n=9/group). **(F, G)** C57BL/6 female mice were subjected to sham or 1 h MCAO followed by vehicle or 4-EG (100 mg/kg) i.v. administration at 2 h post-reperfusion. **(F)** Three representative TTC-stained brain samples of sham, and vehicle- and 4-EG-treated MCAO are shown, and **(G)** the infarct volumes of sham (n=5), and vehicle- and 4-EG- treated MCAO female mice (n=10/group) were assessed. ***p<0.01* by the Kruskal–Wallis test.

survival in ischemic stroke animals, suggesting that 4-EG exerts a therapeutic potential for the treatment of ischemic stroke.

3.2 4-EG Suppresses MG Activation and Neuroinflammation in Ischemic Stroke

In response to ischemic cerebral injury, MG are rapidly activated and produce inflammatory cytokines and chemokines (18). Activated MG upregulate co-stimulatory molecules, such as CD80 and CD86 (19). Furthermore, CD68, a lysosomal protein, is also highly upregulated in activated MG (20). To explore the effect of 4-EG on MG activation in ischemic stroke, we measured the expression of maturation markers, CD68 and CD86, on MG. The ischemic brains were harvested from sham, and vehicle- and 4-EG-treated MCAO mice followed by mononuclear cell isolation, and the isolated cells were then subjected to the staining of CD45 and CD11b in the combination with CD68 or CD86 followed by flow cytometry analysis. We determined the MG population in the isolated mononuclear cells based on their intermediate expression of CD45 ($CD45^{int}$) and positive expression of CD11b ($CD11b^{+}$), and the gating strategy of flow cytometry analysis is presented in **Supplementary Figure 3A**. Our results showed that a low level of CD68 expression ($CD68^{L}$) was detected in MG isolated from the ipsilateral hemisphere of sham controls as well as the contralateral hemisphere of vehicle- and 4-EG-treated MCAO mice, suggesting that MG express a basal level of CD68 under non-inflamed conditions (**Figure 2A**). Notably, ischemic stroke enhanced the microglial expression of CD68 ($CD68^{H}$) in the ipsilateral hemisphere of the ischemic brain. However, 4-EG was capable of suppressing ischemia-enhanced microglial CD68 expression in the ipsilateral hemisphere (**Figure 2A**). Furthermore, we observed that

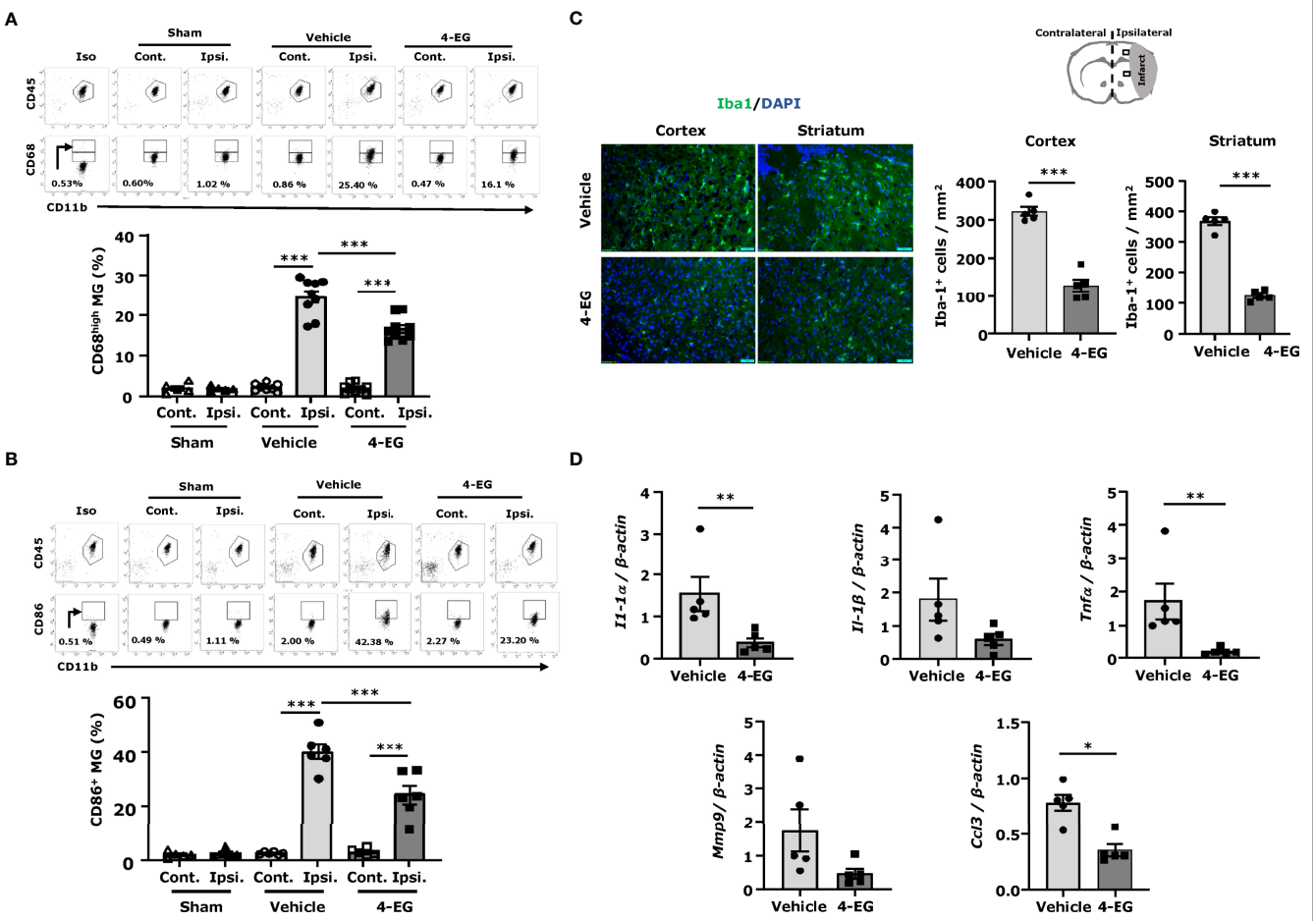

FIGURE 2 | 4-EG suppresses MG activation and neuroinflammation in ischemic stroke. C57BL/6 male mice were subjected to sham or 40 min MCAO followed by the i.v. administration of vehicle or 4-EG (100 mg/kg) at 2 h post-reperfusion. At 16–20 h post-injury, the ipsilateral and contralateral hemispheres of sham, and vehicle- and 4-EG-treated MCAO mice were harvested and subjected to mononuclear cell isolation. The isolated mononuclear cells were then stained with antibodies against CD45 and CD11b in the combination with CD68 or CD86 followed by flow cytometry analysis. MG were determined based on their surface intermediate expression of CD45 and positive expression of CD11b ($CD45^{int}CD11b^{+}$). Isotype controls (Iso) were used as a negative control to determine $CD45^{int}CD11b^{+}$ MG positive for CD68 or CD86 expression. **(A)** The gating of CD68 low ($CD68^{L}$) was based on the basal expression of CD68 in MG in sham controls, and the expression level of CD68 higher than $CD68^{L}$ was then determined as CD68 high ($CD68^{H}$). The frequency of $CD68^{H}$ MG in the contralateral and ipsilateral hemispheres of sham (n=5), and vehicle- and 4-EG-treated MCAO mice (n=9/group) was then measured and quantified. ****p<0.001* by two-way AVONA. **(B)** The frequency of CD86 expression in the contralateral and ipsilateral hemispheres of sham (n=5), and vehicle- and 4-EG-treated MCAO mice (n=6/group) was also determined. ****p<0.001* by two-way ANOVA. **(C)** At 20 h post-injury, the brain tissues of vehicle- and 4-EG-treated MCAO mice were harvested and subjected to IHC to assess Iba1 expression (n = 5/group). The representative images of $Iba1^{+}$ cells in the ipsilateral cortex and striatum of vehicle- and 4-EG-treated MCAO mice are shown. Cell nuclei were stained by DAPI. Scale bar, 50 μm. The number of $Iba1^{+}$ cells in the ipsilateral cortex and striatum was quantified. ****p < 0.001* by unpaired *t*-test. **(D)** The mRNA expression of IL-1α, IL-1β, TNFα, MMP9, and CCL3 in the ischemic brain of vehicle- and 4-EG-treated MCAO mice (n=5/group) was measured. **p<0.05, **p<0.01* by the Kruskal–Wallis test.

ischemia stroke increased $CD86^{+}$ MG in the ipsilateral hemisphere of vehicle-treated MCAO mice compared to that of sham controls (**Figure 2B**). Consistent with its effect on CD68 expression in MG, 4-EG-treated MCAO mice exhibited a decreased frequency of $CD86^{+}$ MG compared to vehicle-treated MCAO mice (**Figure 2B**). Moreover, we subjected ischemic brain tissues to IHC to assess the level of $Iba1^{+}$ cells in vehicle- and 4-EG-treated MCAO mice. MG, displaying an activated amoeboid morphology with a large soma size and short branching processes, were observed in the ischemic brain of vehicle-treated MCAO mice. In contrast, MG, exhibiting a resting ramified morphology with a small soma size and long branching processes, were found in the ischemic brain of 4-EG-treated MCAO mice (**Figure 2C** left). Further quantification of IHC results revealed that the number of $Iba1^{+}$ cells in the ipsilateral cortex and striatum was significantly lower in 4-EG-treated MCAO mice compared to vehicle-treated MCAO controls (**Figure 2C** right). Finally, we measured the expression of inflammatory molecules in the ischemic brain of vehicle- and 4-EG-treated MCAO mice. We found that 4-EG treatment suppressed the expression of inflammatory molecules, including IL-1α, IL-1β,

TNFα, MMP9, and CCL3, in the ischemic brain (**Figure 2D**). Taken altogether, these results demonstrate that 4-EG exerts anti-inflammatory effects on the suppression of MG activation and inhibition of inflammatory cytokine expression, leading to attenuated neuroinflammation in ischemic stroke.

3.3 4-EG Alleviates BBB Disruption and Represses Peripheral Immune Cell Infiltration of the CNS in Ischemic Stroke

Following cerebral ischemia, BBB disruption plays an important role in causing neurological dysfunction in ischemic stroke (21). To determine whether 4-EG alleviated ischemia-induced BBB disruption, mice were subjected to MCAO with 3 h occlusion to induce a severe BBB disruption followed by the administration of vehicle or 4-EG, and the level of BBB disruption was determined by Evans blue leakage at 3.5 h post-reperfusion. We found that cerebral ischemia induced a severe BBB disruption, exhibiting a profound leakage of Evans blue in the ipsilateral hemisphere, whereas 4-EG treatment markedly mitigated ischemia-induced BBB disruption, displaying a significant reduction of Evans blue leakage in the ischemic brain (**Figure 3A**).

Reperfusion following cerebral ischemia recruits peripheral inflammatory immune cells into the ischemic brain that further exacerbates brain injury, leading to the secondary brain injury (22). To explore whether attenuated brain infarct and alleviated BBB disruption observed in 4-EG-treated MCAO mice were correlated with repressed peripheral immune cell infiltration of the CNS, the ischemic brains were harvested from vehicle- and 4-EG-treated MCAO mice and subjected to mononuclear cell isolation followed by flow cytometry analysis to assess the level of peripheral cell infiltrates in the ischemic brain. Our previous studies have demonstrated that the contralateral hemisphere of MCAO mice and sham controls displayed a similar pattern of cell infiltrates (23). Thus, the contralateral hemispheres could serve as a proper control as sham controls. We observed that the contralateral hemisphere of vehicle- and 4-EG-treated MCAO mice only had a very few cell infiltrates (**Figure 3B**). However, we found that the frequency and number of $CD45^{hi}CD11b^{+}$ monocytes/macrophages were significantly increased in the ipsilateral hemisphere compared to the contralateral hemisphere in vehicle-treated MCAO mice. In contrast, the frequency and number of $CD45^{hi}CD11b^{+}$ monocytes/macrophages were significantly decreased in the ipsilateral hemisphere of 4-EG-treated MCAO mice compared to that of vehicle-treated MCAO controls (**Figure 3B**). Taken altogether, our results demonstrate that 4-EG lessens ischemia-induced BBB disruption that may subsequently suppresses peripheral immune cell infiltration of the CNS, leading to alleviated reperfusion-induced secondary brain injury in ischemic stroke.

3.4 4-EG Inhibits Brain Endothelial Adhesion Molecule Expression in the Ischemic Brain

Studies have shown that the adhesion molecules, such as E-selectin, P-selectin, ICAM-1, and VCAM-1, are upregulated on the surface of brain endothelial cells within hours after ischemic stroke that promotes the influx of inflammatory cells into the ischemic brain (24, 25). To explore whether 4-EG modulated brain endothelial adhesion molecule expression, the ischemic brains harvested from sham controls, and vehicle- and 4-EG-treated MCAO mice were subjected to microvasculature isolation followed by flow cytometry analysis to assess the level of adhesion molecule expression on the surface of brain endothelial cells. The brain endothelial cells were determined based on their positive expression of CD31, and the gating strategy of flow cytometry analysis is presented in **Supplementary Figure 3B**. Our results showed that ischemic stroke increased the frequency of $ICAM\text{-}1^{+}$, $E\text{-}selectin^{+}$, and $VCAM\text{-}1^{+}$ $CD31^{+}$ brain endothelial cells in the ipsilateral hemisphere of vehicle-treated MCAO mice compared to that of sham controls and the contralateral hemisphere of vehicle-treated MCAO mice (**Figure 4A**). Notably, the frequency of $ICAM\text{-}1^{+}$, $E\text{-}selectin^{+}$, and $VCAM\text{-}1^{+}$ $CD31^{+}$ brain endothelial cells was decreased in the ipsilateral hemisphere of 4-EG-treated MCAO mice compared to that of vehicle-treated MCAO mice (**Figure 4A**). The modulatory effect of 4-EG on adhesion molecule expression was further confirmed in the brain endothelial cell line, bEnd.3 cells, *in vitro*. We found that ICAM-1 and E-selectin were upregulated by TNFα stimulation in bEnd.3 cells. In contrast, 4-EG suppressed TNFα-upregulated ICAM-1 and E-selectin expression in bEnd.3 cells (**Figure 4B**). Taken altogether, our results demonstrate that 4-EG suppresses the upregulation of adhesion molecule expression in the brain endothelial cells of MCAO mice *in vivo* and in TNFα-activated bEnd.3 cells *in vitro*.

3.5 4-EG Promotes HO-1 Expression in MG *In Vivo* and *In Vitro*

Previous studies have demonstrated that HO-1 overexpression significantly attenuates the infarct volume, and HO-1 deficiency results in exacerbated brain injury in ischemic stroke (26–28). Studies from other and our groups have shown that 4-EG induced HO-1 expression in THP-1 human monocytes and in the spinal cord of mice subjected to EAE, respectively (12, 29). Therefore, we explored whether 4-EG induced HO-1 expression in the ischemic brain to confer protection against ischemic stroke. As MG were reported to be the main producers of HO-1 in the CNS (30, 31), we therefore assessed whether MG displayed HO-1 expression following ischemic brain injury in vehicle- and 4-EG-treated MCAO mice. The ischemic brains were harvested from sham, and vehicle- and 4-EG-treated MCAO mice followed by mononuclear cell isolation, and the isolated cells were then subjected to the surface staining of CD45 and CD11b followed by the intracellular staining of HO-1. The expression of HO-1 in $CD45^{int}CD11b^{+}$ MG was determined by flow cytometry analysis, and the gating strategy of analysis is presented in **Supplementary Figure 3A**. We found that ischemic stroke induced HO-1 expression in MG in the ipsilateral but not contralateral hemisphere (**Figure 5A**), suggesting that cerebral ischemic insults induce oxidative stress that promotes HO-1 upregulation in the ischemic brain. Importantly, we found that 4-EG treatment further enhanced HO-1 expression in

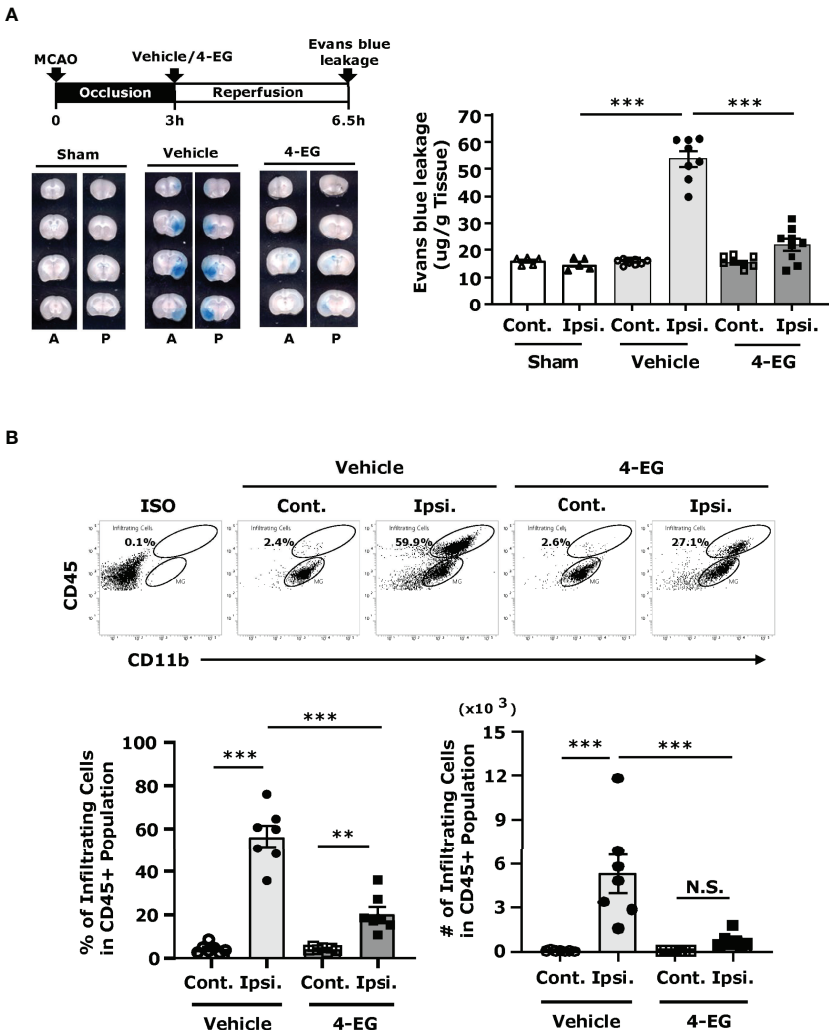

FIGURE 3 | 4-EG alleviates BBB disruption and represses peripheral immune cell infiltration of the CNS in ischemic stroke. **(A)** C57BL/6 male mice were subjected to sham or 3 h MCAO followed by vehicle or 4-EG administration. At 2.5 h post-reperfusion, mice were i.v.-administered Evans blue. 1 h after Evans blue injection, ischemic brains were harvested and sectioned. The representative brain images of sham, and vehicle- and 4-EG-treated MCAO mice are shown (A, anterior surface; P, posterior surface), and the Evans blue extravasation in the contralateral (Cont.) and ipsilateral (Ipsi.) hemispheres of sham (n=5), and vehicle- and 4-EG-treated MCAO mice (n=8/group) was determined. ****p<0.001* by two-way ANOVA. **(B)** C57BL/6 male mice subjected to 40 min MCAO were i.v. administered vehicle or 4-EG (100 mg/kg) at 2 h post-reperfusion. At 48 h post-injury, the ischemic brains harvested from vehicle- and 4-EG-treated MCAO mice were separated into the contralateral and ipsilateral hemispheres followed by mononuclear cell isolation (n=7/group). The isolated mononuclear cells were stained with antibodies against CD45 and CD11b and then analyzed by flow cytometry analysis. Isotype controls (Iso) were used as a negative control to determine $CD45^{int}CD11b^{+}$ MG and $CD45^{hi}CD11b^{+}$ infiltrating immune cells. The percentage and number of $CD45^{hi}CD11b^{+}$ infiltrating cells were then determined. ***p<0.01, ****p<0.001*, N.S., no significant differences by two-way ANOVA.

MG, as the frequency of HO-1-expressing MG was markedly increased in the ischemic brain of 4-EG-treated MCAO mice compared to that of vehicle-treated MCAO mice (**Figure 5A**). To further confirm the observed results, we subjected brain tissues to IHC to assess HO-1 expression. We observed HO-1 expression in the ipsilateral cortex and striatum of vehicle-treated MCAO mice. Consistently, 4-EG treatment further enhanced HO-1 expression in the ipsilateral cortex and striatum compared to vehicle treatment in MCAO mice (**Figure 5B**). Notably, HO-1 expression was co-localized with $Iba1^{+}$ cells in the ischemic brain, although HO-1 expression was also observed in non-$Iba1^{+}$ cells (**Figure 5B**). Finally, the effect of 4-EG on the induction of HO-1 was confirmed *in vitro* by using primary MG, BV2, and primary macrophages. Cells were activated with TNFα in the absence or presence of different doses of 4-EG followed by flow cytometry to determine HO-1 expression. The gating strategy of flow cytometry analysis is presented in **Supplementary Figure 4**. Our results showed that 4-EG dose-dependently upregulated HO-1 expression in these cells (**Figure 5C**). Altogether, our results demonstrate that 4-EG upregulates HO-1 expression in ischemia-activated MG *in vivo* and in TNFα-activated MG *in vitro*.

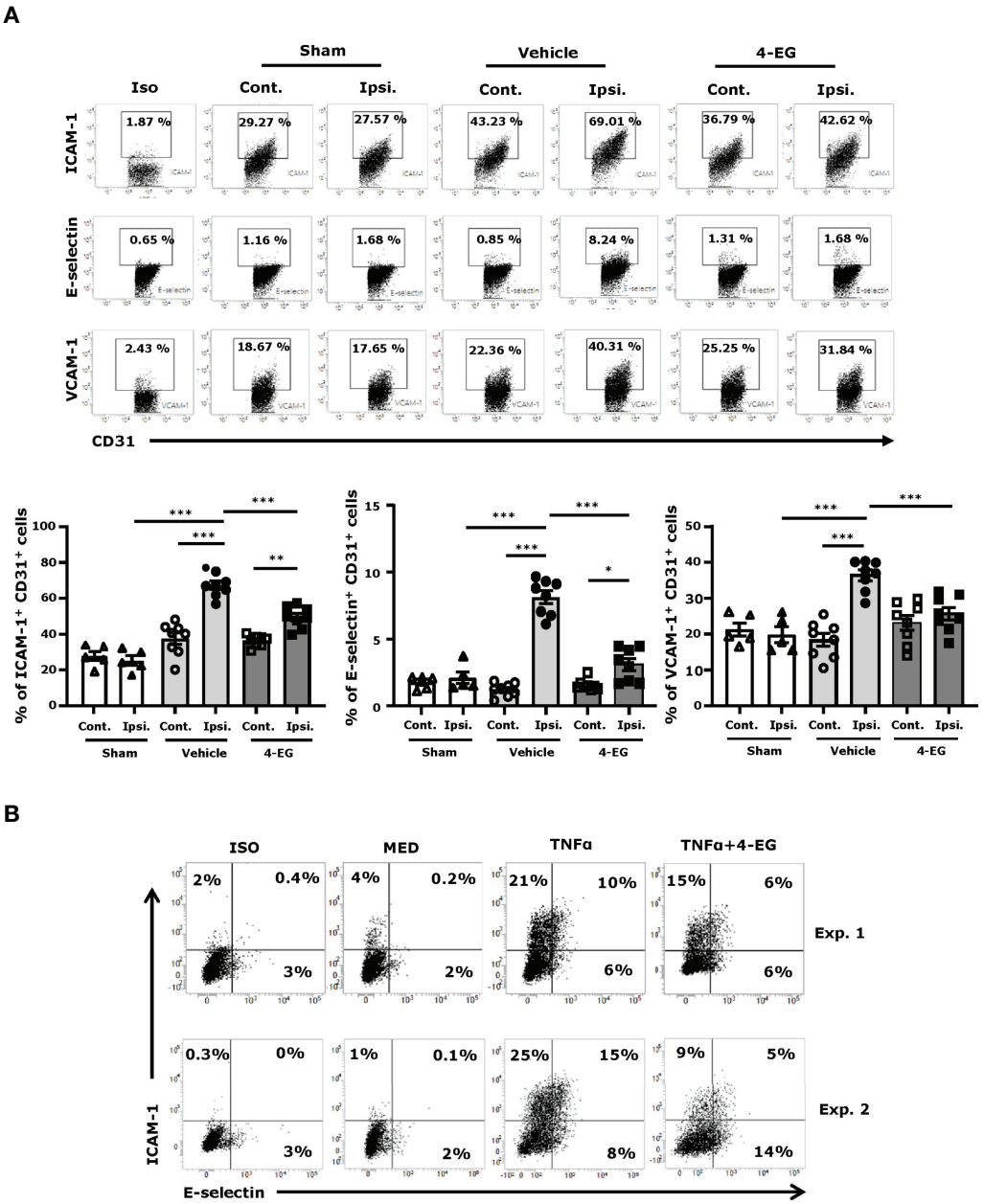

FIGURE 4 | 4-EG inhibits brain endothelial adhesion molecule expression in the ischemic brain. **(A)** C57BL/6 male mice were subjected to sham or 40 min MCAO followed by the i.v. administration of vehicle or 4-EG (100 mg/kg) at 2 h post-reperfusion. At 16–20 h post-injury, the contralateral and ipsilateral hemispheres of sham (n=5), and vehicle- and 4-EG- treated MCAO mice (n=8/group) were harvested and subjected to microvasculature isolation. The isolated cells were then stained with CD31 in the combination with ICAM-1, E-selectin, or VCAM-1 followed by flow cytometry analysis. Isotype controls (Iso) were used as a negative control to determine $CD31^+$ brain endothelial cells positive for ICAM-1, E-selectin, or VCAM-1 expression. The frequency of ICAM-1^+, E-selectin$^+$, and VCAM-1^+ $CD31^+$ cells was determined. *$p<0.05$, **$p<0.01$, ***$p<0.001$ by two-way ANOVA. **(B)** bEnd.3 cells were pretreated with 4-EG 200 μM for 1 h followed by TNFα 50 ng/ml stimulation for 4 h. Cells were then harvested and stained with ICAM-1 and E-selectin followed by flow cytometry analysis. Two representative flow cytometry results of five independent experiments are shown.

3.6 Inhibition of Nrf2/HO-1 Pathway Reverses the Protection Effect of 4-EG in Ischemic Stroke

To confirm whether the induction of the Nrf2/HO-1 pathway was required for the protective effect of 4-EG in ischemic stroke, male *Nrf2*$^{-/-}$ mice were subjected to MCAO followed by the administration of vehicle or 4-EG. 48 h post-injury, vehicle- and 4-EG-treated *Nrf2*$^{-/-}$ MCAO mice were sacrificed and the cerebral infarct was determined to assess the level of ischemic brain injury. Our results showed that the protective effect of 4-

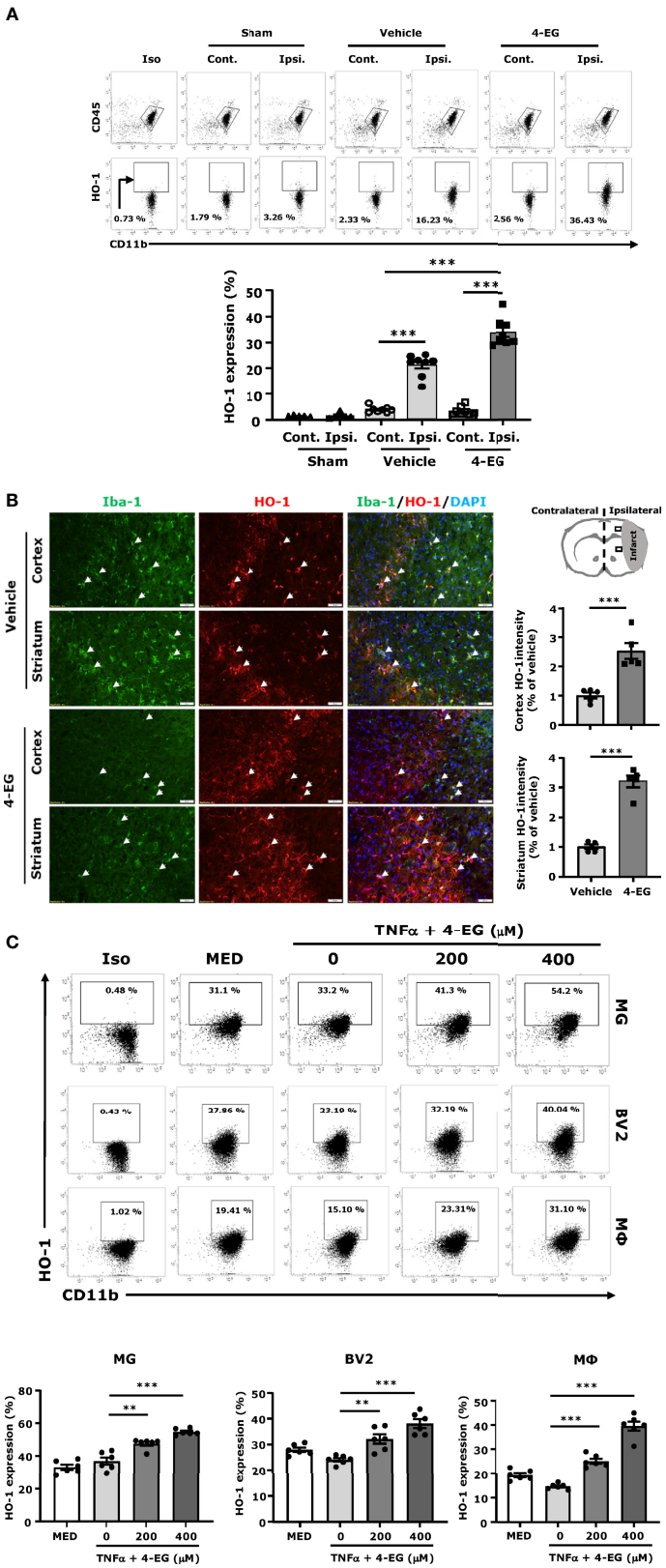

FIGURE 5 | Continued

FIGURE 5 | 4-EG promotes HO-1 expression in MG *in vivo* and *in vitro*. **(A)** C57BL/6 male mice were subjected to sham or 40 min MCAO followed by vehicle or 4-EG (100 mg/kg) i.v. administration at 2 h post-reperfusion. At 16–20 h post-injury, the contralateral and ipsilateral hemispheres of sham (n=5), vehicle- and 4-EG-treated MCAO mice (n=8/group) were harvested followed by mononuclear cell isolation. The isolated mononuclear cells were subjected to the surface staining of CD45 and CD11b and then the intracellular staining of HO-1 followed by flow cytometry analysis. Isotype controls (Iso) were used as a negative control to determine $CD45^{int}CD11b^{+}$ MG positive for HO-1 expression. The frequency of HO-1 expression in $CD45^{int}CD11b^{+}$ MG was measured. ***$p<0.001$ by two-way ANOVA. **(B)** At 20 h post-injury, the brain tissues of vehicle- and 4-EG-treated MCAO mice (n = 5/group) were subjected to IHC analysis to determine Iba1 and HO-1 expression. The representative images of Iba1 and HO-1 staining in the ipsilateral cortex and striatum of vehicle- and 4-EG-treated MCAO mice are shown. White arrows indicate the examples of Iba1/HO-1co-localization. The fluorescence intensity of HO-1 in the ipsilateral cortex and striatum was also quantified. Scale bar, 50 μm. ***$p<0.001$ by unpaired *t*-test. **(C)** MG, BV2, and macrophages (MΦ) were pretreated with 4-EG 200 μM or 400 μM for 1 h followed by TNFα 100 ng/ml stimulation for 24 h (n=6/treatment group). Cells were then collected and subjected to the surface staining of CD11b and then the intracellular staining of HO-1 followed by flow cytometry analysis. Isotype controls (Iso) were used as a negative control to determine $CD11b^{+}$ cells positive for HO-1 expression. **$p<0.01$, ***$p<0.001$ by one-way ANOVA.

EG in ischemic stroke was reversed in *Nrf2*$^{-/-}$ MCAO mice, as vehicle- and 4-EG-treated *Nrf2*$^{-/-}$ MCAO mice exhibited a comparable level of cerebral infarct (vehicle 110.2 ± 12.5 mm^3 vs. 4-EG 92.2 ± 12.4 mm^3; **Figure 6A**). The reversed protective effect of 4-EG in *Nrf2*$^{-/-}$ MCAO mice was due to Nrf2 deficiency that subsequently led to attenuated HO-1 expression in the ischemic brain, as we observed 4-EG-induced HO-1 upregulation in MG was abolished in *Nrf2*$^{-/-}$ MCAO mice (**Supplementary Figure 5**). Furthermore, we determined the protective effect of 4-EG in female stroke mice with Nrf2 deficiency. Female *Nrf2*$^{-/-}$ mice were subjected to MCAO followed by vehicle or 4-EG treatment to determine the level of brain injury in ischemic stroke. Similarly, female vehicle- and 4-EG-treated *Nrf2*$^{-/-}$ MCAO mice displayed a comparable size of infarct (vehicle 106.2 ± 9.7 mm^3 vs. 4-EG 96.2 ± 10.7 mm^3; **Figure 6B**). Collectively, these results indicate that the activation of the Nrf2 pathway is essential for 4-EG-conferred protection against ischemic stroke.

To further confirm whether the induction of HO-1 was required for the protective effect of 4-EG in ischemic stroke, male and female mice were treated with vehicle or ZnPP, an HO-1 inhibitor, and then subjected to MCAO followed by 4-EG administration. The control MCAO mice were subjected to vehicle treatments only. At 48 h post-injury, MCAO mice were sacrificed and infarct volumes were determined. Our results showed that both male and female MCAO mice treated with ZnPP and 4-EG exhibited significant larger infarct volumes than MCAO mice treated with 4-EG only, but displayed slightly decreased or comparable infarct volumes compared to vehicle-treated male or female MCAO mice, respectively (**Figures 6C, D**). These results indicate that the inhibition of HO-1 by ZnPP reverses the protective effect of 4-EG in ischemic stroke. Taken altogether, our results demonstrate that the induction of the Nrf2/HO-1 pathway plays an essential role in 4-EG-conferred protection against ischemic stroke.

4 DISCUSSION

In the present study, we demonstrate the efficacy of 4-EG treatment in ischemic stroke. Our *in vivo* results show that 4-EG treatment attenuates brain infarct, alleviates BBB disruption, improves neurological deficits, and increases survival in MCAO mice. At the cellular levels, 4-EG suppresses MG activation, leading to decreased CD86 and CD68 expression, and suppressed brain endothelial cell activation, resulting in reduced ICAM-1, E-selectin, and VCAM-1 expression in the ischemic brain. Mechanistically, 4-EG promotes HO-1 expression in MG to alleviate ischemic brain injury, as the protective effect of 4-EG in ischemic stroke is abolished in *Nrf2*$^{-/-}$ MCAO mice and MCAO mice treated with an HO-1 inhibitor. Thus, our results reveal that 4-EG exerts promising therapeutic effects on the attenuation of ischemic brain injury, suggesting that 4-EG could be developed as a novel therapeutic agent for the treatment of ischemic stroke.

Following ischemic stroke, neuroinflammation is a significant contributor to the pathological process of ischemic stroke (32–34). Inflammatogenic self-molecules derived from damaged tissue are generally called damage-associated molecular patterns (DAMPs), which are released from ischemic brain cells and stimulate DAMP receptors to induce the production of inflammatory cytokines and chemokines by MG that subsequently recruits peripheral immune cells infiltrating the injured brain (34). Thus, MG activation and peripheral immune cell infiltration contribute to the induction and aggravation of neuroinflammation in the ischemic brain, respectively (33, 35). In this study, we observed that 4-EG attenuated MG activation, as we found that the number of CD68- and CD86-expressing MG, and $Iba1^{+}$ cells was largely reduced in 4-EG-treated MCAO mice compared to vehicle-treated MCAO controls. Furthermore, we observed a significant decrease of immune cell infiltrates in the ischemic brain of 4-EG-treated MCAO mice compared to that of vehicle-treated MCAO controls. Altogether, our results demonstrate that 4-EG suppresses MG activation and inhibits peripheral immune cell infiltration of the ischemic brain in MCAO mice, suggesting that the protective effects of 4-EG in ischemic stroke may be partly mediated through its modulatory effects on both the CNS and peripheral immune cells, leading to attenuated neuroinflammation.

Ischemic stroke–induced brain damage is a complex pathophysiological process including multichannel damages (36, 37). Studies have demonstrated that BBB dysfunction is a decisive event during the progression of stroke (38, 39). Because BBB integrity plays an important role in maintaining the microenvironment and homeostasis of the brain (40), protecting the BBB from disruption is a prospective strategy for the prevention and treatment of ischemic stroke. Adhesion molecules expressed on the surface of brain endothelial cells play a vital role in the recruitment of leukocytes, especially neutrophils, into the CNS after ischemic brain injury (21). Targeting these molecules to block immune cell recruitment and minimize secondary inflammatory responses in stroke has been a reliable strategy for ischemic stroke treatment (21, 41). Leukocyte migration involves

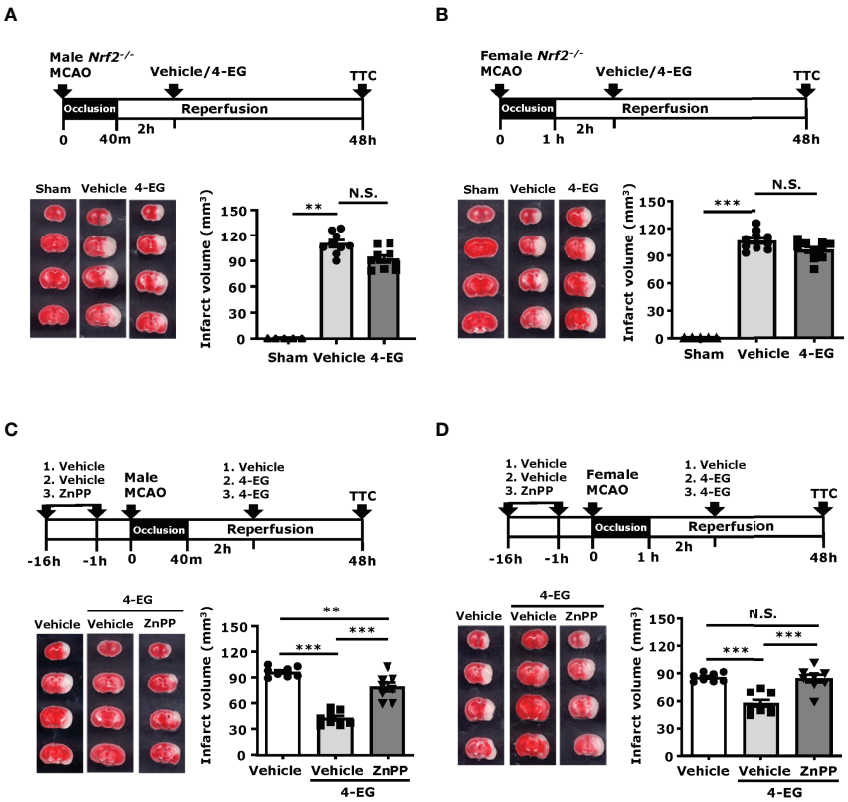

FIGURE 6 | Inhibition of Nrf2/HO-1 pathway reverses the protection effect of 4-EG in ischemic stroke. **(A, B)** Male and female *Nrf2*$^{-/-}$ mice were subjected to sham or MCAO followed by vehicle or 4-EG (100 mg/kg) administration at 2 h post-reperfusion. At 48 h post-injury, mice were sacrificed, and the ischemic brains were harvested, sliced, and stained with TTC. **(A)**. The representative TTC-stained brain samples of sham, and vehicle- and 4-EG-treated male *Nrf2*$^{-/-}$ MCAO mice are shown (left panel), and the infarct volumes of sham (n=5), and vehicle- and 4-EG-treated male *Nrf2*$^{-/-}$ MCAO mice (n=9/group) were measured (right panel). ***p<0.01*, N.S., no significant differences by the Kruskal–Wallis test. **(B)** The representative TTC-stained brain samples of sham, and vehicle- and 4-EG-treated female *Nrf2*$^{-/-}$ MCAO mice are shown (left panel), and the infarct volumes of sham (n=5), and vehicle- and 4-EG-treated female *Nrf2*$^{-/-}$ MCAO mice (n=10/group) were measured (right panel). ****p<0.001*, N.S., no significant differences by the Kruskal–Wallis test. **(C)** Male and **(D)** female C57BL/6 mice were pretreated with either vehicle or ZnPP (30 mg/kg) overnight and 1 h prior to MCAO. At 2 h post-reperfusion, vehicle-treated MCAO mice were treated with vehicle or 4-EG, and ZnPP-treated MCAO mice were treated with 4-EG. At 48 h post-injury, mice were sacrificed, and ischemic brains were harvested and subjected to TTC staining. The representative TTC-stained brain samples are shown (left panel), and the infarct volumes of vehicle-, 4-EG-, and ZnPP+4-EG-treated MCAO (n=8/group) mice were measured (right panel). ***p<0.01, ***p<0.001*, N.S., no significant differences by one-way ANOVA.

the processes of rolling, adherence, and transendothelial migration, and these processes are needed for peripheral immune cells to access the ischemic brain through the BBB (21, 22). Cellular interactions between the endothelium and circulating leukocytes are mainly mediated by three groups of cell adhesion molecules, namely, selectins (such as E-selectin), the immunoglobulin superfamily (such as ICAM-1 and VCAM-1), and integrins (21, 41). The increased expression of E-selectin has been documented in the animal models of cerebral ischemia and has been shown to participate in neuroinflammation and brain injury after ischemic stroke (42). Furthermore, ICAM-1 has been shown to play a key role in psychiatric disorders, and it is a marker for inflammation (41). Moreover, studies have shown that the blockade of leukocyte adhesion by targeting the interactions among the various adhesion molecules prevents leukocytes from entering the ischemic tissue, resulting in reduced neuronal damage (12). In this study, we found that 4-EG treatment repressed the expression of ICAM-1, VCAM-1, and E-selectin in brain endothelial cells, and diminished Evans blue leakage in ischemic stroke. Taken altogether, our results suggest that 4-EG could potentially modulate cellular interactions between the endothelium and circulating leukocytes to improve BBB integrity after ischemic stroke.

Nrf2 plays a central role in cellular defense against oxidative stress (28, 43). Under the condition of redox imbalance, Nrf2 activation promotes the production of various detoxifying and antioxidant enzymes, including HO-1, NQO1, and Gclc, through binding to antioxidant response elements (AREs). It has been reported to HO-1 has the most AREs on its promoter, making it a promising therapeutic target against brain injury in ischemic stroke (28, 43). Notably, HO-1 knockout mice exhibited a larger infarct compared to their WT controls after ischemic stroke, and MCAO mice treated with adenoviral vector overexpressing HO-1, resulting in decreased infarct volumes and attenuated neurologic deficits (28). Since MG were reported to be the main producers of

HO-1 in the CNS, we therefore conducted the assays of flow cytometry and IHC to determine the induction of HO-1 by 4-EG in MG following ischemic stroke. In the flow cytometry assay, MG were identified by their intermediate expression of CD45 and positive expression of CD11b, and their expression of CD45 and CD11b was not significantly altered following ischemic injury. We observed a low level of HO-1 expression in MG in both hemispheres of sham controls and the contralateral hemisphere of vehicle- and 4-EG treated MCAO mice, suggesting HO-1 is not induced under non-injured conditions in MG. In contrast, HO-1 was upregulated in MG in the ipsilateral hemisphere of vehicle-treated MCAO mice, and HO-1 expression was further upregulated in MG in the ipsilateral hemisphere of 4-EG-treated MCAO mice compared to that of vehicle-treated MCAO mice. These results demonstrate that ischemic insults induce HO-1 expression and 4-EG further upregulates HO-1 expression in MG in ischemic stroke. In the IHC assay, we found that Iba1 expression was downregulated in the ischemic brain of 4-EG-treated MCAO mice compared to that of vehicle-treated MCAO mice, suggesting that 4-EG suppresses MG activation. Notably, an increased level of HO-1 expression was observed in the ischemic brain of 4-EG-treated MCAO mice compared to that of vehicle-treated MCAO mice, and the co-localization of Iba1 and HO-1 immunoactivity was also detected in the ischemic cortex and striatum of vehicle- and 4-EG-treated MCAO mice. Collectively, these results demonstrate that 4-EG induces HO-1 upregulation in MG following ischemic stroke. Finally, we conducted *in vitro* studies to confirm our observation of the 4-EG-mediated induction of HO-1 expression *in vivo* by utilizing three different cell types, including primary MG, MG cell line BV2, and primary macrophages. Cells were activated with TNFα to mimic the inflammatory microenvironment in the ischemic brain, as previous studies have shown that TNFα was induced in the ischemic brain (44–46) and we also observed TNFα expression in the ischemic brain. Our results showed that 4-EG was capable of enhancing HO-1 expression in primary MG, BV2, and primary macrophages stimulated with TNFα. Altogether, our findings strongly demonstrate that 4-EG induces HO-1 expression in MG *in vitro* as well as *in vivo*.

Our observation of 4EG-induced HO-1 expression in the ischemic brain prompted us to investigate whether the induction of the Nrf2/HO-1 pathway was required for 4-EG-mediated protection against ischemic stroke. With the approach of inducing ischemic stroke in *Nrf2*$^{-/-}$ mice, we observed that the protective effect of 4-EG in ischemic stroke was reversed in *Nrf2*$^{-/-}$ MCAO mice. Importantly, we found that 4-EG-induced HO-1 upregulation in MG was abolished in *Nrf2*$^{-/-}$ MCAO mice. Furthermore, using the HO-1 inhibitor, ZnPP, we observed that the protective effect of 4-EG in ischemic stroke was also reversed in MCAO mice. Interesting, we noticed that the protective effect of 4-EG in ischemic stroke was not totally abolished in *Nrf2*$^{-/-}$ and ZnPP-treated MCAO mice, as 4-EG was still able to slightly attenuate brain infarct in *Nrf2*$^{-/-}$ and ZnPP-treated MCAO mice. These results suggest that the 4-EG-induced Nrf2/HO-1 pathway plays an essential role in alleviating brain injury induced by ischemic insults; however, 4-EG may induce additional protective mechanisms to offer protection against ischemic stroke. Indeed, 4-EG was previously reported to modulate NFκB and NLRP3 inflammasome activation (11), and the activation of NFκB and NLRP3 inflammasome was reported to induce brain injury in ischemic stroke (47, 48). Further studies would be required to investigate whether 4-EG directly inhibits NFκB and NLRP3 inflammasome activation to modulate brain injury in ischemic stroke.

There are limitations in our current study and that would be worthy of discussion. First, it is unknown whether 4-EG can cross the BBB, as there are no studies demonstrating their ability of crossing intact BBB. However, based on ChemDraw (PerkinElmer Informatics), 4-EG has a LogP value of 2.35 and it has been reported that drugs with LogP values above two are the most BBB penetrant (49). In addition, studies have shown that ischemic stroke induces BBB disruption (39), and in this study 4-EG was administered to MCAO mice at 2 h post-reperfusion that would facilitate their entering of the CNS through the disrupted BBB. Second, it is unknown what is the half-life of 4-EG *in vivo*. Although it is beyond the scope of the current study, future studies to investigate the pharmacokinetic properties of 4-EG would provide valuable data regarding its potential as a therapeutic agent for the treatment of ischemic stroke.

5 CONCLUSIONS

Our present study showed that 4-EG conferred protection against ischemic stroke. We observed that 4-EG suppressed MG activation, inhibited inflammatory molecule expression, and repressed the peripheral immune cell of infiltration of the CNS in ischemic stroke. Furthermore, we found that 4-EG suppressed brain endothelial cell adhesion molecule upregulation and alleviated BBB disruption in the ischemic brain. Finally, we revealed that 4-EG induced HO-1 expression in MG in the ischemic brain, and the inhibition of the Nrf2/HO-1 pathway reversed the protective effect of 4-EG in ischemic stroke. In summary, our results suggest that 4-EG, a natural compound, could be developed as a potential therapeutic agent for the treatment of ischemic stroke through its immunomodulatory and anti-inflammatory properties.

DATA AVAILABILITY STATEMENT

The original contributions presented in the study are included in the article/**Supplementary Material**. Further inquiries can be directed to the corresponding author.

ETHICS STATEMENT

The animal study was reviewed and approved by Purdue Animal Care and Use Committee.

AUTHOR CONTRIBUTIONS

W-TW performed experiments, analyzed data, and wrote the manuscript. P-CK performed experiments and analyzed data. BS

and HP performed experiments. DB and I-CY contributed to study discussion and manuscript editing. J-HY conceived the study, designed experiments, and wrote the manuscript. All authors read and approved the final manuscript.

FUNDING

This work was supported by IU start-up fund and in part by NIH R01NS102449 to J-HY.

SUPPLEMENTARY MATERIAL

The Supplementary Material for this article can be found online at: https://www.frontiersin.org/articles/10.3389/fimmu.2022.887000/full#supplementary-material

Supplementary Figure 1 | Genotyping of *Nrf2*$^{-/-}$ mouse by PCR. Genomic DNA extracted from mouse tails of wildtype (WT) (n=2) and *Nrf2*$^{-/-}$ mice (n=8) was amplified by PCR with multi-primers for genotyping. The primers used are as follows: Forward primer: 5'-GCCTGAGAGCTGTAGGCCC-3', WT reverse primer: 5'-GGAATGGAAAATAGCTCCTGCC-3', mutant reverse primer: 5'-GACAGTATCGGCCTCAGGAA-3'. PCR products of 262 and 400 bp correspond to WT and *Nrf2*$^{-/-}$ alleles, respectively.

Supplementary Figure 2 | The dose effect of 4-EG in ischemic stroke. C57BL/6 male mice were subjected to sham or 40min MCAO followed by vehicle or different doses of 4-EG (50, 100, or 150 mg/kg) i.v. administration at 2 h post-reperfusion (n=8/group). At 48 h post-injury, the ischemic brains were harvested and sliced (2 mm) followed by TTC staining. **(A)** Two representative TTC-stained brain samples of vehicle- and 4-EG-treated MCAO mice are shown, and **(B)** the infarct volumes of survived vehicle- and 4-EG-treated MCAO male were measured. ****p<0.001* by one-way ANOVA. **(C)** The survive rate of vehicle- and 4-EG-treated MCAO mice was also calculated.

Supplementary Figure 3 | Gating strategy of flow cytometry analysis *in vivo*. **(A)** Mononuclear cells isolated from the brains of sham and MCAO mice were subjected to surface staining of CD11b and CD45 in the presence of 7-AAD followed by surface staining of CD86 or intracellular staining of CD68 or HO-1. 7-AAD negative live cells were then gated followed by singlet gating. CD45^{int}CD11b^{+} cells were gated to identify MG, and isotype controls (Iso) were used as negative controls to determine CD45^{int}CD11b^{+} MG positive for the expression of CD86, CD68, or HO-1. **(B)** Microvascular cells isolated from the brains of sham or MCAO mice were subjected to surface staining of CD31 in the presence of 7-AAD followed by surface staining of ICAM-1, E-selectin, or VCAM-1. 7-AAD negative live cells were gated followed by singlet gating. CD31^{+} cells were then gated to identify brain endothelial cells, and isotype controls (Iso) were used as a negative control to determine CD31^{+} cells positive for the surface expression of ICAM-1, E-selectin, or VCAM-1.

Supplementary Figure 4 | Gating strategy of flow cytometry analysis *in vitro*. MG, BV2, and macrophages (MΦ) were subjected to surface staining of CD11b in the presence of 7-AAD followed by intracellular staining of HO-1. 7-AAD negative live cells were gated followed by singlet gating. Isotype controls (Iso) were used as negative controls to determine CD11b^{+} cells positive for the expression of HO-1.

Supplementary Figure 5 | 4-EG-induced HO-1 expression in MG is abolished in *Nrf2*$^{-/-}$ MCAO mice. *Nrf2*$^{-/-}$ male mice were subjected to 40 min MCAO followed by vehicle or 4-EG (100 mg/kg) i.v. administration at 2 h post-reperfusion (n=8/group). At 16-20 h post-injury, the contralateral and ipsilateral hemispheres of vehicle- and 4-EG-treated *Nrf2*$^{-/-}$ MCAO mice were harvested followed by mononuclear cell isolation. The isolated mononuclear cells were subjected to surface staining of CD45 and CD11b and then intracellular staining of HO-1 followed by flow cytometry analysis. Isotype controls (Iso) were used as a negative control to determine CD45^{int}CD11b^{+} MG positive for HO-1 expression. The frequency of HO-1 expression in CD45^{int}CD11b^{+} MG was measured. ***p<0.01; ***p<0.001*, N.S; no significant differences by one-way ANOVA.

REFERENCES

1. Fisher M, Saver JL. Future Directions of Acute Ischaemic Stroke Therapy. *Lancet Neurol* (2015) 14:758–67. doi: 10.1016/S1474-4422(15)00054-X
2. Esposito E, Ahn BJ, Shi J, Nakamura Y, Park JH, Mandeville ET, et al. Brain-To-Cervical Lymph Node Signaling After Stroke. *Nat Commun* (2019) 10:5306. doi: 10.1038/s41467-019-13324-w
3. Ma Y, Wang J, Wang Y, Yang GY. The Biphasic Function of Microglia in Ischemic Stroke. *Prog Neurobiol* (2017) 157:247–72. doi: 10.1016/j.pneurobio.2016.01.005
4. Ishrat T, Mohamed IN, Pillai B, Soliman S, Fouda AY, Ergul A, et al. Thioredoxin-Interacting Protein: A Novel Target for Neuroprotection in Experimental Thromboembolic Stroke in Mice. *Mol Neurobiol* (2015) 51:766–78. doi: 10.1007/s12035-014-8766-x
5. Kim E, Cho S. Microglia and Monocyte-Derived Macrophages in Stroke. *Neurotherapeutics* (2016) 13:702–18. doi: 10.1007/s13311-016-0463-1
6. Zhang QY, Wang ZJ, Miao L, Wang Y, Chang LL, Guo W, et al. Neuroprotective Effect of SCM-198 Through Stabilizing Endothelial Cell Function. *Oxid Med Cell Longev* (2019) 2019:7850154. doi: 10.1155/2019/7850154
7. Prakash R, Carmichael ST. Blood-Brain Barrier Breakdown and Neovascularization Processes After Stroke and Traumatic Brain Injury. *Curr Opin Neurol* (2015) 28:556–64. doi: 10.1097/WCO.0000000000000248
8. Krueger M, Bechmann I, Immig K, Reichenbach A, Härtig W, Michalski D. Blood-Brain Barrier Breakdown Involves Four Distinct Stages of Vascular Damage in Various Models of Experimental Focal Cerebral Ischemia. *J Cereb Blood Flow Metab* (2015) 35:292–303. doi: 10.1038/jcbfm.2014.199
9. Graf BA, Milbury PE, Blumberg JB. Flavonols, Flavones, Flavanones, and Human Health: Epidemiological Evidence. *J Med Food* (2005) 8:281–90. doi: 10.1089/jmf.2005.8.281
10. Arts IC, Hollman PC. Polyphenols and Disease Risk in Epidemiologic Studies. *Am J Clin Nutr* (2005) 81:317s–25s. doi: 10.1093/ajcn/81.1.317S
11. Zhao DR, Jiang YS, Sun JY, Li HH, Luo XL, Zhao MM. Anti-Inflammatory Mechanism Involved in 4-Ethylguaiacol-Mediated Inhibition of LPS-Induced Inflammation in THP-1 Cells. *J Agric Food Chem* (2019) 67:1230–43. doi: 10.1021/acs.jafc.8b06263
12. Weng WT, Kuo PC, Brown DA, Scofield BA, Furnas D, Paraiso HC, et al. 4-Ethylguaiacol Modulates Neuroinflammation and Th1/Th17 Differentiation to Ameliorate Disease Severity in Experimental Autoimmune Encephalomyelitis. *J Neuroinflamm* (2021) 18:110. doi: 10.1186/s12974-021-02143-w
13. Kuo PC, Yu IC, Scofield BA, Brown DA, Curfman ET, Paraiso HC, et al. 3h-1,2-Dithiole-3-Thione as a Novel Therapeutic Agent for the Treatment of Ischemic Stroke Through Nrf2 Defense Pathway. *Brain Behav Immun* (2017) 62:180–92. doi: 10.1016/j.bbi.2017.01.018
14. Kuo PC, Weng WT, Scofield BA, Furnas D, Paraiso HC, Intriago AJ, et al. Interferon-Beta Alleviates Delayed tPA-Induced Adverse Effects *via* Modulation of MMP3/9 Production in Ischemic Stroke. *Blood Adv* (2020) 4:4366–81. doi: 10.1182/bloodadvances.2020001443
15. Kreutzberg GW. Microglia: A Sensor for Pathological Events in the CNS. *Trends Neurosci* (1996) 19:312–8. doi: 10.1016/0166-2236(96)10049-7
16. Paraiso HC, Wang X, Kuo PC, Furnas D, Scofield BA, Chang FL, et al. Isolation of Mouse Cerebral Microvasculature for Molecular and Single-Cell Analysis. *Front Cell Neurosci* (2020) 14:84. doi: 10.3389/fncel.2020.00084
17. Hooper KM, Yen JH, Kong W, Rahbari KM, Kuo PC, Gamero AM, et al. Prostaglandin E2 Inhibition of IL-27 Production in Murine Dendritic Cells: A

Novel Mechanism That Involves Irf1. *J Immunol* (2017) 198:1521–30. doi: 10.4049/jimmunol.1601073
18. Jian Z, Liu R, Zhu X, Smerin D, Zhong Y, Gu L, et al. The Involvement and Therapy Target of Immune Cells After Ischemic Stroke. *Front Immunol* (2019) 10:2167. doi: 10.3389/fimmu.2019.02167
19. Greter M, Lelios I, Croxford AL. Microglia Versus Myeloid Cell Nomenclature During Brain Inflammation. *Front Immunol* (2015) 6:249. doi: 10.3389/fimmu.2015.00249
20. Bennett ML, Bennett FC, Liddelow SA, Ajami B, Zamanian JL, Fernhoff NB, et al. New Tools for Studying Microglia in the Mouse and Human CNS. *Proc Natl Acad Sci USA* (2016) 113:E1738–1746. doi: 10.1073/pnas.1525528113
21. Yang C, Hawkins KE, Doré S, Candelario-Jalil E. Neuroinflammatory Mechanisms of Blood-Brain Barrier Damage in Ischemic Stroke. *Am J Physiol Cell Physiol* (2019) 316:C135–c153. doi: 10.1152/ajpcell.00136.2018
22. Planas AM. Role of Immune Cells Migrating to the Ischemic Brain. *Stroke* (2018) 49:2261–7. doi: 10.1161/STROKEAHA.118.021474
23. Kuo PC, Scofield BA, Yu IC, Chang FL, Ganea D, Yen JH. Interferon-Beta Modulates Inflammatory Response in Cerebral Ischemia. *J Am Heart Assoc* (2016) 5:1-15. doi: 10.1161/JAHA.115.002610
24. Lindsberg PJ, Carpen O, Paetau A, Karjalainen-Lindsberg ML, Kaste M. Endothelial ICAM-1 Expression Associated With Inflammatory Cell Response in Human Ischemic Stroke. *Circulation* (1996) 94:939–45. doi: 10.1161/01.CIR.94.5.939
25. Zhang R, Chopp M, Zhang Z, Jiang N, Powers C. The Expression of P- and E-Selectins in Three Models of Middle Cerebral Artery Occlusion. *Brain Res* (1998) 785:207–14. doi: 10.1016/S0006-8993(97)01343-7
26. Panahian N, Yoshiura M, Maines MD. Overexpression of Heme Oxygenase-1 Is Neuroprotective in a Model of Permanent Middle Cerebral Artery Occlusion in Transgenic Mice. *J Neurochem* (1999) 72:1187–203. doi: 10.1111/j.1471-4159.1999.721187.x
27. Shah ZA, Nada SE, Doré S. Heme Oxygenase 1, Beneficial Role in Permanent Ischemic Stroke and in Gingko Biloba (EGb 761) Neuroprotection. *Neuroscience* (2011) 180:248–55. doi: 10.1016/j.neuroscience.2011.02.031
28. Bereczki DJr., Balla J, Bereczki D. Heme Oxygenase-1: Clinical Relevance in Ischemic Stroke. *Curr Pharm Des* (2018) 24:2229–35. doi: 10.2174/1381612824666180717101104
29. Vijayan V, Wagener F, Immenschuh S. The Macrophage Heme-Heme Oxygenase-1 System and Its Role in Inflammation. *Biochem Pharmacol* (2018) 153:159–67. doi: 10.1016/j.bcp.2018.02.010
30. Zhang Y, Chen K, Sloan SA, Bennett ML, Scholze AR, O'Keeffe S, et al. An RNA-Sequencing Transcriptome and Splicing Database of Glia, Neurons, and Vascular Cells of the Cerebral Cortex. *J Neurosci* (2014) 34:11929–47. doi: 10.1523/JNEUROSCI.1860-14.2014
31. Kuo PC, Weng WT, Scofield BA, Furnas D, Paraiso HC, Yu IC, et al. Immunoresponsive Gene 1 Modulates the Severity of Brain Injury in Cerebral Ischaemia. *Brain Commun* (2021) 3:fcab187. doi: 10.1093/braincomms/fcab187
32. Dziedzic T. Systemic Inflammation as a Therapeutic Target in Acute Ischemic Stroke. *Expert Rev Neurother* (2015) 15:523–31. doi: 10.1586/14737175.2015.1035712
33. Pluta R, Januszewski S, Czuczwar SJ. Neuroinflammation in Post-Ischemic Neurodegeneration of the Brain: Friend, Foe, or Both? *Int J Mol Sci* (2021) 22:1-16. doi: 10.3390/ijms22094405
34. Nakamura K, Shichita T. Cellular and Molecular Mechanisms of Sterile Inflammation in Ischaemic Stroke. *J Biochem* (2019) 165:459–64. doi: 10.1093/jb/mvz017
35. Jayaraj RL, Azimullah S, Beiram R, Jalal FY, Rosenberg GA. Neuroinflammation: Friend and Foe for Ischemic Stroke. *J Neuroinflamm* (2019) 16:142. doi: 10.1186/s12974-019-1516-2
36. Ahmad M, Dar NJ, Bhat ZS, Hussain A, Shah A, Liu H, et al. Inflammation in Ischemic Stroke: Mechanisms, Consequences and Possible Drug Targets. *CNS Neurol Disord Drug Targets* (2014) 13:1378–96. doi: 10.2174/1871527313666141023094720
37. Manzanero S, Santro T, Arumugam TV. Neuronal Oxidative Stress in Acute Ischemic Stroke: Sources and Contribution to Cell Injury. *Neurochem Int* (2013) 62:712–8. doi: 10.1016/j.neuint.2012.11.009
38. Bernardo-Castro S, Sousa JA, Bras A, Cecilia C, Rodrigues B, Almendra L, et al. Pathophysiology of Blood-Brain Barrier Permeability Throughout the Different Stages of Ischemic Stroke and Its Implication on Hemorrhagic Transformation and Recovery. *Front Neurol* (2020) 11:594672. doi: 10.3389/fneur.2020.594672
39. Abdullahi W, Tripathi D, Ronaldson PT. Blood-Brain Barrier Dysfunction in Ischemic Stroke: Targeting Tight Junctions and Transporters for Vascular Protection. *Am J Physiol Cell Physiol* (2018) 315:C343–56. doi: 10.1152/ajpcell.00095.2018
40. Saïghi S, Mayr CG, Serrano-Gotarredona T, Schmidt H, Lecerf G, Tomas J, et al. Plasticity in Memristive Devices for Spiking Neural Networks. *Front Neurosci* (2015) 9. doi: 10.3389/fnins.2015.00051
41. Müller N. The Role of Intercellular Adhesion Molecule-1 in the Pathogenesis of Psychiatric Disorders. *Front Pharmacol* (2019) 10:1-9. doi: 10.3389/fphar.2019.01251
42. Yang C, Hawkins K. E., Doré S, Candelario-Jalil E. Neuroinflammatory mechanisms of blood-brain barrier damage in ischemic stroke. *Am J Physiol Cell Physiol* (2019) 316:C135–153. doi: 10.1152/ajpcell.00136.2018
43. Lu X, Chen-Roetling J, Regan RF. Systemic Hemin Therapy Attenuates Blood-Brain Barrier Disruption After Intracerebral Hemorrhage. *Neurobiol Dis* (2014) 70:245–51. doi: 10.1016/j.nbd.2014.06.005
44. Chen X, Zhang X, Wang Y, Lei H, Su H, Zeng J, et al. Inhibition of Immunoproteasome Reduces Infarction Volume and Attenuates Inflammatory Reaction in a Rat Model of Ischemic Stroke. *Cell Death Dis* (2015) 6:e1626. doi: 10.1038/cddis.2014.586
45. Li YH, Fu HL, Tian ML, Wang YQ, Chen W, Cai LL, et al. Neuron-Derived FGF10 Ameliorates Cerebral Ischemia Injury *via* Inhibiting NF-kappaB-Dependent Neuroinflammation and Activating PI3K/Akt Survival Signaling Pathway in Mice. *Sci Rep* (2016) 6:19869. doi: 10.1038/srep19869
46. Pan Z, Cui M, Dai G, Yuan T, Li Y, Ji T, et al. Protective Effect of Anthocyanin on Neurovascular Unit in Cerebral Ischemia/Reperfusion Injury in Rats. *Front Neurosci* (2018) 12:947. doi: 10.3389/fnins.2018.00947
47. Harari OA, Liao JK. NF-kappaB and Innate Immunity in Ischemic Stroke. *Ann N Y Acad Sci* (2010) 1207:32–40. doi: 10.1111/j.1749-6632.2010.05735.x
48. Ismael S, Zhao L, Nasoohi S, Ishrat T. Inhibition of the NLRP3-Inflammasome as a Potential Approach for Neuroprotection After Stroke. *Sci Rep* (2018) 8:5971. doi: 10.1038/s41598-018-24350-x
49. Hansch C, Steward AR, Anderson SM, Bentley D. The Parabolic Dependence of Drug Action Upon Lipophilic Character as Revealed by a Study of Hypnotics. *J Med Chem* (1968) 11:1–11. doi: 10.1021/jm00307a001

Conflict of Interest: The authors declare that the research was conducted in the absence of any commercial or financial relationships that could be construed as a potential conflict of interest.

frontiers | Frontiers in Cellular Neuroscience

TYPE Review
PUBLISHED 21 October 2022
DOI 10.3389/fncel.2022.1013905

OPEN ACCESS

EDITED BY
Jui-Hung Jimmy Yen,
Indiana University School of Medicine, United States

REVIEWED BY
Takashi Shichita,
Tokyo Metropolitan Institute of Medical Science, Japan
Linglei Kong,
Chinese Academy of Medical Sciences and Peking Union Medical College, China
Yutong Jiang,
Third Affiliated Hospital of Sun Yat-sen University, China

*CORRESPONDENCE
Yu Cui
cuiyu1210@126.com

SPECIALTY SECTION
This article was submitted to Cellular Neuropathology, a section of the journal Frontiers in Cellular Neuroscience

RECEIVED 08 August 2022
ACCEPTED 03 October 2022
PUBLISHED 21 October 2022

CITATION
Zhang Z, Lv M, Zhou X and Cui Y (2022) Roles of peripheral immune cells in the recovery of neurological function after ischemic stroke. *Front. Cell. Neurosci.* 16:1013905. doi: 10.3389/fncel.2022.1013905

Roles of peripheral immune cells in the recovery of neurological function after ischemic stroke

Zhaolong Zhang[1], Mengfei Lv[2,3], Xin Zhou[2,3] and Yu Cui[2,3]*

[1]Department of Interventional Radiology, The Affiliated Hospital of Qingdao University, Qingdao, Shandong, China, [2]Institute of Neuroregeneration and Neurorehabilitation, Qingdao University, Qingdao, Shandong, China, [3]Qingdao Medical College, Qingdao University, Qingdao, Shandong, China

Stroke is a leading cause of mortality and long-term disability worldwide, with limited spontaneous repair processes occurring after injury. Immune cells are involved in multiple aspects of ischemic stroke, from early damage processes to late recovery-related events. Compared with the substantial advances that have been made in elucidating how immune cells modulate acute ischemic injury, the understanding of the impact of the immune system on functional recovery is limited. In this review, we summarized the mechanisms of brain repair after ischemic stroke from both the neuronal and non-neuronal perspectives, and we review advances in understanding of the effects on functional recovery after ischemic stroke mediated by infiltrated peripheral innate and adaptive immune cells, immune cell-released cytokines and cell-cell interactions. We also highlight studies that advance our understanding of the mechanisms underlying functional recovery mediated by peripheral immune cells after ischemia. Insights into these processes will shed light on the double-edged role of infiltrated peripheral immune cells in functional recovery after ischemic stroke and provide clues for new therapies for improving neurological function.

KEYWORDS

ischemic stroke, functional recovery, T cells, monocytes and macrophages, B cells, neutrophils, cytokines

Introduction

Stroke is the leading cause of adult disability, and approximately sixty percent of survivors have motor, sensory, memory or language function deficits (Carmichael, 2006). There are two major types of strokes: ischemic stroke and intracerebral hemorrhage. Ischemic stroke occurs when a vessel supplying blood to the brain is obstructed, and accounts for 70–80% of all stroke cases (Feigin et al., 2009). Ischemic stroke can initiate neuronal death, which further result in blood–brain barrier (BBB) disruption and neuroinflammation cascades, leading to severe neurological deficits

(Iadecola and Anrather, 2011; Lyu et al., 2021). Generally, the adult brain is considered to have an extremely limited capacity for regeneration. Nevertheless, a growing body of literature suggests that diseases or injuries can trigger molecular, vascular, glial, neuronal, or environmental events that regulate brain repair (Cramer and Riley, 2008; Varadarajan et al., 2022). Likewise, both neuronal and non-neuronal mechanisms, such as neurogenesis, angiogenesis, astrogliosis and oligodendrogenesis, contribute to the improvement of behavioral deficits in the long-term after ischemic stroke (Font et al., 2010; Hu et al., 2015). Considering the lack of therapeutic drugs that can be administered during the late stage of stroke, it is of great importance to illuminate the mechanisms underlying the complicated repair processes.

As immune cells are essential for both initiating and resolving inflammatory responses, the regulation of brain injury and repair of immune cells are becoming increasingly understood (Seifert and Pennypacker, 2014; Prinz and Priller, 2017; Carrasco et al., 2022). Ischemic damage-induced sterile neuroinflammation, which is caused by recognition by danger/damage-associated molecular patterns (DAMPs) such as ATP, HMGB1 and damaged DNA, and specific pattern-recognition receptors (PRRs), occurs within a few days after stroke onset, during which innate immune cells, including microglia, macrophages, and neutrophils, play a major role. After the acute phase (Days 1–3 post-ischemia), adaptive immunity-associated immune cells such as distinct types of T cells and B cells, have been observed to infiltrate the brain by different means and last for weeks or months, indicating the involvement of these cells in functional recovery (Jayaraj et al., 2019; Iadecola et al., 2020). To date, the contribution of neuroinflammation in the primary injury caused by the initial ischemic event or secondary injury of the brain created by a series of biological and functional changes has long been investigated. The effects of these infiltrated immune cells in the chronic phase of functional restoration are poorly understood.

This review discusses the role of infiltrating peripheral immune cells in the functional recovery of ischemic stroke. Besides peripheral immune cells, the brain also harbors some immune cells, which are essential for brain development and function and regulate ischemic stroke (Colonna and Butovsky, 2017; Smolders et al., 2018; Badimon et al., 2020). Many previous studies have thoroughly reviewed the role of brain resident immune cells in ischemic stroke as well as immune cells in the regulation of the acute injury phase (Iadecola and Anrather, 2011; Hu et al., 2015; Jian et al., 2019; Iadecola et al., 2020). Here, we provide focused attention only on the role of peripheral innate and adaptive immune cells in the recovery of neurological function during the subacute (Days 4–8 post-ischemia) and chronic phases (exceeding 9 days post-ischemia) of ischemic stroke (**Figure 1**), and highlight outstanding questions for future studies.

Neuronal and non-neuronal mechanisms of functional recovery after ischemic stroke

Ischemic stroke-induced injury can trigger some repair processes, such as neurogenesis, axon sprouting, oligodendrogenesis, angiogenesis, and astrogliosis, the degree of which depends on the severity and topography of the injury. For many decades, findings from human and animal studies have continued to shed light on the molecular, vascular, glial, neuronal, and environmental events that regulate neurological recovery during the weeks after ischemic stroke (Carmichael, 2006; Cramer and Riley, 2008). In the following section, we briefly summarize the main aspects from the neuronal and non-neuronal perspectives (**Table 1**).

Tremendous efforts have been devoted to characterizing the cellular and molecular mechanisms of neuronal regeneration. Methods to promote neuron regeneration in the brain, such as by blocking inhibitory factors for myelination and promoting axon sprouting, have met with mixed success, albeit some challenges. For example, in many experiments, increased axon sprouting or neuronal survival has been observed after treatment (Barker et al., 2018; Joy et al., 2019; Hu et al., 2020); however, approaches to fully restore circuit function are lacking. In addition, the differences in reactions and effects in animal models and human patients make it difficult for clinical trials (Carmichael, 2006; Carmichael et al., 2017; Varadarajan et al., 2022). These discoveries cannot be ignored as they reveal possible neuronal regeneration mechanisms existing in stroke models weeks and months after acute damage and raise important strategies to intervene in neuronal regeneration and functional recovery, which include neurogenesis, axon sprouting and extension, synapse reformation and stimulation-based refinement of newly formed circuits (Small et al., 2013; Joy and Carmichael, 2021; Shi X. et al., 2021; Varadarajan et al., 2022). To achieve better functional connectivity, methods targeting multifaceted processes are needed.

Besides neuronal injury, ischemic stroke can also result in marked damage to the BBB and neurovascular unit dysfunction, and induce inflammatory responses in glial cells in human and animal models (Jiang et al., 2018; Jayaraj et al., 2019). These changes further lead to events including (1) angiogenesis, which is mediated by endothelial cells; (2) the astrogliosis of astrocytes; (3) oligodendrogenesis, which is regulated by oligodendrocyte progenitor cells (OPCs); and (4) changes in inflammatory phenotypes and phagocytic capacity of innate immune cells (Hatakeyama et al., 2020; Shibahara et al., 2020; Zhu et al., 2021). The capacity of neuronal regeneration and the ultimate recovery of sensorimotor and language deficits or neuropsychiatric sequelae depend on these processes in the long-term.

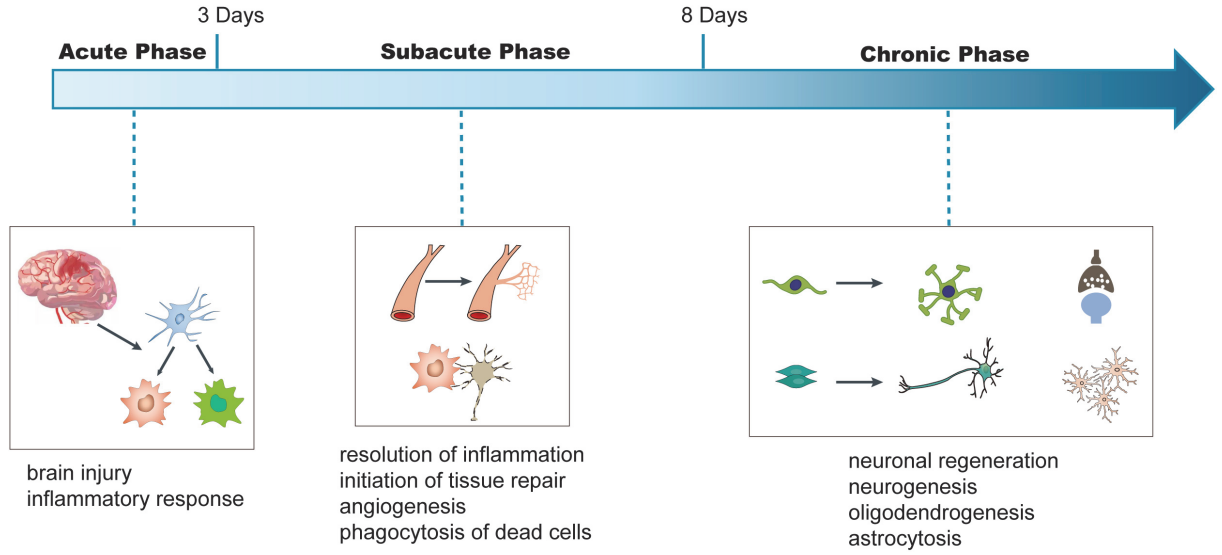

FIGURE 1
Schematic viewing of time-dependent key injury and repair processes after ischemic stroke. In this review, we refer to Days 1–3 after stroke onset as the acute phase, Days 3–8 being subacute phase, and days exceeding 8 being chronic phase. We illustrate the conceptual changes in each phase. In the acute phase, ischemia in the brain leads to the injury of the brain and inflammatory responses. In the subacute phase, the resolution of inflammatory response and phagocytosis of dead neurons were observed and tissue repair processes, such as angiogenesis, are initiated. During the chronic phase, processes, such as neurogenesis, oligodendrogenesis, and astrocytosis are initiated to regulate neuronal regeneration and functional recovery.

TABLE 1 Mechanisms of peripheral immune system in functional recovery after ischemic stroke.

	Mechanism	Immune cells or factors	Effects on functional recovery
Neuronal	Neurogenesis	Treg cells (Brifault et al., 2015), MMs (Jones et al., 2018), IL-6 (Alia et al., 2017), IL-17A (Miron et al., 2013), B cells (Chen et al., 2022)	Improvement (Treg cells, B cells, IL-6, IL-17A); Exacerbation (MMs)
	Axon sprouting and Extension	Not reported	
	Synaptic plasticity	Not reported	
	Circuit Reformation	Not reported	
Non-neuronal	Angiogenesis	Neutrophil (Otxoa-de-Amezaga et al., 2019), MMs (Gendron et al., 2002; Chamorro et al., 2012)	Improvement (Neutrophils, MMs)
	Astrogliosis	Treg cells (Qiu et al., 2021)	Improvement (Treg cells)
	Oligodendrogenesis	Treg cells (Martinez and Gordon, 2014), IL-4 (Laterza et al., 2017)	Improvement (Treg cells)
	M1/M2 polarization	IL-4 (Ma et al., 2017), Treg cells (Martinez and Gordon, 2014), MMs (Jin et al., 2006; Lei et al., 2012; Roy Choudhury et al., 2014; Kanazawa et al., 2019; Hatakeyama et al., 2020; Zhu et al., 2021)	Improvement (IL-4, Treg cells, MMs)
	Phagocytosis	MMs (Iwai et al., 2010; Zhang et al., 2010, 2013; Chu et al., 2014; Choudhury and Ding, 2016; Sims and Yew, 2017)	Improvement (MMs)

MMs, myeloid and macrophages; Treg cell, Regulatory T cells; IL-4, interleukin 4; IL-6, interleukin 6; IL-17A, interleukin 17A.

Angiogenesis is thought to contribute to functional recovery in two ways. First, new blood vessels that are formed after ischemia enhance neurogenesis by facilitating the migration of neural stem/progenitor cells (NSCs/NPCs) toward the infarct region by supplying nutrients, oxygen and soluble factors, promoting the proliferation and differentiation of NSCs/NPCs *via* the expression of extracellular signals and supplying oxygen and growth factors (Grade et al., 2013; Ruan et al., 2015;

Lange et al., 2016; Kanazawa et al., 2019). Second, postischemic angiogenesis contributes to axonal outgrowth by vascular endothelial growth factors (VEGFs) and laminin/β1-integrin signaling (Jin et al., 2006; Lei et al., 2012; Hatakeyama et al., 2020). After ischemic injury, some activated astrocytes can transform into reactive astrocytes, which causes astrogliosis or forms glial scars. Although some studies have shown that reactive astrogliosis with compact glial scar formation may impede axonal regeneration and hinder functional recovery process (Zhang et al., 2010; Roy Choudhury et al., 2014), other studies have also demonstrated that reactive astrogliosis can be neuroprotective by generating and releasing factors or proteins such as glial-derived neurotrophic factor (GDNF), VEGF and heterodimeric glycoprotein, clusterin 1 (Choudhury and Ding, 2016; Sims and Yew, 2017). Stroke acutely induces mature oligodendrocyte damage, leading to loss of myelin. During the recovery phase of ischemic stroke, there is a significant increase in the generation of OPCs, and some of them become mature myelinating oligodendrocytes, which are essential for white matter repair and long-term functional recovery after ischemic stroke (Iwai et al., 2010; Zhang et al., 2013). The role of inflammatory phenotypes and phagocytic capacity of innate immune cells in functional recovery are complex and discussed in detail in the peripheral immune cell and functional recovery sections.

Effects and mechanisms of peripheral immune cells in functional recovery after ischemic stroke

Immediately following ischemic stroke, brain-resident immune cells such as microglia and astrocytes are activated to respond to ischemia injury. Subsequently, peripheral immune cells are activated and recruited to the brain to assist in the immune response (Chu et al., 2014; Jones et al., 2018). In the following days, peripheral immunodepression can occur, with a subsequent increased risk for systemic infections, especially in patients with large strokes (Gendron et al., 2002). The extent of these local and peripheral immune responses to stroke is variable, and this plays an important role in determining patient outcomes and overall functional recovery in the acute and chronic phases after stroke (Chamorro et al., 2012; Hu et al., 2015). In the following part, we summarized the roles of peripheral immune cells in two perspectives: (1) the roles of main immune cells on functional recovery (see section "Peripheral immune cells and functional recovery"); (2) roles of interactions and communications between peripheral immune cells and brain resident cells on functional recovery (see section "Roles of interactions and communications between peripheral immune cells and brain resident cells in functional recovery").

Peripheral immune cells and functional recovery

Innate immune cells

Neutrophils

Neutrophils are traditionally recognized as the first line of innate immune defense against pathogens (Amulic et al., 2012). Similarly, neutrophils are the first responders to infiltrate the brain after ischemic injury as they were observed to attach the brain endothelial cells within a few minutes and peak at 1–3 days (Perez-de-Puig et al., 2015; Ma et al., 2021). After activation, neutrophils produce cytokines to recruit other immune cells, engulf microbes *via* receptor-mediated phagocytosis, and further release granular antimicrobial molecules as well as the formation of neutrophil extracellular traps (NETs) (Amulic et al., 2012). Consistent with their infiltration time, neutrophils mainly function in the acute injury events, such as regulation of BBB integrity and inflammation-mediated brain infarction (Jickling et al., 2015; Cai et al., 2020; Ma et al., 2021).

Recently, one study showed that neutrophils accumulate in the peri-infarct area during all stages of ischemic stroke, and depletion of neutrophils reduces the breakdown of BBB and enhances neovascularization at Day 14 (Kang et al., 2020). Mechanistically, NETs formation promotes subsequent activation of STING-dependent type I IFN production, which potentially induces vascular remodeling to enhance functional recovery (Kang et al., 2020). Notably, a unique immature neutrophil subset, that secretes growth factors to promote axon regeneration in the optic nerve and spinal cord has been identified in a recent report (Sas et al., 2020). Whether this type of neutrophils also enhance axon sprouting in ischemic stroke is unknown.

Similar to monocytes and macrophages (MMs), neutrophils can also be derived into proinflammatory N1 and anti-inflammatory N2 subtypes; the N1 type is generally considered neurotoxic and the N2 type is neuroprotective during the acute injury phase of ischemic stroke (Cuartero et al., 2013; Jickling et al., 2015; Wanrooy et al., 2021). Whether type N2 neutrophil-induced resolution of neuroinflammation facilitates functional recovery remains unknown. In addition, studies have shown that microglia mediate phagocytosis of neutrophils, which may help to restore the homeostasis of the brain and retain neuronal function and survivability after stroke (Neumann et al., 2008; Otxoa-de-Amezaga et al., 2019) (**Figure 2**). The role of different neutrophil subsets in other points of neuroplasticity remains unclear.

Monocytes and macrophages

Monocytes and macrophages are mononuclear phagocytes and are derived from macrophage/dendritic cell progenitors in the bone marrow (BM). At least two subtypes of monocytes have been reported in mice: Ly6C^{hi} classical inflammatory monocytes and Ly6C^{low} non-classical patrolling monocytes.

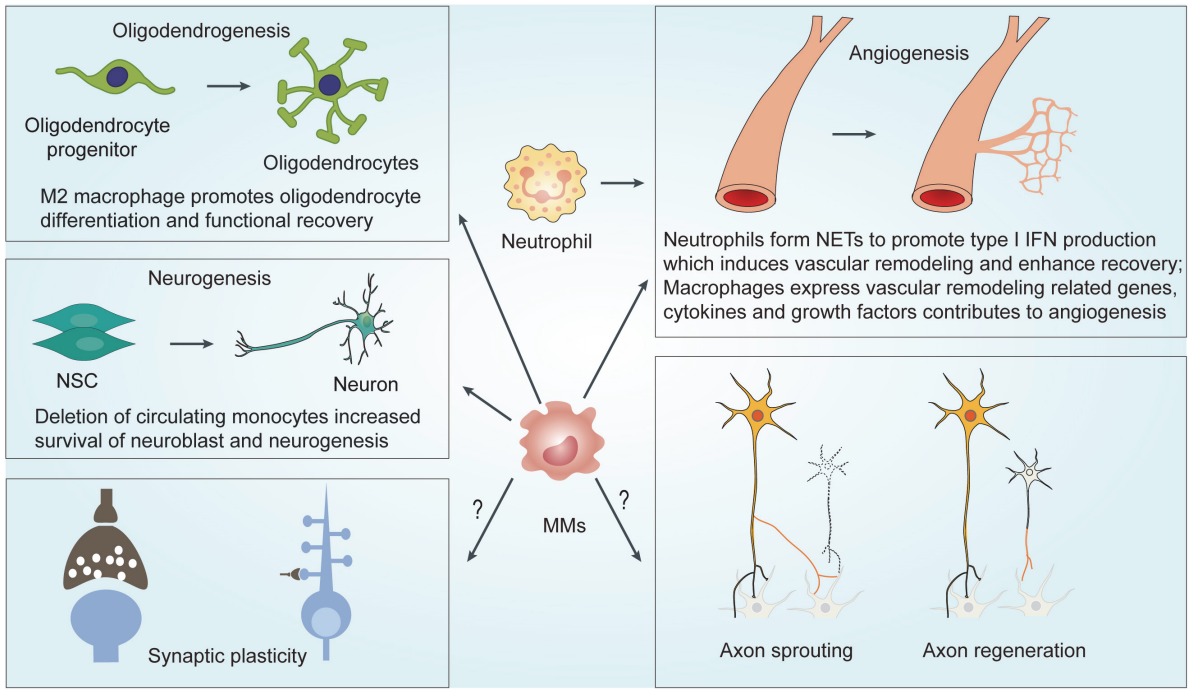

FIGURE 2
Mechanisms underlying MMs and neutrophils-mediated effects on functional recovery after ischemic stroke. MMs regulates functional recovery by modulating neurogenesis, angiogenesis and oligodendrogenesis. NETs formation of neutrophils induces vascular remodeling and angiogenesis to enhance functional recovery. MMs, Monocytes and macrophage; NSC, neural stem cell; NET, neutrophil extracellular traps; IFN, interferons.

Ly6C^{low} monocytes are derived from Ly6C^{hi} monocytes in the blood or common monocyte progenitor (cMoP) in the BM (Ginhoux and Jung, 2014). During disease progression, they can exit to the circulatory system in a C-C chemokine receptor 2 (CCR2)-dependent manner and enter tissues to give rise to tissue macrophages referred to as monocyte-derived macrophages (MDMs), which express high levels of CD68 (Auffray et al., 2009; Ginhoux and Jung, 2014; Li and Barres, 2018; Han et al., 2020).

Monocyte and macrophage responses and functional recovery after ischemic stroke

(1) Neuroinflammation and functional recovery

Previous studies showed that the number of monocytes peaks at Day 3 after ischemic stroke, and they differentiate into MDMs (Wattananit et al., 2016; Fang et al., 2018). During ischemic stroke, dying/dead neurons release DAMPs, such as ATP, HMGB1, damaged DNA and peroxiredoxin family proteins, which can be recognized by pattern recognition receptors (PRRs), including Toll-like receptor (TLR)-2 and TLR-4, expressed by some innate immune cells, such as MMs, microglia and neutrophils (Shichita et al., 2012).

Many studies showed that activated MMs can polarize into distinct subtypes, including the well-known M1 and M2 subpopulations (**Figure 3A**). The M1 subtype secretes proinflammatory cytokines, such as tumor necrosis factor alpha (TNF-α), interleukin (IL)-1β, IL-12, and IL-6, and can be distinguished by cell surface markers CD16 and CD32. The M2 phenotype produces TGF-β, IL-4, IL-10, and IL-13, and expresses CD206 and Arg1. The activation of MM subpopulations and other innate immune cells leads to neuroinflammation (Hu et al., 2012; Wattananit et al., 2016; Fang et al., 2018), the role of which has been well characterized in the acute phase of ischemic brain injury (Jayaraj et al., 2019; Qiu et al., 2021). During the subsequent 2 weeks, MMs gradually shift from the proinflammatory M1 phenotype to the alternatively activated M2 phenotype, facilitating the resolution of inflammation (Wattananit et al., 2016; Fang et al., 2018). However, such definition may not fully illustrate all different activation scenarios. As many reports proposed that there are some other subtypes between M1 and M2, such as M2a, M2b, and M2c (Martinez and Gordon, 2014). With the development of single-cell sequencing technique, the different phenotypes of MMs subpopulations during different stages of ischemic stroke needs further investigation.

Early studies showed that strategies to switch MMs from the proinflammatory phenotype to the anti-inflammatory phenotype promote long-term functional recovery (Brifault et al., 2015; Zheng et al., 2019; Hou et al., 2021; Liu et al.,

2021). For example, delayed pituitary adenylate cyclase-activating polypeptide delivery after cerebral ischemia enhances functional recovery by inducing the polarization of MMs toward M2 phenotype (Brifault et al., 2015). Poststroke treatment with TGFβ-activated kinase 1 (TAK1)-specific inhibitor 5Z-7-oxozeaenol (OZ) causes a phenotypic shift in microglia/macrophages toward an inflammation-resolving state, which effectively promotes the integrity of both gray matter and white matter and long-term neurological recovery (Jickling et al., 2015). In addition, MMs can also express receptors, such as Mannose receptors and macrophage scavenger receptor-1 Msr1, to facilitate the clearance of DAMPs, and contributes to inflammation resolution and brain repair (Giraldi-Guimaraes et al., 2012; Shichita et al., 2017). Moreover, one study showed that modulation of monocytes by supplementation with ursolic acid prevents monocyte dysfunction in diabetic mice and protects mice against atherosclerosis and loss of renal function (Ullevig et al., 2014). Given that many metabolites are altered after ischemic stroke (Wang X. et al., 2020), whether modulation of metabolic of MMs can alter their cytokine profile and affect functional recovery deserve further investigation. For microglia, the polarization from the M1 to the M2 phenotype promotes functional recovery by facilitating neurovascular remodeling, neurogenesis, white matter integrity, and neuroplasticity (Hu et al., 2015; Lyu et al., 2021). Whether the phenotypic switch from M1 to M2 of MMs also promotes brain repair as microglia do still needs further investigation.

(2) **Phagocytosis and functional recovery**

Phagocytosis of dead/dying neurons or myelin debris is another important response of MMs to modulate brain repair (**Figure 3B**). When ischemic stroke occurs, several substances, including ATPs, sphingosine-1-phosphate, and chemokines, are released by injured neurons that act as "find me" signals, which attract neighboring phagocytes to migrate to the injury site. Phagocytes can sense and recognize specific "eat me" signals, such as phospholipid phosphatidylserine, calreticulin, or the complement components C1q and C3b, which are present on the dead or dying cells *via* specific receptors, including TREM2, lipoprotein receptor-related protein LRP and complement receptor CR3 to mediate phagocytosis (Jia et al., 2021; Chen et al., 2022). On one hand, the phagocytosis of dead neurons or myelin debris can help to prevent the release of cytotoxic intracellular contents, which act as DAMPs to promote inflammation and lead to secondary damage, and on the other hand, the phagocytosis of dead/dying neurons modulates tissue reconstruction and neuronal network reorganization to promote functional recovery (Jia et al., 2021; Lyu et al., 2021).

At present, compared with microglia, whose regulatory mechanisms and cellular pathways of phagocytosis, and their resulting effects in neural regeneration are well studied, the detailed mechanism of action of peripheral MMs is less understood. RNA-seq results showed that a large number of genes related to chemotaxis, the recognition of dead cells, engulfment, and the processing of phagosomes are upregulated in brain-infiltrating macrophages after ischemic stroke, and they promote the phagocytosis of dying neurons, which facilitates inflammation resolution, and finally the recovery of neurological functions (Zhang W. et al., 2019). Factors such as CD36, TREM2, Kv1.3, and STAT6/Arg1 contribute to the MM-mediated phagocytosis of dying neurons and enhance functional recovery (Woo et al., 2016; Cai et al., 2019; Gao et al., 2019; Hu et al., 2021). Moreover, the microvascular pericytes colocalize with macrophages within the infarct area and potentiate the clearance activity of recruited macrophages toward myelin debris, which subsequently stimulates oligodendrogenesis and remyelination after ischemia (Shibahara et al., 2020).

In conclusion, during ischemic stroke, MM-mediated inflammation and phagocytosis are dynamically altered. The inflammatory and phagocytic response of MMs can be different in the acute, subacute, and chronic phase by time, and in the ischemic core or the peri-infarct region by location (Chen et al., 2022). In addition, the M1 and M2 phenotype have different phagocytosis capacities, although they both express phagocytic receptors. The M2 phenotype is more efficient at clearing dead cells than the M1 phenotype (Kapellos et al., 2016). Currently, it remains unknown, how the inflammatory phenotype and phagocytic capacity of MMs are cross-regulated, and even less is known about the detailed molecular mechanisms and their effects on functional recovery after ischemic stroke. Therefore, future studies need to consider the inflammatory phenotype and the phagocytosis of MMs in the context of time and location to optimize treatment for improving functional recovery.

Diverse ways of monocytes and macrophages in regulating functional recovery after ischemic stroke

(1) **Neurogenesis and angiogenesis**

Accumulating evidence suggests that microglia can regulate functional outcomes after ischemic stroke *via* diverse mechanisms including neurogenesis, angiogenesis, oligodendrogenesis, and neuroplasticity (Ma et al., 2017; Jia et al., 2021; Lyu et al., 2021). Similarly, MMs also seem to regulate neurological function from these aspects besides some differences. Depletion of circulating monocytes by using CCR2 antibody MC-21 early after stroke enhances neurogenesis in the subventricular zone (SVZ) as well as migration of neuroblasts toward the damaged striatum (Laterza et al., 2017). Pro-reparative monocytes facilitate angiogenesis and improve behavioral performance after ischemic stroke (Pedragosa et al., 2020). Further transcriptome analysis of infiltrated MMs in a mouse model of permanent focal cerebral ischemia indicated that neurovascular remodeling associated genes, such as Wnt,

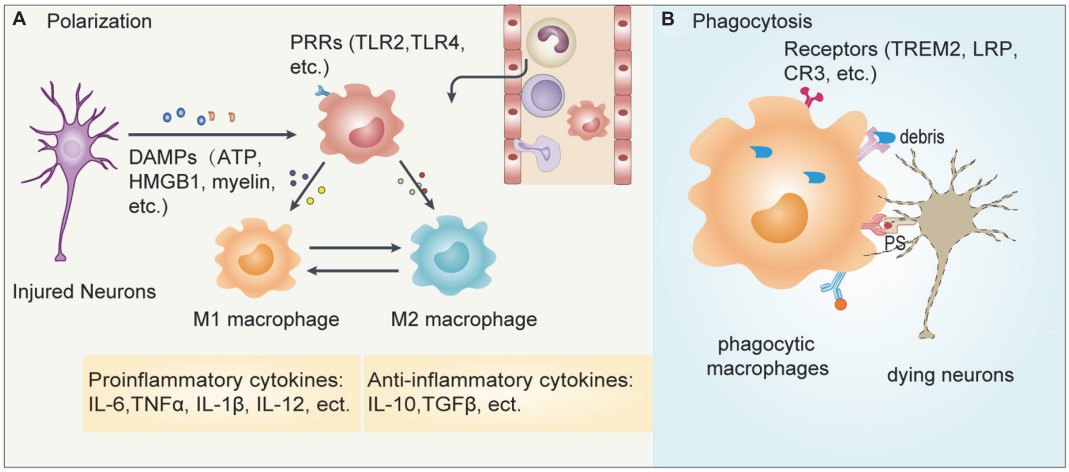

FIGURE 3
Responses of MMs after ischemic stroke. Cerebral ischemia leads to the release of many inflammatory mediators which contributes to the recruitment of peripheral immune cells into the infarct brain. **(A)** The dying/dead neurons release damage-associated molecular patterns (DAMPs) such as ATP, HMGB1, myelin, etc., which can be recognized by pattern recognition receptors (PRRs) such as TLR2 and TLR4 expressed on MMs. The activated macrophages can then polarize into pro-inflammatory M1 or anti-inflammatory M2 cells. **(B)** In addition, macrophages can also recognize phosphatidylserine (PS) expressed on apoptotic neurons or myelin debris released from injured neurons, which is mediated by some specific receptors including TREM2, lipoprotein receptor-related protein LRP and complement receptor CR3, leading to phagocytosis. These two events coordinately regulate the outcome of ischemic stroke.

epidermal growth factor receptor (EGFR), and Notch signaling-related genes involved in angiogenesis and neurogenesis, and cytokines, growth factors that contribute to angiogenesis and neuroplasticity, are overexpressed. Myeloid cell-specific deletion of PPARc reduced poststroke angiogenesis and neurogenesis, and exacerbated neurological deficits (Wang R. et al., 2020). These data suggest that MMs modulate functional recovery *via* neurogenesis and angiogenesis, although the detailed molecular mechanism remains unclear.

(2) **Neuroplasticity**

Neuroplasticity enables the restoration of neural networks and rewiring of functional connections after ischemic stroke (Alia et al., 2017). In recent years, increasing evidence demonstrated the involvement of microglia in the regulation of neuroplasticity (Hu et al., 2015; Ma et al., 2017; Lyu et al., 2021). For MMs, a close anatomical association between activated macrophages and sprouting dopaminergic axons was observed, and macrophages at the wound edges highly express neurotrophic factors that support axon sprouting (Batchelor et al., 2002). Oligodendrogenesis, mediated *via* OPC proliferation and differentiation, promotes remyelination, which influences the integrity of white matter and affects signal transmission efficiency and neuroplasticity after ischemic stroke (Miron et al., 2013). An *in vivo* study showed that depletion of M2 cells including M2 macrophages inhibits oligodendrocyte differentiation (Miron et al., 2013). Consistent with this finding, OPC differentiation can be stimulated by macrophage-conditioned medium with myelin debris *in vitro* (Shibahara et al., 2020). In addition, proinflammatory cytokines, such as IL-6 and IL-1β, play an important role in synaptogenesis and long-term potentiation during development (Katsuki et al., 1990; Faust and Schafer, 2021), although the role of pro-inflammatory or anti-inflammatory cytokines in the modulation of synaptic plasticity and thus potentially brain plasticity is far less clear. Illuminating cellular mechanisms of MMs in the functional recovery of ischemic stroke as well as the detailed molecular mechanisms may lead to novel therapeutic strategies.

Adaptive immune cells

T cells

T cells are key players in cellular adaptive immunity, which functions in a variety of neurological diseases (Prinz and Priller, 2017; Carrasco et al., 2022). In response to the upregulation of adhesion molecules on endothelial cells and the exposed CNS antigens from the injured brain, T cells can be activated and then invade the brain. Three different routes of T lymphocyte migration exist: (1) the BBB pathway, (2) the meninges and choroid plexus (ChP) infiltration routes, and (3) the ChP stroma pathway (Llovera et al., 2017; Benakis et al., 2018). According to the previous reports, the day of T-cells infiltration peak varied, with some studies showing an infiltration peak within 24 h, some around Day 3 to Day 7, and some in the chronic phase, which may result from different stroke models and testing methods (Gronberg et al., 2013; Stubbe et al., 2013; Chu et al., 2014).

The role of different T-cell subsets in ischemic stroke in the acute damage phase remains controversial (Zhang et al., 2021). Blocking $CD8^+$ T-cell expansion and activation through the administration of IL-2 or IL-15 neutralizing antibody, or depletion of $CD8^+$ T cells with anti-CD8α antibody could significantly reduce brain infarct volume and attenuate the associated behavioral deficits in two ischemia models that rely on the production of perforin (Mracsko et al., 2014; Lee et al., 2018; Zhou et al., 2019). The mode of $CD4^+$ T-cell differentiation in response to brain injury ultimately determines stroke outcome. IFN-γ released from Th1 cells appears to either worsen outcomes (Lambertsen et al., 2004; Yilmaz et al., 2006) or have an effect on brain infarct volume (Shichita et al., 2009). Loss of IL-4 or neutralization of IL-4, the main cytokines released from Th2 cells, exert a neuroprotective effect (Korhonen et al., 2015; Xiong et al., 2015; Zhang et al., 2018). Interestingly, the infiltrating IL-17 producing cells in the brain are not $CD4^+$ Th cells, but γδ T lymphocytes (Swardfager et al., 2013). The balance in the peripheral Treg/Th17 cells ratio is altered after stroke which in turn modifies stroke pathophysiology. For example, conditional knockout of ACC1 (acetyl coenzyme A carboxylase 1), a key enzyme involved in *de novo* fatty acid synthesis, profoundly alleviates ischemic brain injury by preserving the balance of Treg/Th17 cells (Wang et al., 2019), indicating the involvement of cell metabolism in stroke pathogenesis. Inconsistent with the long existence of T cells in the brain after ischemic stroke, the role of different T-cell subsets, especially Treg cells in the chronic phase of functional recovery is being exposed.

Treg cells are essential for maintaining immune homeostasis by suppressing conventional T cell activation and function (Zhu et al., 2010). Accumulating evidence indicates that Treg cells migrate into the brain in the chronic phase of ischemic stroke and last for several months, during which Treg cells exhibit multifaceted roles to promote functional recovery (Wang et al., 2015; Ito et al., 2019; Shi L. et al., 2021). First, Treg cells release AREG to suppress astrogliosis and increase brain recovery (Ito et al., 2019). Second, Treg cell-derived osteopontin can act through integrin receptors on microglia to enhance microglial reparative activity, consequently facilitating oligodendrocyte regeneration and white matter integrity (Shi L. et al., 2021). Third, NSC proliferation in the SVZ of normal and ischemic brain can also be enhanced by activated Treg cells *via* IL-10 (Wang et al., 2015) (**Figure 4**). The role of Treg cells on neuroplasticity especially axon sprouting and synaptic function, and other T cell subsets in the functional recovery remain to be established.

Similar to $CD4^+$ T cells, $CD8^+$ T cells also persist in the injured brain for weeks. One study showed that mice with higher ipsilesional $CD8^+$ T cells at Day 30 exhibited worse functional recovery. The Depletion of $CD8^+$ T cells beginning 10 days post-tMCAO improved motor recovery (Selvaraj et al., 2021). Notably, one recent report discovered a new CD8+ T regulatory-like cells ($CD8^+CD122^+CD49d^{lo}$), which could reprogram to upregulate leukemia inhibitory factor (LIF) receptor, epidermal growth factor–like transforming growth factor (ETGF), and interleukin 10 (IL-10) to exert neuroprotection and promoted long-term neurological recovery (Cai et al., 2022). In contrast, traumatic brain injury activates $CD8^+$ T cells, which causes long-term neurological impairment in mice (Daglas et al., 2019). The role of $CD8^+$ T cells in neuroplasticity is worth investigation.

B cells

B cells were originally identified through studies searching for the cellular source of antibodies. As the key player in humoral immunity, B cells contribute to immunity through antigen presentation, antibody production and cytokine secretion (Jain and Yong, 2021). The role of B cells in the acute phase of ischemic stroke is inconclusive. Some studies found no effect on infarct and stroke outcome (Kleinschnitz et al., 2010; Schuhmann et al., 2017). However, others observed a beneficial role of B cells (Ren et al., 2011; Offner and Hurn, 2012).

Given that the adaptive immune response specific for CNS antigens develops later than the innate immune response, the role of B cells in the subacute and chronic phase of ischemic stroke attracts has attracted the attention of some researchers'. Ischemic injury induces significant bilateral B-cell diapedesis into remote brain regions to regulate motor and cognitive functions by supporting neuronal viability and dendritic arborization (Ortega et al., 2020). In a distal middle cerebral artery occlusion (dMCAO) model, B cells were found to infiltrate the infarct region and secrete IgA and IgG in the chronic phase after stroke, which may directly impact cognition after stroke (Doyle et al., 2015; **Figure 4**). Notably, multiple sclerosis studies have raised the notion that B cells contribute to CNS pathology independent of antibody production (Li et al., 2018). Consistent with this finding, B cells have been reported to produce several neurotrophins including brain-derived neurotrophic factor (BDNF) and nerve growth factor (NGF) (Edling et al., 2004; Fauchais et al., 2008). Whether B cells regulates other events in neurological recovery in an antibody-production-independent manner is a field worth future study.

Natural killer cells

Natural killer (NK) cells are a type of cytotoxic lymphocyte that play an important role in innate immunity (Abel et al., 2018; Chen et al., 2019). NK cells were reported to accumulate in the brain during the acute injury phase. Kinetic experiments showed that NK cells accumulated as early as 3 hours, peaking at Day 3 after tMCAO (Gan et al., 2014). In human ischemic brain, the infiltrations of NK cells peaked at Days 2–5 (Zhang et al., 2014). Consistent with their infiltration time, NK cells contribute to brain injury in various ways: they induce the necrosis of neural cells *via* IFN-γ (Chen et al., 2019); damage the BBB in response

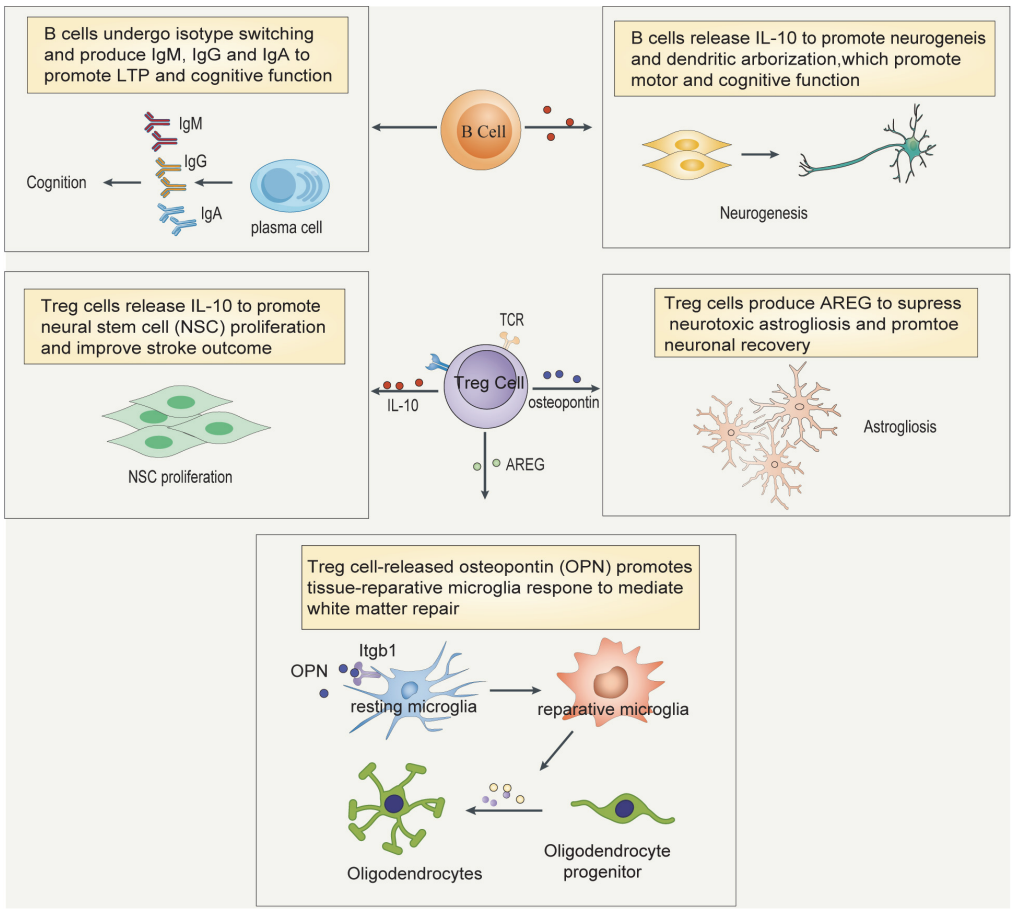

FIGURE 4
Mechanisms underlying Treg cell and B cell-mediated impacts on functional recovery after ischemic stroke. Treg cells promotes functional recovery after ischemic stroke by the following means: Treg cells release IL-10 to directly promote neural stem cell proliferation or restrict proinflammatory cytokine production; Treg cells release AREG to inhibit astrogliosis and facilitate neuronal recovery; Treg cell-derived osteopontin act through integrin receptors on microglia to enhance microglial reparative activity, as both anti-inflammatory cytokines and genes encoding proteins involved in brain repair are upregulated, consequently facilitating oligodendrocyte regeneration and white matter integrity. B cells release IL-10 to promote neurogenesis and dendritic arborization, which promote motor and cognitive function, and in addition, B cells also undergo isotype switching and produce IgM, IgG and IgA to promote cognitive function. TCR, T cell receptor; ILRs, interleukin receptors; AREG, amphiregulin; NSC, neural stem cell.

to interferon-inducible protein-10 (IP-10) (Zhang et al., 2014); mediate cytolytic killing of ischemic neurons *via* perforin (Gan et al., 2014); act in cooperation with monocytes and platelets to propagate thrombosis and activate the complement system (Eltzschig and Eckle, 2011). At present, the function of NK cells on neurofunctional recovery is poorly understood.

Stroke-induced systemic immunosuppression was first described in the 1970s and is characterized by severe lymphopenia in the peripheral blood, thymus, and spleen, which affects the mortality and functional recovery of patients with ischemic stroke (Offner et al., 2006; Klehmet et al., 2009; Wong, 2019). Currently, stroke-induced immunosuppression is considered both detrimental and beneficial to the human body. Stroke-induced immunosuppression is deleterious, as it increases the incidence of poststroke infections, especially pneumonia and urinary tract infection (Iadecola and Anrather, 2011; Chamorro et al., 2012). Several studies have provided a mechanistic basis for this phenomenon and demonstrated that T lymphocytes and iNKT cells play critical roles in regulating poststroke induced immunosuppression as well as subsequent infections (Prass et al., 2003; Wong et al., 2011; Roth et al., 2021). The spleen is reported to exacerbate brain injury and contributes to long-term neurodegenerations (Ajmo et al., 2008; Pennypacker and Offner, 2015). After brain ischemia, spleen atrophy and peripheral NK Cell cells were observed. NK cells display remarkably distinct temporal and transcriptome profiles in the brain and spleen. Catecholaminergic and hypothalamic-pituitary-adrenal (HPA) axis innervations suppress peripheral NK cells after ischemic stroke. Correspondingly, modulation of neurogenic

pathways preserves NK cell function and improves host immune defense against poststroke infections (Liu et al., 2017).

Roles of interactions and communications between peripheral immune cells and brain resident cells in functional recovery

Accumulating evidence shows that the infiltrated peripheral immune cells interact with brain resident cells in complex ways, that may be either detrimental or supportive for brain injury and repair. After ischemic stroke, the bidirectional neuroimmune interactions and communications of infiltrated peripheral immune cells and brain resident cell allow these cell populations to influence each other in multiple ways, including releasing factors to affect each other and direct cell–cell interactions (Kamel and Iadecola, 2012; Alia et al., 2021; Muhammad et al., 2021).

Communications-mediated by cytokines or other factors and functional recovery

After brain injury, various DAMPs, such as ATP, HMGB1, damaged DNA and peroxiredoxin family proteins and brain-derived antigens, can be released after ischemic insult into the periphery, which activates the peripheral immune cells and leads to further infiltration into the brain owing to a compromised BBB (Javidi and Magnus, 2019; Stanzione et al., 2022). These infiltrated activated immune cells or autoreactive adaptive immune cells can then polarize or differentiate into different populations, such as M1/M2 subtypes and different Th subsets, which further interact with other brain resident cells to modulate brain repair. For example, brain infiltrating Treg cells can on one hand release AREG to suppress astrogliosis and increase brain recovery (Ito et al., 2019), and, on the other hand, produce osteopontin to activate integrin receptors on microglia and enhance microglial reparative activity to facilitate oligodendrocyte regeneration and white matter integrity (Shi L. et al., 2021). In addition, during autoimmune disease or tumor progression, the interaction between macrophage and T cells was observed and their interaction affect the progression of the disease (Han et al., 2012; Cess and Finley, 2020). On one hand, cytokines or chemokines produced by T cells can lead to recruitment and activation of macrophages, which further produce additional inflammatory mediators and become effector cells in pathogenesis (Yoon and Jun, 1999); On the other hand, macrophages can present antigen to T cells, which induce their activation and differentiation to affect disease progression (Underhill et al., 1999). The role of macrophage and T cell interaction in the functional recovery of ischemic stroke is still unclear.

After activation, both adaptive and innate immune cells secrete cytokines, which play multiple and vital roles in neurological disease progression (Kerschensteiner et al., 2010; Cui and Wan, 2019). Some studies have supplemented certain cytokines during ischemic stroke to study their direct effects (**Table 1**).

Interleukin-4 (IL-4) is an anti-inflammatory cytokine produced by a variety of immune cells, including Th2 cells, mast cells, eosinophils and basophils (Gadani et al., 2012), and can drive macrophages into M2 phenotype in the presence of IL-13 (Murray, 2017). Loss of IL-4 promotes the M1 phenotype in microglia/macrophages after ischemic stroke and exacerbates long-term sensorimotor dysfunction as well as cognitive deficits after ischemia, while infusion of IL-4 into the cerebroventricular after ischemic stroke improves neurological functions (Liu et al., 2016). In addition to promoting M2 phenotype polarization, intranasal delivery of IL-4 nanoparticles poststroke also improves white matter integrity by acting directly on OPCs to enhance oligodendrocyte differentiation mediated by the PPARγ axis, which reduces long-term sensorimotor and cognitive deficits (Zhang Q. et al., 2019).

Tumor necrosis factor alpha and IL-33 have also been found to confer a protective effect on regulation of white matter integrity. TNFα directly protected OPCs and oligodendrocytes against oxygen and glucose deprivation (OGD)-induced cell death, but did not affluence on OPC differentiation, which is mediated by the EGFR and the downstream transcription factor STAT3 on oligodendrocyte lineage cells (Dai et al., 2020). IL-33 also protected oligodendrocytes and OPCs against ischemic injury but in a microglia/macrophage-dependent manner by promoting a beneficial response *via* the ST2-ATAT6 axis (Xie et al., 2021).

In contrast to IL-4, IL-6 is a proinflammatory cytokine secreted by some innate immune cells. Mice treated with recombinant IL-6 exhibited significantly increased proliferation and neural differentiation of NPCs in the ipsilateral SVZ, as well as functional recovery. However, IL-6 neutralizing antibody confer the opposite effects (Meng et al., 2015). Injection of IL-6 in pregnant mice or developing embryos increases glutamatergic synapse density and overall hyperconnectivity in the offspring (Mirabella et al., 2021); thus future studies should clarify the role of IL-6 in poststroke synapse plasticity.

Leukemia inhibitory factor is a multi-functional cytokine belongs to the IL-6 cytokine family. LIF modulates post-stroke responses and reduces infarct volume (Davis et al., 2017; Davis and Pennypacker, 2018). In addition, LIF also preserves white matter injury and improves functional outcomes when administered to rats subjected to pMCAO. Mechanistically, LIF reduces superoxide dismutase activity through increasing peroxiredoxin 4 (Prdx4) transcripts *via* the Akt signaling (Rowe et al., 2014). Likewise, IL-17A, another proinflammatory cytokine, also enhances the survival and neuronal differentiation

of NPCs and subsequent synaptogenesis, which modestly ameliorates functional deficits after stroke (Lin et al., 2016). The role of other cytokines and chemokines in chronic functional recovery still needs further investigation.

Besides the influence of cytokines-released from peripheral innate and adaptive immune cells on brain resident cells, brain resident cells can also regulate peripheral immune cell function through neuroinflammation. After ischemia-induced cell death, activation of microglia and astrocytes were observed and neuroinflammation is initiated (Cekanaviciute and Buckwalter, 2016; Xu et al., 2020). The released cytokines and chemokines can further mediate peripheral immune cell infiltration and modulate their differentiation, which further affects functional recovery (da Fonseca et al., 2014; Dudvarski Stankovic et al., 2016).

Direct cell–cell interactions and functional recovery

Peripheral immune cells and brain-resident cells can directly interact with each other and affect neurological function recovery. For example, infiltrating peripheral immune cells are able to interact with brain resident cells, and resolve inflammation and promote functional recovery *via* phagocytosis. *In vitro* studies showed that in organotypic brain slices, externally invading polymorphonuclear neutrophils massively enhanced ischemic neurotoxicity, and microglia exerted protection through the rapid engulfment of apoptotic and motile neutrophils within brain slices. Consistently, in an *in vivo* ischemic stroke model, neutrophils reach the perivascular spaces of brain vessels, and reactive microglia can interact and engulf neutrophils at the periphery of the ischemic lesion to help restore the homeostasis of the brain (Neumann et al., 2008; Otxoa-de-Amezaga et al., 2019). Moreover, pericytes can colocalize with macrophages within the infarct area and potentiate the clearance of debris by recruited macrophages, which subsequently stimulates remyelination after ischemic stroke (Shibahara et al., 2020).

These important and intricate communications and interactions indicate the complexity of therapeutic strategies for clinical application. For example, in the acute phase, some immune cells can produce cytokines and growth factors, which serve as important resources for neuronal sprouting, neurogenesis, angiogenesis, and matrix reorganization (Alia et al., 2021; Varadarajan et al., 2022). If the production of these cytokines or growth factors is blocked, acute brain injury may be reduced, but brain repair may be hindered in the long term hinder. Therefore, attempts to treat stroke patients by modifying these interactions or communications must be made with caution. Future studies should test the proper concentration of the inhibitors or neutralization antibodies, the time to administer these blockers, and specific type of cytokines or growth factors in order to drive the development of immunotherapies of ischemic stroke.

Discussion

In summary, this review provides a systematic summary of the important role of the innate and adaptive immune systems in regulating brain repair after ischemic stroke and raises some currently unresolved questions. Monocytes and macrophages actively participate in neurogenesis, angiogenesis, and oligodendrogenesis after the acute phase of cerebral ischemia, during which their polarization and phagocytotic function are engaged. Neutrophils can impair revascularization and vascular remodeling by releasing extracellular traps. In addition, evidence for the critical role of Treg cells in facilitating functional recovery has accumulated. B cells may regulate neurological function in an antibody-dependent manner. More importantly, these cells can interact and communicate with each other and the brain resident cells in a very complex way to influence ischemic injury severity and functional recovery. Thus, future clinical trials must consider these stage-specific effects and the complex neuroimmune interactions.

From the reviews above, we could easily realize that there is still a long way to go to understand the regulation of immune cells in neurological recovery in depth, as so many questions remain unknown. For example: (1) What are the effects of the innate and adaptive immune cells on neuroplasticity after ischemic stroke, especially axon sprouting and synaptic plasticity? (2) What are the impacts of the adaptive immune cells on neuropsychiatric consequences of stroke? (3) Is the response of the infiltrating immune cells distinct in different regions of the brain after ischemic stroke? The development of single-cell sequencing technologies may help resolve this question. (4) How the immune cells, especially macrophages, balance their survival, inflammation and phagocytotic function during ischemic stroke? Currently, the progress of metabolomics and chromatin-related technologies such as ATAC-seq, chromatin conformation capture 3C, Hi-C may bring some new prospective. (5) In the microscale or molecular level, how the immune cells interact with neurons or other brain-resident cells, to transmit signals and affect functional prognosis? With the improvement of the resolution of microscopy, to see the interaction between cells at the molecular level may not be impossible. Resolving these questions would move forward the immunity-based translational research focusing on recovery-specific therapy.

Author contributions

ZZ was involved in the writing, reading literature, design of the figures. ML and XZ contributed to the literature search and editing of the manuscript. YC was involved in the overall

supervision of the review and editing of the manuscript. All authors approved the submitted version.

Funding

This work was supported by the National Natural Science Foundation of China (31900634) to YC, National Natural Science Foundation of China (82101380) and Natural Science Foundation of Shandong Province (ZR202102280316) to ZZ.

Acknowledgments

We are grateful for support from the Institute of Neuroregeneration and Neurorehabilitation of Qingdao University.

Conflict of interest

The authors declare that the research was conducted in the absence of any commercial or financial relationships that could be construed as a potential conflict of interest.

Publisher's note

All claims expressed in this article are solely those of the authors and do not necessarily represent those of their affiliated organizations, or those of the publisher, the editors and the reviewers. Any product that may be evaluated in this article, or claim that may be made by its manufacturer, is not guaranteed or endorsed by the publisher.

References

Abel, A. M., Yang, C., Thakar, M. S., and Malarkannan, S. (2018). Natural killer cells: Development, maturation, and clinical utilization. *Front. Immunol.* 9:1869. doi: 10.3389/fimmu.2018.01869

Ajmo, C. T. Jr., Vernon, D. O., Collier, L., Hall, A. A., Garbuzova-Davis, S., Willing, A., et al. (2008). The spleen contributes to stroke-induced neurodegeneration. *J. Neurosci. Res.* 86, 2227–2234. doi: 10.1002/jnr.21661

Alia, C., Cangi, D., Massa, V., Salluzzo, M., Vignozzi, L., Caleo, M., et al. (2021). Cell-to-cell interactions mediating functional recovery after stroke. *Cells* 10:3050. doi: 10.3390/cells10113050

Alia, C., Spalletti, C., Lai, S., Panarese, A., Lamola, G., Bertolucci, F., et al. (2017). Neuroplastic changes following brain ischemia and their contribution to stroke recovery: Novel approaches in neurorehabilitation. *Front. Cell. Neurosci.* 11:76. doi: 10.3389/fncel.2017.00076

Amulic, B., Cazalet, C., Hayes, G. L., Metzler, K. D., and Zychlinsky, A. (2012). Neutrophil function: From mechanisms to disease. *Annu. Rev. Immunol.* 30, 459–489. doi: 10.1146/annurev-immunol-020711-074942

Auffray, C., Sieweke, M. H., and Geissmann, F. (2009). Blood monocytes: Development, heterogeneity, and relationship with dendritic cells. *Annu. Rev. Immunol.* 27, 669–692. doi: 10.1146/annurev.immunol.021908.132557

Badimon, A., Strasburger, H. J., Ayata, P., Chen, X., Nair, A., Ikegami, A., et al. (2020). Negative feedback control of neuronal activity by microglia. *Nature* 586, 417–423. doi: 10.1038/s41586-020-2777-8

Barker, R. A., Gotz, M., and Parmar, M. (2018). New approaches for brain repair-from rescue to reprogramming. *Nature* 557, 329–334. doi: 10.1038/s41586-018-0087-1

Batchelor, P. E., Porritt, M. J., Martinello, P., Parish, C. L., Liberatore, G. T., Donnan, G. A., et al. (2002). Macrophages and microglia produce local trophic gradients that stimulate xonal sprouting toward but not beyond the wound edge. *Mol. Cell. Neurosci.* 21, 436–453. doi: 10.1006/mcne.2002.1185

Benakis, C., Llovera, G., and Liesz, A. (2018). The meningeal and choroidal infiltration routes for leukocytes in stroke. *Ther. Adv. Neurol. Disord.* 11:1756286418783708. doi: 10.1177/1756286418783708

Brifault, C., Gras, M., Liot, D., May, V., Vaudry, D., and Wurtz, O. (2015). Delayed pituitary adenylate cyclase-activating polypeptide delivery after brain stroke improves functional recovery by inducing m2 microglia/macrophage polarization. *Stroke* 46, 520–528. doi: 10.1161/STROKEAHA.114.006864

Cai, W., Dai, X., Chen, J., Zhao, J., Xu, M., Zhang, L., et al. (2019). STAT6/Arg1 promotes microglia/macrophage efferocytosis and inflammation resolution in stroke mice. *JCI Insight* 4:e131355. doi: 10.1172/jci.insight.131355

Cai, W., Liu, S., Hu, M., Huang, F., Zhu, Q., Qiu, W., et al. (2020). Functional dynamics of neutrophils after ischemic stroke. *Transl. Stroke Res.* 11, 108–121. doi: 10.1007/s12975-019-00694-y

Cai, W., Shi, L., Zhao, J., Xu, F., Dufort, C., Ye, Q., et al. (2022). Neuroprotection against ischemic stroke requires a specific class of early responder T cells in mice. *J. Clin. Invest.* 132:e157678. doi: 10.1172/JCI157678

Carmichael, S. T. (2006). Cellular and molecular mechanisms of neural repair after stroke: Making waves. *Ann. Neurol.* 59, 735–742. doi: 10.1002/ana.20845

Carmichael, S. T., Kathirvelu, B., Schweppe, C. A., and Nie, E. H. (2017). Molecular, cellular and functional events in axonal sprouting after stroke. *Exp. Neurol.* 287, 384–394. doi: 10.1016/j.expneurol.2016.02.007

Carrasco, E., Gomez de Las Heras, M. M., Gabande-Rodriguez, E., Desdin-Mico, G., Aranda, J. F., and Mittelbrunn, M. (2022). The role of T cells in age-related diseases. *Nat. Rev. Immunol.* 22, 97–111. doi: 10.1038/s41577-021-00557-4

Cekanaviciute, E., and Buckwalter, M. S. (2016). Astrocytes: Integrative regulators of neuroinflammation in stroke and other neurological diseases. *Neurotherapeutics* 13, 685–701. doi: 10.1007/s13311-016-0477-8

Cess, C. G., and Finley, S. D. (2020). Multi-scale modeling of macrophage-T cell interactions within the tumor microenvironment. *PLoS Comput. Biol.* 16:e1008519. doi: 10.1371/journal.pcbi.1008519

Chamorro, A., Meisel, A., Planas, A. M., Urra, X., van de Beek, D., and Veltkamp, R. (2012). The immunology of acute stroke. *Nat. Rev. Neurol.* 8, 401–410. doi: 10.1038/nrneurol.2012.98

Chen, C., Ai, Q. D., Chu, S. F., Zhang, Z., and Chen, N. H. (2019). NK cells in cerebral ischemia. *Biomed. Pharmacother.* 109, 547–554. doi: 10.1016/j.biopha.2018.10.103

Chen, W., Zhang, Y., Zhai, X., Xie, L., Guo, Y., Chen, C., et al. (2022). Microglial phagocytosis and regulatory mechanisms after stroke. *J. Cereb. Blood Flow Metab.* 42, 1579–1596. doi: 10.1177/0271678X221098841

Choudhury, G. R., and Ding, S. (2016). Reactive astrocytes and therapeutic potential in focal ischemic stroke. *Neurobiol. Dis.* 85, 234–244. doi: 10.1016/j.nbd.2015.05.003

Chu, H. X., Kim, H. A., Lee, S., Moore, J. P., Chan, C. T., Vinh, A., et al. (2014). Immune cell infiltration in malignant middle cerebral artery infarction: Comparison with transient cerebral ischemia. *J. Cereb. Blood Flow Metab.* 34, 450–459. doi: 10.1038/jcbfm.2013.217

Colonna, M., and Butovsky, O. (2017). Microglia function in the central nervous system during health and neurodegeneration. *Annu. Rev. Immunol.* 35, 441–468. doi: 10.1146/annurev-immunol-051116-052358

Cramer, S. C., and Riley, J. D. (2008). Neuroplasticity and brain repair after stroke. *Curr. Opin. Neurol.* 21, 76–82. doi: 10.1097/WCO.0b013e3282f36cb6

Cuartero, M. I., Ballesteros, I., Moraga, A., Nombela, F., Vivancos, J., Hamilton, J. A., et al. (2013). N2 neutrophils, novel players in brain inflammation after stroke:

Modulation by the PPARgamma agonist rosiglitazone. *Stroke* 44, 3498–3508. doi: 10.1161/STROKEAHA.113.002470

Cui, Y., and Wan, Q. N. K. T. (2019). Cells in neurological diseases. *Front. Cell. Neurosci.* 13:245. doi: 10.3389/fncel.2019.00245

da Fonseca, A. C., Matias, D., Garcia, C., Amaral, R., Geraldo, L. H., Freitas, C., et al. (2014). The impact of microglial activation on blood-brain barrier in brain diseases. *Front. Cell. Neurosci.* 8:362. doi: 10.3389/fncel.2014.00362

Daglas, M., Draxler, D. F., Ho, H., McCutcheon, F., Galle, A., Au, A. E., et al. (2019). Activated CD8(+) T cells cause long-term neurological impairment after traumatic brain injury in mice. *Cell Rep.* 29:e1176. doi: 10.1016/j.celrep.2019.09.046

Dai, X., Chen, J., Xu, F., Zhao, J., Cai, W., Sun, Z., et al. (2020). TGFalpha preserves oligodendrocyte lineage cells and improves white matter integrity after cerebral ischemia. *J. Cereb. Blood Flow Metab.* 40, 639–655. doi: 10.1177/0271678X19830791

Davis, S. M., and Pennypacker, K. R. (2018). The role of the leukemia inhibitory factor receptor in neuroprotective signaling. *Pharmacol. Ther.* 183, 50–57. doi: 10.1016/j.pharmthera.2017.08.008

Davis, S. M., Collier, L. A., Leonardo, C. C., Seifert, H. A., Ajmo, C. T. Jr., and Pennypacker, K. R. (2017). Leukemia inhibitory factor protects neurons from ischemic damage via upregulation of superoxide dismutase 3. *Mol. Neurobiol.* 54, 608–622. doi: 10.1007/s12035-015-9587-2

Doyle, K. P., Quach, L. N., Sole, M., Axtell, R. C., Nguyen, T. V., Soler-Llavina, G. J., et al. (2015). B-lymphocyte-mediated delayed cognitive impairment following stroke. *J. Neurosci.* 35, 2133–2145. doi: 10.1523/JNEUROSCI.4098-14.2015

Dudvarski Stankovic, N., Teodorczyk, M., Ploen, R., Zipp, F., and Schmidt, M. H. H. (2016). Microglia-blood vessel interactions: A double-edged sword in brain pathologies. *Acta Neuropathol.* 131, 347–363. doi: 10.1007/s00401-015-1524-y

Edling, A. E., Nanavati, T., Johnson, J. M., and Tuohy, V. K. (2004). Human and murine lymphocyte neurotrophin expression is confined to B cells. *J. Neurosci. Res.* 77, 709–717. doi: 10.1002/jnr.20176

Eltzschig, H. K., and Eckle, T. (2011). Ischemia and reperfusion–from mechanism to translation. *Nat. Med.* 17, 1391–1401. doi: 10.1038/nm.2507

Fang, W., Zhai, X., Han, D., Xiong, X., Wang, T., Zeng, X., et al. (2018). CCR2-dependent monocytes/macrophages exacerbate acute brain injury but promote functional recovery after ischemic stroke in mice. *Theranostics* 8, 3530–3543. doi: 10.7150/thno.24475

Fauchais, A. L., Lalloue, F., Lise, M. C., Boumediene, A., Preud'homme, J. L., Vidal, E., et al. (2008). Role of endogenous brain-derived neurotrophic factor and sortilin in B cell survival. *J. Immunol.* 181, 3027–3038. doi: 10.4049/jimmunol.181.5.3027

Faust, T. E., and Schafer, D. P. (2021). IL-6 boosts synaptogenesis STAT! *Immunity* 54, 2444–2446. doi: 10.1016/j.immuni.2021.10.010

Feigin, V. L., Lawes, C. M., Bennett, D. A., Barker-Collo, S. L., and Parag, V. (2009). Worldwide stroke incidence and early case fatality reported in 56 population-based studies: A systematic review. *Lancet Neurol.* 8, 355–369. doi: 10.1016/S1474-4422(09)70025-0

Font, M. A., Arboix, A., and Krupinski, J. (2010). Angiogenesis, neurogenesis and neuroplasticity in ischemic stroke. *Curr. Cardiol. Rev.* 6, 238–244. doi: 10.2174/157340310791658802

Gadani, S. P., Cronk, J. C., Norris, G. T., and Kipnis, J. (2012). IL-4 in the brain: A cytokine to remember. *J. Immunol.* 189, 4213–4219. doi: 10.4049/jimmunol.1202246

Gan, Y., Liu, Q., Wu, W., Yin, J. X., Bai, X. F., Shen, R., et al. (2014). Ischemic neurons recruit natural killer cells that accelerate brain infarction. *Proc. Natl. Acad. Sci. U.S.A.* 111, 2704–2709. doi: 10.1073/pnas.1315943111

Gao, T., Raza, S. A., Ramesha, S., Nwabueze, N. V., Tomkins, A. J., Cheng, L., et al. (2019). Temporal profiling of Kv1.3 channel expression in brain mononuclear phagocytes following ischemic stroke. *J. Neuroinflammation* 16:116. doi: 10.1186/s12974-019-1510-8

Gendron, A., Teitelbaum, J., Cossette, C., Nuara, S., Dumont, M., Geadah, D., et al. (2002). Temporal effects of left versus right middle cerebral artery occlusion on spleen lymphocyte subsets and mitogenic response in Wistar rats. *Brain Res.* 955, 85–97. doi: 10.1016/s0006-8993(02)03368-1

Ginhoux, F., and Jung, S. (2014). Monocytes and macrophages: Developmental pathways and tissue homeostasis. *Nat. Rev. Immunol.* 14, 392–404. doi: 10.1038/nri3671

Giraldi-Guimaraes, A., de Freitas, H. T., Coelho Bde, P., Macedo-Ramos, H., Mendez-Otero, R., Cavalcante, L. A., et al. (2012). Bone marrow mononuclear cells and mannose receptor expression in focal cortical ischemia. *Brain Res.* 1452, 173–184. doi: 10.1016/j.brainres.2012.03.002

Grade, S., Weng, Y. C., Snapyan, M., Kriz, J., Malva, J. O., and Saghatelyan, A. (2013). Brain-derived neurotrophic factor promotes vasculature-associated migration of neuronal precursors toward the ischemic striatum. *PLoS One* 8:e55039. doi: 10.1371/journal.pone.0055039

Gronberg, N. V., Johansen, F. F., Kristiansen, U., and Hasseldam, H. (2013). Leukocyte infiltration in experimental stroke. *J. Neuroinflammation* 10:115. doi: 10.1186/1742-2094-10-115

Han, D., Liu, H., and Gao, Y. (2020). The role of peripheral monocytes and macrophages in ischemic stroke. *Neurol. Sci.* 41, 3589–3607. doi: 10.1007/s10072-020-04777-9

Han, Y. L., Li, Y. L., Jia, L. X., Cheng, J. Z., Qi, Y. F., Zhang, H. J., et al. (2012). Reciprocal interaction between macrophages and T cells stimulates IFN-gamma and MCP-1 production in Ang II-induced cardiac inflammation and fibrosis. *PLoS One* 7:e35506. doi: 10.1371/journal.pone.0035506

Hatakeyama, M., Ninomiya, I., and Kanazawa, M. (2020). Angiogenesis and neuronal remodeling after ischemic stroke. *Neural. Regen. Res.* 15, 16–19. doi: 10.4103/1673-5374.264442

Hou, Y., Yang, D., Wang, X., Wang, H., Zhang, H., Wang, P., et al. (2021). Pseudoginsenoside-F11 promotes functional recovery after transient cerebral ischemia by regulating the microglia/macrophage polarization in rats. *Int. Immunopharmacol.* 99:107896. doi: 10.1016/j.intimp.2021.107896

Hu, M., Lin, Y., Men, X., Wang, S., Sun, X., Zhu, Q., et al. (2021). High-salt diet downregulates TREM2 expression and blunts efferocytosis of macrophages after acute ischemic stroke. *J. Neuroinflammation* 18:90. doi: 10.1186/s12974-021-02144-9

Hu, S., Zheng, J., Du, Z., and Wu, G. (2020). Knock down of lncRNA H19 promotes axon sprouting and functional recovery after cerebral ischemic stroke. *Brain Res.* 1732:146681. doi: 10.1016/j.brainres.2020.146681

Hu, X., Leak, R. K., Shi, Y., Suenaga, J., Gao, Y., Zheng, P., et al. (2015). Microglial and macrophage polarization-new prospects for brain repair. *Nat. Rev. Neurol.* 11, 56–64. doi: 10.1038/nrneurol.2014.207

Hu, X., Li, P., Guo, Y., Wang, H., Leak, R. K., Chen, S., et al. (2012). Microglia/macrophage polarization dynamics reveal novel mechanism of injury expansion after focal cerebral ischemia. *Stroke* 43, 3063–3070. doi: 10.1161/STROKEAHA.112.659656

Iadecola, C., and Anrather, J. (2011). The immunology of stroke: From mechanisms to translation. *Nat. Med.* 17, 796–808. doi: 10.1038/nm.2399

Iadecola, C., Buckwalter, M. S., and Anrather, J. (2020). Immune responses to stroke: Mechanisms, modulation, and therapeutic potential. *J. Clin. Invest.* 130, 2777–2788. doi: 10.1172/JCI135530

Ito, M., Komai, K., Mise-Omata, S., Iizuka-Koga, M., Noguchi, Y., Kondo, T., et al. (2019). Brain regulatory T cells suppress astrogliosis and potentiate neurological recovery. *Nature* 565, 246–250. doi: 10.1038/s41586-018-0824-5

Iwai, M., Stetler, R. A., Xing, J., Hu, X., Gao, Y., Zhang, W., et al. (2010). Enhanced oligodendrogenesis and recovery of neurological function by erythropoietin after neonatal hypoxic/ischemic brain injury. *Stroke* 41, 1032–1037. doi: 10.1161/STROKEAHA.109.570325

Jain, R. W., and Yong, V. W. (2021). B cells in central nervous system disease: Diversity, locations and pathophysiology. *Nat. Rev. Immunol.* 22, 513–524. doi: 10.1038/s41577-021-00652-6

Javidi, E., and Magnus, T. (2019). Autoimmunity after ischemic stroke and brain injury. *Front. Immunol.* 10:686. doi: 10.3389/fimmu.2019.00686

Jayaraj, R. L., Azimullah, S., Beiram, R., Jalal, F. Y., and Rosenberg, G. A. (2019). Neuroinflammation: Friend and foe for ischemic stroke. *J. Neuroinflammation* 16:142. doi: 10.1186/s12974-019-1516-2

Jia, J., Yang, L., Chen, Y., Zheng, L., Chen, Y., Xu, Y., et al. (2021). The role of microglial hagocytosis in ischemic stroke. *Front. Immunol.* 12:790201. doi: 10.3389/fimmu.2021.790201

Jian, Z., Liu, R., Zhu, X., Smerin, D., Zhong, Y., Gu, L., et al. (2019). The involvement and therapy target of immune cells after ischemic stroke. *Front. Immunol.* 10:2167. doi: 10.3389/fimmu.2019.02167

Jiang, X., Andjelkovic, A. V., Zhu, L., Yang, T., Bennett, M. V. L., Chen, J., et al. (2018). Blood-brain barrier dysfunction and recovery after ischemic stroke. *Prog. Neurobiol.* 16, 144–171. doi: 10.1016/j.pneurobio.2017.10.001

Jickling, G. C., Liu, D., Ander, B. P., Stamova, B., Zhan, X., and Sharp, F. R. (2015). Targeting neutrophils in ischemic stroke: Translational insights from experimental studies. *J. Cereb. Blood Flow Metab.* 35, 888–901. doi: 10.1038/jcbfm.2015.45

Jin, K., Mao, X. O., and Greenberg, D. A. (2006). Vascular endothelial growth factor stimulates neurite outgrowth from cerebral cortical neurons via rho kinase signaling. *J. Neurobiol.* 66, 236–242. doi: 10.1002/neu.20215

Jones, K. A., Maltby, S., Plank, M. W., Kluge, M., Nilsson, M., Foster, P. S., et al. (2018). Peripheral immune cells infiltrate into sites of secondary neurodegeneration after ischemic stroke. *Brain Behav. Immun.* 67, 299–307. doi: 10.1016/j.bbi.2017.09.006

Joy, M. T., and Carmichael, S. T. (2021). Encouraging an excitable brain state: Mechanisms of brain repair in stroke. *Nat. Rev. Neurosci.* 22, 38–53. doi: 10.1038/s41583-020-00396-7

Joy, M. T., Ben Assayag, E., Shabashov-Stone, D., Liraz-Zaltsman, S., Mazzitelli, J., Arenas, M., et al. (2019). CCR5 is a therapeutic target for recovery after stroke and traumatic brain injury. *Cell* 176:e1113. doi: 10.1016/j.cell.2019.01.044

Kamel, H., and Iadecola, C. (2012). Brain-immune interactions and ischemic stroke: Clinical implications. *Arch. Neurol.* 69, 576–581. doi: 10.1001/archneurol.2011.3590

Kanazawa, M., Takahashi, T., Ishikawa, M., Onodera, O., Shimohata, T., and Del Zoppo, G. J. (2019). Angiogenesis in the ischemic core: A potential treatment target? *J. Cereb. Blood Flow Metab.* 39, 753–769. doi: 10.1177/0271678X19834158

Kang, L., Yu, H., Yang, X., Zhu, Y., Bai, X., Wang, R., et al. (2020). Neutrophil extracellular traps released by neutrophils impair revascularization and vascular remodeling after stroke. *Nat. Commun.* 11:2488. doi: 10.1038/s41467-020-16191-y

Kapellos, T. S., Taylor, L., Lee, H., Cowley, S. A., James, W. S., Iqbal, A. J., et al. (2016). A novel real time imaging platform to quantify macrophage phagocytosis. *Biochem. Pharmacol.* 116, 107–119. doi: 10.1016/j.bcp.2016.07.011

Katsuki, H., Nakai, S., Hirai, Y., Akaji, K., Kiso, Y., and Satoh, M. (1990). Interleukin-1 beta inhibits long-term potentiation in the CA3 region of mouse hippocampal slices. *Eur. J. Pharmacol.* 181, 323–326. doi: 10.1016/0014-2999(90)90099-r

Kerschensteiner, M., Meinl, E., and Hohlfeld, R. (2010). Neuro-immune crosstalk in CNS diseases. *Results Probl. Cell Differ.* 51, 197–216. doi: 10.1007/400_2009_6

Klehmet, J., Harms, H., Richter, M., Prass, K., Volk, H. D., Dirnagl, U., et al. (2009). Stroke-induced immunodepression and post-stroke infections: Lessons from the preventive antibacterial therapy in stroke trial. *Neuroscience* 158, 1184–1193. doi: 10.1016/j.neuroscience.2008.07.044

Kleinschnitz, C., Schwab, N., Kraft, P., Hagedorn, I., Dreykluft, A., Schwarz, T., et al. (2010). Early detrimental T-cell effects in experimental cerebral ischemia are neither related to adaptive immunity nor thrombus formation. *Blood* 115, 3835–3842. doi: 10.1182/blood-2009-10-249078

Korhonen, P., Kanninen, K. M., Lehtonen, S., Lemarchant, S., Puttonen, K. A., Oksanen, M., et al. (2015). Immunomodulation by interleukin-33 is protective in stroke through modulation of inflammation. *Brain Behav. Immun.* 49, 322–336. doi: 10.1016/j.bbi.2015.06.013

Lambertsen, K. L., Gregersen, R., Meldgaard, M., Clausen, B. H., Heibol, E. K., Ladeby, R., et al. (2004). A role for interferon-gamma in focal cerebral ischemia in mice. *J. Neuropathol. Exp. Neurol.* 63, 942–955. doi: 10.1093/jnen/63.9.942

Lange, C., Turrero Garcia, M., Decimo, I., Bifari, F., Eelen, G., Quaegebeur, A., et al. (2016). Relief of hypoxia by angiogenesis promotes neural stem cell differentiation by targeting glycolysis. *EMBO J.* 35, 924–941. doi: 10.15252/embj.201592372

Laterza, C., Wattananit, S., Uoshima, N., Ge, R., Pekny, R., Tornero, D., et al. (2017). Monocyte depletion early after stroke promotes neurogenesis from endogenous neural stem cells in adult brain. *Exp. Neurol.* 297, 129–137. doi: 10.1016/j.expneurol.2017.07.012

Lee, G. A., Lin, T. N., Chen, C. Y., Mau, S. Y., Huang, W. Z., Kao, Y. C., et al. (2018). Interleukin 15 blockade protects the brain from cerebral ischemia-reperfusion injury. *Brain Behav. Immun.* 73, 562–570. doi: 10.1016/j.bbi.2018.06.021

Lei, W. L., Xing, S. G., Deng, C. Y., Ju, X. C., Jiang, X. Y., and Luo, Z. G. (2012). Laminin/beta1 integrin signal triggers axon formation by promoting microtubule assembly and stabilization. *Cell Res.* 22, 954–972. doi: 10.1038/cr.2012.40

Li, Q., and Barres, B. A. (2018). Microglia and macrophages in brain homeostasis and disease. *Nat. Rev. Immunol.* 18, 225–242. doi: 10.1038/nri.2017.125

Li, R., Patterson, K. R., and Bar-Or, A. (2018). Reassessing B cell contributions in multiple sclerosis. *Nat. Immunol.* 19, 696–707. doi: 10.1038/s41590-018-0135-x

Lin, Y., Zhang, J. C., Yao, C. Y., Wu, Y., Abdelgawad, A. F., Yao, S. L., et al. (2016). Critical role of astrocytic interleukin-17 A in post-stroke survival and neuronal differentiation of neural precursor cells in adult mice. *Cell Death Dis.* 7:e2273. doi: 10.1038/cddis.2015.284

Liu, Q., Jin, W. N., Liu, Y., Shi, K., Sun, H., Zhang, F., et al. (2017). Brain ischemia suppresses immunity in the periphery and brain via different neurogenic innervations. *Immunity* 46, 474–487. doi: 10.1016/j.immuni.2017.02.015

Liu, X., Liu, J., Zhao, S., Zhang, H., Cai, W., Cai, M., et al. (2016). Interleukin-4 is essential for microglia/macrophage M2 polarization and long-term recovery after cerebral ischemia. *Stroke* 47, 498–504. doi: 10.1161/STROKEAHA.115.012079

Liu, Y., Li, S., Wang, R., Pu, H., Zhao, Y., Ye, Q., et al. (2021). Inhibition of TGFbeta-activated kinase 1 promotes inflammation-resolving microglial/macrophage responses and recovery after stroke in ovariectomized female mice. *Neurobiol. Dis.* 151:105257. doi: 10.1016/j.nbd.2021.105257

Llovera, G., Benakis, C., Enzmann, G., Cai, R., Arzberger, T., Ghasemigharagoz, A., et al. (2017). The choroid plexus is a key cerebral invasion route for T cells after stroke. *Acta Neuropathol.* 134, 851–868. doi: 10.1007/s00401-017-1758-y

Lyu, J., Xie, D., Bhatia, T. N., Leak, R. K., Hu, X., and Jiang, X. (2021). Microglial/macrophage polarization and function in brain injury and repair after stroke. *CNS Neurosci. Ther.* 27, 515–527. doi: 10.1111/cns.13620

Ma, Y., Wang, J., Wang, Y., and Yang, G. Y. (2017). The biphasic function of microglia in ischemic stroke. *Prog. Neurobiol.* 157, 247–272. doi: 10.1016/j.pneurobio.2016.01.005

Ma, Y., Yang, S., He, Q., Zhang, D., and Chang, J. (2021). The role of immune cells in post-stroke angiogenesis and neuronal remodeling: The known and the unknown. *Front. Immunol.* 12:784098. doi: 10.3389/fimmu.2021.784098

Martinez, F. O., and Gordon, S. (2014). The M1 and M2 paradigm of macrophage activation: Time for reassessment. *F1000Prime Rep.* 6:13. doi: 10.12703/P6-13

Meng, C., Zhang, J. C., Shi, R. L., Zhang, S. H., and Yuan, S. Y. (2015). Inhibition of interleukin-6 abolishes the promoting effects of pair housing on post-stroke neurogenesis. *Neuroscience* 307, 160–170. doi: 10.1016/j.neuroscience.2015.08.055

Mirabella, F., Desiato, G., Mancinelli, S., Fossati, G., Rasile, M., Morini, R., et al. (2021). Prenatal interleukin 6 elevation increases glutamatergic synapse density and disrupts hippocampal connectivity in offspring. *Immunity* 54:e2618. doi: 10.1016/j.immuni.2021.10.006

Miron, V. E., Boyd, A., Zhao, J. W., Yuen, T. J., Ruckh, J. M., Shadrach, J. L., et al. (2013). M2 microglia and macrophages drive oligodendrocyte differentiation during CNS remyelination. *Nat. Neurosci.* 16, 1211–1218. doi: 10.1038/nn.3469

Mracsko, E., Liesz, A., Stojanovic, A., Lou, W. P., Osswald, M., Zhou, W., et al. (2014). Antigen dependently activated cluster of differentiation 8-positive T cells cause perforin-mediated neurotoxicity in experimental stroke. *J. Neurosci.* 34, 16784–16795. doi: 10.1523/JNEUROSCI.1867-14.2014

Muhammad, S., Chaudhry, S. R., Kahlert, U. D., Niemela, M., and Hanggi, D. (2021). Brain immune interactions-novel emerging options to treat acute ischemic brain injury. *Cells* 10:2429. doi: 10.3390/cells10092429

Murray, P. J. (2017). Macrophage polarization. *Annu. Rev. Physiol.* 79, 541–566. doi: 10.1146/annurev-physiol-022516-034339

Neumann, J., Sauerzweig, S., Ronicke, R., Gunzer, F., Dinkel, K., Ullrich, O., et al. (2008). Microglia cells protect neurons by direct engulfment of invading neutrophil granulocytes: A new mechanism of CNS immune privilege. *J. Neurosci.* 28, 5965–5975. doi: 10.1523/JNEUROSCI.0060-08.2008

Offner, H., and Hurn, P. D. (2012). A novel hypothesis: Regulatory B lymphocytes shape outcome from experimental stroke. *Transl. Stroke Res.* 3, 324–330. doi: 10.1007/s12975-012-0187-4

Offner, H., Subramanian, S., Parker, S. M., Wang, C., Afentoulis, M. E., Lewis, A., et al. (2006). Splenic atrophy in experimental stroke is accompanied by increased regulatory T cells and circulating macrophages. *J. Immunol.* 176, 6523–6531. doi: 10.4049/jimmunol.176.11.6523

Ortega, S. B., Torres, V. O., Latchney, S. E., Whoolery, C. W., Noorbhai, I. Z., Poinsatte, K., et al. (2020). B cells migrate into remote brain areas and support neurogenesis and functional recovery after focal stroke in mice. *Proc. Natl. Acad. Sci. U.S.A.* 117, 4983–4993. doi: 10.1073/pnas.1913292117

Otxoa-de-Amezaga, A., Miro-Mur, F., Pedragosa, J., Gallizioli, M., Justicia, C., Gaja-Capdevila, N., et al. (2019). Microglial cell loss after ischemic stroke favors brain neutrophil accumulation. *Acta Neuropathol.* 137, 321–341. doi: 10.1007/s00401-018-1954-4

Pedragosa, J., Miro-Mur, F., Otxoa-de-Amezaga, A., Justicia, C., Ruiz-Jaen, F., Ponsaerts, P., et al. (2020). CCR2 deficiency in monocytes impairs angiogenesis and functional recovery after ischemic stroke in mice. *J. Cereb. Blood Flow Metab.* 40, S98–S116. doi: 10.1177/0271678X20909055

Pennypacker, K. R., and Offner, H. (2015). The role of the spleen in ischemic stroke. *J. Cereb. Blood Flow Metab.* 35, 186–187. doi: 10.1038/jcbfm.2014.212

Perez-de-Puig, I., Miro-Mur, F., Ferrer-Ferrer, M., Gelpi, E., Pedragosa, J., Justicia, C., et al. (2015). Neutrophil recruitment to the brain in mouse and human ischemic stroke. *Acta Neuropathol.* 129, 239–257. doi: 10.1007/s00401-014-1381-0

Prass, K., Meisel, C., Hoflich, C., Braun, J., Halle, E., Wolf, T., et al. (2003). Stroke-induced immunodeficiency promotes spontaneous bacterial infections and is mediated by sympathetic activation reversal by poststroke T helper cell type 1-like immunostimulation. *J. Exp. Med.* 198, 725–736. doi: 10.1084/jem.20021098

Prinz, M., and Priller, J. (2017). The role of peripheral immune cells in the CNS in steady state and disease. *Nat. Neurosci.* 20, 136–144. doi: 10.1038/nn.4475

Qiu, M., Xu, E., and Zhan, L. (2021). Epigenetic regulations of microglia/macrophage polarization in ischemic stroke. *Front. Mol. Neurosci.* 14:697416. doi: 10.3389/fnmol.2021.697416

Ren, X., Akiyoshi, K., Dziennis, S., Vandenbark, A. A., Herson, P. S., Hurn, P. D., et al. (2011). Regulatory B cells limit CNS inflammation and neurologic deficits in murine experimental stroke. *J. Neurosci.* 31, 8556–8563. doi: 10.1523/JNEUROSCI.1623-11.2011

Roth, S., Cao, J., Singh, V., Tiedt, S., Hundeshagen, G., Li, T., et al. (2021). Post-injury immunosuppression and secondary infections are caused by an AIM2 inflammasome-driven signaling cascade. *Immunity* 54:e648. doi: 10.1016/j.immuni.2021.02.004

Rowe, D. D., Collier, L. A., Seifert, H. A., Chapman, C. B., Leonardo, C. C., Willing, A. E., et al. (2014). Leukemia inhibitor factor promotes functional recovery and oligodendrocyte survival in rat models of focal ischemia. *Eur. J. Neurosci.* 40, 3111–3119. doi: 10.1111/ejn.12675

Roy Choudhury, G., Ryou, M. G., Poteet, E., Wen, Y., He, R., Sun, F., et al. (2014). Involvement of p38 MAPK in reactive astrogliosis induced by ischemic stroke. *Brain Res.* 1551, 45–58. doi: 10.1016/j.brainres.2014.01.013

Ruan, L., Wang, B., ZhuGe, Q., and Jin, K. (2015). Coupling of neurogenesis and angiogenesis after ischemic stroke. *Brain Res.* 1623, 166–173. doi: 10.1016/j.brainres.2015.02.042

Sas, A. R., Carbajal, K. S., Jerome, A. D., Menon, R., Yoon, C., Kalinski, A. L., et al. (2020). A new neutrophil subset promotes CNS neuron survival and axon regeneration. *Nat. Immunol.* 21, 1496–1505. doi: 10.1038/s41590-020-00813-0

Schuhmann, M. K., Langhauser, F., Kraft, P., and Kleinschnitz, C. (2017). B cells do not have a major pathophysiologic role in acute ischemic stroke in mice. *J Neuroinflammation* 14:112. doi: 10.1186/s12974-017-0890-x

Seifert, H. A., and Pennypacker, K. R. (2014). Molecular and cellular immune responses to ischemic brain injury. *Transl. Stroke Res.* 5, 543–553. doi: 10.1007/s12975-014-0349-7

Selvaraj, U. M., Ujas, T. A., Kong, X., Kumar, A., Plautz, E. J., Zhang, S., et al. (2021). Delayed diapedesis of CD8 T cells contributes to long-term pathology after ischemic stroke in male mice. *Brain Behav. Immun.* 95, 502–513. doi: 10.1016/j.bbi.2021.05.001

Shi, X., Luo, L., Wang, J., Shen, H., Li, Y., Mamtilahun, M., et al. (2021). Stroke subtype-dependent synapse elimination by reactive gliosis in mice. *Nat. Commun.* 12:6943. doi: 10.1038/s41467-021-27248-x

Shi, L., Sun, Z., Su, W., Xu, F., Xie, D., Zhang, Q., et al. (2021). Treg cell-derived osteopontin promotes microglia-mediated white matter repair after ischemic stroke. *Immunity* 54:e1528. doi: 10.1016/j.immuni.2021.04.022

Shibahara, T., Ago, T., Tachibana, M., Nakamura, K., Yamanaka, K., Kuroda, J., et al. (2020). Reciprocal interaction between pericytes and macrophage in poststroke tissue repair and functional recovery. *Stroke* 51, 3095–3106. doi: 10.1161/STROKEAHA.120.029827

Shichita, T., Ago, T., Kamouchi, M., Kitazono, T., Yoshimura, A., and Ooboshi, H. (2012). Novel therapeutic strategies targeting innate immune responses and early inflammation after stroke. *J. Neurochem.* 123(Suppl. 2), 29–38. doi: 10.1111/j.1471-4159.2012.07941.x

Shichita, T., Ito, M., Morita, R., Komai, K., Noguchi, Y., Ooboshi, H., et al. (2017). MAFB prevents excess inflammation after ischemic stroke by accelerating clearance of damage signals through MSR1. *Nat. Med.* 23, 723–732. doi: 10.1038/nm.4312

Shichita, T., Sugiyama, Y., Ooboshi, H., Sugimori, H., Nakagawa, R., Takada, I., et al. (2009). Pivotal role of cerebral interleukin-17-producing gammadeltaT cells in the delayed phase of ischemic brain injury. *Nat. Med.* 15, 946–950. doi: 10.1038/nm.1999

Sims, N. R., and Yew, W. P. (2017). Reactive astrogliosis in stroke: Contributions of astrocytes to recovery of neurological function. *Neurochem. Int.* 107, 88–103. doi: 10.1016/j.neuint.2016.12.016

Small, S. L., Buccino, G., and Solodkin, A. (2013). Brain repair after stroke–a novel neurological model. *Nat. Rev. Neurol.* 9, 698–707. doi: 10.1038/nrneurol.2013.222

Smolders, J., Heutinck, K. M., Fransen, N. L., Remmerswaal, E. B. M., Hombrink, P., Ten Berge, I. J. M., et al. (2018). Tissue-resident memory T cells populate the human brain. *Nat. Commun.* 9:4593. doi: 10.1038/s41467-018-07053-9

Stanzione, R., Forte, M., Cotugno, M., Bianchi, F., Marchitti, S., and Rubattu, S. (2022). Role of DAMPs and of leukocytes infiltration in ischemic stroke: Insights from animal models and translation to the human disease. *Cell. Mol. Neurobiol.* 42, 545–556. doi: 10.1007/s10571-020-00966-4

Stubbe, T., Ebner, F., Richter, D., Engel, O., Klehmet, J., Royl, G., et al. (2013). Regulatory T cells accumulate and proliferate in the ischemic hemisphere for up to 30 days after MCAO. *J. Cereb. Blood Flow Metab.* 33, 37–47. doi: 10.1038/jcbfm.2012.128

Swardfager, W., Winer, D. A., Herrmann, N., Winer, S., and Lanctot, K. L. (2013). Interleukin-17 in post-stroke neurodegeneration. *Neurosci. Biobehav. Rev.* 37, 436–447. doi: 10.1016/j.neubiorev.2013.01.021

Ullevig, S. L., Kim, H. S., Nguyen, H. N., Hambright, W. S., Robles, A. J., Tavakoli, S., et al. (2014). Ursolic acid protects monocytes against metabolic stress-induced priming and dysfunction by preventing the induction of Nox4. *Redox Biol.* 2, 259–266. doi: 10.1016/j.redox.2014.01.003

Underhill, D. M., Bassetti, M., Rudensky, A., and Aderem, A. (1999). Dynamic interactions of macrophages with T cells during antigen presentation. *J. Exp. Med.* 190, 1909–1914. doi: 10.1084/jem.190.12.1909

Varadarajan, S. G., Hunyara, J. L., Hamilton, N. R., Kolodkin, A. L., and Huberman, A. D. (2022). Central nervous system regeneration. *Cell* 185, 77–94. doi: 10.1016/j.cell.2021.10.029

Wang, J., Xie, L., Yang, C., Ren, C., Zhou, K., Wang, B., et al. (2015). Activated regulatory T cell regulates neural stem cell proliferation in the subventricular zone of normal and ischemic mouse brain through interleukin 10. *Front. Cell. Neurosci.* 9:361. doi: 10.3389/fncel.2015.00361

Wang, X., Zhang, L., Sun, W., Pei, L. L., Tian, M., Liang, J., et al. (2020). Changes of metabolites in acute ischemic stroke and its subtypes. *Front. Neurosci.* 14:580929. doi: 10.3389/fnins.2020.580929

Wang, R., Liu, Y., Ye, Q., Hassan, S. H., Zhao, J., Li, S., et al. (2020). RNA sequencing reveals novel macrophage transcriptome favoring neurovascular plasticity after ischemic stroke. *J. Cereb. Blood Flow Metab.* 40, 720–738. doi: 10.1177/0271678X19888630

Wang, X., Zhou, Y., Tang, D., Zhu, Z., Li, Y., Huang, T., et al. (2019). ACC1 (Acetyl coenzyme A carboxylase 1) is a potential immune modulatory target of cerebral ischemic stroke. *Stroke* 50, 1869–1878. doi: 10.1161/STROKEAHA.119.024564

Wanrooy, B. J., Wen, S. W., and Wong, C. H. (2021). Dynamic roles of neutrophils in post-stroke neuroinflammation. *Immunol. Cell Biol.* 99, 924–935. doi: 10.1111/imcb.12463

Wattananit, S., Tornero, D., Graubardt, N., Memanishvili, T., Monni, E., Tatarishvili, J., et al. (2016). Monocyte-derived macrophages contribute to spontaneous long-term functional recovery after stroke in mice. *J. Neurosci.* 36, 4182–4195. doi: 10.1523/JNEUROSCI.4317-15.2016

Wong, C. H. Y. (2019). Effects of stroke beyond the brain. *Nat. Rev. Immunol.* 19:719. doi: 10.1038/s41577-019-0234-4

Wong, C. H., Jenne, C. N., Lee, W. Y., Leger, C., and Kubes, P. (2011). Functional innervation of hepatic iNKT cells is immunosuppressive following stroke. *Science* 334, 101–105. doi: 10.1126/science.1210301

Woo, M. S., Yang, J., Beltran, C., and Cho, S. (2016). Cell surface CD36 protein in monocyte/macrophage contributes to phagocytosis during the resolution phase of ischemic stroke in mice. *J. Biol. Chem.* 291, 23654–23661. doi: 10.1074/jbc.M116.750018

Xie, D., Liu, H., Xu, F., Su, W., Ye, Q., Yu, F., et al. (2021). IL33 (Interleukin 33)/ST2 (Interleukin 1 receptor-like 1) axis drives protective microglial responses and promotes white matter integrity after stroke. *Stroke* 52, 2150–2161. doi: 10.1161/STROKEAHA.120.032444

Xiong, X., Xu, L., Wei, L., White, R. E., Ouyang, Y. B., and Giffard, R. G. (2015). IL-4 is required for sex differences in vulnerability to focal ischemia in mice. *Stroke* 46, 2271–2276. doi: 10.1161/STROKEAHA.115.008897

Xu, S., Lu, J., Shao, A., Zhang, J. H., and Zhang, J. (2020). Glial cells: Role of the immune response in ischemic stroke. *Front. Immunol.* 11:294. doi: 10.3389/fimmu.2020.00294

Yilmaz, G., Arumugam, T. V., Stokes, K. Y., and Granger, D. N. (2006). Role of T lymphocytes and interferon-gamma in ischemic stroke. *Circulation* 113, 2105–2112. doi: 10.1161/CIRCULATIONAHA.105.593046

Yoon, J. W., and Jun, H. S. (1999). Cellular and molecular roles of beta cell autoantigens, macrophages and T cells in the pathogenesis of autoimmune diabetes. *Arch. Pharm. Res.* 22, 437–447. doi: 10.1007/BF02979150

Zhang, D., Hu, X., Qian, L., O'Callaghan, J. P., and Hong, J. S. (2010). Astrogliosis in CNS pathologies: Is there a role for microglia? *Mol. Neurobiol.* 41, 232–241. doi: 10.1007/s12035-010-8098-4

Zhang, D., Ren, J., Luo, Y., He, Q., Zhao, R., Chang, J., et al. (2021). T cell response in ischemic stroke: From mechanisms to translational insights. *Front. Immunol.* 12:707972. doi: 10.3389/fimmu.2021.707972

Zhang, W., Zhao, J., Wang, R., Jiang, M., Ye, Q., Smith, A. D., et al. (2019). Macrophages reprogram after ischemic stroke and promote efferocytosis and inflammation resolution in the mouse brain. *CNS Neurosci. Ther.* 25, 1329–1342. doi: 10.1111/cns.13256

Zhang, Q., Zhu, W., Xu, F., Dai, X., Shi, L., Cai, W., et al. (2019). The interleukin-4/PPARgamma signaling axis promotes oligodendrocyte differentiation and remyelination after brain injury. *PLoS Biol.* 17:e3000330. doi: 10.1371/journal.pbio.3000330

Zhang, R., Chopp, M., and Zhang, Z. G. (2013). Oligodendrogenesis after cerebral ischemia. *Front. Cell. Neurosci.* 7:201. doi: 10.3389/fncel.2013.00201

Zhang, S. R., Piepke, M., Chu, H. X., Broughton, B. R., Shim, R., Wong, C. H., et al. (2018). IL-33 modulates inflammatory brain injury but exacerbates systemic immunosuppression following ischemic stroke. *JCI Insight* 3:e121560. doi: 10.1172/jci.insight.121560

Zhang, Y., Gao, Z., Wang, D., Zhang, T., Sun, B., Mu, L., et al. (2014). Accumulation of natural killer cells in ischemic brain tissues and the chemotactic effect of IP-10. *J. Neuroinflammation* 11:79. doi: 10.1186/1742-2094-11-79

Zheng, Y., He, R., Wang, P., Shi, Y., Zhao, L., and Liang, J. (2019). Exosomes from LPS-stimulated macrophages induce neuroprotection and functional improvement after ischemic stroke by modulating microglial polarization. *Biomater. Sci.* 7, 2037–2049. doi: 10.1039/c8bm01449c

Zhou, Y. X., Wang, X., Tang, D., Li, Y., Jiao, Y. F., Gan, Y., et al. (2019). IL-2mAb reduces demyelination after focal cerebral ischemia by suppressing CD8(+) T cells. *CNS Neurosci. Ther.* 25, 532–543. doi: 10.1111/cns.13084

Zhu, J., Yamane, H., and Paul, W. E. (2010). Differentiation of effector CD4 T cell populations (*). *Annu. Rev. Immunol.* 28, 445–489. doi: 10.1146/annurev-immunol-030409-101212

Zhu, Y. M., Lin, L., Wei, C., Guo, Y., Qin, Y., Li, Z. S., et al. (2021). The key regulator of necroptosis, RIP1 kinase, contributes to the formation of astrogliosis and glial scar in ischemic stroke. *Transl. Stroke Res.* 12, 991–1017. doi: 10.1007/s12975-021-00888-3

frontiers | Frontiers in Immunology

TYPE Original Research
PUBLISHED 09 December 2022
DOI 10.3389/fimmu.2022.1080482

OPEN ACCESS

EDITED BY
Yan Wang,
Peking University Third Hospital, China

REVIEWED BY
Friederike Ebner,
Free University of Berlin, Germany
Jinming Han,
Capital Medical University, China

*CORRESPONDENCE
Ruslan Rust
ruslan.rust@irem.uzh.ch

SPECIALTY SECTION
This article was submitted to Multiple Sclerosis and Neuroimmunology, a section of the journal Frontiers in Immunology

RECEIVED 26 October 2022
ACCEPTED 22 November 2022
PUBLISHED 09 December 2022

CITATION
Weber RZ, Mulders G, Perron P, Tackenberg C and Rust R (2022) Molecular and anatomical roadmap of stroke pathology in immunodeficient mice. *Front. Immunol.* 13:1080482. doi: 10.3389/fimmu.2022.1080482

Molecular and anatomical roadmap of stroke pathology in immunodeficient mice

Rebecca Z. Weber[1,2], Geertje Mulders[3], Patrick Perron[1], Christian Tackenberg[1,2] and Ruslan Rust[1,2]*

[1]Institute for Regenerative Medicine, University of Zurich, Schlieren, Switzerland, [2]Neuroscience Center Zurich, University of Zurich and Eidgenössische Technische Hochschule (ETH) Zurich, Zurich, Switzerland, [3]Department of Health Sciences and Technology, Eidgenössische Technische Hochschule (ETH) Zurich, Zurich, Switzerland

Background: Stroke remains a leading cause of disability and death worldwide. It has become apparent that inflammation and immune mediators have a predominant role in initial tissue damage and long-term recovery. Still, different immunosuppressed mouse models are necessary in stroke research e.g., to evaluate therapies using human cell grafts. Despite mounting evidence delineating the importance of inflammation in the stroke pathology, it is poorly described to what extent immune deficiency influences overall stroke outcome.

Methods: Here, we assessed the stroke pathology of popular genetic immunodeficient mouse models, i.e., NOD scid gamma (NSG) and recombination activating gene 2 ($Rag2^{-/-}$) mice as well as pharmacologically immunosuppressed mice and compared them to immune competent, wildtype (WT) C57BL/6J mice three weeks after injury. We performed histology, gene expression, blood serum and behavioural analysis to identify the impact of immunosuppression on stroke progression.

Results: We detected changes in microglia activation/macrophage infiltration, scar-forming and vascular repair in immune-suppressed mice three weeks after injury. Transcriptomic analysis of stroked tissue revealed the strongest deviation from WT was observed in NSG mice affecting immunological and angiogenic pathways. Pharmacological immunosuppression resulted in the least variation in gene expression compared with the WT. These anatomical and genetic changes did not affect functional recovery in a time course of three weeks. To determine whether timing of immunosuppression is critical, we compared mice with acute and delayed pharmacological immunosuppression after stroke. Mice with delayed immunosuppression (7d) showed increased inflammatory and scarring responses compared to animals acutely treated with tacrolimus, thus more closely resembling WT pathology. Transplantation of human cells in the brains of immunosuppressed mice led to prolonged cell survival in all immunosuppressed mouse models, which was most consistent in NSG and $Rag2^{-/-}$ mice.

Conclusions: We detected distinct anatomical and molecular changes in the stroke pathology between individual immunosuppressed mouse models that should be considered when selecting an appropriate mouse model for stroke research.

KEYWORDS

ischemia, immune deficiency, immune suppression, cell therapy, photothrombotic stroke, rodent, transcriptomics, histology

Introduction

Stroke is a major cause of disability and death due to the brain's limited capacity to regenerate damaged tissue (1). To promote recovery, cell-based therapy has been proposed as an emerging treatment and potential regenerative strategy for stroke patients with remaining neurologic deficits (2). Recent advances in induced pluripotent stem cells (iPSC) technology facilitated the generation of human neuronal cells as a suitable and scalable cell source. To test the human-derived graft's efficacy and safety for cell therapy, preclinical research requires the immunosuppression in mice to avoid xenograft rejection (3–7). The use of immunosuppressed mice allows the evaluation of long-term effects of cell therapies in mice with the drawback that general immunosuppression may substantially alter the stroke pathology (8, 9).

Acutely after stroke, inflammation plays a critical role in early ischemic damage that both promotes further injury resulting in cell death but conversely has also been shown to contribute to regeneration and remodelling (10). Despite mounting evidence delineating the importance of inflammation in the stroke pathology, it is poorly described to what extent partial immune deficiency influences the overall stroke outcome. Several immunosuppressed mouse models have been used in preclinical stroke research, most prominent: (a) pharmacological immunosuppression with calcineurin inhibitory drugs (e.g., tacrolimus) that block the development and proliferation of T cells; (b) genetically deficient mice that lack recombination activating gene 2 protein ($Rag2^{-/-}$) required for the generation of mature B and T lymphocytes; and (c) NOD scid gamma (NSG) mice that lack mature T and B lymphocytes, natural killer (NK) cells and have deficiencies in multiple cytokine signalling and innate immunity (11, 12). However, it is unclear to what extent the immunosuppression in these mouse models alter the natural pathology of stroke and may affect the outcome of therapies that require immunosuppression such as human cell-based therapies.

Here, we hypothesize that different aspects of stroke pathology may be altered depending on the mouse model of immunosuppression. Therefore, we compare the stroke pathology of most popular genetic mouse models using $Rag2^{-/-}$ mice and NSG mice, as well as tacrolimus immunosuppressed mice, to immune competent, WT control. We identify changes in tissue responses and gene expression after stroke affecting especially inflammatory, scar-forming and angiogenic remodelling processes in all immunosuppressed mice compared to immune competent WT controls three weeks after injury. These changes were mitigated if the tacrolimus treatment was deferred beyond the acute stroke phase. The anatomical, genetic, and systemic changes did not affect functional deficits and recovery in a time course of three weeks. Local intraparenchymal cell transplantation led to prolonged graft survival in all immunodeficient mouse models compared to WT, which, however, was more profound in the genetically immunodeficient $Rag2^{-/-}$ and NSG animals. These changes in anatomy, physiology, and gene expression after stroke across the tested immunodeficient mouse models are relevant to understand the role of immunosuppression in the stroke pathology and for evaluating the preclinical efficacy of cell-based therapies.

Abbreviations: BL, baseline; BLI, bioluminescence imaging; cc, corpus callosum; CD, cluster of differentiation; ctx, cortex; dpi, days post injury; EdU, 5-ethynyl-2′-deoxyuridine; eGFP, enhanced green fluorescent protein; GFAP, glial fibrillary acidic protein; HuNu, Human nuclei; IFN, interferon; IL, interleukin; iPSC, induced pluripotent stem cells; NF-H, Neurofilament heavy chain; NF-L, Neurofilament light chain; NK cells, natural killer cells; NOD, non-obese diabetic; NPC, neural progenitor cells; NSG, NOD scid gamma; PFA, paraformaldehyde; ph, photons; RAG2, recombination activating gene 2; RNAseq RNA sequencing; ROI, region of interest; sbr, signal background ratio; SD, standard deviation; SNR, signal to noise ratio; sr, steradian; Tacr, Tacrolimus; Tukey HSD, Tukey honest significant differences; WT, wildtype.

Materials and methods

Experimental design

Stroke pathology was compared between (1) wildtype (WT) C57BL/J mice with three immunosuppressant mouse models (2): WT C57BL/J mice that were immunosuppressed with

tacrolimus (3) Rag2$^{-/-}$ mice and (4) NSG mice. All mice received a large photothrombotic stroke to the right sensorimotor cortex and underwent regular behavioral tests at baseline, 3, 7, 14, 21 days after stroke induction. At 21 days after stroke, mice from each group were divided into two subgroups: Brains from the first subgroup were collected, fixed and histologically analysed; brains from the other group were microdissected around the stroke region and prepared for RNAseq analysis. We chose the time point based on previous findings showing functional differences starting from three weeks following regenerative therapies (13). To test the effects of delayed tacrolimus treatment, we compared between (1) wildtype C57BL/J mice with (2) WT C57BL/J mice that were acutely immunosuppressed mice with tacrolimus (0 dpi) and (3) WT C57BL/J mice that received tacrolimus delayed at 7 dpi. The brains were treated equivalently to the previous set-up to obtain comparable histology and RNAseq data.

Long-term survival and successful immunosuppression were tested by local intraparenchymal transplantation of human NPCs to 1) WT C57BL/J mice (2) WT C57BL/J mice that were immunosuppressed with tacrolimus (3) Rag2$^{-/-}$ mice and (4) NSG mice. Luciferase expressing NPCs were tracked over 35 days using *in vivo* bioluminescence imaging and brain tissue was collected to identify the transplanted cells in brain sections.

Animals

All procedures were conducted in accordance with governmental, institutional (University of Zurich), and ARRIVE guidelines and had been approved by the Veterinarian Office of the Canton of Zurich (license: 209/2019). In total, 20 WT (WT) mice (histology: 7, RNAseq: 8, cell therapy: 5) with C57BL/6 background mice, 17 tacrolimus treated WT mice (histology: 8, RNAseq: 4, cell therapy: 5), 19 Rag2$^{-/-}$ mice (histology: 5, RNAseq: 9, cell therapy: 5) and 19 NSG mice (histology: 10, RNAseq: 4, cell therapy: 5) were used. Mice that were used for histology and RNAseq both performed the behavioral tasks. We used both sex female and male and mice were 3 months of age. Breeding of Rag2$^{-/-}$ mice and NSG mice was performed at Laboratory Animal Services Center (LASC) in Schlieren, CH. WT animals were provided by Charles River Laboratories, Germany. All animals were housed in standard type II/III cages on a 12h day/light cycle (6:00 A.M. lights on) with food and water ad libitum. All mice were acclimatized for at least a week to environmental conditions before set into experiment.

Photothrombotic lesion

Anaesthesia was performed using isoflurane (5% induction, 1.5-2% maintenance, Attane, Provet AG) and adequate sedation was confirmed by tail pinch. Novalgin (1mg/ml) was applied *via* drinking water; 24 h prior to the procedure and for three consecutive days directly after stroke surgery. Cerebral ischemia was induced by photothrombotic stroke surgery as previously described (13, 14). Briefly, animals were fixed in a stereotactic frame (David Kopf Instruments), the surgical area was sanitized, and the skull was exposed through a cut along the midline. A cold light source (Olympus KL 1,500LCS, 150W, 3,000K) was positioned over the right forebrain cortex (anterior/posterior: −1.5–+1.5 mm and medial/lateral 0 mm to +2 mm relative to Bregma). Rose Bengal (15 mg/ml, in 0.9% NaCl, Sigma) was injected intraperitoneally 5 min prior to illumination and the region of interest was subsequently illuminated through the intact skull for 12 min. To restrict the illuminated area, an opaque template with an opening of 3 × 4 mm was placed directly on the skull. The wound was closed using a 6/0 silk suture and animals were allowed to recover.

Blood perfusion by Laser Doppler imaging

Cortical perfusion was evaluated using Laser Doppler Imaging (Moor Instruments, MOORLDI2-IR). Briefly, animals were fixed in a stereotactic frame and the region of interest was shaved and sanitized. To expose the skull, a cut was made along the midline and the brain was scanned using the repeat image measurement mode. All data were exported and quantified in terms of total flux in the ROI using Fiji (ImageJ).

Tacrolimus pump implantation

For pharmacological immunosuppression, Alzet osmotic pumps (Model 1004, Cupertino, CA, USA) filled with 100µl tacrolimus solved in a mixture of DMSO and PEG 300 (50mg/ml; 7.56mg/ml concentration) were implanted subcutaneously on the back according to the manufacturer's protocol. Briefly, animals were anesthetized using isoflurane (5% induction, 1.5-2% maintenance, Attane, Provet AG), the surgical area was sanitized and shaved. The implantation site was exposed through a mid-scapular incision. An implantation pocket was created using a hemostat. The pump was inserted into the pocket and the wound was closed with sutures.

Tissue processing and immunofluorescence

Animals were euthanized using pentobarbital (i.p, 150 mg/kg body weight, Streuli Pharma AG) and perfused transcardially with Ringer solution (containing 5 ml/l Heparin, B. Braun) followed by paraformaldehyde (PFA, 4%, in 0.2 M phosphate

buffer, pH 7). Brain tissue was collected and post-fixed for 6 h in 4% PFA. For cryoprotection, tissue was transferred to 30% sucrose and stored at 4°C. Coronal sections were cut at a thickness of 40 µm using a sliding microtome (Microm HM430, Leica), collected, and stored as free-floating sections in cryoprotectant solution at −20°C.

For immunostaining, brain sections were blocked with 5% normal donkey serum for 1 h at room temperature and incubated with primary antibodies (rabbit anti-GFAP 1:200, Dako, #GA524; goat anti-Iba1, 1:500 Wako, #011-27991; NeuroTrace™ 1:200, Thermo Fischer; mouse anti-NeuN Antibody 1:500, Merck, #MAB377; rabbit anti-Neurofilament 200 antibody 1:200, Merck, #N4142; guinea pig anti-Neurofilament L, 1:200, Synaptic Systems, rat anti-CD31 antibody 1:50, BD Biosciences, #MEC13.3; goat anti-CD13, 1:200; R&D Systems, #AF2335) overnight at 4°C. The next day, sections were incubated with corresponding secondary antibodies (1:500, Thermo Fischer Scientific). Nuclei were counterstained with DAPI (1:2,000 in 0.1 M PB, Sigma). Mounting was performed using Mowiol.

Vascular quantification

Vascular parameters (vessel area fraction, length, branching and nearest distance) were identified using an automated ImageJ script as previously described for brain and retinal vasculature (15, 16). Briefly, for total vessel area fraction, the area covered by anti-CD31 staining was quantified using ImageJ after applying a constant threshold. The vascular length was evaluated using the "skeleton length" tool and number of branches was calculated with the "analyse skeleton" tool. Results were normalized per mm^2 of brain tissue for vascular length and number of branches.

EdU administration

5-ethynyl-2'-deoxyuridine (EdU, 50 mg/kg body weight, ThermoFischer) was applied intraperitoneally on day 7 after stroke to label proliferating vascular endothelial cells. EdU incorporation was detected 21 days after stroke using the Click-it EdU Alexa Fluor 647 Imaging Kit (ThermoFischer) on 40 µm coronal sections.

Blood plasma multiplex cytokine analysis

Blood was collected through the tail-vein at baseline, 7- and 21-days post injury. Blood plasma cytokines levels (of IFN-γ, IL-1β, IL-2, IL-4, IL-5, IL-6, KC/GRO, IL-10, IL-12p70, and TNF-α) were measured using the Proinflammatory Panel 1 Mouse kit, a chemiluminescence-based assays from Meso Scale Discovery (MSD, Gaithersburg, MD, USA) according to the manufacturer's protocol. Analyses were done using a QuickPlex SQ 120 instrument (MSD) and DISCOVERY WORKBENCH® 4.0 software.

Gene expression analysis

Total RNA of stroked cortical tissue and the corresponding contralesional site was isolated using TRIzol extraction followed by the RNeasy RNA isolation kit (Qiagen) including a DNase treatment to digest residual genomic DNA. All samples had a RIN value of >8.5.

Library preparation, sequencing, read processing, read alignment, and read counting was performed at the Functional Genomics Center Zurich (FGCZ) core facility. For library preparation, the TruSeq stranded RNA kit (Illumina Inc.) was used according to the manufacturer's protocol. The mRNA was purified by polyA selection, chemically fragmented and transcribed into cDNA before adapter ligation. Analysis of RNA sequencing data and gene set enrichment analysis was performed using EdgeR (17) and clusterProfiler 4.0 (18).

Transcriptomic raw data are available to readers *via* Gene Expression Omnibus with identifier GSE208605.

Behavioral studies

Animals were tested on the (1) runway (2), ladder rung test and (3) the rotarod test. All animals were tested 3 days before surgery to establish baseline performance and 3, 7, 14 and 21 days after stroke induction. Performance on the runway and the ladder rung was evaluated using a recently established deep learning-based protocol (19).

A runway walk was performed to assess whole body coordination during overground locomotion as described previously (18). Briefly, mice were recorded crossing a runway with a high-definition video camera (GoPro Hero 7) at a resolution of 4000 × 3000 and a rate of 60 frames per second from three perspectives. In a first step, the animals were acclimatized to the apparatus in daily training sessions until they crossed the runway at a constant speed and voluntarily (without external intervention). Then, each animal was placed individually on one end of the transparent plexiglas basin and was allowed to walk for 3 minutes.

The ladder rung test was performed using the same set-up as for the runway to assess skilled locomotion; with the only difference that the runway was replaced with a horizontal ladder on which the spacing of the rungs is variable. The animals were trained to cross the ladder without external reinforcement. A total of at least three runs per animal and per session were recorded. A step was defined as misstep when the toe tips of the animal reached a threshold of >0.5 cm below the ladder height.

The rotarod test is a standard sensory-motor test to investigate the animals' ability to stay and run on an accelerated rod (Ugo Basile, Gemonio, Italy). All animals were pre-trained to stay on the accelerating rotarod (slowly increasing from 5 to 50 rpm in 300s) until they could remain on the rod for > 60 s. During the performance, the time and speed was measured until the animals fell or started to rotate with the rod without running. The test was always performed three times and means were used for statistical analysis. The recovery phase between the trials was at least 10 min.

Cell transplantations

Induced pluripotent stem cell (iPSC)-derived neural progenitor cells (NPCs) were generated as previously described (20). In brief, NPCs at passage number < 11 were used in all experiments. Intraparenchymal cell transplantation was performed as previously described (21). In brief $eGFP^+/Luc^+$ NPCs were thawed, washed, and diluted to a final concentration of 8×10^4 cells/µL in sterile 1x PBS (pH 7.4, without calcium or magnesium; Thermo Fisher Scientific). Cells were stored on ice until transplantation. Mice were anesthetized using isoflurane (5% induction, 1.5% maintenance: Attane, Provet AG). Analgesic (Rimadyl; Pfizer) was administered subcutaneously prior to surgery (5 mg/kg body weight). Animals were fixed in a stereotactic frame (David Kopf Instruments), the surgical area was sanitized, and the skull was exposed through a midline skin incision to reveal lambda and bregma points. Coordinates were calculated (the coordinates of interest chosen for this protocol were: AP: + 0.5, ML: + 1.5, DV: −0.8 relative to bregma) and a hole was drilled using a surgical dental drill (Foredom, Bethel CT) (20). Mice were injected with 1.6×10^5 cells (2µL/injection) using a 10-µL Hamilton microsyringe (33-gauge) and a micropump system with a flow rate of 0.3 µL/min (injection) and 1.5 µl/min (withdrawal). The wound was closed with suture.

In vivo bioluminescence imaging and analysis

Bioluminescence imaging (BLI) experiments were performed with the IVIS Spectrum CT (PerkinElmer). Animals were imaged in regular intervals starting 2h after transplantation for up to 35 days. 30mg/ml D-luciferin potassium salt (PerkinElmer) was dissolved in 1x PBS (pH 7.4, without calcium or magnesium; Thermo Fisher Scientific) and sterilized through a 0.22 µm syringe filter. Luciferin was injected intraperitoneally with a final dose of 300 mg/kg body weight before isoflurane anaesthesia (5% induction, 1.5% maintenance; Attane, Provet AG). The head region was shaved before imaging. Image acquisition was performed for 20 min using the following settings: Field of View: A, Subject height: 1.5 cm, Binning: 16, F/Stop: 2. Exposure time (ranging from 1s to 60s) was set automatically by the system to reach the most sensitive setting. Imaging parameters and measurement procedures were kept consistent between mice.

The regions of interest (ROIs) were manually drawn based on anatomical landmarks (eyes, ears and snout) on each image. Plotting and statistical analysis was performed using RStudio. The brain-specific signal was calculated and corrected for nonspecific signal taken from a ROI on the skin of the animal's back and for noise taken from a ROI outside the mouse. Signal-to-noise ratio (SNR) was calculated by dividing the total photon flux (ph/s/cm^2/sr) by the standard deviation of the noise. Bioluminescent signal was calculated by subtracting the background flux from the total photon flux per ROI.

Statistical analysis

Statistical analysis was performed using RStudio (4.04 (2021-02-15). Sample sizes were designed with adequate power according to our previous studies (13, 22, 23) and to the literature (3, 24). All data were tested for normal distribution by using the Shapiro-Wilk test. Multiple comparisons (NSG, $Rag2^{-/-}$, WT-Tacr, WT) were initially tested for normal distribution with the Shapiro-Wilk test. The significance of mean differences between normally distributed multiple comparisons was assessed using repeated measures ANOVA with post-hoc analysis (p adjustment method = holm). Normally distributed data ($WT\text{-}Tacr_{acute}$ vs. $WT\text{-}Tacr_{delayed}$) were tested for differences with a two-tailed unpaired one-sample *t*-test to compare changes between the two groups. Variables exhibiting a skewed distribution were transformed, using natural logarithms before the tests to satisfy the prerequisite assumptions of normality. Data are expressed as means ± SD, and statistical significance was defined as $*p < 0.05$, $**p < 0.01$, and $***p < 0.001$.

Results

Immunodeficient mice exhibit altered inflammation, scarring and vascular remodelling in the peri-infarct brain tissue

To identify stroke-related changes in immunodeficient mouse models, we induced a photothrombotic stroke in the right sensorimotor cortex in (1) C57BL/6J wildtype (WT) mice (2) C57BL/6J WT mice that were continuously immunosuppressed with tacrolimus (WT-Tacr); as well as genetically immunodeficient (3) $Rag2^{-/-}$ and (4) NSG mice (Figure 1A). A successful stroke was confirmed in all groups by ≈ 70% reduction of cerebral blood flow in the lesioned right hemisphere 24h after

10.3389/fimmu.2022.1080482

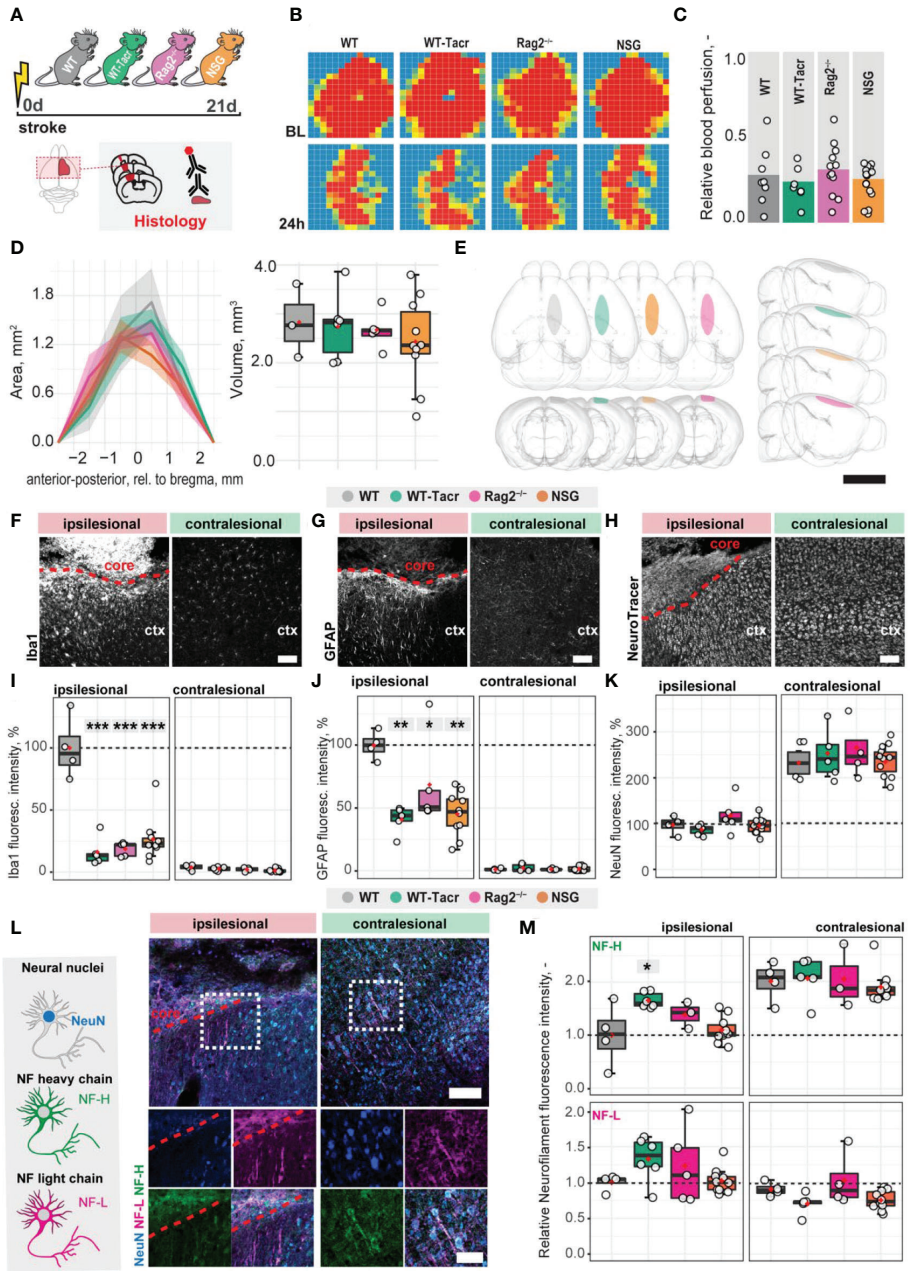

FIGURE 1
Anatomical changes in the stroke pathology of immunosuppressed mice. **(A)** Schematic representation of experimental set-up and groups of mice: C57BL/6J wildtype (WT), tacrolimus immunosuppressed wildtype (WT-Tacr), recombination activating gene 2 deficient mice (Rag2$^{-/-}$) and NOD scid gamma mice (NSG). **(B)** Representative images of relative blood perfusion at baseline and 24 h after stroke induction. **(C)** Quantification of cerebral blood perfusion of the injured hemisphere at 24 h following injury relative to baseline blood perfusion. **(D)** Quantification of stroke area and stroke volume at 21 dpi. **(E)** 3D reconstruction of stroke location within a brain template. Scale bar: 1 cm. **(F)** Representative histological overview of activated microglia/macrophages (Iba1^{+}) **(G)** reactive astrocytes (GFAP^{+}) and **(H)** neural nuclei (NeuroTracer) at the ipsi- and contralesional hemisphere of WT mouse. Scale bar: 100 µm. **(I)** Quantification of relative **(J)** Iba1^{+}, **(J)** GFAP^{+} and **(K)** NeuN signal in the contra- and ipsilesional cortex 21 days following injury. **(L)** Representative histological overview of neural nuclei (NeuN^{+}, blue) and neurofilament light (NF-L, magenta) and heavy chain (NF-H, green) of WT mice. Scale bar: 50 µm. **(M)** Quantification of relative neurofilament light and heavy chain signal in the ischemic and contralesional cortex. Data are shown as mean distributions where the red dot represents the mean. Boxplots indicate the 25% to 75% quartiles of the data. For boxplots: each dot in the plots represents one animal. Line graphs are plotted as mean ± sem. Significance of mean differences between the groups (baseline hemisphere, contralesional hemisphere, and ipsilesional hemisphere) was assessed using Tukey's HSD. Asterisks indicate significance: *P < 0.05, **P < 0.01, ***P < 0.001. ctx, cortex; d, days; BL, baseline; dpi, days post injury; NF, neurofilament.

stroke induction (WT = −72%; WT-Tacr = −76%; Rag2$^{-/-}$ = -69% NSG = −74%, all p > 0.5, Figures 1B, C). Twenty-one days post injury (dpi), brain tissue was collected and revealed comparable stroke volumes and a near complete overlap (> 99%) of affected brain areas in mice from all groups (WT = 2.8 ± 0.7 mm; WT-Tacr = 2.7 ± 0.7 mm^3; Rag2$^{-/-}$ = 2.6 ± 0.4 mm^3; NSG = 2.4 ± 0.3 mm^3, all p = 1, Figures 1D, E; Supplementary Figure 1). To identify stroke-related tissue responses such as inflammation, scarring and neuronal remodelling, we quantified the fluorescence intensities in the contralesional cortex as well as 300-µm cortical peri-infarct regions adjacent to the ipsilesional stroke core three weeks after injury. As expected, inflammatory as well as scarring signals were elevated in the ipsilesional compared to the contralesional cortex (Figures 1F–H). In the peri-infarct areas, microglial activation/macrophage infiltration (Iba1$^+$) and glial scarring (GFAP$^+$) signals were reduced in all immunosuppressed mouse models compared to WT controls (Iba1$^+$: WT-Tacr: −84%, Rag2$^{-/-}$: −82%, NSG: −74%, all p < 0.001; GFAP$^+$: WT-Tacr: −60%, p = 0.002; Rag2$^{-/-}$: −32%, p = 0.015, NSG: −55%; p = 0.002, Figures 1I, J). On the unaffected contralesional side however, no significant differences were detected. The quantity of mature neurons indicated by NeuN$^+$ expression was reduced in the lesioned regions in all groups by 50-60% but no changes have been observed in NeuN$^+$ expression between the groups (Figure 1K). The expression of neurofilament light and heavy chain, major proteins of the neuronal cytoskeleton, was also altered after stroke (Figure 1L). Interestingly, we observed a significantly lower loss of Neurofilament H in WT-Tacr mice (WT-Tacr: +66%, p = 0.02) but no differences in the other immunosuppressed Rag2$^{-/-}$ and NSG mice (Rag2$^{-/-}$: +39%, p = 0.37; NSG = +10%, p = 0.95) compared to WT control (Figure 1M). No changes have also been observed between the groups for Neurofilament L expression in the injured regions (WT-Tacr: +33%, Rag2$^{-/-}$: +23%, NSG: +2%, all p > 0.5, Figure 1M).

Next, we asked if vascular remodelling after stroke may be altered in immunosuppressed mice, because inflammatory responses are known to affect angiogenesis (25). We quantified the vascular density and maturation as well as identified newly formed vessels in the contralesional and ipsilesional cortex three weeks after injury. The overall vascular density, number of branches and total length of the vascular network was increased in the peri-infarct areas in all immunodeficient groups compared to the WT control (Figures 2A–C). Most prominent, Rag2$^{-/-}$ mice had an increase of +70% (p < 0.001) in vascular network density, +215% (p < 0.001) in the number of branches and +79% (p < 0.001) in the vascular length compared to WT mice. Importantly, no vascular differences between the groups were observed in the contralesional brain tissue (all p >0.05, Figure 2D). To confirm that the blood vessels in the ischemic border zone were newly formed, the nucleotide analogue 5-ethynyl-2′-deoxyuridine (EdU) was systemically applied at the peak of poststroke angiogenesis at day 7 (Figures 2E–G). NSG mice had an increase in EdU$^+$ blood vessels per mm^2 in the ischemic border zone compared to WT controls (NSG: 109.4 ± 32.4 mm^{-2}; WT: 39.2 ± 46.9 mm^{-2}; p = 0.03, Figure 2G). As newly formed blood vessels after stroke may be associated with immature vessels that lack stabilizing pericytes (CD13$^+$) we investigated whether CD31 and CD13 markers were colocalized (Figures 2H, I). Pericyte coverage in the ipsilesional site was ≈ 70% lower compared to the contralesional site in all groups but was comparable between the groups in the peri-infarct areas as indicated by the ratio of pericyte covered vasculature (CD13$^+$CD31$^+$) to total vasculature (CD31$^+$) (WT: 0.36 ± 0.15, WT-Tacr: 0.15 ± 0.14, Rag2$^{-/-}$: 0.23 ± 0.12, NSG = 0.23 ± 0.1; all p > 0.4, Figure 2J).

To test if also systemic inflammatory responses were altered following stroke, we measured serum cytokine levels at baseline, 3 and 21 days after stroke using MSD multiplex assays (Figure 2K). We identified that all immunosuppressed mice showed a changed cytokine signature compared to WT mice. The strongest deviation from WT was present in cytokine levels of NSG mice, particularly in the reduced levels of IFNy, IL-2, IL-5 and increased Il-1b, Il-4 (Figure 2K).

Motor performance and gait alterations after stroke are comparable between immunodeficient and wildtype mice

Large damage of the sensorimotor cortex by photothrombotic stroke causes long-term impairment in fore and hindlimb function and locomotion [13,23]. To test whether the anatomical and systemic changes following immunosuppression may affect functional recovery, motor performance and gait analysis was performed at baseline and at repeated intervals after stroke for 21 days (Figure 3A).

We determined in all groups, except of NSG mice, an acute deficit in the rotarod performance indicated by a ≈ 40% shorter time spent on the rod acutely after stroke (3dpi to bl: WT: −48%, p = 0.020, WT-Tacr: −35%, p = 0.048; Rag2$^{-/-}$ = −43%, p = 0.037; NSG = −22%, p = 0.549) with a gradual recovery (Figure 3B). NSG mice had also a striking higher intra-group variability between individual animals in the rotarod task (Figure 3B).

Next, we applied a recently established deep learning algorithm to videos of mice during a voluntary run to identify specific gait changes after stroke (19, 26). We confirmed that the body parts of interest including tail base, iliac crest, hip, back ankles, back toe, shoulder, wrist, elbow, front toe, and head could be reliably detected from three perspectives (Figures 3C, D). The ratio of confident labels (>95% likelihood of detection) to total labels ranged from 93-99% (Figure 3E). Data points that did not pass the likelihood of detection of 95% were excluded. We confirmed that previously identified key parameters (19) were altered in all groups of animals after stroke. For instance, an asymmetric stride pattern describing the non-simultaneous

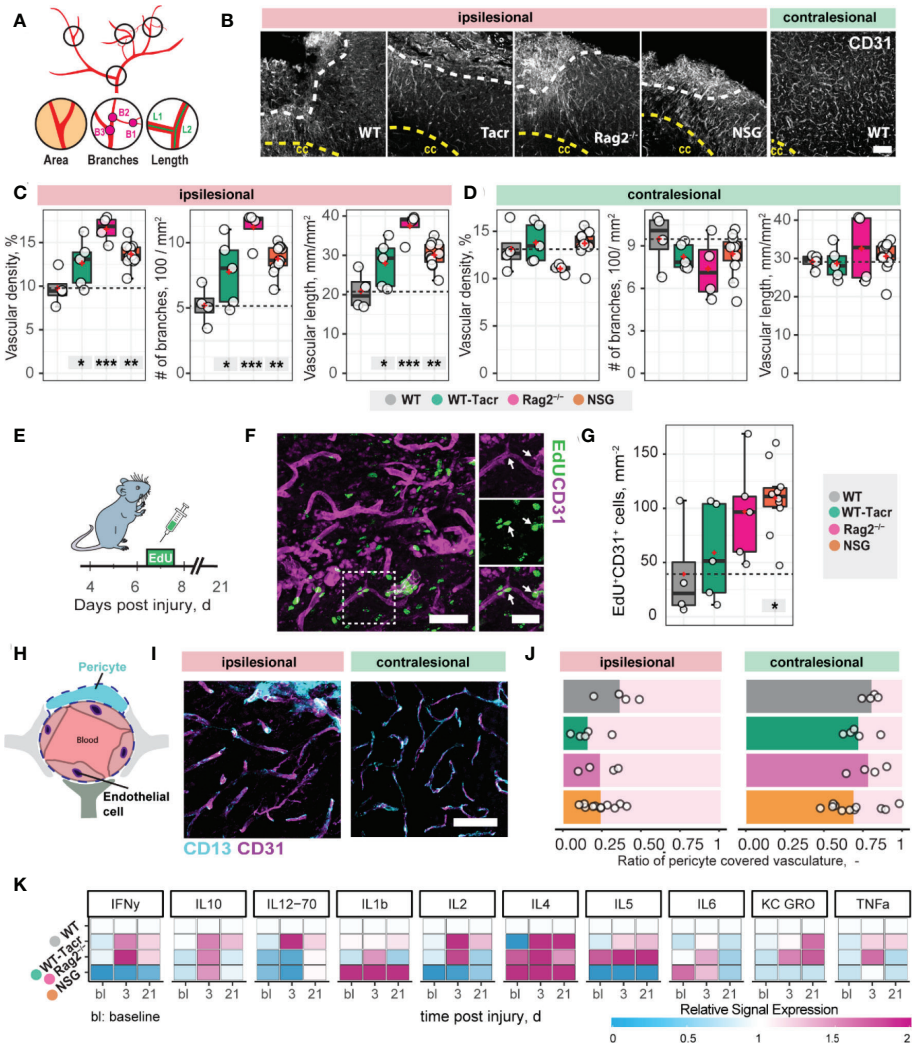

FIGURE 2
Vascular repair and remodelling of immunosuppressed mice after stroke. **(A)** Schematic representation of vascular parameters. **(B)** Representative images of CD31$^+$ vasculature in the ipsi- and contralesional cortex in WT mouse. Scale bar: 100 µm. **(C)** Quantification of vascular density, number of vascular branches and vascular length of ipsi- and **(D)** contralesional cortex 21 dpi. **(E)** Schematic representation of EdU injection to label proliferating cells 7 dpi. **(F)** Representative image of EdU incorporating CD31$^+$ blood vessels in the ipsilesional site at 21 dpi. Arrow shows EdU$^+$ vasculature. **(G)** Quantification of EDU$^+$CD31$^+$ cells per mm^2 in the ipsilesional site. **(H)** Schematic representation of blood brain barrier components. **(I)** Representative image of CD31$^+$ cells covered by CD13$^+$ pericytes in the ipsi-and contralesional site of WT mice at 21 dpi. Scale bar: 25 µm. **(J)** Quantitative ratio of vasculature covered by pericytes in ipsi- and contralesional site. **(K)** Blood plasma cytokine analysis of pro-inflammatory factors at baseline, 3 and 21 dpi. Data are shown as mean distributions where the red dot represents the mean. Boxplots indicate the 25% to 75% quartiles of the data. For boxplots: each dot in the plots represents one animal. Significance of mean differences between the groups (baseline hemisphere, contralesional hemisphere, and ipsilesional hemisphere) was assessed using Tukey's HSD. Asterisks indicate significance: *P < 0.05, **P < 0.01, ***P < 0.001. ctx, cortex; cc, corpus callosum; bl, baseline; d, days.

placement of opposed front and back toes, was observed acutely after stroke in all groups (3dpi: all $p < 0.05$) (Figure 3F). The asymmetric stride pattern reversed to baseline with time in all groups (Figure 3F). Also, we detected comparable irreversible gait changes in all groups such as a reduced range of motion in the contralesional left front paw (3dpi to bl: WT: −1.2 ± 1.4 mm, WT-Tacr: −0.9 ± 0.5 mm, Rag2$^{-/-}$: −0.8 ± 0.6 mm, NSG: −0.7 ± 0.3 mm, all $p < 0.05$) that gradually recovered but did not reach baseline levels throughout the time course (21dpi to bl: WT: −1.0 ± 0.8 mm, WT-Tacr: −0.5 ± 0.3 mm, Rag2$^{-/-}$: −0.5 ± 0.4 mm, NSG: −0.4± 0.3 mm, all $p < 0.05$, Figure 3G).

To detect fine motor deficits, we additionally performed a deep learning assisted irregular ladder rung test and quantified the ratio of stepping errors (19, 27). We achieved a high ratio of confident labels of 92-93% (Figure 3H) and excluded all data points that did not pass the confidence threshold. Errors

10.3389/fimmu.2022.1080482

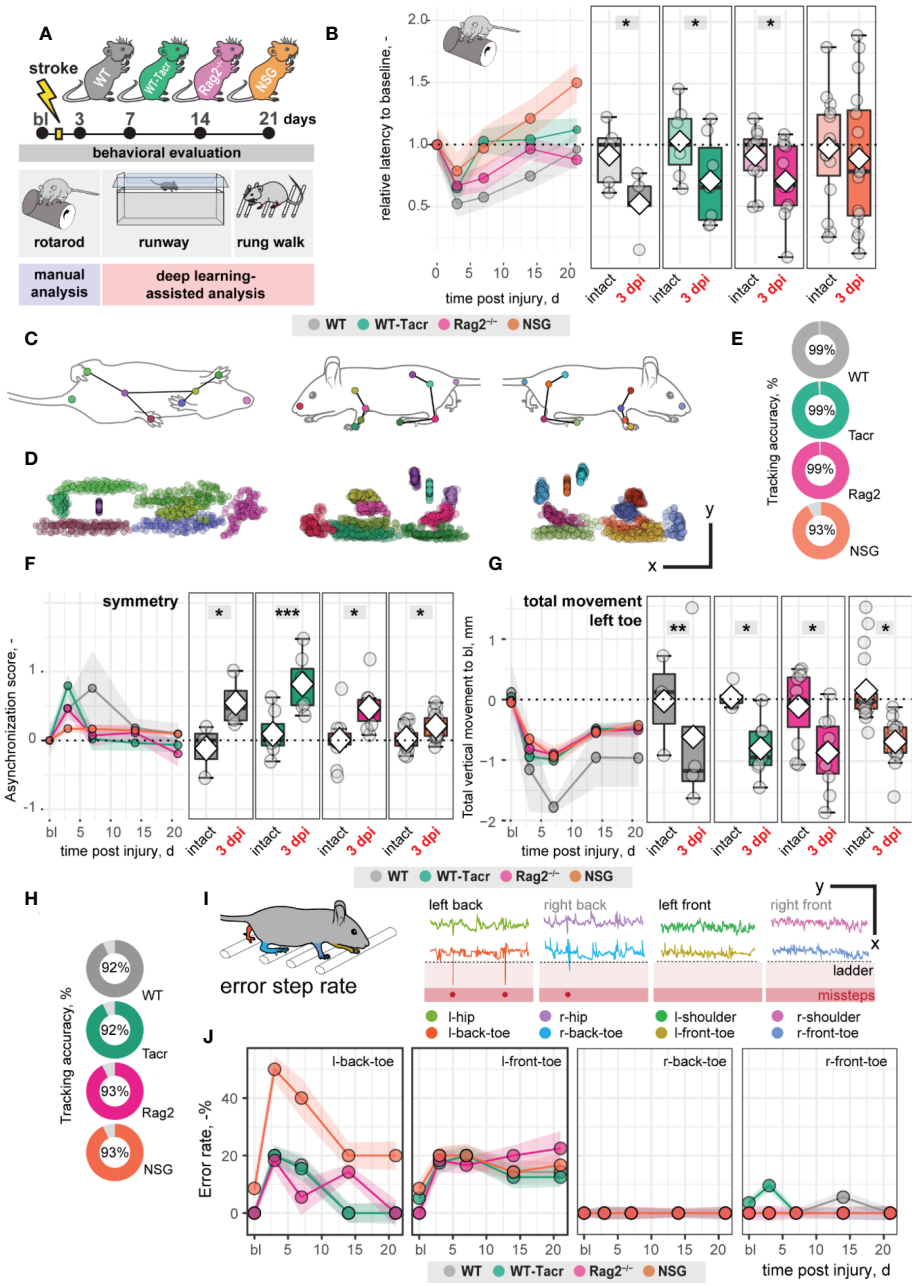

FIGURE 3
Gait and motor performance of immunosuppressed mice after stroke. **(A)** Schematic time course of experimental interventions. **(B)** Rotarod test showing the relative latency at baseline and 3, 7, 14, 21 dpi. **(C, D)** Walking profile normalized to the hip coordinates of randomly selected non-injured mice. Each dot represents an anatomical landmark. **(E)** Likelihood of a confident labelling for individual body parts in the runway. **(F)** Ratio of asynchronization at baseline, 3, 7, 14, 21 dpi. (0 = ideal synchronization). **(G)** Absolute vertical movement of left (contralesional) toe at baseline and 3, 7, 14, 21 dpi. **(H)** Likelihood of a confident labelling for individual body parts in the ladder rung test **(I)** Representation of an individual ladder rung walk of WT mice at 3 dpi, selected body parts are tracked including hip, back toe, shoulder, and front toe. **(J)** Time course of error rate during ladder rung test in the individual paws. Data are shown as mean distributions where the white dot represents the mean. Boxplots indicate the 25% to 75% quartiles of the data. For boxplots: each dot in the plots represents one animal. Line graphs are plotted as mean ± sem. For line graphs: the dots represent the mean of the data. Significance of mean differences between the groups was assessed using repeated ANOVA with post-hoc (emmeans) analysis. Asterisks indicate significance: *P < 0.05, **P < 0.01, ***P < 0.001.

were defined if the front or back toe dropped lower than the ladder height due to a misstep or a slip (Figure 3I). All groups of mice showed acutely increased error rates that were most pronounced in the contralateral left back (3dpi: WT: +20%, WT-Tacr: +20%, Rag2$^{-/-}$: +18%, NSG: +50%, all $p < 0.05$) and left front toe (3dpi: WT: +20%, WT-Tacr: +10%, Rag2$^{-/-}$: +18%, NSG: +18%, all $p < 0.05$) compared to baseline misstep rates (Figure 3J). NSG mice tend to have a higher overall error rate, most prominent in the left back toe after injury (Figure 3J).

In sum, the motor performance and gait alterations between immunosuppressed and WT mice were largely comparable. NSG mice deviated in few behavioral readouts from the functional deficits in WT mice. However, the data indicates that the observed anatomical and systemic changes did not lead to major changes in functional recovery between the groups in a time course of three weeks.

Immunodeficient mice have distinct gene expression profile after stroke

To further dissect molecular changes in the ischemic brain, we performed RNA sequencing of ischemic brain tissue from immunodeficient and WT mice (Figure 4A). Three weeks after stroke, the majority of the significantly altered genes were upregulated in all groups of mice (Figure 4B). Principal component analysis and a heatmap of the most differentially expressed genes demonstrate a clear separation between naïve mice from their stroked littermates (Figures 4B, C). As expected, we also observed a strong separation between non-stroked and stroked NSG mice to the other groups presumably because of their different background (NSG mice have a NOD-background; all other groups of mice had a C57Bl/J background, Supplementary Figures 2A, B). Most enriched gene sets between non-stroked NSG and WT mice affected pathways related to the adaptive immune system (Supplementary Figure 3).

After stroke, there was an overlap of 32% of the top$_{1000}$ upregulated genes but only 3% of the top$_{1000}$ downregulated genes in all groups of mice compared to their respective non-stroke controls (Figure 4D). WT-Tacr mice showed the closest gene expression profile to WT; and NSG mice deviated most from WT gene expression after stroke. Still, many of the top$_{30}$ upregulated genes were present in all groups of animals such as Mmp12, CD5l, Mmp3, C3, Apoc4, Tgm1, Clec7a, Lcn2 and Lilr4b. (Figure 4E). However, no top$_{30}$ downregulated genes were present in all groups (Supplementary Figure 4).

The majority of the enriched pathways in all groups after stroke were related to the innate and adaptive immune system e.g., leukocyte migration, positive regulation of cytokine production, and regulation of immune effector process (Figures 5A, B). While 80% of the top 10 enriched pathways after stroke overlapped between WT-Tacr, Rag2$^{-/-}$ and WT, only 40% of pathways were identical between NSG and WT (Figures 5A, B).

Next, we analysed gene expression differences among the immunosuppressed stroked groups that were normalized for their respective non-stroked genotype to WT stroked mice (Figure 6A). The majority of differentially expressed genes in the different immunosuppressed stroked mice were unique (Figure 6B). As expected, the enriched pathways were mostly associated with inflammatory responses such as, innate immune response, regulation of cytokine production and lymphocyte activation (Supplementary Figures 5A–C).

Interestingly, a second cluster of pathways that was enriched in immunosuppressed stroked mice compared to WT stroked mice was linked to angiogenic responses (Figures 6C, D). Surprisingly, these pathways were highly positively enriched in NSG and Rag2$^{-/-}$ mice (Figure 6D) but negatively enriched in WT-Tacr mice at 3 weeks after injury (Figure 6D), indicating a reduced angiogenic response at 21 dpi in tacrolimus immunosuppressed mice.

In sum, we observed distinct gene expression and pathway enrichment changes between the immunosuppressed and WT mice three weeks after stroke. The strongest deviation was observed in NSG mice. Apart from inflammatory responses, angiogenesis related genes were most significantly altered.

Delayed immunosuppression results in altered stroke progression that more closely resembles wildtype pathology

Transient angiogenic responses have been previously reported after stroke (28) and may explain the enhanced vascular repair mediated by tacrolimus with concomitant downregulation of angiogenesis related genes and pathways three weeks after stroke. We therefore asked if the anatomical and gene expression differences in the stroke pathology between tacrolimus treated and WT mice could be reduced by delaying the tacrolimus administration by one week. This time window was chosen to mimic a clinically relevant scenario. In most studies, cell transplantation usually happens around one week after injury to avoid the very acute and hostile phase; and immunosuppression will be applied shortly before delivery (29). To test this hypothesis, we induced a photothrombotic stroke in (1) WT (2), acute (0 dpi) tacrolimus immunosuppressed mice (WT-Tacr$_{acute}$) and (3) delayed (7 dpi) tacrolimus immunosuppressed mice (WT-Tacr$_{delayed,}$ Figure 7A).

First, we performed brain tissue analysis of inflammatory and scarring responses at 21 dpi. (Figure 7B). Histological analysis in the peri-infarct region revealed an increased glial scar signal (GFAP^{+}) in WT-Tacr$_{delayed}$ (+21% to WT) compared to WT-Tacr$_{acute}$ (−58% to WT) mice ($p = 0.025$, Figure 7C).

10.3389/fimmu.2022.1080482

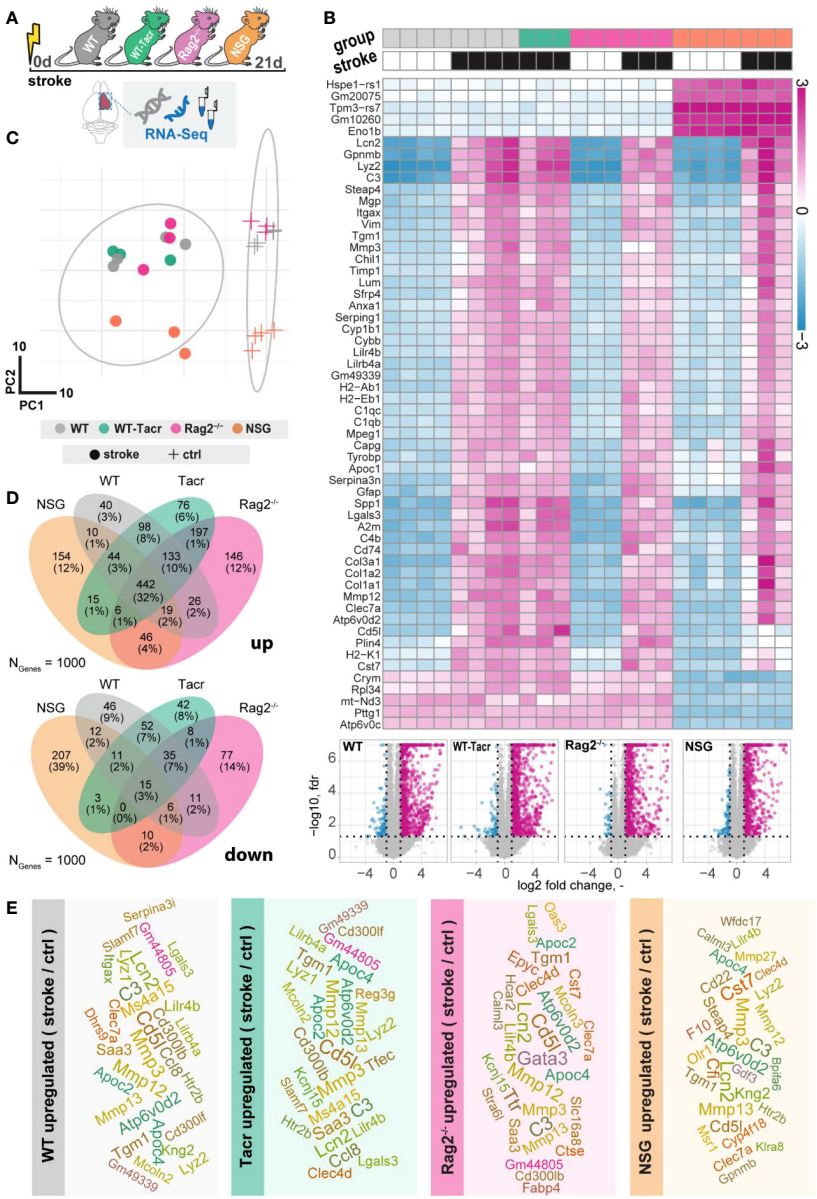

FIGURE 4
Gene expression changes in immunodeficient mouse models after stroke. **(A)** Schematic overview of experimental time course and groups of mice: C57BL/6J wildtype (WT), tacrolimus immunosuppressed wildtype (WT-Tacr), recombination activating gene 2 deficient mice (Rag2$^{-/-}$) and NOD scid gamma mice (NSG). **(B)** Heatmap of most differentially expressed genes and volcano plot of stroked (black boxes) to non-stroked (white boxes) WT, WT-Tacr, Rag2$^{-/-}$, NSG mice. **(C)** Principal component analysis, circles indicate stroked mice, crosses indicate non-stroked mice. **(D)** Venn diagram of common and differentially expressed top1000 genes in all groups of immunodeficient mice. **(E)** List of top 30 upregulated genes after stroke in the respective group of immunodeficient mice, font size represents strength of upregulation.

Inflammatory Iba1$^+$ levels were also amplified in WT-Tacr$_{delayed}$ (−25% to WT) compared to WT-Tacr$_{acute}$ (−60% to WT) mice ($p = 0.04$, Figure 7D). The number of newly formed Iba1$^+$ cells (Iba1$^+$EdU$^+$) around the stroke was increased between Tacr$_{delayed}$ (+1% to WT) compared to WT-Tacr$_{acute}$ (−59% to WT) mice ($p = 0.001$, Figure 7E), indicating overall that post-stroke scarring and inflammation in WT-Tacr$_{delayed}$ mice is closer to WT tissue responses.

No differences have been observed in the stroke volumes between the groups (WT-Tacr$_{acute}$ = 2.85 ± 0.62 mm^3, WT-

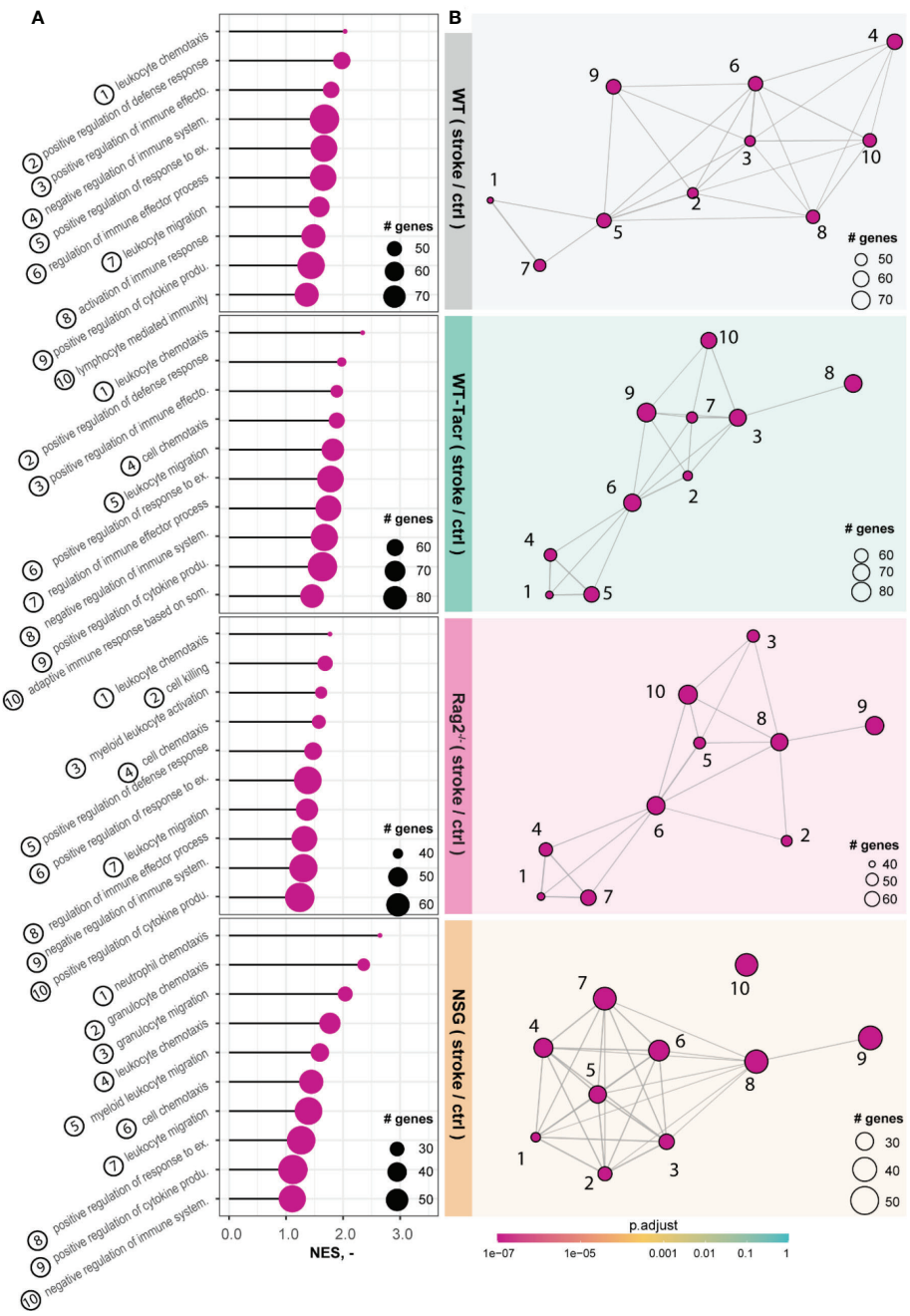

FIGURE 5
Gene set enrichment analysis in stroked mice. **(A)** Lollipop plot and **(B)** enrichment map (EMAP) of top 10 pathways enriched in stroked C57BL/6J wildtype (WT), tacrolimus immunosuppressed wildtype (WT-Tacr), recombination activating gene 2 deficient mice (Rag2$^{-/-}$) and NOD scid gamma mice (NSG). mice compared to their non-stroked littermates. Size of dots represents the number of genes in the pathway and color of dots represents adjusted p value.

$Tacr_{delayed}$ = 3.31 ± 0.61 mm^3, WT = 3.30 ± 0.71 mm^3, p >0.05, Figure 7F). Additionally, delayed tacrolimus administration reduced the vascular density (−35%, p = 0.048) and number of branches (−60%, p = 0.032) but did not influence the number of newly formed blood vessels compared to WT-$Tacr_{acute}$ ($CD31^+EDU^+$: WT-$Tacr_{acute}$ = 56.3 ± 3.2 cells/mm^2, WT-$Tacr_{delayed}$ = 59.3± 8.1 cells/mm^2, p > 0.05, Figures 7G–I). The ratio of pericyte coverage of total vasculature remained unchanged in the peri-infarct region between the groups (WT-$Tacr_{acute}$ = 0.25 ± 0.15, WT-$Tacr_{delayed}$ = 0.29 ± 0.08, p > 0.05, Figures 7J).

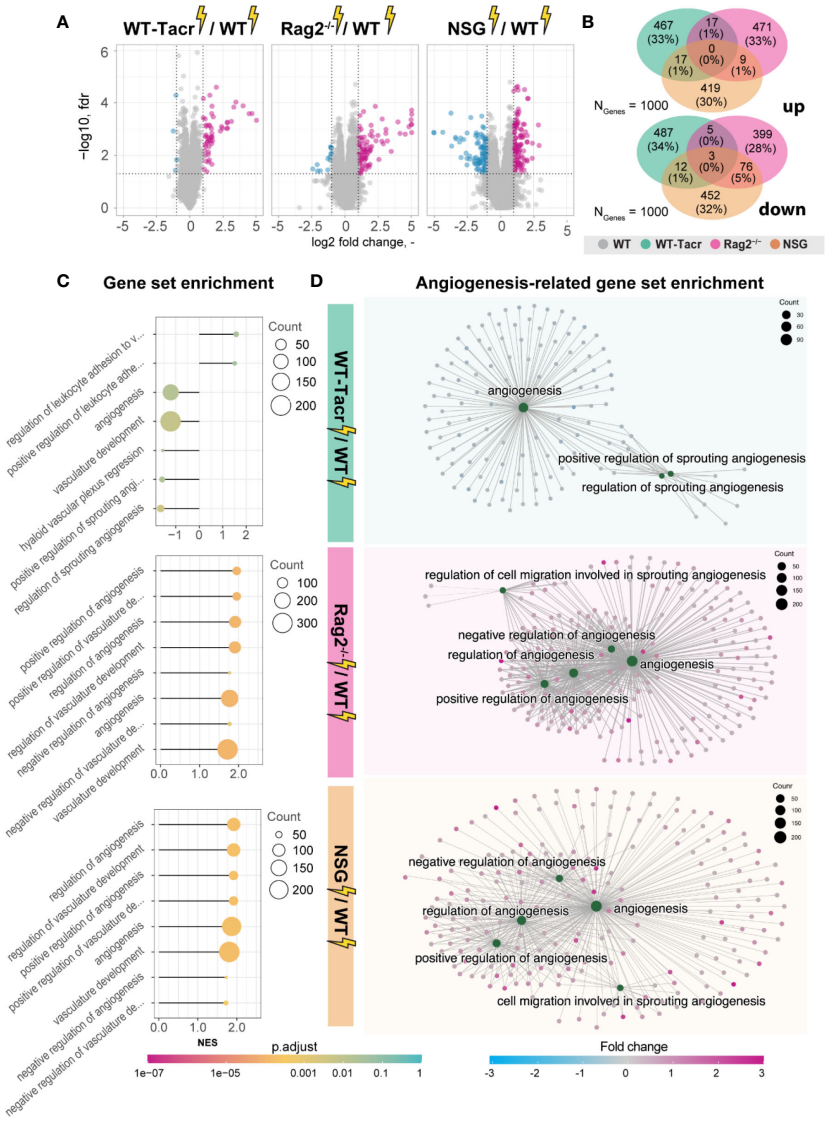

FIGURE 6
Gene expression changes and gene set enrichment between immunodeficient stroked mice and wildtype stroke pathology. **(A)** Volcano plot of differentially expressed genes identified between immunodeficient stroked mice and wildtype stroked mice. Magenta dots indicate upregulated gene expression, and blue dots indicate downregulated gene expression. **(B)** Venn diagram of common and differentially expressed top1000 genes in all groups of stroked immunodeficient mice. **(C)** Gene set enrichment shown in a lollipop plot in immunodeficient stroked mice compared to wildtype stroked mice. Size of dots represents the number of genes in the pathway and color of dots represents adjusted p value. **(D)** CNET plot describing linkages of genes and biological processes for angiogenesis-related pathways. Size of dots represents the number of genes in the pathway and color of dots represents fold changes.

Interestingly, gene expression analysis of ischemic brain tissue reveals an increased gene set enrichment for cytokine production and pro-angiogenic responses in WT-Tacr$_{delayed}$ mice (Figures 7K–M, Supplementary Figure 6). This may indicate that the increased angiogenic responses in WT-Tacr$_{acute}$ mice may be transient and/or that delayed immunosuppression shifts the angiogenic response towards a later timepoint after stroke.

These data indicate that a 7-day delayed pharmacological immunosuppression with tacrolimus shifts the course of stroke more towards the WT pathology.

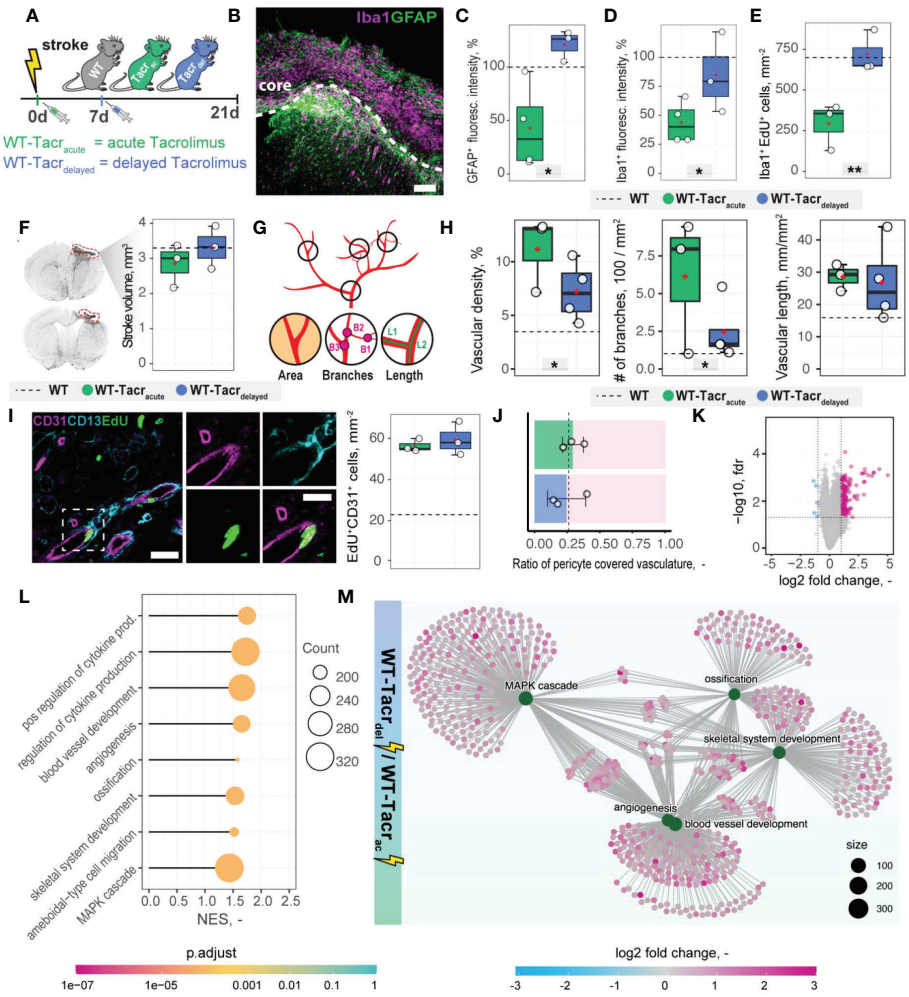

FIGURE 7
Anatomical and gene expression changes in the stroke pathology of acute and delayed pharmacological immunosuppression. **(A)** Schematic representation of experimental set-up and groups of mice: C57BL/6J wildtype (WT), acute (0 dpi) tacrolimus immunosuppressed wildtype (WT-Tacr$_{acute}$), and delayed tacrolimus (7 dpi) immunosuppressed wildtype (WT-Tacr$_{delayed}$) mice. **(B)** Representative image of Iba1$^+$ inflammatory cells (Iba1, magenta) and reactive astrocytes (GFAP$^+$, green) in the ipsilesional cortex at 21 dpi. Scale bar: 100 µm. **(C)** Quantification of GFAP$^+$, and **(D)** Iba1$^+$ fluorescence intensity in the peri-infarct regions at 21 dpi. **(E)** Quantification of Iba1$^+$ EDU$^+$ cells in per-infarct region. **(F)** Stroke volume quantification at 21 dpi. **(G)** Schematic overview of vascular parameters **(H)** Quantification of vascular density, number of vascular branches and vascular length in the peri-infarct region at 21 dpi. **(I)** Representative image of newly formed blood vessels (CD31$^+$, magenta) covered by pericytes (CD13$^+$, cyan) and incorporating a nucleotide analogue that was injected at 7 dpi (EdU$^+$, green). Scale bars: Overview: 20 µm. Closeup: 10 µm. Quantification of EdU$^+$CD31+ cells per mm^2 in the peri-infarct region at 21 dpi. **(J)** Pericyte coverage assessed by the ratio of CD13$^+$/CD31$^+$ cells at 21dpi. **(K)** Volcano plot of gene expression differences between delayed and acute immunosuppressed mice. **(L)** Lollipop chart of gene set enrichment terms for "biological process" in delayed tacrolimus immunosuppressed mice. **(M)** Visualization of top five gene set enrichments terms with respective genes. Data are shown as mean distributions where the white dot represents the mean. Boxplots indicate the 25% to 75% quartiles of the data. For boxplots: each dot in the plots represents one animal. Dotted line represents mean of WT mice. *P < 0.05, **P < 0.01.

Grafted human NPCs survive long-term in genetically immunodeficient Rag2$^{-/-}$ and NSG mice

Next, we evaluated long-term survival of intracerebrally transplanted grafts in (1) WT mice (2) WT mice that were continuously immunosuppressed with tacrolimus (WT-Tacr); and genetically immunodeficient (3) Rag2$^{-/-}$ and (4) NSG mice (Figure 8A). As a cell source, we used recently generated human neural progenitor cells (NPCs) derived from induced pluripotent stem cells (iPSCs) (20). The NPCs were transduced with a dual reporter consisting of a bioluminescent firefly luciferase (rFluc) and a fluorescent eGFP. A successful transplantation in all groups of mice was confirmed by comparable levels of luciferase signal directly after transplantation (Figures 8B, C). As expected, we observed the absence of the graft in WT mice 14

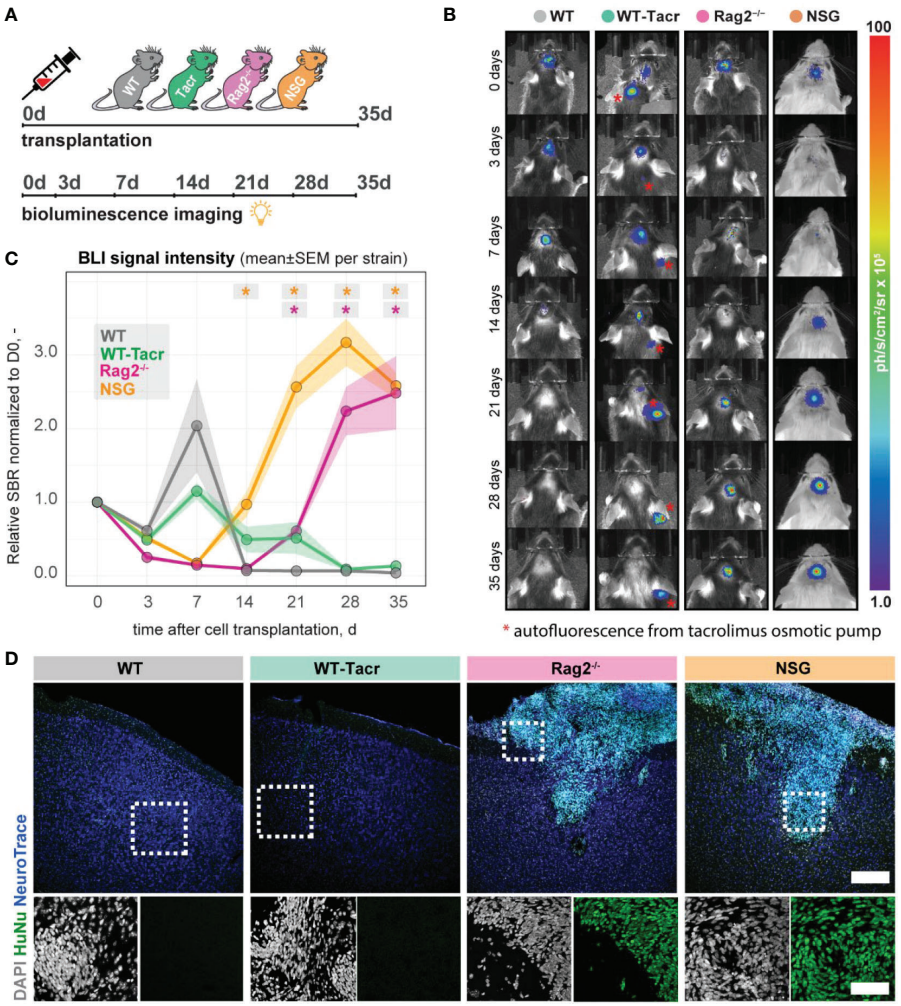

FIGURE 8
In vivo tracking of transplanted NPCs in immunodeficient mouse models. **(A)** Schematic overview of experimental time course **(B)** Representative bioluminescence images of luciferase-expressing NPCs transplanted in immunodeficient and WT mouse models at 0, 3, 7, 14, 21, 28, 35 days after transplantation. **(C)** Bioluminescence signal intensity over time after transplantation. **(D)** Representative images of transplanted human NPCs 35 days after transplantation stained with anti-human nuclei antibody (HuNu, green), NeuroTrace (fluorescent Nissl, blue) and counterstained with DAPI (grey). Scale bar: 50 um. Line graphs are plotted as mean ± sem. d, days; BLI, bioluminescence imaging; sbr = signal background ratio; ph, photons; sr, steradian. *P < 0.05.

days after transplantation presumably due to xenogenic immune rejection. In contrast, the immunosuppressed mice showed all a prolonged graft survival. However, only in Rag2$^{-/-}$ and NSG mice, we observed a strong bioluminescence signal during the entire time course of more than 1 month after transplantation (Figures 8B, C). After 35 days, surviving graft cells were identified using human-specific antibodies in brain sections of NSG and Rag2$^{-/-}$ mice but were not detectable in WT and WT-Tacr mice (Figure 8D).

These data suggests that genetic immunosuppression is more reliable for graft survival, especially in long-term studies.

Discussion

Immunodeficient mouse models are commonly used in preclinical stroke research to evaluate e.g., the efficacy of human cell-based therapies. As changes to the inflammatory responses after stroke may considerably alter overall stroke outcome, it is important to understand the stroke pathology of commonly used immunodeficient mouse models. Here, we identified distinct anatomical, gene expression and systemic changes in the stroke pathology between pharmacologically and genetically immunodeficient mice after stroke. These changes were most prominent in NSG mice that have deficiencies in the innate and

adaptive immune system and less pronounced in Rag2$^{-/-}$ and pharmacologically immunosuppressed mice with tacrolimus. The changes mainly affected the inflammatory and vascular responses after stroke. However, long-term graft survival was most consistent in NSG and Rag2$^{-/-}$ mice.

A variety of cell types are responsible for postinjury inflammation in the brain after stroke. These cells may locally arise from resident microglia and astrocytes or are recruited from the peripheral blood circulation. Especially cells from the innate immune system such as neutrophils and monocytes have been extensively studied in experimental stroke (10). It is assumed that these cells may predominantly be responsible for the secondary inflammatory injury by releasing proinflammatory factors, reactive oxygen species (ROS) and proteases (30). Although neutrophils and monocytes constitute most of the remaining mouse immune cells in the immunodeficient NSG mice, dendritic cells and macrophages have been described to be detective because of the genetic NOD background (31). We further observed an altered pattern in serum cytokines in NSG mice. These findings are directly in line with previous findings describing deficiencies of NSG mice in cytokines release (31). These deficiencies in the cytokine and innate immune system may explain the strong deviation of the NSG gene expression profile after stroke to the other mouse models with intact innate immune systems. These differences also persisted after correcting for the genetic NOD background.

In contrast to the innate immune system, the role of the adaptive immune system after stroke is less clear. B and T lymphocytes are scarce in the CNS but can be found in the postischemic brain, which may be caused by cytokine signalling from the brain to the periphery or by the compromised blood-brain barrier after stroke. For instance, infiltration and activation of B and T lymphocytes in the brain have been associated with increased cognitive decline in an experimental stroke model and blocking adaptive immune responses has been suggested as a potential therapeutic target after stroke (32). Both, the here used Rag2$^{-/-}$ as well as tacrolimus immunosuppressed mice have deficiencies in the adaptive immune system and are lacking matured B- and T- lymphocytes (Rag2$^{-/-}$) or respectively suppressed T-lymphocyte activation (tacrolimus). The lack of adaptive immune response caused a marked change in the brain tissue pathology as well as in the inflammatory and angiogenic gene expression signature. The main advantage in using pharmacological immunosuppression is that their time point of application can be chosen according to the experimental set-up. For instance, most studies using human cell-based strategies for stroke avoid the very acute phase for cell transplantations because of the hostile environment in the damaged brain regions; and choose transplantation around one week after stroke induction (3, 29). This set-up would facilitate to immunosuppress mice shortly before cell transplantation and allow a natural stroke progression for the first week. Tacrolimus has also been already successfully used in clinics for cell-based therapies in stroke and Parkinson's and has therefore direct translational potential (33, 34). On the other hand, genetic mouse models are easier to handle and show generally a more consistent survival of the graft, as we have also observed in this study. Alternatively, future studies may use immune deficient mice such as NSG or Rag2$^{-/-}$ Il2$^{-/-}$ and CD47$^{-/-}$ (Tripple KO) mice that are reconstituted with a humanised immune system and HLA-matched to the donor cells. Humanised mice may show a closer pathology to the WT (35), although these mice still have several limitations, including limited lifespan, incomplete human immune function and graft-versus-host disease etc (36).

Contrary to previous findings that described a reduced stroke volume of several immunodeficient mice (37, 38), we did not observe anatomical changes in stroke outcome compared to immunocompetent WT mice. One reason for these inconsistencies may be the time point of stroke volume evaluation. Many studies evaluated stroke volume at 24 h after stroke induction to investigate acute effects of the stroke pathology. However, we were interested in long-term effects as regenerative cell therapies may have a therapeutic time course of weeks to months. At three weeks following stroke, major structural reorganisations occur, pushing the corpus callosum towards the brain surface, which in turn can affect the stroke volume estimates (39).

Findings from a growing number of preclinical and clinical studies suggest that post-stroke angiogenesis is a key restorative process for tissue preservation and repair, leading to improved outcome (13, 24, 40, 41). In our study, we observed marked upregulation of vascular repair in the peri-infarct regions of WT-Tacr, Rag2$^{-/-}$ and NSG mice compared to immunocompetent WT mice 21 days after stroke. The improved vascular repair in histological brain sections was abolished if immunosuppressive tacrolimus was administered delayed at 7 dpi. As post-stroke angiogenesis starts from 3 dpi (42) and depends on the acute inflammatory and cytokine microenvironment in the injured brain, a delayed immunosuppression by 1 week seems to ensure that levels of vascular repair are more similar to that of control WT mice.

However, the pro-angiogenic responses in continuously immunosuppressed mice did not lead to improved functional outcome in our set-up. One explanation for the absence of improved functional recovery in immunodeficient mice could be that the observed angiogenesis only occurred transiently, as has been described previously (28, 42). The downregulation of angiogenesis-related genes at 21 dpi in the acutely tacrolimus immunosuppressed mice compared with mice receiving tacrolimus treatment 7 dpi further suggests the transient nature of post-stroke angiogenesis resulting from immunosuppression. Additionally, it is well known that the growth of new capillaries carries the risk for immature vessel formation, which may enhance haemorrhagic transformation and BBB damage; and mature vessels are associated with better functional outcomes (24, 43). We observed in all groups of animals a low pericyte

coverage in the peri-infarct regions that tend to decrease especially in Rag2$^{-/-}$ animals, which had the highest vascular density in the injured brain regions. These changes in vascular responses following stroke are important to consider when evaluating the effects of cell-based therapies in immunosuppressed mice, as vascularization is often one of the important readouts to observe the effectiveness of a cell therapy (44, 45).

One limitation of our study is that we used mice with different genetic backgrounds. Although we corrected the gene expression findings to the background of the mice, there might be confounding effects that are difficult to account for. For instance, mice with different backgrounds may have variable weight and size effects, time required to learn behavioral tasks or natural stroke recovery due to cerebral vascular architecture (46, 47). We used two cohorts of animals for the gene expression and anatomical studies after stroke, which may add to the variability of the data. Future studies may profit from recent advances in spatially resolved transcriptomics approaches that could directly associate gene expression signatures to anatomical changes in the same animal (48). However, the natural temporal delay in gene expression and anatomical and functional recovery may complicate understanding of complex processes *in vivo*, such as whether angiogenesis occurs transiently after stroke.

Microglia, the resident immune cells of the central nervous system (CNS), become activated as a response to stroke and accumulate in damaged brain areas. In mice, activated microglia obtain an amoeboid morphology, thus becoming indistinguishable from infiltrating macrophages (10, 49). Iba-1, the marker used in this study, is expressed by both cell types, making it difficult to determine the ratio of residual activated microglia and infiltrating macrophages. Future studies may consider using additional cell markers, such as TMEM119 or P2RY12, to better distinguish between cell populations following brain injury (49).

The pharmacological immunosuppression with tacrolimus occurred *via* osmotic mini pumps that ensured a constant delivery rate previously validated in other studies (50–52); however, we do not know the spatiotemporal distribution and delivery efficacy of tacrolimus to the injured brain regions, an irregular delivery may influence the survival of the grafted cells. Furthermore, tacrolimus may additionally influence the survival of the graft independent of the calcineurin-pathway (53). Future studies may compare different routes and different time points of delivery for tacrolimus, such as daily i.p. injections instead of using osmotic mini pumps, as this has already been shown to provide long-term cell survival in animal stroke models (3). Additionally, alternative immunosuppressive regimes should be investigated to optimize graft survival.

Conclusion

In sum, our study identifies key changes in anatomy, physiology, and gene expression of popular immunosuppressed mouse models after stroke. We found significantly decreased microglial activation/macrophage infiltration and glial scarring signals in immune-suppressed animals in and around the stroked area three weeks after injury compared to immune-competent WT animals. The overall vascular density, number of branches and total length of the vascular network was increased in the peri-infarct areas in all immunodeficient groups compared to the WT, most prominent in Rag2$^{-/-}$ animals. Transcriptomic analysis of stroked tissue revealed the strongest deviation from WT was observed in NSG mice affecting immunological and angiogenic pathways. Pharmacological immunosuppression resulted in the least variation in gene expression compared with the WT group. These changes in stroke progression should be considered when investigating molecular mechanisms of stroke or evaluating therapies that require immunosuppression.

Data availability statement

Transcriptomic raw data are available to readers *via* Gene Expression Omnibus with identifier GSE208605. All other raw data are available upon request.

Ethics statement

The animal study was reviewed and approved by Veterinarian Office of the Canton of Zurich (license: 209/2019).

Author contributions

RW, CT, and RR designed the study. RW, RR prepared the Figures and wrote the manuscript. RW, GM, PP, and RR carried out the experiments. RW, GM, PP, CT, and RR proofread and revised the manuscript. All authors read and approved the final manuscript. All authors contributed to the article and approved the submitted version.

Funding

The authors acknowledge funding from Mäxi Foundation, Swiss 3R Competence Center (OC-2020-002) and the Swiss National Science Foundation (CRSK-3_195902).

Acknowledgments

The authors thank the Functional Genomics Center Zurich (FGCZ) for support with the RNASeq data.

Conflict of interest

The authors declare that the research was conducted in the absence of any commercial or financial relationships that could be construed as a potential conflict of interest.

Publisher's note

All claims expressed in this article are solely those of the authors and do not necessarily represent those of their affiliated organizations, or those of the publisher, the editors and the reviewers. Any product that may be evaluated in this article, or claim that may be made by its manufacturer, is not guaranteed or endorsed by the publisher.

Supplementary material

The Supplementary Material for this article can be found online at: https://www.frontiersin.org/articles/10.3389/fimmu.2022.1080482/full#supplementary-material

References

1. GBD 2016 Stroke Collaborators. Global, regional, and national burden of stroke, 1990-2016: a systematic analysis for the global burden of disease study 2016. *Lancet Neurol* (2019) 18:439–58. doi: 10.1016/S1474-4422(19)30034-1

2. Krause M, Phan TG, Ma H, Sobey CG, Lim R. Cell-based therapies for stroke: Are we there yet? *Front Neurol* (2019) 10. doi: 10.3389/fneur.2019.00656

3. Wang Y, Zhao Z, Rege SV, Wang M, Si G, Zhou Y, et al. 3K3A-APC stimulates post-ischemic neuronal repair by human neural stem cells in mice. *Nat Med* (2016) 22:1050–5. doi: 10.1038/nm.4154

4. Lam J, Lowry WE, Carmichael ST, Segura T. Delivery of iPS-NPCs to the stroke cavity within a hyaluronic acid matrix promotes the differentiation of transplanted cells. *Adv Funct Mater* (2014) 24:7053–62. doi: 10.1002/adfm.201401483

5. Andres RH, Horie N, Slikker W, Keren-Gill H, Zhan K, Sun G, et al. Human neural stem cells enhance structural plasticity and axonal transport in the ischaemic brain. *Brain J Neurol* (2011) 134:1777–89. doi: 10.1093/brain/awr094

6. Moshayedi P, Nih LR, Llorente IL, Berg AR, Cinkornpumin J, Lowry WE, et al. Systematic optimization of an engineered hydrogel allows for selective control of human neural stem cell survival and differentiation after transplantation in the stroke brain. *Biomaterials* (2016) 105:145–55. doi: 10.1016/j.biomaterials.2016.07.028

7. Rust R, Tackenberg C. Stem cell therapy for repair of the injured brain: Five principles. *Neuroscientist* (2022) 1–7. doi: 10.1177/10738584221110100

8. Wong CHY. Effects of stroke beyond the brain. *Nat Rev Immunol* (2019) 19:719–9. doi: 10.1038/s41577-019-0234-4

9. Meisel C, Meisel A. Suppressing immunosuppression after stroke. *N Engl J Med* (2011) 365:2134–6. doi: 10.1056/NEJMcibr1112454

10. Jayaraj RL, Azimullah S, Beiram R, Jalal FY, Rosenberg GA. Neuroinflammation: friend and foe for ischemic stroke. *J Neuroinflammation* (2019) 16:142. doi: 10.1186/s12974-019-1516-2

11. Belizário JE. Immunodeficient mouse models: An overview. *Open Immunol J* (2009) 2:79–85. doi: 10.2174/1874226200902010079

12. Hwang JW, Myeong SH, Lee N-H, Kim H, Son HJ, Chang JW, et al. Immunosuppressant drugs mitigate immune responses generated by human mesenchymal stem cells transplanted into the mouse parenchyma. *Cell Transpl* (2021) 30:1–13. doi: 10.1177/09636897211019025

13. Rust R, Grönnert L, Gantner C, Enzler A, Mulders G, Weber RZ, et al. Nogo-a targeted therapy promotes vascular repair and functional recovery following stroke. *Proc Natl Acad Sci* (2019) 116:14270–9. doi: 10.1073/pnas.1905309116

14. Labat-gest V, Tomasi S. Photothrombotic ischemia: a minimally invasive and reproducible photochemical cortical lesion model for mouse stroke studies. *J Vis Exp.* (2013) (76):50370. doi: 10.3791/50370

15. Rust R, Kirabali T, Grönnert L, Dogancay B, Limasale YDP, Meinhardt A, et al. A practical guide to the automated analysis of vascular growth, maturation and injury in the brain. *Front Neurosci* (2020) 14:244/full. doi: 10.3389/fnins.2020.00244/full

16. Rust R, Grönnert L, Dogançay B, Schwab ME. A revised view on growth and remodeling in the retinal vasculature. *Sci Rep* (2019) 9:3263. doi: 10.1038/s41598-019-40135-2

17. Robinson MD, McCarthy DJ, Smyth GK. edgeR: a bioconductor package for differential expression analysis of digital gene expression data. *Bioinformatics* (2010) 26:139–40. doi: 10.1093/bioinformatics/btp616

18. Wu T, Hu E, Xu S, Chen M, Guo P, Dai Z, et al. clusterProfiler 4.0: A universal enrichment tool for interpreting omics data. *Innovation* (2021) 2:100141. doi: 10.1016/j.xinn.2021.100141

19. Weber RZ, Mulders G, Kaiser J, Tackenberg C, Rust R. Deep learning based behavioral profiling of rodent stroke recovery. *BMC Biol* (2021) 20:232. doi: 10.1101/2021.08.11.455647v1

20. Rust R, Weber RZ, Generali M, Kehl D, Bodenmann C, Uhr D, et al. Xeno-free induced pluripotent stem cell-derived neural progenitor cells for in vivo applications. *J Transl Med* (2022) 20:421. doi: 10.1101/2022.01.18.476253v1

21. Weber R, Bodenmann C, Uhr D, Zurcher K, Wanner D, Generali M, et al. Intracerebral transplantation and *In vivo* bioluminescence tracking of human neural progenitor cells in the mouse brain. *J Vis Exp* (2022) 179:e63102. https://www.jove.com/v/63102/intracerebral-transplantation-vivo-bioluminescence-tracking-human. doi: 10.3791/63102

22. Weber RZ, Grönnert L, Mulders G, Maurer MA, Tackenberg C, Schwab ME, et al. Characterization of the blood brain barrier disruption in the photothrombotic stroke model. *Front Physiol* (2020) 11:586226/abstract. doi: 10.3389/fphys.2020.586226/abstract

23. Rust R, Weber RZ, Grönnert L, Mulders G, Maurer MA, Hofer A-S, et al. Anti-Nogo-A antibodies prevent vascular leakage and act as pro-angiogenic factors following stroke. *Sci Rep* (2019) 9:1–10. doi: 10.1038/s41598-019-56634-1

24. Nih LR, Gojgini S, Carmichael ST, Segura T. Dual-function injectable angiogenic biomaterial for the repair of brain tissue following stroke. *Nat Mater* (2018) 17:642. doi: 10.1038/s41563-018-0083-8

25. Zhu H, Zhang Y, Zhong Y, Ye Y, Hu X, Gu L, et al. Inflammation-mediated angiogenesis in ischemic stroke. *Front Cell Neurosci* (2021) 15:652647. doi: 10.3389/fncel.2021.652647

26. Mathis A, Mamidanna P, Cury KM, Abe T, Murthy VN, Mathis MW, et al. DeepLabCut: markerless pose estimation of user-defined body parts with deep learning. *Nat Neurosci* (2018) 21:1281–9. doi: 10.1038/s41593-018-0209-y

27. Metz GA, Whishaw IQ. The ladder rung walking task: A scoring system and its practical application. *J Vis Exp* (2009) 1204. doi: 10.3791/1204

28. Yu SW, Friedman B, Cheng Q, Lyden PD. Stroke-evoked angiogenesis results in a transient population of microvessels. *J Cereb Blood Flow Metab* (2007) 27:755–63. doi: 10.1038/sj.jcbfm.9600378

29. Park YJ, Niizuma K, Mokin M, Dezawa M, Borlongan CV. Cell-based therapy for stroke. *Stroke* (2020) 51:2854–62. doi: 10.1161/STROKEAHA.120.030618

30. Martynov MY, Gusev EI. Current knowledge on the neuroprotective and neuroregenerative properties of citicoline in acute ischemic stroke. *J Exp Pharmacol* (2015) 7:17–28. doi: 10.2147/JEP.S63544

31. Serreze DV, Gaedeke JW, Leiter EH. Hematopoietic stem-cell defects underlying abnormal macrophage development and maturation in NOD/Lt mice: defective regulation of cytokine receptors and protein kinase c. *Proc Natl Acad Sci U S A* (1993) 90:9625–9. doi: 10.1073/pnas.90.20.9625

32. Weitbrecht L, Berchtold D, Zhang T, Jagdmann S, Dames C, Winek K, et al. CD4+ T cells promote delayed b cell responses in the ischemic brain after

experimental stroke. *Brain Behav Immun* (2021) 91:601–14. doi: 10.1016/j.bbi.2020.09.029

33. Takahashi J. iPS cell-based therapy for parkinson's disease: A Kyoto trial. *Regen Ther* (2020) 13:18–22. doi: 10.1016/j.reth.2020.06.002

34. Zhang G, Li Y, Reuss JL, Liu N, Wu C, Li J, et al. Stable intracerebral transplantation of neural stem cells for the treatment of paralysis due to ischemic stroke. *Stem Cells Transl Med* (2019) 8:999–1007. doi: 10.1002/sctm.18-0220

35. Dash PK, Gorantla S, Poluektova L, Hasan M, Waight E, Zhang C, et al. Humanized mice for infectious and neurodegenerative disorders. *Retrovirology* (2021) 18:13. doi: 10.1186/s12977-021-00557-1

36. Allen TM, Brehm MA, Bridges S, Ferguson S, Kumar P, Mirochnitchenko O, et al. Humanized immune system mouse models: progress, challenges and opportunities. *Nat Immunol* (2019) 20:770–4. doi: 10.1038/s41590-019-0416-z

37. Hurn PD, Subramanian S, Parker SM, Afentoulis ME, Kaler LJ, Vandenbark AA, et al. T- and b-cell-deficient mice with experimental stroke have reduced lesion size and inflammation. *J Cereb Blood Flow Metab* (2007) 27:1798–805. doi: 10.1038/sj.jcbfm.9600482

38. Kleinschnitz C, Schwab N, Kraft P, Hagedorn I, Dreykluft A, Schwarz T, et al. Early detrimental T-cell effects in experimental cerebral ischemia are neither related to adaptive immunity nor thrombus formation. *Blood* (2010) 115:3835–42. doi: 10.1182/blood-2009-10-249078

39. Minassian A, Dobrivojevic Radmilovic M, Vogel S, Diedenhofen M, Nelles M, Stoeber M, et al. Cortical tissue loss and major structural reorganization as result of distal middle cerebral artery occlusion in the chronic phase of nude mice. *Sci Rep* (2019) 9:6823. doi: 10.1038/s41598-019-43341-0

40. Szpak GM, Lechowicz W, Lewandowska E, Bertrand E, Wierzba-Bobrowicz T, Dymecki J. Border zone neovascularization in cerebral ischemic infarct. *Folia Neuropathol* (1999) 37:264–8.

41. Krupinski J, Kaluza J, Kumar P, Kumar S, Wang JM. Role of angiogenesis in patients with cerebral ischemic stroke. *Stroke* (1994) 25:1794–8. doi: 10.1161/01.STR.25.9.1794

42. Rust R. Insights into the dual role of angiogenesis following stroke. *J Cereb Blood Flow Metab* (2020) 40:1167–71. doi: 10.1177/0271678X20906815

43. Zhang ZG, Zhang L, Jiang Q, Zhang R, Davies K, Powers C, et al. VEGF enhances angiogenesis and promotes blood-brain barrier leakage in the ischemic brain. *J Clin Invest* (2000) 106:829–38. doi: 10.1172/JCI9369

44. Rascón-Ramírez FJ, Esteban-García N, Barcia JA, Trondin A, Nombela C, Sánchez-Sánchez-Rojas L. Are we ready for cell therapy to treat stroke? front. *Cell Dev Biol* (2021) 9:621645. doi: 10.3389/fcell.2021.621645

45. Boese AC, Le Q-SE, Pham D, Hamblin MH, Lee J-P. Neural stem cell therapy for subacute and chronic ischemic stroke. *Stem Cell Res Ther* (2018) 9:154. doi: 10.1186/s13287-018-0913-2

46. El Amki M, Lerouet D, Garraud M, Teng F, Beray-Berthat V, Coqueran B, et al. Improved reperfusion and vasculoprotection by the Poly(ADP-Ribose) Polymerase inhibitor PJ34 after stroke and thrombolysis in mice. *Mol Neurobiol* (2018) 55:9156–68. doi: 10.1007/s12035-018-1063-3

47. Brooks SP, Pask T, Jones L, Dunnett SB. Behavioural profiles of inbred mouse strains used as transgenic backgrounds. I: motor tests. *Genes Brain Behav* (2004) 3:206–15. doi: 10.1111/j.1601-183X.2004.00072.x

48. Ortiz C, Navarro JF, Jurek A, Märtin A, Lundeberg J, Meletis K. Molecular atlas of the adult mouse brain. *Sci Adv* (2020) 6:eabb3446. doi: 10.1126/sciadv.abb3446

49. Ruan C, Elyaman W. A new understanding of TMEM119 as a marker of microglia. *Front Cell Neurosci* (2022) 16:902372. doi: 10.3389/fncel.2022.902372

50. Rojanathammanee L, Floden AM, Manocha GD, Combs CK. Attenuation of microglial activation in a mouse model of alzheimer's disease *via* NFAT inhibition. *J Neuroinflammation* (2015) 12:42. doi: 10.1186/s12974-015-0255-2

51. Moisseiev E, Smit-McBride Z, Oltjen S, Zhang P, Zawadzki RJ, Motta M, et al. Intravitreal administration of human bone marrow CD34+ stem cells in a murine model of retinal degeneration. *Invest Ophthalmol Vis Sci* (2016) 57:4125–35. doi: 10.1167/iovs.16-19252

52. De la Vega RE, Coenen MJ, Müller SA, Nagelli CV, Quirk NP, Lopez de Padilla C, et al. Effects of FK506 on the healing of diaphyseal, critical size defects in the rat femur. *Eur Cell Mater* (2020) 40:160–71. doi: 10.22203/eCM.v040a10

53. Sachewsky N, Hunt J, Cooke MJ, Azimi A, Zarin T, Miu C, et al. Cyclosporin a enhances neural precursor cell survival in mice through a calcineurin-independent pathway. *Dis Model Mech* (2014) 7:953–61. doi: 10.1242/dmm.014480

frontiers | Frontiers in Immunology

TYPE Original Research
PUBLISHED 31 March 2023
DOI 10.3389/fimmu.2023.1148069

OPEN ACCESS

EDITED BY
Marcela Pekna,
University of Gothenburg, Sweden

REVIEWED BY
Vladimer Darsalia,
Karolinska Institutet (KI), Sweden
Yu-Yo Sun,
University of Virginia, United States

*CORRESPONDENCE
Jui-Hung Jimmy Yen
jimyen@iu.edu

SPECIALTY SECTION
This article was submitted to Multiple Sclerosis and Neuroimmunology, a section of the journal Frontiers in Immunology

RECEIVED 19 January 2023
ACCEPTED 22 February 2023
PUBLISHED 31 March 2023

CITATION
Kuo P-C, Weng W-T, Scofield BA, Paraiso HC, Bojrab P, Kimes B, Yu I-CI and Yen J-HJ (2023) Interferon-β modulates microglial polarization to ameliorate delayed tPA-exacerbated brain injury in ischemic stroke.
Front. Immunol. 14:1148069.
doi: 10.3389/fimmu.2023.1148069

Interferon-β modulates microglial polarization to ameliorate delayed tPA-exacerbated brain injury in ischemic stroke

Ping-Chang Kuo[1], Wen-Tsan Weng[1], Barbara A. Scofield[1], Hallel C. Paraiso[2], Paul Bojrab[3], Brandon Kimes[3], I-Chen Ivorine Yu[2] and Jui-Hung Jimmy Yen[1*]

[1]Department of Microbiology and Immunology, Indiana University School of Medicine, Fort Wayne, IN, United States, [2]Department of Anatomy, Cell Biology and Physiology, Indiana University School of Medicine, Fort Wayne, IN, United States, [3]Doctor of Medicine Program, Indiana University School of Medicine, Fort Wayne, IN, United States

Tissue plasminogen activator (tPA) is the only FDA-approved drug for the treatment of ischemic stroke. Delayed tPA administration is associated with increased risks of blood-brain barrier (BBB) disruption and hemorrhagic transformation. Studies have shown that interferon beta (IFNβ) or type I IFN receptor (IFNAR1) signaling confers protection against ischemic stroke in preclinical models. In addition, we have previously demonstrated that IFNβ can be co-administered with tPA to alleviate delayed tPA-induced adverse effects in ischemic stroke. In this study, we investigated the time limit of IFNβ treatment on the extension of tPA therapeutic window and assessed the effect of IFNβ on modulating microglia (MG) phenotypes in ischemic stroke with delayed tPA treatment. Mice were subjected to 40 minutes transient middle cerebral artery occlusion (MCAO) followed by delayed tPA treatment in the presence or absence of IFNβ at 3h, 4.5h or 6h post-reperfusion. In addition, mice with MG-specific IFNAR1 knockdown were generated to validate the effects of IFNβ on modulating MG phenotypes, ameliorating brain injury, and lessening BBB disruption in delayed tPA-treated MCAO mice. Our results showed that IFNβ extended tPA therapeutic window to 4.5h post-reperfusion in MCAO mice, and that was accompanied with attenuated brain injury and lessened BBB disruption. Mechanistically, our findings revealed that IFNβ modulated MG polarization, leading to the suppression of inflammatory MG and the promotion of anti-inflammatory MG, in delayed tPA-treated MCAO mice. Notably, these effects were abolished in MG-specific IFNAR1 knockdown MCAO mice. Furthermore, the protective effect of IFNβ on the amelioration of delayed tPA-exacerbated ischemic brain injury was also abolished in these mice. Finally, we identified that IFNβ-mediated modulation of MG phenotypes played a role in maintaining BBB integrity, because the knockdown of IFNAR1 in MG partly reversed the protective

effect of IFNβ on lessening BBB disruption in delayed tPA-treated MCAO mice. In summary, our study reveals a novel function of IFNβ in modulating MG phenotypes, and that may subsequently confer protection against delayed tPA-exacerbated brain injury in ischemic stroke.

KEYWORDS

tissue plasminogen activator, interferon beta, type I interferon receptor, blood brain barrier, microglial polarization, ischemic stroke

Introduction

Stroke is a leading cause of death and results in permanent disability in up to 30% of survivors. There are two types of strokes, ischemic stroke and hemorrhagic stroke, in which ischemic stroke accounts for more than 80% of stroke cases. Currently, tissue plasminogen activator (tPA) is the only FDA-approved drug for ischemic stroke. Mechanistically, tPA functions to dissolve blood clots that leads to reestablish the cerebral blood flow in the ischemic brain. However, tPA-induced reperfusion promotes the recruitment of peripheral inflammatory immune cells into the infarct core that subsequently results in the secondary brain injury (1). Furthermore, studies have shown that tPA induces microglia (MG) activation that exacerbates brain injury in ischemic stroke (2, 3). Moreover, the administration of tPA beyond its therapeutic window of 3-4.5h post-injury significantly increases the risk of blood brain barrier (BBB) disruption and hemorrhagic transformation (HT) after ischemic stroke (4–7).

MG activation plays an important role in the immunopathogenesis of the central nervous system (CNS) diseases. Following ischemic stroke, MG are rapidly activated and exert detrimental effects on ischemic brain injury. MG activation can be determined by detecting the expression of inflammatory markers, such as CD86 and CD16, and the upregulation of pro-inflammatory cytokines, including IL-1α, IL-β, TNF-α, and IL-6. Studies have shown that inflammatory MG markers and cytokines display an increased trend during the first 14 days following ischemic stroke (8). On the other hand, anti-inflammatory MG were also observed in the ischemic brain. Anti-inflammatory MG phenotype can be assessed by the expression of surface marker, macrophage mannose receptor 1 (CD206), and the upregulation of anti–inflammatory molecules, including IL– 10, arginase–1 (Arg1), Ym1, and TGF–β. Studies have shown that the expression of anti-inflammatory MG markers and molecules was increased at day 1 and peaked at day 5-7 post stroke. Importantly, anti-inflammatory MG exert protective effects on promoting brain repair and prognosis in ischemic stroke (8–10). Thus, modulating MG transformation from inflammatory to anti-inflammatory phenotype represents a critical strategy for attenuating neuroinflammation and ameliorating brain injury in ischemic stroke.

Interferon beta (IFNβ) is an FDA-approved therapy for the treatment of multiple sclerosis, and its immunomodulatory and anti-inflammatory properties were well characterized (11, 12). Hence, IFNβ exerts a potential to be utilized as an anti-inflammatory agent for the treatment of ischemic stroke. Indeed, we have previously demonstrated that IFNβ ameliorates brain injury through inhibiting MG activation and suppressing inflammatory immune cell infiltration of the CNS in stroke animals (13). In addition, studies from other groups showed that IFNβ and/or type I IFN receptor (IFNAR1) signaling confer protection against brain injury in ischemic stroke animal models (14–19). Moreover, our recent study showed that IFNβ can be co-administered with tPA to ameliorate delayed tPA-exacerbated brain injury in ischemic stroke (20). Collectively, studies from our and other groups demonstrate the beneficial effects of IFNβ treatment in ischemic stroke.

Our previous study demonstrated that IFNβ extended tPA therapeutic window to 3h post-injury in ischemic stroke in which IFNβ ameliorated delayed tPA-exacerbated ischemic brain injury and lessened tPA-aggravated BBB disruption and HT (20). In the present study, we investigated the time limit of IFNβ treatment on the extension of tPA therapeutic window and assessed the effect of IFNβ on the modulation of MG phenotypes in delayed tPA-treated stroke animals. Furthermore, mice with MG-specific IFNAR1 knockdown were generated to validate the effects of IFNβ on modulating MG phenotypes, ameliorating brain injury, and lessening BBB disruption in delayed tPA-treated stroke animals. In sum, our findings reveal that IFNβ exerts protective effects on modulating MG phenotypes, leading to the suppression of inflammatory MG and the induction of anti-inflammatory MG, and that subsequently confers protection against delayed tPA-exacerbated brain injury in ischemic stroke.

Abbreviations: tPA, Tissue plasminogen activator; BBB, Blood-brain barrier; IFNβ, Interferon beta; IFNAR1, Type I IFN receptor; MG, Microglia; MCAO, Middle cerebral artery occlusion; CNS, Central nervous system; CD206, Macrophage mannose receptor 1; Arg1, Arginase–1; TAM, Tamoxifen; TTC, Triphenyltetrazolium chloride; TCA, Trichloroacetic acid; CBF, Cerebral blood flow; NVU, Neurovascular unit.

Materials and methods

Mice

Animal experimental procedures were approved by the Purdue Animal Care and Use Committee and performed in strict

compliance with the National Institutes of Health Guide for the Care and Use of Laboratory Animals. C57BL/6, *Ifnar1*$^{fl/fl}$, and *Cx3cr1*$^{CreERT2/CreERT2}$ mice were purchased from the Jackson Laboratory (Bar Harbor, ME) and bred in our animal facility. *Ifnar1*$^{fl/fl}$ mice were crossed with *Cx3cr1*$^{CreERT2/CreERT2}$ mice to generate *Ifnar1*$^{fl/+}$-*Cx3cr1*$^{CreERT2/+}$ mice. *Ifnar1*$^{fl/+}$-*Cx3cr1*$^{CreERT2/+}$ mice were then crossed with *Ifnar1*$^{fl/+}$-*Cx3cr1*$^{CreERT2/+}$ mice to generate *Ifnar1*$^{fl/fl}$-*Cx3cr1*$^{CreERT2/+}$ and *Cx3cr1*$^{CreERT2/+}$ mice. *Ifnar1*$^{fl/fl}$-*Cx3cr1*$^{CreERT2/+}$ mice at 7-8 weeks old were subjected to *i.p.* injection of 75mg/kg Tamoxifen (TAM) for a total of 5 consecutive days to induce IFNAR1 knockdown in MG/macrophages. TAM-treated *Ifnar1*$^{fl/fl}$-*Cx3cr1*$^{CreERT2/+}$ mice were housed for additional 7-8 weeks to allow peripheral monocyte/macrophages to be replenished and then subjected to ischemic stroke. *Cx3cr1*$^{CreERT2/+}$ control mice were subjected to the same procedure of TAM treatment followed by ischemic stroke induction. Mice were housed and bred with controlled humidity, temperature and 12h:12h light-dark cycle in the animal facility with food and water available ad libitum.

Reagents

IFNβ was purchased from PBL Interferon Source (Piscataway, NJ), and tPA was purchased from Genentech (San Francisco, CA). Evans blue was purchased from Sigma-Aldrich (St. Louis, MO). Triphenyltetrazolium chloride (TTC) and trichloroacetic acid (TCA) were purchased from Alfa Aesar (Tewksbury, MA). Antibodies of Alexa Fluor 488 anti-CD45 (Clone: 30-F11), FITC anti-CD11a (Clone: M17/4), PE/Cy7 anti-Ly6C (Clone: HK1.4), APC anti-CD11b (Clone: M1/70), PE/Cy7 anti-CD68 (Clone: FA-11), PE/Cy7 anti-CD86 (Clone: GL-1), PE/Cy7 anti-CD206 (Clone: C068C2), APC anti-IFNAR1 (Clone: MAR1-5A3), and PE anti-IL-1α (Clone: ALF-161) were purchased from BioLegend (San Diego, CA). APC anti-Arg1 antibody was purchase from R&D Systems. APC anti-IL-1β (Clone: NJTEN3) antibody was purchase from eBioscience (Waltham, MA).

Middle cerebral artery occlusion model

Cerebral ischemia was induced in 3-4 months old male and female mice as previously described (13, 20). Briefly, mice were subjected to intraluminal occlusion of right middle cerebral artery by the insertion of silicone-coated nylon monofilament (Doccol Corp, Sharon, MA). A laser doppler flowmetry was used to measure the cerebral blood flow (CBF). The filament was withdrawn to allow reperfusion after 40min or 4.5h occlusion. Animal's body temperature was maintained at ~37°C throughout the surgery by a warming lamp and heating pad. Sham controls were subjected to the same surgical procedure without monofilament insertion. After surgery, mice were placed in the recovery cage in which the temperature was maintained at 37°C for 1h to recover from anesthesia. Mice that had a reduction of the CBF more than 80% during the occlusion were included in the study and assigned randomly to receive *i.v.* administration of vehicle (PBS), tPA (5mg/kg), or tPA+IFNβ (10,000U) at the indicated time points. tPA+IFNβ-treated MCAO mice received an additional dose of IFNβ at day 1 post-injury if they were sacrificed at day 2 or day 7. The doses of tPA and IFNβ used in this study were based on the previous studies (13, 20–22). The investigators who performed the experiments were blinded to the animal groups.

Infarct volume measurements

Mice were perfused with PBS, and the ischemic brains were harvested and subjected to 2 mm coronal slicing with a rodent brain matrix. Brain sections were than stained with 1% TTC followed by scanning, and the infarct volumes were calculated by using ImageJ as previously described (13).

Evans blue extravasation assay

Mice were *i.v.* administered 4 ml/kg 2% (w/v) Evans blue dye/0.9% saline solution through lateral tail vein. One hour after injection, mice were then anesthetized deeply and perfused with PBS to remove intravascular Evans blue. The brains were harvested and sliced. The brain sections were then subjected to scanning to obtain images. Subsequently, the hemispheres of brain sections were separated and weighted followed by homogenization with 50% TCA solution. After centrifugation, the supernatants were collected and diluted with 95% ethanol at the ratio of 1:3. The amount of extravascular Evans blue in the supernatants was then determined by measuring the fluorescence with excitation at 540/25nm and emission at 645/40nm using a BioTek Synergy HT microplate reader.

Mononuclear cells isolation and FACS analysis

Mice subjected to MCAO were anesthetized deeply and transcardially perfused with PBS at indicated time points. The brains were harvested, and the meninge, olfactory bulb, and cerebellum were removed. The forebrains were then homogenized with 1x Hanks' balanced salt solution (HBSS) buffer followed by filtration through a 70μm nylon cell strainer. Following centrifugation, cells were resuspended in 30% Percoll and underlayered with 70% Percoll. After centrifugation, the mononuclear cells were then isolated from the interface between 30% and 70% Percoll. For intracellular cytokine staining, the isolated cells were *ex-vivo* cultured in the presence of GolgiPlug for 4.5h. Cells were then collected and stained with antibodies of CD45 and CD11b followed by fixation and permeabilization. After wash, cells were stained with IL-1α and IL-1β antibodies followed by FACS analysis. For cell surface staining, the isolated cells were stained with antibodies of CD45 and CD11b in the presence of CD86 or CD11a and Ly6C antibodies followed by FACS analysis. For intracellular staining, the isolated cells were stained with antibodies of CD45 and CD11b followed by fixation and

permeabilization. After wash, cells were stained with CD68, Arg1, or CD206 antibody followed by FACS analysis. The gating strategy of flow cytometry analysis to identify the population of MG with the intermediate expression of CD45 ($CD45^{int}$) and positive expression of CD11b ($CD11b^{+}$) is presented in Supplementary Figure 1. For *in vitro* intracellular cytokine staining, cells were treated with indicated conditions and harvested at the indicated time points. GolgiPlug was added to the culture 4.5h prior cell harvesting. Cells were then fixed and permeabilized, and subsequently subjected to IL-1β antibody staining followed by FACS analysis. For *in vitro* intracellular staining, cells treated with indicated conditions were harvested at the indicated time points followed by fixation and permeabilization. After wash, cells were then stained with Arg1 and CD206 antibodies followed by FACS analysis.

Rotarod test

Motor coordination was assessed in MCAO mice by using the rotarod test (Model 47600, Ugo Basile, Varese, Italy). Prior to MCAO surgery, mice were trained on the rotarod apparatus with a setting of accelerating speed from 4 to 80 rpm over a 5min period for three trials with a 30min resting interval every day for three consecutive days. Following MCAO, mice were given three trials with a 30min resting interval at day 2, 4, and 6 post-injury. Motor function was assessed based on the latency to fall.

Cell culture

Primary MG were generated from neonatal mice as previously described (23). Briefly, cerebral cortical cells were collected from 1-2 days old neonatal mice and seeded in T75 flasks containing Dulbecco's modified eagle medium/nutrient mixture F-12 (DMEM/F12) complete media. After removing media, the flasks were replenished with complete media containing 10ng/ml GM-CSF on day 3 and 6 after plating. MG were harvested by shaking the flasks at 250rpm for 40min at 37°C on day 13 or 14. Cells were then seeded in cell culture wells followed by treatments.

Quantitative polymerase chain reaction

mRNA expression was measured by Q-PCR analysis as previously described (24). The primers used were *Il-1α*: 5'-CGCTT GAGTCGGCAAAGAAAT-3' and 5'-CTTCCCGTTGCTTG ACGTT G-3'; *Il-1β*: 5'-CCCTGCAGCTGGAGAGTGTGGA-3' and 5'-TGTGCTCTGCTTGTGAGGTG CTG-3'.

Statistical analysis

All results in this study were given as mean ± SEM. Sample sizes were determined by power calculations based on our previous studies. The normal distribution of the data was confirmed by Shapiro-Wilk test. Comparisons among multiple groups were performed by one-way ANOVA (one variable) or two-way ANOVA (two variables) followed by Tukey *post hoc* test. Comparisons between two groups were performed by unpaired *t* test. Statistical analyses were performed by using GraphPad Prism 9 software. Statistical significance was determined as $p<0.05$.

Results

IFNβ confers protection against delayed tPA-exacerbated brain injury in ischemic stroke

We have previously demonstrated that delayed but not early tPA treatment exacerbated brain injury in ischemic stroke, and IFNβ ameliorated ischemic brain injury in MCAO mice subjected to delayed tPA treatment (20). In this study, we aimed to investigate the time limit of IFNβ on the extension of tPA therapeutic window in ischemic stroke. As we have previously shown that IFNβ administered at 3h post-reperfusion ameliorated ischemic brain injury (13), we first assessed the time limit of IFNβ-conferred protection against ischemic brain injury. C57BL/6 mice were subjected to 40min MCAO followed by IFNβ administration at 4.5h or 6h post-reperfusion, and MCAO mice were sacrificed at day 2 post-injury to determine the level of brain injury. Our results showed that IFNβ administered at 4.5h but not 6h post-reperfusion significantly attenuated infarct volumes in MCAO mice (Supplementary Figure 2). We then determined the therapeutic potential of IFNβ on the extension of tPA therapeutic window in MCAO mice at different time points. Mice subjected to 40min MCAO were treated with tPA at 40min post-injury or with tPA in the presence or absence of IFNβ at 3h, 4.5h, or 6h post-reperfusion. Consistent with our previous findings (20), tPA administered at 40min post-injury did not alter the level of brain injury in MCAO mice compared to vehicle-treated MCAO controls. However, delayed tPA treatment at 3h, 4.5h, or 6h post-reperfusion exacerbated brain injury in MCAO mice, and the level of brain injury was comparable among these animals at day 1 post-injury (Figure 1A). Importantly, we found that IFNβ attenuated ischemic brain injury-exacerbated by delayed tPA treatment at 3h and 4.5h post-reperfusion (Figure 1A). Although there was a trend that IFNβ reduced brain infarct in MCAO mice treated with tPA at 6h post-reperfusion, it did not reach statistical significance (Figure 1A). Furthermore, the detrimental effect of delayed tPA treatment at 4.5h post-reperfusion on ischemic brain injury and the protective effect of IFNβ on delayed tPA-exacerbated brain injury were observed in MCAO mice at day 2 post-injury (Figure 1B). Finally, we investigated the observed effects in female MCAO mice. Our results showed that delayed tPA treatment at 4.5h post-reperfusion exacerbated brain injury, and consistently IFNβ ameliorated delayed tPA-exacerbated brain injury in female MCAO mice (Figure 1C). Notably, we observed a smaller infarct in vehicle-treated female MCAO mice compared to vehicle-treated male MCAO mice. Similarly, delayed tPA-exacerbated brain injury was

10.3389/fimmu.2023.1148069

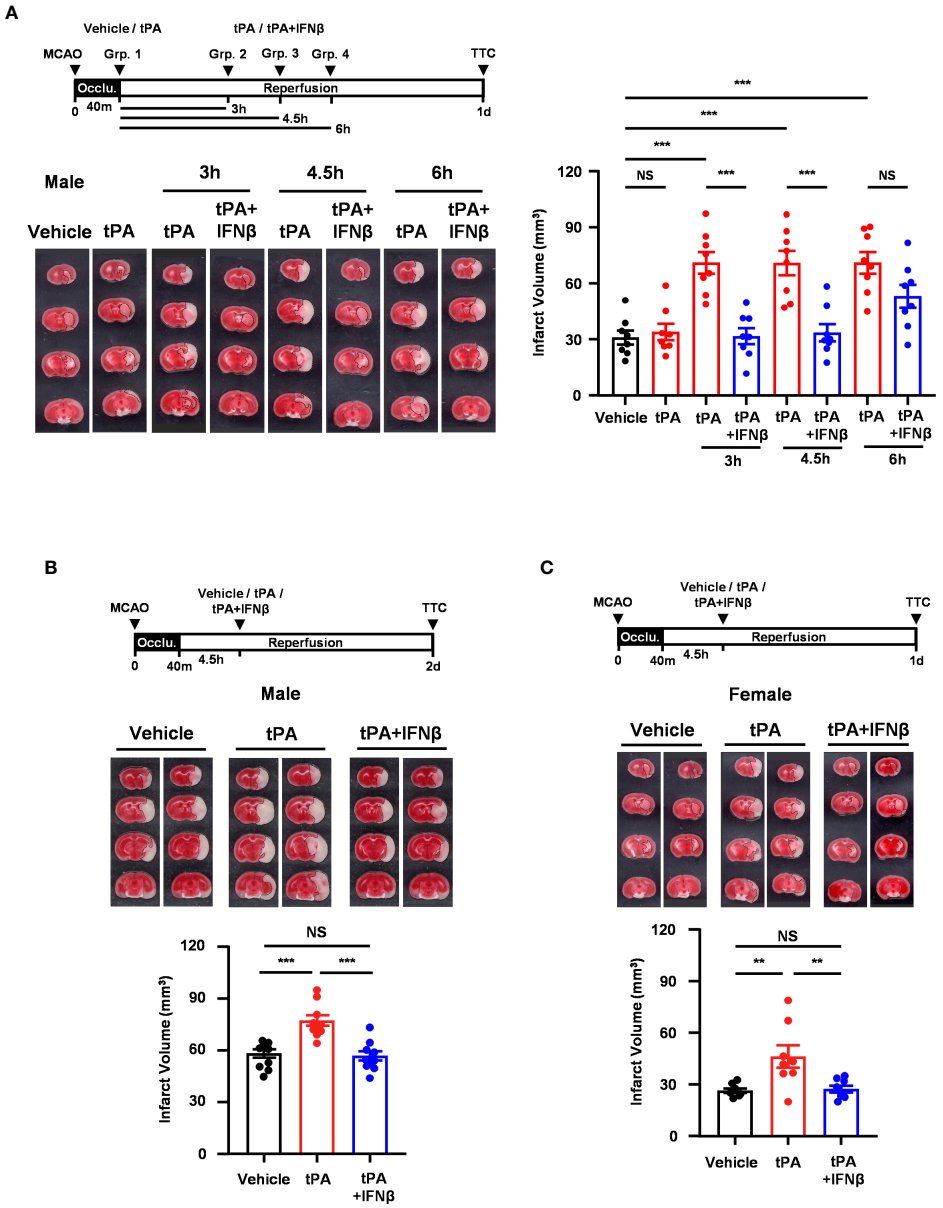

FIGURE 1
IFNβ confers protection against delayed tPA-exacerbated brain injury in ischemic stroke. **(A)** Male C57BL/6 mice were subjected to 40min MCAO followed by the administration of vehicle or tPA right after the onset of reperfusion or of tPA in the presence or absence of IFNβ at 3h, 4.5h, or 6h post-reperfusion (n=8/group). At day 1 post-injury, the ischemic brains were harvested and subjected to TTC staining. One representative TTC-stained brain sample of each group is shown, and the infarct volumes were also measured. **(B)** Male C57BL/6 mice subjected to 40min MCAO were administered vehicle, tPA, or tPA +IFNβ at 4.5h post-reperfusion (n=10/group). At day 2 post-injury, the ischemic brains were harvested and subjected to TTC staining. Two representative TTC-stained brain samples of each group are shown, and the infarct volumes were also measured. **(C)** Female C57BL/6 mice subjected to 40min MCAO were administered vehicle, tPA, or tPA+IFNβ at 4.5h post-reperfusion (n=8/group). At day 1 post-injury, the ischemic brains were harvested and subjected to TTC staining. Two representative TTC-stained brain samples of each group are shown, and the infarct volumes were also measured. ***p<0.01; ***p<0.001;* NS, no significant difference by one-way ANOVA. Occlu., occlusion; Grp., group.

less severe in female MCAO mice compared to male MCAO mice (Figures 1A vs. 1C). These results suggest that female mice exhibit less severe brain injury compared to male mice following ischemic stroke, consistent with the previous findings (25, 26). Collectively, our results demonstrate that delayed tPA treatment exacerbates ischemic brain injury, and IFNβ exerts a therapeutic potential to extend tPA therapeutic window to 4.5h post-injury and ameliorate delayed tPA-exacerbated brain injury in ischemic stroke.

IFNβ confers long-term protection against ischemic stroke with delayed tPA treatment

To further evaluate whether IFNβ conferred long-term protection against ischemic stroke with delayed tPA treatment, mice were subjected to 40min MCAO followed by vehicle, tPA, or tPA+IFNβ administration at 4.5h post-reperfusion, and the survival assay was

performed. Our results showed that tPA-treated MCAO mice displayed reduced survival compared to vehicle-treated MCAO mice at day 7 post-injury. Notably, tPA+IFNβ-treated MCAO mice exhibited increased survival compared to tPA-treated MCAO mice and displayed a similar level of survival as vehicle-treated MCAO mice at day 7 post-injury (Figure 2A). Furthermore, the rotarod test was performed to assess the effect of delayed tPA treatment in the presence or absence of IFNβ on motor coordination in MCAO mice. Our results showed that tPA-treated MCAO mice had a poor performance on the rotarod test compared to vehicle-treated MCAO mice. In contrast, tPA+IFNβ-treated MCAO mice exhibited an improved performance on the rotarod test compared to tPA-treated MCAO mice (Figure 2B). Finally, we assessed the level of brain injury in MCAO mice treated with delayed tPA in the presence or absence of IFNβ at day 7 post-injury. Our results showed that tPA+IFNβ-treated MCAO mice exhibited reduced infarct volumes compared to tPA-treated MCAO mice, and the infarct volumes were comparable between vehicle- and tPA+IFNβ-treated MCAO mice (Figure 2C). Altogether, our results demonstrate that IFNβ confers long-term protection against ischemic stroke with delayed tPA treatment, and that was accompanied with attenuated brain infarct volumes, improved motor coordination, and increased survival.

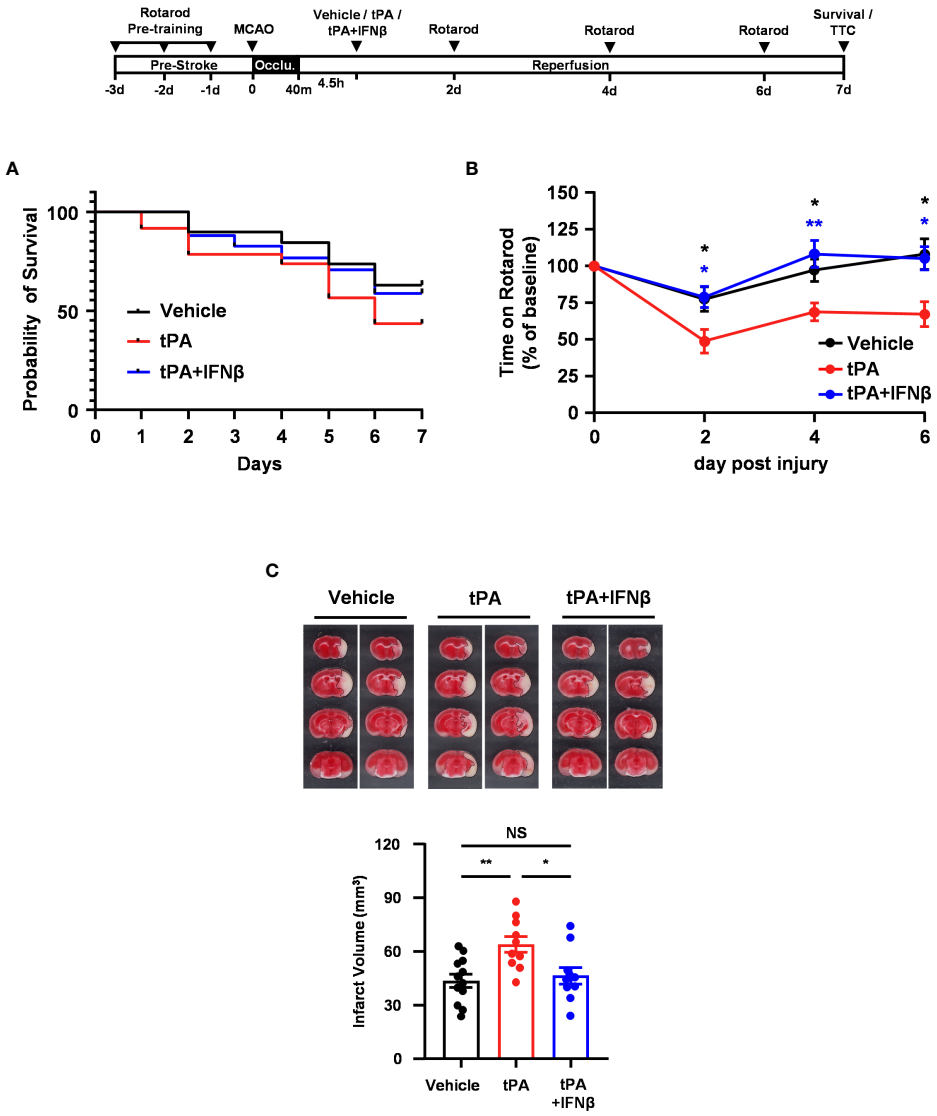

FIGURE 2
IFNβ confers long-term protection against ischemic stroke with delayed tPA treatment. Male C57BL/6 mice were subjected to 40min MCAO followed by the administration of vehicle, tPA, or tPA+IFNβ at 4.5h post-reperfusion. MCAO mice were then subjected to **(A)** survival assay for 7 days and **(B)** rotarod tests at day 2, 4, and 6 post-injury. **p<0.05, **p<0.01* compared to tPA by unpaired *t*-test. **(C)** At day 7 post-injury, the survived MCAO mice (vehicle: n=12; tPA: n=10; tPA+IFNβ: n=10) were sacrificed and subjected to TTC staining. Two representative TTC-stained samples of each group are shown, and the infarct volumes were measured. **p<0.05; **p<0.01;* NS, no significant difference by one-way ANOVA.

10.3389/fimmu.2023.1148069

IFNβ modulates MG polarization in delayed tPA-treated ischemic stroke

To elucidate whether IFNβ modulated MG phenotypes to confer protection against delayed tPA-exacerbated ischemic brain injury, we assessed MG inflammatory and anti-inflammatory phenotypes in 40min MCAO mice treated with vehicle, tPA, or tPA+IFNβ at 4.5h post-reperfusion. MG were determined as $CD45^{int}CD11b^{+}$ cells in the ischemic brain. As previous studies showed that $CD45^{high}$ ($CD45^{hi}$) infiltrating monocytes/macrophages might become $CD45^{int}$ MG-like phenotypes following ischemic brain injury (27–29), we measured the expression of macrophage markers, CD11a and Ly6C, in the population of $CD45^{int}CD11b^{+}$ cells in the ischemic brain. We found that $CD45^{int}CD11b^{+}$ cells did not express CD11a and Ly6C in the ischemic brain of MCAO mice at day 1 post-injury (Supplementary Figure 3A). We then determined MG phenotypes in the ischemic brain of vehicle-, tPA-, and tPA+IFNβ-treated MCAO mice. Our results showed that ischemic stroke induced MG activation, and that was accompanied with increased CD86 expression and upregulated IL-1α and IL-1β production in the ipsilateral hemisphere of vehicle-treated MCAO mice compared to the ipsilateral hemisphere of sham controls and the contralateral hemisphere of vehicle-treated MCAO mice at day 1 post-injury (Figures 3A–C). Notably, delayed tPA treatment aggravated MG inflammatory phenotype, because the expression of CD86, IL-1α, and IL-1β in MG was further upregulated in the ipsilateral hemisphere of tPA-treated MCAO mice compared to that of vehicle-treated MCAO mice (Figures 3A–C). Importantly, IFNβ was able to suppress delayed tPA-induced CD86, IL-1α, and IL-1β upregulation in MG following MCAO (Figures 3A–C).

We then evaluated whether IFNβ promoted MG anti-inflammatory phenotype to confer protection against delayed tPA-exacerbated ischemic brain injury. The expression of anti-inflammatory molecules, Arg1 and CD206, and anti-inflammatory cytokine IL-10 in MG was assessed in MCAO mice treated with vehicle, tPA, or tPA+IFNβ at 4.5h post-reperfusion. We found ischemic stroke enhanced MG Arg1 and CD206

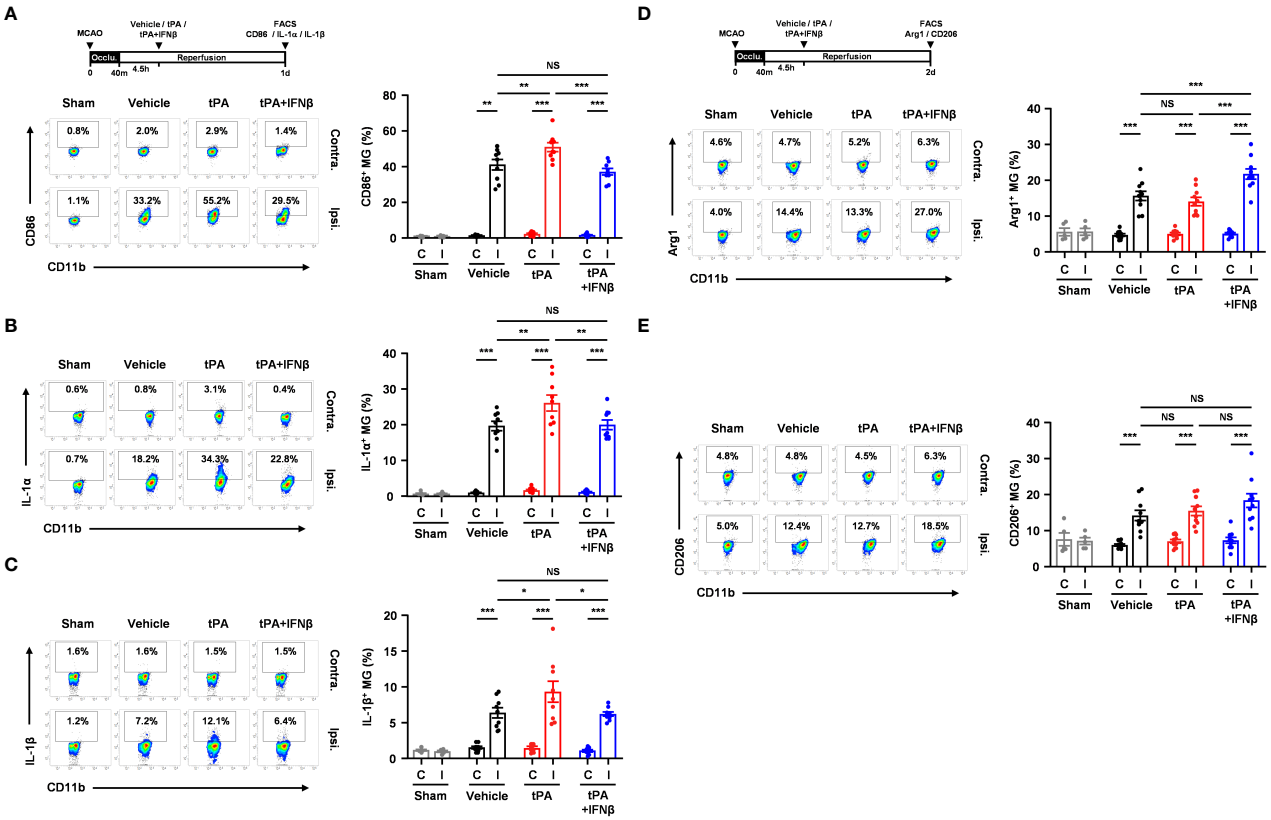

FIGURE 3
IFNβ modulates MG polarization in delayed tPA-treated ischemic stroke. Male C57BL/6 mice were subjected to sham or 40min MCAO followed by the administration of vehicle, tPA, or tPA+IFNβ at 4.5h post-reperfusion. **(A–C)** At day 1 post-injury, the contralateral (Contra.; C) and ipsilateral (Ipsi.; I) hemispheres of sham (n=6), and vehicle-, tPA-, and tPA+IFNβ-treated MCAO mice (n=9/group) were harvested followed by mononuclear cell isolation. **(A)** The isolated cells were stained with CD45 and CD11b antibodies in the presence of CD86 antibody to determine the surface expression of CD86 in $CD45^{int}CD11b^{+}$ MG. **(B, C)** The isolated mononuclear cells were ex-vivo cultured in the presence of GolgiPlug for 4.5h followed by staining with CD45 and CD11b antibodies. After fixation and permeabilization, cells were then stained with IL-1α and IL-1β antibodies to determine the intracellular expression of IL-1α and IL-1β in $CD45^{int}CD11b^{+}$ MG by flow cytometry. **(D, E)** At day 2 post-injury, the isolated mononuclear cells were stained with CD45 and CD11b antibodies. Following fixation and permeabilization, cells were then stained with Arg1 and CD206 antibodies to determine the expression of Arg1 and CD206 in $CD45^{int}CD11b^{+}$ MG by flow cytometry. *$p<0.05$; **$p<0.01$; ***$p<0.001$; NS, no significant difference by two-way ANOVA.

expression in the ipsilateral hemisphere of vehicle-treated MCAO mice compared to that of sham controls at day 2 post-injury (Figures 3D, E). However, delayed tPA treatment did not alter MG Arg1 and CD206 expression compared to vehicle treatment in MCAO mice. Importantly, IFNβ upregulated MG Arg1 expression, as the expression level of Arg1 in MG was higher in the ipsilateral hemisphere of tPA+IFNβ-treated MCAO mice than that of tPA-treated MCAO mice (Figure 3D). Interestingly, the frequency of $Ly6C^{+}$ cells in the $CD45^{int}CD11b^{+}$ population was higher in tPA-treated MCAO mice than vehicle- or tPA+IFNβ-treated MCAO mice, although it did not reach statistically significant differences (Supplementary Figure 3B). However, we found $Arg1^{+}$ cells was mostly associated with $Ly6C^{-}CD45^{int}CD11b^{+}$ cells but not $Ly6C^{+}CD45^{int}CD11b^{+}$ cells in the ischemic brain of tPA+IFNβ-treated MCAO mice (Supplementary Figure 3C), suggesting IFNβ mainly modulates the phenotype of resident MG in the ischemic brain. Finally, we observed a trend that IFNβ enhanced MG CD206 expression in tPA+IFNβ-treated MCAO mice compared to tPA-treated MCAO mice (Figure 3E). However, we did not observe an induction of IL-10 in MG in vehicle, tPA, or tPA+IFNβ-treated MCAO mice (Data not shown). Collectively, our results demonstrate that delayed tPA treatment aggravates MG inflammatory phenotype; in contrast, IFNβ diminishes delayed tPA-aggravated MG inflammatory phenotype in ischemic stroke. Furthermore, we identify that IFNβ promotes MG anti-inflammatory phenotype in delayed tPA-treated ischemic stroke. Thus, our results suggest that IFNβ exerts protective effects in ischemic stroke with delayed tPA treatment through suppressing tPA-aggravated inflammatory MG and promoting anti-inflammatory MG in the ischemic brain.

IFNβ-conferred protection against delayed tPA-exacerbated ischemic brain injury is abolished in MCAO mice with MG-specific IFNAR1 knockdown

Since we observed IFNβ modulated MG phenotypes and ameliorated brain injury in delayed tPA-treated MCAO mice, we thought to assess whether IFNβ-mediated activation of IFNAR1 signaling in MG plays an essential role in ameliorating delayed tPA-exacerbated brain injury in ischemic stroke. Thus, we generated $Ifnar1^{fl/fl}$-$Cx3cr1^{CreERT2/+}$ mice and subjected mice to TAM treatment to induce IFNAR1 knockdown specifically in MG (Supplementary Figure 4A). $Ifnar1^{fl/fl}$-$Cx3cr1^{CreERT2/+}$ and control $Cx3cr1^{CreERT2/+}$ mice were then subjected to 40min MCAO followed by tPA or tPA+IFNβ treatment at 4.5h post-reperfusion, and sacrificed at day 1 or day 2 post-injury to assess the level of brain injury. We confirmed whether IFNAR1 was deleted from MG in MCAO mice. Our results showed that MG in the ischemic brain of tPA- and tPA+IFNβ-treated control $Cx3cr1^{CreERT2/+}$ MCAO mice expressed a comparable level of IFNAR1. As expected, MG in the ischemic brain of tPA- and tPA+IFNβ-treated $Ifnar1^{fl/fl}$-$Cx3cr1^{CreERT2/+}$ MCAO mice exhibited IFNAR1 knockdown (Supplementary Figure 4B). We then compared the level of brain injury in $Cx3cr1^{CreERT2/+}$ and $Ifnar1^{fl/fl}$-$Cx3cr1^{CreERT2/+}$ MCAO mice subjected to tPA or tPA+IFNβ treatment. Our results showed that IFNβ ameliorated delayed tPA-exacerbated brain injury in $Cx3cr1^{CreERT2/+}$ MCAO mice at day 1 and day 2 post-injury (Figures 4A, B), and these findings are consistent with the results of C57BL/6 MCAO mice treated with delayed tPA in the presence or absence of IFNβ (Figure 1B). In contrast, the protective effect of IFNβ on ameliorating delayed tPA-exacerbated brain injury was abolished in $Ifnar1^{fl/fl}$-$Cx3cr1^{CreERT2/+}$ MCAO mice (Figures 4A, B). Collectively, our results demonstrate that IFNβ-induced IFNAR1 signaling activation in MG plays an essential role in conferring protection against delayed tPA-exacerbated brain injury in ischemic stroke.

MG-specific IFNAR1 knockdown abolishes IFNβ-mediated modulation of MG phenotypes in delayed tPA-treated ischemic stroke

To determine whether IFNβ failed to provide a protective effect in MG-specific IFNAR1 knockdown MCAO mice with delayed tPA treatment was due to the abrogated effect of IFNβ on modulating MG phenotypes, $Ifnar1^{fl/fl}$-$Cx3cr1^{CreERT2/+}$ and $Cx3cr1^{CreERT2/+}$ mice were subjected to 40min MCAO followed by tPA or tPA+IFNβ treatment at 4.5h post-reperfusion and the ischemic brains were then harvested to assess the expression of inflammatory and anti-inflammatory molecules in MG. Our results showed that the inflammatory molecules, CD86 and CD68, and the inflammatory cytokines, IL-1α and IL-1β, were suppressed in MG in the ipsilateral hemisphere of tPA+IFNβ-treated $Cx3cr1^{CreERT2/+}$ MCAO mice compare to that of tPA-treated $Cx3cr1^{CreERT2/+}$ MCAO mice (Figures 5A–D). These results are consistent with the results of C57BL/6 MCAO mice subjected to delayed tPA treatment in the presence or absence of IFNβ (Figures 3A–C). On the contrary, IFNβ-mediated suppression of delayed tPA-enhanced CD86, CD68, IL-1α, and IL-1β expression in MG was abolished in $Ifnar1^{fl/fl}$-$Cx3cr1^{CreERT2/+}$ MCAO mice (Figures 5A–D). Furthermore, we observed that the expression of anti-inflammatory marker Arg1 in MG was upregulated in tPA+IFNβ-treated $Cx3cr1^{CreERT2/+}$ MCAO mice compared to tPA-treated $Cx3cr1^{CreERT2/+}$ MCAO mice (Figure 5E), consistent with the results observed in C57BL/6 MCAO mice (Figure 3D). Similar to C57BL/6 MCAO mice, there was a trend of CD206 upregulation in tPA+IFNβ-treated $Cx3cr1^{CreERT2/+}$ MCAO mice compared to tPA-treated $Cx3cr1^{CreERT2/+}$ MCAO mice (Figure 5F). However, IFNβ-mediated upregulation of Arg1 and CD206 expression in MG was abolished in $Ifnar1^{fl/fl}$-$Cx3cr1^{CreERT2/+}$ MCAO mice with tPA treatment (Figures 5E, F). Altogether, our results demonstrate that the knockdown of IFNAR1 specifically in MG abolishes IFNβ-mediated modulation of MG phenotypes that may subsequently abrogate the protective effect of IFNβ on the amelioration of delayed tPA-exacerbated brain injury in ischemic stroke.

10.3389/fimmu.2023.1148069

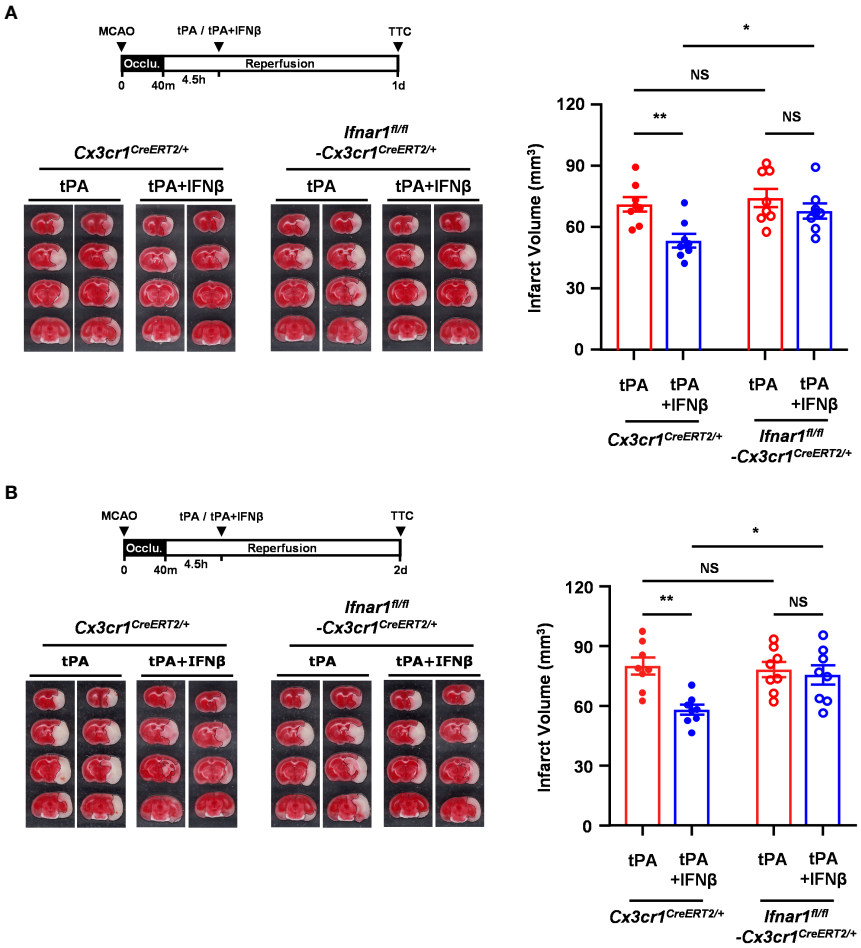

FIGURE 4
IFNβ-conferred protection against delayed tPA-exacerbated ischemic brain injury is abolished in MCAO mice with MG-specific IFNAR1 knockdown. Male *Cx3cr1*$^{CreERT2/+}$ and *Ifnar1*$^{fl/fl}$-*Cx3cr1*$^{CreERT2/+}$ mice were subjected to 40min MCAO followed by tPA or tPA+IFNβ treatment at 4.5h post-reperfusion (n=8/group). **(A)** At day 1 or **(B)** day 2 post-injury, the ischemic brains were harvested and subjected to TTC staining. Two representative TTC-stained brain samples of each group are shown, and the infarct volumes were also measured. **p<0.05; **p<0.01;* NS, no significant difference by two-way ANOVA.

IFNβ inhibits inflammatory MG and promotes anti-inflammatory MG *in vitro*

To confirm our *in vivo* findings that IFNβ modulated MG phenotypes in tPA-treated MCAO mice, we assessed the effect of tPA and IFNβ on regulating the expression of inflammatory and anti-inflammatory molecules in primary MG. Because studies reported that TNFα was induced in the ischemic brain to induce neuroinflammation (20, 30–32), we therefore activated MG with TNFα or TNFα+tPA in the presence or absence of IFNβ followed by Q-PCR and flow cytometry analysis to assess the expression of inflammatory and ant-inflammatory molecules. Our results showed that TNFα upregulated IL-1α and IL-1β mRNA expression in MG, and tPA further enhanced the expression of these inflammatory cytokines, indicating tPA promotes MG activation (Figure 6A). Importantly, IFNβ attenuated IL-1α and IL-1β mRNA expression in TNFα+tPA-treated MG (Figure 6A). Our flow cytometry analysis confirmed that tPA enhanced IL-1β expression in TNFα-treated MG, and IFNβ suppressed TNFα+tPA-induced IL-1β expression in MG (Figure 6B). Furthermore, we assessed the effect of IFNβ on the expression of anti-inflammatory molecules in MG. Our results showed that IFNβ upregulated Arg1 and CD206 expression in TNFα+tPA-treated MG (Figure 6C). Collectively, our results demonstrate that IFNβ suppresses inflammatory cytokine expression and promotes anti-inflammatory molecule expression in TNFα+tPA-treated MG *in vitro*, and that confirms our *in vivo* observation of IFNβ-mediated suppression of inflammatory MG and promotion of anti-inflammatory MG in tPA-treated MCAO mice.

IFNβ confers protection against delayed tPA-exacerbated brain injury and BBB disruption in ischemic stroke subjected to 4.5h occlusion

We observed that IFNβ conferred protection against tPA-exacerbated brain injury in 40min MCAO mice with delayed tPA

10.3389/fimmu.2023.1148069

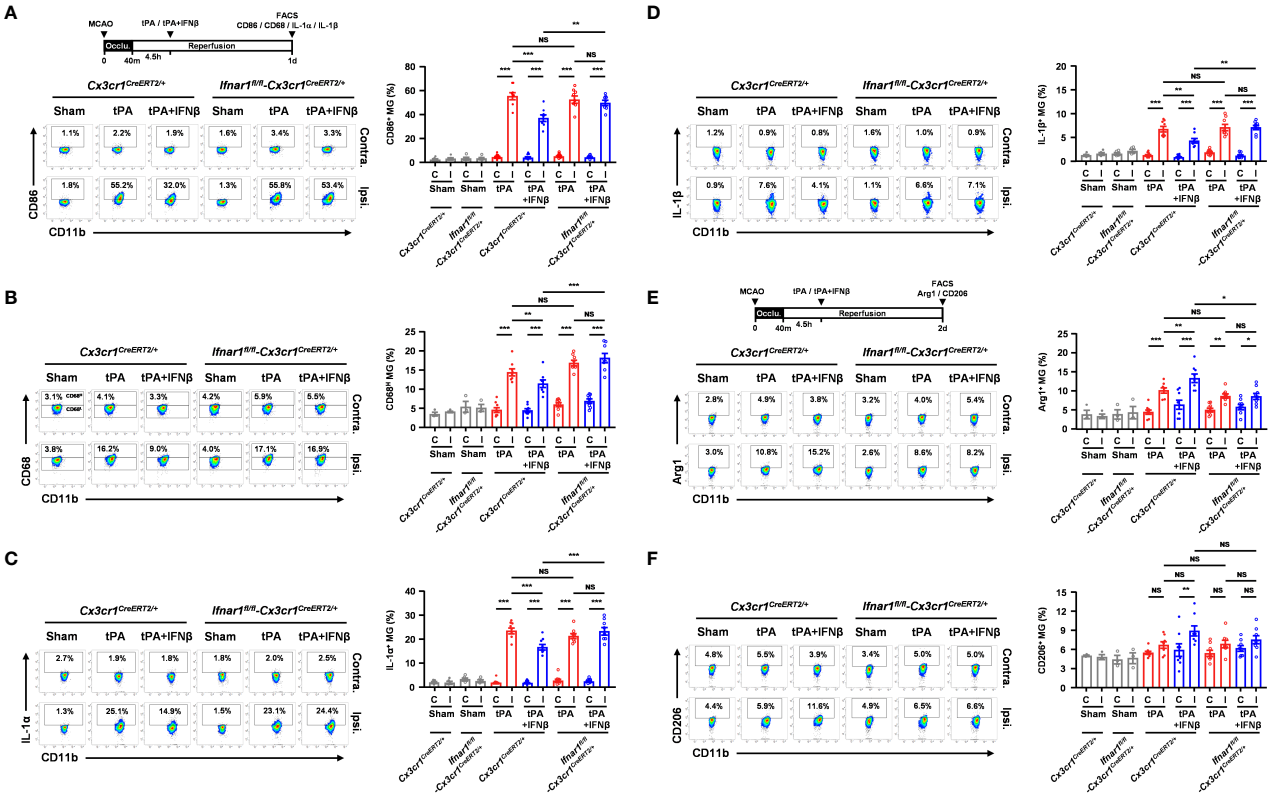

FIGURE 5
MG-specific IFNAR1 knockdown abolishes IFNβ-mediated modulation of MG phenotypes in delayed tPA-treated ischemic stroke. Male *Cx3cr1*$^{CreERT2/+}$ and *Ifnar1*$^{fl/fl}$-*Cx3cr1*$^{CreERT2/+}$ mice were subjected to sham (n=3-4) or 40min MCAO followed by *i.v.* administration of tPA or tPA +IFNβ at 4.5h post-reperfusion (n=8/group). **(A, B)** At day 1 post-injury, the contralateral (Contra.; C) and ipsilateral (Ipsi.; I) hemispheres of sham, and tPA- and tPA+IFNβ-treated MCAO mice were harvested followed by mononuclear cell isolation. The isolated mononuclear cells were stained with CD45 and CD11b antibodies followed by surface staining of CD86 antibody or intracellular staining of CD68 antibody. The expression of CD86 and CD68 in CD45^{int}CD11b^{+} MG was then determined by flow cytometry. The gating of CD68 low (CD68^{L}) was based on the basal expression of CD68 in MG in sham controls, and the expression level of CD68 higher than CD68^{L} was then determined as CD68 high (CD68^{H}). **(C, D)** The isolated cells were *ex-vivo* cultured in the presence of GolgiPlug for 4.5h and then stained with CD45 and CD11b antibodies. Following fixation and permeabilization, cells were subjected to the staining of IL-1α and IL-1β antibodies to determine the intracellular expression of IL-1α and IL-1β in CD45^{int}CD11b^{+} MG by flow cytometry. **(E, F)** At day 2 post-injury, the isolated mononuclear cells were stained with CD45 and CD11b antibodies followed by fixation and permeabilization. The isolated cells were then stained with Arg1 and CD206 antibodies followed by flow cytometry analysis to assess the expression of Arg1 and CD206 in CD45^{int}CD11b^{+} MG. *$p<0.05$; **$p<0.01$; ***$p<0.001$; NS, no significant difference by two-way ANOVA.

treatment at 4.5h post-reperfusion. To closely mimic the clinical condition, we subjected mice to a long-term occlusion of 4.5h followed immediately by vehicle, tPA, or tPA+IFNβ treatment. The ischemic brains were harvested at day 1 post-injury to assess the severity of brain injury. Our results showed that tPA treatment at 4.5h post-injury exacerbated brain injury in MCAO mice, and importantly IFNβ was able to ameliorate delayed tPA-exacerbated ischemic brain injury (Figure 7A). Similarly, we observed that tPA treatment at 4.5h post-injury exacerbated brain injury in female 4.5h MCAO mice, and IFNβ attenuated delayed tPA-exacerbated brain injury in female MCAO mice (Figure 7B). In addition, tPA administration beyond its therapeutic window has been shown to aggravate BBB disruption in ischemic stroke (20). We therefore assessed whether delayed tPA treatment at 4.5h post-injury aggravated BBB disruption and whether IFNβ lessened delayed tPA-aggravated BBB disruption in 4.5h MCAO mice. Indeed, our results showed that delayed tPA treatment aggravated BBB disruption, leading to enhanced Evans blue leakage in the ipsilateral hemisphere of tPA-treated MCAO mice compared to that of vehicle-treated MCAO mice (Figure 7C). Importantly, we observed IFNβ lessened delayed tPA-aggravated BBB disruption, resulting in attenuated Evans blue leakage in the ipsilateral hemisphere of tPA+IFNβ-treated MCAO mice compared to that of tPA-treated MCAO mice (Figure 7C). Furthermore, we assessed whether IFNβ offered protection against delayed tPA-aggravated BBB disruption in female MCAO mice. Although the level of BBB disruption was less severe in female MCAO mice compared to male MCAO mice because of sex-mediated differences in ischemic brain injury (25, 26), our results showed that delayed tPA treatment aggravated BBB disruption and IFNβ lessened delayed tPA-aggravated BBB disruption in female MCAO mice (Figure 7D), consistent with the results of male MCAO mice (Figure 7C). Altogether, our results demonstrate that IFNβ ameliorates delayed tPA-exacerbated brain injury and lessens delayed tPA-aggravated BBB disruption in MCAO mice subjected to 4.5h occlusion.

10.3389/fimmu.2023.1148069

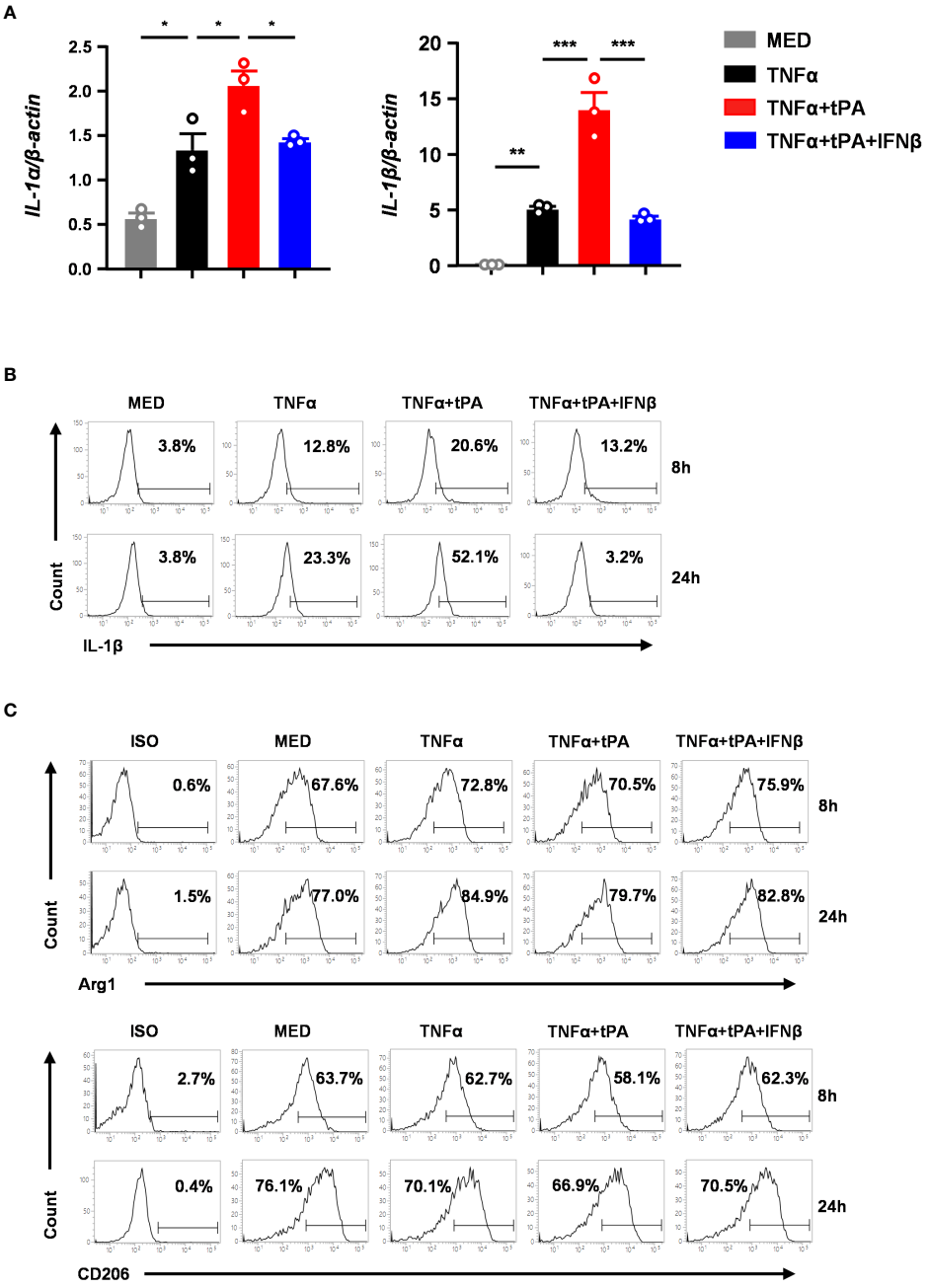

FIGURE 6
IFNβ inhibits inflammatory MG and promotes anti-inflammatory MG *in vitro*. Primary MG were treated with TNFα (50ng/ml) or TNFα+tPA (10μg/ml) in the presence or absence of IFNβ (1000U/ml). **(A)** At 8h after treatment, cells were harvested and subjected to Q-PCR analysis for IL-1α and IL-1β mRNA expression (n=3 technique replicates per group). The results represent 3-4 independent biological replicates with similar results. *$p<0.05$; **$p<0.01$; ***$p<0.001$ by one-way ANOVA. **(B)** At 8h and 24h post-treatment, cells were fixed and permeabilized followed by intracellular staining of IL-1β. The frequency (%) of IL-1β expression was measured. The experiments were repeated for 6 times with similar results obtained. **(C)** At 8h and 24h post-treatment, cells were fixed and permeabilized followed by staining of Arg1 and CD206. The frequency (%) of Arg1 and CD206 expression was measured. The experiments were repeated for 3 times with similar results obtained.

MG-specific IFNAR1 knockdown partly reverses IFNβ-lessened delayed tPA-aggravated BBB disruption in ischemic stroke

To further investigate whether IFNβ-mediated modulation of MG phenotypes contributes to the protective effect of IFNβ on lessening delayed tPA-aggravated BBB disruption in ischemic stroke, we assessed the severity of BBB disruption in *Ifnar1*$^{fl/fl}$-*Cx3cr1*$^{CreERT2/+}$ and *Cx3cr1*$^{CreERT2/+}$ MCAO mice treated with delayed tPA in the presence or absence of IFNβ. Our results showed that IFNβ lessened BBB disruption in tPA-treated *Cx3cr1*$^{CreERT2/+}$ MCAO mice, resulting in attenuated Evans blue leakage in the ischemic brain of tPA+IFNβ-treated *Cx3cr1*$^{CreERT2/+}$

10.3389/fimmu.2023.1148069

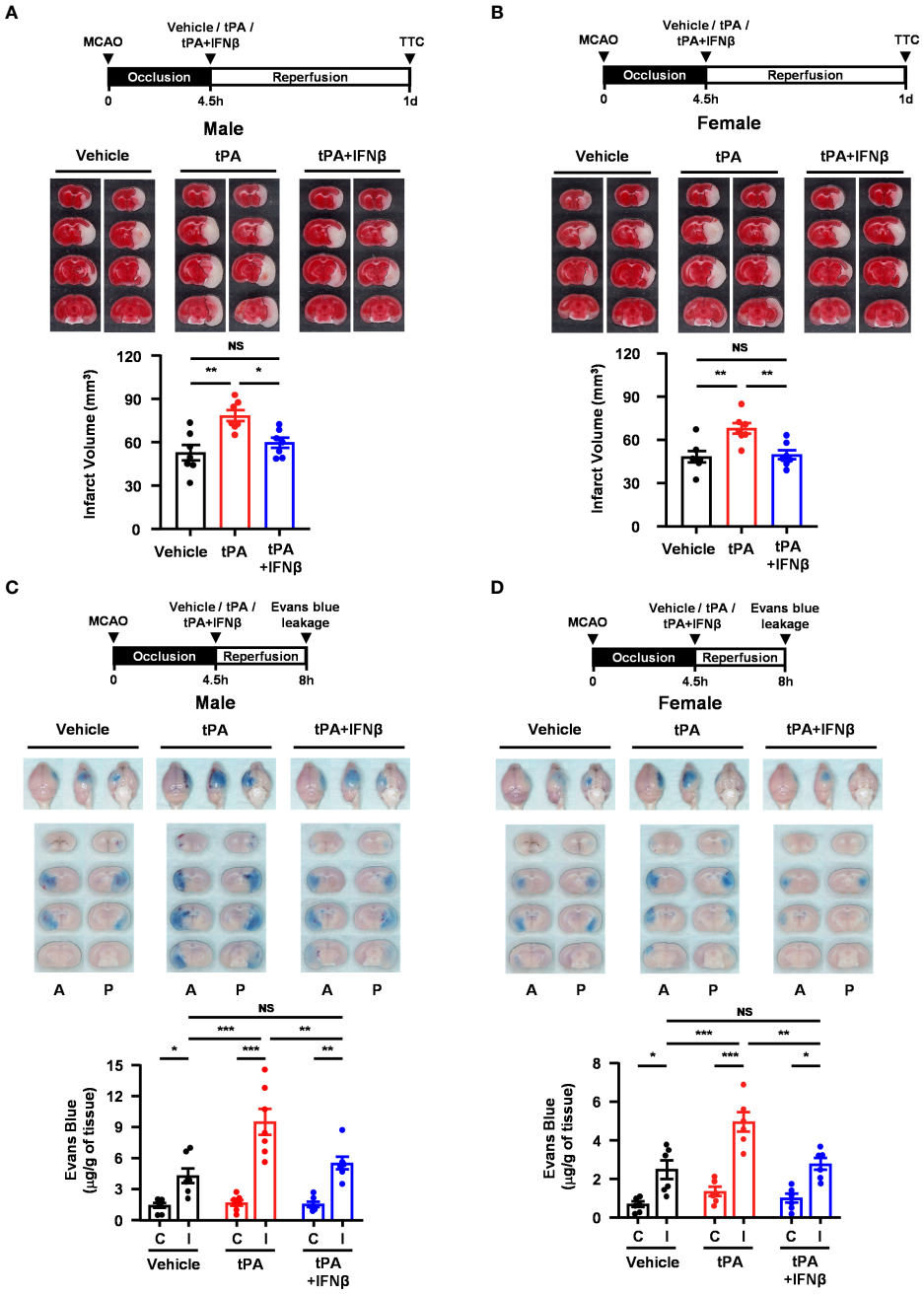

FIGURE 7
IFNβ confers protection against delayed tPA-exacerbated brain injury and BBB disruption in ischemic stroke subjected to 4.5h occlusion. **(A)** Male and **(B)** female C57BL/6 mice were subjected to 4.5h MCAO followed immediately by vehicle, tPA, or tPA+IFNβ administration. At day 1 post-injury, the ischemic brains were harvested and subjected to TTC staining. Two representative TTC-stained brain samples of each group are shown, and the infarct volumes were measured (n=7/group). *$p<0.05$; **$p<0.01$; NS: no significant difference by one-way ANOVA. **(C)** Male and **(D)** female C57BL/6 mice were subjected to 4.5h MCAO followed immediately by *i.v.* administration of vehicle, tPA, or tPA+IFNβ. Mice were injected with Evans blue 1h prior to euthanasia, and the ischemic brains were harvested at 8h post-injury followed by imaging and sectioning. The Evans blue leakage in the contralateral and ipsilateral hemispheres was quantified (male: n=7/group; female: n=6/group). A, anterior surface; P, posterior surface; C, contralateral hemisphere; I, ipsilateral hemisphere. *$p<0.05$; **$p<0.01$; ***$p<0.001$; NS, no significant difference by two-way ANOVA.

MCAO mice compared to that of tPA-treated *Cx3cr1*$^{CreERT2/+}$ MCAO mice (Figure 8A). Interestingly, we found that the protective effect of IFNβ on lessening delayed tPA-aggravated BBB disruption was partly but not fully reversed in *Ifnar1*$^{fl/fl}$-*Cx3cr1*$^{CreERT2/+}$ MCAO mice, as there was no statistically significant difference in the Evans blue leakage between *Ifnar1*$^{fl/fl}$-*Cx3cr1*$^{CreERT2/+}$ and *Cx3cr1*$^{CreERT2/+}$ MCAO mice treated with tPA +IFNβ (Figure 8A). The similar results were also observed in female MCAO mice (Figure 8B). Collectively, our results suggest that IFNβ-mediated modulation of MG phenotypes may partly contribute to lessening delayed tPA-aggravated BBB disruption in ischemic stroke.

10.3389/fimmu.2023.1148069

Discussion

The use of tPA is limited by its narrow therapeutic window of 3 to 4.5h post-onset of ischemic stroke, and the administration of tPA beyond its therapeutic window has been linked to increased risks of aggravated BBB disruption and HT induction. Studies have reported that only less than 10% of patients with acute ischemic stroke were able to receive tPA treatment (33, 34). Thus, developing a therapy that can be co-administered with tPA to ameliorate ischemia-induced neuroinflammation and extend tPA therapeutic window would be of clinical importance. We have previously demonstrated that IFNβ conferred protection against ischemic stroke (13). In our follow-up study, we further demonstrated that IFNβ was able to extend tPA therapeutic window to 3h post-injury. Mechanistically, we identified that IFNβ attenuated delayed tPA-induced brain injury exacerbation, BBB disruption aggravation, and HT induction in ischemic stroke, and these protective effects were partly mediated through IFNβ-exerted suppression of MMP3 and MMP9 in the ischemic brain (20). In the present study, we further investigated the time limit of IFNβ on the extension of tPA therapeutic window in ischemic stroke. Our results demonstrated that IFNβ was able to extend tPA therapeutic window to 4.5h post-injury and that was accompanied with ameliorated brain injury and lessened BBB disruption in ischemic stroke. These findings are clinically significant. As previous studies reported that the rodent time is about 40 times faster than human time and one human year is equivalent to nine mice days (35), the extension of tPA therapeutic window to 4.5h post-injury in MACO mice would be considered a significant extension of tPA therapeutic window for human ischemic stroke. Thus, our results demonstrate the

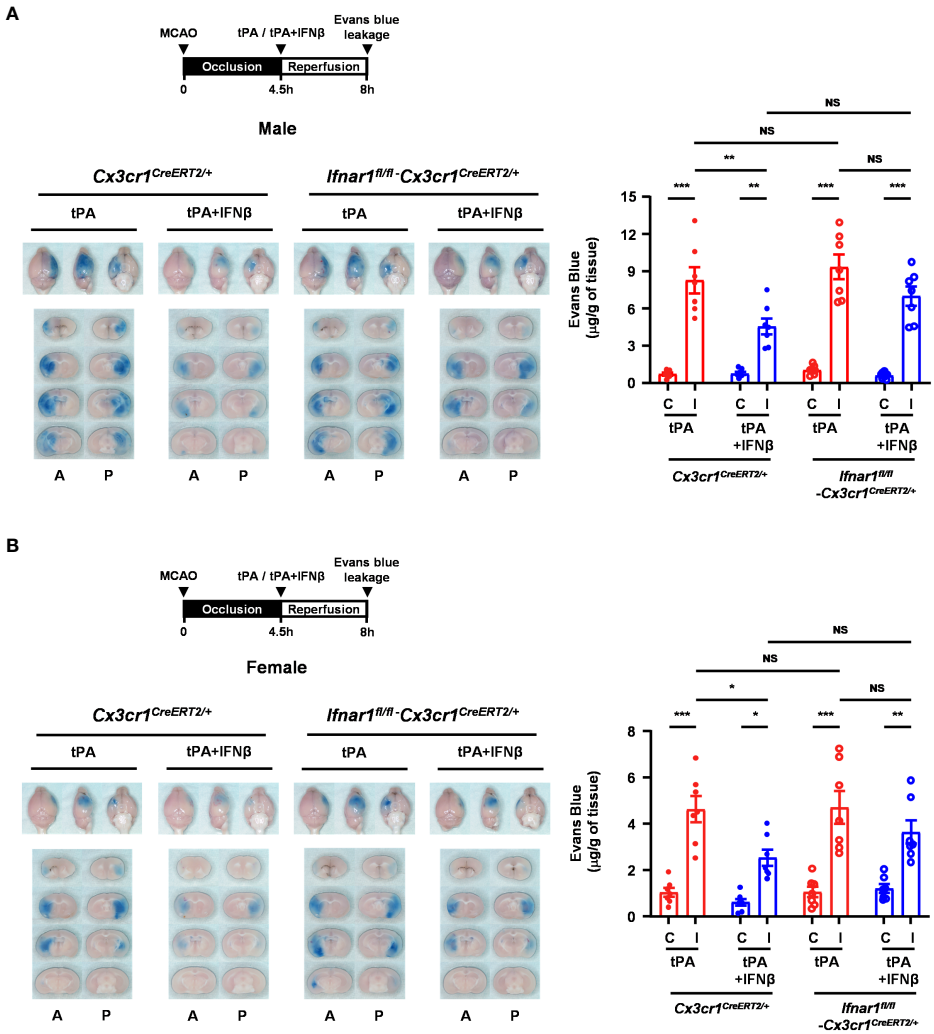

FIGURE 8
MG-specific IFNAR1 knockdown partly reverses IFNβ-lessened delayed tPA-aggravated BBB disruption in ischemic stroke. **(A)** Male and **(B)** female *Cx3cr1*$^{CreERT2/+}$ and *Ifnar1*$^{fl/fl}$-*Cx3cr1*$^{CreERT2/+}$ mice were subjected to 4.5h MCAO followed immediately by tPA or tPA+IFNβ administration. Mice were then injected with Evans blue 1h prior to euthanasia, and the ischemic brains were harvested at 8h post-injury followed by imaging and sectioning. The Evans blue leakage in the contralateral and ipsilateral hemispheres was quantified (male: n=7/group; female: n=7/group). A, anterior surface; P, posterior surface; C, contralateral hemisphere; I, ipsilateral hemisphere. *$p<0.05$; **$p<0.01$; ***$p<0.001$; NS, no significant difference by two-way ANOVA.

beneficial effects of IFNβ on the extension of tPA therapeutic window for ischemic stroke treatment.

Studies have shown that MG-mediated inflammatory response is an important pathological mechanism in ischemic stroke (36, 37). MG can be activated by various stimuli to secrete factors that exert proinflammatory or anti-inflammatory effects (38, 39). Previous studies show that inflammatory MG exert detrimental effects, whereas anti-inflammatory MG possess neuroprotective effects in the CNS (8, 9). Thus, it is beneficial to promote anti-inflammatory and inhibit inflammatory phenotypes of MG in ischemic stroke. Since cerebral ischemia induces MG activation and tPA was shown to further promote MG activation (2, 3), we assessed whether IFNβ modulated MG phenotypes to confer protection against delayed tPA-exacerbated brain injury in ischemic stroke. Indeed, the effect of IFNβ on the induction of anti-inflammatory myeloid cells has been documented previously. For instance, IFNβ has been shown to induce anti-inflammatory macrophages that express M2 genes, including Arg1 and Fizz1 (40). In addition, studies reported that IFNAR1 signaling is required for LPS-induced IL-10 upregulation in macrophages (41). Furthermore, we have previously demonstrated that IFNβ exerts differential effects on inflammatory and anti-inflammatory cytokine production, leading to the suppression of proinflammatory cytokines, IL-12 and IL-23, and the promotion of anti-inflammatory cytokine IL-10 in dendritic cells (42). Moreover, TLR3-induced upregulation of IL-10 was reported to be mediated by IFNβ in MG (43). Finally, the production of IFNβ by macrophages has been shown to promote the resolution of bacterial inflammation, and this effect is potentially mediated through IFNβ-induced IL-10 production in macrophages *in vivo* (44). In the present study, our findings revealed that IFNβ attenuated tPA-upregulated inflammatory molecules, CD86, IL-1α, and IL-1β, and promoted anti-inflammatory molecules, Arg1 and CD206, in MG during the acute phase of ischemic stroke. Notably, the effects of IFNβ on modulating MG phenotypes and ameliorating delayed tPA-exacerbated brain injury in ischemic stroke were abolished in mice with the conditional knockdown of IFNAR1 in MG. Finally, our *in vitro* studies showed that IFNβ suppressed TNFα+tPA-induced inflammatory molecules, IL-1α and IL-1β, and enhanced anti-inflammatory molecules, Arg1 and CD206, in primary MG, consistent with our *in vivo* findings. Altogether, our results provide the first evidence that IFNβ exerts modulatory effects on suppressing inflammatory and promoting anti-inflammatory MG, and that may subsequently lead to attenuated neuroinflammation and ameliorated brain injury in delayed tPA-treated ischemic stroke.

Previous studies showed that infiltrating monocytes/macrophages become MG-like phenotypes following phagocytosis, leading to the conversion of $CD45^{hi}$ macrophages into $CD45^{int}$ macrophages, and this conversion was observed in the ischemic brain of stroke animals at the later time points of day 3 and day 7 post-injury (27–29). In this study, we determined MG based on their intermediate expression of CD45 and positive expression of CD11b, and the expression of pro-inflammatory and anti-inflammatory markers in $CD45^{int}CD11b^{+}$ MG was assessed at day 1 and day 2 post-injury, respectively. We verified whether the population of $CD45^{int}CD11b^{+}$ cells contained infiltrating macrophages by measuring the expression of CD11a and Ly6C in $CD45^{int}CD11b^{+}$ cells, as these two markers are well defined surface markers for macrophages (28, 45, 46). We did not observe $CD45^{int}CD11b^{+}$ cells expressed CD11a or Ly6C in the ischemic brain of day 1 MCAO mice. However, a slight increase of $Ly6C^{+}$ cells in the population of $CD45^{int}CD11b^{+}$ cells was observed in the ischemic brain of day 2 MCAO mice. Interestingly, a further increased frequency of $Ly6C^{+}CD45^{int}CD11b^{+}$ cells was found in the ischemic brain of tPA-treated mice compared to that of vehicle- or tPA+IFNβ-treated MCAO mice. We speculated that increased $Ly6C^{+}CD45^{int}CD11b^{+}$ cells in the ischemic brain of tPA-treated MCAO might be due to increased cell infiltrates converting into MG-like phenotypes following reperfusion. Notably, we observed that $Arg1^{+}$ cells were largely associated with $Ly6C^{-}CD45^{int}CD11b^{+}$ cells but not $Ly6C^{+}CD45^{int}CD11b^{+}$ cells in the ischemic brain of vehicle-, tPA-, and tPA+IFNβ-treated MCAO mice. Taken altogether, our findings suggest that ischemic stroke promotes a low frequency of infiltrating $Ly6C^{+}CD45^{hi}CD11b^{+}$ cells converting into $Ly6C^{+}CD45^{int}CD11b^{+}$ MG-like cells in the ischemic brain at day 2 but not day 1 post-injury. Most importantly, we found that IFNβ-mediated attenuation of inflammatory phenotype (day 1) and augmentation of anti-inflammatory phenotype (day 2) of MG in tPA-treated MCAO mice were largely associated with $Ly6C^{-}CD45^{int}CD11b^{+}$ resident MG but not $Ly6C^{+}CD45^{int}CD11b^{+}$ MG-like infiltrating cells. Thus, our findings suggest that IFNβ mainly modulates resident MG phenotypes and that may then alleviate tPA-aggravated neuroinflammation in ischemic stroke.

The BBB possesses an essential role in maintaining the CNS homeostasis. The integrity of BBB is maintained by physical and biochemical characteristics, including tight junction protein complexes and transporters (47). In addition, its function is supported by astrocytes, pericytes, neurons, and MG that form the neurovascular unit (NVU). The cellular components of NVU can be activated upon sterile inflammation or disease induction that contributes to the BBB remodeling (48). This is particularly true for MG, because MG can be polarized into inflammatory or anti-inflammatory phenotype that exerts different impacts on BBB integrity. Studies have shown that inflammatory MG promote BBB dysfunction, whereas anti-inflammatory MG contribute to maintaining BBB integrity (49–51). Notably, our results showed that delayed tPA treatment promoted the inflammatory phenotype of MG, and that was correlated with aggravated BBB disruption in MCAO mice with delayed tPA treatment. In contrast, IFNβ suppressed tPA-enhanced inflammatory MG and promoted anti-inflammatory MG, and that was linked to lessened BBB disruption in delayed tPA-treated MCAO mice. Importantly, we found that the effect of IFNβ on inflammatory MG suppression and anti-inflammatory MG promotion was abrogated in delayed tPA-treated MCAO mice with MG-specific IFNAR1 deletion. Interestingly, we observed the protective effect of IFNβ on lessening delayed tPA-aggravated BBB disruption was partly but

not fully abolished in these animals. Altogether, these results suggest that IFNβ-mediated modulation of MG phenotypes contributes to the alleviation of BBB disruption in ischemic stroke with delayed tPA treatment.

There are limitations with our current study. First, further studies would be required to identify the signaling pathways activated by IFNβ/IFNAR1 axis modulating MG polarization in delayed tPA-treated ischemic stroke. IFNAR1 signaling activates STAT1, STAT2, and STAT3. Studies have shown that STAT1 and STAT2 mediate the antiviral and inflammatory effects of IFNAR1 signaling (52–55). However, IFNAR1 signaling-induced STAT3 activation has been shown to inhibit STAT1-dependent gene activation, thereby downregulating IFNAR1 activation-induced inflammatory mediators (52). In addition, STAT3 activation has been shown to promote Arg1 and IL-10 upregulation (56). Thus, it is possible that IFNAR1 signaling induces STAT3 activation, leading to the suppression of tPA-enhanced inflammatory molecules, IL-1α, IL-1β and CD86, expression and the promotion of anti-inflammatory molecules, Arg1 and CD206, upregulation in MG in delayed tPA-treated stroke animals. Further studies of silencing STAT3 specifically in MG would provide insight into whether the activation of STAT3 *via* IFNAR1 signaling is required for IFNβ-mediated modulation of MG phenotypes in ischemic stroke with delayed tPA treatment. Second, we observed that the protective effect of IFNβ on lessening delayed tPA-aggravated BBB in ischemic stroke was partly reversed in MCAO mice with MG-specific IFNAR1 knockdown, suggesting that IFNβ-mediated modulation of MG phenotypes plays a role in lessening delayed tPA-aggravated BBB disruption in ischemic stroke. Since IFNAR1 is highly expressed in brain endothelial cells (57, 58), it is possible that IFNβ acts on brain endothelial cells to offer partial protection in MG-specific IFNAR1 knockdown MCAO mice subjected to delayed tPA treatment. Indeed, our previous study showed that IFNβ attenuated adhesion molecules, ICAM-1 and E-selectin, upregulation in TNFα-stimulated bEnd.3 cells *in vitro* and in the ischemic brain *in vivo* (13), suggesting IFNβ exerts a direct effect on the suppression of brain endothelial cell activation. Thus, further studies using conditional knockout mice in which IFNAR1 is specifically knockout in brain endothelial cells are warranted to elucidate the direct effect of IFNβ on modulating brain endothelial cells to lessen delayed tPA-aggravated BBB disruption in ischemic stroke. Finally, in this study we used the intraluminal suture MCAO model to evaluate the effect of IFNβ on the amelioration of delayed tPA-exacerbated brain injury in ischemic stroke. It is recognized that the suture MCAO model produces stable and consistent outcomes of ischemic brain injury. Thus, this model benefits our cellular and molecular mechanism studies to decipher the protective effect of IFNβ on ameliorating delayed tPA-exacerbated brain injury in ischemic stroke. Nevertheless, the suture MCAO model has limitations on assessing tPA thrombolytic effects *in vivo*. Thus, studies utilizing the thromboembolic MCAO model would be needed to further confirm the observed mechanism of IFNβ-exerted modulation of MG phenotypes in delayed tPA-treated MCAO mice.

In summary, we report that IFNβ extends tPA therapeutic window to 4.5h post-injury in ischemic stroke. Furthermore, we show that IFNβ exerts protective effects on attenuating delayed tPA-exacerbated brain injury, lessening delayed tPA-aggravated BBB disruption, and reducing delayed-tPA enhanced mortality in ischemic stroke. Mechanistically, we identify that IFNβ modulates MG phenotypes, leading to the suppression of inflammatory MG and the promotion of anti-inflammatory MG in delayed tPA-treated MCAO animals. Importantly, we find that MG-mediated modulation of MG phenotypes plays an important role in ameliorating delayed tPA-exacerbated ischemic brain injury, because the knockdown of IFNAR1 specifically in MG abrogates the effect of IFNβ on modulating MG polarization, abolishes the protective effect of IFNβ on ameliorating brain injury, and partly reverses the beneficial effect of IFNβ on lessening BBB disruption in delayed tPA-treated MCAO animals. In summary, our current study reveals a novel function of IFNβ on the modulation of MG polarization toward anti-inflammatory phenotype that may subsequently confer protection against delayed tPA-exacerbated brain injury in ischemic stroke. Thus, our findings open a new venue for the use of IFNβ in the combination of tPA to attenuate neuroinflammation and extend tPA therapeutic window in ischemic stroke.

Data availability statement

The original contributions presented in the study are included in the article/Supplementary Material. Further inquiries can be directed to the corresponding author.

Ethics statement

The animal study was reviewed and approved by Purdue Animal Care and Use Committee.

Author contributions

P-CK performed the experiments, analyzed data, and wrote the manuscript. W-TW, BS, HP, PB, and BK performed the experiments. I-CIY reviewed and edited the manuscript. J-HJY. conceived the study, designed the experiments, and wrote the manuscript. All authors contributed to the article and approved the submitted version.

Funding

This study was supported by research funding from NIH R01NS102449 to J-HJY.

Conflict of interest

The authors declare that the research was conducted in the absence of any commercial or financial relationships that could be construed as a potential conflict of interest.

Publisher's note

All claims expressed in this article are solely those of the authors and do not necessarily represent those of their affiliated organizations, or those of the publisher, the editors and the reviewers. Any product that may be evaluated in this article, or claim that may be made by its manufacturer, is not guaranteed or endorsed by the publisher.

Supplementary material

The Supplementary Material for this article can be found online at: https://www.frontiersin.org/articles/10.3389/fimmu.2023.1148069/full#supplementary-material

References

1. Jin R, Yang G, Li G. Inflammatory mechanisms in ischemic stroke: Role of inflammatory cells. *J Leukoc Biol* (2010) 87:779–89. doi: 10.1189/jlb.1109766

2. Pineda D, Ampurdanes C, Medina MG, Serratosa J, Tusell JM, Saura J, et al. Tissue plasminogen activator induces microglial inflammation *via* a noncatalytic molecular mechanism involving activation of mitogen-activated protein kinases and akt signaling pathways and AnnexinA2 and galectin-1 receptors. *Glia* (2012) 60:526–40. doi: 10.1002/glia.22284

3. Won S, Lee JK, Stein DG. Recombinant tissue plasminogen activator promotes, and progesterone attenuates, microglia/macrophage M1 polarization and recruitment of microglia after MCAO stroke in rats. *Brain Behav Immun* (2015) 49:267–79. doi: 10.1016/j.bbi.2015.06.007

4. Powers WJ, Rabinstein AA, Ackerson T, Adeoye OM, Bambakidis NC, Becker K, et al. Guidelines for the early management of patients with acute ischemic stroke: 2019 update to the 2018 guidelines for the early management of acute ischemic stroke: A guideline for healthcare professionals from the American heart Association/American stroke association. *Stroke* (2019) 50:e344–418. doi: 10.1161/STR.0000000000000211

5. Zhang J, Yang Y, Sun H, Xing Y. Hemorrhagic transformation after cerebral infarction: current concepts and challenges. *Ann Transl Med* (2014) 2:81. doi: 10.3978/j.issn.2305-5839.2014.08.08

6. Chapman SN, Mehndiratta P, Johansen MC, McMurry TL, Johnston KC, Southerland AM. Current perspectives on the use of intravenous recombinant tissue plasminogen activator (tPA) for treatment of acute ischemic stroke. *Vasc Health Risk Manag* (2014) 10:75–87. doi: 10.2147/VHRM.S39213

7. Rosell A, Foerch C, Murata Y, Lo EH. Mechanisms and markers for hemorrhagic transformation after stroke. *Acta Neurochir Suppl* (2008) 105:173–8. doi: 10.1007/978-3-211-09469-3_34

8. Hu X, Li P, Guo Y, Wang H, Leak RK, Chen S, et al. Microglia/macrophage polarization dynamics reveal novel mechanism of injury expansion after focal cerebral ischemia. *Stroke* (2012) 43:3063–70. doi: 10.1161/STROKEAHA.112.659656

9. Hu X, Leak RK, Shi Y, Suenaga J, Gao Y, Zheng P, et al. Microglial and macrophage polarization-new prospects for brain repair. *Nat Rev Neurol* (2015) 11:56–64. doi: 10.1038/nrneurol.2014.207

10. Mizuma A, Yenari MA. Anti-inflammatory targets for the treatment of reperfusion injury in stroke. *Front Neurol* (2017) 8:467. doi: 10.3389/fneur.2017.00467

11. Cheriyan J, Kim S, Wolansky LJ, Cook SD, Cadavid D. Impact of inflammation on brain volume in multiple sclerosis. *Arch Neurol* (2012) 69:82–8. doi: 10.1001/archneurol.2011.674

12. Kasper LH, Reder AT. Immunomodulatory activity of interferon-beta. *Ann Clin Transl Neurol* (2014) 1:622–31. doi: 10.1002/acn3.84

13. Kuo PC, Scofield BA, Yu IC, Chang FL, Ganea D, Yen JH. Interferon-beta modulates inflammatory response in cerebral ischemia. *J Am Heart Assoc* (2016) 5: 1-15. doi: 10.1161/JAHA.115.002610

14. Cruz SA, Hari A, Qin Z, Couture P, Huang H, Lagace DC, et al. Loss of IRF2BP2 in microglia increases inflammation and functional deficits after focal ischemic brain injury. *Front Cell Neurosci* (2017) 11:201. doi: 10.3389/fncel.2017.00201

15. Dixon BJ, Chen D, Zhang Y, Flores J, Malaguit J, Nowrangi D, et al. Intranasal administration of interferon beta attenuates neuronal apoptosis *via* the JAK1/STAT3/BCL-2 pathway in a rat model of neonatal hypoxic-ischemic encephalopathy. *ASN Neuro* (2016) 8: 1-14. doi: 10.1177/1759091416670492

16. Inacio AR, Liu Y, Clausen BH, Svensson M, Kucharz K, Yang Y, et al. Endogenous IFN-beta signaling exerts anti-inflammatory actions in experimentally induced focal cerebral ischemia. *J Neuroinflamm* (2015) 12:211. doi: 10.1186/s12974-015-0427-0

17. Liu H, Xin L, Chan BP, Teoh R, Tang BL, Tan YH. Interferon-beta administration confers a beneficial outcome in a rabbit model of thromboembolic cerebral ischemia. *Neurosci Lett* (2002) 327:146–8. doi: 10.1016/S0304-3940(02)00371-3

18. Marsh B, Stevens SL, Packard AE, Gopalan B, Hunter B, Leung PY, et al. Systemic lipopolysaccharide protects the brain from ischemic injury by reprogramming the response of the brain to stroke: A critical role for IRF3. *J Neurosci* (2009) 29:9839–49. doi: 10.1523/JNEUROSCI.2496-09.2009

19. Veldhuis WB, Derksen JW, Floris S, van der Meide PH, De Vries HE, Schepers J, et al. Interferon-beta blocks infiltration of inflammatory cells and reduces infarct volume after ischemic stroke in the rat. *J Cereb Blood Flow Metab* (2003) 23:1029–39. doi: 10.1097/01.WCB.0000080703.47016.B6

20. Kuo PC, Weng WT, Scofield BA, Furnas D, Paraiso HC, Intriago AJ, et al. Interferon-beta alleviates delayed tPA-induced adverse effects *via* modulation of MMP3/9 production in ischemic stroke. *Blood Adv* (2020) 4:4366–81. doi: 10.1182/bloodadvances.2020001443

21. Zhang L, Zhang ZG, Zhang R, Morris D, Lu M, Coller BS, et al. Adjuvant treatment with a glycoprotein IIb/IIIa receptor inhibitor increases the therapeutic window for low-dose tissue plasminogen activator administration in a rat model of embolic stroke. *Circulation* (2003) 107:2837–43. doi: 10.1161/01.CIR.0000068374.57764.EB

22. Zhang L, Zhang ZG, Buller B, Jiang J, Jiang Y, Zhao D, et al. Combination treatment with VELCADE and low-dose tissue plasminogen activator provides potent neuroprotection in aged rats after embolic focal ischemia. *Stroke* (2010) 41:1001–7. doi: 10.1161/STROKEAHA.109.577288

23. Kuo PC, Yu IC, Scofield BA, Brown DA, Curfman ET, Paraiso HC, et al. 3H-1,2-Dithiole-3-thione as a novel therapeutic agent for the treatment of ischemic stroke through Nrf2 defense pathway. *Brain Behav Immun* (2017) 62:180–92. doi: 10.1016/j.bbi.2017.01.018

24. Weng WT, Kuo PC, Brown DA, Scofield BA, Furnas D, Paraiso HC, et al. 4-ethylguaiacol modulates neuroinflammation and Th1/Th17 differentiation to ameliorate disease severity in experimental autoimmune encephalomyelitis. *J Neuroinflamm* (2021) 18:110. doi: 10.1186/s12974-021-02143-w

25. Hayashi S, Ueyama T, Kajimoto T, Yagi K, Kohmura E, Saito N. Involvement of gamma protein kinase c in estrogen-induced neuroprotection against focal brain ischemia through G protein-coupled estrogen receptor. *J Neurochem* (2005) 93:883–91. doi: 10.1111/j.1471-4159.2005.03080.x

26. Patrizz AN, Moruno-Manchon JF, O'Keefe LM, Doran SJ, Patel AR, Venna VR, et al. Sex-specific differences in autophagic responses to experimental ischemic stroke. *Cells* (2021) 10: 1-16. doi: 10.3390/cells10071825

27. Ju H, Park KW, Kim ID, Cave JW, Cho S. Phagocytosis converts infiltrated monocytes to microglia-like phenotype in experimental brain ischemia. *J Neuroinflamm* (2022) 19:190. doi: 10.1186/s12974-022-02552-5

28. Chen HR, Sun YY, Chen CW, Kuo YM, Kuan IS, Tiger Li ZR, et al. Fate mapping *via* CCR2-CreER mice reveals monocyte-to-microglia transition in development and neonatal stroke. *Sci Adv* (2020) 6:eabb2119. doi: 10.1126/sciadv.abb2119

29. Grassivaro F, Menon R, Acquaviva M, Ottoboni L, Ruffini F, Bergamaschi A, et al. Convergence between microglia and peripheral macrophages phenotype during development and neuroinflammation. *J Neurosci* (2020) 40:784–95. doi: 10.1523/JNEUROSCI.1523-19.2019

30. Chen X, Zhang X, Wang Y, Lei H, Su H, Zeng J, et al. Inhibition of immunoproteasome reduces infarction volume and attenuates inflammatory reaction in a rat model of ischemic stroke. *Cell Death Dis* (2015) 6:e1626. doi: 10.1038/cddis.2014.586

31. Li YH, Fu HL, Tian ML, Wang YQ, Chen W, Cai LL, et al. Neuron-derived FGF10 ameliorates cerebral ischemia injury *via* inhibiting NF-kappaB-dependent neuroinflammation and activating PI3K/Akt survival signaling pathway in mice. *Sci Rep* (2016) 6:19869. doi: 10.1038/srep19869

32. Pan Z, Cui M, Dai G, Yuan T, Li Y, Ji T, et al. Protective effect of anthocyanin on neurovascular unit in cerebral Ischemia/Reperfusion injury in rats. *Front Neurosci* (2018) 12:947. doi: 10.3389/fnins.2018.00947

33. Schwamm LH, Ali SF, Reeves MJ, Smith EE, Saver JL, Messe S, Fonarow GC, et al. Temporal trends in patient characteristics and treatment with intravenous thrombolysis among acute ischemic stroke patients at get with the guidelines-stroke hospitals. *Circ Cardiovasc Qual Outcomes* (2013) 6:543–9. doi: 10.1161/CIRCOUTCOMES.111.000095

34. Reeves MJ, Arora S, Broderick JP, Frankel M, Heinrich JP, Hickenbottom S, et al. Acute stroke care in the US: Results from 4 pilot prototypes of the Paul coverdell national acute stroke registry. *Stroke* (2005) 36:1232–40. doi: 10.1161/01.STR.0000165902.18021.5b

35. Dutta S, Sengupta P. Men and mice: Relating their ages. *Life Sci* (2016) 152:244–8. doi: 10.1016/j.lfs.2015.10.025

36. Guruswamy R, ElAli A. Complex roles of microglial cells in ischemic stroke pathobiology: New insights and future directions. *Int J Mol Sci* (2017) 18: 1-16. doi: 10.3390/ijms18030496

37. Zhang S. Microglial activation after ischaemic stroke. *Stroke Vasc Neurol* (2019) 4:71–4. doi: 10.1136/svn-2018-000196

38. Herder V, Iskandar CD, Kegler K, Hansmann F, Elmarabet SA, Khan MA, et al. Dynamic changes of Microglia/Macrophage M1 and M2 polarization in theiler's murine encephalomyelitis. *Brain Pathol* (2015) 25:712–23. doi: 10.1111/bpa.12238

39. Lyu J, Xie D, Bhatia TN, Leak RK, Hu X, Jiang X. Microglial/Macrophage polarization and function in brain injury and repair after stroke. *CNS Neurosci Ther* (2021) 27:515–27. doi: 10.1111/cns.13620

40. Tong Y, Zhou L, Yang L, Guo P, Cao Y, Qin FX, et al. Concomitant type I IFN and m-CSF signaling reprograms monocyte differentiation and drives pro-tumoral arginase production. *EBioMedicine* (2019) 39:132–44. doi: 10.1016/j.ebiom.2018.11.062

41. Chang EY, Guo B, Doyle SE, Cheng G. Cutting edge: Involvement of the type I IFN production and signaling pathway in lipopolysaccharide-induced IL-10 production. *J Immunol* (2007) 178:6705–9. doi: 10.4049/jimmunol.178.11.6705

42. Yen JH, Kong W, Hooper KM, Emig F, Rahbari KM, Kuo PC, et al. Differential effects of IFN-beta on IL-12, IL-23, and IL-10 expression in TLR-stimulated dendritic cells. *J Leukoc Biol* (2015) 98:689–702. doi: 10.1189/jlb.3HI0914-453R

43. Lobo-Silva D, Carriche GM, Castro AG, Roque S, Saraiva M. Interferon-beta regulates the production of IL-10 by toll-like receptor-activated microglia. *Glia* (2017) 65:1439–51. doi: 10.1002/glia.23172

44. Kumaran Satyanarayanan S, El Kebir D, Soboh S, Butenko S, Sekheri M, Saadi J, et al. IFN-beta is a macrophage-derived effector cytokine facilitating the resolution of bacterial inflammation. *Nat Commun* (2019) 10:3471. doi: 10.1038/s41467-019-10903-9

45. Shukla AK, McIntyre LL, Marsh SE, Schneider CA, Hoover EM, Walsh CM, et al. CD11a expression distinguishes infiltrating myeloid cells from plaque-associated microglia in alzheimer's disease. *Glia* (2019) 67:844–56. doi: 10.1002/glia.23575

46. Getts DR, Terry RL, Getts MT, Muller M, Rana S, Shrestha B, et al. Ly6c+ "inflammatory monocytes" are microglial precursors recruited in a pathogenic manner in West Nile virus encephalitis. *J Exp Med* (2008) 205:2319–37. doi: 10.1084/jem.20080421

47. Weiss N, Miller F, Cazaubon S, Couraud PO. The blood-brain barrier in brain homeostasis and neurological diseases. *Biochim Biophys Acta* (2009) 1788:842–57. doi: 10.1016/j.bbamem.2008.10.022

48. Tohidpour A, Morgun AV, Boitsova EB, Malinovskaya NA, Martynova GP, Khilazheva ED, et al. Neuroinflammation and infection: Molecular mechanisms associated with dysfunction of neurovascular unit. *Front Cell Infect Microbiol* (2017) 7:276. doi: 10.3389/fcimb.2017.00276

49. Taylor RA, Sansing LH. Microglial responses after ischemic stroke and intracerebral hemorrhage. *Clin Dev Immunol* (2013) 2013:746068. doi: 10.1155/2013/746068

50. Dudvarski Stankovic N, Teodorczyk M, Ploen R, Zipp F, Schmidt MHH. Microglia-blood vessel interactions: A double-edged sword in brain pathologies. *Acta Neuropathol* (2016) 131:347–63. doi: 10.1007/s00401-015-1524-y

51. Zhao X, Eyo UB, Murugan M, Wu LJ. Microglial interactions with the neurovascular system in physiology and pathology. *Dev Neurobiol* (2018) 78:604–17. doi: 10.1002/dneu.22576

52. Ho HH, Ivashkiv LB. Role of STAT3 in type I interferon responses. negative regulation of STAT1-dependent inflammatory gene activation. *J Biol Chem* (2006) 281:14111–8. doi: 10.1074/jbc.M511797200

53. Tsai MH, Pai LM, Lee CK. Fine-tuning of type I interferon response by STAT3. *Front Immunol* (2019) 10:1448. doi: 10.3389/fimmu.2019.01448

54. Au-Yeung N, Mandhana R, Horvath CM. Transcriptional regulation by STAT1 and STAT2 in the interferon JAK-STAT pathway. *JAKSTAT* (2013) 2:e23931. doi: 10.4161/jkst.23931

55. Platanias LC. Mechanisms of type-i- and type-II-interferon-mediated signalling. *Nat Rev Immunol* (2005) 5:375–86. doi: 10.1038/nri1604

56. Li Q, Li Q, Hao Z, Zheng X, He W. A novel polysaccharide from rhizoma panacis japonica exerts anti-inflammatory effects *via* STAT3 signal pathway. *RSC Adv* (2018) 8:26371–6. doi: 10.1039/C8RA02923G

57. Vanlandewijck M, He L, Mae MA, Andrae J, Ando K, Del Gaudio F, et al. A molecular atlas of cell types and zonation in the brain vasculature. *Nature* (2018) 554:475–80. doi: 10.1038/nature25739

58. He L, Vanlandewijck M, Mae MA, Andrae J, Ando K, Del Gaudio F, et al. Single-cell RNA sequencing of mouse brain and lung vascular and vessel-associated cell types. *Sci Data* (2018) 5:180160. doi: 10.1038/sdata.2018.160

Frontiers in Immunology

Explores novel approaches and diagnoses to treat immune disorders.

The official journal of the International Union of Immunological Societies (IUIS) and the most cited in its field, leading the way for research across basic, translational and clinical immunology.

Discover the latest Research Topics

See more →

Frontiers

Avenue du Tribunal-Fédéral 34
1005 Lausanne, Switzerland
frontiersin.org

Contact us

+41 (0)21 510 17 00
frontiersin.org/about/contact